REPORT NO. 153

JUNE 1966

FULL SCALE WIND TUNNEL TEST REPORT

LIFT FAN FLIGHT RESEARCH AIRCRAFT PROGRAM

GENERAL ELECTRIC

REPORT NUMBER 153

FULL SCALE WIND TUNNEL TEST REPORT

XV-5A Lift Fan Flight Research Aircraft

Contract No. DA 44-177-TC-715

June, 1966

ADVANCED TECHNOLOGY & DEMONSTRATOR PROGRAMS DEPARTMENT
GENERAL ELECTRIC COMPANY
CINCINNATI, OHIO 45215

CONTENTS

(Continued)

(Continued)

(Continued)

(Continued)

SECTION		PAGE

(Continued)

BLANK PAGE

LIST OF FIGURES

(Continued)

FIGURE

(Continued)

(Continued)

(Continued)

FIGURE

(Continued)

FIGURE

(Continued)

FIGURE

(Continued)

FIGURE

(Continued)

FIGURE

(Continued)

FIGURE

1.0 SUMMARY

The XV-5A Aircraft Serial Number 62-4505 was tested in the NASA-Ames Research Center Wind Tunnel facilities between April 29, 1964 and July 9, 1964. These tests were performed in accordance with Contract DA 44-177-TC-715 and represented a total of thirty-seven test hours, twenty-one of which were with the fans operating. The test program included aerodynamic, thermodynamic and mechanical evaluation of the complete flight type aircraft system at flight speeds equivalent to hover up through 100 knots in both the conventional and fan power modes of flight.

This report summarizes the more important aerodynamic performance obtained during the test program. The data are presented graphically in coefficient form to provide a consistent basis of comparison.

The aerodynamic results obtained during these tests may be summarized by saying that the aircraft, as designed and tested, has adequate control power, lift, horizontal thrust and static stability to permit safe transitional flight between a hover lift-off and conversion to the jet mode of flight.

The results of this wind tunnel test program have proven to be a valuable asset during conduct of the flight test program. Using these data, predictions of aircraft performance have been verified by actual measured flight data.

BLANK PAGE

2.0 INTRODUCTION

This report represents a summary of the results of the full-scale wind tunnel tests of the XV-5A flight aircraft, Serial Number 62-4505. These tests were performed in the NASA, Ames Research Center, 40 X 80 foot wind tunnel and the outdoor static thrust stand. Only minimum modifications of the aircraft were used in preparing for the wind tunnel tests, in order to test, as near as possible, the systems as they would exist during actual aircraft flight. This required that all control actuation be performed using the conventional control devices such as conventional stick, throttles, etc., as designed into the aircraft systems.

After preparing the aircraft for testing, that is, installing the actuation and instrumentation systems, testing was initiated on April 29, 1964 and was concluded on July 9, 1964. The total test program included four test phases, two on the static thrust stand and two in the 40 X 80 foot wind tunnel. During the test program, performance data were obtained for simulated flight conditions from zero flight speed, equivalent to hover in the fan mode, up through and above maximum fan supported flight. Tests of the aircraft in the conventional configuration were performed for a range of aircraft configurations, such as variable flap deflections and the intermediate configurations experienced during conversions between the two modes of flight. For each set of test conditions approximating near trimmed flight, the effects of control pertubations around the given test conditions were obtained as well as changes in the aircraft attitude. This report presents the principle results of these test conditions in suitable coefficient forms. Typical procedures for using these coefficients in analysis of actual flight conditions is also presented.

Additional data are at the General Electric Company for review but have not been prepared in multiple copies. The data include log sheets, instrumentation calibration curves, inspection records, test procedures, maintenance records and all recorded data in both absolute units and in coefficient notation. Copies of these data will be provided on request from authorized agencies or personnel.

Photographs of the aircraft installed in the wind tunnel and the static thrust stand are shown in Figures 1 and 2. Figure 1 shows two views of the aircraft installed in the wind tunnel test section. The aircraft as shown is in the "pre-conversion" configuration. Figure 2 shows the aircraft mounted on the outdoor static thrust stand. Here also, the aircraft is shown in the pre-conversion configuration and located at a height above the ground of approximately 62 inches based on gear-height. This is a height at which ground effects are assumed to have diminished to a relatively small value.

3.0 AIRCRAFT AND APPARATUS

3.1 AIRCRAFT

The basic test article used during this program was the flight quality XV-5A Aircraft, Serial Number 62-4505. The basic design intent of the aircraft was maintained during the tests except when particular modifications unique to the wind tunnel installation were required. Figure 3 shows the general arrangement of the aircraft in a three view drawing. Some of the more significant aircraft geometric data is tabulated below.

3.1.1 Areas

Wing Area (including 49 square feet of fuselage)	260.3 Sq. Ft.
Horizontal Tail Area	52.9 Sq. Ft.
Vertical Tail Area	51.0 Sq. Ft.
Flap Area	25.4 Sq. Ft.
Aileron Area (aft of hinge line), Total	20.1 Sq. Ft.
Elevator Area (aft of hinge line), Total	12.0 Sq. Ft.
Rudder Area (aft of hinge line)	6.4 Sq. Ft.
Wing Fan Annulus Area, Total	35.6 Sq. Ft.
Wing Fan Total Area (fan tip)	42.6 Sq. Ft.
Pitch Fan Annulus Area	5.64 Sq. Ft.

3.1.2 Dimensional Data

Wings:	
Span:	29.83 Ft.
Chord:	
Root	12.08 Ft.
at break in quarter chord	9.09 Ft.
theoretical tip	3.58 Ft.
mean aerodynamic	9.41 Ft.
Sweep at 25% chord:	
inboard panel	15.0 Deg.
outboard panel	28.3 Deg.
Leading edge of M.A.C.	FS-211.1 In.
Aspect ratio	3.42

Ailerons:	
Span	6.37 Ft.
Chord	29.6 Percent
Centroid of aileron area	BL-139.6 In.
Flaps: (single slotted)	
Span	43.0 Percent
Chord (average)	19.6 Percent
Horizontal Tail:	
Span	13.18 Ft.
Chord:	
root	5.46 Ft.
tip	2.56 Ft.
Sweep of leading edge	19.5 Deg.
Aspect ratio	3.29
Pivot point	FS-496.7 In.
Distance of 1/4 M.A.C. from wing 1/4 M.A.C.	21.17 Ft.
Elevators:	
Span (per side)	5.47 Ft.
Chord:	
root (BL 4.3)	1.337 Ft.
tip (BL 69.9)	0.854 Ft.
Location of 1/4 M.A.C.	FS-521.1 In.
Vertical Tail:	
Sweep of leading edge	35.4 Deg.
Aspect ratio	1.178
Distance of 1/4 M.A.C. to wing 1/4 M.A.C.	18.25 Ft.
Rudder:	
Span	5.20 Ft.
Chord:	
root	1.470 Ft.
tip	0.980 Ft.
Location of 1/4 M.A.C.	FS-507.4 In.

Wing Fans:

Centerline:

lengthwise	FS-256 In.
spanwise	BL-61 In.

Pitch Fan:

Centerline located at	FS-58.5 In.

3.1.3 Center of Gravity

Center #1 (aft)	WL-112 In.
	FS-246 In.
Center #2 (forward)	WL-112 In.
	FS-240 In.

3.1.4 Control Movements

The following motions are nominal design values of maximum deflections. Actual measured data will be presented in results of test.

Rudder - 25 degrees trailing edge left and right.

Rudder pedals - 3 1/4 inches forward and aft.

Elevator - 25 degrees trailing edge up and down.

Longitudinal control stick - 15 degrees aft and forward.

Ailerons (flaps at 0 degrees) - 19 degrees trailing edge up and 15 degrees trailing edge down.

Ailerons (flaps at 45 degrees) - 8 degrees trailing edge up and 27 degrees trailing edge down.

Lateral control stick - 7 1/2 degrees left and right.

Horizontal stabilizer - 20 degrees leading edge up and 5 degrees leading edge down.

Flaps - 45 degrees trailing edge down.

Pitch fan modulator door - 68 degrees total travel.

Wing fan yaw control (differential vector) - 32 degrees maximum at zero vector angle.

Wing fan roll control (differential stagger) - 24 degrees maximum.

Wing fan collective control (collective stagger) - 13 degrees minimum - 37 degrees maximum.

Wing fan vector control (collective vector) - minus 5 degrees to plus 50 degrees.

3.2 AIRCRAFT MOUNTING

The aircraft was supported in both the wind tunnel and the static stand by a three point mounting system. Mounting was accomplished by adapting to existing jack pad points provided on the aircraft.. Figure 4 shows schematically the mount arrangement of the aircraft in the wind tunnel test section. Also shown are location details of the three mounting points used for the tunnel testing.

For the static stand testing, each of the ball sockets were replaced with calibrated strain gaged load cells. Details of this mounting system used on the static thrust stand may be observed in Figure 2.

3.3 AIRCRAFT CONTROL ACTUATION

In order to provide for remote operation of the aircraft system while installed in the tunnel, an actuation system capable of operating the conventional pilot operated controls was provided in the aircraft. This system consisted of an array of electric actuators, bars and linkages capable of moving each of the basic system control inputs. These included collective stick, rudder pedals, longitudinal and lateral stick and both engine throttles. The remote console for control of the actuators was located in the wind tunnel control room.

Control motions were transmitted to direct reading dials attached to the remote concole to provide continuous monitoring of the various control inputs.

Other functions controlled through the remote console were:

- flap position
- vector angle command
- mode selection
- horizontal tail trim
- diverter valve actuation

Note: Independent operation of the diverter valve cannot be accomplished normally on the aircraft, but was provided in the wind tunnel as a safety device.

3.4 PROPULSION SYSTEM OPERATION AND CONTROL

To monitor the propulsion system operation, the following engine instruments were located in the wind tunnel control room:

- Engine RPM
- Engine EGT
- Engine Fuel Flow
- Engine Oil Pressure
- Hydraulic System Pressure
- Wing Fan RPM
- Pitch Fan RPM
- Engine Ignition Control

Observation and actuation of the aircraft's safety systems (structural overhead, fire warning, and fire extinguishing) were available in the wind tunnel control room, plus an auxiliary fire extinguishing system installed within the aircraft structure.

3.5 SPECIAL TEST EQUIPMENT

Three basic aircraft modifications were investigated during this test program which differed from the flying configuration.

The first modification provided a means of simulating fan mode operation with the pitch fan inoperative. Blank-off plates were installed in the pitch fan ducts during certain test conditions, shutting off the gas flow to the pitch fan. In addition, spacers were added to the diverter valves that would open the valve sufficiently to bleed flow through the tailpipe equivalent to that previously ducted to the pitch fan. This diverter valve adjustment precluded retrimming of the wing fan scroll areas and maintained equivalent gas generator operating conditions.

Various horizontal stabilizer geometry configurations were investigated. Tip extensions were employed to increase the horizontal tail area from 52.9 to 59.4 square feet. The effects of a leading edge slat of approximately 15 percent chord extending over the entire stabilizer leading edge were also investigated.

A separate remote hydraulic supply was provided to drive the wing fan exit louver actuation system. This was accomplished to allow full exit louver travel when it became evident that the existing aircraft system (hydraulic system and louver actuators) could not sustain the aerodynamic loads experienced by the louvers.

3.6 INSTRUMENTATION

3.6.1 Aircraft Forces

For testing the aircraft in the wind tunnel, six components of the forces were measured on the conventional beam balance system provided in the NASA facility. The force data were recorded by the DATEX System which is part of the wind tunnel facility.

Instrumented flexure load cells were used for force measurements on the static thrust stand. During the first static thrust test program, only five force components were recorded; side force was omitted, while in the second test phase all six components were recorded. The load cell outputs were recorded on continuously running Sanborn oscillographs during each test run. Conventional forces and moments were obtained by applying the appropriate load cell mounting geometry.

3.6.2 Research Instrumentation

This category includes all measurements taken during the test program in excess of propulsion system operating parameters and aircraft force data.

- Structural temperatures
- Cooling air and gas temperatures
- Control stick and surface positions
- Cooling system pressures
- Hydraulic, gearbox and engine oil temperatures
- Stick forces and wing fan closure forces
- Wing and pitch fan blade stresses
- Wing fan inlet vane stresses
- Fan and engine vibrations
- Engine and fan RPM's
- Aircraft angle of pitch and yaw indicator deflections

Most of the above measurements were recorded using a high speed recording digital voltmeter system. This recording equipment consisted of a switching system capable of scanning data at the rate of five per second. The system recorded the data in two forms as well as on a visual indicating voltmeter. The two forms of recorded data were a typed set of measurements available for monitoring during the conduct of the test and a coded punched tape that was applicable to automatic machine reduction of data. This equipment had the capability of recording all measurements in approximately forty seconds; compatible with the time required for a complete force reading. This allowed for rapid setting and acquisition of data at each test point. Under normal conditions of test, data points were obtained at approximately two minute intervals.

Table ˉ gives a listing of the measurements recorded on the digital system. The mea.urements are listed by nomenclature as well as the normal symbols that were assigned to these measurements at the initiation of the XV-5A program.

Engine and fan vibration levels were monitored on CEC vibration meters fitted with filters for removing the low frequency vibration levels of the aircraft. The fan system was fitted with a hi-pass filter with a cut-off frequency of 30 CPS while the engine cut-off frequency was 60 CPS. The vibration levels were periodically recorded on log sheets.

Fan and vane stresses were monitored on a scope presentation system during the testing and simultaneously recorded on a multi-channel tape system to allow for further analysis and evaluation under laboratory controlled conditions.

Additional inputs of data included wind tunnel temperature, pressure and velocity. These inputs were obtained from the tunnel instrumentation and hand fed into the data handling system.

The digital recording system referred to in Table I was a high speed digital voltmeter system. The system recorded the data on a coded, punched tape and presented the data during the tests in a typed format and on a visual indicating voltmeter. A scanning rate of five per second was available with all measurements recorded in approximately 40 seconds; this made it compatible with the time required for a complete set of force readings.

4.0 TEST PROCEDURES

4.1 WIND TUNNEL TESTS

4.1.1 Fan Powered

Engines were started using a mobile air-impingement start cart. After engine start, the tunnel speed was increased to 20 kts. and the propulsion system was diverted to the fan mode.

To obtain the test conditions, the tunnel speed and fan speeds were set at the desired values, then the aircraft was trinned. Trim was obtained by zeroing the drag using vector angle command, then zeroing the pitching moment about the desired reference moment center with the longitudinal control.

After the aircraft was trimmed, pertubations of the particular test variable were made about the trimmed condition. The variables tested included:

- Angle of attack (-4 degrees to +20 degrees)
- Angle of side slip (+10 degrees to -10 degrees)
- Vector command (0 degrees to 50 degrees)
- Tail incidence (-5 degrees to +20 degrees)
- Longitudinal stick position
- Lateral stick position
- Rudder pedal position
- Collect ve stick position

During these pertubations, the gas generator power setting and tunnel speeds were held constant.

At each test point, a complete force reading and scan of the digital data were taken at approximately the same interval. Periodically during the data points recordings of stresses and vibrations were taken.

Testing was performed at two power settings in the fan mode equivalent to approximately 65 percent and 95 percent fan speed while tunnel velocity was varied from zero to approximately 100 knots.

4.1.2 Conventional

Testing of the aircraft in the conventional mode (non-fan powered) was conducted whenever possible without the engines running. Complete power-off operation was possible because all conventional control systems are mechanical, except the ailerons which require hydraulic boost. The remote hydraulic supply was capable of supplying this boost separate from the aircraft system.

Only the tunnel speed needed adjustment; 80 knots was used for this type of testing throughout the test program.

To test the aircraft in the "pre-conversion" and "VTOL-converted" conditions, the engines were operated at idle power to maintain hydraulic pressure on the wing fan louvers, closure doors and pitch fan modulator systems (the remote hydraulic system was not plumbed to these units).

4.2 STATIC THRUST STAND TESTS

4.2.1 Phase I

The Phase I testing on the static thrust stand was run primarily to demonstrate the capability of the aircraft to run for sustained periods of time, 30 minutes or longer, without apparent structure heating problems, and to obtain a general checkout of the actuation and instrumentation system. Any force and moment data obtained was of secondary importance. Also during this period of testing, the apparent inadequacy of the louver actuation system was investigated.

The procedure used during the Phase I tests was to start the engines, then clear the area under and around the aircraft. The Sanborn and digital recorders were turned on, then the aircraft was diverted to the fan mode and the engines adjusted to the desired power levels. Control inputs were made and force and digital data recorded. Periodically, complete scans of the temperature data were taken to insure that the aircraft structural temperatures were within limit values.

For the louver force surveys, the louver actuators were replaced with fixed instrumented load links, whose outputs were recorded by the digital system. The engines were started and diverted to the fan mode. As the engines were accelerated and decelerated slowly, the fan speeds and louver link loads were recorded continuously. This procedure was repeated for various louver positions.

Because of the severe reingestion levels experienced during these ramp runs, as well as high levels of aircraft vibration in the force measurement system, questionable force data were obtained and were not used as a basis in future analysis.

4.2.2 Phase II

In preparation for the second static thrust stand runs, the instrumentation systems were modified in two ways:

- The load or force measurements were fitted with filters to attenuate the aircraft vibration force levels.
- Fan speeds and inlet temperatures, as well as forces, were recorded continuously on Sanborn oscillograph equipment during each system run.

The procedure used during this test phase was to start the Sanborn equipment prior to starting the engines. The engines were then started, diverted to the fan mode, and accelerated to the desired power setting. With the recording systems still operating, the desired control excursions were made and data recorded.

4.3 SUMMARY OF TEST RUNS AND TIMES

4.3.1 Wind Tunnel Tests

Table II shows a summary of the thirty-three runs performed during the wind tunnel tests, listing the range of variables and configurations tested.

4.3.2 Static Thrust Stand Tests

Tables III and IV summarize the tests performed during the two phases of the static thrust stand runs.

4.3.3 Operating Times

Table V presents a summary of the total operating times accumulated on the aircraft and propulsion system during conduct of this test program.

BLANK PAGE

5.0 DATA REDUCTION PROCEDURES

5.1 WIND TUNNEL TESTS

5.1.1 Force Data

Force data gathered during the wind tunnel tests were reduced to conventional aircraft coefficient form using electronic data processing methods established by NASA for all wind tunnel data. The data obtained for the power-off configurations were corrected for the effects of wind tunnel wall interferences in the following manner:

$$C_L = C_{Lu} + 0.58\ C_{Lu}$$

$$C_D = C_{Du} + 0.0102\ (C_{Lu})^2$$

$$C_m = C_{mu} + 0.0131\ C_{Lu}$$

"u" denoted measured coefficients

A drag correction due to the strut system was also applied to the data which amounted to the following:

$$C_D = C_{Du} + 0.0133$$

$$C_m = C_{mu} - 0.0066 - 0.0123 \sin \alpha$$

No corrections due to wall interference effects were applied to the power-on fan mode data, since the effects of fan airflow on wind tunnel corrections are unknown.

5.1.2 Digital Data

The coded punched tape of the digital system was processed through electronic computers to convert the coded data into engineering units, for example, temperatures in degrees F, forces in pounds, and positions in degrees. The process involved a simple conversion of the coded data into engineering units by use of a previously obtained set of calibration curves.

The output of this process was a printed listing of all the data with proper identification of run and reading number as well as the measurement symbol. Table VI presents a typical listing of data for one particular run and reading.

In addition to the printed listing, certain propulsion system operating parameters were stored on a punched card output for use in the coefficient reduction methods described below.

5.1.3 Performance Calculations

Performance calculations for the complete system were processed on electronic computers in a manner similar to both the force and digital data. The input data for this program was obtained from the card outputs of the force as well as the digital data programs described above. The inputs to this program consisted of the following measurements.

- Forces and moments in conventional coefficients
- Angle of attack and sideslip
- Wind tunnel velocity head in #/ft.^{2}
- J-85 engine speeds
- Wing fan and pitch fan RPM
- Fan and engine inlet temperature
- Wind tunnel temperature and total pressure

These inputs were then used to calculate the aircraft performance in three different systems of coefficients; conventional, slipstream and fan. Non-dimensional velocity ratios and fan speed ratios were also computed. Table VII shows a typical listing of the computed data obtained from this program.

To perform these calculations, certain basic assumptions concerning fan performance at hover conditions were necessary, particularly for computing fan speed ratios and slipstream velocity head, qs. This data is shown in Figures 7 through 9. Figure 7 shows the assumed fan disc loading that was used in the computation of slipstream velocity head, qs. Figures 8 and 9 show the basic engine speed - horsepower - fan speed relationships used in calculation of the fan speed ratios throughout the transition envelope. Although these curves are estimated data, agreement with measured static performance in the tunnel and on the thrust stand was well within expected measurement accuracies, and for practical purposes these curves show real performance. Agreement should be good since these estimates were based on average fan performance obtained during flightworthiness and acceptance tests of these fan systems.

Appendix B presents the relationships that exist between the three forms of fan performance coefficients. In this report only two coefficient forms will be used for showing the data. Conventional coefficients will be used for power-off (fans-off) data and fan coefficients (H's) will be used for all the fan-powered data.

5.2 STATIC THRUST STAND TESTS

Data acquisition methods used during Phase I of the static thrust stand runs were not refined to the point where automatic data processing was possible. The most important set of data obtained during this test phase was the louver load data as described in detail in Appendix A.

For the Phase II test program, the instrumentation system was improved to the condition that allowed for automatic performance calculations. A specific reduction program using electronic computers was set up to accept the data visually read from the Sanborn charts. The necessary calculations of forces and moments were then performed. The reduced data was presented in absolute force measurements as well as fan and slipstream coefficients.

BLANK PAGE

6.0 TEST RESULTS

The significant results of both the wind tunnel and static thrust stand tests will be discussed in the following sections. The aircraft is in the normal as-designed configuration unless otherwise specified. Similarly all data will be referenced to Moment Center (MC) #2 (FS-240, WL-112). Some data will include Moment Center #1 (FS-246, W-112), however, MC #2 is the center of gravity location closest to that anticipated for use during the flight test program. When not specifically designated, the data will be presented for MC #2.

6.1 AIRCRAFT RIGGING

Prior to presentation or analysis of any of the wind tunnel test data, it is desirable to describe in detail the rigging of the aircraft control systems as it existed during this test program. In particular, it is necessary to understand the corresponding motions of the fan exit louvers and pitch fan modulator doors with respect to the possible control inputs. Prior to conduct of the tests, the aircraft was rigged according to specification. The following data presents the control surface motions that were experienced during conduct of the test program when the specific control inputs were commanded.

6.1.1 Vector Command

The vector command function is the means used for control of collective vector of the wing fan louvers. Collective vector, B_v, is defined as the average louver angle of the fan system. In the normal aircraft, control of this function is obtained by a roller switch on the conventional control stick grip. A cockpit dial for vector command indication is provided on the instrument panel. Vector command is the readings as presented on the dial.

Figure 10 shows the variation of the individual louvers with respect to vector command for approximately neutral controls; 50 percent collective will be referred to as neutral and variations of longitudinal stick do not effect the vector command function. Figure 11 shows the same data in terms of average louver angle and stagger angle for the left and right wing fans. This data shows that the rigging, although within rigging tolerances, has a slight yaw left and roll right input at the louvers for approximately neutral controls.

6.1.2 Longitudinal Stick

The longitudinal control stick controls the motion of the pitch fan modulator door in the fan-mode as well as the conventional elevator. The authority of the longitudinal stick motion on the elevator is fixed while the authority on the pitch door is programmed with respect to the vector command function.

Figure 12 shows the pitch fan door and elevator positions for corresponding longitudinal stick position for a range of vector command angles. The reduction of longitudinal stick authority on the pitch fan door with increasing vector command is clearly apparent from this data. Similarly, the constant elevator authority is apparent. By comparison of the pitch fan door angle and rigging tolerances, it may be concluded that a 13 degree forward stick motion is the limit value.

Figure 13 shows the variation of pitch fan door position, at neutral stick, with vector command. Gearing ratios for pitch fan door with respect to vector command angle and longitudinal stick angle are presented as a function of the other variables.

6.1.3 Collective Stick

Collective stick control is a control function characteristic of fan mode flight only. Collective stick motions have control authority over collective stagger of the wing fans as well as a small amount of pitch modulator control. The authority of the collective control diminishes rapidly at high vector angles. It begins to diminish at a vector command of about 15 degrees and is completely washed out by about 30 degrees.

Figure 14 shows the effects of collective stick position on wing fan vector and stagger angles for three vector angles of 0 degrees, 16 degrees, and 29 degrees. Also shown is the control authority of the collective stick on the pitch fan modulator.

Figure 15 shows the gearing ratios for collective control of the wing fan stagger and pitch fan modulator door angle. The wash-out of collective authority is clearly apparent from the lower figure.

6.1.4 Lateral Stick

Motion of the lateral stick controls two functions similar to the case of longitudinal stick motions. In addition to controlling the aileron motions, the lateral stick controls louver stagger (differentially). This then provides for continuous roll control from zero speed where fan momentum control is used up to high transition speeds where aerodynamic control effectiveness becomes predominant.

Figure 16 shows the variation of louver stagger and vector angles for each fan system versus lateral stick position. These are shown for vector command angles of 0 degrees, 11 degrees, 16 degrees, and 29 degrees. At vector angles above 30 degrees there is no corresponding change in stagger angle with lateral stick motions. Also shown in Figure 16 is the corresponding aileron motions with lateral stick position. This aileron motion applies to 45 degrees flap deflection and the corresponding 15 degree aileron droop. At neutral stick it may be observed that both ailerons are deflected to about 15 degrees trailing edge down.

Figure 17 shows the louver stagger (differential) gearing ratios as a function of vector command. This data clearly shows the wash-out of the lateral control function in the fan louver system.

6.1.5 Directional Rigging

Directional control or rudder pedal deflections cause a combined fan louver and conventional rudder motion. However, when a rudder pedal input is applied there is not only a corresponding change in louver vector angle, right to left, but also an associated louver differential stagger input in the direction of a favorable roll control input. This built in programming was anticipated in the control system design in order to correct for an adverse roll that would occur with yaw control inputs during the fan mode of flight.

Figures 18 and 19 show the corresponding louver vector and stagger angles experienced by the fans for a complete range of vector command angles. Rudder inputs at neutral lateral control as well as at full reverse roll inputs are shown. Figure 20 shows this data in the form of differential vector and stagger angles versus rudder input and vector command. This is a more direct method of looking at the basic control authorities. Using this data, the gearing of vector and stagger angles with rudder pedal input was obtained and is shown in Figure 21.

6.1.6 Conventional Aircraft Control Rigging

The deflections of the rudder, elevator and ailerons with the corresponding stick motions were previously discussed for the case of operating in the fan mode. In addition to this rigging, there are additional control motions more characteristic of the conventional flight configuration.

Figure 22 shows the relationship of aileron deflections with lateral stick motion for a range of flap deflections. This change in aileron gearing is a result of the aileron droop variation with flap angle setting.

Another characteristic of the rigging of the aircraft conventional controls is shown in Figures 23 and 24. Figure 23 shows the relationship of elevator deflection with longitudinal stick for a range of horizontal stabilizer settings. From this data it may be shown that the elevator gearing ratio is related to the stabilizer incidence angle. This effect is shown in the upper curve in Figure 24 as a function of stabilizer incidence angle. The lower figure shows some additional data relating the change in elevator angle with the longitudinal stick fixed as the stabilizer is moved through the complete incidence range.

6.2 CONVENTIONAL AIRCRAFT PERFORMANCE

As part of the complete test program, numerous tests were performed on the aircraft in the conventional flight configuration. These tests were run at a velocity of 80 knots (q = 21 psf). The following discussion will present the results of this part of the test program.

6.2.1 Longitudinal (Angle of Attack) Characteristics

Figures 25 through 29 show the variation of longitudinal characteristics with angle of attack for a number of conventional flight configurations. Figures 25 and 26 show the effects of flap setting on conventional lift, drag and pitching moments. Note that the horizontal stabilizer incidence angle was set at -4.5 degrees during the 30 degree flap setting as compared to zero degrees during the zero and 45 degree flap settings.

Figures 27 and 28 show the longitudinal characteristics of the two aircraft configurations that exist during the intervals between the conventional mode of flight and the fan powered mode. Figure 27 is for the "pre-conversion" configuration that occurs during flight when the aircraft is prepared for conversion by opening up the fan louvers, pitch fan inlet and pitch fan modulator doors. The aircraft must be capable of sustained flight in this condition. Note that in order to test this configuration, the engines were running at idle power setting in order to provide hydraulic pressure for restraining the wing fan louvers and pitch modulator doors. Figure 31 shows the estimated lift, drag and moment contributions due to this level of engine power.

Figure 28 shows the longitudinal characteristics as obtained for the aircraft in the "VTOL-converted" condition. This condition of the aircraft is a transient situation that occurs during the short interval between the time the wing fan doors open and the time the diverter valve actuates and the fans pick up speed.

Figure 29 shows the effects of landing gear on the lift, drag and pitching moments for a flap setting of 30 degrees. During the tests when this set of data was obtained hydraulic boost was not maintained on the ailerons, and as a result, the ailerons tended to float upwards as compared to the normal droop position. Figure 30 shows a comparison of the aileron angles for this set of test data, and the normal aileron angles. Corrections were estimated for this change in aileron droop and are shown in Figure 29. The drag and lift corrections were negligible, the only significant correction is in the pitching moment as shown.

6.2.2 Lateral - Directional (Sideslip) Characteristics

Figures 32 through 36 show the variation of longitudinal and lateral characteristics with angle of sideslip for a number of conventional flight configurations. Figures 32 and 33 show longitudinal and lateral-directional characteristics for variable sideslip angles at an angle of attack of zero degrees and +8 degrees. Figure 32 is for flaps at zero degrees and Figure 33 for flaps at 45 degrees.

Figures 34 and 35 show the longitudinal and lateral-directional characteristics for a range of sideslip angles for the two intermediate aircraft configurations that occur during the conversion cycle. Figure 36 shows effects of landing gear on the lateral-directional characteristics during sideslip.

6.2.3 Control Power

Figures 37 through 42 show the effectiveness of each of the control systems for the conventional aircraft configuration. Figures 37 and 38 show the force and moment capability of the longitudinal control systems. These include the horizontal stabilizer incidence and longitudinal stick motions.

Figures 39 through 41 show the lateral control effectiveness of the ailerons for three different flap settings. These three different flap settings are equivalent to three different aileron droop values at which the effectiveness was measured. It should be noted here that there is a corresponding change in longitudinal stick position with lateral stick motions and conversely. This cross-coupling is due to the mechanics of the actuation system used to move the controls. Figure 43 shows this relationship between longitudinal and lateral stick motions.

Figure 42 shows the aircraft forces and moments as a result of rudder pedal deflections with the flaps at 45 degrees.

6.3 FAN POWERED AIRCRAFT PERFORMANCE

The following discussion will be concerned with the presentation of data obtained for the normal, unmodified aircraft while operating in the fan mode of flight from hover speed up through maximum fan-supported flight speeds. The test philosophy used in gathering the data was to first approximately trim the aircraft in drag and pitch moments at a given set of tunnel and fan speed conditions. Then changes in all control functions and aircraft attitudes from this trimmed condition were tested. The following is a discussion of this data which is shown in Figures 44 through 74.

6.3.1 Longitudinal Characteristics (Angle of Attack)

Figures 44 and 45 show the variation of lift, drag and pitching moments with angle of attack for a range of cross-flow velocity ratios, μ, from 0.11 to 0.26. These values of μ are equivalent to true airspeeds of from approximately 40 knots to 110 knots at full engine power.

The more important results shown in these figures are:

- Lift increases with increased angle of attack.
- Drag increases with increased angle of attack.
- Moments decrease with increased angle of attack for MC #2 up to a certain angle, after which they begin to increase with a farther angle of attack increase. Decreasing moments with angle of attack indicates a longitudinal statically-stable aircraft.

6.3.2 Lateral - Directional Characteristics

Figures 46 through 48 present the lateral-directional characteristics for the fan mode of operation in the form of forces and moments versus angle of sideslip. Angle of attack is zero unless otherwise noted.

6.3.3 Vector Command Effectiveness

Figures 49 through 53 show the variation of forces and moments with changes in the vector command function. Each figure shows the effects of changing vector command at a particular cross-flow ratio. For each range of test data, all other control functions were held fixed. However, it should be noted that even with the longitudinal stick fixed, changes in vector command will produce changes in the pitch modulator door as shown by the rigging data in Figure 12.

The data shown in Figure 49 were obtained during the Phase II Static Thrust Stand Tests while all other performance is a result of the wind tunnel tests.

6.3.4 Longitudinal Control Effectiveness

Longitudinal control effectiveness is shown in Figures 54 through 58 for a range of cross-flow ratios at approximately trimmed conditions of exit louver vector command. These figures show the control effectiveness for the fan mode of flight where motions of the longitudinal stick produce both elevator and pitch modulator door motions. Therefore, the moments and forces as shown represent the sum of both reaction and aerodynamic control.

Figure 54 shows the effectiveness at zero flight speed as obtained during the Phase II Static Thrust Stand runs. During these tests, problems in strain gage load cells caused drifting during the conduct of the tests. This drifting shows itself mostly in the measured moments, in particular the pitch moment. Even though this drift did occur and the absolute level of the measurements are in error, the small changes due to longitudinal stick motions should be valid because of the rapidity at which the data was taken for each series of runs.

6.3.5 Lateral Control Effectiveness

Figures 59 through 65 show the effectiveness of the lateral control system in changing forces and moments of the aircraft. Here again, the lateral control function operates the conventional ailerons in conjunction with movement of the fan exit louvers as shown in the previous rigging of the system.

The variation of lateral control effectiveness for a range of trimmed cross-flow ratios is shown in Figures 59 through 63 at a wing angle of attack of zero. Figures 64 and 65 show the lateral control effectiveness for some extreme angles of pitch and sideslip in the lower flight speed conditions.

6.3.6 Collective Control Effectiveness

Collective control is purely a fan thrust (lift) control function. Measured force and moment variations due to movement of this control are shown in Figures 66 through 68. Again, the data shown for zero flight speed in Figure 66 were obtained on the static thrust stand and drifting of moments, both pitch and roll, is apparent. For these test runs there was a re-rigging of the collective authority over fan stagger. This changed rigging, as shown, gave a collective authority range of from 13 to 30 degrees of stagger. Previous rigging was from 13 to 37 degrees of stagger. When using this data appropriate rigging corrections must be applied.

6.3.7 Directional Control Effectiveness

Force and moment changes due to rudder pedal inputs are depicted in Figures 69 through 74. Each curve presents forces and moments for a given cross-flow ratio versus rudder pedal position. Most of the figures include an excursion of rudder pedals for neutral lateral stick position as well as full reverse control inputs. There is no equivalent rudder effectiveness presented at zero flight speed due to insufficient test data at the time this test condition was run.

6.3.8 Horizontal Stabilizer Effectiveness

The effectiveness of the horizontal tail as a trim device was tested at one of the higher cross-flow ratios equivalent to near maximum fan supported flight. This is shown in Figure 75 in terms of lift, drag and pitch moment variations versus horizontal stabilizer incidence angle.

6.4 FAN POWERED AIRCRAFT PERFORMANCE - PITCH FAN "OFF"

The wind tunnel test program included a series of tests to investigate the performance of the aircraft in the fan mode with the pitch fan "off". The system used for shutting off the pitch fan was described in Paragraph 3.5. Figure 76A shows the estimated tailpipe thrust component resulting from the equivalent pitch fan flow discharge. Figure 76B shows the estimated lift and thrust components in coefficient form for a range of power settings. A thrust angle of 5.5 degrees and a reasonable fan-to-engine speed ratio was used to obtain the estimates.

Th[illegible] fan "off" performance data presented in this report do not include the above corrections.

6.4.1 Longitudinal Characteristics (Angle of Attack)

Variations of lift, drag and pitching moments with angle of attack are shown in Figure 77. This data was obtained at two different power levels for the conditions of near-trimmed lift and moments at zero angle of attack. Angle of attack variations were made holding control and power settings constant.

6.4.2 Lateral - Directional Characteristics (Angle of Sideslip)

Figures 78 and 79 show the variation of forces and moments with angle of sideslip for two representative trimmed flight conditions.

6.4.3 Vector Command Effectiveness

With the aircraft approximately trimmed in drag and moments, excursions of vector command were run with all other variables held fixed. This data is shown in Figures 80 through 83 for a range of cross-flow velocity ratios approximating flight speed from about 50 to 100 knots.

6.4.4 Longitudinal Control Effectiveness

With the pitch fan inoperative, longitudinal control is provided solely by the aerodynamic controls (stabilizer-elevator system). Figures 84 through 87 show the measured changes in forces and moments due to longitudinal stick inputs and the attendant elevator motions.

6.4.5 Lateral Control Effectiveness

Inputs from the lateral stick produce the same motions of the fan louver system and conventional ailerons whether the pitch fan is operating or not. As a check on possible influences of pitch fan operation on the flow distributions over the wings and fan, lateral control effectiveness was measured and the resulting data plotted in Figures 88 and 89 for two different cross-flow ratios.

6.4.6 Directional Control Effectiveness

Although the mechanical operation of the directional control system is not effected by the shutdown of the pitch fan, directional control effectiveness tests were run with the pitch fan "off", and the results are shown in Figures 90 and 91.

6.4.7 Horizontal Stabilizer Effectiveness

Figures 92 and 93 present the effectiveness of the horizontal stabilizer in controlling the pitching moments of the system. This data is shown as lift, drag and pitching moments versus tail incidence angle at two cross-flow ratios.

6.5 FAN SPEED RATIOS

Throughout the complete test program, measurements of fan and engine RPM's as well as inlet temperatures were obtained at each test point. Using the measured engine RPM and inlet temperature data in association with the estimated performance shown in Figures 8 and 9, a hover or zero flight speed fan RPM was calculated. This established a base on reference speed for the gas generator power setting being employed. This base speed when compared to the measured fan speed provides a correlation parameter called fan speed ratio. In summary, this correlating parameter is the ratio of fan RPM that would exist at a given flight condition, to the fan RPM that would exist at zero flight speed and the same gas generator power (RPM) setting.

During the test program, it became apparent that this fan speed ratio is influenced by almost every variable tested. The following data presents these speed ratios in a systematic fashion.

6.5.1 Variable Forward Speed

Figures 94 and 95 show the variation of speed ratio with crossflow for the three fan systems. These data were obtained at near trimmed drag conditions. The vector command angle required is shown on the figures. Figure 94 was obtained at the hi power setting while Figure 95 was at the lo power level. These figures show the speed trends to be as follows:

- Pitch fan speed changes very little with cross-flow.
- Both wing fans exhibit a fan speed increase of between 9 to 10% from hover speed at the same power setting.
- At a cross-flow ratio of 0.25 there appears to be the possibility that the fan speed ratio has reached a peak value.

6.5.2 Variable Angle of Attack

The variation of wing and pitch fan speed ratios with angle of attack of the aircraft is shown in Figures 96 through 98. Figures 96 and 97, taken at different fan speed levels, show a definite fan speed increase with angle of attacks from -5 degrees to about +5 degrees. As for the pitch fan speeds shown in Figure 98, a steady rise in speed with increased angle of attack is apparent for all speed conditions.

6.5.3 Variable Angle of Sideslip

Figure 99 shows the variation of wing fan and pitch fan speeds with angle of yaw or sideslip. Figure 105 shows only the wing fan speeds with yaw or sideslip since the pitch fan is "off".

6.5.4 Variable Control Inputs

Figures 100 through 104 show the variation of some of the significant fan speed changes with control system inputs. Data taken at zero flight speeds are not presented because the data were obtained during conditions of severe reingestion. These conditions produce fluctuations in fan speeds of much larger levels than would be expected from the basic control inputs. Therefore, valid data could not be obtained during these conditions.

Some of the more interesting points apparent in these figures are:

- Input of roll or lateral control causes fan speed changes only at low flight speeds where the roll authority on louver stagger is greatest.
- A similar situation occurs for collective control inputs at low speeds. Full-down collective when maximum stagger occurs causes highest fan speeds.
- Very little or no fan speed changes occur due to rudder inputs, with or without full lateral stick inputs.
- Pitch fan speed changes with longitudinal stick inputs are small, less than 1 percent.

6.6 HORIZONTAL STABILIZER MODIFICATIONS

As a result of early test results, a sequence of runs were performed in an attempt to improve the longitudinal stability of the aircraft system at high angle of attacks. These tests included the addition of a leading edge slat on the normal horizontal tail as well as increasing the total horizontal tail area by the use of tip extensions. The following data summarizes the results of this phase of the wind tunnel tests.

6.6.1 Longitudinal Characteristics (Angle of Attack)

Figures 106 through 108 show the variation of lift, drag, and moments for a range of approximate trimmed flight conditions and for three different tail configurations. Figure 106 shows performance for the normal tail configuration with the leading edge slat installed. Figure 107 and 108 show performance for the tail with tip extensions, both with and without the leading edge slat. All sets of data show the characteristic increases in lift and drag with angle of attack. The moment data show a positive (stable) stability at low angles of attack followed by a negative (unstable) stability at the higher angles.

Figures 109 and 110 present longitudinal characteristics for a range of fixed control settings at two equivalent speeds of about 40 to 60 knots. The change in longitudinal stability (change in moments with respect to angle of attack) is apparent in both figures at the high positive (nose down) values of longitudinal stick setting.

6.6.2 Horizontal Stabilizer and Longitudinal Control Effectiveness

The effectiveness of the horizontal stabilizer in terms of moment, lift and drag change with angle of incidence is shown in Figures 111 through 118.

Figures 119 through 121 show the longitudinal control effectiveness at two values of cross-flow ratio for each of the three tail configurations.

6.7 PITCH INDICATOR CALIBRATION

During part of the test program, the flow angle as measured by the pitch or angle of attack indicator was recorded for a range of aircraft attitudes and flight speeds. Figures 122 and 123 present the variations of the measured angle of attack versus the geometric angle of the aircraft in the tunnel. The data are shown for a range of cross-flow ratios for both the pitch fan "on" as well as the special cases with it "off". Also shown is the lines of zero deviation or the true indication.

Using this data, it is possible to summarize the characteristics as a zero intercept and a slope for a range of cross-flow ratios. This has been done and is shown in Figure 124. This figure shows that both the zero intercept as well as the slope increase with decreasing cross-flow ratio. At very low speeds the values are indetermediate because the velocity at the nose boom is essentially zero. The zero deviation line shown in Figures 122 and 123 is defined by the condition; that as the cross-flow ratio approaches infinity, the zero intercept should approach zero and the slope should be 1.0. Figure 125 shows the test data replotted against the inverse of the cross-flow ratio, and a reasonable fairing of the data through the zero intercept is possible for both the slope and the zero angle of attack error. The analysis tends to show that the pitch attitude calibration as obtained is a correct set of data and these errors or deviations angles are apparently due to flow distortion at the nose boom. It is not known whether this distortion is due to the fan-wing effects or due to wind tunnel flow angularities as a result of fan operation.

BLANK PAGE

7.0 ANALYSIS OF RESULTS

The following discussion will be concerned primarily with the development of a series of basic curves and characteristics that will summarize the complete low flight speed operating envelope of the aircraft system. The methods to be used in summarizing the data will be to first obtain a reference set of trimmed flight characteristics and then provide a means of perturbating from this reference. First the performance of the conventional aircraft system will be presented, followed by the fan powered mode of flight.

7.1 CONVENTIONAL PERFORMANCE

Figures 126 and 127 show the estimated trimmed lift, drag and longitudinal control characteristics for the three flap settings tested. To obtain these curves the basic untrimmed polars shown in Figures 25 through 29 were first trimmed using the horizontal stabilizer effectiveness and elevator effectiveness shown in Figures 37 and 38. For the power-on characteristics, the thrust component of the propulsion system was assumed to act at a 5.5 degree inclination relative to the aircraft reference plane. For trimmed thrust components, the lift increment was computed and the moment contribution assumed to be negligible. This resulted in the curves shown in Figure 127.

Figure 128 is a comparison of trimmed lift, drag and longitudinal control for the three intermediate configurations that exist during a conversion cycle. All of the data are presented for the gear-up condition.

The gear lift, drag and moment increments are shown in Figure 129. These characteristics were obtained from Figure 29 using corrections for differences in longitudinal control settings as well as the floating ailerons. Ailerons floated because of failure to have hydraulic boost on the system.

All of characteristics are very close to predictions, with the largest deviation being the existence of an exceptionally favorable large lift increment due to full-flap deflection. The more significant stability and control parameters for the conventional aircraft configuration are presented in Table VIII. This table presents the significant static deviations of forces and moments for both longitudinal and directional motions of the aircraft as well as those due to control inputs.

This table along with Figures 126 through 129 summarizes the conventional aircraft performance obtained during this test program.

7.2 FAN POWERED PERFORMANCE

The techniques to be used in summarizing the test results during the fan powered mode of flight will be to present all data in the form of partial derivatives with respect to a single variable - all other variables remaining fixed. This means that the significant forces and moments effected by any aircraft attitude or control displacement will be reduced to the closest linear approximation and be presented as a derivative. This derivative may then be used in conjunction with a set of trimmed transition characteristics to obtain system performance for small perturbations from the trimmed condition. This is normally the way, only slightly untrimmed, the aircraft will be flown in the fan powered mode. The following discussion will be concerned with the sources of data used and presentation of the basic set of performance parameters.

7.2.1 Effects of Aircraft Attitude

The effects of aircraft attitude will be presented as derivatives of forces and moments with respect to angles of attack and sideslip. No interaction between the two axes will be assumed in presenting this data.

The longitudinal characteristics (angle of attack variable) as shown in Figures 44 and 45 were used to obtain the derivatives of lift, drag and pitching moments with respect to angle of attack. Prior to obtaining these derivatives, it was first observed that a definite break occurs in the moment variation with angle of attack. This break was traced to a pitch fan type of interference effect. However, for the normal aircraft configuration for near trimmed condition, the angle at which this break occurs may be definitely defined. Figure 130 presents a summary of data for the break angle of attack versus cross-flow ratio. In obtaining the derivatives of moment with respect to angle of attack, two values were taken at angles both below and above the pitching moment break point.

Figure 131 presents the derivatives with respect to angle of attack for the complete fan powered envelope. The values at hover speeds, cross-flow equal to zero, were estimated using static fan performance and rigging of the aircraft louver and pitch modulator door systems. It is interesting to note the following concerning the longitudinal stability derivatives shown in the figure.

- Lift changes with angle of attack are very nearly equal to those of the conventional aircraft.
- Longitudinal stability (moment change with respect to angle of attack) is always stable but is about 1/2 the value of the conventional aircraft. This is true at angles below the break in moments; at angles above this break the aircraft is unstable.
- Change in horizontal thrust or drag with angle of attack is nearly constant throughout the flight envelope.

Figure 132 presents the data from Figures 46 through 48 in terms of lateral stability derivatives. The data show an increase in both lateral and directional stability over that experienced by the conventional aircraft configuration.

7.2.2 Control Characteristics

The aircraft when in the fan powered mode of flight is subject to all normal conventional type controls as well as some new type control systems characteristic of the fan system. The control inputs, other than engine power levels are:

- Longitudinal stick
- Lateral stick
- Rudder pedals
- Collective stick
- Vector command
- Horizontal stabilizer incidence

The first three control inputs operate on both fan control as well as conventional control systems. The next two, collective and vector command, are strictly fan power control functions. The last, horizontal stabilizer incidence, is a pure aerodynamic control system. The following discussion will be concerned with the significant forces and moments that are affected by these control motions. The sources of this data were Figures 49 through 75.

Figure 133 through 138 present the control derivatives. The more important conclusions from these characteristics are as follows:

- Figure 133 shows that at high speed ($\mu = 0.25$) and vector angles, the derivatives of drag with vector command approaches zero which indicates no additional increase in horizontal thrust or speed may be obtained due to increased vector. The lift reduction with increasing vector along with the drag change tends to indicate the approach of limit flight speed in the fan mode.
- Longitudinal, lateral, and directional control sensitivities do not change appreciably throughout the fan mode of flight. Each tends to approach the conventional, jet mode, control sensitivity at the high flight speeds where fan control components are rapidly phased out.
- A favorable roll with yaw control exists throughout the complete fan flight mode, while a slightly adverse yaw with roll is apparent.
- Collective effectiveness is essentially constant until phase-out at a vector command angle of about 30 degrees is achieved.

In final summary, it may be concluded from these results presented in form of derivatives, that control sensitivity should remain relatively constant throughout the complete transition envelope as long as near trimmed conditions of vector command and power level are maintained.

7.2.3 Trimmed Transition Envelope

A trimmed transition envelope in this case is defined as the variation of lift versus cross-flow ratio for the special case of all forces and moments trimmed to zero except for lift, which is allowed to vary as required. The angle of attack and sideslip are set at zero degrees. As a result of trimming the aircraft, a schedule of vector command and longitudinal stick position versus flight speed is also obtained.

Throughout the test program, numerous test points were obtained at near trimmed conditions. The failure to provide a true trimmed condition at each test point was due to the slight variations of test conditions. Taking this data and correcting to trimmed conditions, using the derivatives previously discussed, the curves shown in Figures 139 and 140 were obtained. Figure 139 is for the fans operating at hi power while Figure 140 is for the lo power setting. These curves are presented for the case of neutral or 50 percent collective setting. Some of the more interesting conclusions apparent from these curves are:

- Lift approaches a minimum at the intermediate cross-flow ratio of about 0.15. At high speed, lift continues to decrease rapidly due to reduction in lift with increased vector. The exact cause of this lift reduction at μ = 0.15 is not fully understood but is partially due to nose-down trim required in conjunction with a considerable residual stagger in the fan louver system (see Figure 11).
- Longitudinal trim reaches a maximum of 5 degrees nose down (forward stick) at a cross-flow ratio of about 0.12. This represents a trimmed flight speed of about 45-50 knots. At high flight speeds an increasing amount of nose-up trim is required. However, this may be trimmed out by reduction of the tail incidence from the 20 degree value used in these curves.
- Lift coefficient for the low power setting is considerably lower than for the high power setting. This is because the stagger effectiveness, spoiling of lift, is greater at the low power settings. At the low power setting the louver loads are lower, deflections are less and consequently the spoiling is greater.
- The louver trim schedules for both the high and low power settings are nearly identical.
- The longitudinal trim schedules for both power settings are also almost the same.

These curves will provide the basis of most performance studies that are required for the fan flight mode.

7.2.4 **Composite Transition Characteristics**

Another set of transition characteristics that is interesting to present, but not very useful in performance evaluation, is the variation of lift, drag and pitching moments with vector command angle and cross-flow ratio for all controls fixed at neutral. This type of characteristic is shown in Figure 141. The data points shown on these curves were obtained from the trimmed transition data, vector effectiveness data, and control derivatives. The tail and longitudinal stick were adjusted to neutral using previously presented derivatives.

Figure 141 provided a means of determining the speed-stability of the aircraft. This is defined as the changes in forces and moments with respect to velocity or cross-flow ratio. Figure 142 shows the variation of these derivatives with respect to the trimmed vector command setting. The most interesting characteristic shown in this figure is the change of pitching moment coefficient with respect to speed from a positive value at low speeds to a negative value at high speeds. The negative value indicates a speed instability that is shown by the continuing aft stick required as fan flight speed is increased.

7.3 FAN POWERED PERFORMANCE - PITCH FAN "OFF"

The data obtained during the pitch fan "off" part of the test program may be presented in a form similar to that used for the normal configuration data. Figure 143 shows the composite force and moment variation with speed and vector command. These characteristics are similar to Figure 141 for the case with the pitch fan operating. Figure 143 was used to provide the speed derivatives shown in Figure 144 as a function of vector command at drag trimmed to zero.

The remaining significant derivatives with respect to aircraft attitude and control inputs are shown in Figures 145 through 151. The source of these curves was the control effectiveness shown in the previous data for the pitch fan "off".

7.4 CONTROL EFFECTIVENESS BREAKDOWN

As has been pointed out in the previous discussion, the total control effectiveness about each axis is composed of both a conventional aerodynamic effect as well as a fan power control reaction. The following discussion will be concerned with an analysis of the contributions of each part to the total control, and comparison of the results with measured control effectiveness. To do this, some basic assumptions are required concerning fan performance and conventional control effectiveness. Listed below are these assumptions:

- Fan vector-stagger effectiveness for lift and thrust control are as shown in Figures 152 and 153. These curves are based on measured performance during acceptance and flight worthiness testing prior to installation of the fans in the aircraft. Measured louver stagger-vector rigging of the actual aircraft were also factored into development of these curves.
- Pitch fan thrust modulator effectiveness is as shown in Figure 154. This again is based on factory test results.
- Pitch fan to wing fan speed ratios are as shown in Figure 155.
- Effectiveness of the conventional aerodynamic controls remain the same in the fan mode of flight as they were when measured in the conventional flight mode.

7.4.1 Longitudinal Control

The build-up of longitudinal control using the individual contributions of the elevator and pitch fan modulating doors is shown in Figure 156. The lower curve shows the contributions due to the pitch fan system taking into consideration the gearing ratios of the doors with respect to stick angle as well as the variation of gearing with respect to vector command angle. These gearing ratios are shown in Figure 13. Also shown on this curve is the elevator contribution based on conventional elevator effectiveness.

The upper curve presents a map of the longitudinal control effectiveness throughout the complete flight spectrum. Trimmed longitudinal control effectiveness was obtained using this data and the vector command versus crossflow ratio schedule shown in Figure 139. Comparison of this predicted trim effectiveness with measured data shows excellent agreement; the major discrepancies being attributed to lack of exact trim conditions while taking the actual test data.

7.4.2 Lateral Control

Figure 157 shows a similar breakdown of the lateral control system. Figure 17 shows the fan stagger gearing ratios used during this analysis. The resulting fan roll control effectiveness using the estimated fan static performance is shown in the lower curve for a range of vector command angles. Above a vector command angle of 30 degrees, the fan components have been phased to zero. Also shown in the lower curve is the conventional aileron effectiveness for flaps at 45 degrees.

The total lateral control capability is shown in the upper figure for a range of vector command angles and cross-flow ratios. The measured data when compared to the predicted data of trim indicates a higher control effectiveness. This increased level of control may be attributed to effects of induced lift. When a fan system is unstaggered, the lift increases by virtue of a reduction in fan thrust spoiling and the flow through the fan increases. This increased flow increases the induced lift for the wing in question since it is a well known fact that induced lift is proportional to fan airflow at a given flight speed. This therefore produced a two-fold increase in lift on one wing while a similar two-fold decrease in lift occurs in the opposite wing due to increased stagger on that side. This results in a larger predicted roll control effectiveness in cross-flow than can be accounted for using static fan performance.

7.4.3 Collective Control

Collective control is a pure fan thrust modulating system. A comparison of predicted lift control based on fan static performance and rigging, with measured collective effectiveness is shown in Figure 158. It should be noted that collective stick displacement produces both louver stagger changes as well as motions of the pitch fan modulator doors. The lift change predicted for the pitch modulating door movements is shown in the lower curve of Figure 158. This level of control persists throughout the complete louver schedule even after the collective authority over fan stagger has been phased-out completely.

The agreement of predicted and measured performance is very good. The measured values being slightly higher than predicted may be attributed to induced lift in a manner similar to that previously used in describing induced effects on lateral control.

7.4.4 Directional Control

Figure 159 presents a buildup of the total directional control effectiveness due to rudder pedal deflections. The lower curves show the effectiveness due to the individual fan and conventional control systems using the measured gearing ratios. The upper curve presents the combined control effectiveness with a trimmed schedule for both the predicted and measured test data. The agreement of the predicted and measured data for this case is not nearly as good as for the previously discussed control systems. The reasons for these discrepancies cannot be explained fully by any of the known possible interaction effects. In any case, the measured performance exceeds the predicted results, so the estimated data represents the more conservative approach.

7.4.5 Vector Command

The vector command control function provides a means of rotating the fan thrust vector through a range of angles, thereby providing a means of modulating the propulsive thrust components. Figure 160 shows a comparison of the estimated and measured lift and drag derivatives due to vector command. Also shown is the approximate vector command versus cross-flow for trim where these derivatives were evaluated. The comparison of estimated and test results shows the lift derivative to be lower for the test results. This effect is characteristic of the fan system in cross-flow which shows a lesser reduction in lift due to vector command than experienced at static (speed-zero) condition. It is believed that the exit flow from the fans is skewed aft or rearward at high speeds and the turning requirements of the louvers is reduced appreciably at high cross-flow ratios. Consequently the losses are reduced and the lift components are larger, resulting in a lower derivative of lift than predicted using static test data.

Comparison of estimated and measured drag variations with vector command show the estimate to be lower than the actual test data. This discrepancy is believed to be due to axial thrust components from the pitch fan being a function of pitch modulator door position. Since the pitch modulating door is programmed with respect to vector command (see Figure 13), these thrust levels appear in the drag derivatives with respect to vector command. The levels of these thrust changes with pitch fan door have not been measured during static tests and could not be included in the estimated data.

7.5 LONGITUDINAL TRIM REQUIREMENTS

One of the most potential problem areas anticipated during design of this aircraft was the lack of nose-down trim and control during the critical speed range of from 30 to 70 knots. However, more than adequate design margin is provided. The test results obtained in the wind tunnel verify that adequate longitudinal trim and control does exist in this system. The following analysis will summarize some of the trim capabilities for the two cases tested, that is pitch fan operating as well as shutoff.

Figure 161 presents the trim requirements for both pitch fan "on" and "off". The lower curve in the figure shows the longitudinal stick position for a range of tail settings with the pitch fan operating. At cross-flow ratio less than 0.20 it is not possible to trim the aircraft with the stabilizer alone. The upper curve shows a comparison of tail incidence for trim for the two cases. It is apparent at high speeds that the pitch fan does not add much trim or control. This is due to phase out of the longitudinal stick authority on the pitch fan doors at high vector command angles.

Figure 162 presents the necessary vector command trim schedule that accompanies the trim data in Figure 161. Also shown in this figure is the trimmed lift capability at an angle of attack of zero degrees for the pitch fan "on" and "off". Here it is apparent that the lift for either case is still a minimum at a cross-flow ratio near 0.15 to 0.20. This speed, about 60-70 knots represents the case of minimum lifting capability and therefore may be the most critical operating speed of the system. However, it is recommended that an optimization analysis showing the trade-offs of angle of attack and vector angle be performed at these speeds to see if a higher lift can be obtained. This analysis can be performed easily using the angle of attack and vector command derivatives previously presented.

8.0 APPLICATION OF DATA TO PERFORMANCE ESTIMATES

Since all of the previous data have been presented in coefficient form, it seems desirable that a particular section of the report be devoted to presenting real aircraft performance. Also during this discussion, a simple method of working with the coefficient data will be developed.

The first step in the process is accomplished by noting the relationship between indicated airspeed and the cross-flow parameter. It can be shown that:

$$\mu = \frac{V_{IC}/425}{\% N_f \sqrt{\delta/\theta}}$$

It can also be shown that:

$$L_c = \frac{L}{(\% N_f \sqrt{\delta/\theta})^2} = 43{,}950\ H_L$$

Similarly, the same relationship exists for drag and side force. For the moment coefficients, an appropriate length multiplier must be used.

The above relationships were used to convert the trimmed transition characteristics of Figure 162 into the corrected lift term, L_C. The data are shown in Figure 163 for three collective settings, full-up, neutral, and full-down. The trim requirements such as vector command, tail incidence, and longitudinal stick position are also shown.

The significance of these curves is that they present lift capability for the fans operating at 100 percent physical speed at sea level standard day conditions. It is a known fact that the fans cannot always be operated at 100 percent speed with the gas generator horsepower presently installed in the aircraft. The maximum speed capability of the fans, using the data in Figures 8 and 9, was obtained and is shown in Figure 164. This figure shows the variation of corrected speed with flight speed and ambient temperature. The hashed region to the right of the curve represents the region where the fans are not capable of absorbing all the available gas generator horsepower and in this region the physical speed will be limited to 100 percent.

Using curves 163 and 164, the trimmed lift-flight speed envelope for fan powered flight may be developed and is shown in Figure 165. These characteristics were developed for two atmospheric conditions, sea level standard day and 2500 feet, hot day. Similar techniques may be used to obtain forces and moments throughout the complete transition envelope.

The interesting results of Figure 165 is that a gradual rise in system lifting capability exists at speeds between hover and 80 knots. Above 80 knots there is a rapid decrease in lifting capability as maximum fan mode flight speed is reached. The transition region around 45 to 60 knots is where the height control of the aircraft should be changed from the collective to the engine throttles. At these speeds the collective should be moved to the full-up position in order to avoid the large lift degradation as previously discussed, that is apparent at mid and full-down collective. These curves tend to show that a level transition may be accomplished at constant power setting by using collective control at low speeds and aircraft angle of attack at high speeds.

9.0 CONCLUSIONS

1. Transition from hover to a maximum true air speed of approximately 98 knots can be accomplished with the available gas generator horsepower and within the fan speed limitation of 100 percent physical speed. This is true for an aircraft weight of 10,000 pounds and at a density of greater than 90 percent of standard density.
2. A level transition can be accomplished at essentially constant gas generator power settings and at angles of attack near zero degrees.
3. Throughout a near trimmed transition, the control effectiveness for each axis remains almost constant. That is, the control forces per unit stick throw do not change appreciably. Vectoring ahead of the trimmed flight speed could cause large deteriorations of control effectiveness.
4. Maximum control power at full stick throw does not deteriorate at the worst condition by more than 30 percent from the equivalent hover power levels.
5. The aircraft exhibits static longitudinal and lateral - directional stability throughout the transitional flight speeds from 30 to 100 knots for small pertubations from zero angle of attack and sideslip. For larger excursions of angle of attack, approximately 4 - 8 degrees, stability about the longitudinal axis becomes unstable during fan mode of operation.
6. Conventional aerodynamic performance was very close to predictions based on previous scale model estimates. The largest discrepancy was in flap lift effectiveness which substantially exceeded estimates. Maximum lift coefficient for the flaps at 45 degrees was 1.6 (trimmed power-off).

BLANK PAGE

TABLE I

DATA REDUCTION PROGRAM

SYMBOL DEFINITION

NO.	DIG. POS.	SYMBOL	NOMENCLATURE	UNITS	REMARKS
1	037	TS-602	R/H REAR SPAR LWR CAP BL26	°F	
2	038	TS-604	R/H REAR SPAR LWR CAP BL44	°F	
3	039	TS-606	R/H REAR SPAR LWR CAP BL61	°F	
4	040	TS-608	R/H REAR SPAR LWR CAP BL71	°F	
5	041	TS-612	R/H REAR SPAR UPR CAP BL25	°F	
6	042	TS-610	R/H REAR SPAR UPR CAP BL44	°F	
7	043	TS-634	R/H REAR SPAR - AFT MOUNT	°F	
8	046	TS-618	R/H FRONT SPAR LWR CAP BL61	°F	
9	051	TS-620	R/H PANEL, UPR, FWD, INBD-3	°F	
10	052	TS-622	R/H PANEL, UPR, AFT, INBD-5	°F	
11	080	TS-624	R/H PANEL, LWR, FEW, INBD-7	°F	
12	073	TS-626	R/H PANEL, LWR, AFT, INBD-9	°F	
13	031	TS-603	L/H REAR SPAR LWR CAP BL44	°F	
14	032	TS-605	L/H REAR SPAR LWR CAP BL61	°F	
15	033	TS-607	L/H REAR SPAR LWR CAP BL71	°F	
16	034	TS-611	L/H REAR SPAR UPR CAP BL25	°F	
17	035	TS-609	L/H REAR SPAR UPR CAP BL44	°F	
18	030	TS-633	L/H REAR SPAR - AFT MOUNT	°F	
19	036	TS-613	L/H REAR MOUNT SUPPORT STRUT	°F	
20	044	TS-615	L/H FRONT SPAR LWR CAP BL30	°F	
21	045	TS-617	L/H FRONT SPAR LWR CAP BL61	°F	
22	047	TS-619	L/H PANEL, UPR, FWD, INBD-3	°F	
23	048	TS-621	L/H PANEL, UPR, AFT, INBD-5	°F	
24	071	TS-623	L/H PANEL, LWR, FWD, INBD-7	°F	
25	072	TS-625	L/H PANEL, LWR, AFT, INBD-9	°F	
26	049	TS-627	L/H WING FAIRING INBD BL25	°F	
27	050	TS-629	L/H WING FAIRING INBD BL-56	°F	
28	053	TS-630	L/H WING BRKT. LWR FLG (143W025 - 47)	°F	
29	079	TS-651	L/H FLAP FITTING INBOARD	°F	
30	054	TS-6[illegible]1	FLAP SPAR LWR FLNG (143W010 - 101)	°F	
31	023	TS-301	PITCH FAN SIDE MOUNT - L/H	°F	
32	070	TS-305	PITCH FAN BEARING	°F	
33	017	TS-306	PITCH FAN FRONT FRAME	°F	
34	024	TS-4[illegible]	AFT FUSE, LWR L/H LONG.	°F	
35	025	TS-455	AFT FUSE, LWR LONG @ CONT FRAME	°F	
36	056	TS-457	AFT FUSE VERT STAB FRONT SPAR 143T005	°F	
37	026	TS-458	AFT FUSE CANTERED BULK @ FS400	°F	
38	018	TS-460	D.V. ACT. - L/H	°F	
39	019	TS-461	D.V. ACT. - R/H	°F	
40	081	TS-462	L/H TURB CASE (J-85 ENG.)	°F	
41	082	TS-463	R/H TURB CASE (J-85 ENG.)	°F	
42	027	TS-472	AFT FUSE. CANT. BULK @ FS400 - L/H	°F	
43	028	TS-473	AFT FUSE. CANT. BULK @ FS400 - R/H	°F	
44	077	TS-502	SPC FRM-41 MBR 4 TO 20, STA 251	°F	
45	029	TS-508	CENTER FUS. MLG SILL @ FLAP SUPPORT, L/H	°F	

TABLE I (Cont'd)

NO.	DIG. POS.	SYMBOL	NOMENCLATURE	UNITS	REMARKS
46	078	TS-514	SPC FRM-46, -48 & 18B JCT	°F	
47	012	TS-515	L/H FIRE EXT. BOTTLE	°F	
48	057	TS-705	MLG L/H "V" BRACE WL87	°F	
49	058	TS-707	MLG MODE CHANGE CYL.	°F	EFF RUNS 1 - 28
50	020	TS-721	MLG SHOCK STRUT (TOP OF OLEO)	°F	FOR WNDTNL RUNS 1-15
51	021	TS-725	NOSE GEAR WELL	°F	
52	059	TS 811	MLG WHEEL WELL STA 292	°F	
53	060	TS-813	MLG WHEEL WELL STA 309	°F	
54	055	TS-709	MLG L/H AXLE	°F	FOR WNDTNL RUNS 1-15
55	083	TG-2	L/H EGT	°F	
56	084	TG-3	R/H EGT	°F	
57	008	TG-4	ELEC. COMP. INLET	°F	
58	061	TG-5	L/H UPR X-DUCT COMPT OUTBD	°F	
59	062	TG-6	R/H UPR X-DUCT COMPT OUTBD	°F	
60	063	TG-7	PITCH FAN COMPT AIR INLET	°F	
61	009	TG-8	COCKPIT	°F	
62	065	TG-11	CROSS DUCT COMPT.	°F	
63	010	TG-13	COOLING FAN COMP. INLET	°F	
64	011	TG-15	COOLING FAN INLET	°F	
65	064	TG-16	PITCH FAN EJECTOR INLET	°F	
66	066	TG-17	L/H FWD. FAN EXHAUST	°F	
[illegible]	067	TG-19	L/H AFT. FAN EXHAUST	°F	
68	015	TG-21	COMP SECTION EXHAUST	°F	
69	022	TG-23	ENG TURB SECT AIR	°F	
70	076	TG-25	L/H TAILPIPE EJECTOR	°F	
71	068	TG-27	L/H AFT EJECTOR	°F	
[illegible]	069	TG-29	L/H FWD EJECTOR	°F	
[illegible]	005	TG-32	L/H FAN INLET (4)	°F	
[illegible]	006	TG-31	R/H FAN INLET (4)	°F	
75	003	TG-35	L/H ENGINE INLET (3)	°F	
76	004	TG-36	R/H ENGINE INLET (3)	°F	
77	007	TG-39	PITCH FAN INLET (2)	°F	
78	016	TG-812	MLG WELL	°F	
79	074	TL-1	L/H ENGINE OIL	°F	
80	075	TL-2	R/H ENGINE OIL	°F	
81	013	TL-3	L/H HYDRAULIC RES.	°F	
82	014	TL-4	R/H HYDRAULIC RES.	°F	
83	097	F-1	LATERAL STICK	LBS.	
84	098	F-2	LONGITUDINAL STICK	LBS.	
85	099	F-3	RUDDER PEDAL	LBS.	
86	093	F-11	DOOR OUTRIGGER	LBS.	
87	094	F-12	DOOR OUTRIGGER	LBS.	
88	095	F-13	DOOR OUTRIGGER	LBS.	
89	096	F-14	DOOR OUTRIGGER	LBS.	
90	085	F-21	DOOR ACTUATOR SUPP.	LBS.	
91	086	F-22	DOOR ACTUATOR SUPP.	LBS.	
92	087	F-23	DOOR ACTUATOR SUPP.	LBS.	
93	088	F-24	DOOR ACTUATOR SUPP.	LBS.	
94	089	F-25	DOOR ACTUATOR SUPP.	LBS.	
95	090	F-26	DOOR ACTUATOR SUPP.	LBS.	
96	091	F-27	DOOR ACTUATOR SUPP.	LBS.	
97	092	F-28	DOOR ACTUATOR SUPP.	LBS.	

TABLE I (Cont'd)

NO.	DIG. POS.	SYMBOL	NOMENCLATURE	UNITS	REMARKS
98	101	PO-3	ELEVATOR	DEG	+ TE DN, - TE UP
99	102	PO-4	RUDDER	DEG	EFF RUNS 1-25 + TE LT, - TE RT
100	103	PO-6	L/H AILERON	DEG	+ TE DN, - TE UP
101	112	PO-7	R/H AILERON	DEG	+ TE DN, - TE UP
102	172	PO-9	HORIZONTAL STABILIZER	DEG	+ TE DN, - TE UP
103	105	PO-13	L/H LOUVER - ODD	DEG	
104	106	PO-14	L/H LOUVER - EVEN	DEG	
105	107	PO-15	R/H LOUVER - ODD	DEG	
106	108	PO-16	R/H LOUVER - EVEN	DEG	
107	173	PO-17	VECTOR	DEG	
108	110	PO-22	PITCH FAN DOORS	DEG	MEAS. FROM FULL CLSD.
109	113	PO-32	LATERAL STICK	DEG	-RW DN, +LW DN.
110	114	PO-33	LONGITUDINAL STICK	DEG	+ STK FWD, - STK AFT
111	115	PO-34	RUDDER PEDALS	%	- LT YAW, + RT YAW
112	116	PO-35	COLLECTIVE STICK	%	EFF RUNS 1-25 MEAS. FROM FULL DN
113	117	RPM-1	L/H ENGINE	%RPM	
114	118	RPM-2	R/H ENGINE	%RPM	
115	119	RPM-3	L/H FAN	%RPM	
116	120	RPM-4	R/H FAN	%RPM	
117	121	RPM-5	PITCH FAN	%RPM	
118	125	PG-8	COCKPIT REAR CANOPY INLET	IN.H2O	
119	129	PG-20	L/H ENG TAILPIPE EJEC.	IN.H2O	
120	133	PG-25	CROSS DUCT COMPT.	IN.H2O	
121	137	PG-26	COOLING FAN COMPT INLET	IN.H2O	
122	141	PG-27	COOLING FAN INLET, L/H	IN.H2O	
123	145	PG-28	ELECTRONICS COMPT INLET	IN.H2O	
124	149	PG-29	L/H FWD COOLING FAN EXHAUST	IN.H2O	
125	153	PG-30	PITCH FAN EJECTOR, R/H	IN.H2O	
126	157	PG-31	L/H AFT COOLING FAN EXHAUST	IN.H2O	
127	161	PG-35	L/H AFT FAN EJECTOR	IN.H2O	
128	165	PG-37	L/H FWD FAN EJECTOR	IN.H2O	
129	169	PG-38	R/H BLOWER	IN.H2O	
130		PG-33	L/H P.FAN COMPT COOL. FAN INLET	IN.H2O	EFF RUN 26-33
131		PG-39	L/H ACCESSORY COMPARTMENT	IN.H2O	EFF RUN 26-33
132		PG-40	L/H ENGINE COMPARTMENT	IN.H2O	EFF RUN 26-33
133		PG-24	BOUNDARY LAYER BLEED DUCT	IN.H2O	EFF RUN 26-33
134		PO-17	VECTOR ANGLE COMMAND	DEG	
49	058	TS-.16	R/H FIRE BOTTLE	°F	EFF RUN 29-33
50	020	TS-903	L/H ENG GEAR BOX	°F	EFF WNDTNL RUNS 14-33
54	055	TS-904	R/H ENG GEAR BOX	°F	EFF WNDTNL RUNS 14-33
54	055	TS-901	AFT LOAD CELL	°F	FOR GRD RUNS ONLY
99	102	YAW	ANGLE OF YAW (PO-2)	DEG	+N.R. - N.L. EFF RUNS 26-33
112	116	PITCH	ANGLE OF ATTACK (PO-1)	DEG	+N.U. -N.D. EFF RUNS 26-33

TABLE II SUMMARY OF WIND TUNNEL RUNS

(*Denotes Variable)

RUN	RDG	MODE	V_o	% FAN RPM	δ_f	α	β_v	ψ	i_t	δ_{sa}	δ_{se}	δ_{sr}	δ_{sc}	REMARKS
1	1-14	CTOL	80	0	45	*	90	0	-0.1	-0.2	-0.2	+3	0	
1	15-23	CTOL	80	0	45	*	90	0	+0.1	-0.6	+11.3	+3	0	
1	24-30	CTOL	80	0	45	0	90	0	0.0	*	+11.4	+3	0	
1	30-34	CTOL	80	0	45	0	90	0	0.0	-0.6	+11.4	*	0	
2	1-10	CTOL	80	0	45	*	90	0	-0.1	-0.1	-13.4	+1	0	
2	11-16	CTOL	80	0	45	*	90	0	+0.1	-0.1	-0.1	+2	0	
2	17-25	CTOL	80	0	45	*	90	-5	-0.1	-0.1	0.0	+3	0	
2	26-34	CTOL	80	0	45	*	90	+5	-0.1	-0.1	-0.1	+2	0	
2	35-44	CTOL	80	0	0	*	90	0	-0.1	-0.2	-0.1	+2	0	
2	45-49	CTOL	80	0	0	0	90	0	-0.1	*	-0.4	+3	0	
2	50-54	CTOL	80	0	0	0	90	0	-0.1	*	-13.3	+3	0	
2	55-59	CTOL	80	0	0	0	90	0	-0.1	*	+11.6	+3	0	
3	1-5	VTOL	0	76	45	0	0	0	+20.0	*	0	0	50	
4	1-15	VTOL	40	70	45	*	25	0	+17.5	-0.5	+6.7	+3	50	
5	1	VTOL	20	70	45	0	11	0	+18.1	-0.2	+8.5	+1	50	
5	2-10	VTOL	60	70	45	*	38	0	+17.2	+0.1	+1.5	+1	50	
6	1-8	VTOL	30	70	45	*	18	0	+18.2	-0.2	+9.3	+1	50	
6	9-14	VTOL	70	70	45	*	50	0	+18.1	+0.3	-9.7	+2	50	
8	1-10	CTOL	80	0	45	*	90	0	-4.5	-8.2	-0.6	+4	50	
8	11-19	CTOL	80	0	45	*	90	0	-4.5	+6.9	-0.3	+4	50	
8	20-29	CTOL	80	0	45	*	90	0	-4.5	-0.5	-0.4	+4	50	
9	1-7	CTOL	80	0	45	0	90	*	-4.5	-0.6	-0.3	+4	50	
9	8-15	CTOL	80	0	45	8	90	*	-4.5	-0.6	-0.3	+4	50	
9	16-20	CTOL	80	0	0	0	90	*	-4.5	-0.6	-0.4	+4	50	
9	21-25	CTOL	80	0	0	8	90	*	-4.5	-0.6	-0.4	+4	50	
9	26-31	CTOL	80	0	0	0	90	0	*	-0.6	-0.4	+4	50	
10	1-10	VTOL	40	85	45	*	16	0	+17.8	-0.5	+7.0	-1	50	
10	11-15	VTOL	40	85	45	0	*	0	+17.8	-0.5	+7.2	+1	50	
10	16-17	VTOL	40	85	45	0	16	0	+17.8	+0.2	+7.3	+2	*	
10	18-21	VTOL	40	85	45	0	16	0	+18.0	-0.2	*	+3	50	
10	21-25	VTOL	40	85	45	0	16	0	+18.2	*	+7.5	+2	50	
10	25-27	VTOL	40	85	45	0	16	0	+17.8	-8.3	+7.3	*	50	
10	28-32	VTOL	40	85	45	0	16	0	+17.6	-0.1	+7.6	*	50	

TABLE II (CONTD.)

RUN	RDG	MODE	V_o	% FAN RPM	δ_f	α	B_v	ψ	i_t	δ_{sa}	δ_{se}	δ_{sr}	δ_{sc}	REMARKS
11	1-7	VTOL	60	85	45	*	29	0	+17.9	-0.1	+6.4	+1	50	
12	1-3	VTOL	60	85	45	*	29	0	+18.0	+0.4	+6.8	0	50	
12	4-7	VTOL	60	85	45	0	*	0	+17.2	-0.1	+6.9	+1	50	
12	8-10	VTOL	60	85	45	0	29	0	+17.4	-0.1	*	+1	50	
12	11-13	VTOL	60	85	45	0	29	0	+17.4	-0.1	+6.9	+1	*	
12	13-17	VTOL	60	85	45	0	29	0	+17.4	*	+6.9	+1	50	
13	1	VTOL	60	85	45	0	29	0	+18	+0.1	+6.6	-1	52	
13	2-3	VTOL	60	85	45	0	29	0	+17.8	-7.8	6.4	*	52	
13	4-8	VTOL	60	85	45	0	29	0	+18.2	+0.1	6.7	*	52	
13	9-15	VTOL	80	85	45	*	40	0	+17.8	-0.3	-0.5	0	52	
13	16-19	VTOL	80	85	45	0	*	0	+17.8	0	-1.7	+1	51	
13	20-22	VTOL	80	85	45	0	40	0	+18.1	+0.1	*	+1	51	
13	23-26	VTOL	80	85	45	0	40	0	+17.8	*	-1.8	+2	51	
13	27-29	VTOL	80	85	45	0	40	0	+17.8	-8.1	-2.2	*	51	
14	1-13	VTOL	30	65	45	*	17	0	+13.6	-0.3	+8.4	+1	51	Large Tail
14	14-25	VTOL	40	65	45	*	24	0	+13.5	-0.3	+7.3	+1	51	Large Tail
14	26-28	VTOL	40	65	45	0	24	0	+13.7	+0.1	*	+1	51	Large Tail
14	29-32	VTOL	40	65	45	0	24	0	*	-0.3	+7.2	+1	51	Large Tail
15	1-13	VTOL	60	65	45	*	38	0	+15.0	0	1.3	0	51	Large Tail
15	14-18	VTOL	60	65	45	0	38	0	+14.8	+0.1	*	+1	51	Large Tail
15	18-21	VTOL	60	65	45	0	38	0	*	0	+1	+2	51	Large Tail
15	22-29	VTOL	70	65	45	*	50	0	+12.2	+0.2	-5.6	+2	51	Large Tail
16	1-13	VTOL	30	65	45	*	18	0	12.5	-0.3	+8.6	-1	52	Large Tail/Slat
16	14-16	VTOL	30	65	45	0	18	0	+12.5	+0.2	*	+1	52	Large Tail/Slat
16	17-20	VTOL	30	65	45	0	18	0	*	-0.1	+8.3	+1	52	Large Tail/Slat
16	21-33	VTOL	40	65	45	*	25	0	+14.4	-0.2	+6.7	+1	52	Large Tail/Slat
16	34-36	VTOL	40	65	45	0	25	0	+14.4	+0.4	*	+2	52	Large Tail/Slat
16	36-39	VTOL	40	65	45	0	25	0	*	+0.4	-0.7	+2	52	Large Tail/Slat
16	40-47	VTOL	60	65	45	*	40	0	+13.9	-0.2	+1.7	+2	52	Large Tail/Slat
17	1	VTOL	0	0	45	0	50	0	-5.0	+0.3	+3.9	-1	53	VTOL-Config.
17	2-13	VTOL	80	0	45	*	50	0	-5.0	+0.3	+3.9	-1	53	J85's @ Idle
17	14-18	VTOL	80	0	45	0	50	*	-5.0	+0.3	+3.9	-1	53	in Jet Mode
18	1-13	CTOL	80	0	45	*	50	0	-5.0	-1.5	+5.2	+16	50	Pre-Conv. Config.
18	14-18	CTOL	80	0	45	0	50	*	-5.0	-1.3	+4.7	+17	50	J85's @ Idle
18	19-23	CTOL	80	0	30	0	90	0	-5.0	*	+3.6	+4	52	

TABLE II (CONTD.)

RUN	RDG	MODE	V_o	% FAN RPM	δ_F	α	β_v	ψ'	i_t	δ_{sa}	δ_{se}	δ_{sr}	δ_{sc}	REMARKS
19	1-6	CTOL	*	0	45	0	90	0	-5.0	-0.6	+3.[illegible]	+2	52	Gear Down
19	7-17	CTOL	80	0	45	*	90	0	5.0	-0.6	+3.5	+2	52	
19	18-22	CTOL	80	0	45	0	90	*	-5.0	-0.6	+3.5	+2	52	
21	1-13	VTOL	30	65	45	*	16	0	+15.0	0	+8.7	+1	52	Small Tail/Slat
21	14-26	VTOL	40	65	45	*	27	0	+15.[illegible]	0	+7.4	+1	52	Small Tail/Slat
21	27-28	VTOL	40	65	45	0	27	0	*	0	+7.4	+1	52	Small Tail/Slat
22	1-11	VTOL	40	65	45	*	25	0	+14.5	-0.3	+12.9	0	52	Small Tail/Slat
22	12-21	VTOL	40	65	45	*	25	0	+14.5	-0.2	-14.0	0	52	Small Tail/Slat
22	22-33	VTOL	60	65	45	*	41	0	+15.4	-0.2	+1.2	+2	52	Small Tail/Slat
23	1-11	VTOL	30	65	45	*	17	0	+15.8	0	-14.4	-1	53	Small Tail/Slat
23	12-14	VTOL	30	65	45	0	17	0	*	-0.1	-14.4	+1	53	Small Tail/Slat
23	15-25	VTOL	30	65	45	*	17	0	+14.8	-0.1	-0.8	+1	53	Small Tail/Slat
23	26-28	VTOL	30	65	45	0	17	0	*	-0.1	-0.7	+2	52	Small Tail/Slat
23	29-39	VTOL	40	65	45	*	25	0	+15.0	-0.1	-0.6	+2	53	Small Tail/Slat
23	40-42	VTOL	40	65	45	0	25	0	*	-0.1	-0.6	+3	52	Small Tail/Slat
24	1	VTOL	30	65	45	0	16	0	+19.2	-0.3	+12.6	0	53	Pitch Fan "Off" Small Tail/Slat
24	2-13	VTOL	40	65	45	*	27	0	+19.0	+0.5	+6.6	0	53	
24	14-17	VTOL	40	65	45	0	27	0	*	+0.2	+6.7	0	53	
24	17-19	VTOL	40	65	45	0	27	0	+19.2	+0.1	*	+1	53	
24	20-30	VTOL	60	65	45	*	35	0	+14.8	0	-0.3	+1	53	
25	1-9	VTOL	60	55	45	*	47	0	+10.5	-0.1	-0.5	+1	53	Pitch Fan "Off"
25	10-20	VTOL	40	65	45	*	25	0	+15.2	-0.1	-0.4	+1	53	until Run 29
25	21-24	VTOL	60	65	45	0	40	0	*	-0.1	-0.3	+1	53	Normal Tail
25	25-28	VTOL	60	65	45	0	40	0	+14.7	0	*	+1	53	
25	29-35	VTOL	60	65	45	0	40	*	+15.0	+0.4	-0.2	+1	53	
25	36-39	VTOL	60	65	45	0	*	0	+14.6	+0.3	-0.2	+2	53	
25	40-43	VTOL	40	65	45	0	*	0	+14.6	+0.3	-0.2	+1	53	
25	44-47	VTOL	30	65	45	0	*	0	+14.6	+0.3	-0.1	+1	53	
26	1-8	VTOL	60	85	45	*	23	0	+15.8	+0.4	-0.3	0	50	
26	9-12	VTOL	60	85	45	0	23	0	+15.6	-0.3	*	+1	50	
26	13-18	VTOL	80	85	45	*	35	0	+12.0	0	0	+2	50	
26	19-22	VTOL	80	85	45	0	35	0	+11.7	+0.3	*	+2	50	
26	23-26	VTOL	60	85	45	0	35	0	+12.0	*	-0.1	+2	50	

TABLE II (CONTD.)

RUN	RDC	MODE	V_o	% FAN RPM	δ_F	~	θ_v	ψ	i_t	δ_{sa}	δ_{se}	δ_{sr}	δ_{sc}	REMARKS
26	27-30	VTOL	60	85	45	0	35	0	+12.0	+0.3	-0.2	*	50	
26	31-34	VTOL	80	85	45	0	*	0	+12.2	+0.3	-0.2	+3	50	
27	1-12	VTOL	0	85	45	0	0	0	+15.5	*	+0.3	0	50	
28	1-5	VTOL	60	85	45	0	24	0	+15.6	*	-0.2	+1	50	
28	6-9	VTOL	60	85	45	0	24	0	+15.5	+0.4	+0.2	*	50	
28	10-17	VTOL	60	85	45	0	24	*	+15.5	+0.4	+0.2	+1	50	
28	18-19	VTOL	60	85	45	0	24	0	+15.6	*	-0.2	+1	50	
28	20-21	VTOL	60	85	45	0	24	0	+16.0	+0.2	-0.2	*	50	
28	22	VTOL	60	85	45	0	24	0	+15.4	-8.0	-0.5	-66	50	
28	23-26	VTOL	60	85	45	0	*	0	+15.5	+0.4	-0.2	+1	50	
28	27-29	VTOL	60	85	45	0	24	0	*	+0.2	-0.1	+1	50	
28	30-31	VTOL	100	85	45	0	*	0	+10.4	+0.2	-0.1	+1	50	
29	1-9	VTOL	60	85	45	*	29	0	+18.6	+0.2	+3.6	-1	50	Pitch Fan "On"
29	10-19	VTOL	60	85	45	0	29	*	+19.0	+0.2	*	+2	50	from here to
30	1-4	VTOL	60	85	45	0	29	*	+18.8	+0.1	*	0	50	end of Test
30	4-6	VTOL	60	85	45	0	29	+4	+18.5	*	+3.4	+1	50	
30	7-8	VTOL	60	85	45	0	29	+4	+18.5	-0.1	+3.3	*	50	
30	9	VTOL	60	85	45	0	29	+4	+19.0	+7.2	+3.0	+97	50	
31	1-7	VTOL	100	90	45	*	50	0	+16.0	+0.7	-4.6	+2	50	
32	1-3	VTOL	100	95	45	0	50	0	+16.5	+0.2	*	-1	50	
32	4-6	VTOL	100	95	45	0	50	0	*	0	+3.6	0	50	
32	7-9	VTOL	100	95	45	0	*	-1	+16.5	0	+3.6	+1	50	
32	9-17	VTOL	100	95	45	0	50	-1	+16.3	*	+3.6	+1	50	
32	18-24	VTOL	100	95	45	0	50	-1	+16.2	+0.3	+3.7	*	50	
32	25	VTOL	100	95	45	0	50	-1	+16.2	-4.0	+3.7	-45	50	
32	26	VTOL	100	95	45	0	50	-1	+16.2	-8.1	+3.4	-68	50	
33	1-8	VTOL	30	65	45	*	17	0	+20.0	+0.3	+5.7	-1	50	
33	9-13	VTOL	30	65	45	6	17	*	+20.0	+0.3	+5.7	-1	50	
33	13-15	VTOL	30	65	45	6	17	+8	+19.9	*	+5.7	-1	50	
33	16-17	VTOL	30	65	45	6	17	+8	+19.7	-0.1	+5.8	*	50	
33	18	VTOL	30	65	45	6	17	+8	+19.9	+7.2	+5.3	+97	50	
33	19-21	VTOL	20	65	45	0	11	*	+19.6	0	+4.1	+1	50	
33	21-2[illegible]	VTOL	20	65	45	0	11	+12	+19.8	*	+4.2	+1	50	

TABLE II (CONTD.)

RUN	RDG	MODE	V_o	% FAN RPM	δ_F	α	B_v	ψ	i_t	δ_{sa}	δ_{se}	δ_{sr}	δ_{ac}	REMARKS
33	24-25	VTOL	20	65	45	0	11	+12	+19.5	+0.1	+4.1	*	50	
33	26	VTOL	20	65	45	0	11	+12	+20.0	+7.1	+3.5	+97	50	
33	27-31	VTOL	40	65	45	"	27	0	+19.8	0	-14.2	+2	50	
33	31-36	VTOL	40	65	45	*	27	0	+15.4	0	-14.2	+2	50	

E N D   O F   T E S T

TABLE III - SUMMARY OF STATIC
THRUST STAND RUNS - PHASE I

(Nominal Control Settings Shown)

RUN	RDG	$\%N_{J-85}$	$\%\delta_{sa}$	$\%\delta_{se}$	$\%\delta_{sc}$	$\%\delta_{sr}$	β_v	REMARKS
1	1	*	0	0	50	0	45	Engine checkout Run
2	1	70	0	0	50	0	0	CTOL
	2-3	*	0	0	50	0	0	Lost Instrumentation
3	1	70	0	0	50	0	45	CTOL
	2	85	0	0	0	0	0	
	3	85	0	0	50	0	0	
	4-6	85	*	0	50	0	0	
	7-10	85	0	0	50	0	*	
	11	85	0	0	0	0	0	
	12-15	85	0	*	0	0	0	
4	1	70	0	0	50	0	45	CTOL
	2-4	95	0	0	*	0	0	
	5-7	95	*	0	0	0	0	
	8-10	95	*	0	50	0	0	
	11	95	0	0	50	-100	0	
	12	95	0	0	50	0	0	
	13-15	95	0	0	50	0	*	
	16-18	95	0	*	50	0	0	
	19	95	0	0	*	0	25	
5	1	70	0	0	50	0	0	CTOL
	2	95	0	0	50	0	0	
	3-4	95	*	0	50	0	0	
	5	95	0	0	*	0	0	
	6-7	95	*	0	100	0	0	
	8-9	90	*	0	50	0	0	
	10-11	90	0	0	*	0	0	
	12	90	0	*	100	0	0	
	13-15	95	*	0	50	0	0	
	16-18	90	*	0	50	0	0	
6 (1)	-	*	-	-	-	-	-	$\beta_{VL}=-2.5$, $\beta_{SL}=0$ $\beta_{VR}=-2.5$, $\beta_{SR}=0$
7 (1)	-	*	-	-	-	-	-	$\beta_{VL}=-2.5$, $\beta_{SL}=29$ $\beta_{VR}=-2.5$, $\beta_{SR}=0$
8 (1)	-	*	-	-	-	-	-	$\beta_{VL}=-2.5$, $\beta_{SL}=38$ $\beta_{VR}=-2.5$, $\beta_{SR}=12$
9 (1)	-	*	-	-	-	-	-	$\beta_{VL}=-2.5$, $\beta_{SL}=13$ $\beta_{VR}=-2.5$, $\beta_{SR}=13$
10 (1)	-	-		-	-	-	-	$\beta_{VL}=-2.5$, $\beta_{SL}=13$ $\beta_{VR}=-2.5$, $\beta_{SR}=38$
11 (1)	-	*	-			-	-	$\beta_{VL}=-2.5$, $\beta_{SL}=27$ $\beta_{VR}=-2.5$, $\beta_{SR}=27$
12 (1)	-	*		-	-		-	$\beta_{VL}=-2.5$, $\beta_{SL}=40$ $\beta_{VR}=-2.5$, $\beta_{SR}=40$

TABLE III (CONTD.)

RUN	RDG	% N_J-85	% δ_{sa}	% δ_{se}	% δ_{sc}	% δ_{sr}	B_V	REMARKS
13 ①	-	*	-	-	-	-	-	B_{VL}=-5.5, B_{SL}=6.0 B_{VR}=-5.5, B_{SR}=6.0
14 ①	-	*	-	-	-	-	-	B_{VL}=-11.2, B_{SL}=37.5 B_{VR}=-12.5, B_{SR}=0
15 ①	-	*	-	-	-	-	-	B_{VL}=-17.5 B_{SL}=25 B_{VR}=-17.5, B_{SR}=25
16 ①	-	*	-	-	-	-	-	B_{VL}= 18.2, B_{SL}=36.5 B_{VR}= 18.5, B_{SR}=0
17 ①	-	*	-	-	-	-	-	B_{VL}= 12.5, B_{SL}=27 B_{VR}= 12.5, B_{SR}=27
18 ①	-	*	-	-	-	-	-	B_{VL}= 27.5, B_{SL}=20 B_{VR}= 27.5, B_{SR}=0
19 ①	-	*	-	-	-	-	-	B_{VL}= 45, B_{SL}=0 B_{VR}= 45 B_{SR}=0
20 ①	-	*	-	-	-	-	-	B_{VL}=-2.5, B_{SL}=38 B_{VR}=-2.5, B_{SR}=12
21 ①	-	*	-	-	-	-	-	B_{VL}=-2.5, B_{SL}=12 B_{VR}=-2.5, B_{SR}=12
22 ①	-	*	-	-	-	-	-	B_{VL}=-2.5, B_{SL}=12 B_{VR}=-2.5, B_{SR}=38
23	1	70	0	0	50	0	0	
	2	70	*	0	*	0	0	
	3	90	*	0	*	0	0	
	4	95	*	0	*	0	0	
	-	*	0	0	50	0	0	
	5	95	0	+100	50	0	0	
	6	95	0	-100	50	0	0	
	7	95	0	0	50	+100	0	
	8	95	0	0	50	-100	0	
	9	95	0	+100	50	+100	0	
	10	70	0	+100	50	+100	0	
	11	95	0	-100	50	-100	0	
24	-	95	*	-	-	-	-	Pilot Operated Controls
25	1-2	70	*	0	*	0	0	
	3	90	*	0	*	0	0	
	4	95	*	0	*	0	0	
26	1	95	*	0	50	0	0	
			*	-100	50	0	0	
			*	+100	50	0	0	
			0	0	*	0	0	

① Denotes runs made with fixed links replacing louver actuators for force surveys of actuator loads.

END OF TEST

TABLE IV - SUMMARY OF STATIC THRUST STAND RUNS - PHASE II

(Nominal Control Settings Shown)

RUN	RDG	$\%N_{J-85}$	$\%\delta_{sa}$	$\%\delta_{se}$	$\%\delta_{sc}$	$\%\delta_{sr}$	REMARKS
1	1-5	95	*	0	50	0	$h/D = 1.0$, $B_v = 0^\circ$, $\delta_f = 45^\circ$
1	6-10	95	*	+50	50	0	
1	11-15	95	*	-50	50	0	
1	16-25	95	*	0	50	0	
1	26	95	0	0	50	0	
1	27-31	95	*	0	0	0	
1	32-36	95	*	0	100	0	
1	37-41	95	0	*	50	0	
2	1-21	95	*	0	50	0	$h/D = 1.0$, $B_v = 0^\circ$, $\delta_f = 45^\circ$
2	22-25	95	0	*	50	0	
4	1-5	95	*	0	50	0	$h/D = 1.0$, $B_v = 0^\circ$, $\delta_f = 0^\circ$
4	6-10	95	*	+50	50	0	
4	11-15	95	*	-50	50	0	
4	16-25	95	*	0	50	0	
4	26	95	0	0	50	0	
4	27-31	95	*	0	0	0	
4	32-36	95	*	0	100	0	
4	37-41	95	0	*	50	0	
4	42-47	95	*	0	50	0	$\delta_f = 45^\circ$
5	1-5	95	*	0	50	0	$h/D = 1.0$, $B_v = +10^\circ$, $\delta_f = 45^\circ$
5	6-10	95	*	+50	50	0	
5	11-15	95	*	-50	50	0	
5	16-25	95	*	0	50	0	
5	26	95	0	0	50	0	
5	27-31	95	*	0	0	0	
5	32-36	95	*	0	100	0	
5	37-39	95	*	0	100	0	$B_v = +5^\circ$
6	1-5	0	*	0	50	0	$h/D = 1.0$, $B_v = 0^\circ$, $\delta_f = 45^\circ$
6	6-15	70	*	0	50	0	
6	16-21	85	*	0	50	0	
6	22-35	95	*	0	50	0	
6	36-40	95	*	-50	50	0	
6	41-45	95	*	50	50	0	
6	46-55	70	*	0	50	0	
7	1-8	70	(1)	*	(1)	(1)	Pitch fan door program set at
	9-13	85		*			$B_v = 45^\circ$ schedule
	14-18	95		*			$h/D = 1.0$, $\delta_f = 45^\circ$
8	Rerun of Run 7						
9	1-2	70	(2)	0	(2)	(2)	$h/D = 1.0$, $\delta_f = 45^\circ$
	3	85		0			
	4-8	95		*			PF door set @ $B_v = 45^\circ$ schedule
	9-17	95		*			PF door set @ $B_v = 0^\circ$ schedule
10	1-6	70	(3)	*	(3)	(3)	$h/D = 1.0$, $\delta_f = 45^\circ$
	7-11	85		*			PF door set at $B_v = 0^\circ$ schedule
	12-16	95					
	17-21	95					PF door set at $B_v = 45^\circ$ schedule
11	1-11	85	*	0	50	0	$h/D = 1.0$, $B_v = 0^\circ$, $\delta_f = 45^\circ$
	12-32	95	*	0	50	0	
	33-35	95	0	0	*	0	

TABLE IV (CONTD.)

RUN	RDG	$\% N_{J-85}$	$\% \delta_{sa}$	$\% \delta_{se}$	$\% \delta_{sc}$	$\% \delta_{sr}$	REMARKS
12	1-5	95	*	0	50	0	$h/_D = 2.0$, $B_v = 0^o$, $\delta_f = 45^o$
	6-10	95	*	+50	50	0	
	11-15	95	*	-50	50	0	
	16-26	95	*	0	50	0	
	27-31	95	*	0	0	0	
	32-36	95	*	0	100	0	
13	1-2	95	0	0	50	0	Landing Gear Translated VTOL to CTOL for two cycles.
	3-6	95	*	0	50	0	$h/_D = 2.0$, $B_v = -4$, $\delta_f = 45^o$, $\alpha = -4$
	7-11	95	*	0	50	0	$B_v = 0^o$, $\alpha = -4^o$
	12-16	95	*	0	50	0	$B_v = 0^o$, $\alpha = 0^o$
	17-21	95	*	+50	50	0	$B_v = 0^o$, $\alpha = 0^o$
	22	95	0	0	50	0	

① Louver actuators replaced with fixed links and louver clamps simulating 100% LWD at mid collective and neutral rudder.

② Simulated 100% RWD.

③ Simulated all control neutral

E N D   O F   T E S T

TABLE V - SUMMARY OF OPERATING TIMES

TEST	RUN	TEST TIME (MINS)	ENGINE TIME (MINS)	WING FAN TIME (MINS)	PITCH FAN TIME (MINS)	NO. OF DIVERTS
G-1	1	11	11	0	0	0
	2	10	10	6	6	1
	3	35	35	23	23	1
	4	30	30	24	24	2
	5	38	38	32	32	1
	6	5	5	3	3	1
	7	5	5	3	3	1
	8-10	40	40	12	12	3
	11-13	38	38	12	12	3
	14-15	19	19	8	8	2
	16-17	21	21	8	8	2
	18-19	23	23	8	8	2
	20-22	26	26	12	12	3
	23	31	31	26	26	1
	24	10	10	5	5	1
	25	16	16	13	13	1
	26	8	8	6	6	1
WT-1	1	63	0	0	0	0
	2	102	0	0	0	0
	3-4	52	52	27	27	2
	5	33	33	24	24	1
	6	36	36	27	27	3
	7	48	10	4	4	3
	8	55	0	0	0	0
	9	65	0	0	0	0
	10	51	51	43	43	1
	11	22	22	13	13	1
	12	24	24	22	22	1
	13	69	69	41	41	3
	14	67	67	54	54	2
	15	72	72	49	49	2
	16	82	82	75	75	1
	17	41	41	0	0	0
	18	39	39	0	0	0
	19	53	0	0	0	0
	20	10	0	0	0	0
	21	50	50	42	42	1
	22	70	70	59	59	2
	23	72	72	67	67	1
	24	67	67	53	0	2
	25	78	78	74	0	1
	26	58	58	51	0	1
	27-28	66	66	52	0	2
	29	33	33	26	26	1
	30	22	22	15	15	1
	31	24	24	14	14	1

TABLE V (CONTD.)

TEST	RUN	TEST TIME (MINS)	ENGINE TIME (MINS)	WING FAN TIME (MINS)	PITCH FAN TIME (MINS)	NO. OF DIVERTS
WT-1	32	50	50	32	32	1
	33	61	61	53	53	2
G-2	1-2	35	35	15	15	2
	3-5	57	57	39	39	3
	6	28	28	17	17	1
	7	14	14	9	9	1
	8	9	9	9	6	1
	9	11	11	7	7	1
	10	13	13	7	7	1
	11	18	18	16	16	1
	12	31	31	14	14	1
	13	13	13	8	8	1

TEST SUMMARY:

Test Hours - 37.1
Engine Time - 30.9 hours
Wing Fan Time - 21.0 hours
Pitch Fan Time - 17.1 hours
No. of Starts - 58
No. of Diverts - 75

NOTES:

① Test hours are defined as any time when either engines are running or wind tunnel is blowing.

② G-1 denotes Static Thrust Stand - Phase I
W-1 denotes Wind Tunnel Test
G-2 denotes Static Thrust Stand - Phase II

TABLE VI - TYPICAL DIGITAL DATA LISTING

XV-5A WINDTUNNEL DATA

RUN 10. PO 30.12(HGA) VO 40.KNOTS VECTOR 17. 25.
RDG 5.06 TO 80.(DEG.F)

ENGINEERING UNITS

1	TS-602	101.40	51	TS-725	140.30	101	PO-7	14.88
2	TS-604	140.30	52	TS-811	141.80	102	PO-9	17.55
3	TS-606	172.40	53	TS-813	120.60	103	PO-13	24.56
4	TS-608	128.70	54	TS-709	69.80	104	PO-14	-1.71
5	TS-612	107.00	55	TG-2	1076.00	105	PO-15	27.97
6	TS-610	118.70	56	TG-3	1068.20	106	PO-16	0.11
7	TS-634	182.40	57	TG-4	123.30	107	PO-17	0.
8	TS-618	136.00	58	TG-5	219.60	108	PO-22	60.08
9	TS-620	121.40	59	TG-6	241.80	109	PO-32	-0.46
10	TS-622	143.90	60	TG-7	162.10	110	PO-33	7.14
11	TS-624	150.90	61	TG-8	86.20	111	PO-34	-0.95
12	TS-626	197.60	62	TG-11	173.00	112	PO-35	50.39
13	TS-603	123.60	63	TG-13	95.80	113	RPM-1	95.41
14	TS-605	139.60	64	TG-15	102.30	114	RPM-2	95.43
15	TS-607	108.60	65	TG-16	172.40	115	RPM-3	84.18
16	TS-611	102.00	66	TG-17	121.40	116	RPM-4	85.87
17	TS-609	110.50	67	TG-19	104.10	117	RPM-5	94.16
18	TS-633	168.80	68	TG-21	223.60	118	PG-8	-5.64
19	TS-613	202.10	69	TG-23	193.60	119	PG-20	-1.26
20	TS-615	112.00	70	TG-25	297.80	120	PG-25	-1.78
21	TS-617	142.70	71	TG-27	293.00	121	PG-26	-2.63
22	TS-619	123.30	72	TG-29	185.40	125	PG-30	-5.52
23	TS-621	141.50	73	TG-32	86.80	122	PG-27	-9.12
24	TS-623	177.00	74	TG-31	88.00	123	PG-28	-1.13
25	TS-625	172.40	75	TG-35	83.00	124	PG-29	2.70
26	TS-627	116.30	76	TG-36	83.40	126	PG-31	3.95
27	TS-629	117.80	77	TG-39	81.00	127	PG-35	-29.94
28	TS-630	161.20	78	TG-812	118.40	128	PG-37	0.
29	TS-651	122.60	79	TL-1	318.00	129	PG-38	-5.23
30	TS-661	114.40	80	TL-2	310.00			0.
31	TS-301	198.40	81	TL-3	125.10			0.
32	TS-305	198.40	82	TL-4	126.90			0.
33	TS-306	143.60	83	F-1	90.56			0.
34	TS-452	130.60	84	F-2	39.61			0.
35	TS-455	111.40	85	F-3	14.93			0.
36	TS-457	281.10	86	F-11	63.62			0.
37	TS-458	153.60	87	F-12	163.87			0.
38	TS-460	177.60	88	F-13	200.66			0.
39	TS-461	100.20	89	F-14	-132.47			0.
40	TS-462	1047.20	90	F-21	0.			0.
41	TS-463	1114.00	91	F-22	0.			0.
42	TS-472	102.00	92	F-23	141.07			0.
43	TS-473	103.20	93	F-24	84.98			0.
44	TS-502	211.50	94	F-25	44.71			0.
45	TS-508	98.20	95	F-26	51.65			0.
46	TS-514	251.40	96	F-27	42.21			0.
47	TS-515	86.20	97	F-28	622.05			0.
48	TS-705	85.30	98	PO-3	8.81			0.
49	TS-707	71.30	99	PO-4	-0.33			0.
50	TS-721	63.60	100	PO-6	15.57			0.

BLANK PAGE

TABLE VII - TYPICAL PERFORMANCE COMPUTATION LISTING

XV-5A WINDTUNNEL AERODYNAMIC PERFORMANCE

RUN NO 10

RDG.	1	2	3	4	5	6
ALPHA	0.	0.	-4.0	-2.0	0.	2.0
BETA	-0.	-0.	-0.	-0.	-0.	-0.
QO	5.900	5.440	5.920	5.780	5.730	5.580
MU	0.1107	0.1106	0.1163	0.1157	0.1155	0.1151
TCS	0.9784	0.9784	0.9761	0.9763	0.9764	0.9766
CL	7.0516	7.0781	6.1745	6.4504	6.5246	6.7425
CD	0.0221	0.0176	-0.2179	-0.1537	0.1312	0.2742
CM	-0.1805	-0.2205	-0.1704	-0.2209	-0.2406	-0.2599
CY	0.0145	0.0080	-0.0226	0.0005	-0.0301	0.0187
CN	0.0073	-0.0016	-0.0005	0.0014	0.0132	0.0041
CROLL	-0.0318	-0.0288	-0.0239	-0.0276	-0.0412	-0.0251
ML	0.3157	0.3166	0.3054	0.3159	0.3183	0.3267
MD	0.0010	0.0008	-0.0108	-0.0075	0.0054	0.0133
MM	-0.0146	-0.0178	-0.0153	-0.0196	-0.0212	-0.0228
MY	0.0006	0.0004	-0.0011	0.0000	-0.0015	0.0009
MN	0.0010	-0.0002	-0.0001	0.0002	0.0019	0.0006
MROLL	-0.0042	-0.0038	-0.0035	-0.0040	-0.0059	-0.0036
CLS	0.9350	0.9385	0.9036	0.9353	0.9424	0.9682
CDS	0.0029	0.0023	-0.0319	-0.0223	0.0161	0.0394
CMS	-0.0433	-0.0529	-0.0451	-0.0580	-0.0629	-0.0675
CYS	0.0019	0.0011	-0.0033	0.0001	-0.0043	0.0027
CNS	0.0056	-0.0012	-0.0004	0.0012	0.0109	0.0034
CROLLS	-0.0242	-0.0219	-0.0201	-0.0230	-0.0341	-0.0207
CLS-S	0.9350	0.9385	0.9036	0.9353	0.9424	0.9682
CDS-S	0.0029	0.0023	-0.0319	-0.0223	0.0161	0.0394
CMS-S	-0.0433	-0.0529	-0.0451	-0.0580	-0.0629	-0.0675
CYS-S	0.0019	0.0011	-0.0033	0.0001	-0.0043	0.0027
CNS-S	0.0056	-0.0012	-0.0004	0.0012	0.0109	0.0034
CROLLS-S	-0.0242	-0.0219	-0.0201	-0.0230	-0.0341	-0.0207

TABLE VII - TYPICAL PERFORMANCE COMPUTATION LISTING - CONTINUED

XV-5A WINDTUNNEL AERODYNAMIC PERFORMANCE

RUN NO 10

RDG.	1	2	3	4	5	6
(UT/UTO)L	1.0214	1.0253	1.0178	1.0289	1.0249	1.0223
(UT/UTO)R	1.0118	1.0145	1.0099	1.0165	1.0148	1.0146
(UT/UTO)P	0.9992	1.0011	0.9990	1.0040	0.9989	0.9996
(UP/UT)	0.9856	0.9856	0.9895	0.9867	0.9844	0.9872
T2/TO	1.0086	1.0045	1.0045	0.9985	1.0059	1.0007
T10L/TO	1.0176	1.0122	1.0107	1.0070	1.0126	1.0103
T10R/TO	1.0198	1.0144	1.0164	1.0109	1.0148	1.0103
T20/TO	1.0055	1.0019	1.0041	0.9985	1.0019	1.0011
MU-10	0.1117	0.1113	0.1171	0.1163	0.1163	0.1157
TCS-10	0.9780	0.9781	0.9758	0.9761	0.9761	0.9763
ML-10	0.3216	0.3208	0.3095	0.3188	0.3226	0.3301
MD-10	0.0010	0.0008	-0.0109	-0.0076	0.0055	0.0134
MM-10	-0.0149	-0.0181	-0.0155	-0.0198	-0.0215	-0.0230
CLS-10	0.9521	0.9507	0.9156	0.9435	0.9550	0.9779
CDS-10	0.0030	0.0024	-0.0323	-0.0225	0.0163	0.0398
CMS-10	-0.0441	-0.0536	-0.0457	-0.0585	-0.0637	-0.0682
(UT/UTO)L2	1.0247	1.0268	1.0197	1.0246	1.0290	1.0200
(UT/UTO)R2	1.0132	1.0151	1.0099	1.0109	1.0178	1.0121
(UT/UTO)P2	1.0046	1.0054	1.0022	1.0030	1.0052	0.9999

TABLE VIII - SUMMARY OF STABILITY AND CONTROL DATA - CONVENTIONAL FLIGHT CONFIGURATIONS - LOW SPEED

(Center of gravity at FS-2[illegible]0, WL-11[illegible])

1. Conventional clean configuration - Flaps 3[illegible]0°.

a) Longitudinal

$\partial C_L/\partial \alpha$ = [illegible] (stick fixed)

$\partial C_m/\partial C_L$ = [illegible] (stick fixed)

$\partial C_L/\partial \alpha$ = 0.061 (trimmed)

$\partial C_L/\partial \alpha$ = 0.06[illegible] (power-on, trimmed)

$\partial C_m/\partial \delta_{se}$ = -0.0[illegible]

$\partial C_m/\partial \delta_e$ = -0.01[illegible]

$\partial C_m/\partial i_t$ = -0.02[illegible]

α_0 = -1.[illegible] (angle for zero lift)

C_{D0} = 0.0[illegible]

b) Lateral Directional (β = ± [illegible]°)

$\partial C_Y/\partial \beta$ = [illegible]

$\partial C_n/\partial \beta$ = +[illegible].00[illegible]0 (α = 0°)

$\partial C_l/\partial \beta$ = -0.0010 (α = 0°)

$\partial C_n/\partial \beta$ = +[illegible] (α = +[illegible]°)

$\partial C_l/\partial \beta$ = [illegible] (α = +[illegible]°)

$\partial C_m/\partial |\beta|$ = [illegible] (α = 0°)

$\partial C_l/\partial \delta_{sa}$ = [illegible]

2. **Conventional clean configuration - Flaps @ 30°.**

a) **Longitudinal**

$\partial C_L / \partial \alpha$ = 0.072 (stick fixed)

$\partial C_m / \partial C_L$ = -0.135 (α = 0°)

$\partial C_m / \partial C_L$ = -0.088 (α = +8°)

$\partial C_L / \partial \alpha$ = 0.070 (trimmed)

$\partial C_L / \partial \alpha$ = 0.072 (power-on, trimmed)

C_{D0} = 0.075

b) **Lateral - Directional**

$\partial C_l / \partial \delta_{sa}$ = -0.0044

3. **Conventional clean configuration - Flaps @ 45°.**

a) **Longitudinal**

$\partial C_L / \partial \alpha$ = 0.069 (stick fixed)

$\partial C_m / \partial C_L$ = -0.147 (α = 0°)

$\partial C_m / \partial C_L$ = -0.079 (α = +8°)

$\partial C_L / \partial \alpha$ = 0.068 (trimmed)

$\partial C_L / \partial \alpha$ = 0.071 (power-on, trimmed)

$\partial C_m / \partial \delta_{se}$ = -0.016

$\partial C_m / \partial \delta_e$ = -0.0125

C_{D0} = 0.100

b) **Lateral - Directional**

$\partial C_Y / \partial \beta$ = -0.0123

$\partial C_n / \partial \beta$ = +0.0031 (α = 0°)

$\partial C_l / \partial \beta$ = -0.0015 (α = 0°)

$\partial C_n / \partial \beta$ = +0.0035 (α = +8°)

b) Lateral - Directional (continued)

$\partial C_n/\partial \beta$ = -0.0023 (α = +8°)

[illegible] $/\partial|\delta|$ = -0.005

$\partial C_l/\partial \delta_{sa}$ = -0.0040

$\partial C_Y/\partial \delta_{sr}$ = -0.0006

$\partial C_n/\partial \delta_{sr}$ = +0.00036

$\partial C_Y/\partial \delta_{sr}$ = +0.00012

$\partial C_Y/\partial \delta_r$ = -0.0022

$\partial C_n/\partial \delta_r$ = +0.00133

$\partial C_l/\partial \delta_r$ = -0.00044

[illegible] Pre-Conversion configuration.

a) Longitudinal

$\partial C_L/\partial \alpha$ = 0.0[illegible]6 (stick fixed)

$\partial C_m/\partial C_L$ = -0.1[illegible] (α = 0°)

$\partial C_m/\partial C_L$ = -0.0[illegible] (α = +8°)

$\partial C_L/\partial \alpha$ = [illegible] (trimmed)

C_{D_0} [illegible]

b) Lateral - Directional

$\partial C_Y/\partial \beta$ [illegible]

$\partial C_n/\partial \beta$ [illegible]

$\partial C_l/\partial \beta$ [illegible]

$\partial C_m/\partial|\beta|$ [illegible]

[illegible]

[illegible]

$\partial C_L/\partial \alpha$ [illegible]

$\partial C_m/\partial C_L$ – [illegible] α [illegible]

a) Longitudinal (continued)

$\partial C_m/\partial C_L = -0.204$ ($\alpha = +8^\circ$)

$\partial C_L/\partial\alpha = 0.054$ (trimmed)

$C_{D_0} = 0.130$

b) Lateral - Directional ($B = \pm 5^\circ$)

$\partial C_Y/\partial B = -0.016$

$\partial C_n/\partial B = 0.0023$

$\partial C_l/\partial B = -0.0026$

$\partial C_m/\partial|B| = -0.004$

6. Conventional configuration - gear down - Flaps @ 30°.

a) Longitudinal

$\partial C_L/\partial\alpha = 0.064$ (stick fixed)

$\partial C_m/\partial C_L = -0.135$ ($\alpha = 0^\circ$)

$C_{D_0} = 0.132$

b) Lateral - Directional

$\partial C_Y/\partial B = -0.014$

$\partial C_n/\partial B = +0.0026$

$\partial C_l/\partial B = -0.0029$

APPENDIX A

LOUVER LINK LOAD TESTS - PHASE I STATIC TEST

As part of the Phase I Static Thrust Stand Tests, louver loads, that must be restrained by the louver hydraulic actuator system, were measured. These measurements were taken using instrumented load links in place of the normal hydraulic actuators. The length of each load link was adjustable, thereby permitting each fan louver gang to be set to a predetermined value. The following discussion summarizes the test results obtained during Runs 6 through 22 of the static tests.

For each setting of the louver system, the output of the load links were recorded coincident with fan rotational speed. As the fans were rapidly decelerated, readings of force and speeds were taken. Use of this test procedure minimized the effects of load link drifting due to heating by the fan exhaust flow. Preliminary tests had shown that load link drift with temperature change could be a problem. Figure A-1 shows a typical set of measured louver link loads obtained during a fan deceleration. This figure shows fairly conclusively that the actuator loads are proportional to fan speed squared. The data are faired to go through zero load at zero fan speed by correcting for load link drift.

Since it has been shown that louver loads are proportional to fan speed squared, it is now possible to summarize all data using a non-dimensional coefficient such as:

$$H_{LF} = \frac{FORCE}{\rho U_T^2 A_f}$$

For 100 percent fan speed, standard day, $\rho U_T^2 A_f$ is equal to 21,950 pounds.

Figures A-2 through A-4 present a summary of the measured load data for a range of vector and stagger angles. Figure A-2 shows the effects of stagger at zero vector command angle (louver vector angle = -2.5^o). This condition was felt to be the critical load conditions and the data shows the maximum load factor to be 0.20.

Figures A-3 and A-4 show the effects of combined vector and stagger in the louver system. Converting the coefficient to a sea level standard day and 96 percent fan speed, the absolute louver force is 4040 pounds. The 96 percent fan speed is the maximum attainable speed at full gas generator power.

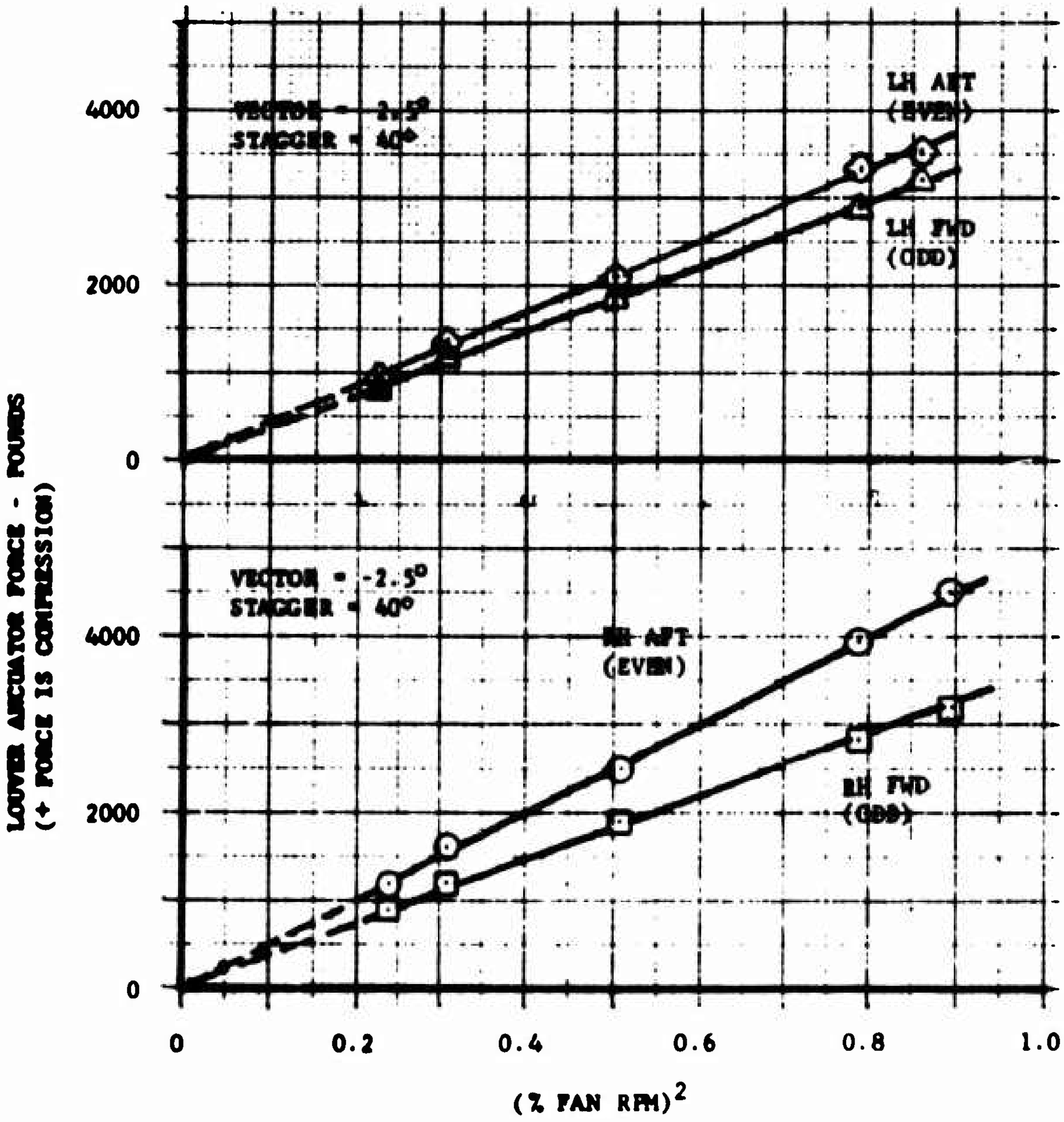

FIGURE A-1

TYPICAL LOUVER LOADS
VERSUS FAN SPEED

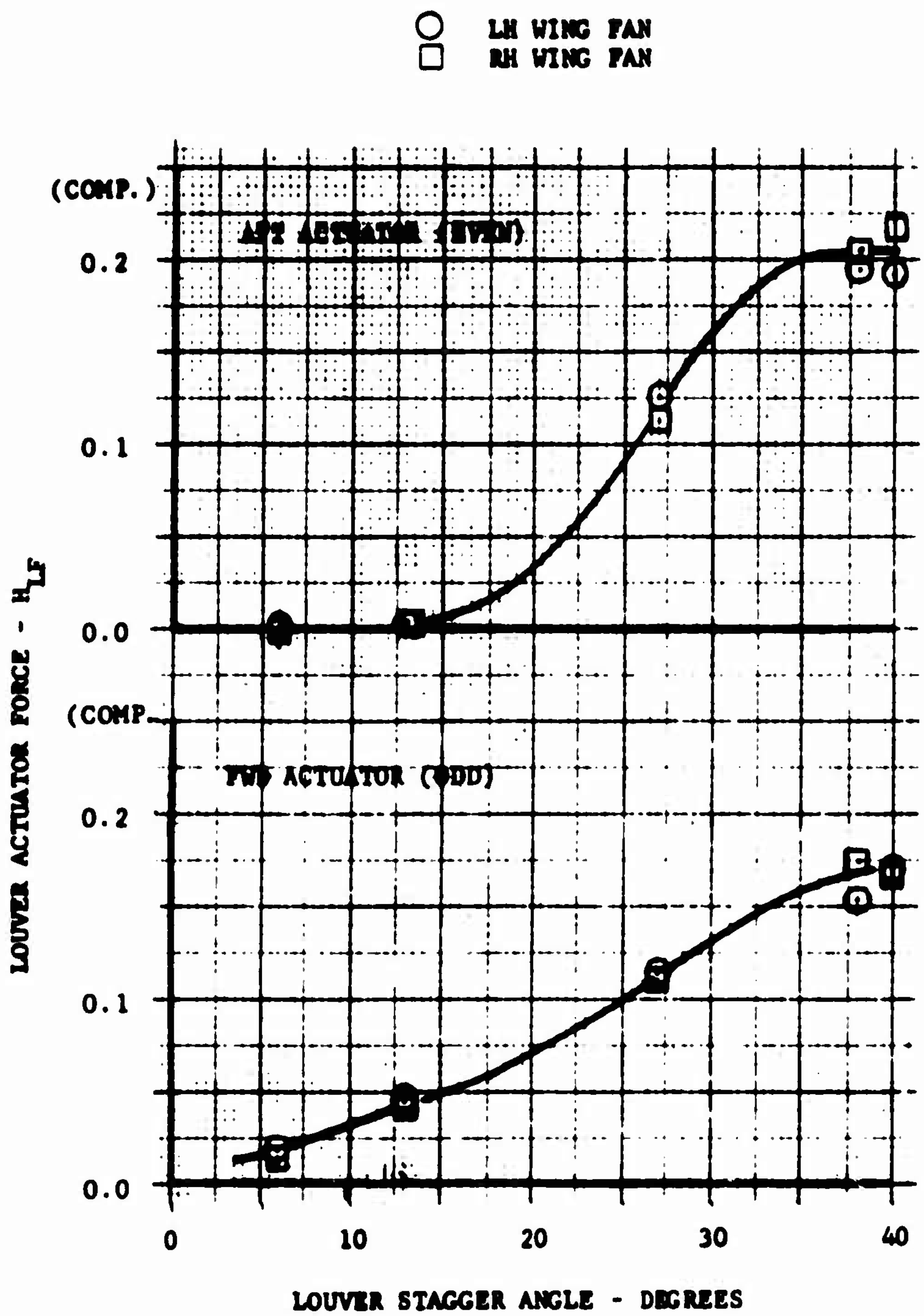

FIGURE A-2

EFFECTS OF LOUVER STAGGER ANGLE
ON LOUVER LOADS AT VECTOR ANGLE OF -2.5°

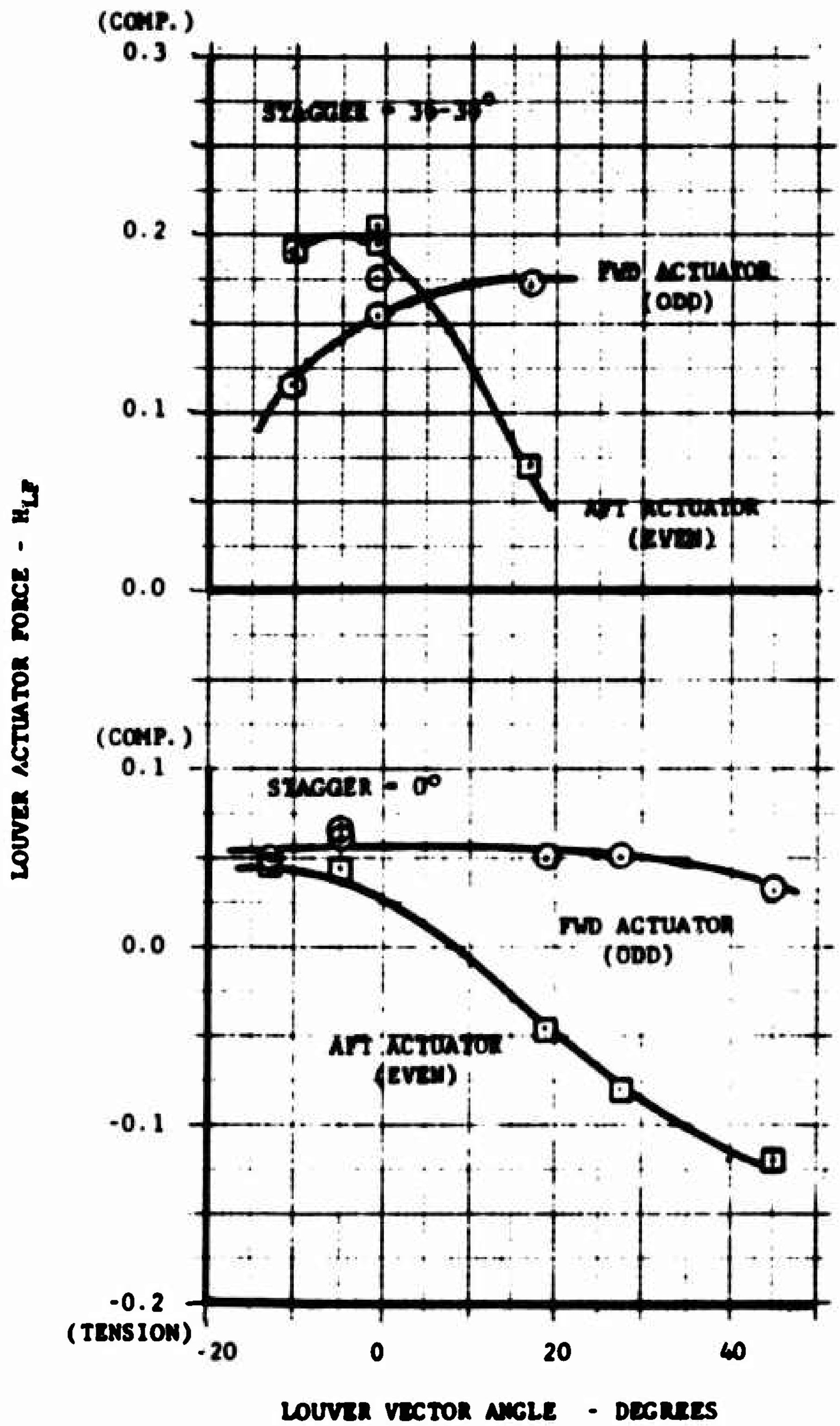

FIGURE A-3

EFFECTS OF LOUVER VECTOR ANGLE ON
LOUVER LOADS AT TWO EXTREME
VALUES OF LOUVER STAGGER

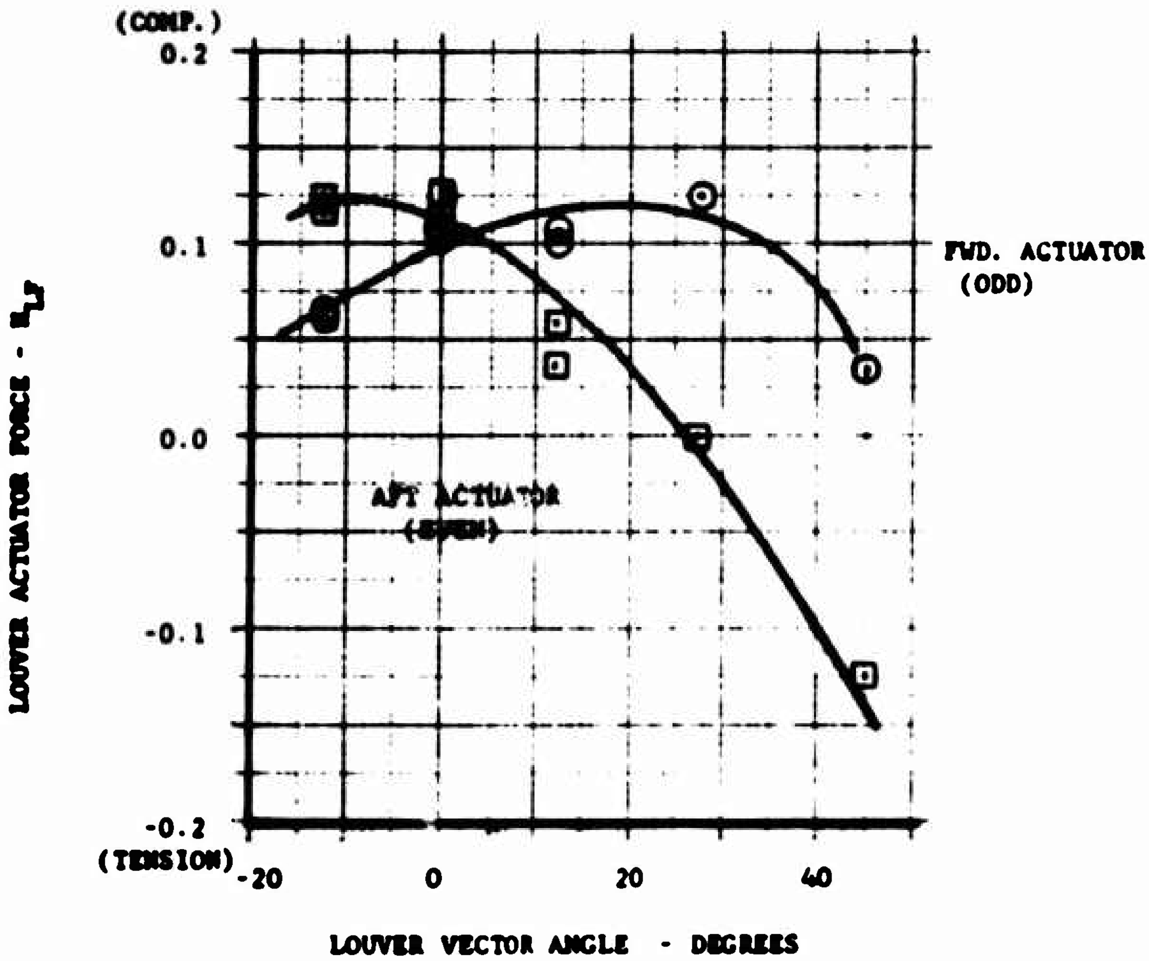

FIGURE A-4

VARIATION OF LOUVER LOADS
WITH VECTOR ANGLE AT
STAGGER ANGLES EQUIVALENT
TO NEUTRAL CONTROLS

APPENDIX B

COMPARISON OF NON-DIMENSIONAL COEFFICIENTS USED FOR PRESENTING FAN-IN-WING PERFORMANCE

In presenting performance of fan-in-wing aircraft system, three types of coefficients have been commonly used. The following discussions will present each system and provide curves and/or charts for converting data between the two systems. These charts and curves will apply only to the XV-5A aircraft and in particular, the configuration run in the NASA-Ames wind tunnel.

The three coefficient systems are identified as follows:

- Conventional aircraft system
- Modified slipstream method
- Fan law notation

The definitions used for presenting forces and moments in coefficient form are defined below. See List of Symbols for definition and units for each symbol.

<u>Conventional Aircraft System</u>

Lift - - - - - - - - - -	$C_L = \dfrac{L}{q_o S_w}$
Drag - - - - - - - - - -	$C_D = \dfrac{D}{q_o S_w}$
Pitch Moment - - - - -	$C_m = \dfrac{m}{q_o S_w C}$
Roll Moment - - - - -	$C_l = \dfrac{l}{q_o S_w b}$
Yaw Moment - - - - - -	$C_n = \dfrac{n}{q_o S_w b}$
Side Force - - - - - -	$C_Y = \dfrac{Y}{q_o S_w}$
Flight Speed - - - - -	$\mu = V_o/U_t$
Fan Power - - - - - -	No Definition

Slipstream Method

Lift - - - - - - $C_L^s = \frac{L}{q_s \; A_F}$

Drag - - - - - - $C_D^s = \frac{D}{q_s \; A_F}$

Pitch Moment - - - - - - - $C_m^s = \frac{m}{q_s \; A_F \; d_f}$

Roll Moment - - - - - - - $C_l^s = \frac{l}{q_s \; A_F \; b}$

Yaw Moment - - - - - - - $C_n^s = \frac{n}{q_s \; A_F \; b}$

Side Force - - - - - - - $C_Y^s = \frac{Y}{q_s \; A_F}$

Flight Speed - - - - - - - $T_C^s = \frac{q_F}{q_s}$

Where: $q_F = T_{ooo}/A_F$

$q_s = q_F + q_o$

Fan Power - - - - - - - $C_P^s = \frac{P \; \rho}{\left[q_F \; \delta/\theta\right]^{3/2} \; \frac{A_F}{2}}$

Fan Law Notation

Lift - - - - - - $H_L = \frac{L}{\rho \; U_T^2 \; A_f}$

Drag - - - - - - $H_D = \frac{D}{\rho \; U_T^2 \; A_f}$

Pitch Moment - - - - - - - $H_m = \frac{m}{\rho \; U_T^2 \; A_f \; d_f}$

Roll Moment - - - - - - - $H_l = \frac{l}{\rho \; U_T^2 \; A_f \; X_f}$

Yaw Moment - - - - - - - $H_n = \frac{n}{\rho \; U_T^2 \; A_f \; X_f}$

Side Force - - - - - - - $H_Y = \frac{Y}{\rho \; U_T^2 \; A_f}$

Flight Speed - - - - - - - $\mu = V_o/U_T$

Power - - - - - - - $N_R = U_T/U_{Tooo}$

For each of the three systems a unique multiplier may be used to convert the coefficients to any other one of the systems. These multipliers are presented in Figures B-1 through B-3.

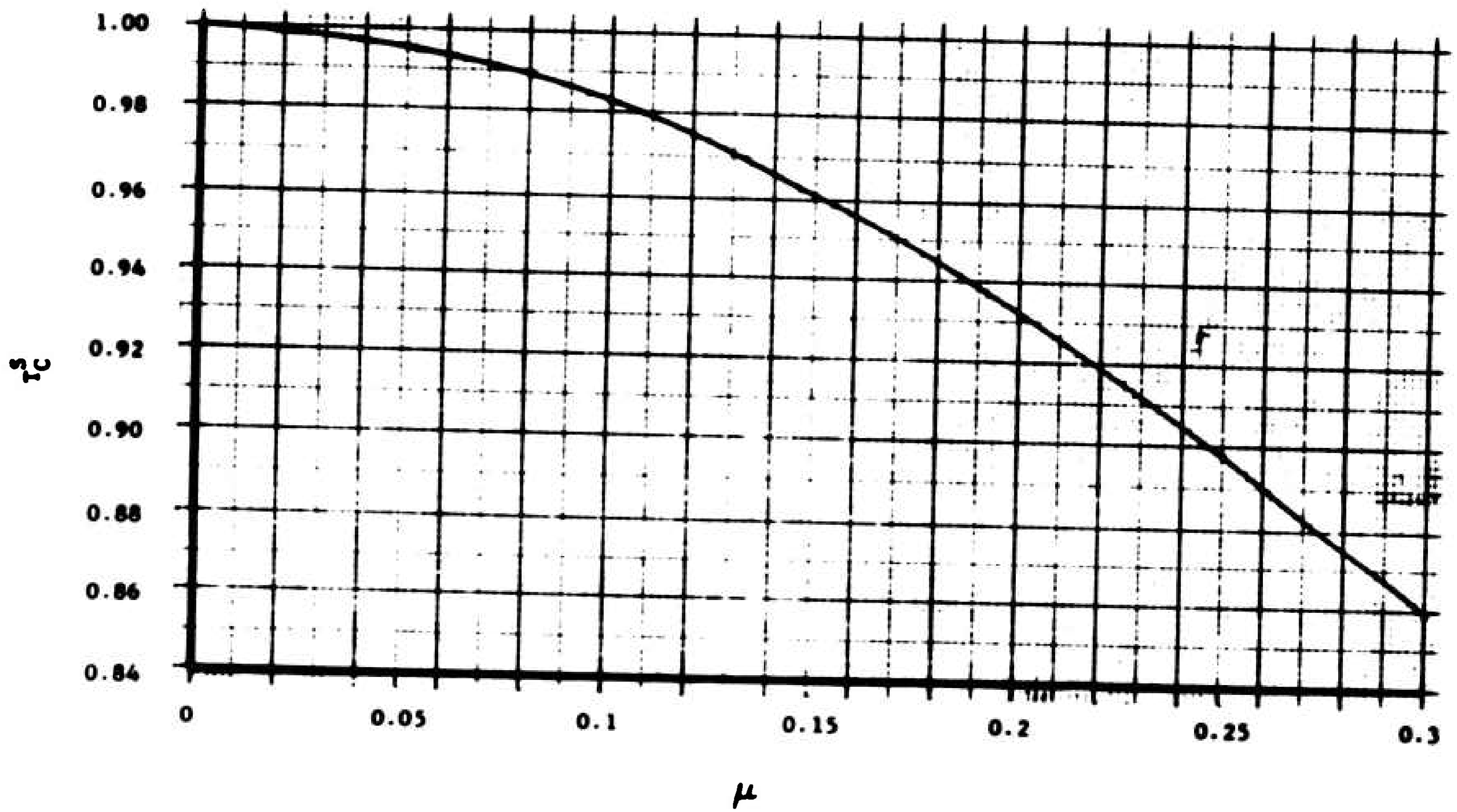

FIGURE B-1

COMPARISON OF T_C^S AND μ METHODS
OF PRESENTING FLIGHT SPEED

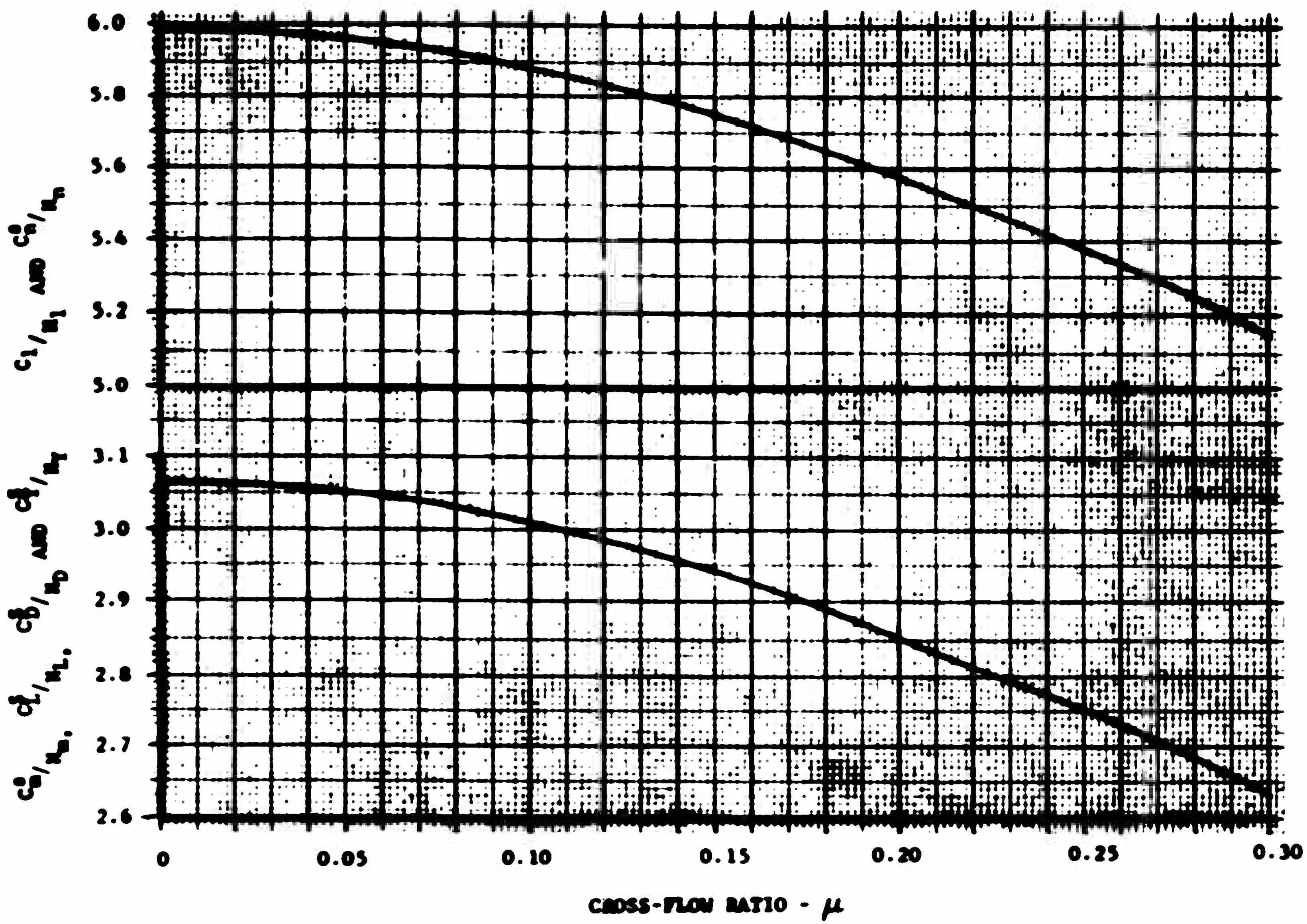

FIGURE B-2

CONVERSION FACTORS - FAN LAW
ROTATION TO SLIPSTREAM COEFFICIENTS

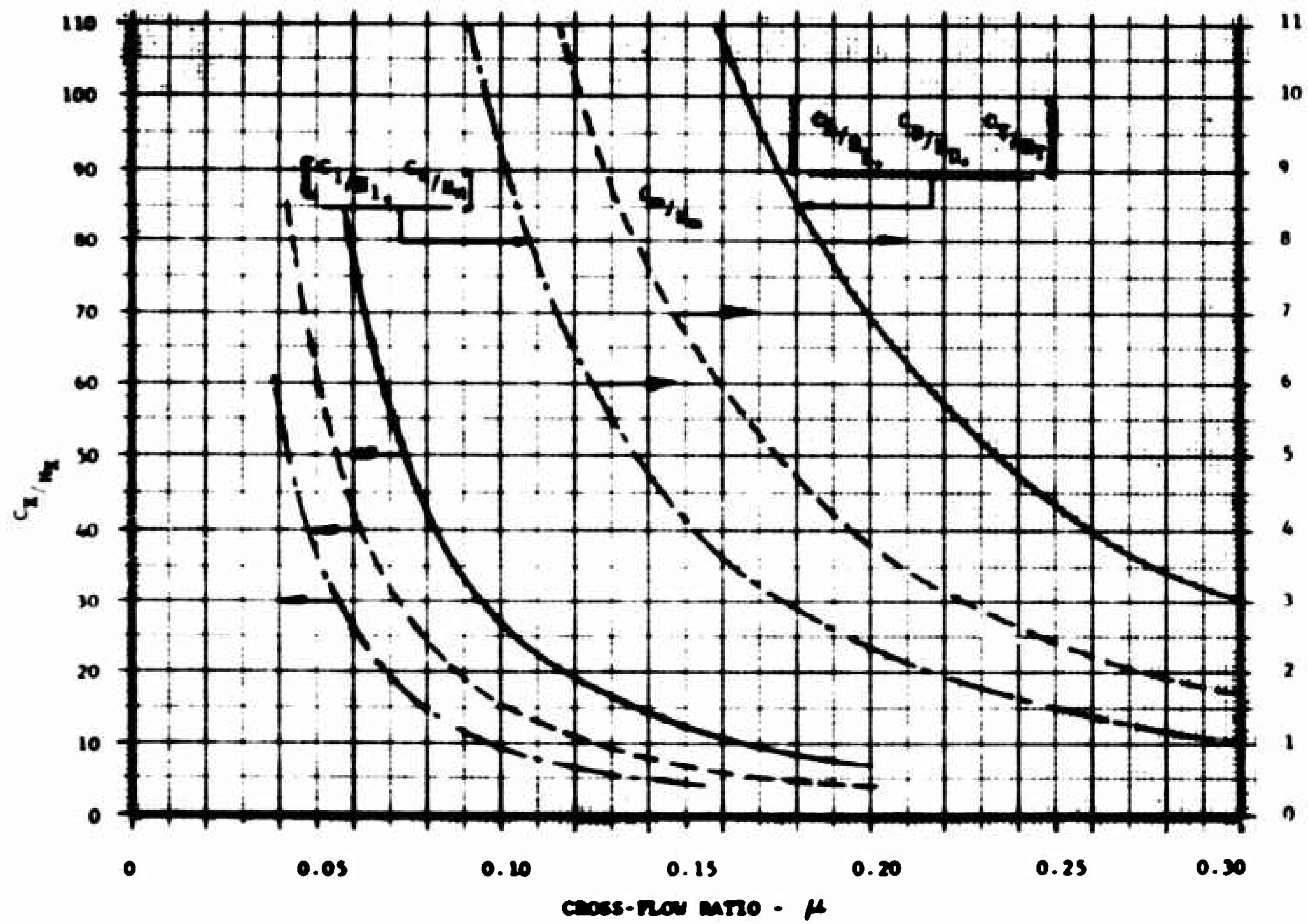

FIGURE B-3

CONVERSION FACTORS - FAN LAW
NOTATION TO CONVENTIONAL COEFFICIENTS

APPENDIX C - SUMMARY OF SYSTEM DISCREPANCIES OBSERVED DURING TEST PROGRAM

DISCREPANCY	POSSIBLE CAUSE	CORRECTION ACTION
1.) At initiation of test program errors in exit louver rigging were observed.	Inadverent movement of control sticks without hydraulic boost pressure on controls.	System was re-rigged according to spec. and movement of controls without hydraulic pressure avoided.
2.) Helicoil inserts used for attaching mount pads on wing spars could not be torqued to required limits.	Holes for inserts were drilled over-size and good thread engagement was not possible.	Larger bolts were used and back up nuts were installed in place of helicoil inserts.
3.) Actuators provided for fan exit louvers were not capable of holding louver positions at high fan power settings.	Louver loads were in excess of design values used in sizing of actuator system.	Provided auxiliary hydraulic supply to these actuators using 4000 psi which increased force sufficiently to hold louvers for tests.
4.) Vector command indicator did not indicate proper positions during louver actuation.	Short, ground or open in position potentiometer in exit louver vector actuator located in mechanical mixer box.	Replaced vector actuator with spare.
5.) Wing fan speeds, left to right, differed by about 2%.	Misadjustment of wing fan scroll areas.	None - Tests were performed with this fan speed discrepancy.
6.) Pitch fan inlet louver developed a crack at one of the ends during Phase I ground tests.	Unknown.	Provided doubler at cracked area-no additional cracks appeared.

APPENDIX C - (CONTD.)

DISCREPANCY	POSSIBLE CAUSE	CORRECTION ACTION
7.) During Phase I ground tests and aircraft inspection, excessive leakage of pitch fan scroll-duct flanges were observed as indicated by high structural temperatures.	Distortion of either pitch fan scroll flange or duct flange.	Realigned flanges and installed stainless steel mesh gasket in flange joint during assembly.
8.) During Phase I ground tests aircraft could not be converted from CTOL to the VTOL mode.	Interlock switches in pitch fan inlet louver actuator malfunctioned and did not indicate that the louvers had opened prior to conversion. Problem was traced to failure of limit switch bracket.	Repaired bracket as well as possible (not flight quality) in order to proceed with testing.
9.) After ground run #4, Phase I, excessive blower gear box leakage began to appear. This problem existed intermittently throughout the test program independent of two gear box changes.	Problem was eventually traced to pressurization of gear box by cooling air flow which, in turn, forced oil out labrinth seals around drive shafts.	One gear box having redesigned seal was installed before W/T Run #14 and leakage ceased. Other gear box was replaced after run #33.
10.) While attempting to light off engines for Run #8, Phase I ground tests, engine failed to start.	Cross-feed fuel shut-off valve would not open when commanded. Shorted solenoid prohibited valve operation.	Valve was removed from aircraft and opened manually, then reinstalled in order to proceed with test program.

APPENDIX C - (CONTD.)

DISCREPANCY	POSSIBLE CAUSE	CORRECTION ACTION
11.) Loosening of rivets and oil canning of structure around lower fuselage structure under cockpit appeared during Phase I ground runs.	Excessive loads in structure due to oscillations of aircraft that were characteristic of static thrust mounting system.	Longitudinal stiffeners were installed in critical areas and loose rivets replaced. Future runs were limited to 95% gas generator power settings to reduce load levels.
12.) During W/T Run #6 at time of divert from VTOL to CTOL, the fire door on right hand side of engine inlet became loose and was ingested by the right wing fan.	At divert, pressure loads on door apparently go through a reversal which jarred the door loose. Door is a "Pop-in" type and is not fastened securely.	Doors were clamped in place using aluminum straps for remainder of test program.
13.) Two false fire warnings occurred during conduct of the wind tunnel tests.	Shorting of fire detector cable to ground was found in both cases.	Removed faulty sections of cable and used remaining cable as fire warning system.
14.) After W/T Run #9, aircraft could not be converted from CTOL to VTOL.	Horizontal stabilizer actuator limit switches would not operate and failed to indicate tail position to conversion system.	Installed jumpers across malfunctioning limit switch in order to proceed with test.

APPENDIX C - (CONTD.)

DISCREPANCY	POSSIBLE CAUSE	CORRECTION ACTION
15.) At end of W/T Run #13 forward inboard circular vane in L/H fan failed completely at forward mount point and was partially ingested by fan. Numerous other vanes had large cracks at juncture of the side and circular vanes. This failure occurred during first test at 80 knots, high fan power setting.	Excessive vibratory loads due to separated flow on vane system in high cross flows.	Vane system was redesigned by addition of stiffeners and rivits. Prior to redesign, tests proceeded using vanes from A/C #2 and power settings held to low levels.
16.) During inspection after W/T Run #13 a crack was observed in J-85 inlet bellmouth. Crack was about 2" long at lower RH outboard lip of inlet.	Unknown	Repaired crack with epoxy and reinforcing glass tape on ›ide surface of inlet.
17.) At conclusion of W/T Run #13 failure of metal tabs inside rubber wing fan door seals was observed. Later during run #29, a 6" piece of the rubber seal detached from the door leading edge but did not fail completely.	Excessive vibratory air loads on leading edges of wing fan doors.	Removed failed part of seal completely and proceeded with tests.

APPENDIX C - (CONTD.)

DISCREPANCY	POSSIBLE CAUSE	CORRECTION ACTION
18.) During W/T Run #28, forward inboard side of wing fan strut fairing failed completely and began to tear loose.	Excessive suction air loads not anticipated during design.	Doublers were installed on the fairings at points of failure. Later fairings were replaced with new parts of heavier metal thickness.
19.) After Run #31 rotor and stator damage of LH wing fan was observed because of ingestion of rotor hub platform.	Damage had occurred because of previous circular vane failure, and resulted in development of fatigue cracking of platforms.	Replaced all platforms of LH fan with spares after conclusion of Run #33.
20.) During aircraft inspection following wind tunnel tests, cooling air duct flapper valves had broken loose at area near hinge line.	Unknown - similar failure appeared at about same time on A/C #2 at Edwards.	Made and installed new flapper valves that were stiffened by rolling over about 1/8" on the edges of plates.
21.) Throughout the wind tunnel tests, fatigue cracks on the sides of the canoe structure occurred.	Oil-canning of the structure due to air loads from wing fan exhaust gas impingement.	Installed doublers on cracked areas and proceeded with tests.
22.) Signs of excessive leakage of fan to wing louver seals was observed during aircraft inspection at conclusion of wind tunnel tests.	Poor seal design and fan to wing fit-up.	None

APPENDIX D

MEASUREMENT OF WING FAN DOOR SUPPORT LOADS DURING WIND TUNNEL TESTS

During the conduct of the wind tunnel test program, the forces associated with the wing fan butterfly door mounting system were measured. These measurements were taken using two types of strain gage instrumentation. The first was a set of steady state strain gages attached to the stabilizing links that fasten the door to the forward and aft ends of the wing fan main strut. These gages were installed on the left-hand wing fan closure system only. The second set of measurements consisted of eight "strain-sert" bolts. These bolts were used to attach the door actuator mechanism to the fan hub assembly and were preloaded to the limit loads that could be transmitted to the fan hub. The "strain-sert" bolt when used in this manner is basically a strain gaged bolt that will indicate when the load being carried exceeds the preload value.

The test results, in general, may be stated by saying that for the range of variables tested, there were no signs of loads in excess of the preload values.

The results of forces obtained from the steady state gages attached to the stabilizing links are summarized in the attached figures. Figures D-1 and D-2 show the support loads when the wing fan doors are open and the fans not operating. The data show the basic aerodynamic loads due to the free stream velocity for a range of angles of attack and yaw. In no case do these loads exceed 100 pounds per link.

Figures D-3 through D-6 show the measured support loads for a complete range of flight speeds with the fans operating at the high power setting. Figures D-7 and D-8 show similar data for a range of yaw angles at two flight speeds. The data indicates that the loads are surprisingly low. It appears that maximum load occurs at the high flight speeds and is about 300 pounds for the forward-inboard link. There is an opposing load of about 100 pounds on the forward-outboard link, so the combined effect is an applied load of less than 200 pounds on the forward door support structure. This is well within design limits. What is more encouraging is the small load changes experienced with angle of yaw or sideslip as shown in Figure D-7 and D-8.

Figure D-9 is a summary of the loads at zero angle of attack for the range of test flight speed, μ. The effects of fan power level are clearly shown. This variation of loads with fan power level is characteristic of all devices placed either in the inlet or exit flow fields of the fan system. This being the case it is possible to present the data in coefficient form, independent of fan power level, as shown in Figure D-10. The data in this figure can be used for obtaining the fan support link loads for any power setting or flight speed.

In summary, it may be concluded that the method of attaching the wing fan closure doors to the fan is adequate and does not transmit excessive loads into the fan structure, as long as reasonable flight attitudes are maintained (α = -5 to +15 degrees, ψ = $\pm$10 degrees).

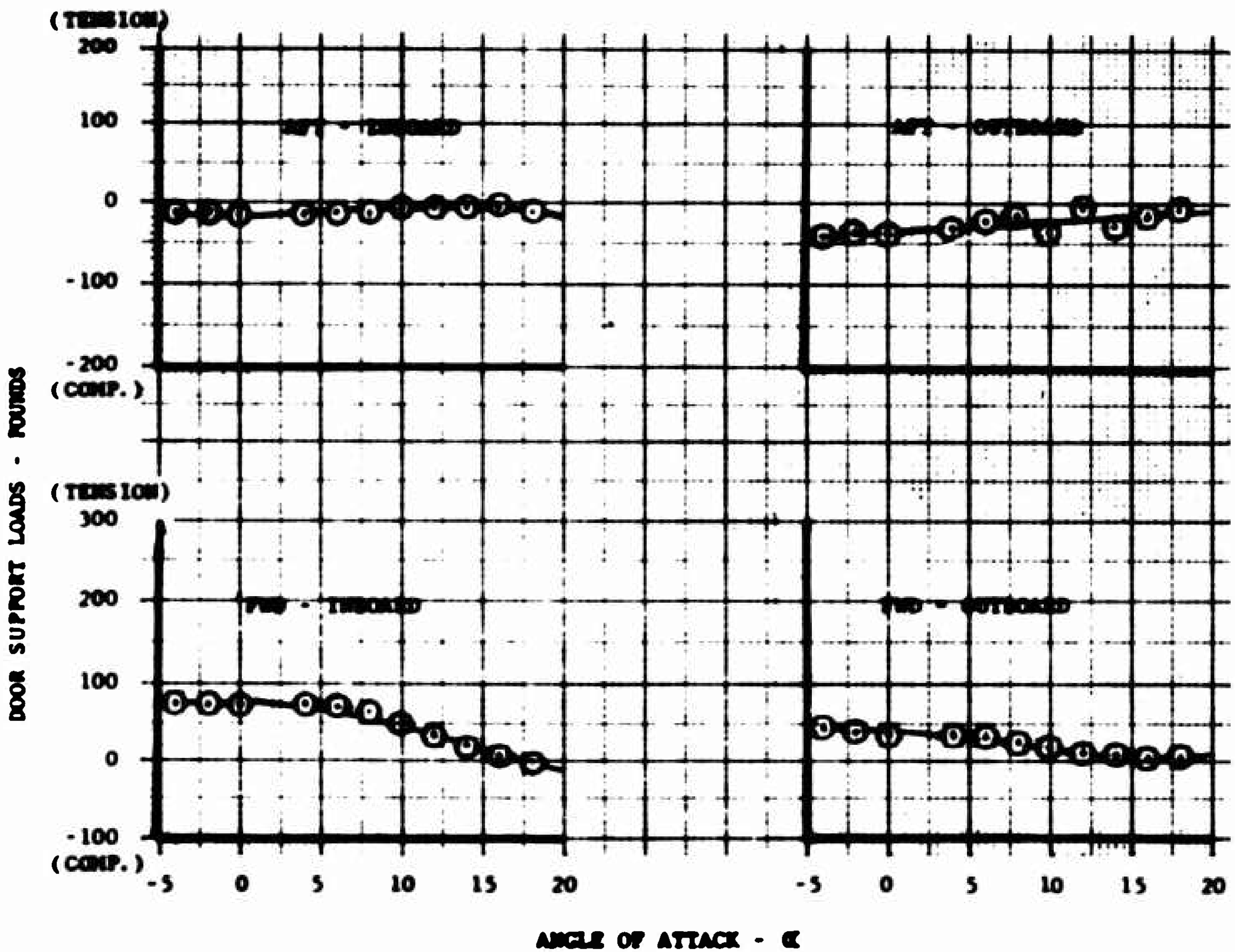

FIGURE D-1

EFFECTS OF ANGLE OF ATTACK ON DOOR SUPPORT LOADS - VTOL CONFIGURATION - FANS NOT OPERATING, q_o - 21.6 psf.

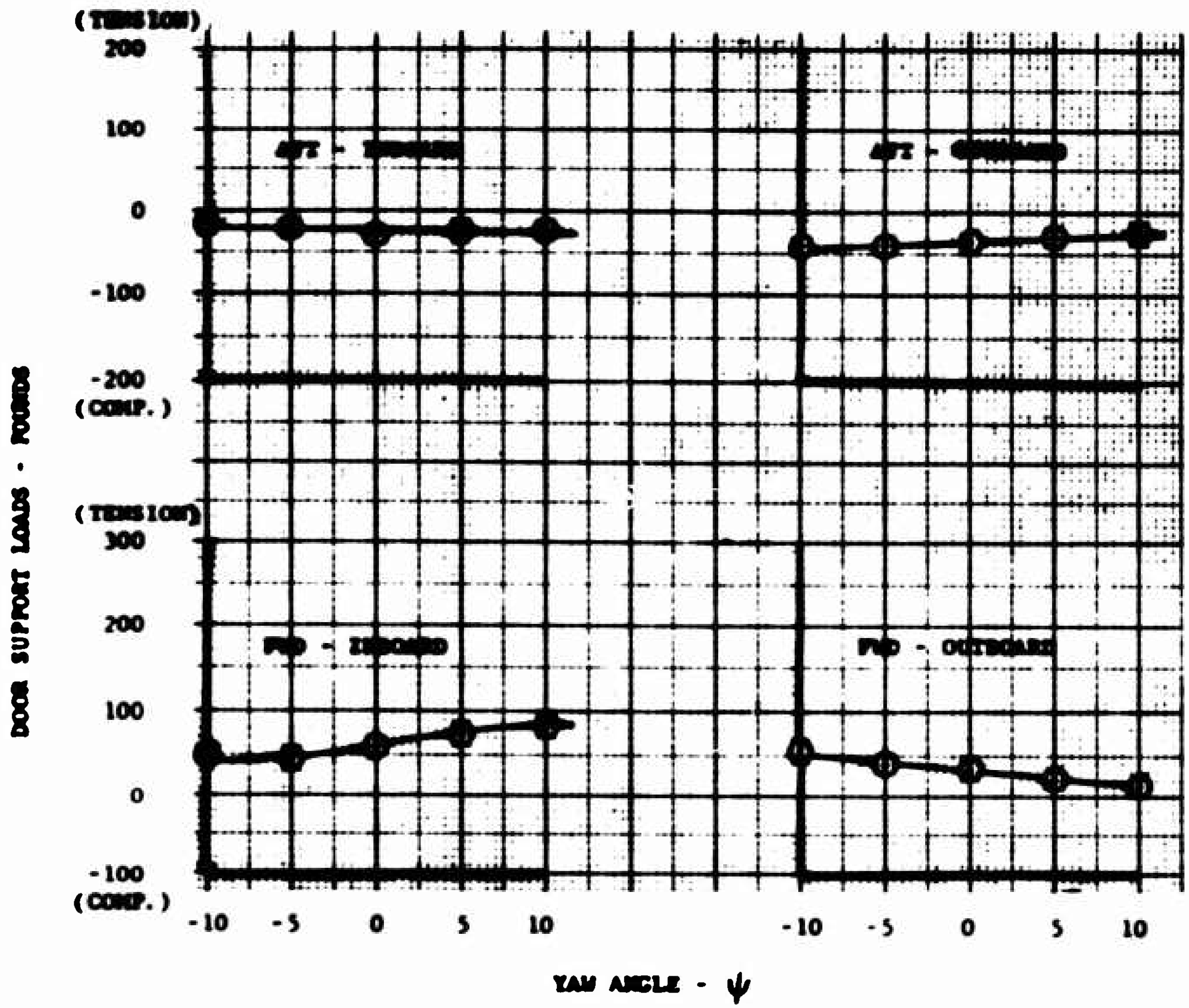

FIGURE D-2

EFFECTS OF YAW ANGLE ON DOOR SUPPORT LOADS - VTOL CONFIGURATION - FANS NOT OPERATING - q_o - 21.6

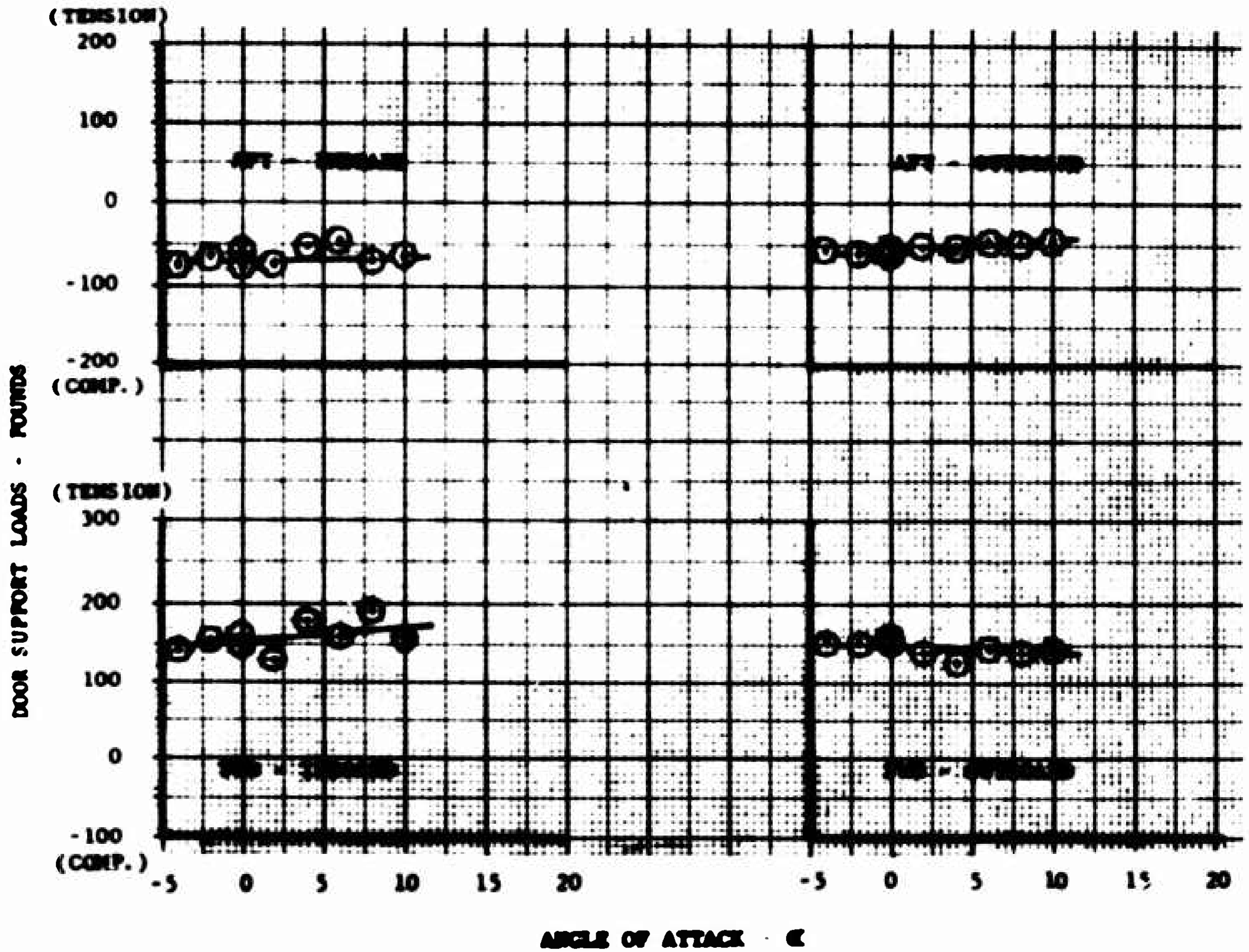

FIGURE - D-3

EFFECTS OF ANGLE OF ATTACK ON DOOR SUPPORT LOADS - FAN POWERED - μ = 0.115 - FAN RPM = 85%

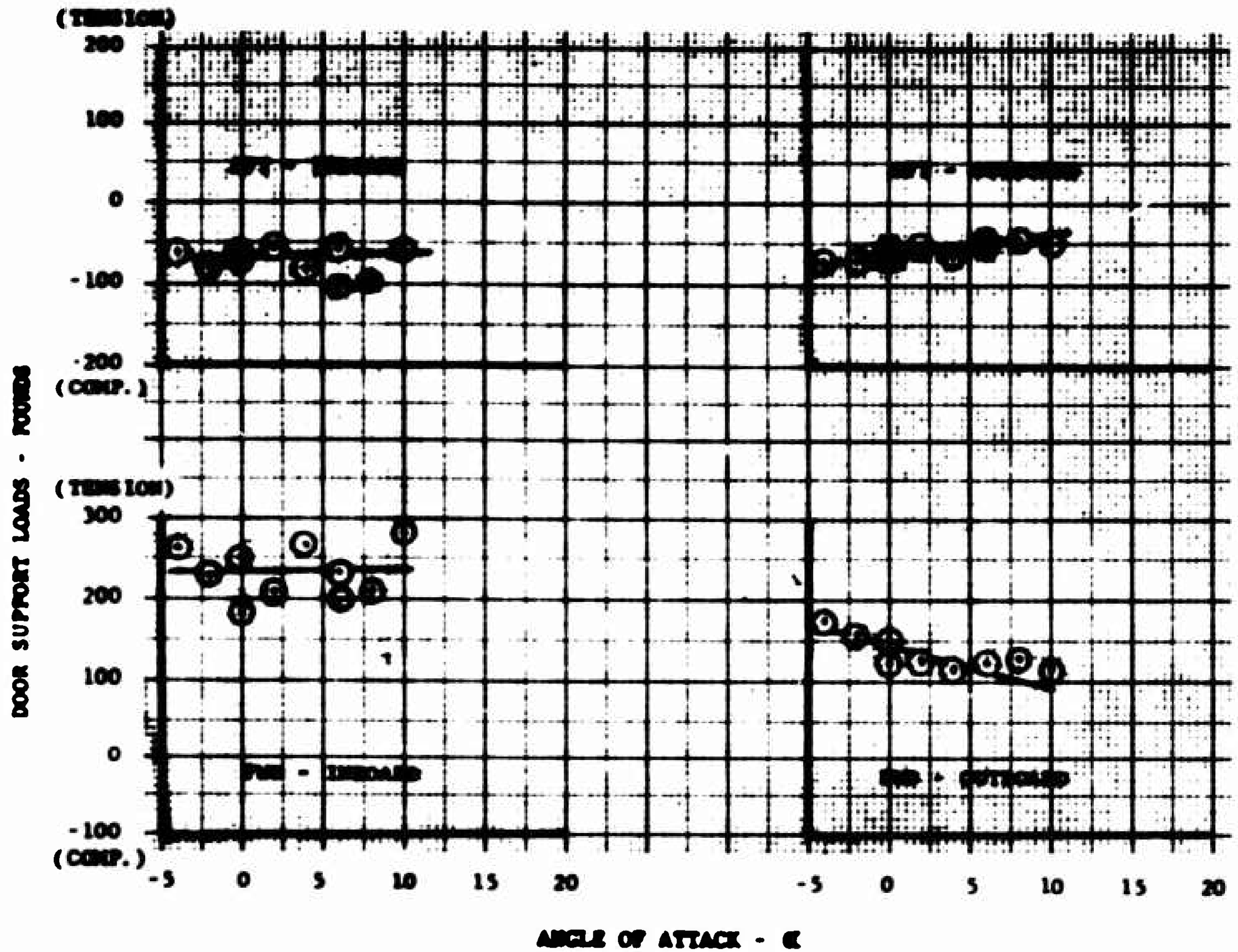

FIGURE D-4

EFFECTS OF ANGLE OF ATTACK ON DOOR SUPPORT LOADS - FAN POWERED - μ = 0.165 - FAN RPM = 87%

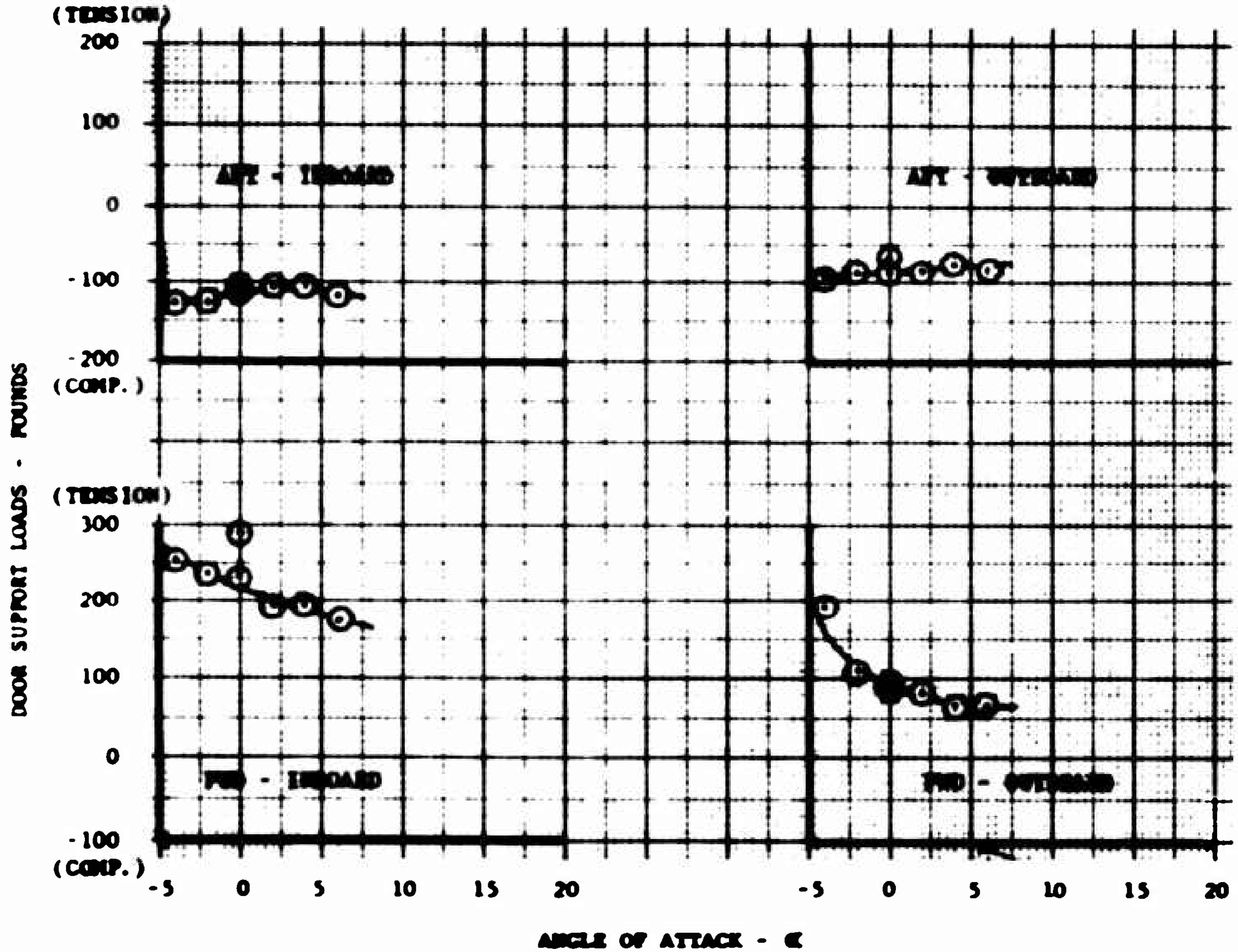

FIGURE D-5

EFFECTS OF ANGLE OF ATTACK ON DOOR
SUPPORT LOADS - FAN POWERED -
μ = 0.215 - FAN RPM = 89%

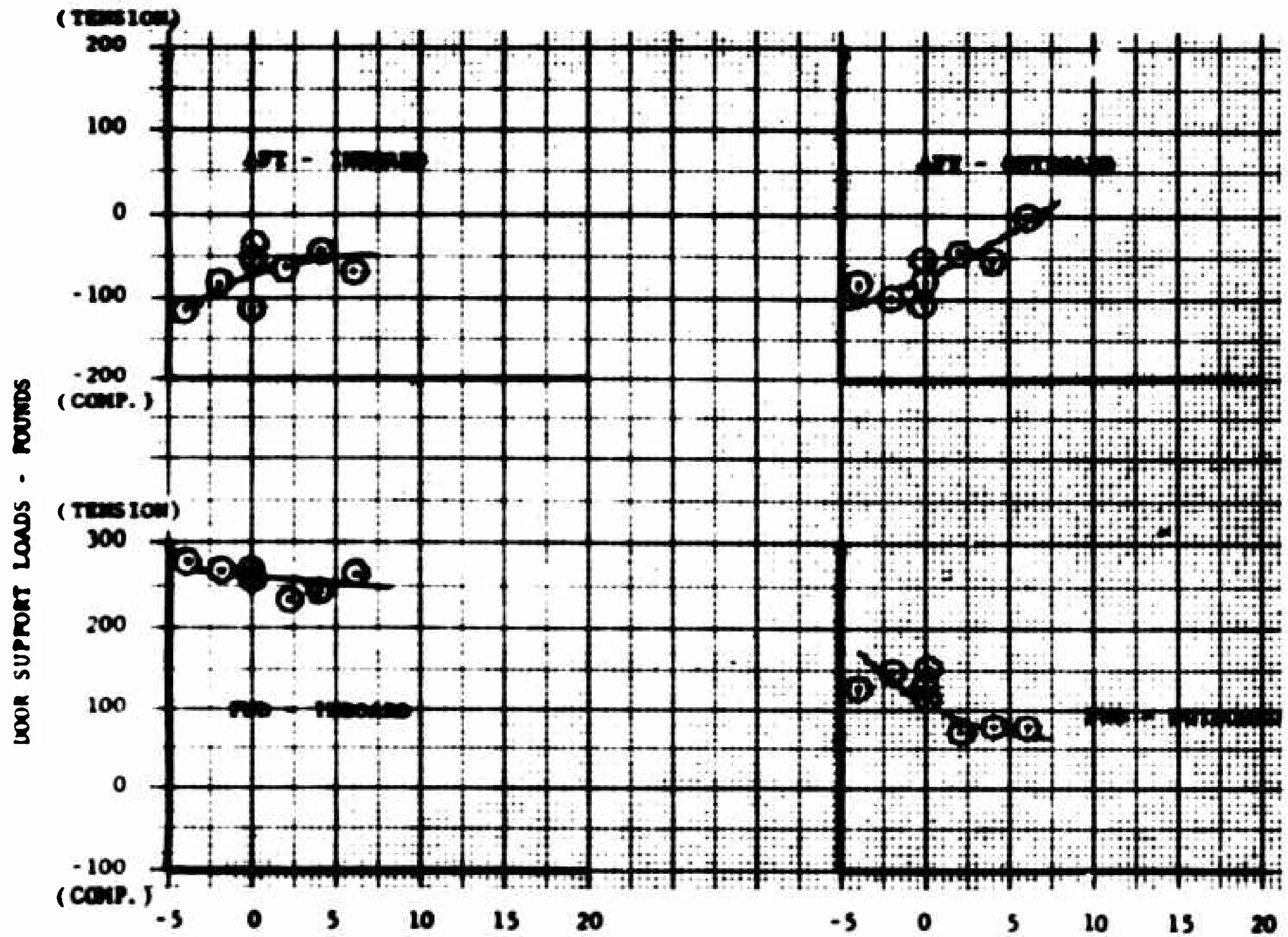

FIGURE D-6

EFFECTS OF ANGLE OF ATTACK ON DOOR
SUPPORT LOADS - FAN POWERED -
μ = 0.26 - FAN RPM = 88%

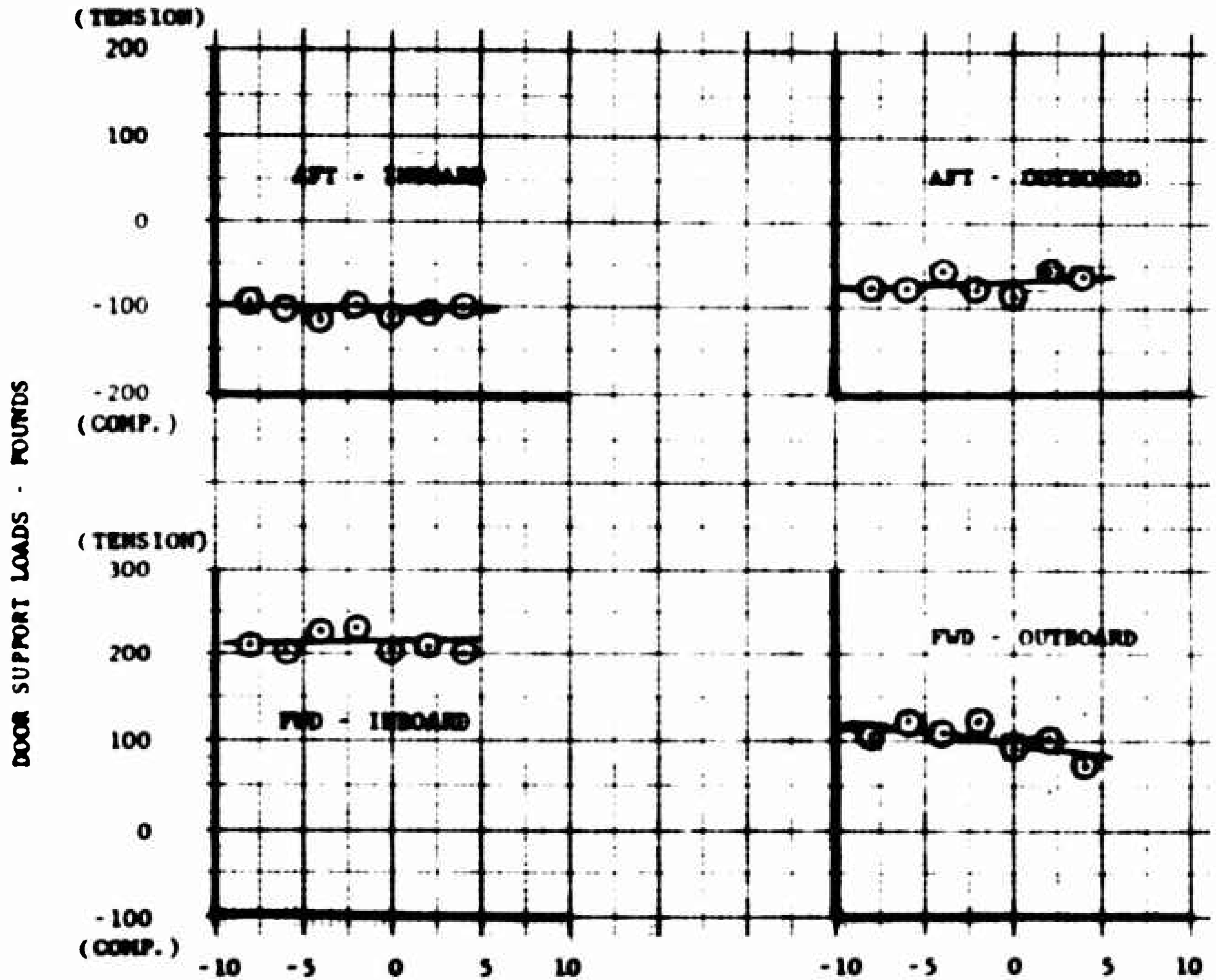

FIGURE D-7

EFFECTS OF ANGLE OF YAW ON DOOR SUPPORT LOADS - FAN POWERED - μ = 0.17
FAN RPM = 84%

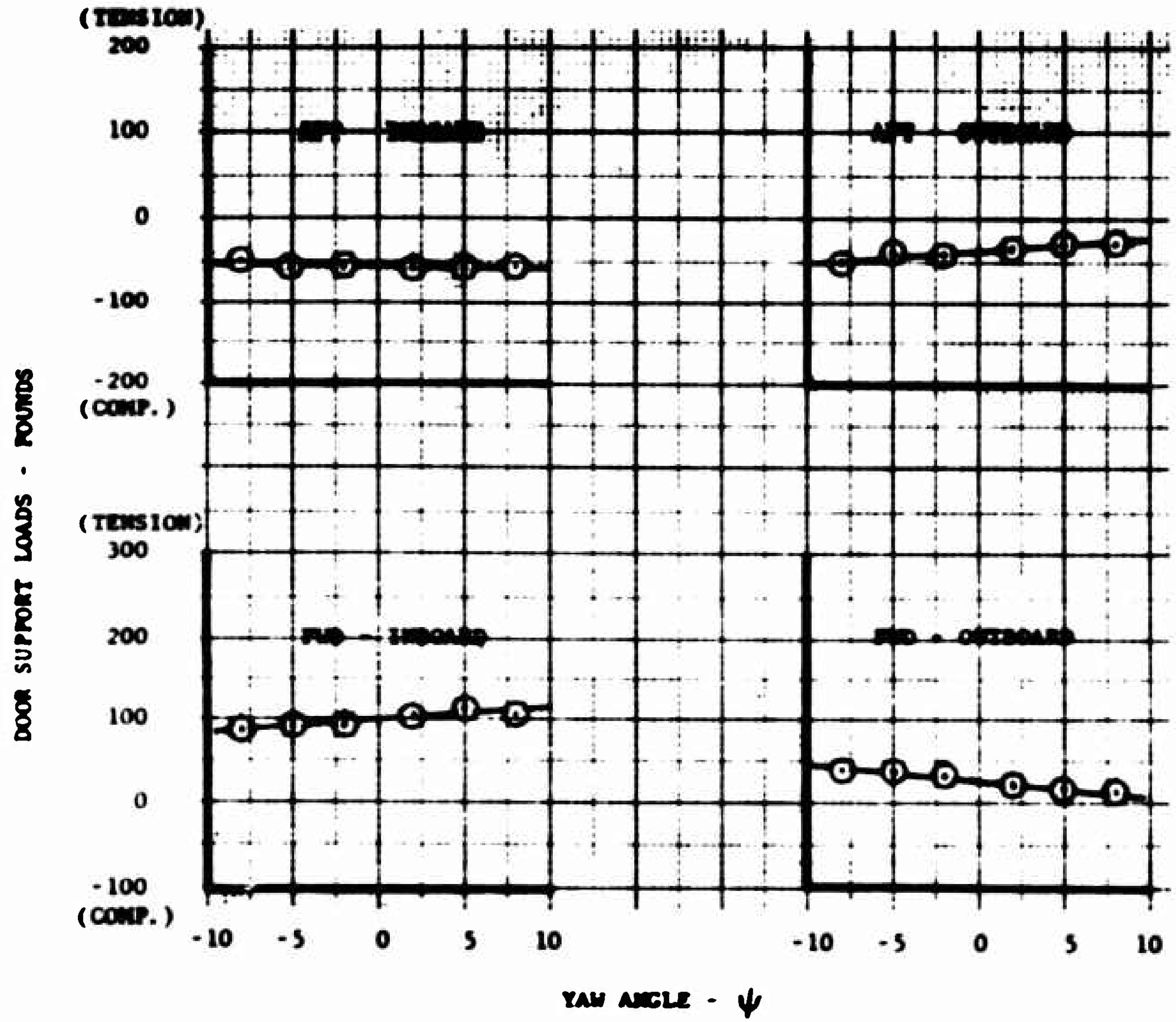

FIGURE D-8

EFFECTS OF ANGLE OF YAW ON DOOR SUPPORT LOADS - FAN POWERED - $\mu = 0.23$ - FAN RPM = 63%

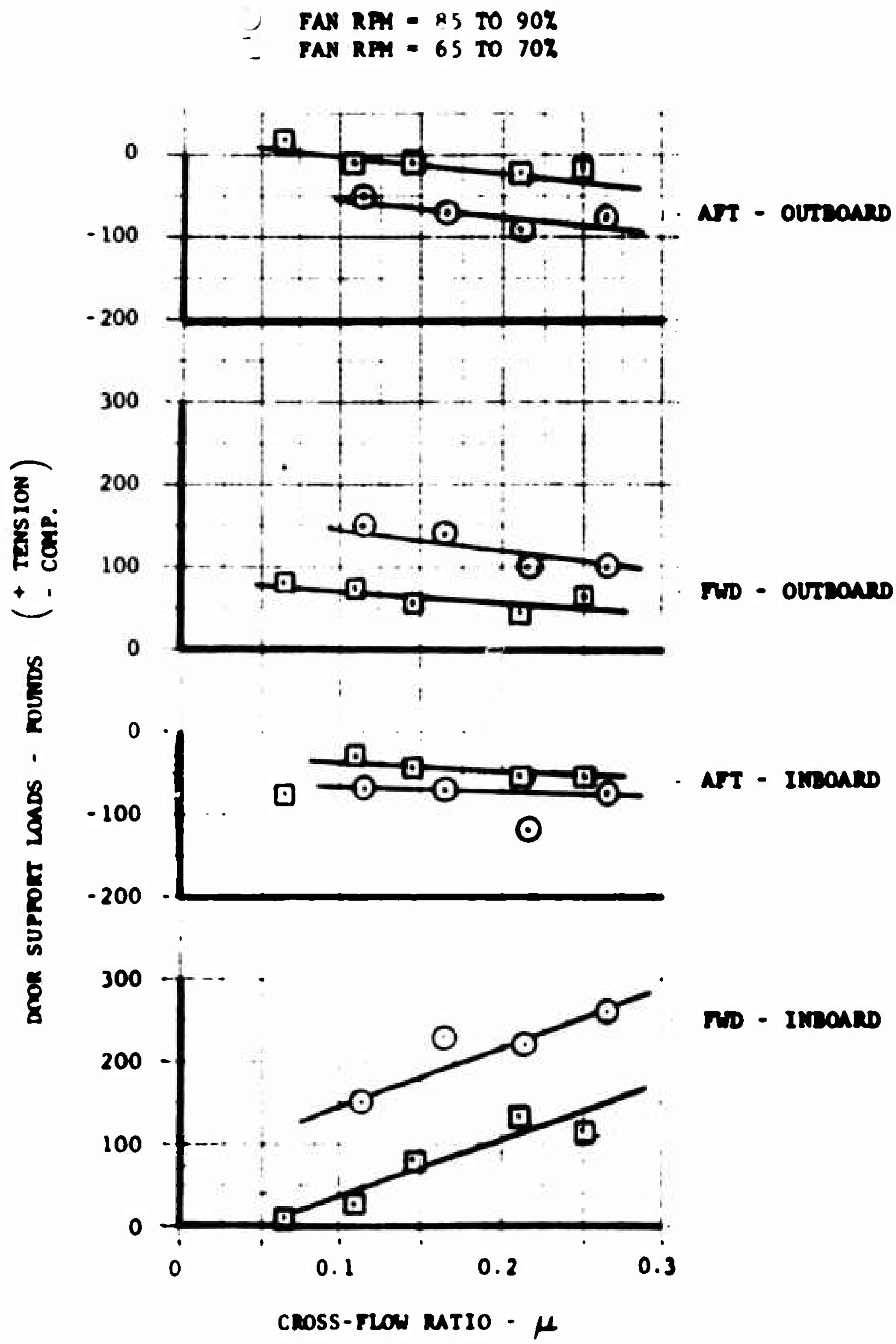

FIGURE D-9

VARIATION OF DOOR SUPPORT
LOADS WITH CROSS-FLOW RATIO FOR BOTH
HIGH AND LOW POWER SETTINGS - $\alpha = 0^{\circ}, \psi = 0^{\circ}$

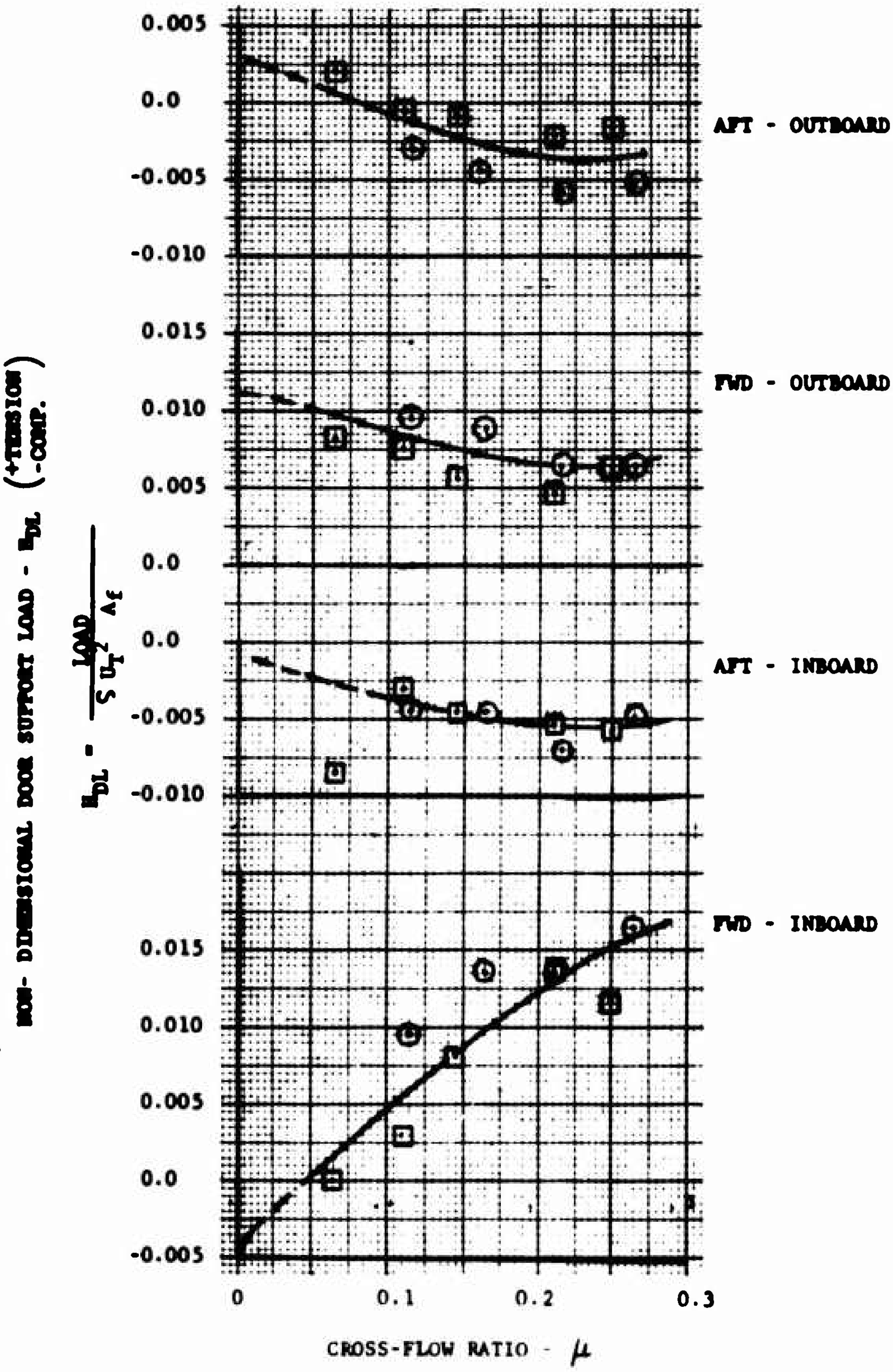

FIGURE D-10

CORRELATION OF DOOR SUPPORT LOADS IN COEFFICIENT FORM VERSUS CROSS-FLOW RATIO

APPENDIX E

STICK FORCES DURING CONVENTIONAL AND FAN POWERED OPERATION

As part of the wind tunnel test program, stick forces for the three control motions, longitudinal and lateral stick and rudder pedals, were measured at each test point. The forces were measured by strain gages applied to one of the control system members for each axis. The outputs of these strain gages were recorded on the digital instrumentation system. Each strain gage system was calibrated by applying known loads to the appropriate control system and recording the strain gage output. The applied calibrating load was then transferred to a convenient reference location where pilot-applied forces act. For example, the rudder pedal force was transferred to the bottom tube of the pedals where the pilot applies toe pressure. The longitudinal and lateral stick forces were transferred to the center of the stick grip. Figures E-1 through E-8 present some typical measurements of stick forces for a range of the more important variables.

Longitudinal Stick Forces

Figures E-1 through E-4 show measured longitudinal stick forces for both conventional and fan powered flight modes. Figure E-1 shows longitudinal stick forces for a range of stick positions and stabilizer incidence settings. These forces are presented in absolute units, pounds, and were taken at a speed of about 80 knots (q_o = 21.2 psf.). This data shows a stick force of about 40 to 50 pounds for full stick throw.

These forces as well as for all others presented in the figures are assigned a direction such that a negative force gradient will occur for a normal restoring force, that is, the change in force per unit control movement is negative. Note that this is control stick or pedal movement not control surface movement.

The upper curve of force versus tail incidence shows an apparent change in stick force with tail incidence angle. However, this is a false indication that may be traced to the changes in elevator angle with tail incidence. Rigging checks show that for a neutral stick, as the tail incidence is changed from zero to maximum incidence, the elevator angle moves from neutral to about 2 degrees trailing edge up. This elevator movement is equivalent to about 1-1/2 degrees of aft stick motion. This stick motion should produce about 4 - 5 pounds of negative stick force. This agrees well with the measured stick change with tail incidence. It can be concluded that the elevator will float, stick free, very close to a streamlined condition.

A similar conclusion may be obtained from the data shown in Figure E-2 which shows stick force variation with angle of attack for a range of conditions. The results indicate that for angle of attack changes above zero degrees, the stick free location will not change appreciably, less than one degree. However, at negative angles of attack, the stick force becomes more positive with reduced angles of attack. With stick free, the stick would move forward as angle of attack is reduced, thereby producing a destabilizing moment. The end result is a reduction in longitudinal stability for the stick free case as compared to the stick-fixed stability condition. This condition is more pronounced at negative tail incidence settings.

Figures E-3A and E-3B show some typical stick force gradients for the fan mode of flight. Data for a range of velocities, vector angles and fan power settings are shown. The stick forces for these flight conditions consists of two types of restoring or centering forces. One is the conventional aerodynamic force due to the elevator balance, and the second is due to an artificial centering force produced by a spring package in the fan control mixer box. The spring package was designed to produce about 12-14 pounds longitudinal force at full stick throw and will phase-out to about 10 percent force at full vector command of 45 degrees. This estimated spring package force gradient is shown as the dashed curves in Figures #3A and 3B.

An interesting breakdown to the total longitudinal stick force gradient is shown in Figure E-4. The lower curve shows the estimated force gradient due to the spring package. Using this gradient, the remaining force shown in Figure E-3 is due to elevator aerodynamic forces. Due to the non-linear nature of these forces, a gradient based on $\pm$ 1/2 stick throw was computed for this aerodynamic component. The gradients are shown in the center curve of Figure E-4 versus free-stream velocity head A linear relationship exists which is desirable for a pure aerodynamic force.

The curve at the top of Figure E-4 presents the map of stick force gradients versus flight speed for the complete vector command range. These curves were generated by summing the individual aerodynamic and spring package gradients.

It should be noted here that all forces when measured during fan mode of operation were adjusted to zero forces at neutral stick by a direct shift of the data. This technique was required because of the considerable shift in strain-gage balance during conduct of the tests when the fans were operating. During fan operation, heating of the strain-gaged links occurred, and even though temperature compensated gages were used, shifts in zero occurred that were at times as large as the forces being measured. The time interval required to make a control excursion during a particular test was relatively short; therefore, shifts in the strain gage outputs were negligible. Thus, the change in force readings due to control changes was valid (delta value), although the absolute level of the force reading was questionable. An angle-of-attack excursion took a considerable period of time and the shifts in data were greater than the actual force change, consequently the data were unuseable. Data are presented for angle-of-attack changes in the conventional mode, since engines were off and data shifts due to temperature were not a problem.

Rudder Pedal Forces

Figures E-5 through E-7 present measured rudder pedal forces similar to those shown for the longitudinal stick. Figure E-5 shows the variation of rudder pedal forces with sideslip angle and rudder pedal deflection.

The lower figure shows a reversal of rudder pedal force at high sideslip angles. However, comparison of these force levels, $\pm$ 5 pounds, with the normal rudder pedal force gradient in the upper figure, shows that they are almost negligible.

Figure E-6 shows the measured rudder pedal force gradients for the fan mode of operation. Here, as for the longitudinal stick, the forces are composed of aerodynamic and spring forces. A breakdown of the two forces is shown in Figure E-7 and again the correlation is excellent. For the rudder pedal system, a spring package force of about 25 pounds for full throw was the design value and to phase-out to zero force at full vector command of 45 degrees.

A map of stick forces versus flight speed for the complete range of vector command angles was developed as shown in the upper curves of Figure E-7.

Lateral Stick Forces

The conventional aircraft lateral control system contains complete hydraulic boost on the ailerons with aerodynamic forces produced by the trim tab system on the ailerons. Artificial feel from a spring package is also used in the fan mode of flight, designed for light control forces of about 2 pounds at full throw.

Because of light forces, it was almost impossible to measure the force gradients with the instrumentation provided. The only reasonable force gradients measured during the test program are shown in Figure E-8. These curves show lateral stick forces for three flap settings. As is apparent from these figures, the force levels are very low and no data could be obtained in the fan mode of flight where drift due to heating occurred.

Conclusions

The results of control force measurements can be summarized as follows:

1.) Lateral stick forces were very light and accurate measurements could not be obtained.

2.) Rudder pedal forces, both conventional and fan powered, appear as predicted and are relatively free of sideslip effects.

3.) Longitudinal stick force gradients are very close to predicted values. Floating tendency of the elevator is very small and will tend to reduce the stability of the aircraft, stick-free as compared to stick-fixed.

4.) At zero stick and elevator position, flaps deflected, there is a stick force tending to move the stick forward. This stick force cannot be trimmed with horizontal tail incidence and exists at all aircraft angles of attack.

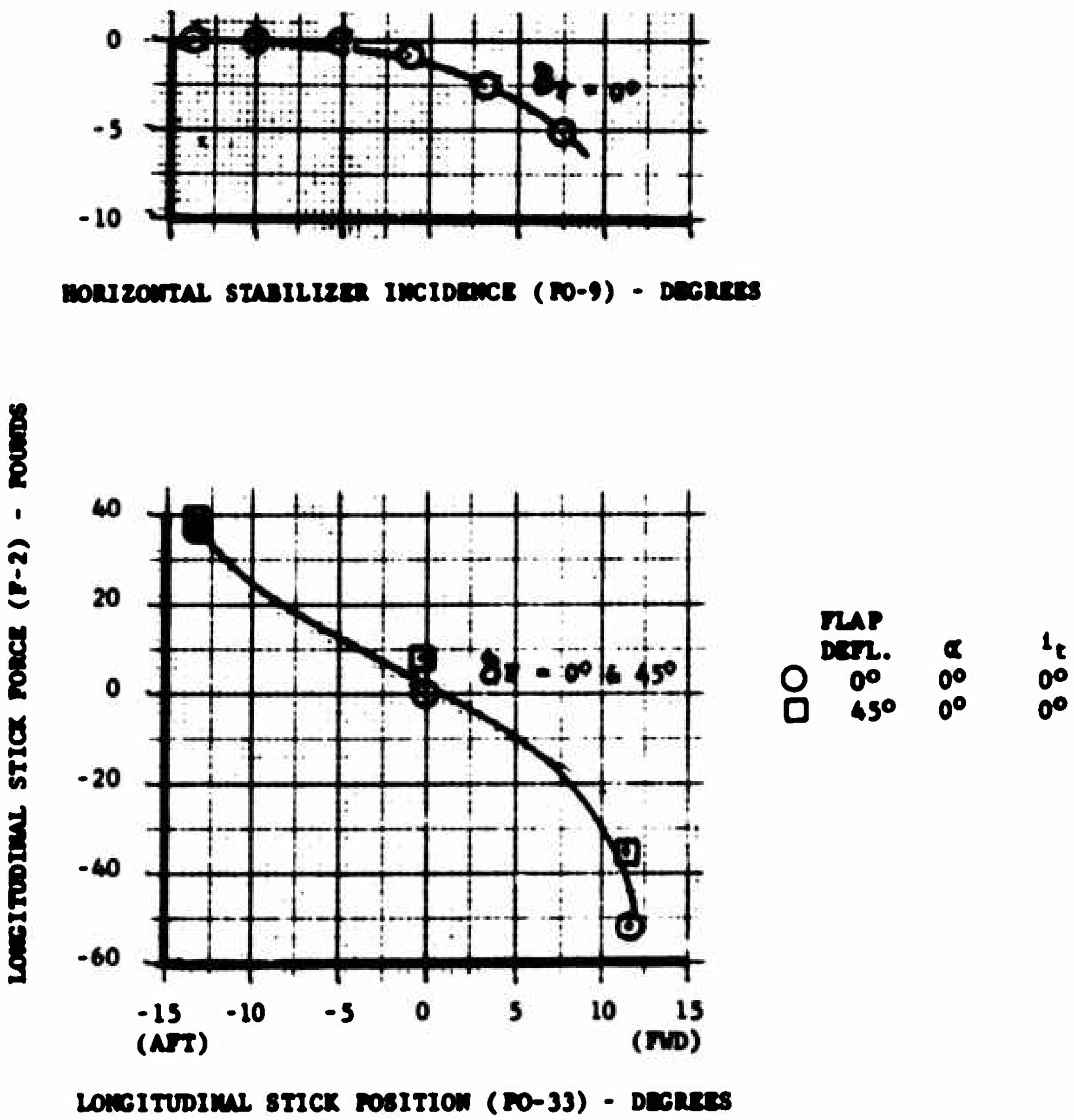

FIGURE E-1

LONGITUDINAL STICK FORCES
VERSUS STICK DEFLECTION AND HORIZONTAL
STABILIZER INCIDENCE - CONVENTIONAL
CONFIGURATION - q_o = 21.2 psf.

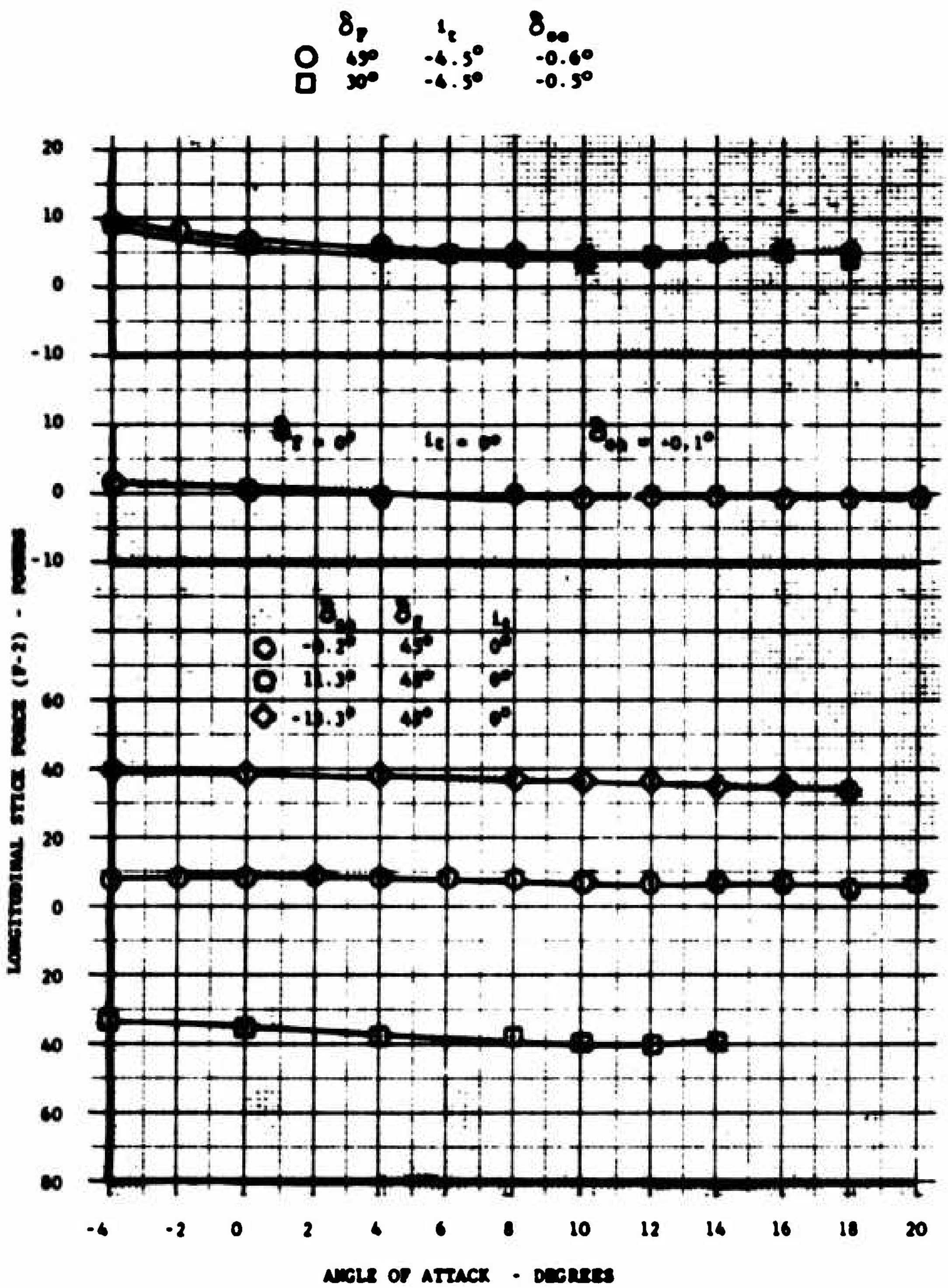

FIGURE E-2

LONGITUDINAL STICK FORCES VERSUS ANGLE OF ATTACK - CONVENTIONAL CONFIGURATION - q_0 = 21.2 psf.

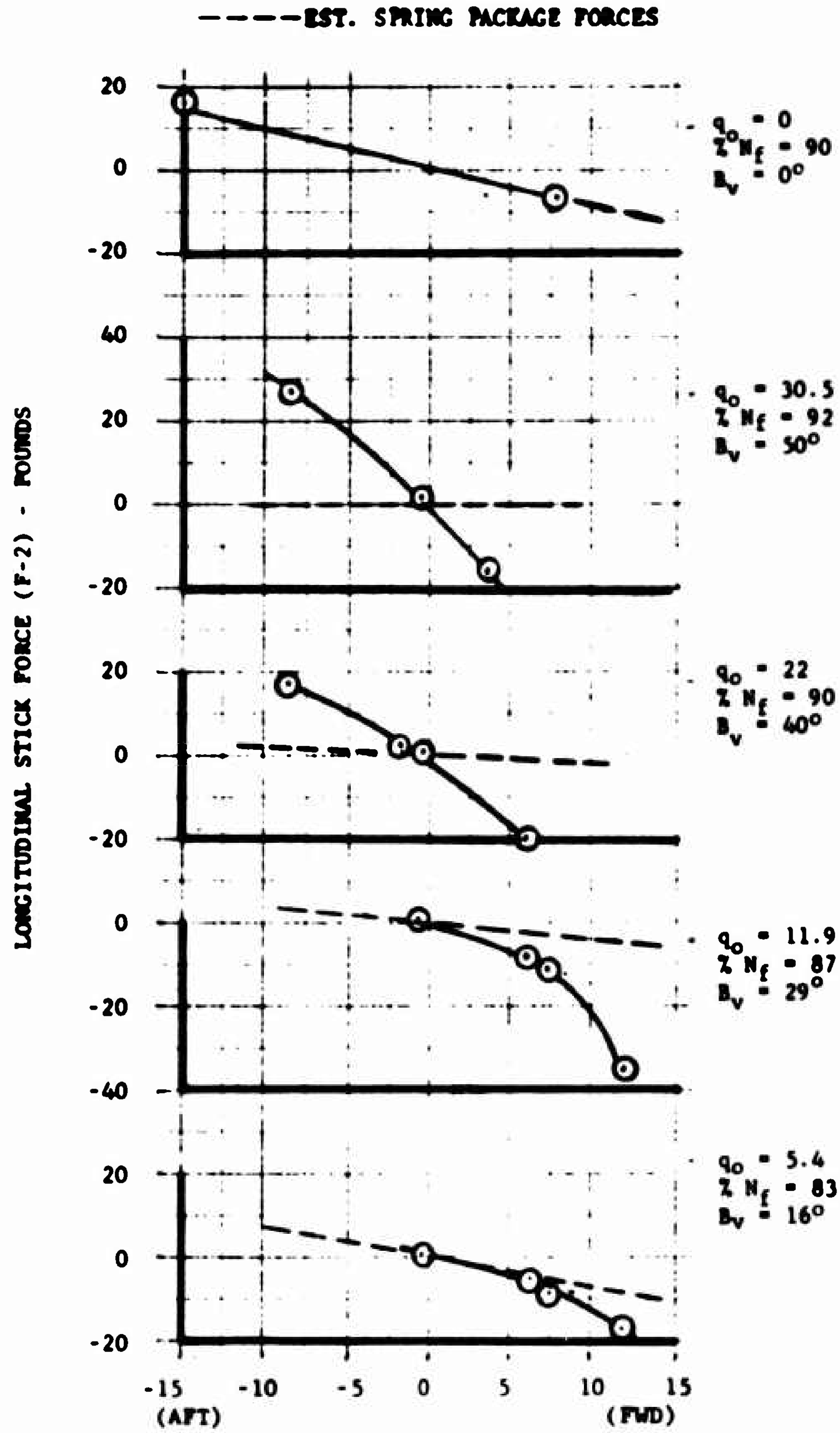

FIGURE E-3A

LONGITUDINAL STICK FORCES VERSUS
FLIGHT SPEED AND VECTOR COMMAND
ANGLE - FAN POWERED

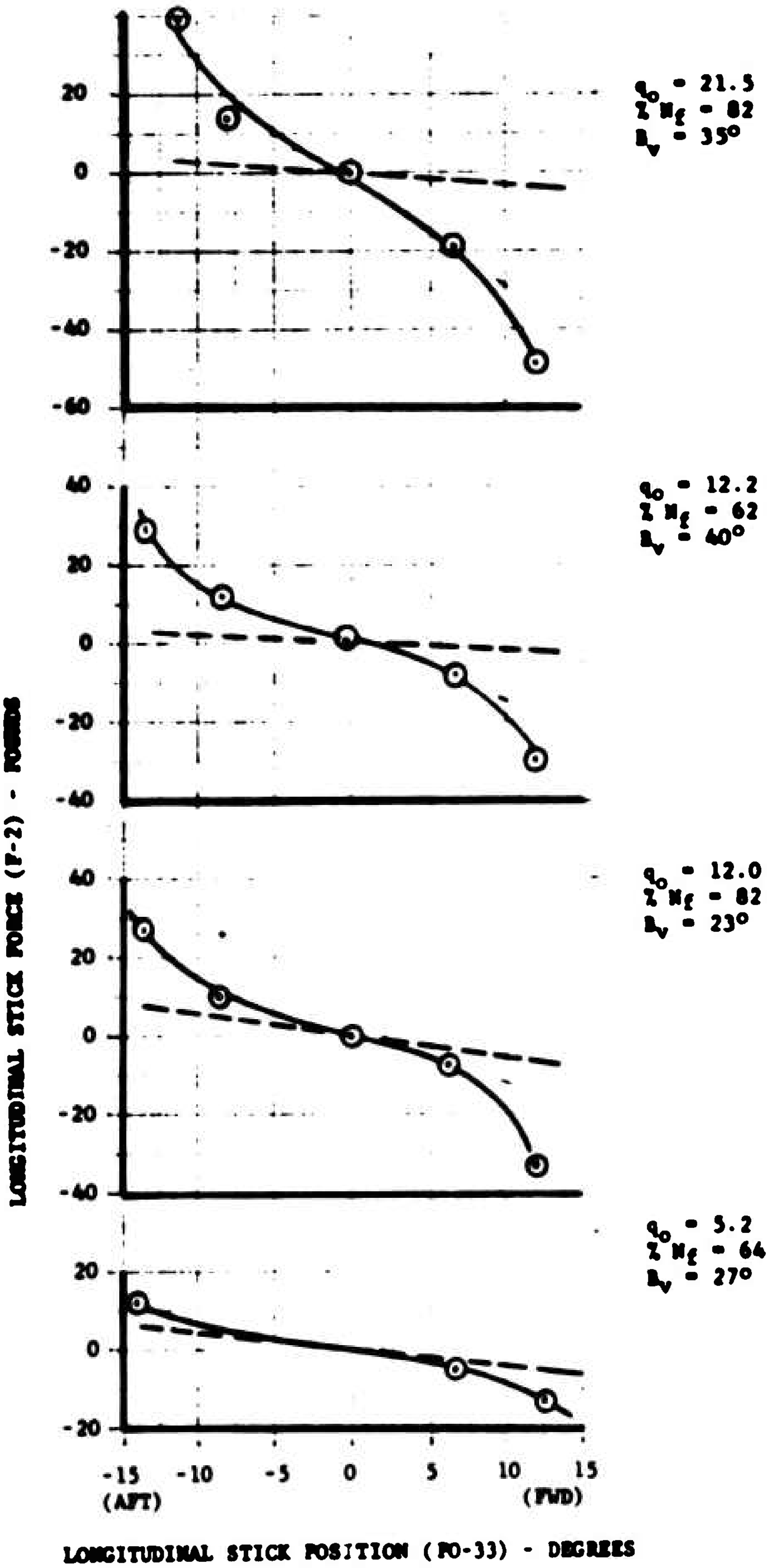

FIGURE E-3B

LONGITUDINAL STICK FORCES VERSUS
FLIGHT SPEED AND VECTOR COMMAND ANGLE - FAN POWERED
(CONTINUED)

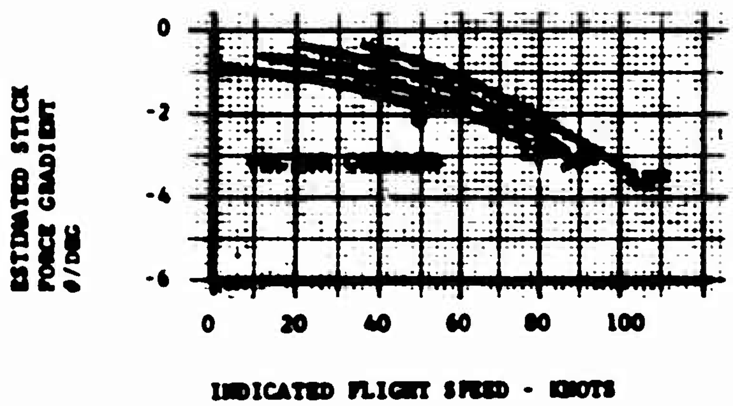

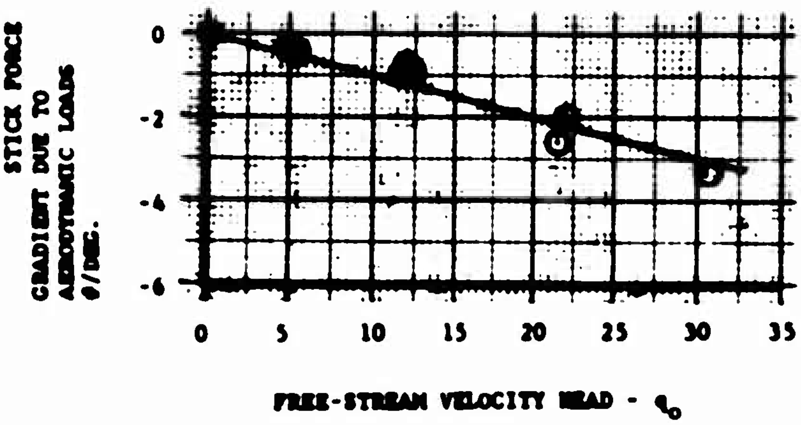

NOTE: GRADIENTS ARE FOR ± 50% STICK THROW AND ARE CORRECTED FOR SPRING PACKAGE GRADIENTS.

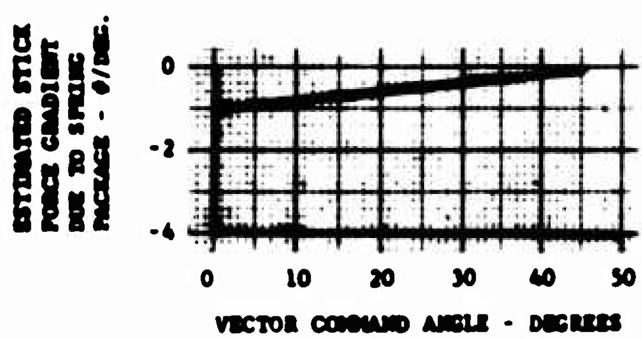

FIGURE E-4

BREAKDOWN OF LONGITUDINAL STICK FORCES INTO CONTRIBUTIONS DUE TO AERODYNAMIC LOADS AND SPRING PACKAGE

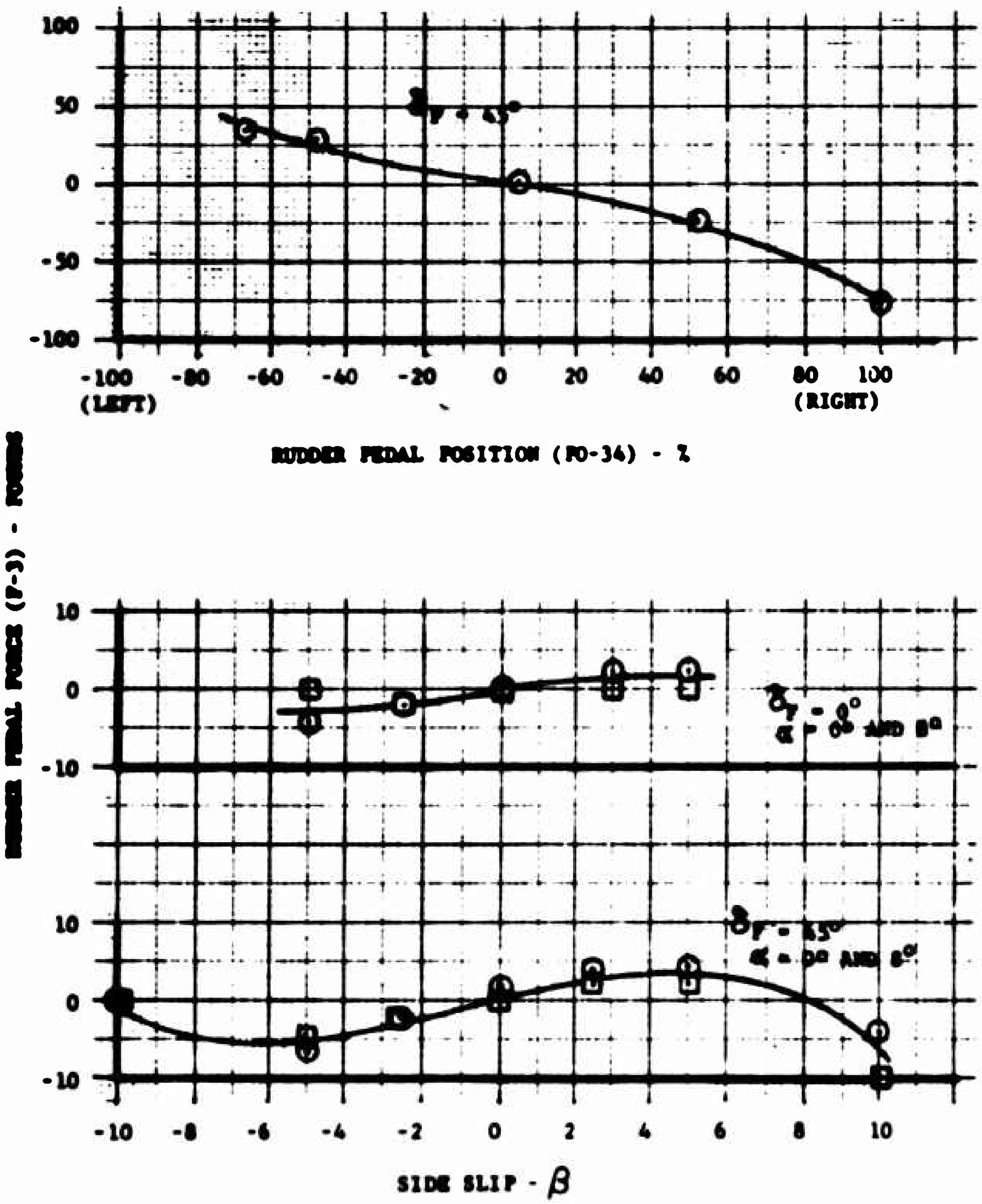

FIGURE E-5

RUDDER PEDAL FORCES VERSUS PEDAL POSITION AND ANGLE OF SIDESLIP - CONVENTIONAL CONFIGURATION
q_o = 21.2 psf

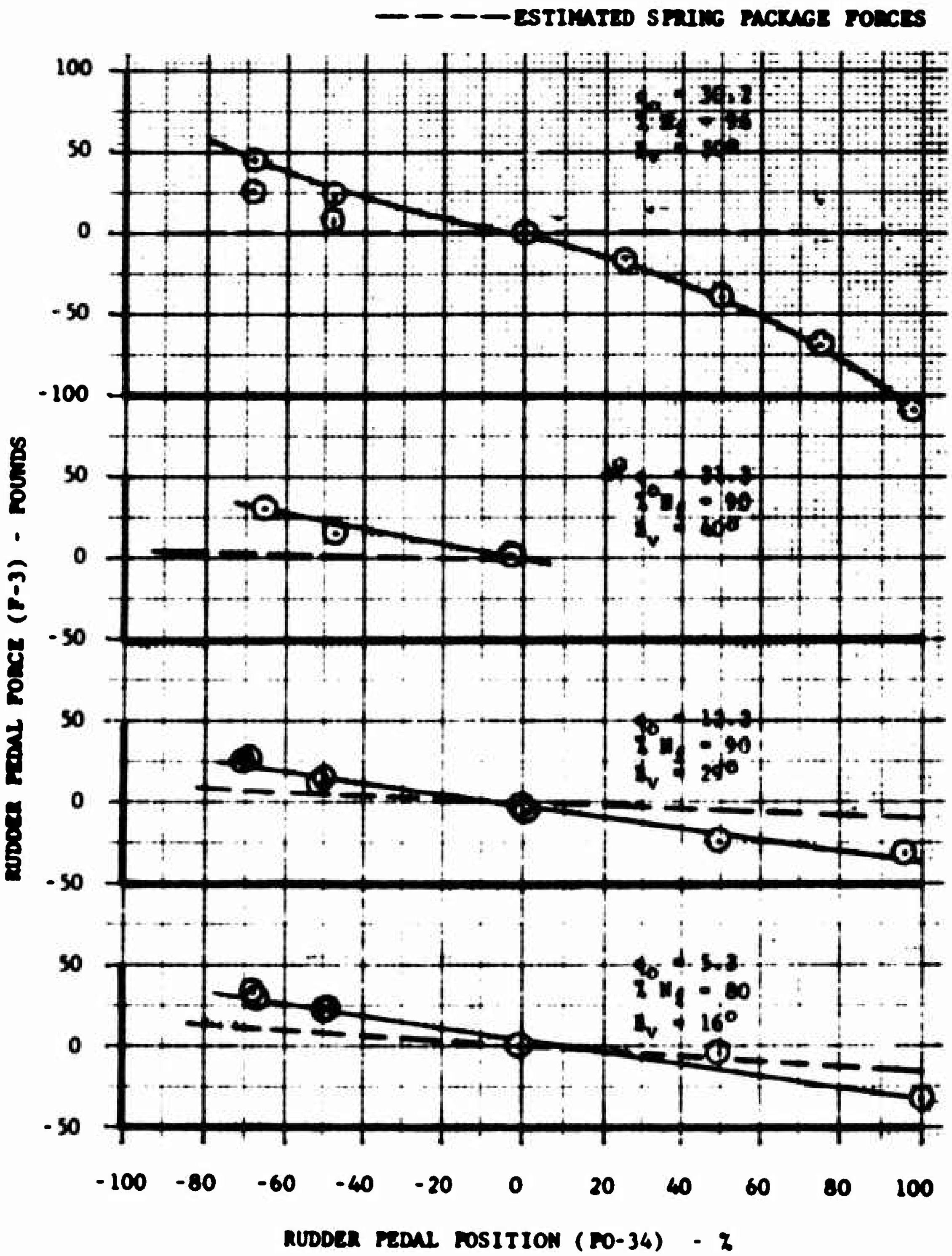

FIGURE E-6

RUDDER PEDAL FORCES VERSUS
FLIGHT SPEED AND VECTOR COMMAND
ANGLE - FAN POWERED

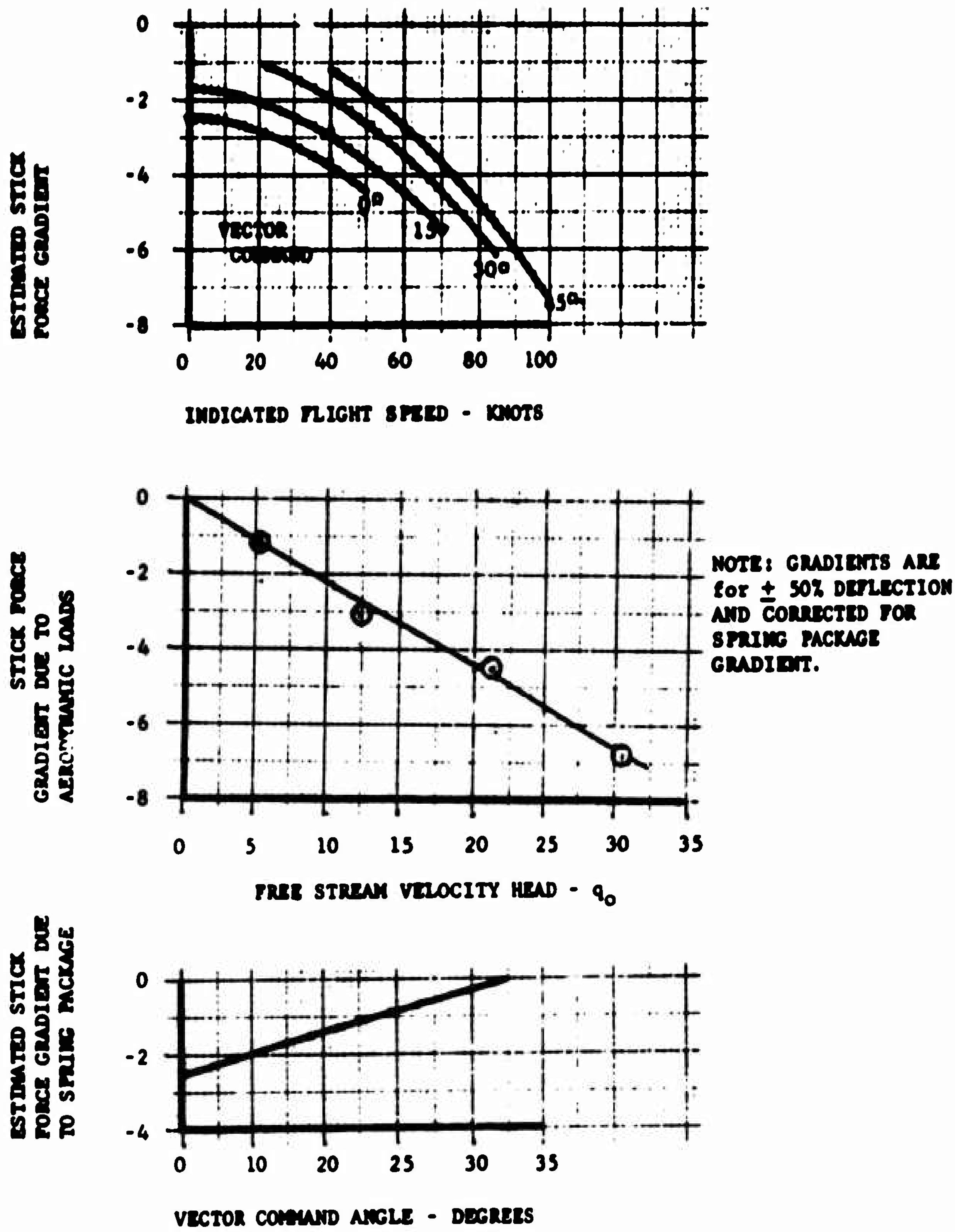

FIGURE E-7

BREAKDOWN OF RUDDER PEDAL FORCES INTO CONTRIBUTION DUE TO AERODYNAMIC LOADS AND SPRING PACKAGE

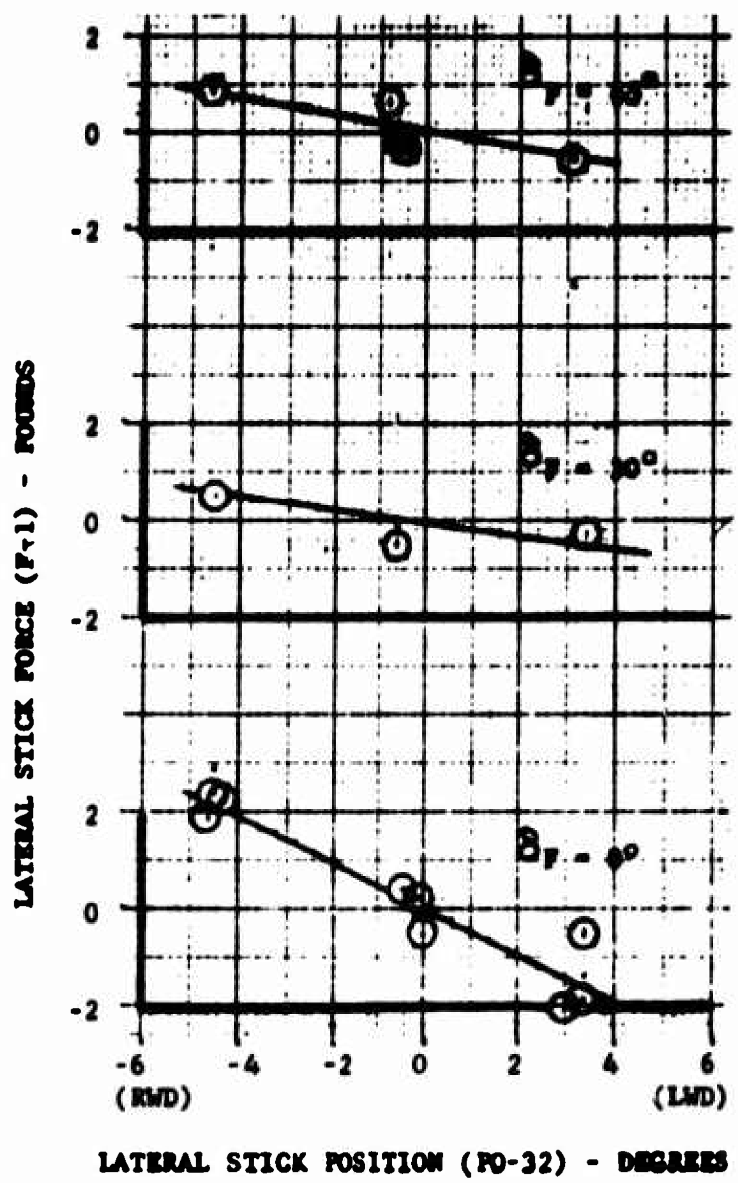

FIGURE E-8

LATERAL STICK FORCES VERSUS
STICK DEFLECTION AND FLAP - DROOP
SETTING - CONVENTIONAL CONFIGURATION -
q_o = 21.5 psf.

BLANK PAGE

APPENDIX F

LIST OF SYMBOLS

Symbol	Parameter	Units
A_f	Fan annulus area	Ft.^{2}
A_F	Fan tip area	Ft.^{2}
A_P	Pitch fan annulus area	Ft.^{2}
b	Wing span	Ft.
B_s	Wing fan louver stagger angle	Deg.
B_v	Vector command angle (cockpit dial)	Deg.
B_{avg}	Wing fan average louver angle (both fans)	Deg.
ΔB_s	Differential stagger angle (left fan louvers minus right)	Deg.
ΔB_v	Differential average louver angle (left fan louvers minus right)	Deg.
c	Chord	Ft.
$\bar{c}$	Mean aerodynamic chord	Ft.
C_x	Conventional coefficients - See Appendix B (x = D, L, Y, m, n, l)	---
C_T	Thrust required in coefficient form ($T/_{qo\ Sw}$)	---
C_x^s	Slipstream coefficient - See Appendix B (x = D, Y, L, m, n, l, P)	---
d_f	Fan tip diameter	Ft.
F	Thrust	Lb.
h	Aircraft height above ground measured from bottom of fans	Ft.
H_x	Fan law coefficients - See Appendix B (x = D, L, Y, m, n, l)	---
H_{LF}	Louver actuator force in coefficient form, LOAD/ $\rho U_T^2 A_f$	---

HDL	Wing fan closure door loads in coefficient form, $LOAD/\rho U_T^2 A_f$	---
HP	Gas generator ideal gas horsepower	---
i_t	Horizontal stabilizer incidence	Deg.
l	Rolling moment	Ft. - Lb.
L	Lift	Lb.
L_C	Corrected lift at 100% fan speed standard day - sea level	Lbs.
m	Pitching moment	Ft. - Lb.
n	Yawing moment	Ft. - Lb.
N_f	Fan rotational speed	%
N_p	Pitch fan rotational speed	%
N_g	Gas generator rotational speed	%
P	Power	
q_F	Two times fan dynamic pressure - See Appendix B	Lb./Ft.^{2}
q_o	Free stream dynamic pressure	Lb./Ft.^{2}
q_s	Slipstream dynamic pressure - See Appendix B	Lb./Ft.^{2}
S_w	Wing projected area	Ft.^{2}
T	Thrust	Lb.
T_{ooo}	Fan lift @ zero flight speed, stagger and vector	Lb.
T_C^S	Flight speed coefficient - See Appendix B	---
U_T	Fan rotational tip speed (720 ft/sec @ 100%)	Ft./Sec.
U_p	Pitch fan rotational tip speed (640 ft/sec @ 100%)	Ft./Sec.

APPENDIX F (Continued)

U_{Tooo}	Fan rotational speed at zero flight speed, vector and stagger at given gas generator power setting	Ft./Sec.
V_o	True airspeed or tunnel speed	Ft./Sec.
V_{IC}	Corrected indicated airspeed	Ft./Sec.
X_f	Distance from aircraft centerline to fan centerline (10.167)	Ft.
Y	Sideforce	Lb.
α	Angle of attack	Deg.
α_i	Angle of attack as indicated by aircraft nose boom	Deg.
α_B	Angle of attack at break or change in slope pitching moments	Deg.
β	Angle of sideslip	Deg.
δ	Control surface movement or Pressure corrected to standard conditions	Deg. ---
δ_S	Control stick movement	---
θ	Temperature corrected to standard conditions	---
ψ	Yaw angle	Deg.
μ	Cross-flow ratio - See Appendix B	---
ρ	Air density	Slugs/Ft.^{3}
$\partial_{()}/\partial_{()}$	Partial derivative - all other parameters fixed	---

Subscripts

a	Aileron or lateral stick
c	Collective stick
d	Droop of ailerons
D	Drag
e	Elevator or longitudinal stick
F	Flap
L	Lift or Left
l	Roll moment
m	Pitch moment
n	Yaw moment

Subscripts (Cont'd)

pm	Pitch modulating doors
R	Right
r	Rudder or rudder pedals
S	Stagger
V	Vector
Y	Sideforce
0	Ambient or free-stream
2	At engine inlet
10	At wing fan inlet
20	At pitch fan inlet

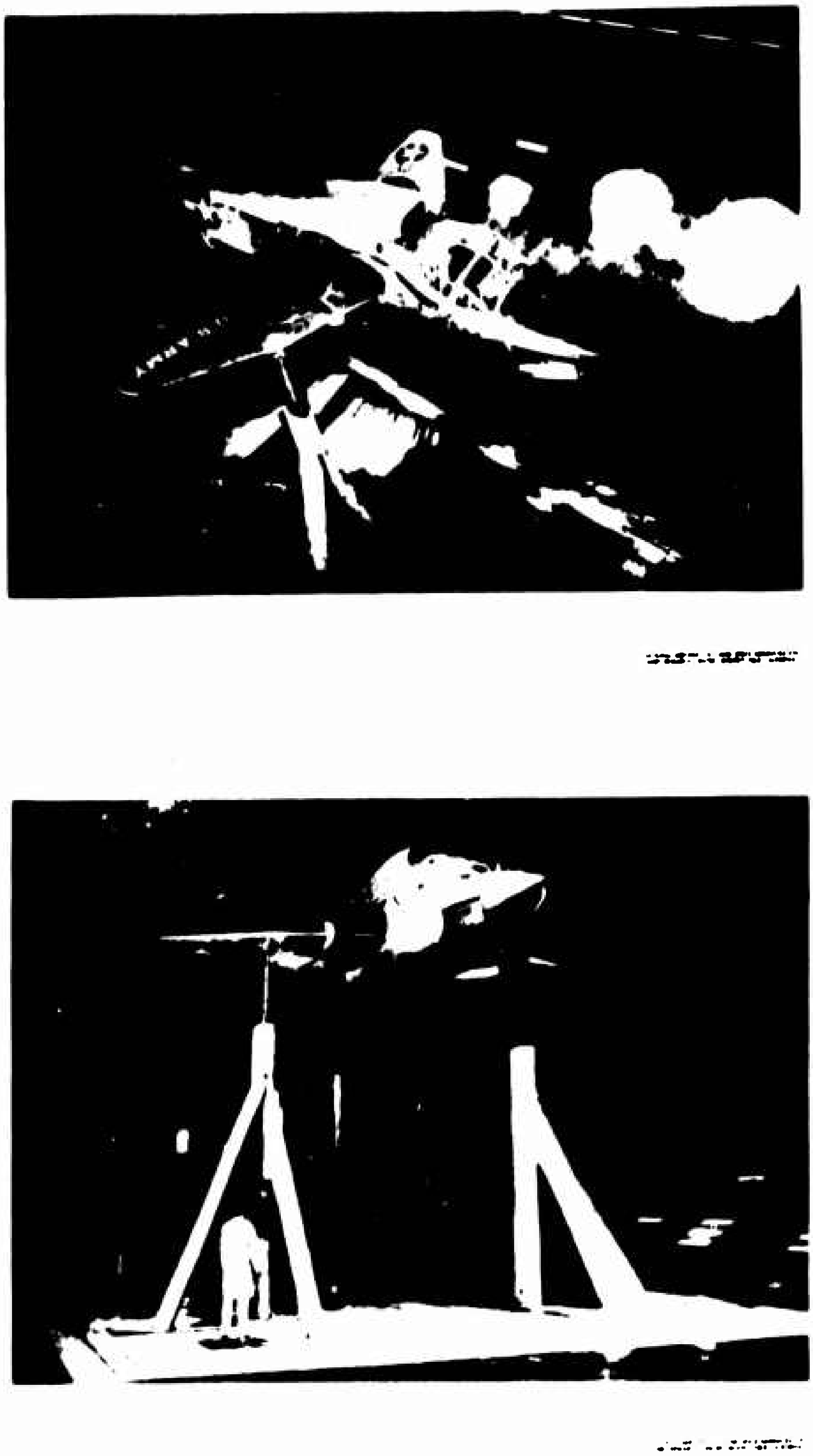

FIGURE 1
PHOTOGRAPHS OF XV-5A AIRCRAFT
INSTALLED IN 40' X 80' WIND TUNNEL

FIGURE 2
PHOTOGRAPH OF XV-5A AIRCRAFT
INSTALLED ON OUTDOOR STATIC THRUST STAND

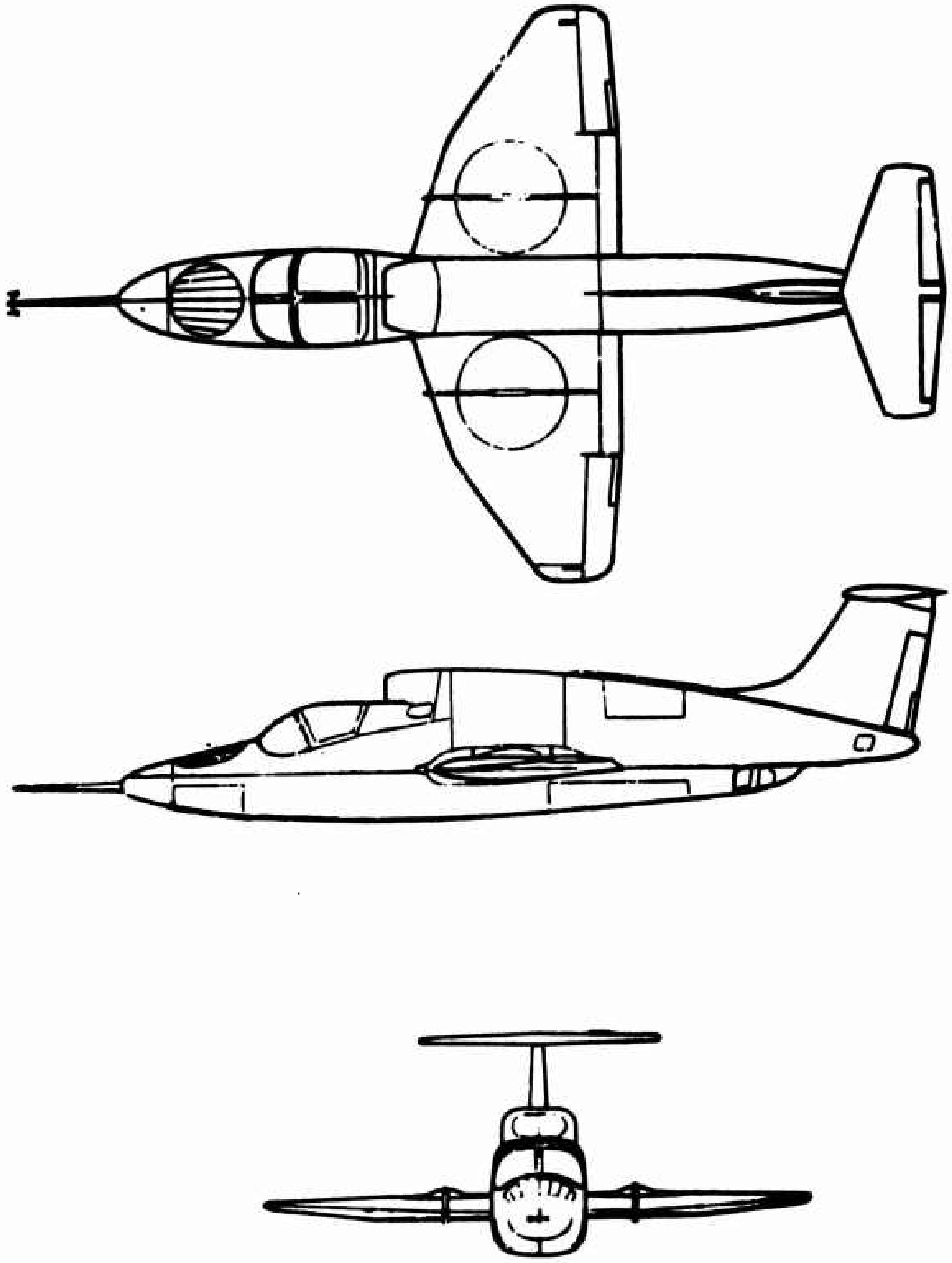

FIGURE 3 THREE VIEW DRAWING OF XV-5A AIRCRAFT

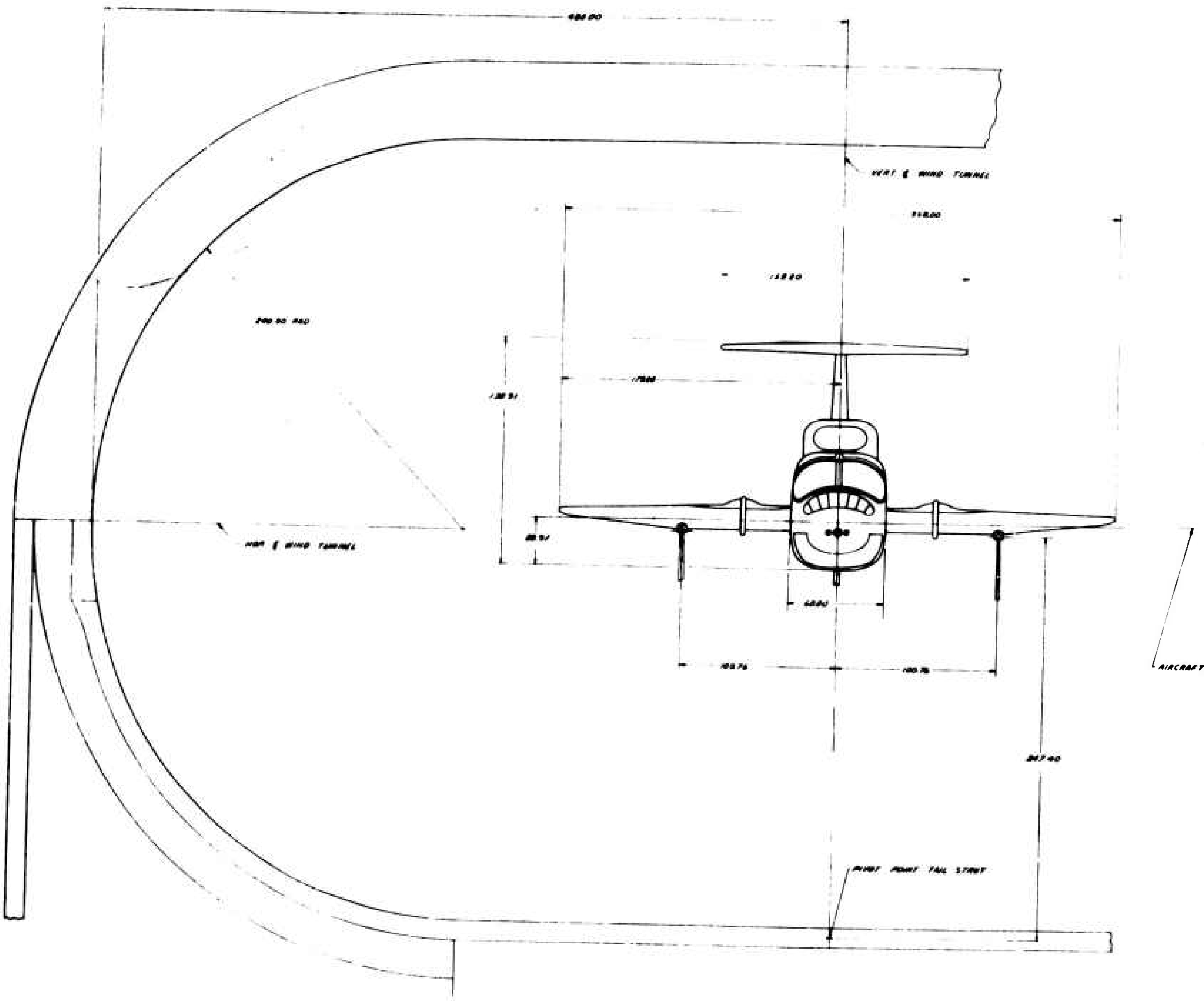
VERT ℄ WIND TUNNEL
240.00 RAD
HOR ℄ WIND TUNNEL
AIRCRAFTS
PIVOT POINT TAIL STRUT

A

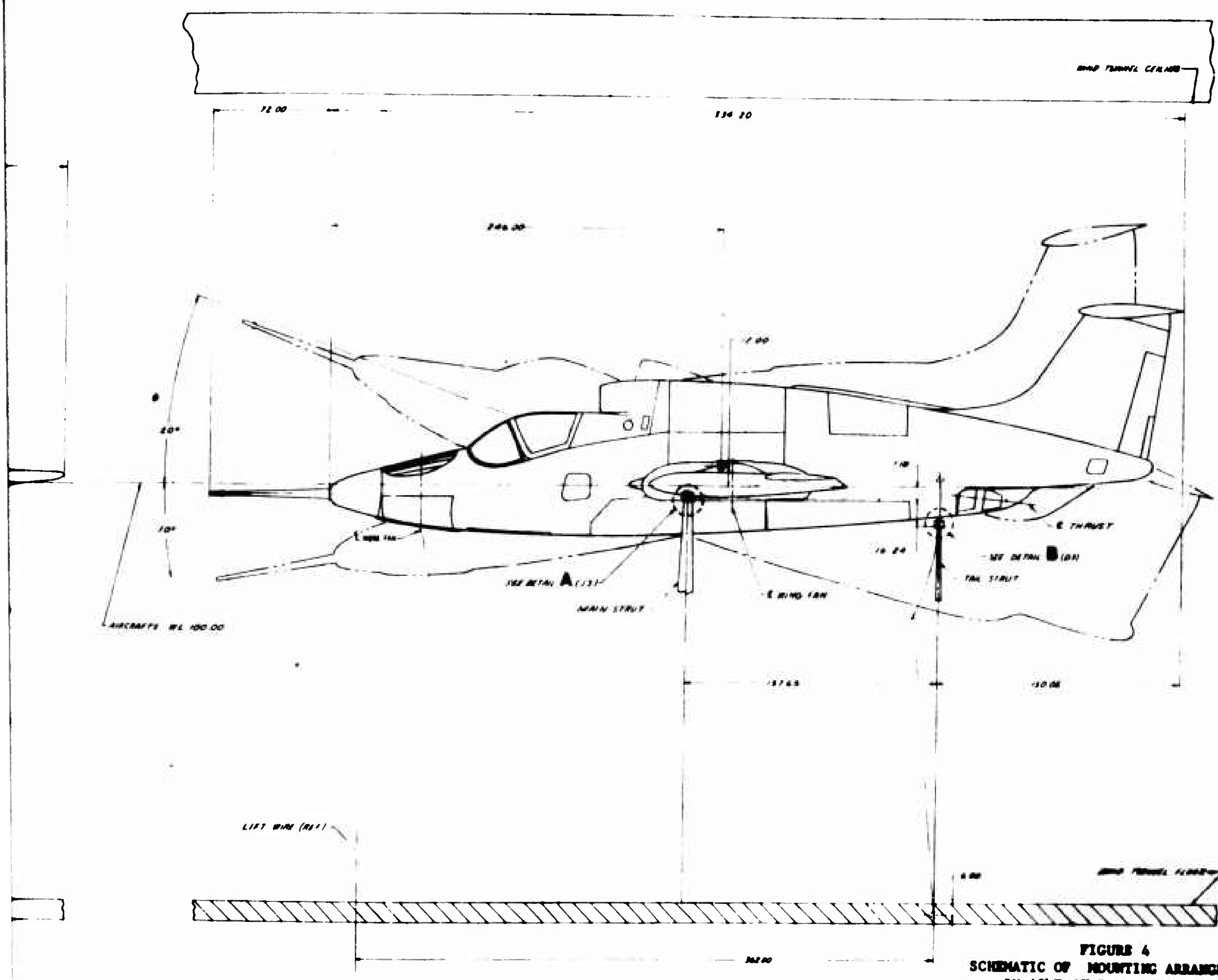

FIGURE 4
SCHEMATIC OF MOUNTING ARRANGEMENT
IN 40' X 80' FOOT WIND TUNNEL

B

BLANK PAGE

FIGURE 5
PHOTOGRAPH OF DIGITAL INSTRUMENTATION CONSOLE

FIGURE 6
PHOTOGRAPH OF STRESS INSTRUMENTATION SYSTEMS

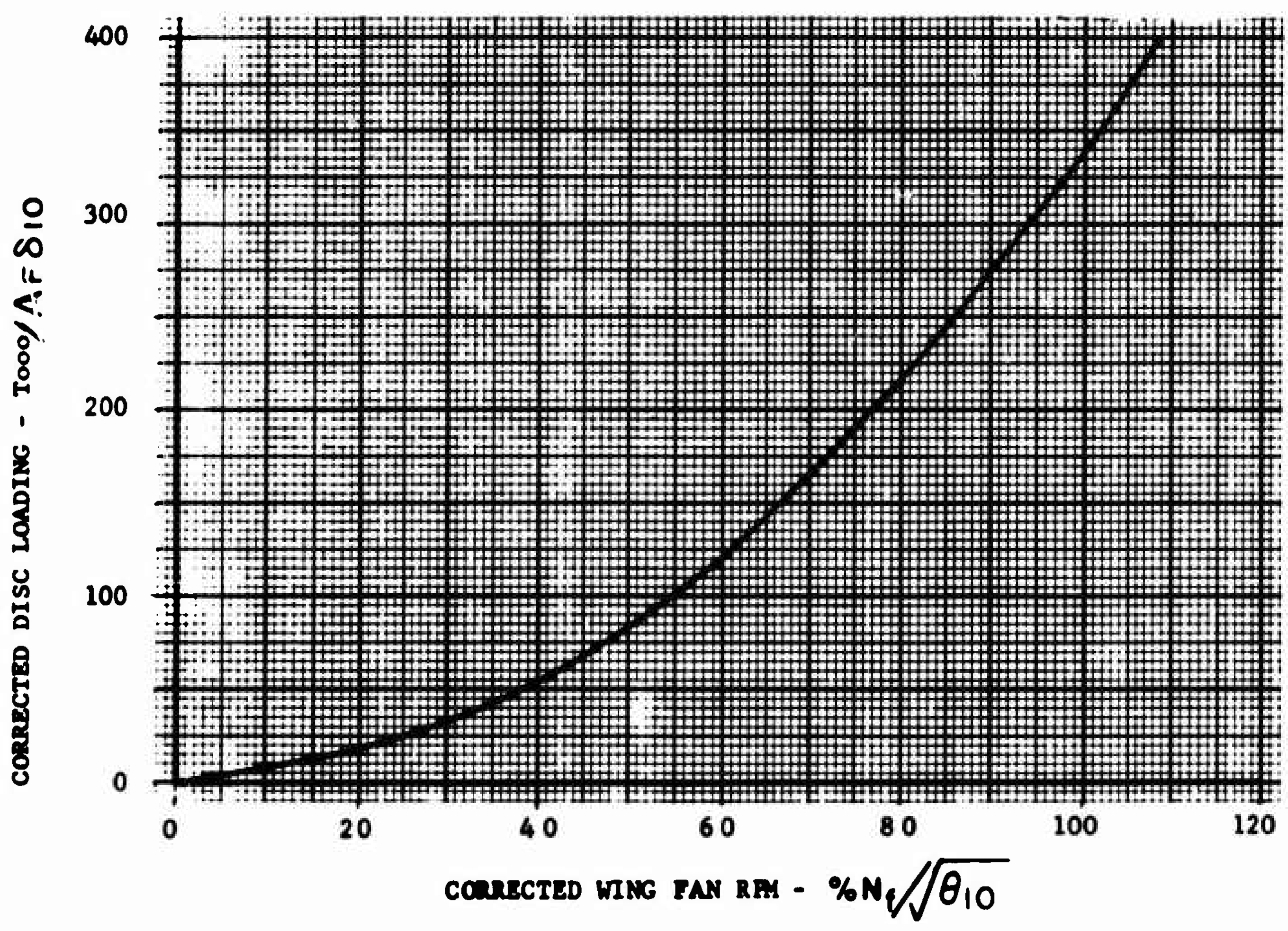

FIGURE 7

ESTIMATED WING FAN DISC LOADING
AT Vo = 0, Bv = 0, Bs = 0
(PER FAN)

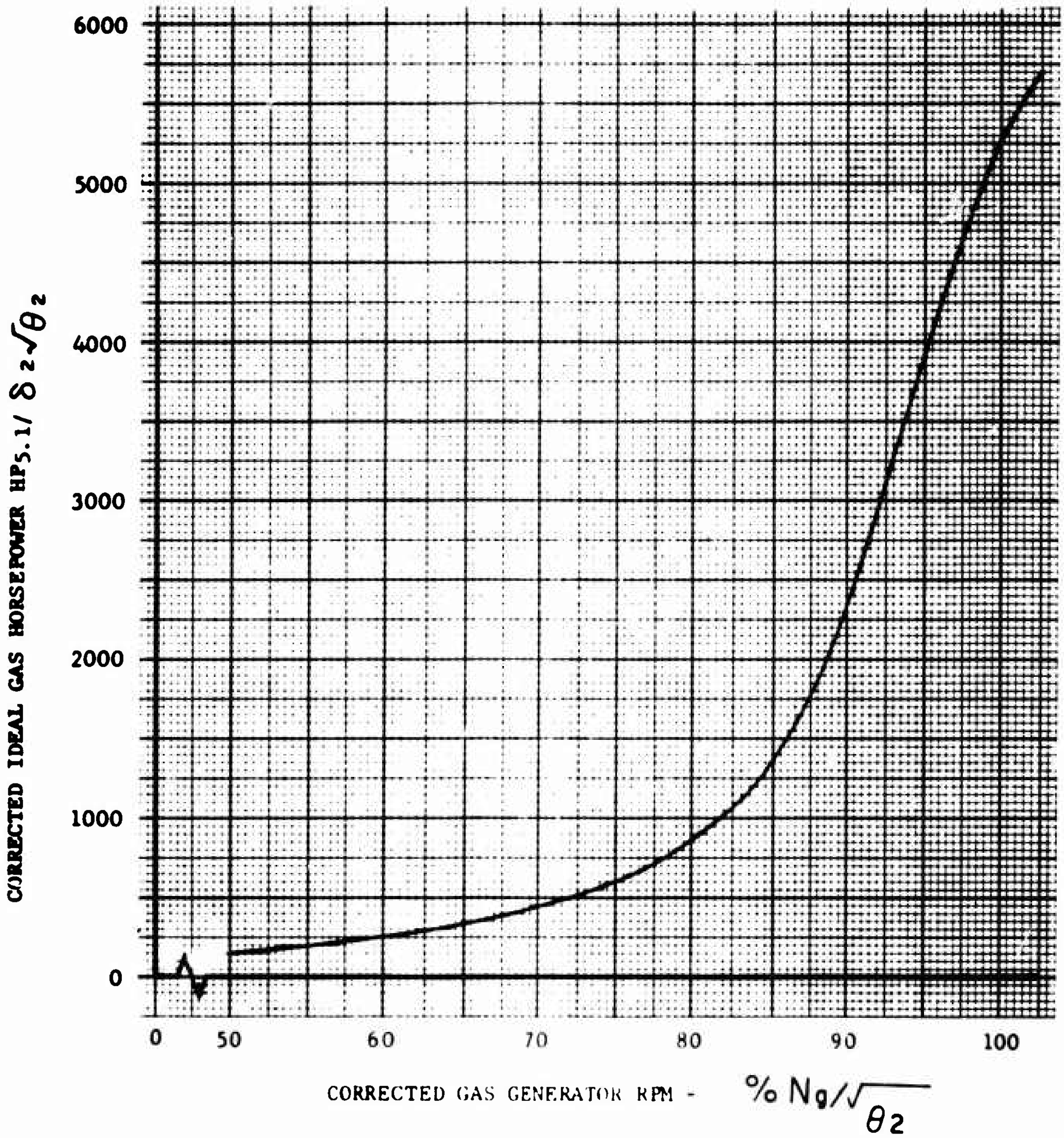

FIGURE 8

ESTIMATED GAS GENERATOR IDEAL HORSEPOWER CHARACTERISTICS

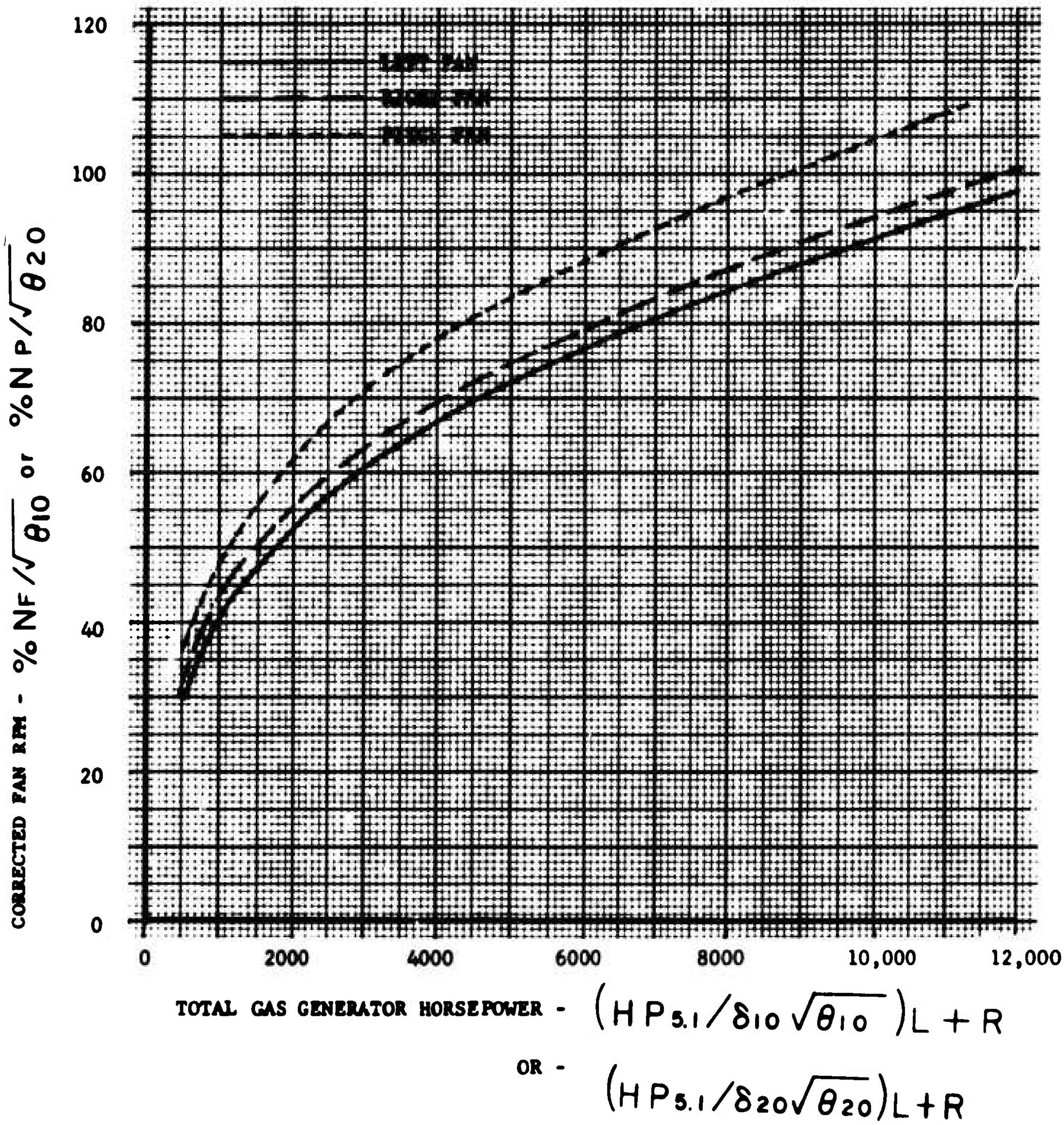

FIGURE 9

ESTIMATED WING FAN AND PITCH FAN SPEED VARIATION WITH TOTAL GAS GENERATOR HORSEPOWER

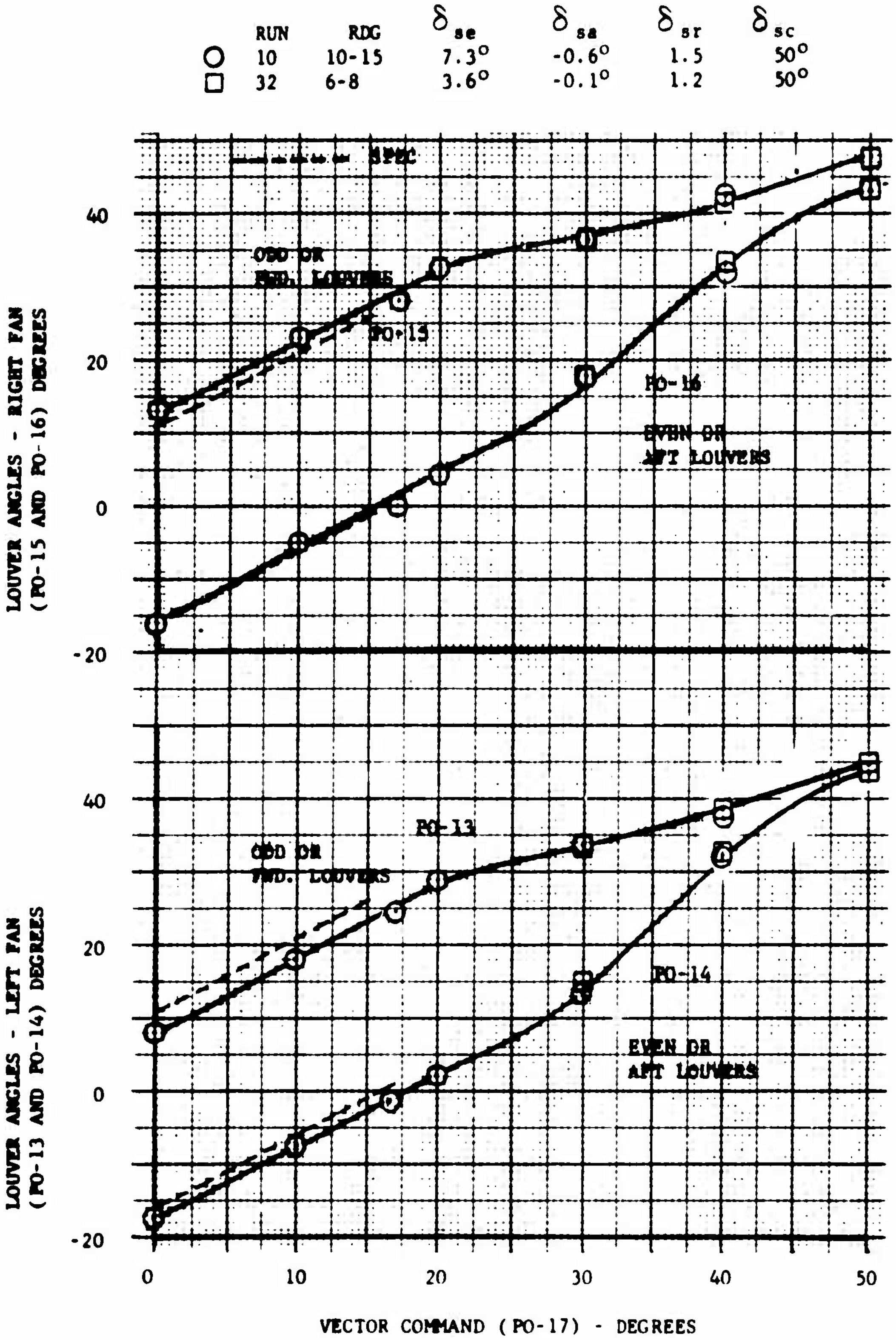

FIGURE 10
EXIT LOUVER RIGGING
VERSUS VECTOR COMMAND

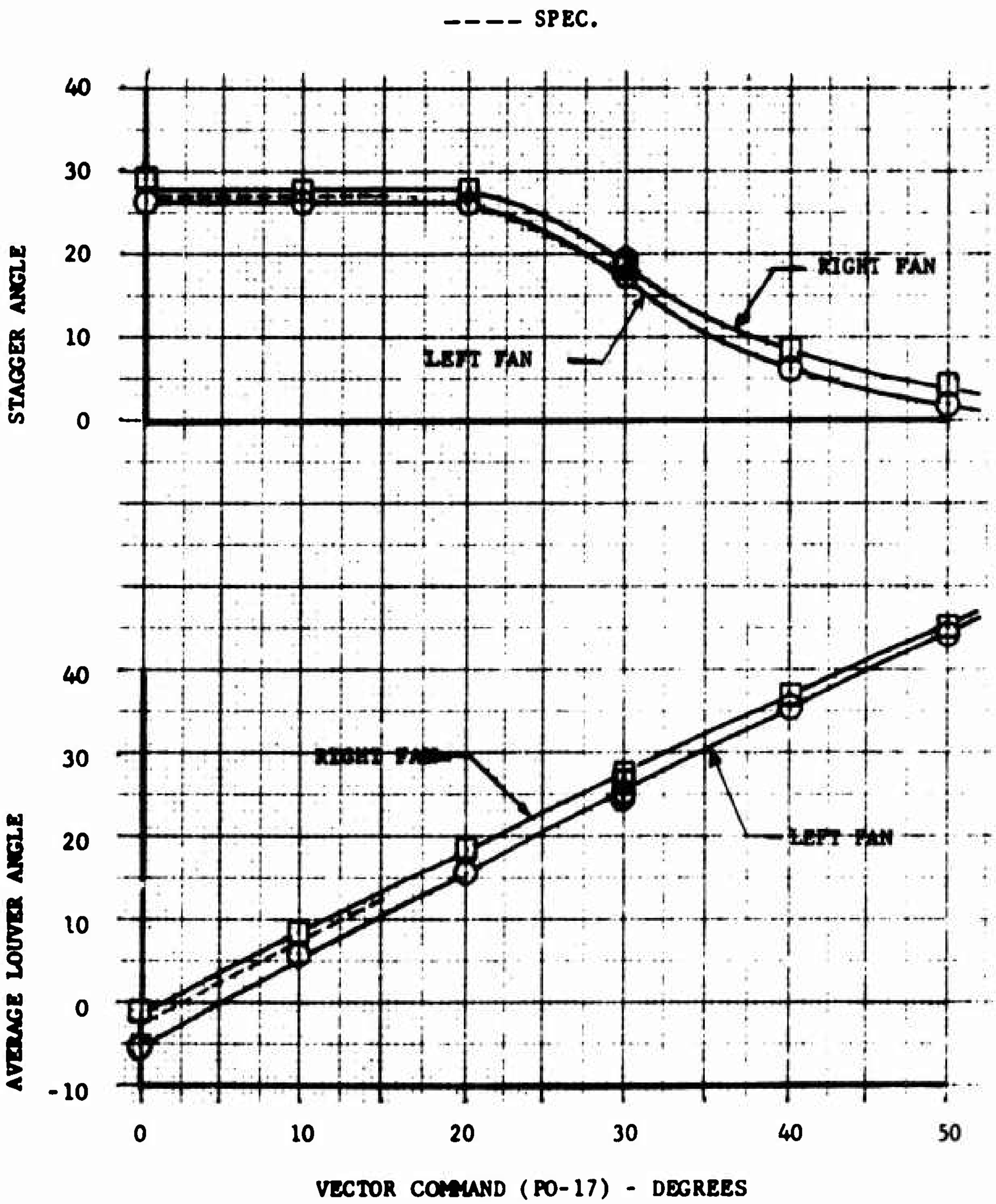

FIGURE 11

STAGGER AND VECTOR ANGLES
VERSUS VECTOR COMMAND
(ALL CONTROLS APPROX. NEUTRAL)

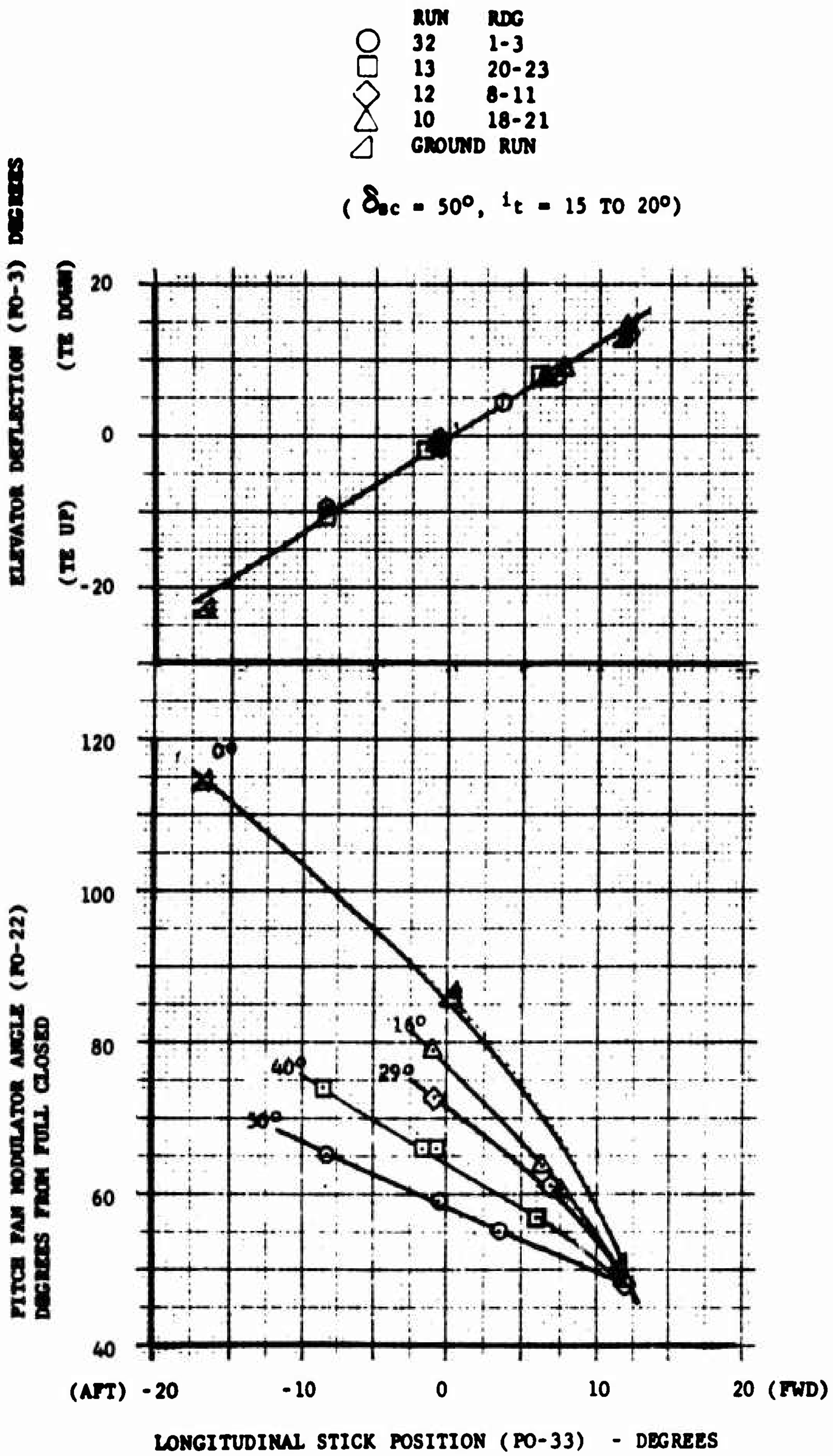

FIGURE 12
LONGITUDINAL RIGGING - PITCH FAN MODULATOR
VERSUS STICK POSITION AND VECTOR COMMAND

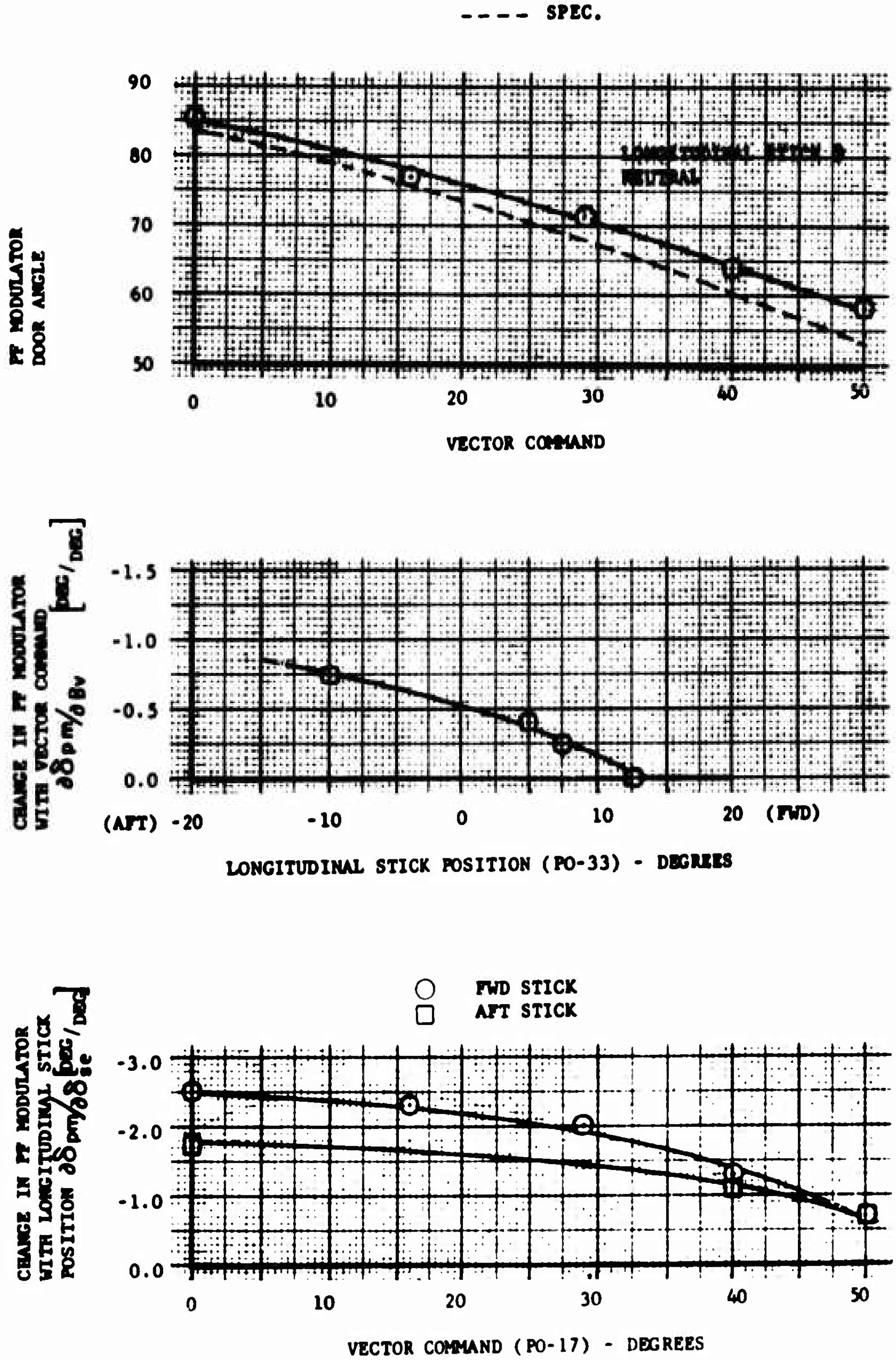

FIGURE 13
PITCH FAN MODULATOR GEARING VERSUS VECTOR COMMAND AND LONGITUDINAL STICK POSITION

(ALL OTHER CONTROLS = NEUTRAL)

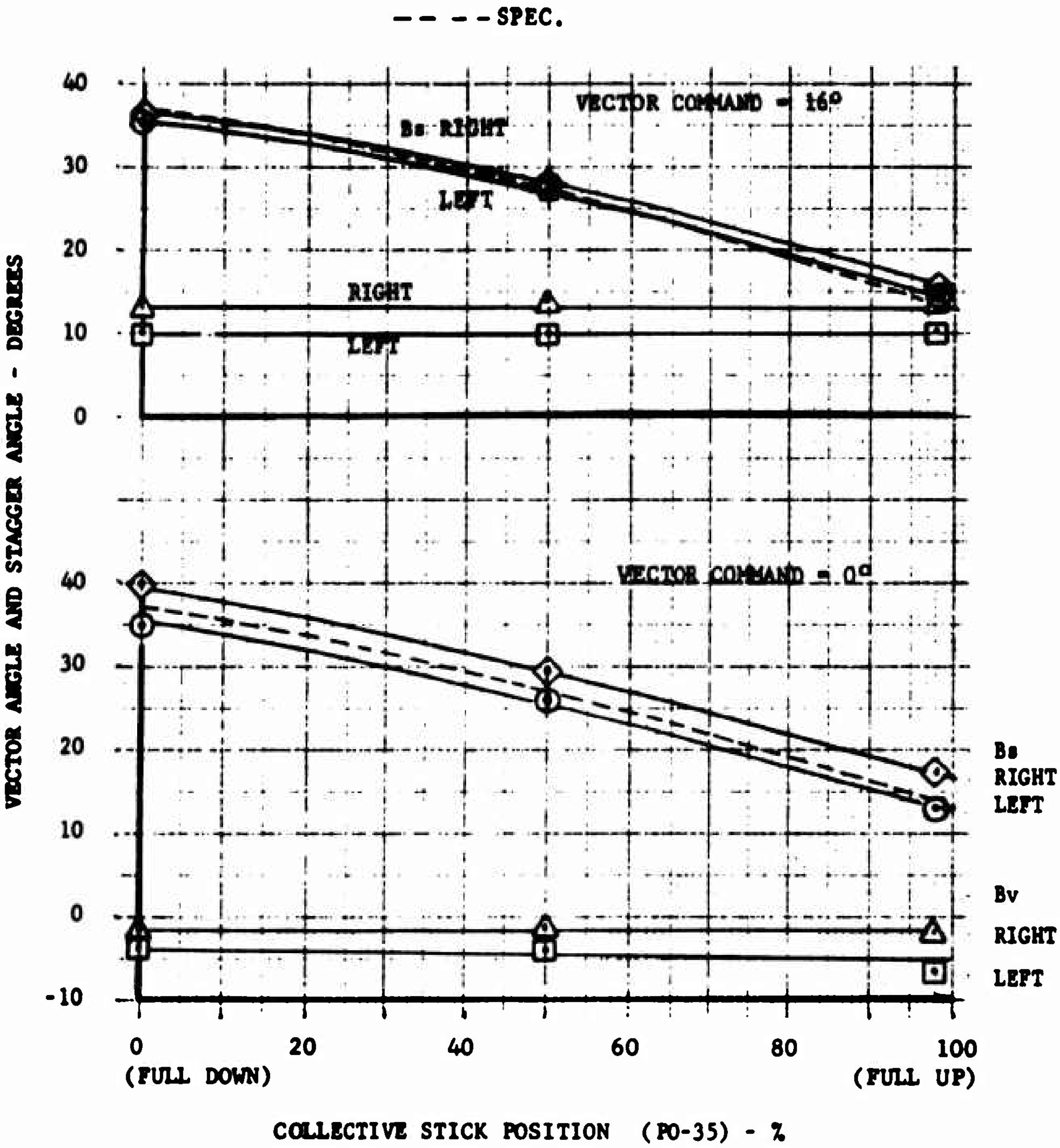

FIGURE 14A

COLLECTIVE RIGGING - LOUVER VECTOR
AND STAGGER ANGLES AND PITCH
FAN MODULATOR DOOR VERSUS
COLLECTIVE SETTING

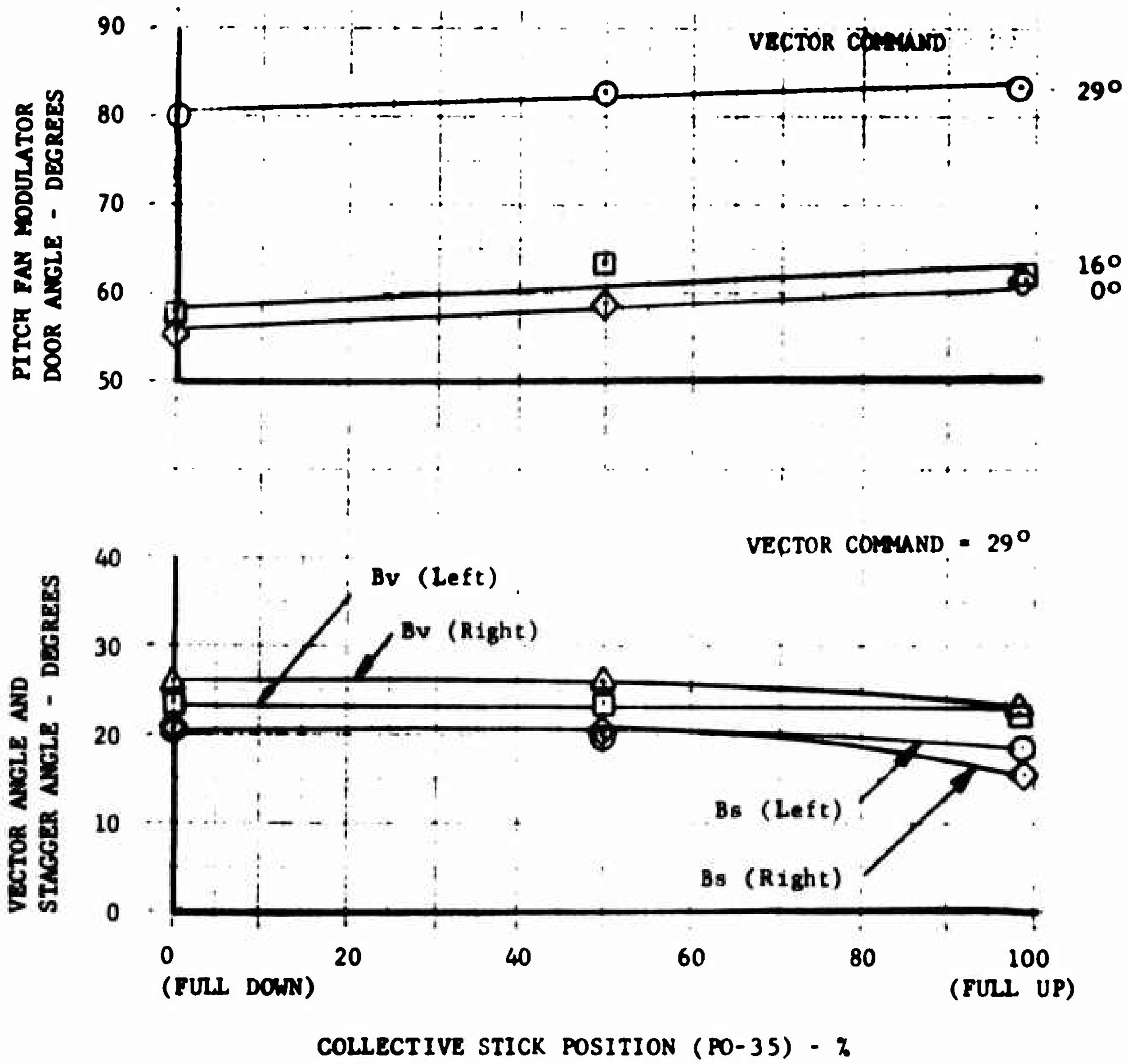

FIGURE 14B

COLLECTIVE RIGGING - CONTINUED

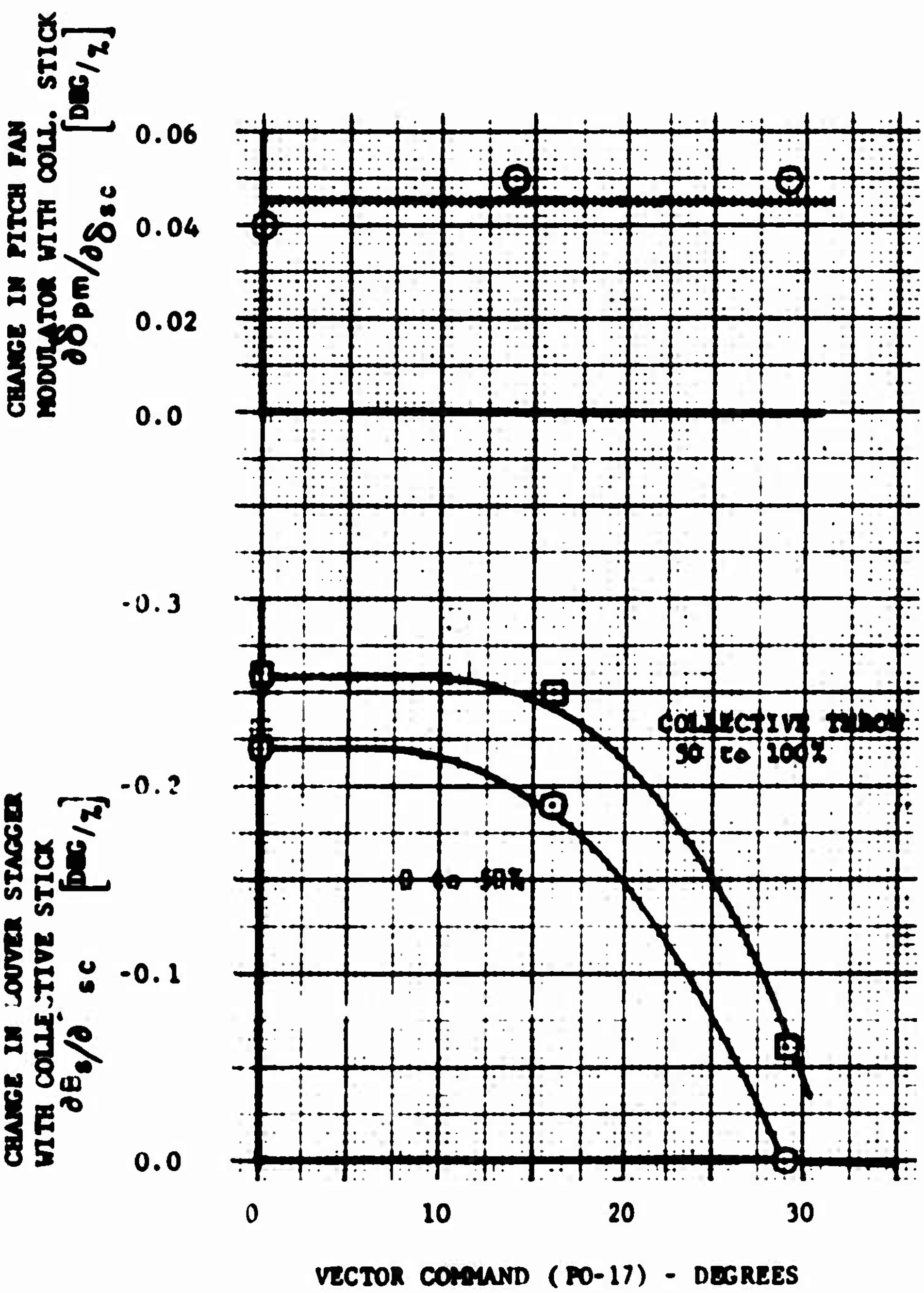

FIGURE 15

LOUVER STAGGER AND PITCH
FAN MODULATOR GEARING
VERSUS VECTOR ANGLE AND
COLLECTIVE STICK POSITION

(ALL CONTROLS = NEUTRAL)

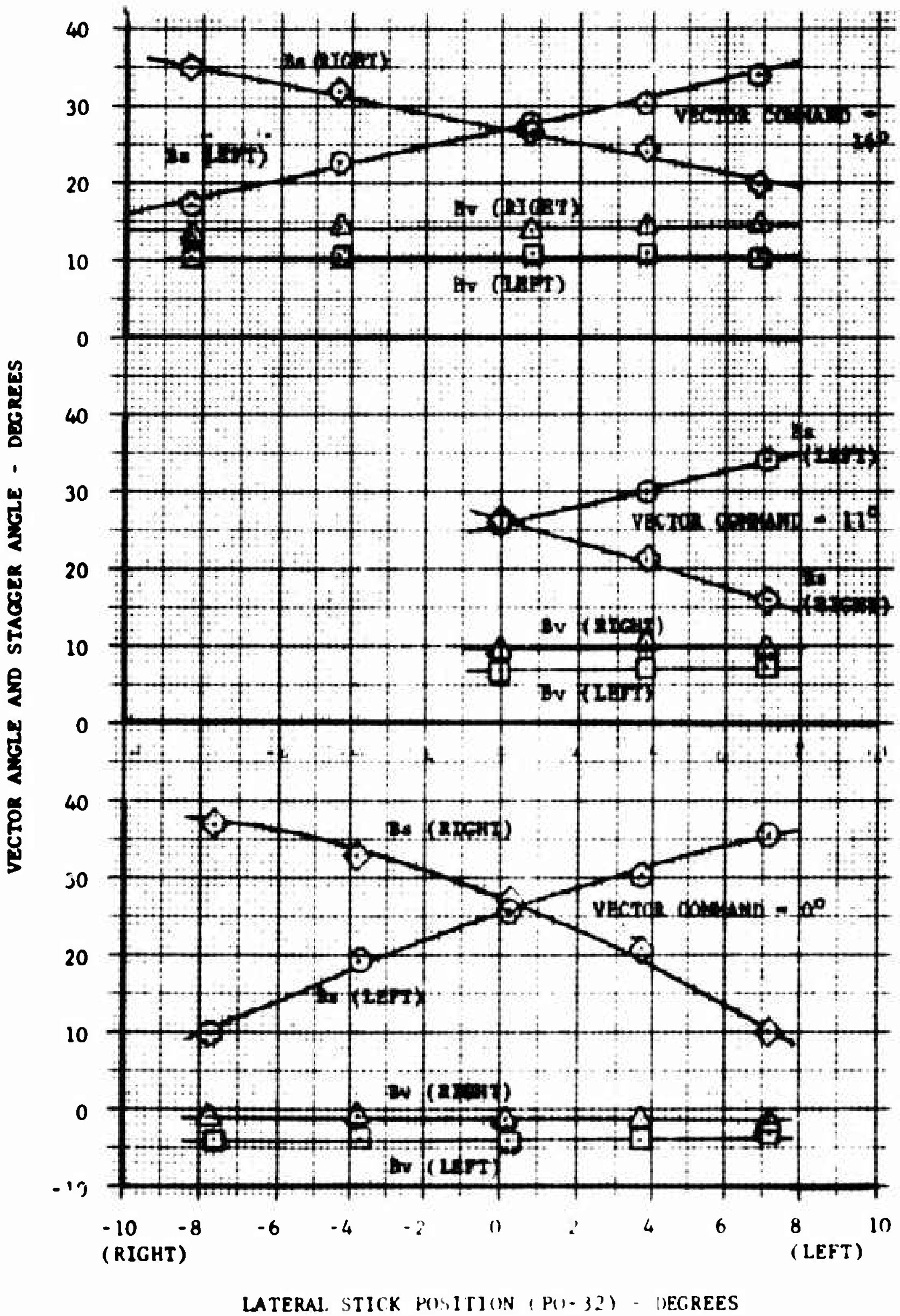

FIGURE 16A
LATERAL RIGGING - VECTOR AND STAGGER ANGLES
VERSUS LATERAL STICK POSITION AND VECTOR COMMAND

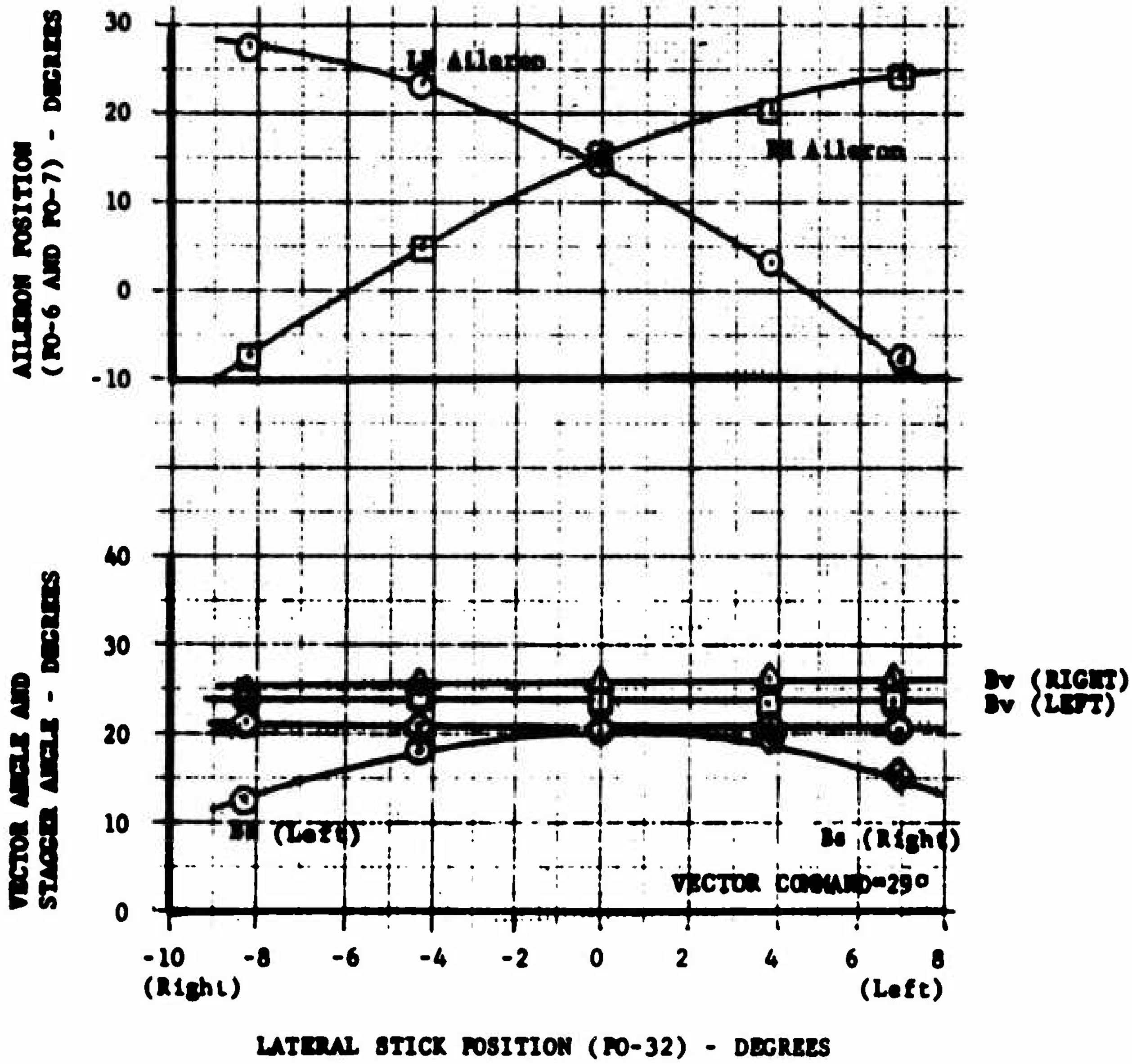

FIGURE 16B

LATERAL RIGGING - CONTINUED

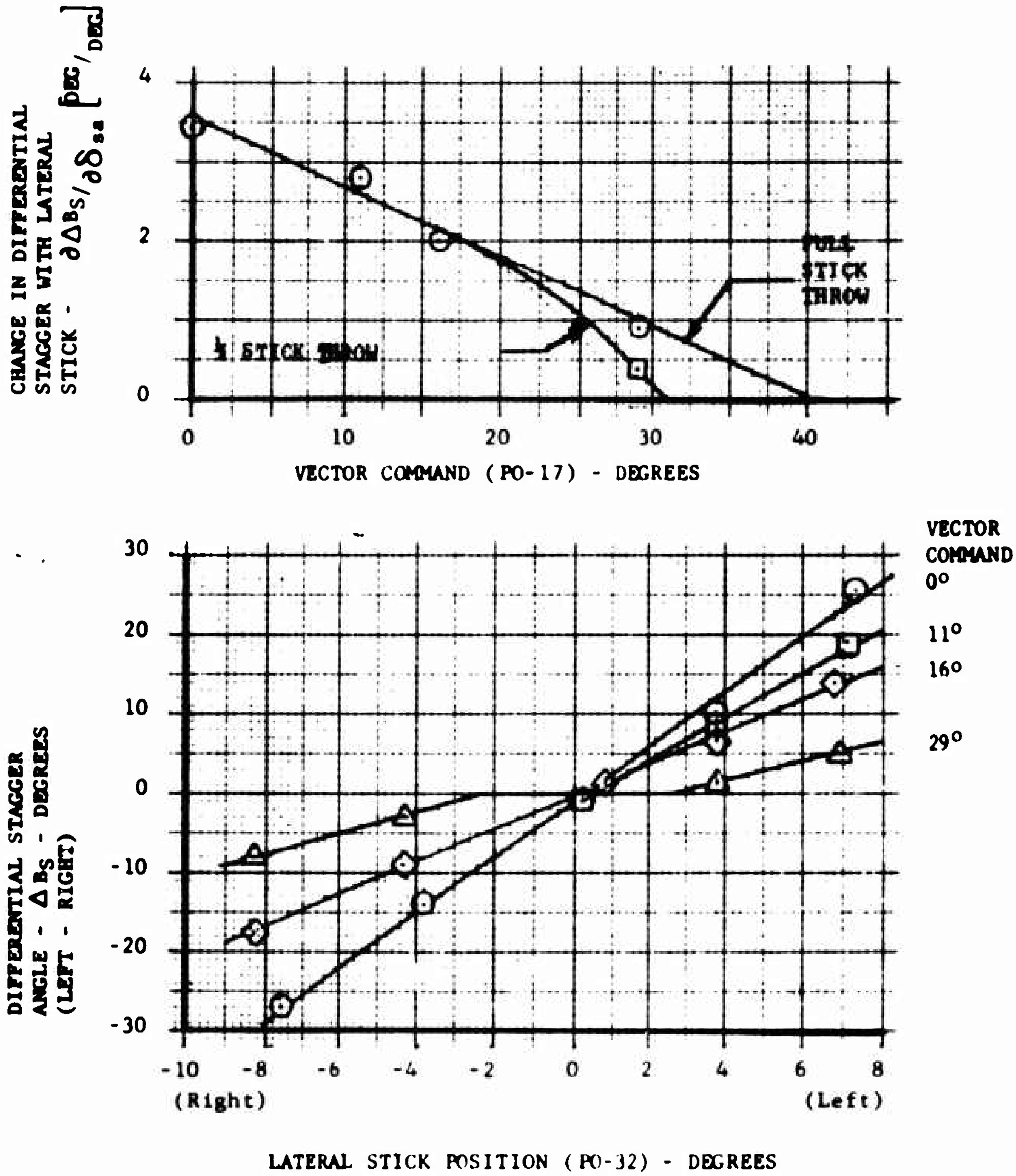

FIGURE 17

LOUVER STAGGER GEARING VERSUS LATERAL STICK AND VECTOR COMMAND ANGLES

(ALL CONTROLS = NEUTRAL)

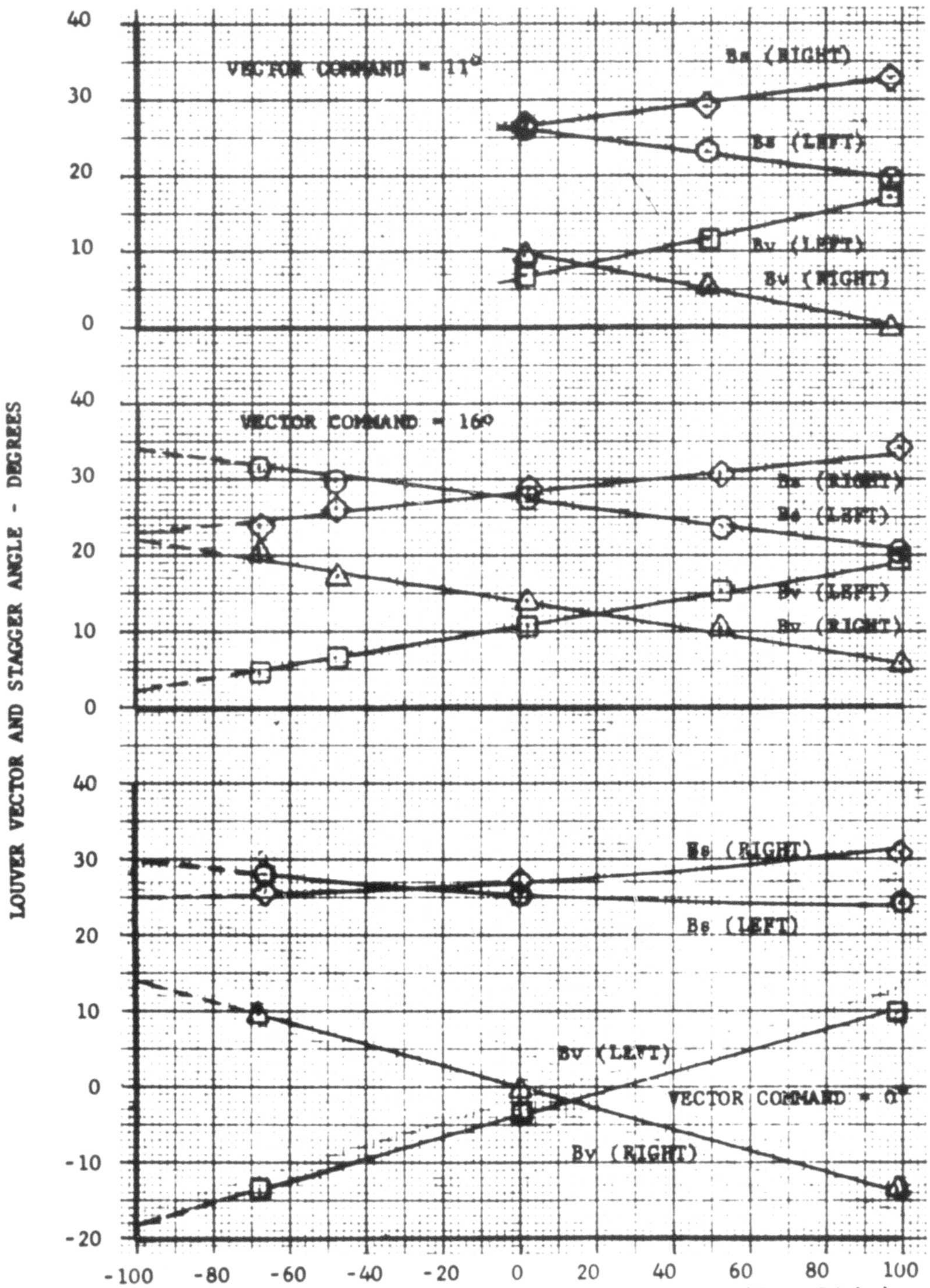

FIGURE 18A
DIRECTIONAL RIGGING - VECTOR AND STAGGER ANGLES
VERSUS RUDDER PEDAL AND VECTOR COMMAND

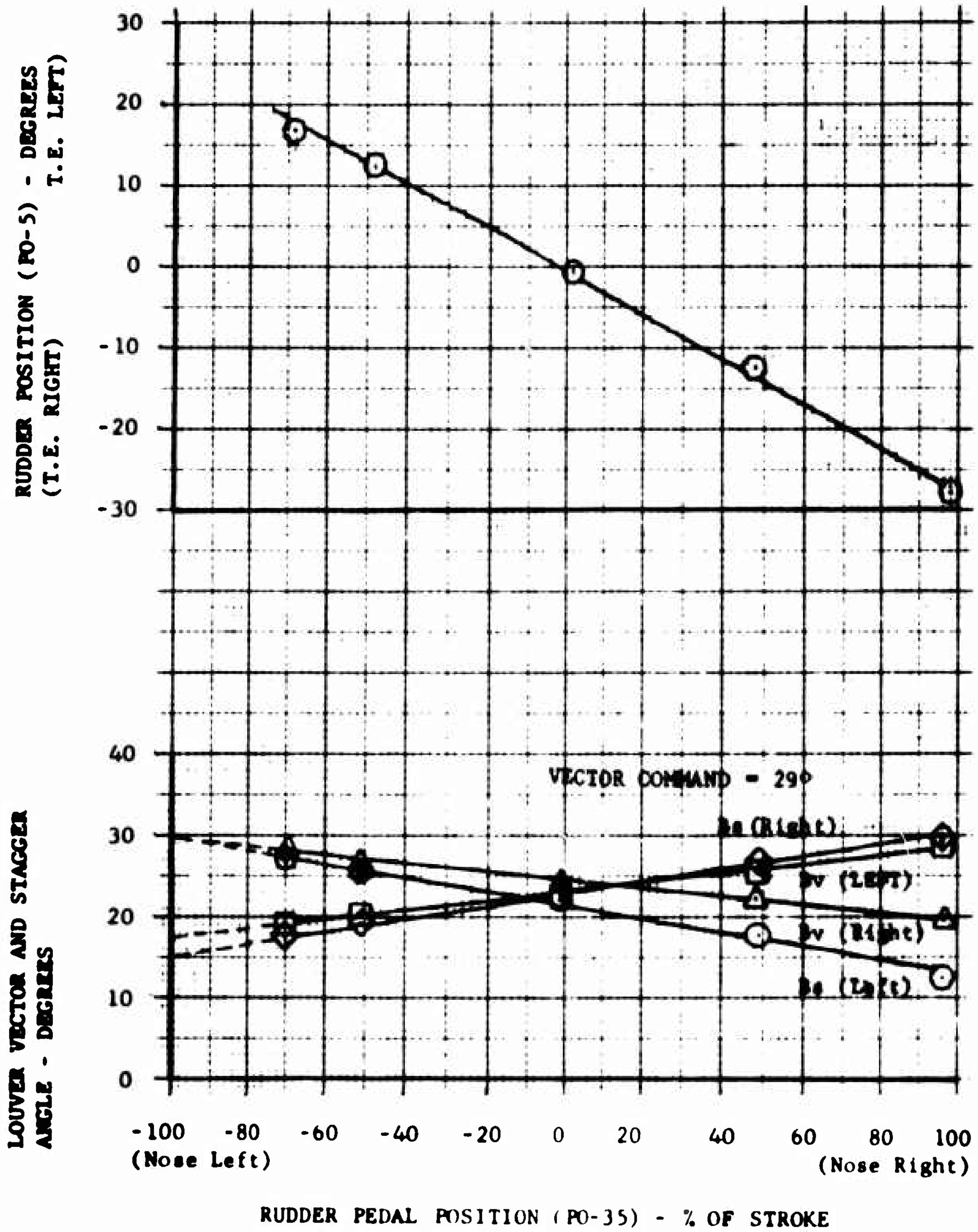

FIGURE 18B

DIRECTIONAL RIGGING - CONTINUED

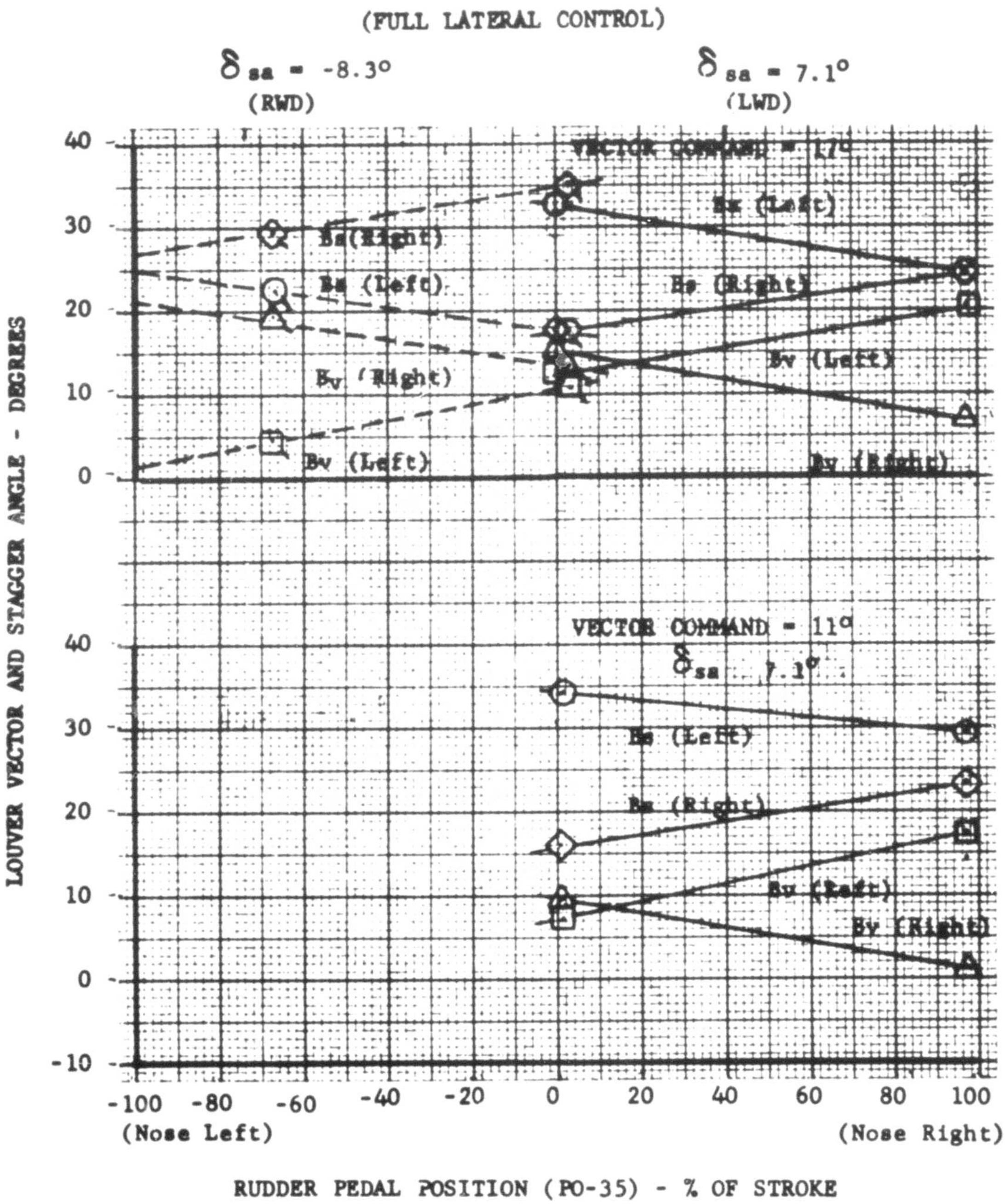

FIGURE 19A

DIRECTIONAL RIGGING - VECTOR AND STAGGER ANGLES VERSUS RUDDER PEDAL AND VECTOR COMMAND

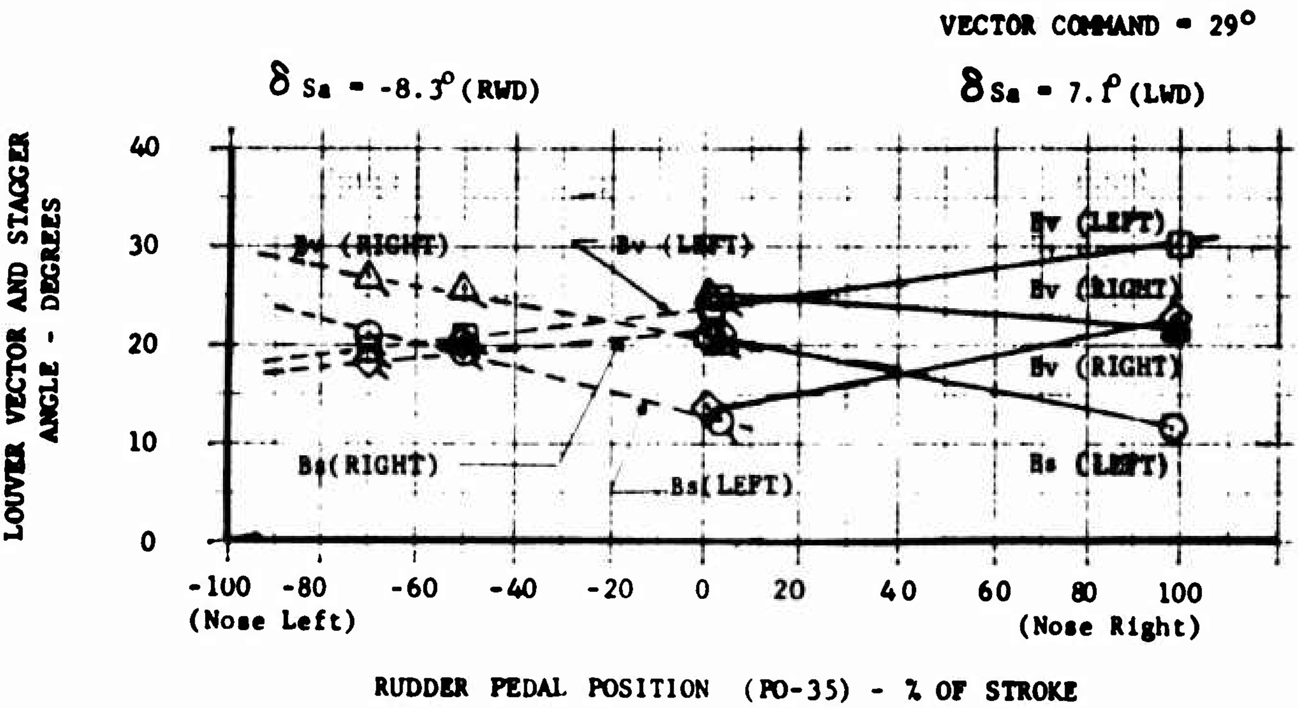

FIGURE 19B

DIRECTIONAL RIGGING - CONTINUED

(NEUTRAL CONTROLS)

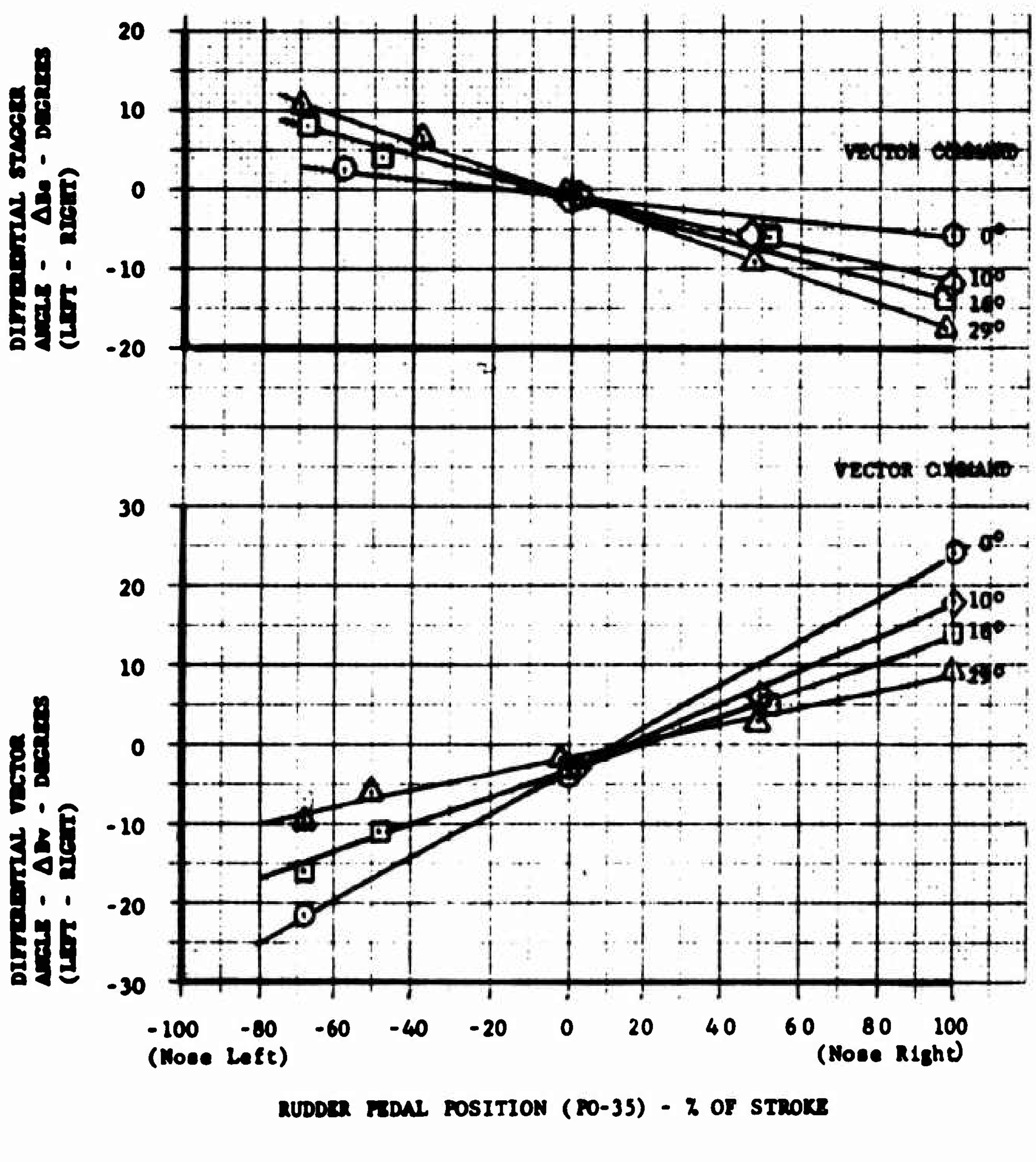

FIGURE 20A

LOUVER VECTOR AND STAGGER GEARING
VERSUS RUDDER PEDAL AND
VECTOR COMMAND

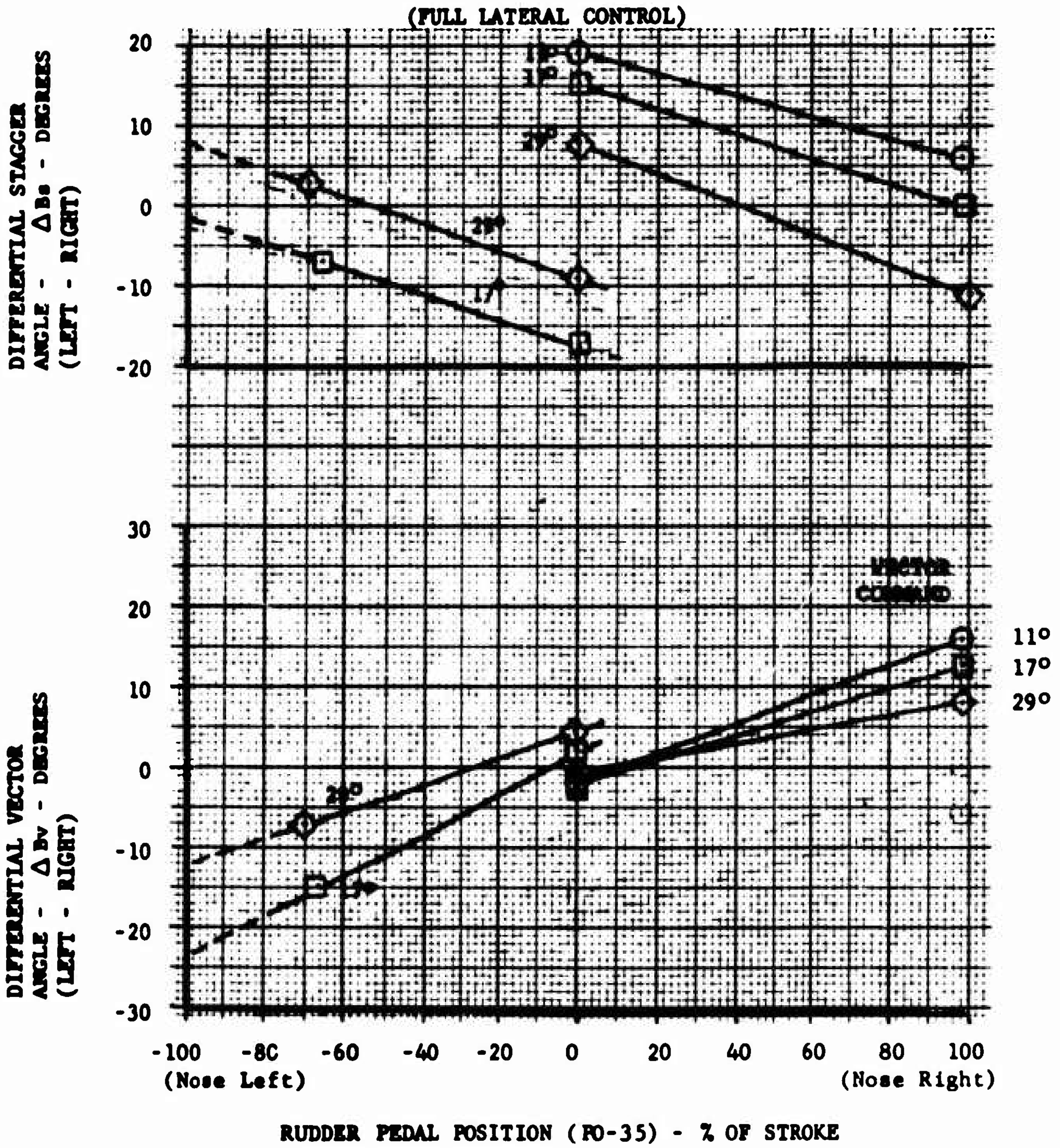

FIGURE 20B

LOUVER VECTOR AND STAGGER GEARING
VERSUS RUDDER PEDAL AND
VECTOR COMMAND

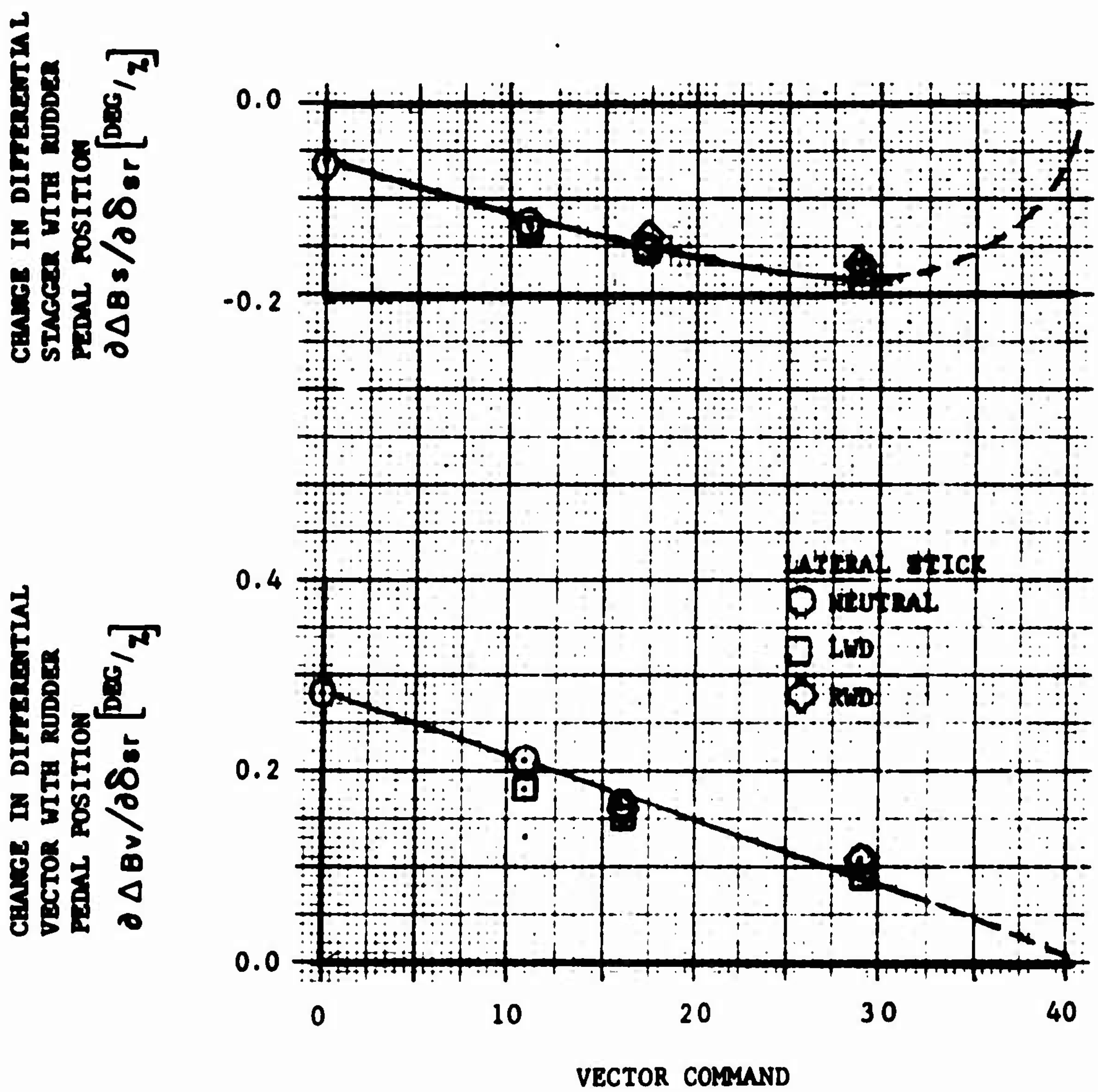

FIGURE 21

DIFFERENTIAL STAGGER AND VECTOR GEARING VERSUS VECTOR COMMAND

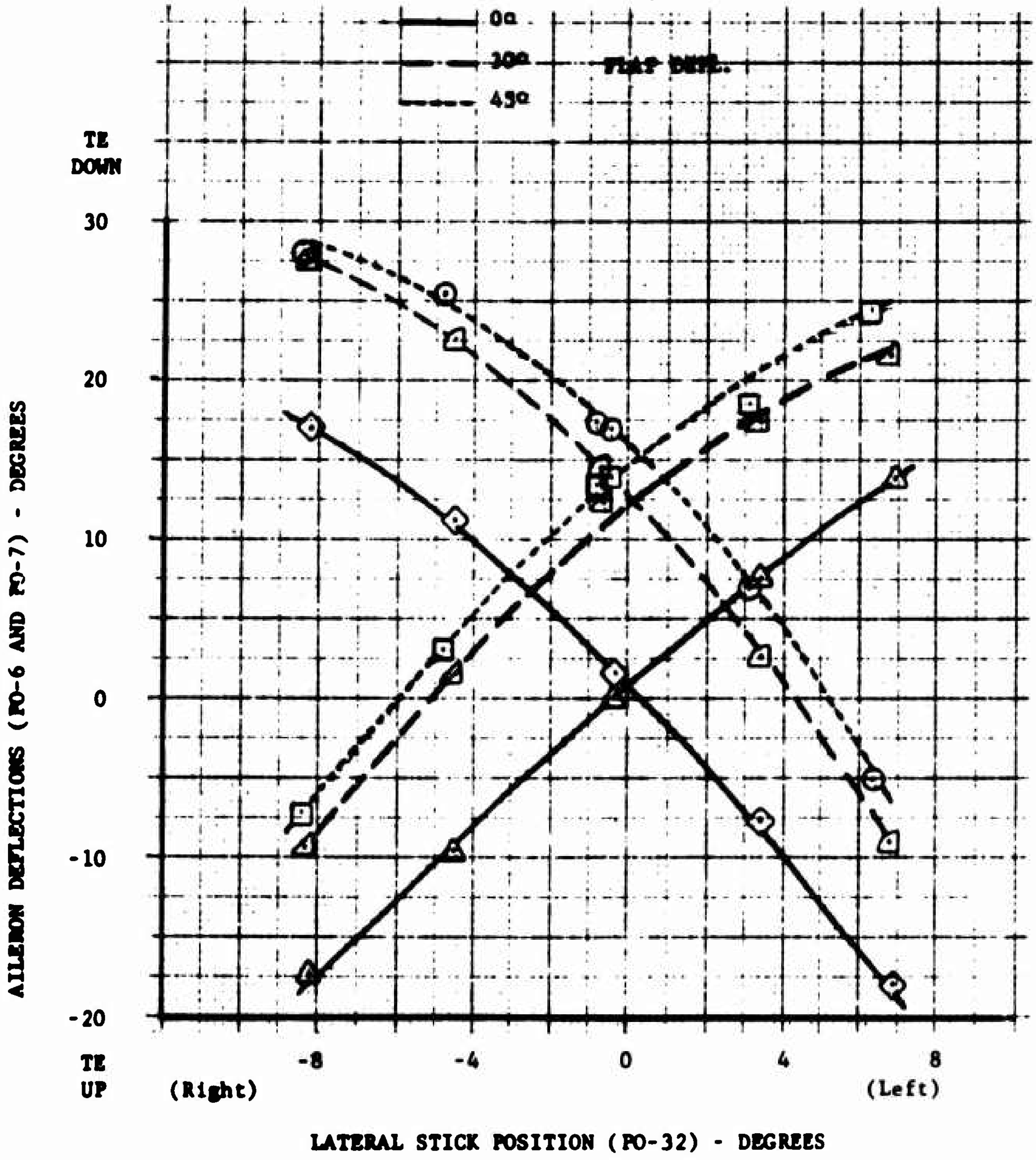

FIGURE 22

LATERAL RIGGING - AILERON
DEFLECTIONS VERSUS LATERAL STICK POSITION
FROM A RANGE OF FLAP SETTINGS

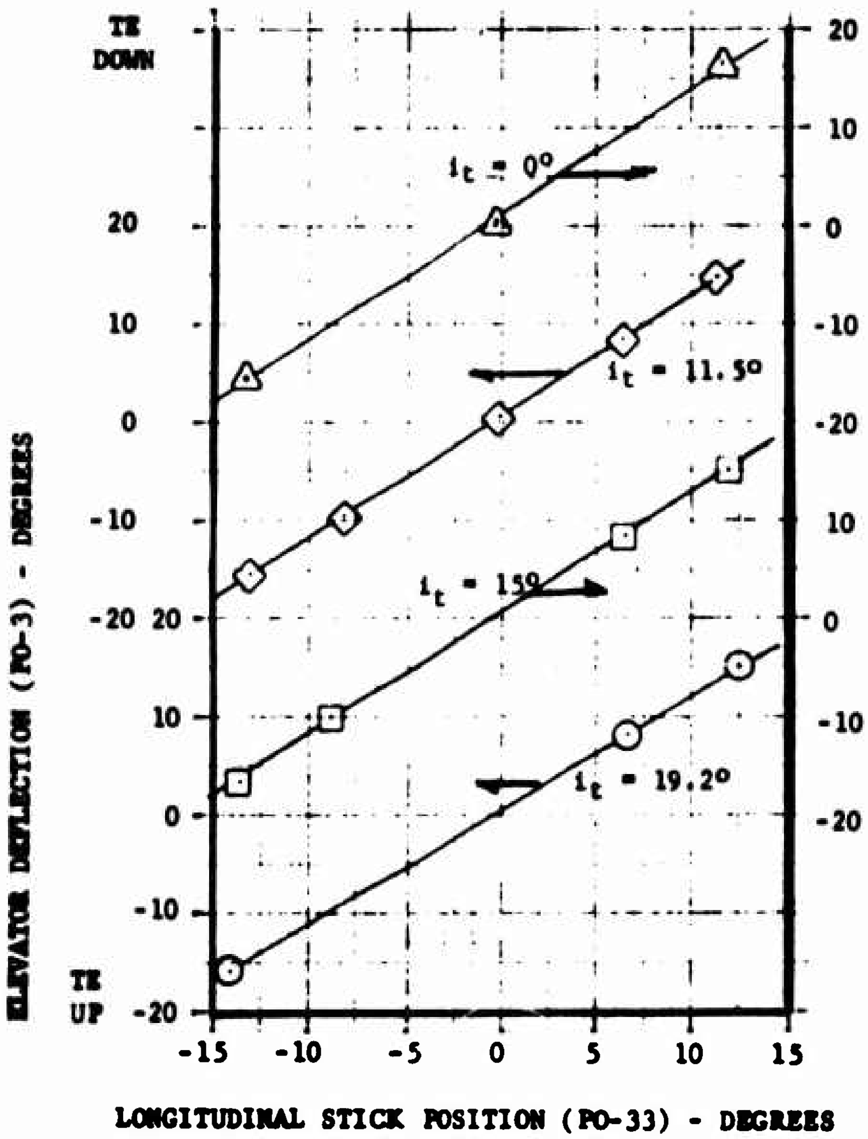

FIGURE 23

LONGITUDINAL RIGGING - ELEVATOR
DEFLECTION VERSUS LONGITUDINAL STICK
POSITION FOR A RANGE OF TAIL INCIDENCE SETTINGS

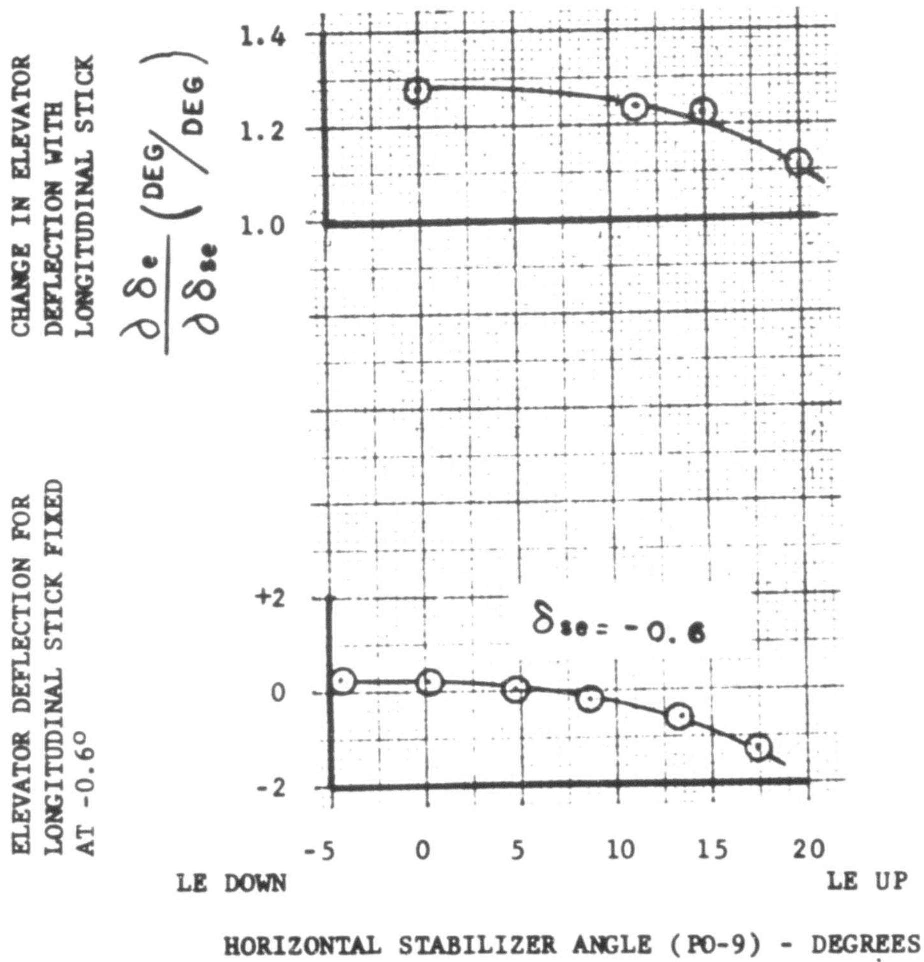

FIGURE 24

ELEVATOR GEARING AND
POSITION FOR NEUTRAL STICK VERSUS
HORIZONTAL STABILIZER ANGLE

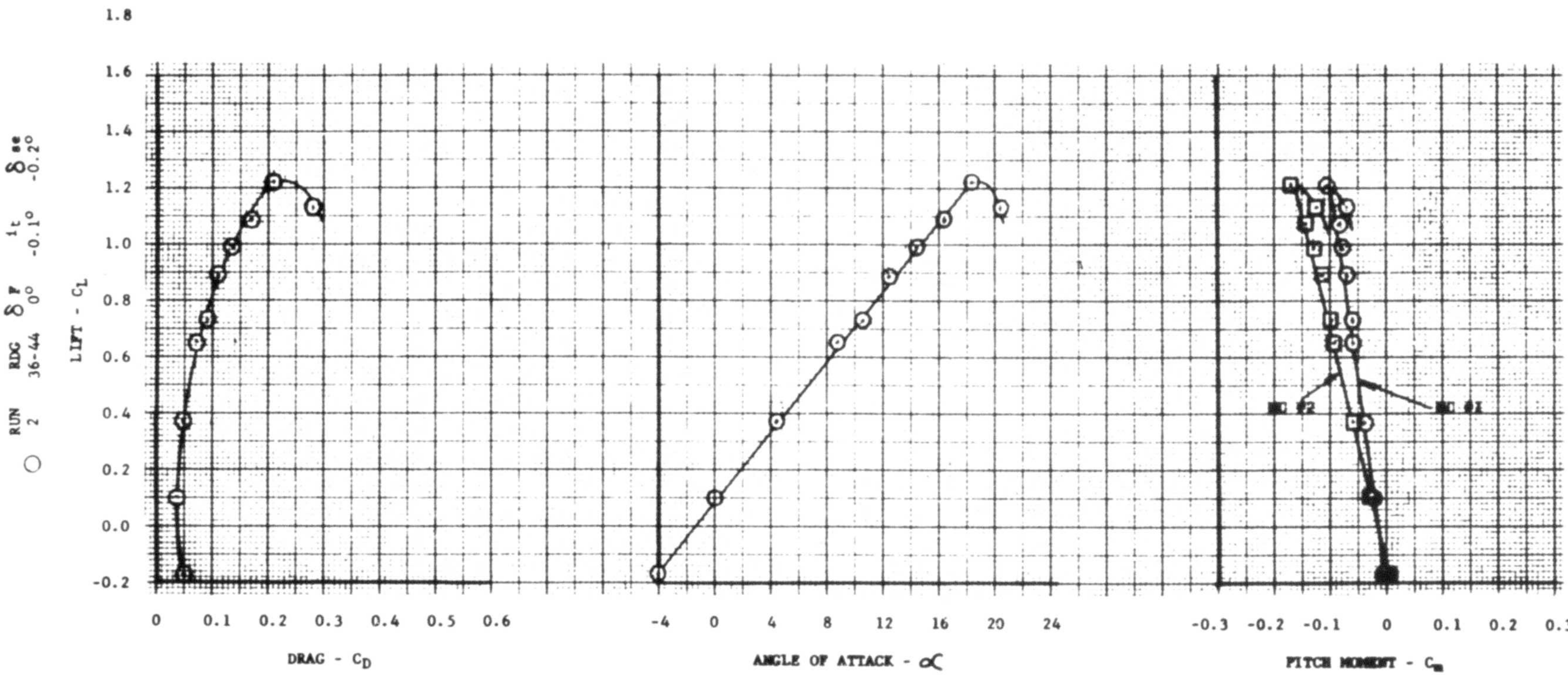

FIGURE 25
LONGITUDINAL CHARACTERISTICS - CONVENTIONAL - POWER OFF
FLAPS AT 0°

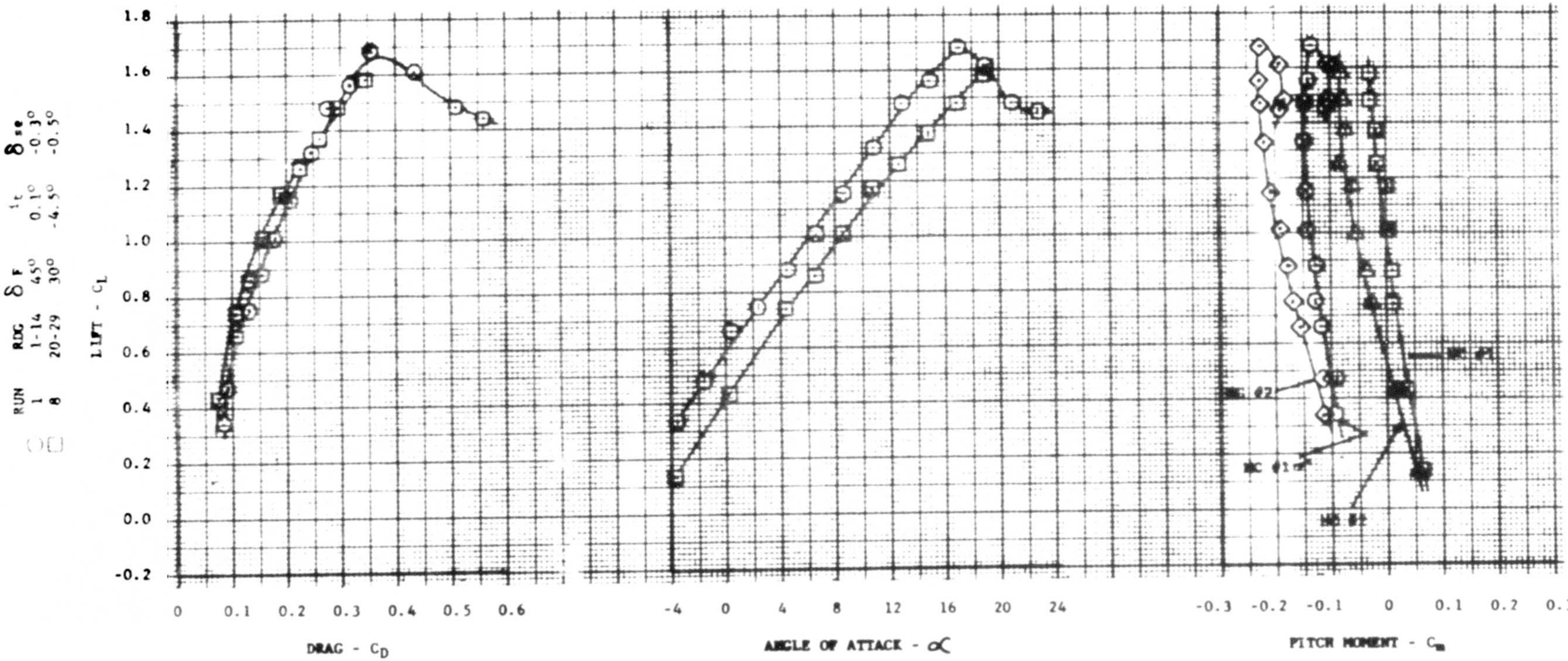

FIGURE 26
LONGITUDINAL CHARACTERISTICS - CONVENTIONAL - POWER OFF
FLAPS AT 45° AND 30°

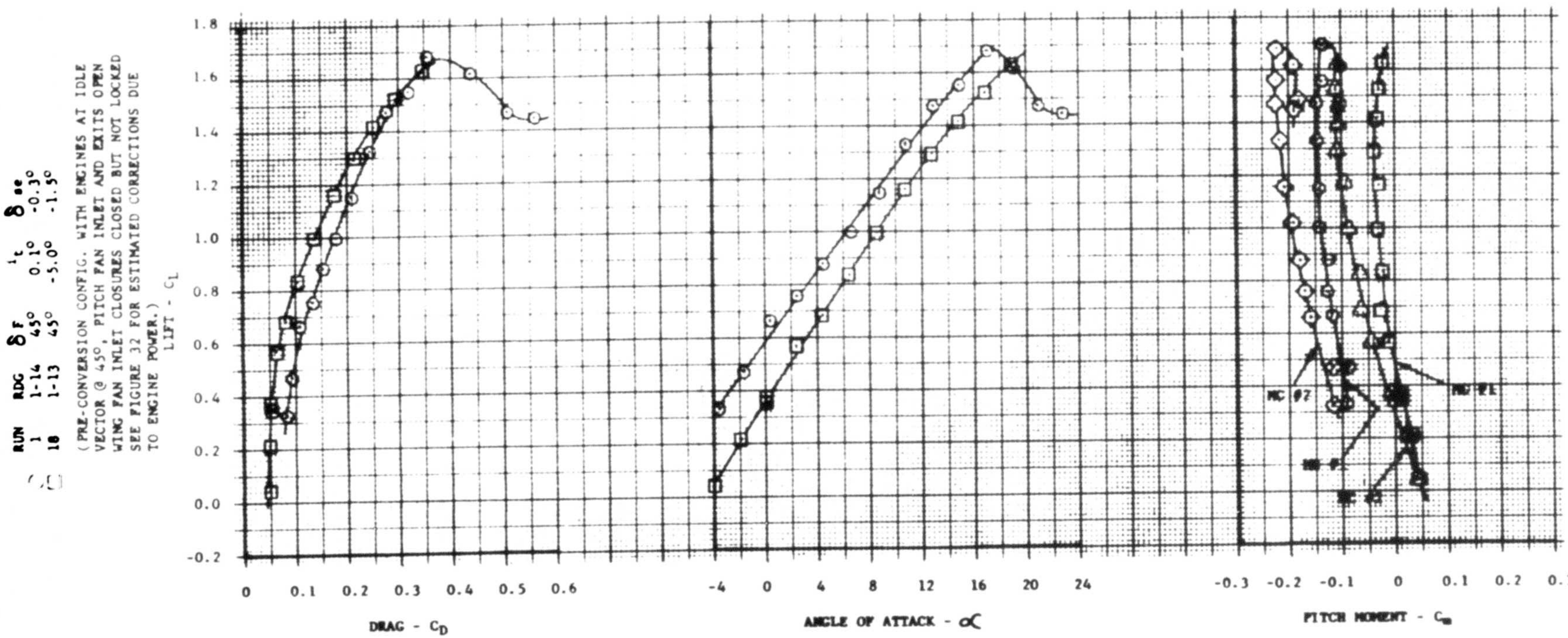

FIGURE 27
LONGITUDINAL CHARACTERISTICS - CONVENTIONAL VERSUS PRE-CONVERSION CONFIGURATIONS

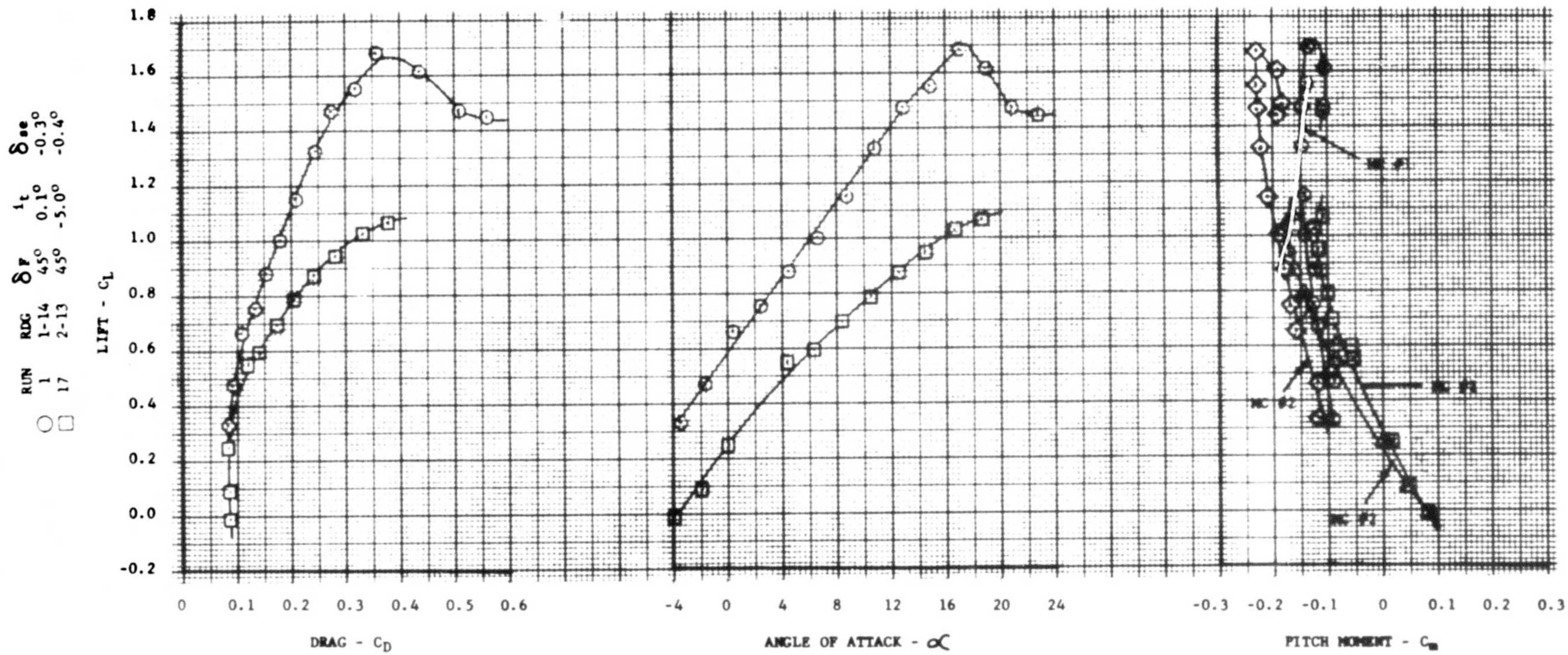

FIGURE 28
LONGITUDINAL CHARACTERISTICS - CONVENTIONAL
VERSUS VTOL-CONVERTED CONFIGURATION

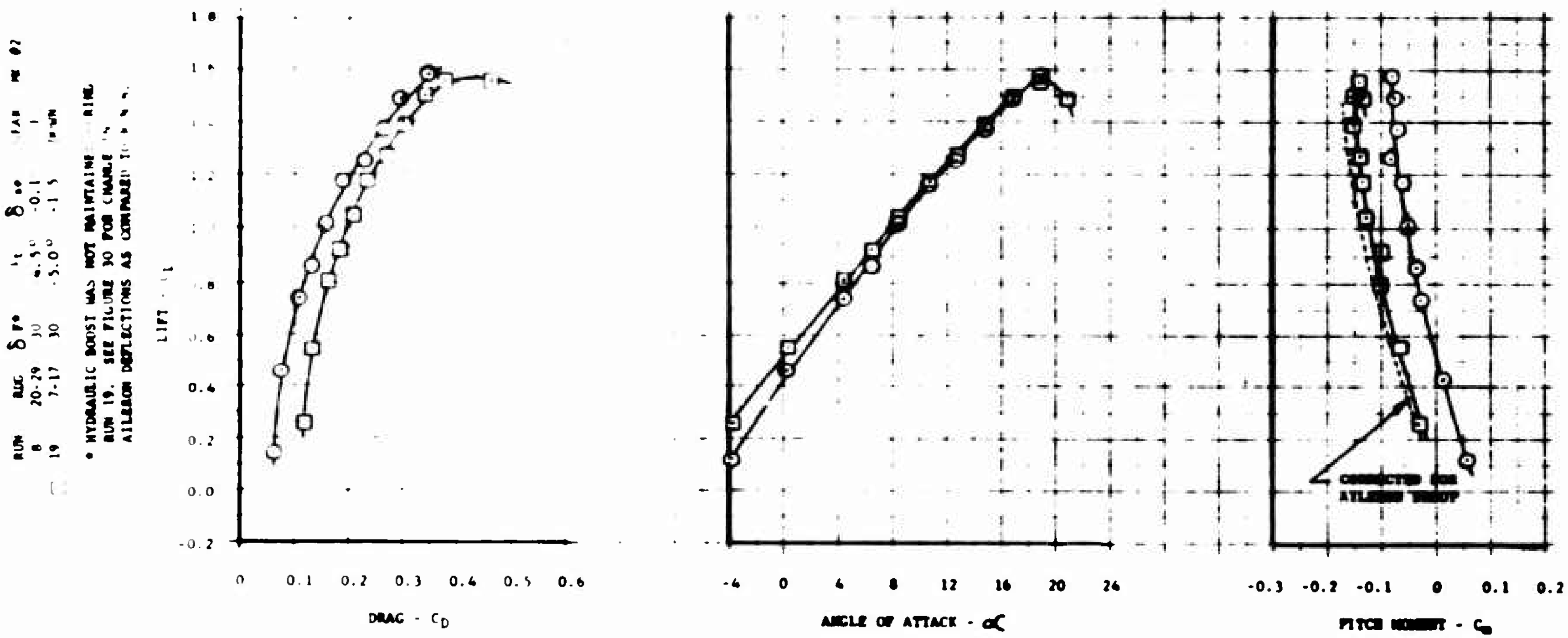

FIGURE 29
LONGITUDINAL CHARACTERISTICS - CONVENTIONAL - POWER OFF
GEAR UP VERSUS GEAR DOWN

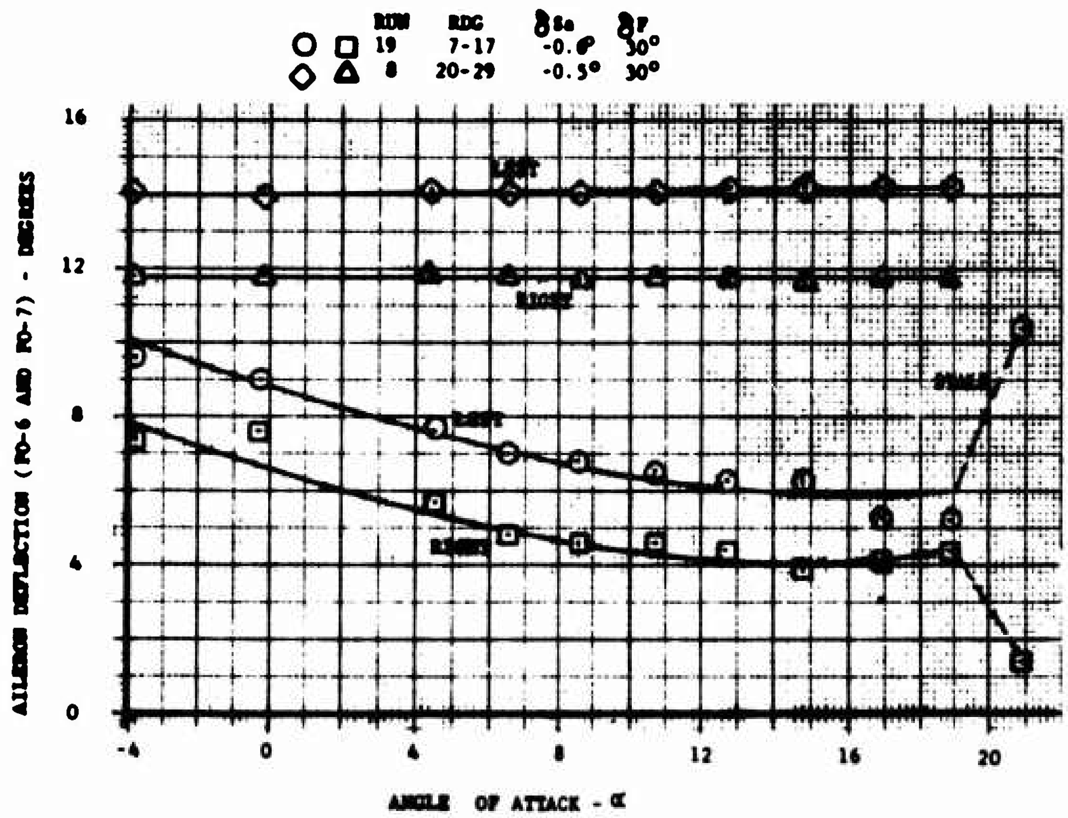

FIGURE 30

CHANGE IN AILERON DEFLECTION WITH ANGLE OF ATTACH FOR RUN 19 - HYDRAULIC BOOST OFF

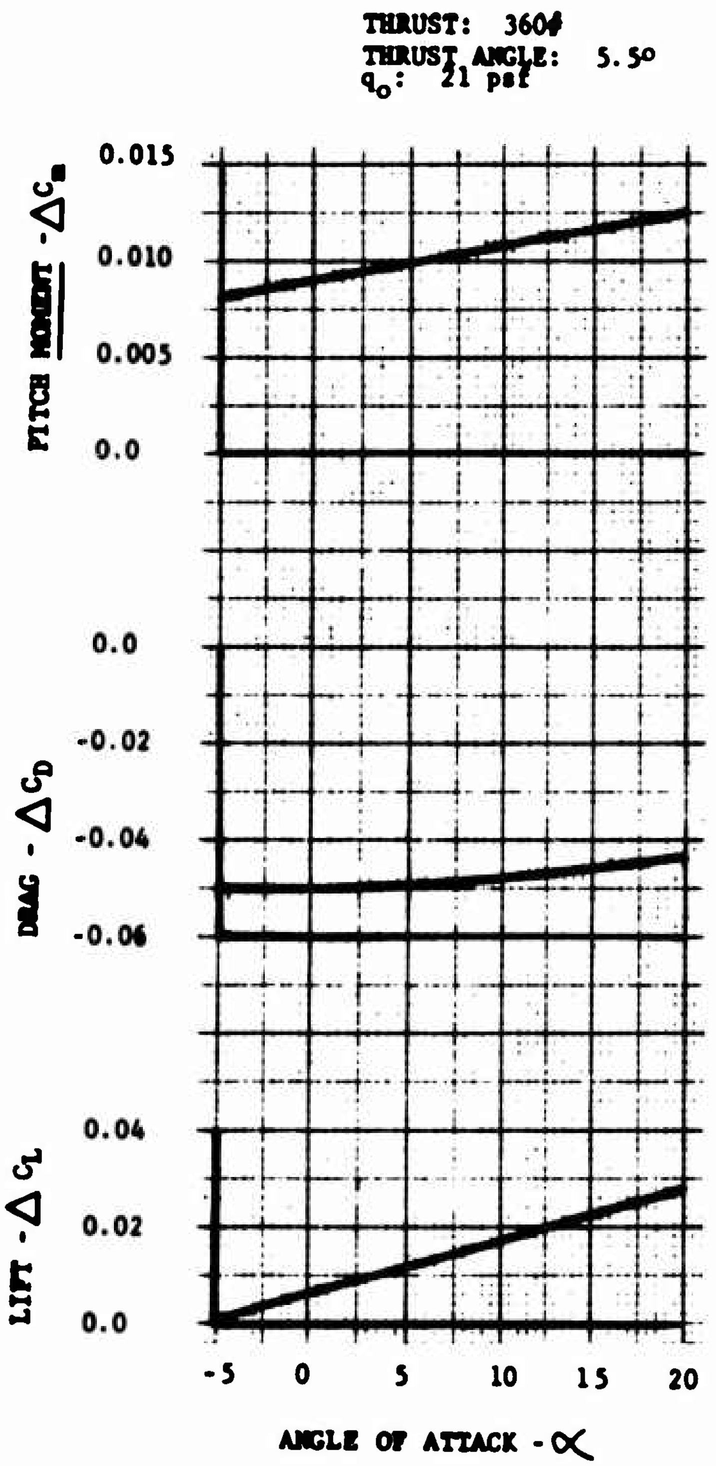

FIGURE 31

ESTIMATED LIFT, DRAG AND MOMENT CONTRIBUTIONS DUE TO TWO ENGINES AT IDLE

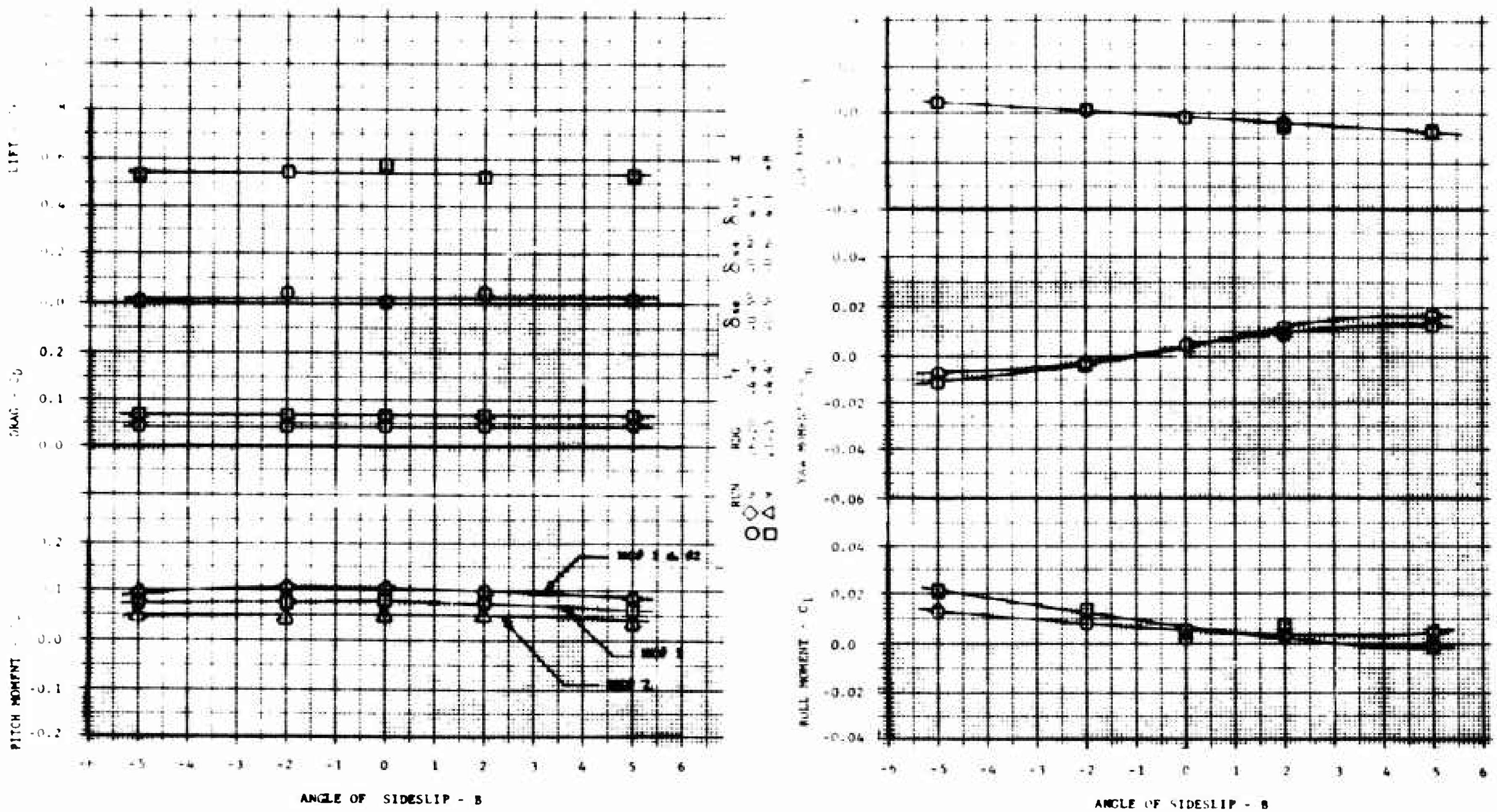

FIGURE 32
LATERAL DIRECTIONAL CHARACTERISTICS - CONVENTIONAL - POWER OFF
FLAPS AT 0° - α = 0 AND α = +8

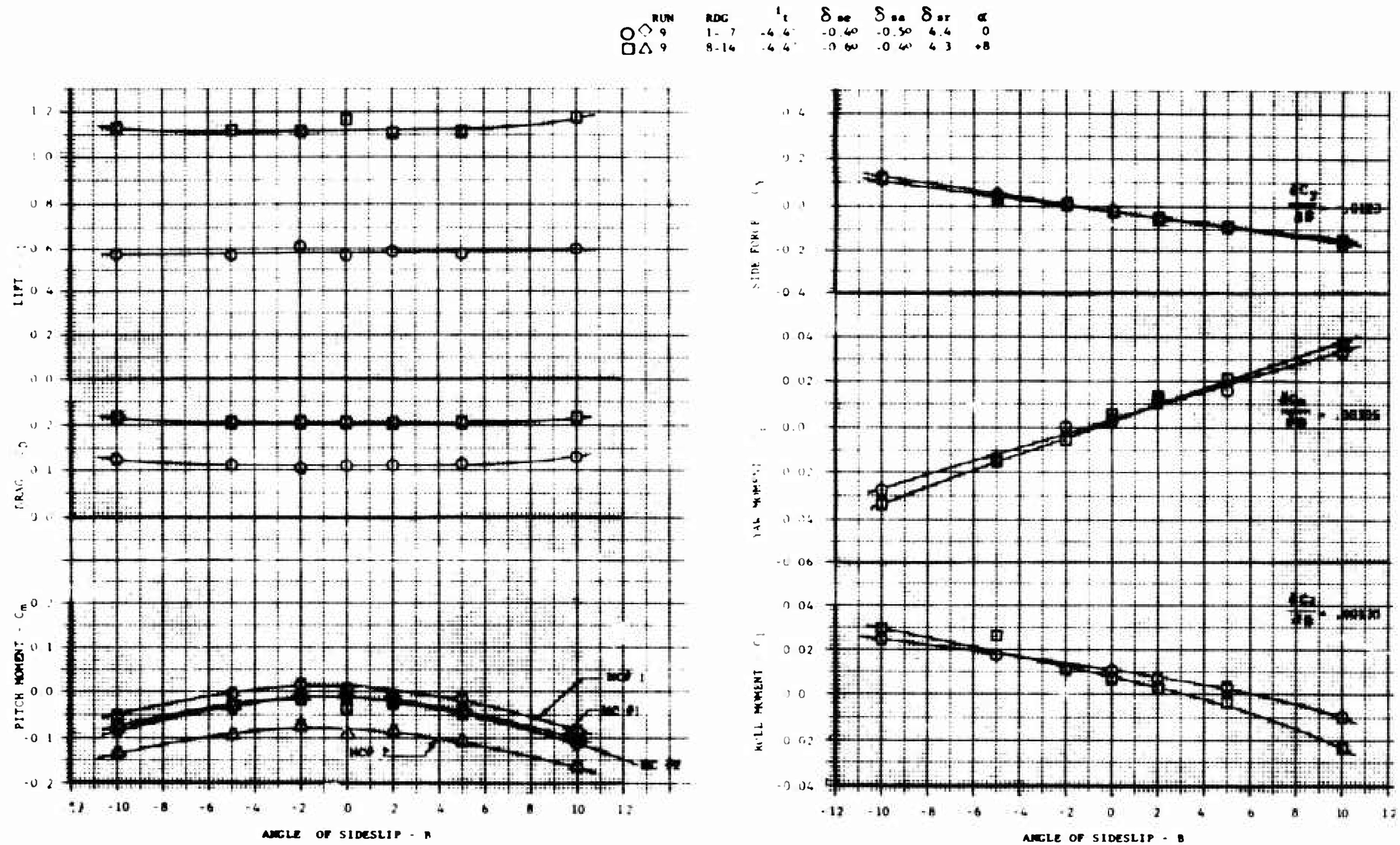

FIGURE 33
LATERAL DIRECTIONAL CHARACTERISTICS - CONVENTIONAL - POWER OFF
FLAPS AT 45° - α = 0 AND +8°

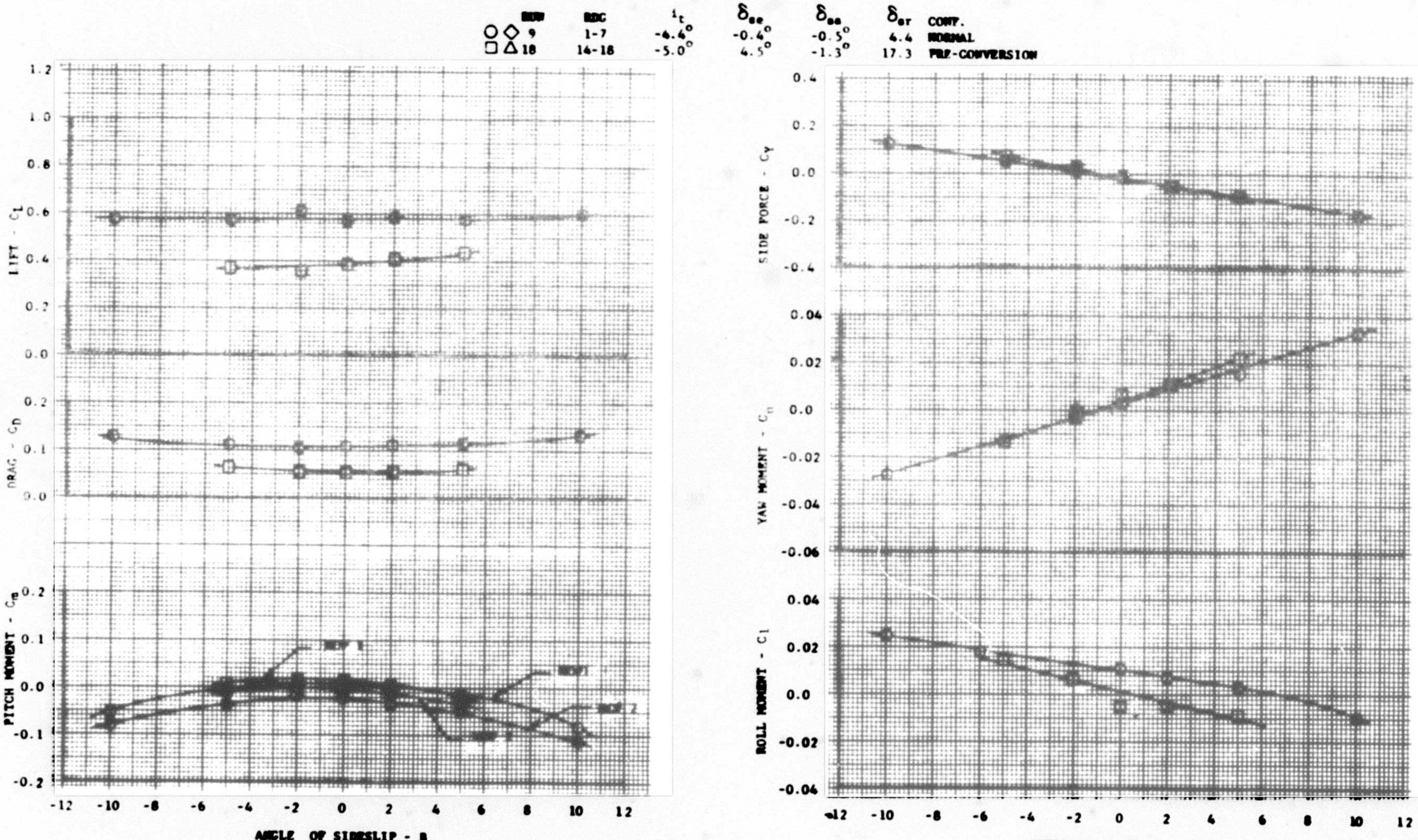

FIGURE 34
LATERAL DIRECTIONAL CHARACTERISTICS
CONVENTIONAL VERSUS PRE-CONVERSION CONFIGURATION - $\alpha = 0°$

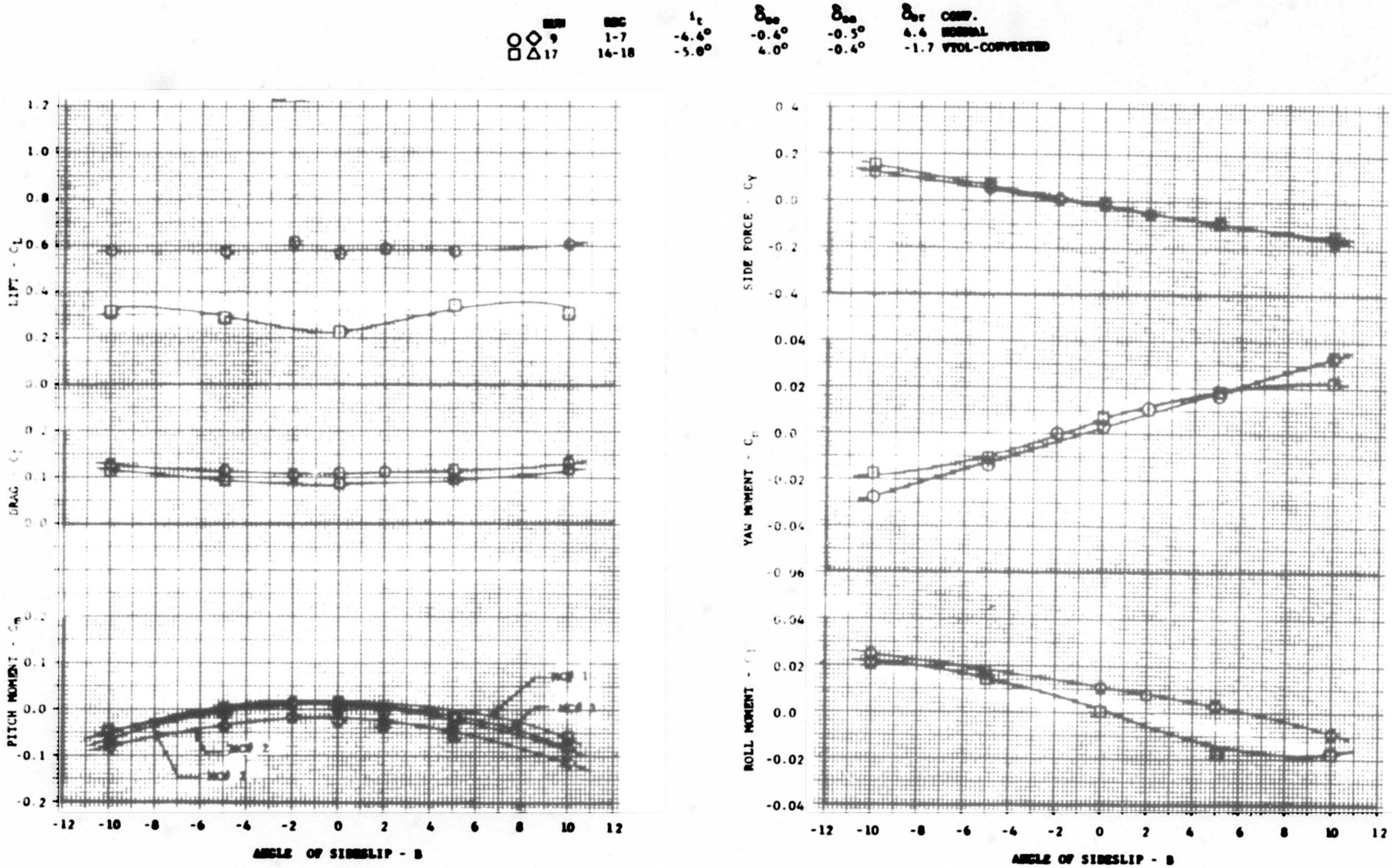

FIGURE 35
LATERAL DIRECTIONAL CHARACTERISTICS
CONVENTIONAL VERSUS VTOL-CONVERTED CONFIGURATION - $\alpha = 0°$

	RUN	BRG	i_t	δ_{se}	δ_{sa}	δ_{sr}	GEAR
○ ◇	9	1-7	-4.4°	-0.4°	-0.5°	4.4	UP
□ △	19	18-22	-5.0°	3.6°	-0.7°	2.5	DOWN

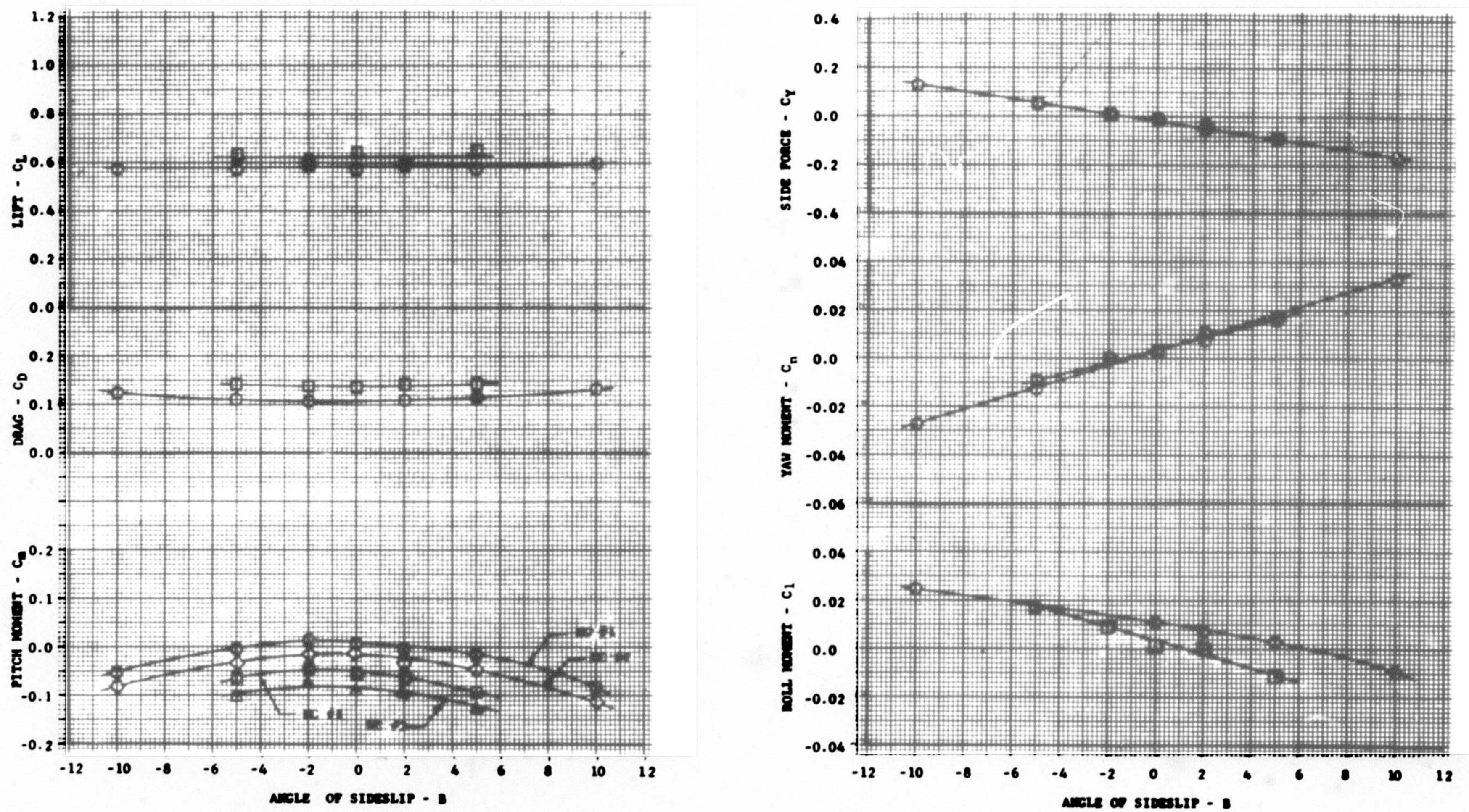

FIGURE 36
LATERAL DIRECTIONAL CHARACTERISTICS - CONVENTIONAL - POWER OFF
GEAR UP VERSUS GEAR DOWN - $\alpha = 0°$

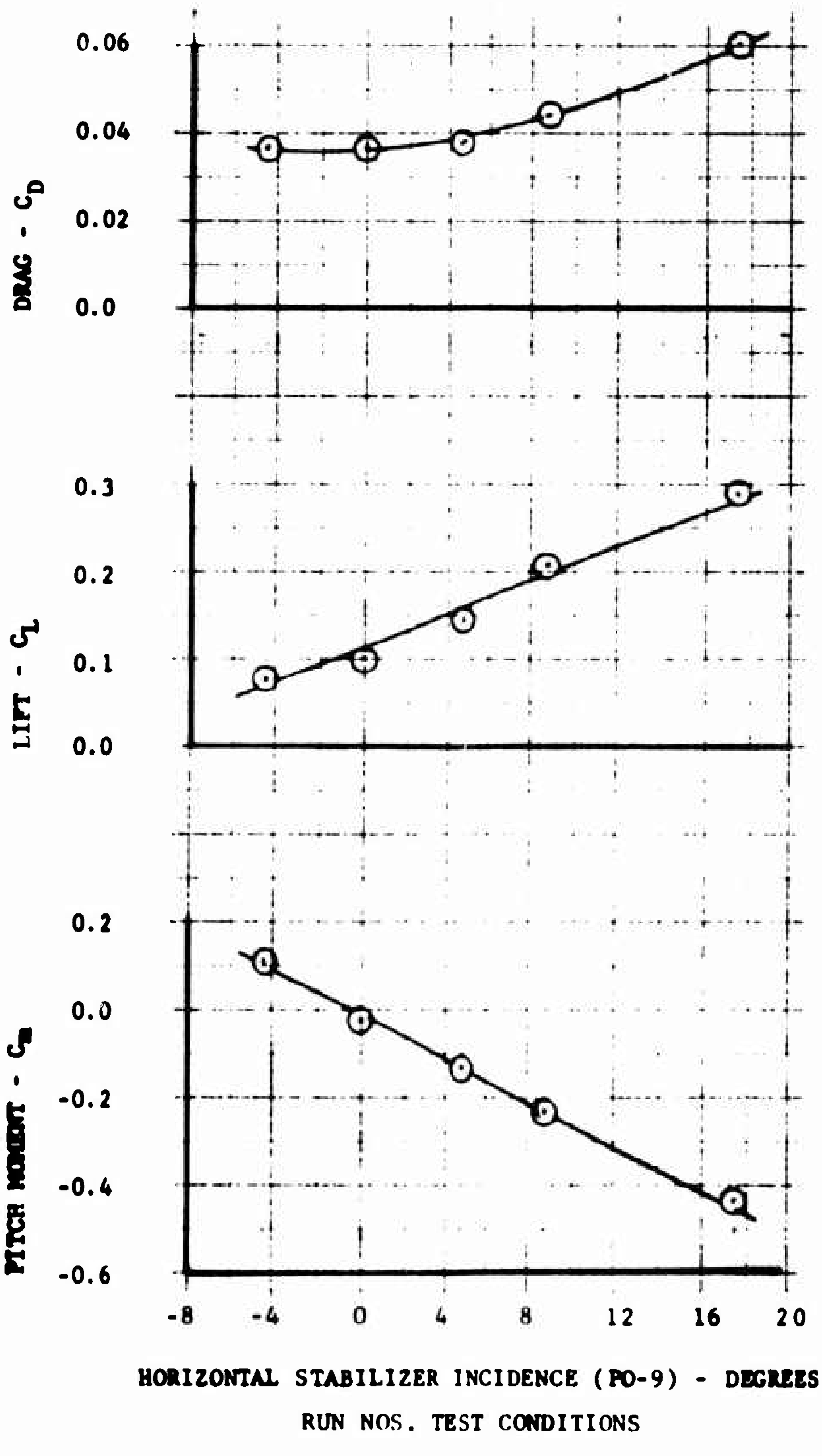

FIGURE 37

HORIZONTAL STABILIZER EFFECTIVENESS
CONVENTIONAL-POWER OFF - FLAPS AT 0° - MC #2

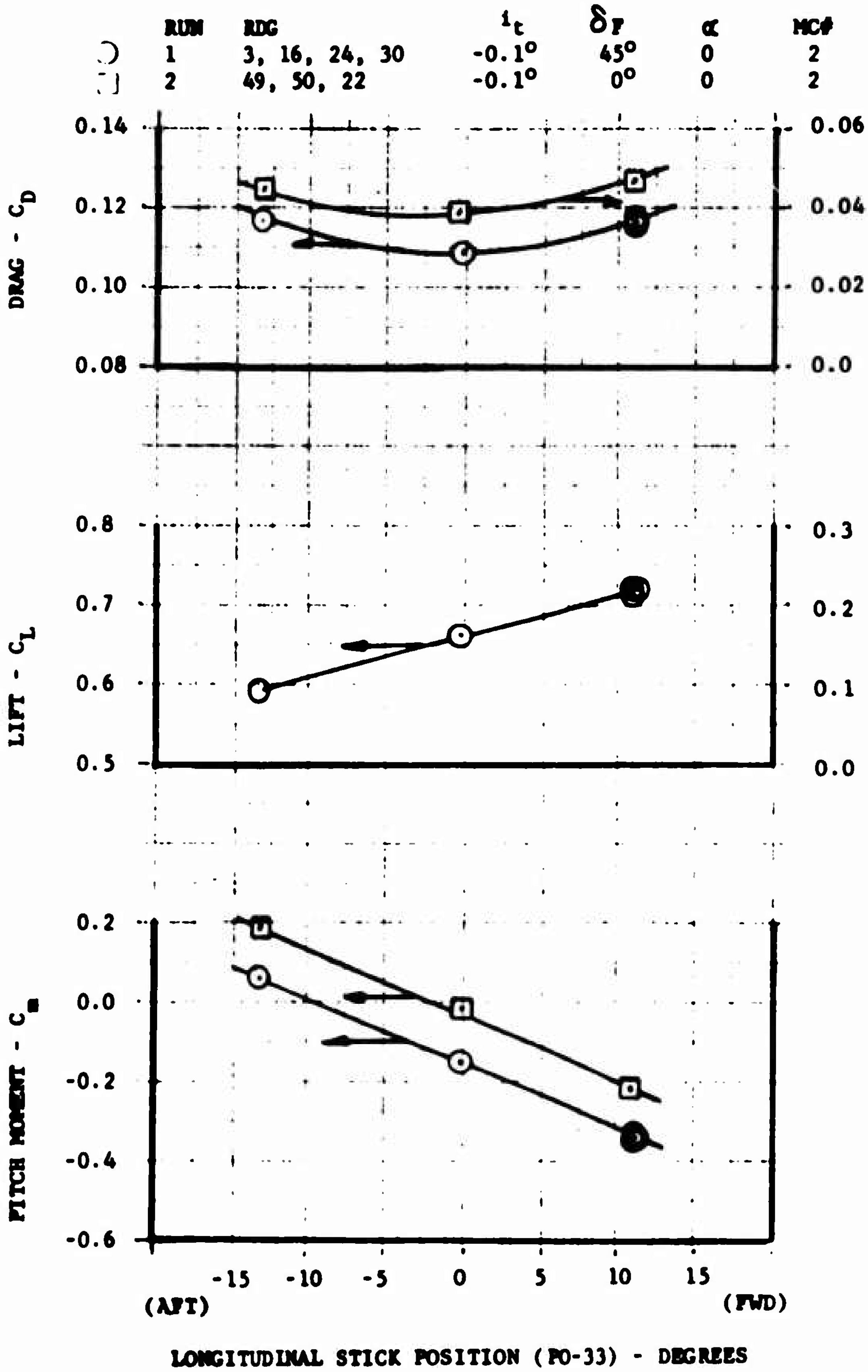

FIGURE 38
LONGITUDINAL CONTROL EFFECTIVENESS
CONVENTIONAL - POWER OFF

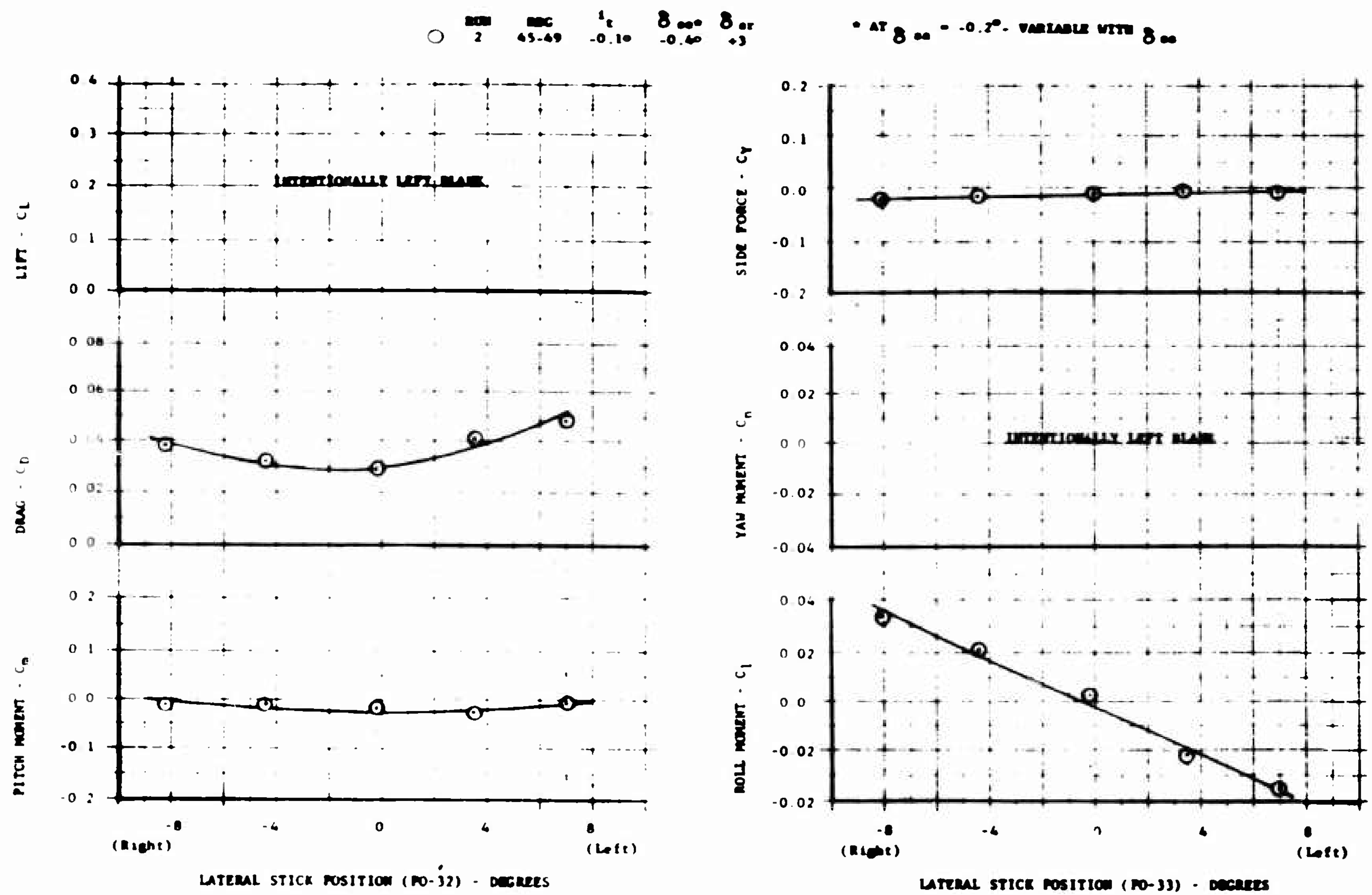

FIGURE 39
LATERAL CONTROL EFFECTIVENESS - CONVENTIONAL
POWER OFF - FLAPS AT 0° - M_c #2

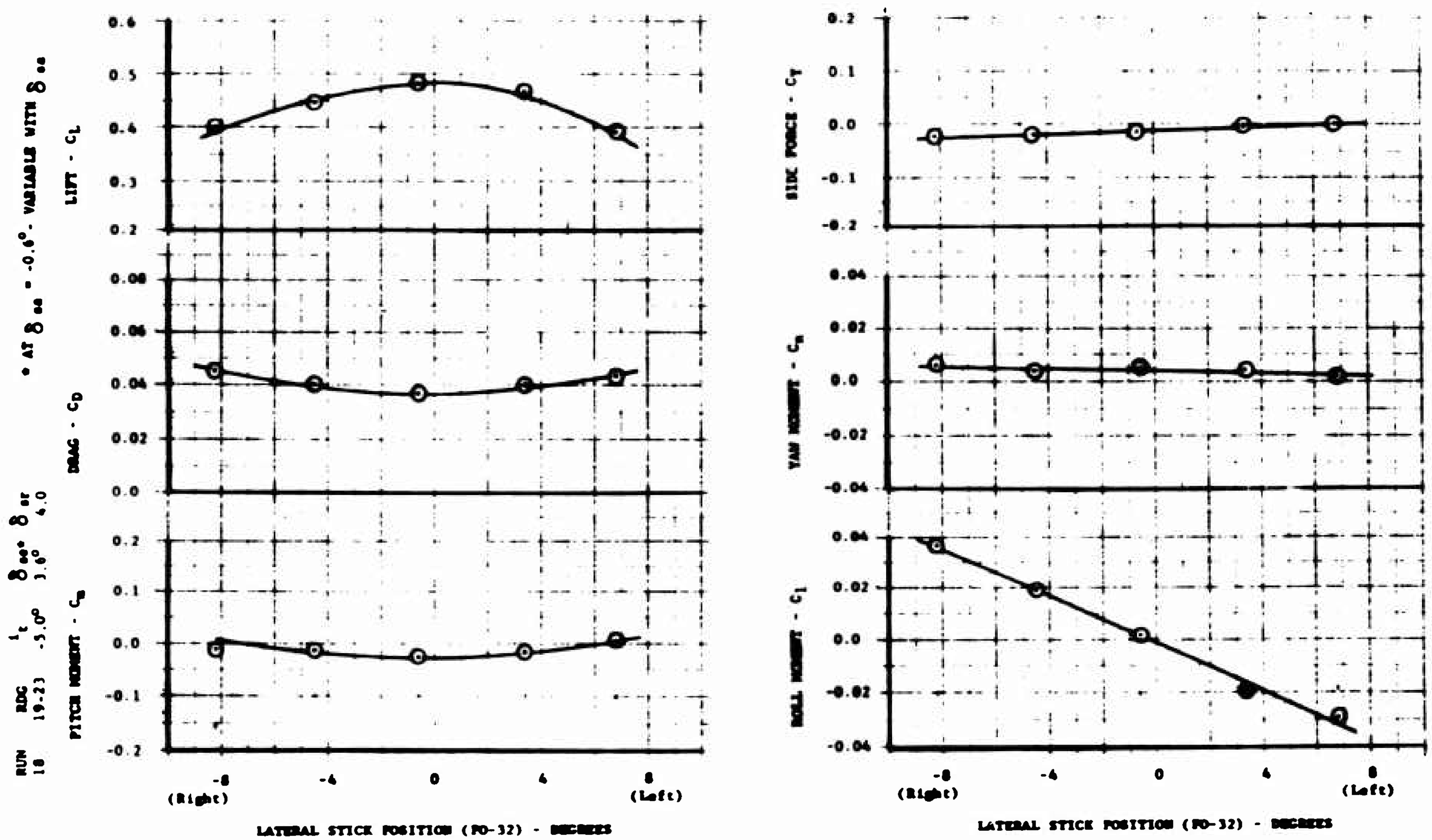

FIGURE 40
LATERAL CONTROL EFFECTIVENESS - CONVENTIONAL
POWER OFF - FLAPS AT 30° - M_c #2

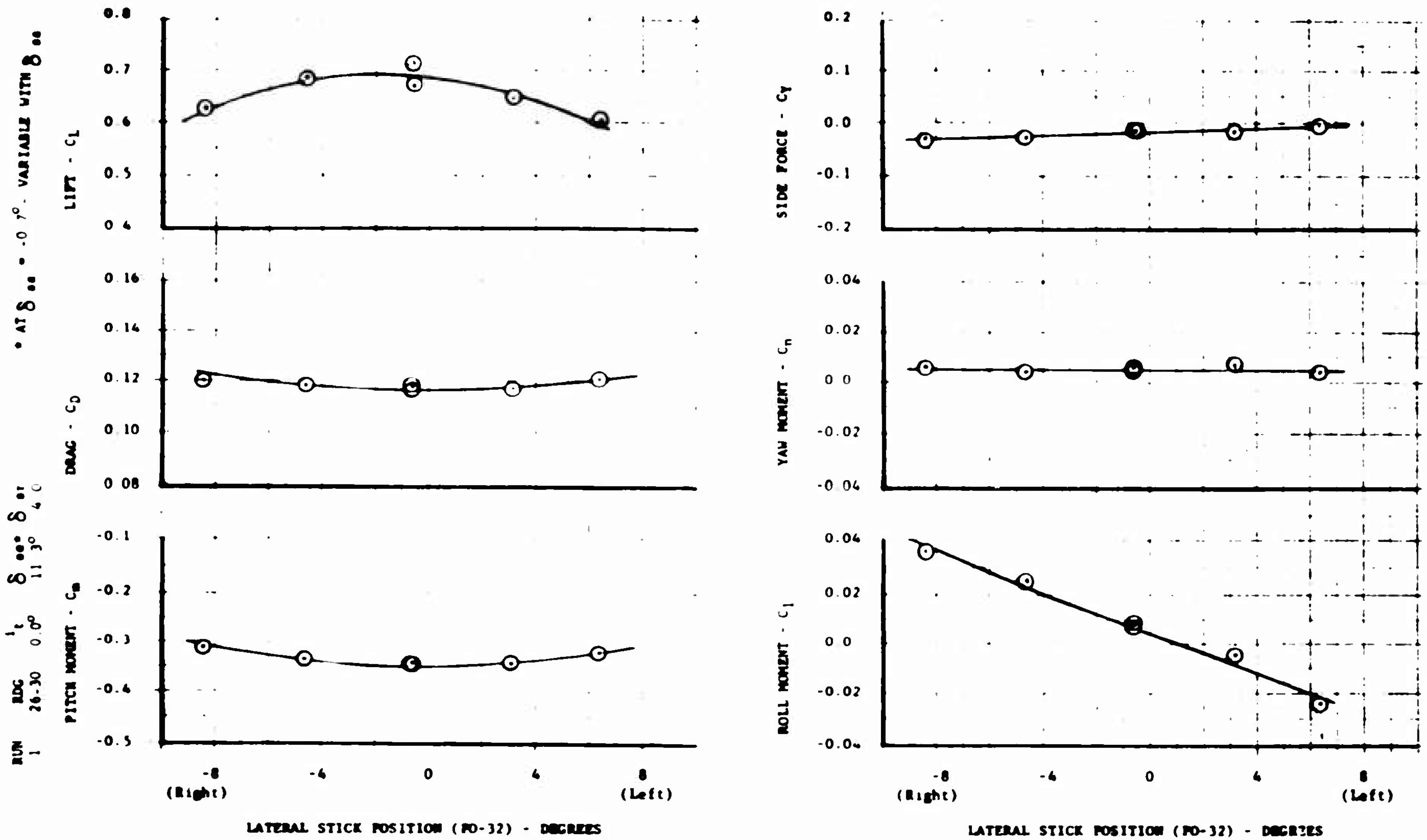

FIGURE 41
LATERAL CONTROL CHARACTERISTICS - CONVENTIONAL
POWER OFF - FLAPS AT 45° - M_c #2

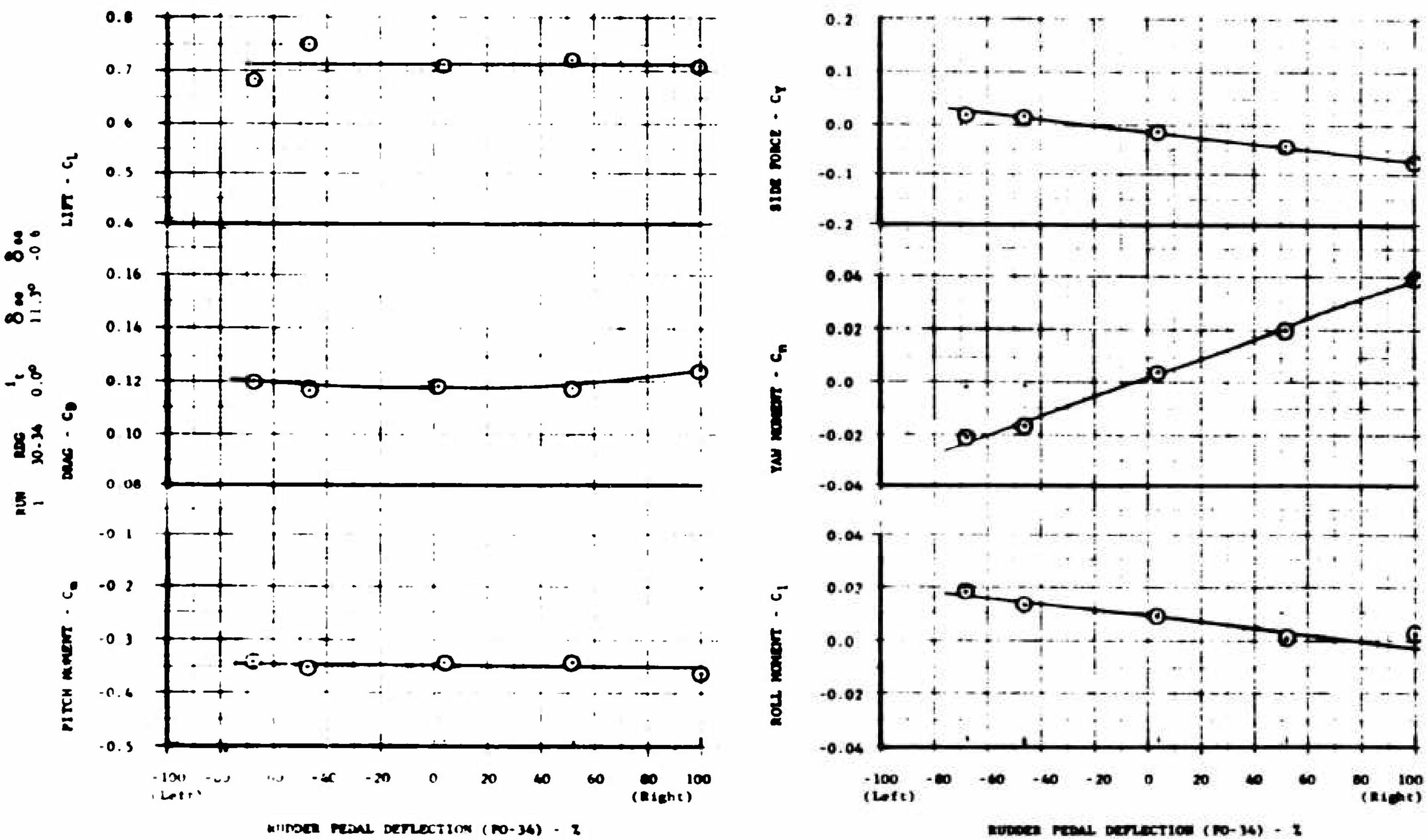

FIGURE 42
DIRECTIONAL CONTROL EFFECTIVENESS - CONVENTIONAL
POWER OFF - FLAPS AT 45° - M_c #2

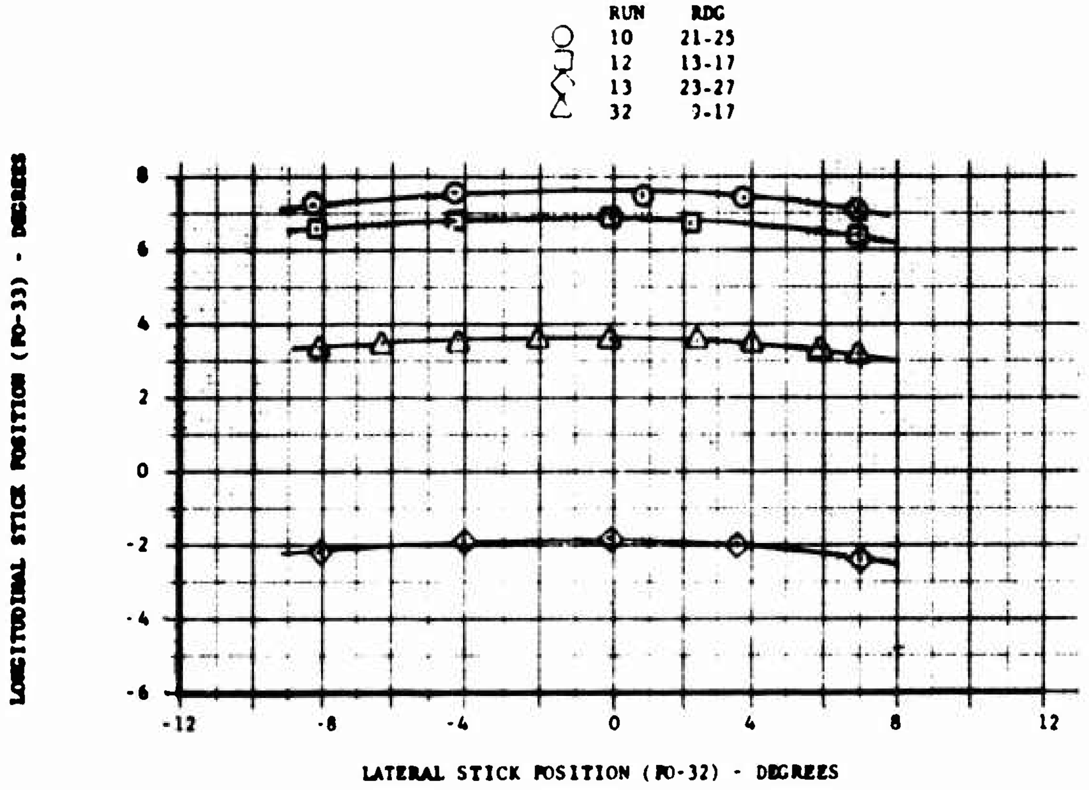

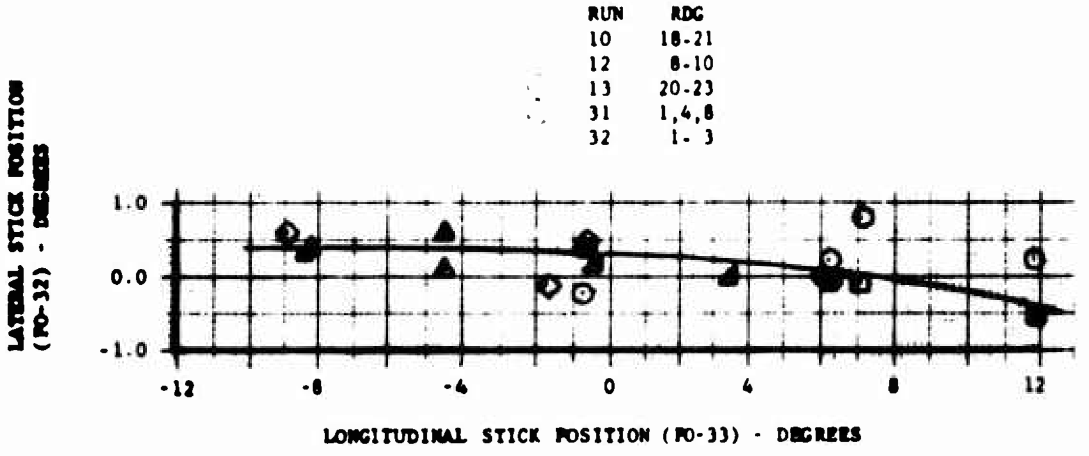

FIGURE 43
CROSS-COUPLING OF LATERAL AND LONGITUDINAL STICK
POSITIONS DUE TO TEST ACTUATION MECHANISM

	RUN	RDG	μ	i_t	δ_{se}	VECTOR COMMAND	β_{avg}	MC #2
○	11	1- 7	.16	17.9°	+6.4°	30°	24.7°	
○	12	1- 3	.16	17.5°	+6.9°	29°	24.1°	
○	29	1- 9	.16	15.6°	3.6°	29°	24.5°	
□	31	1- 7	.26	15.4°	-4.5°	50°	44.6°	
◇	13	9-15	.21	17.6°	-1.7°	42°	36.7°	
△	10	2-10	.11	18.0°	+7.1°	17°	12.9°	

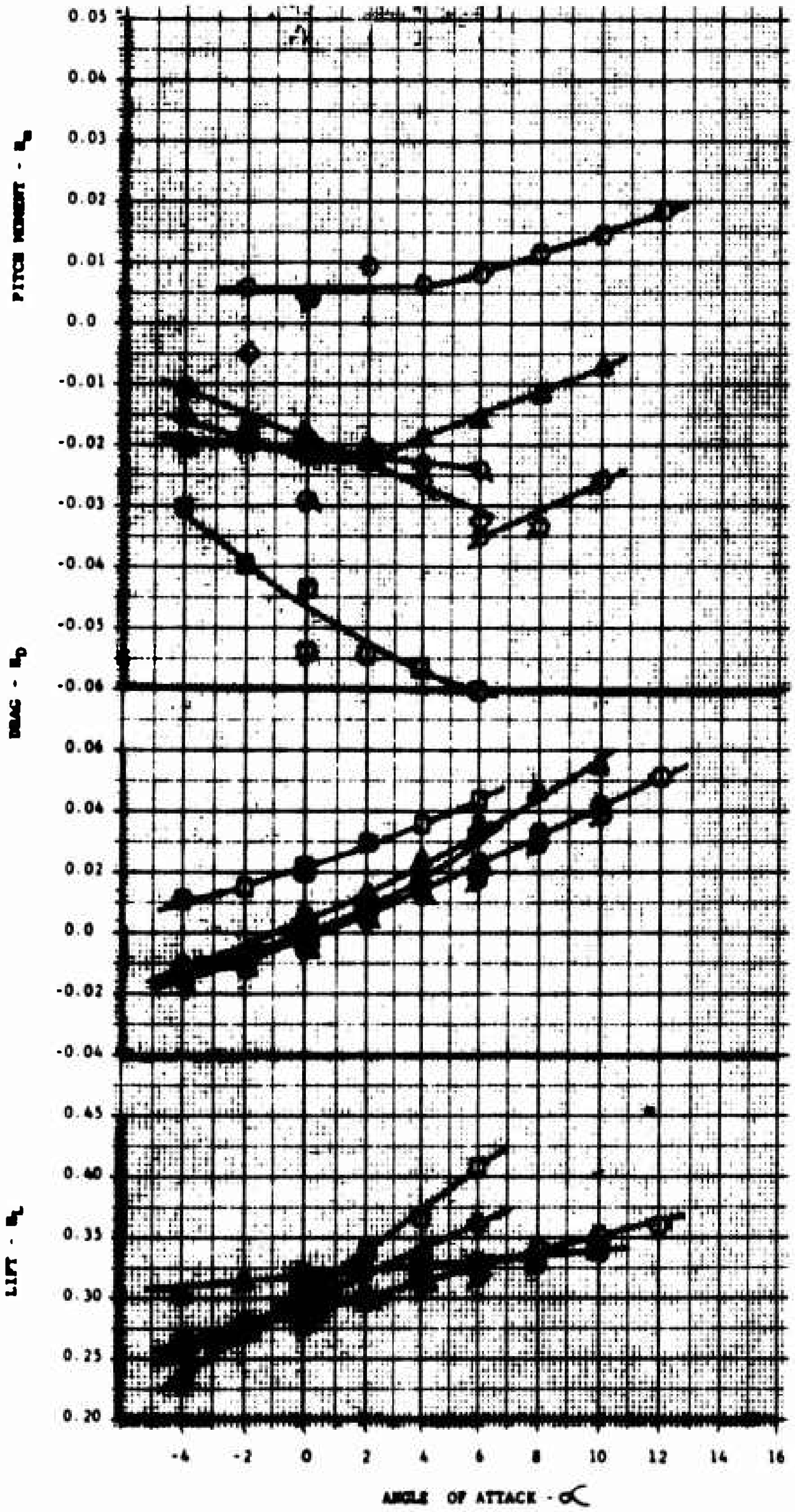

FIGURE 44
LONGITUDINAL CHARACTERISTICS - FAN POWERED (HI-POWER)
NORMAL CONFIGURATION

RUN	RDG	μ	i_t	δ_{ee}	VECTOR COMMAND	B_{avg}
5	1	.06	18.1°	+8.4°	11°	6.9°
6	1- 8	.11	17.8°	+9.3°	18°	13.5°
4	2-15	.14	17.4°	+6.7°	25°	21.3°
5	2-10	.21	16.3°	+1.5°	38°	32.2°
6	9-19	.25	18.0°	-9.6°	50°	44.3°

OPEN SYMBOLS - MC #1
SOLID SYMBOLS - MC #2

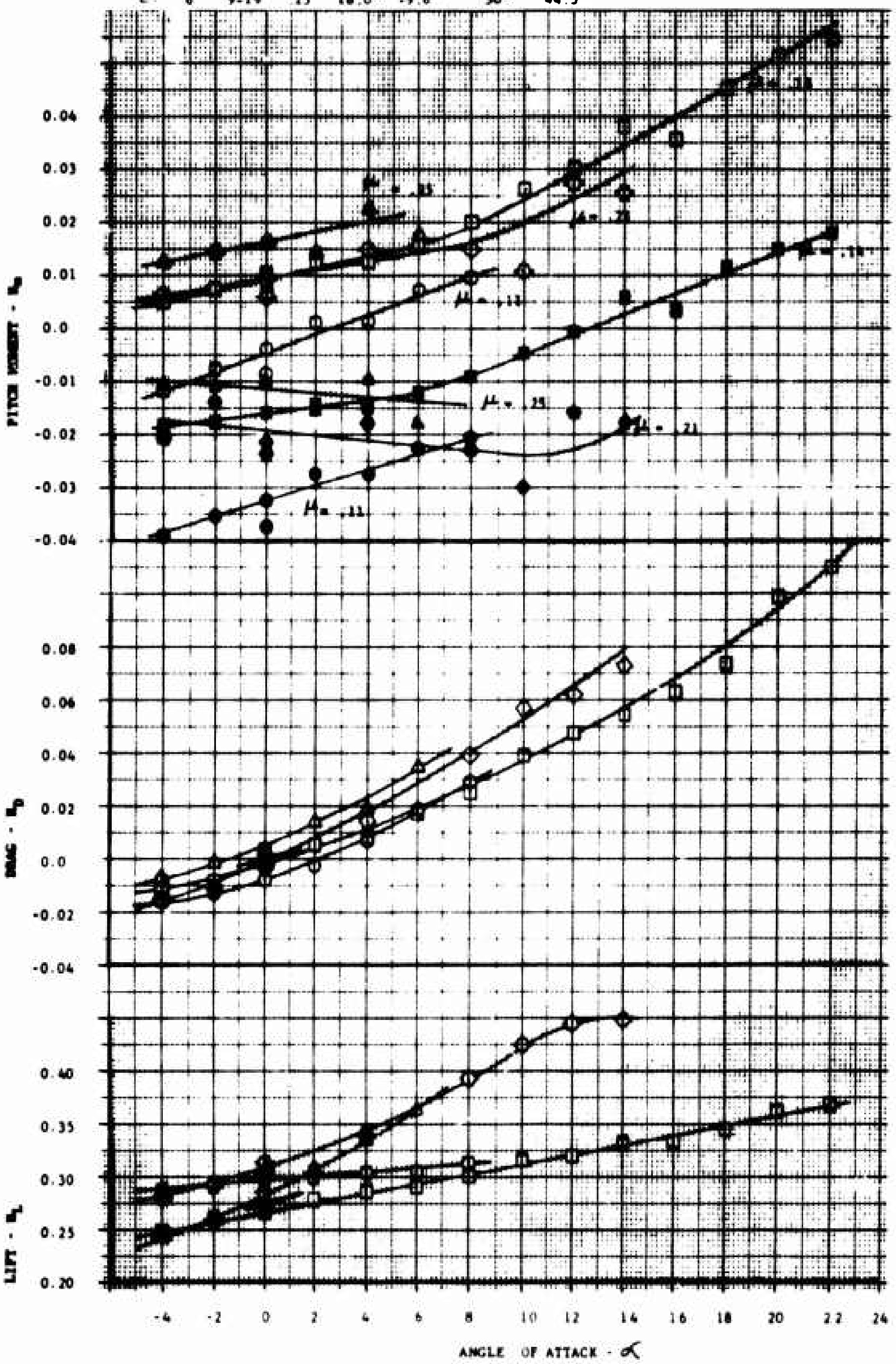

FIGURE 45A
LONGITUDINAL CHARACTERISTICS - FAN POWERED (LO-POWER)
NORMAL CONFIGURATION

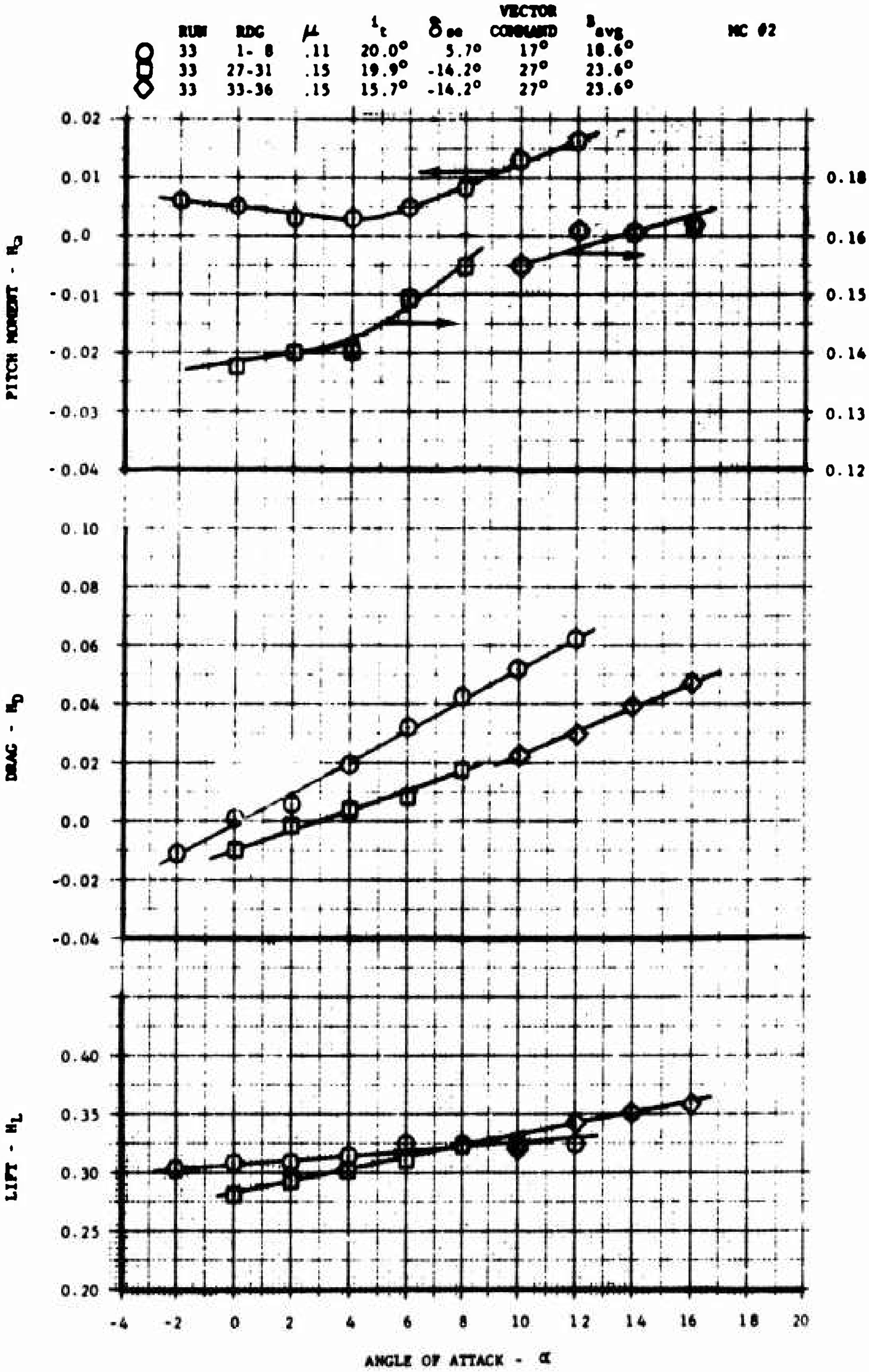

FIGURE 45B
LONGITUDINAL CHARACTERISTICS - FAN POWERED (LO-POWER)
NORMAL CONFIGURATION

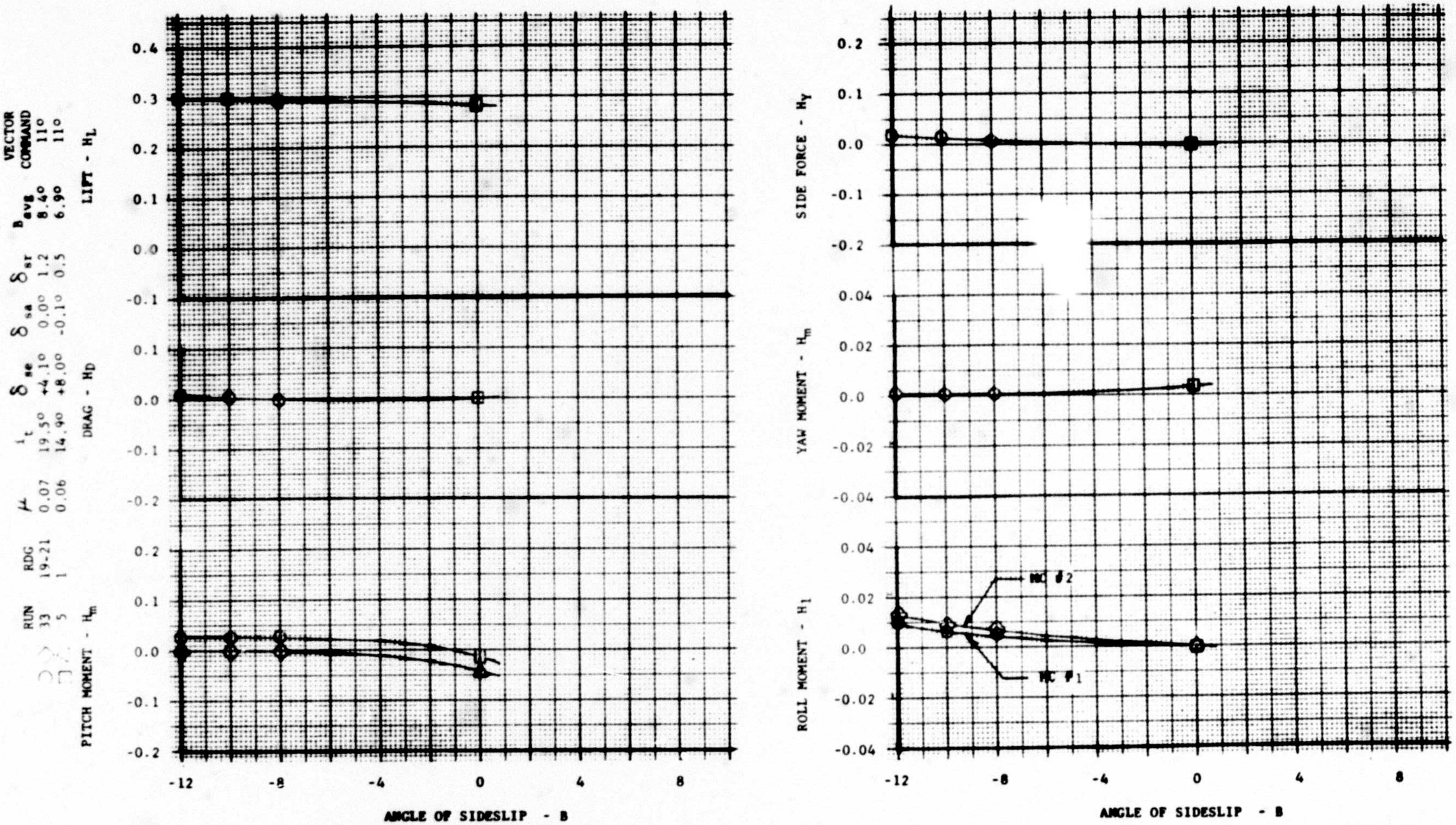

FIGURE 46
LATERAL DIRECTIONAL CHARACTERISTICS - FAN POWERED (LO-POWER)
NORMAL CONFIGURATION - $\mu = 0.07$

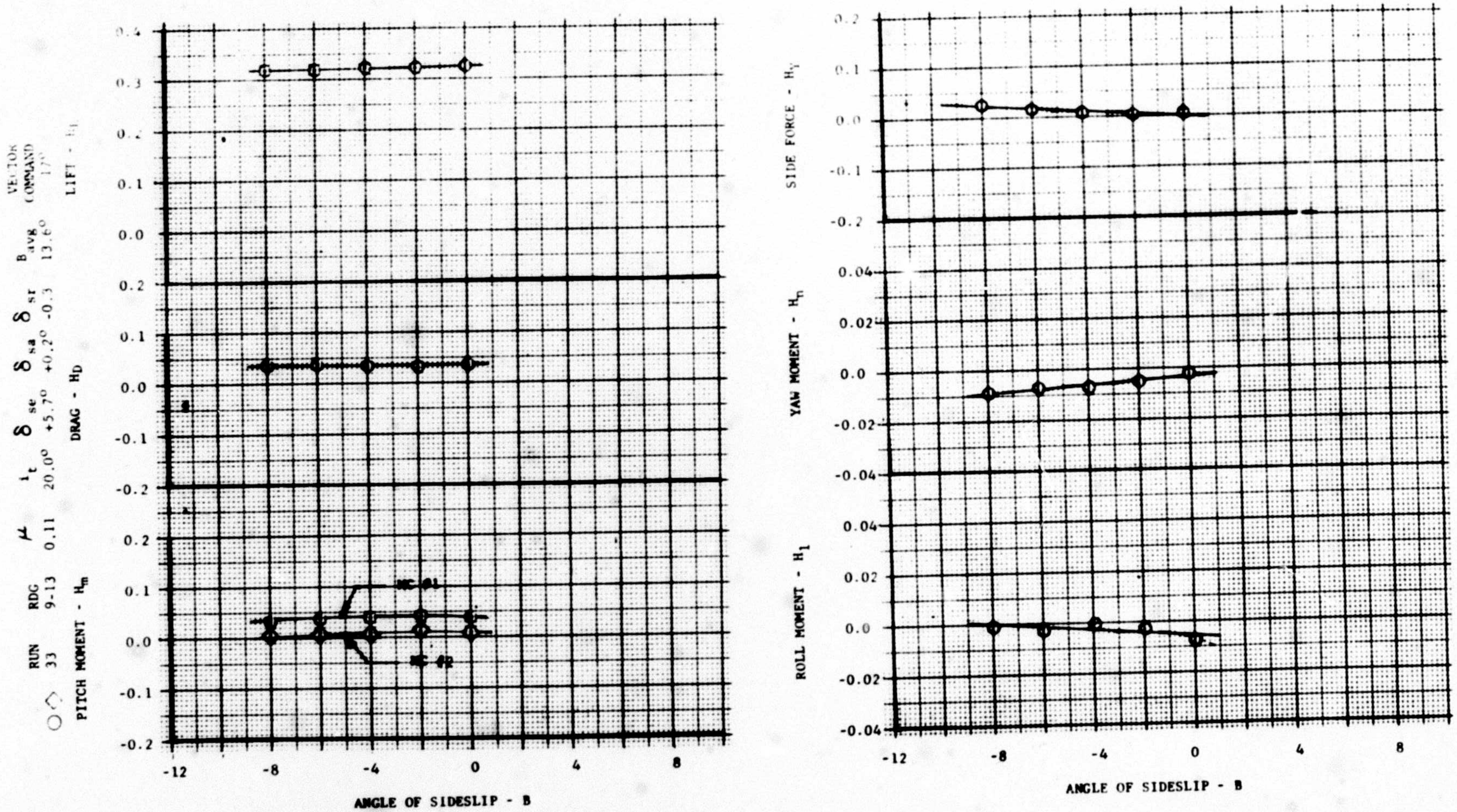

FIGURE 47
LATERAL DIRECTIONAL CHARACTERISTICS - FAN POWERED (LO-POWER)
NORMAL CONFIGURATION - $\mu = 0.11$, $\alpha = +6°$

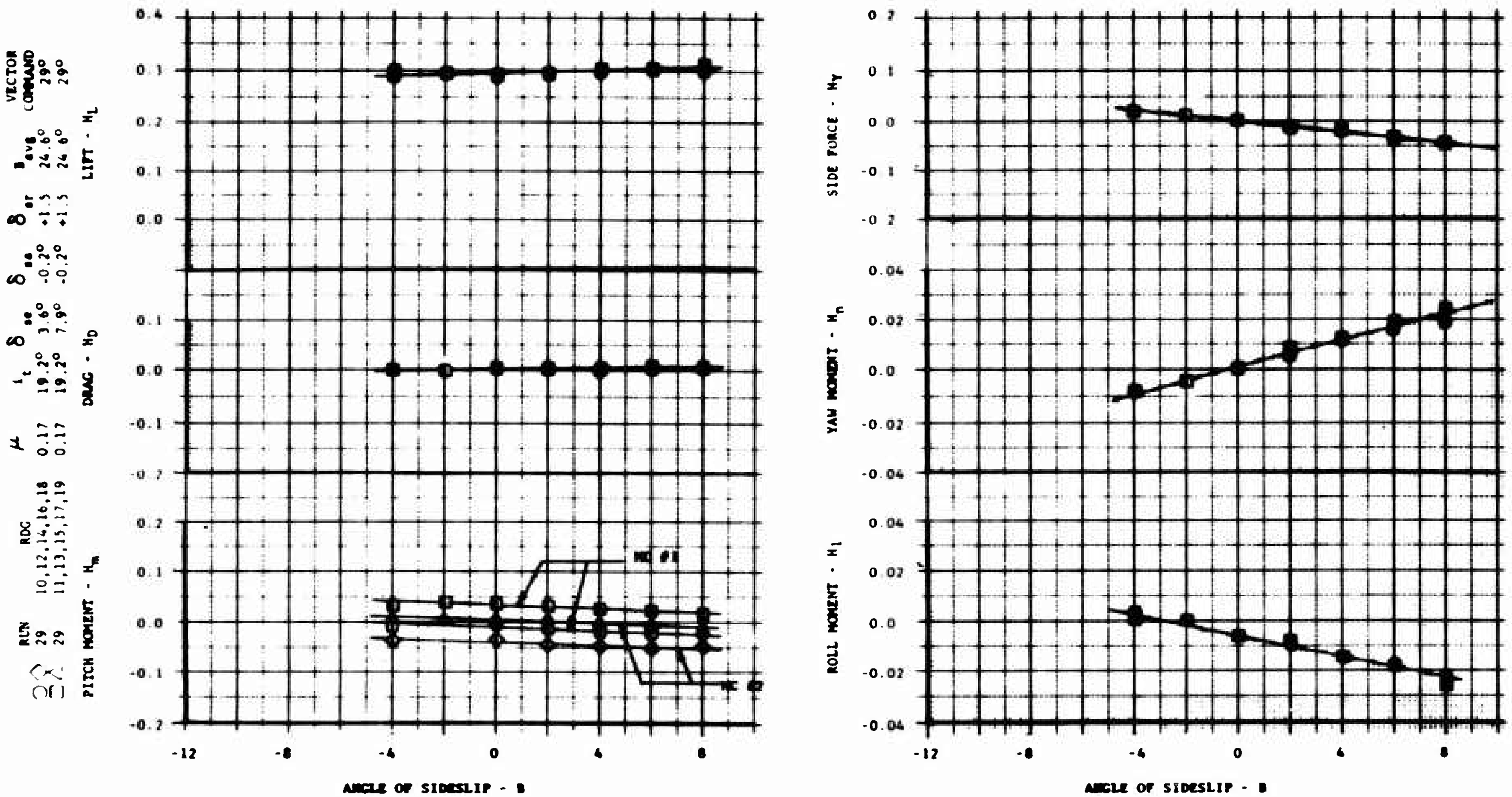

FIGURE 48
LATERAL DIRECTIONAL CHARACTERISTICS - FAN POWERED (LO-POWER)
NORMAL CONFIGURATION - μ = 0.17

RUN	RDG	μ	i_t	δ_{se}	δ_{sa}	δ_{sr}	δ_{sc}	VECTOR COMMAND	MC#
4G	1,3,5	0.0	20°	1.8°	0.7°	-1	50	0°	2
5G	1,3,5	0.0	20°	0.8°	1.1°	-5		10°	2

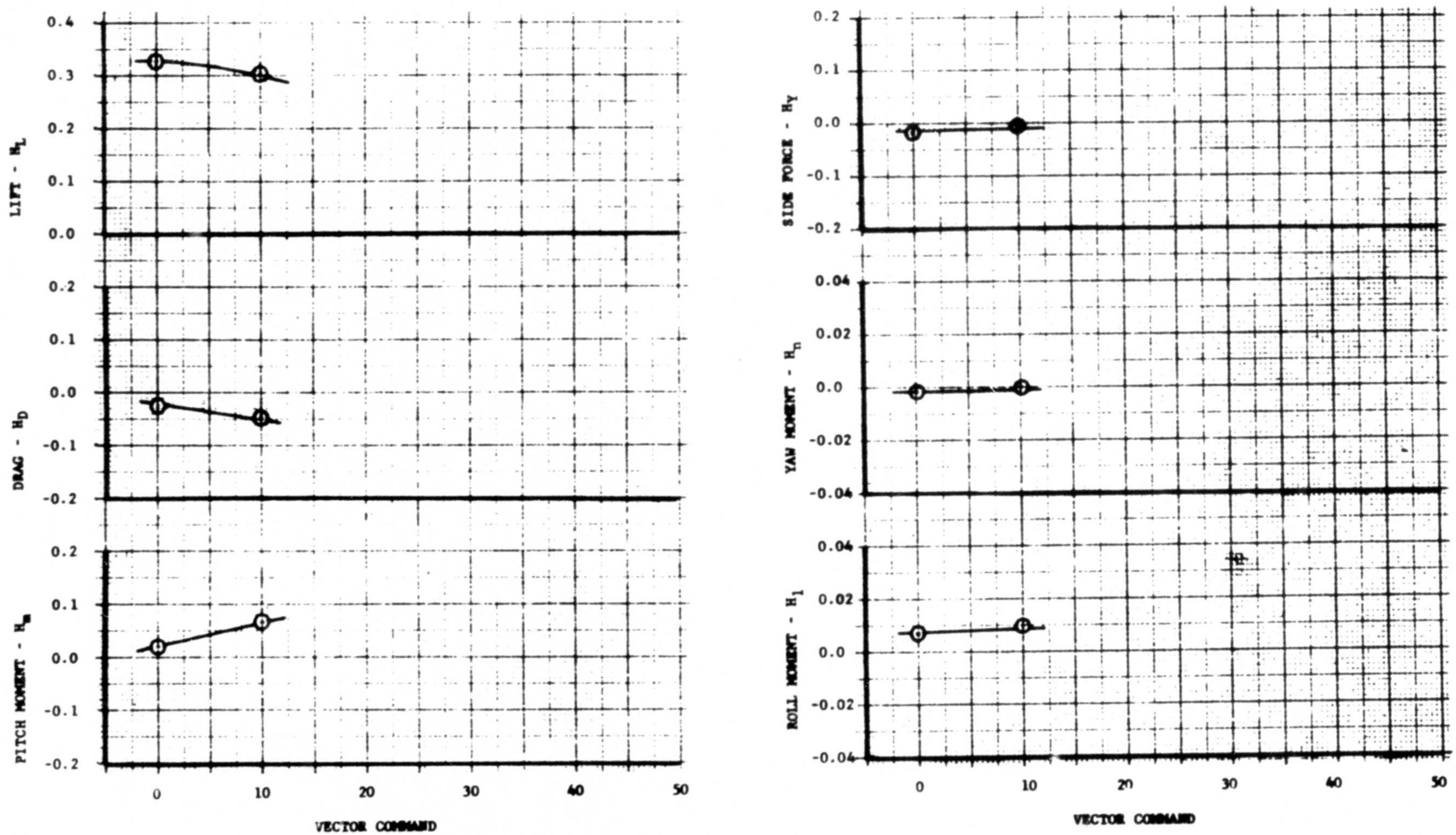

FIGURE 49

VECTOR EFFECTIVENESS - FAN POWERED (HI-POWER) $\mu = 0.0$

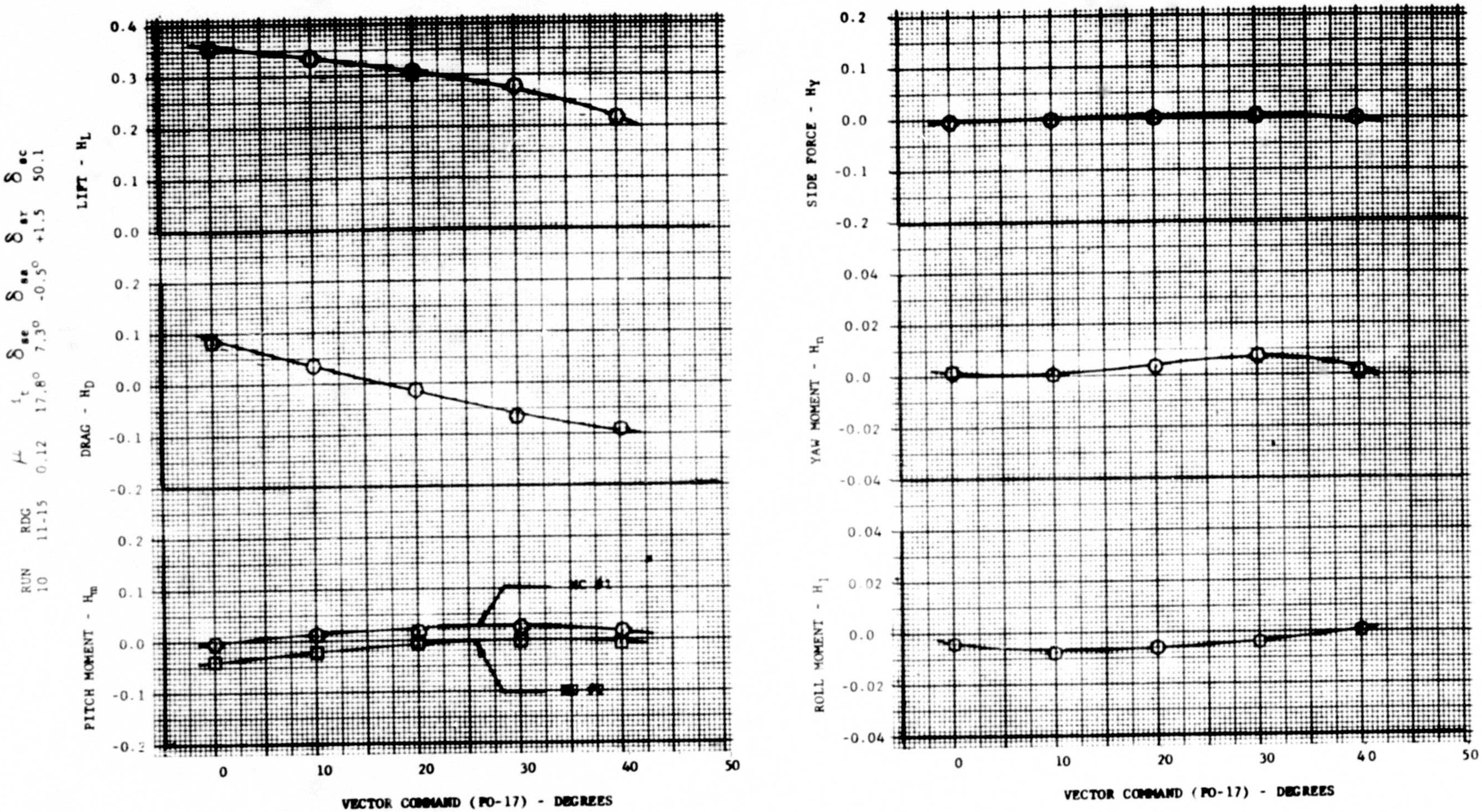

FIGURE 50
VECTOR EFFECTIVENESS - FAN POWERED (HI-POWER) - $\mu = 0.12$

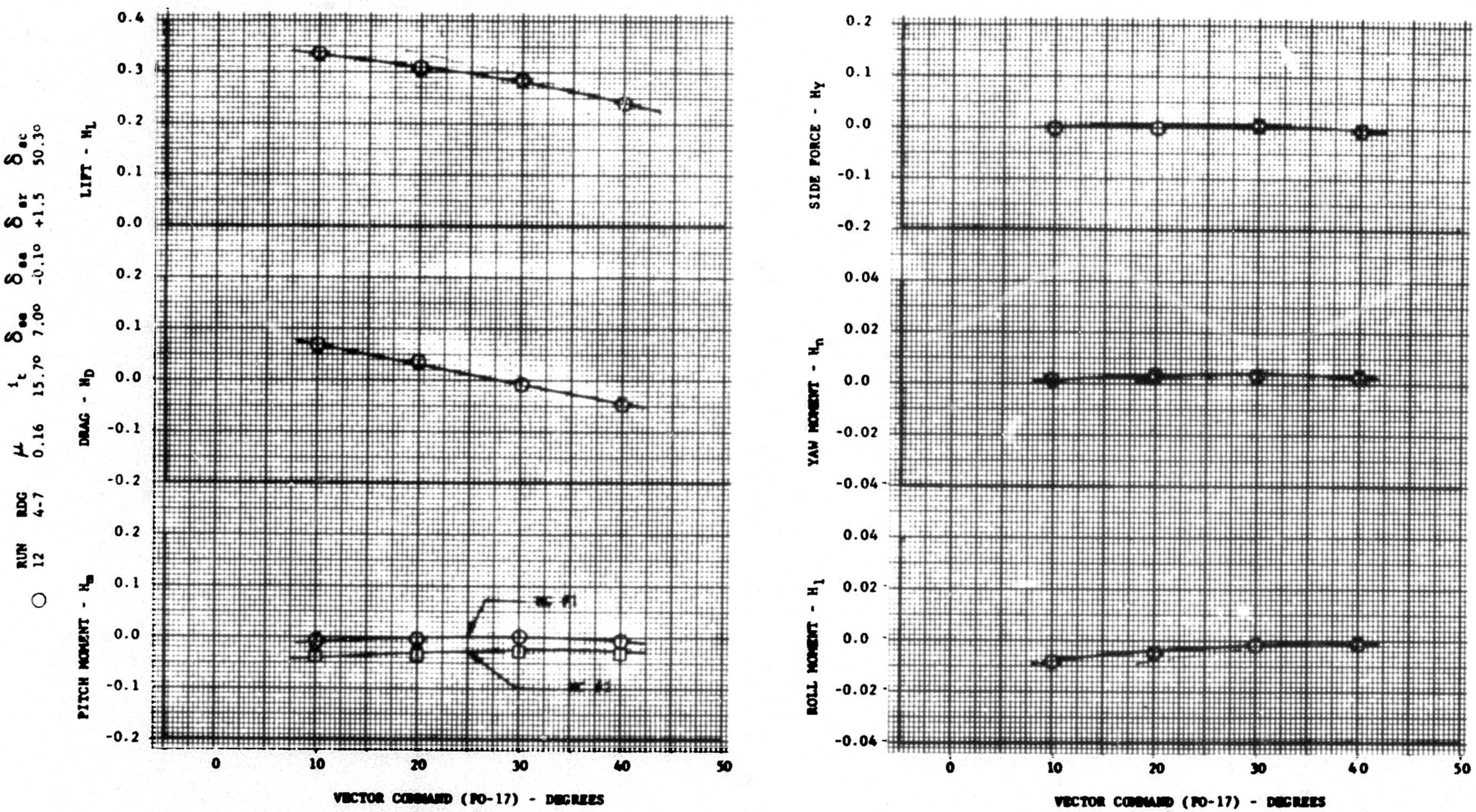

FIGURE 51
VECTOR EFFECTIVENESS - FAN POWERED (HI-POWER) - μ = 0.16

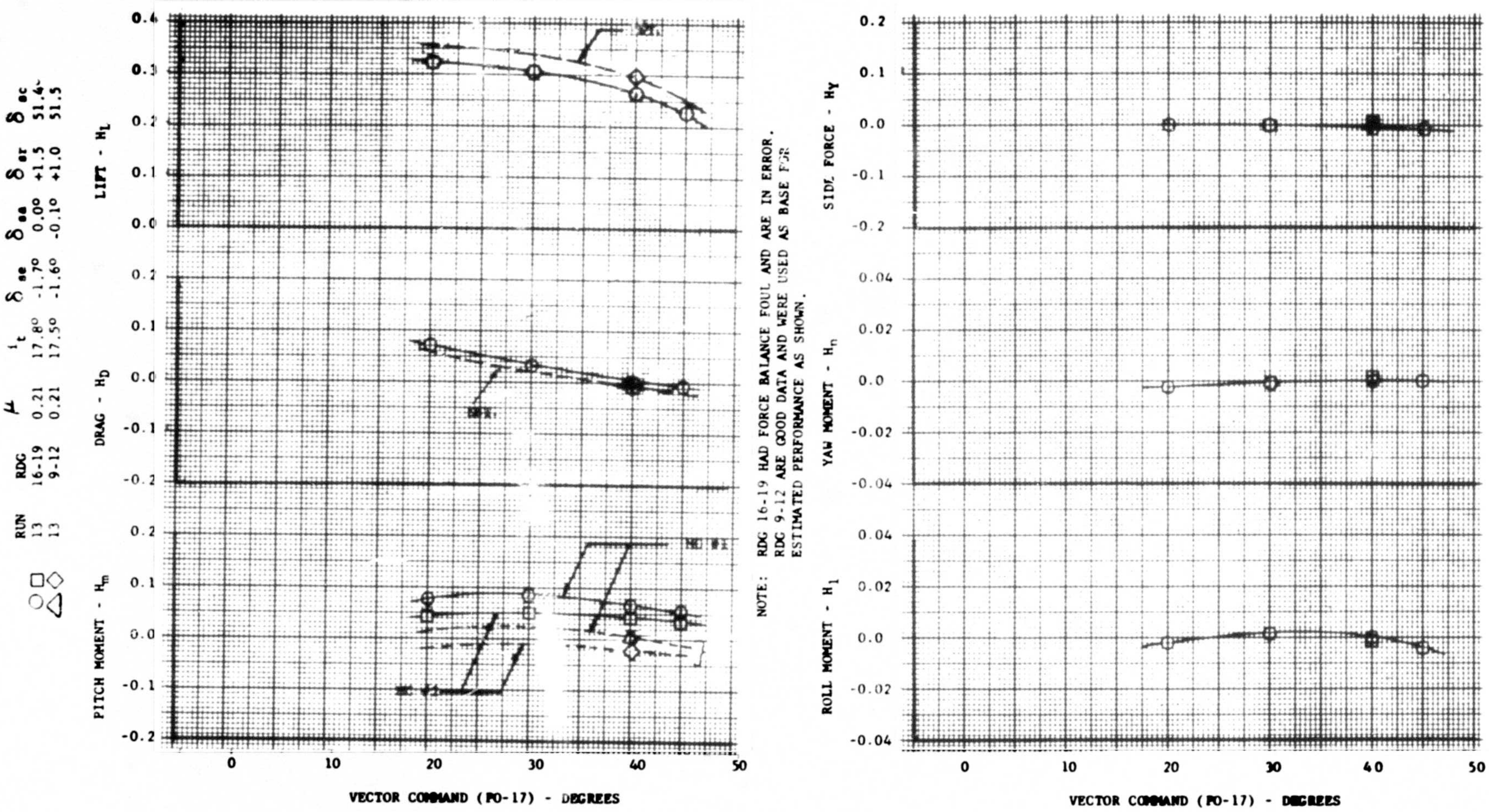

FIGURE 52
VECTOR EFFECTIVENESS - FAN POWERED (HI-POWER) - μ = 0.21

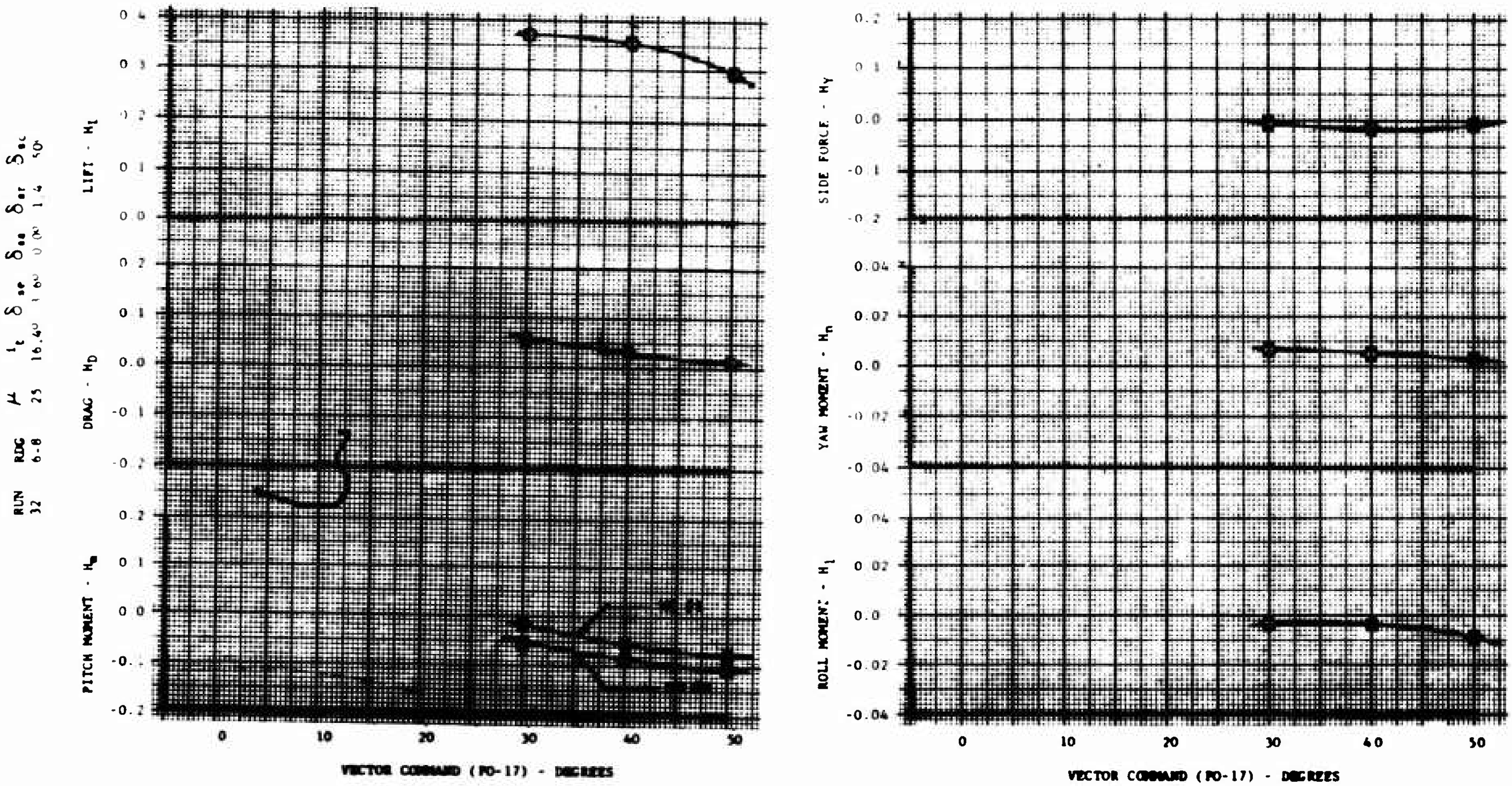

FIGURE 53
VECTOR EFFECTIVENESS - FAN POWERED (HI-POWER) - μ= 0.25

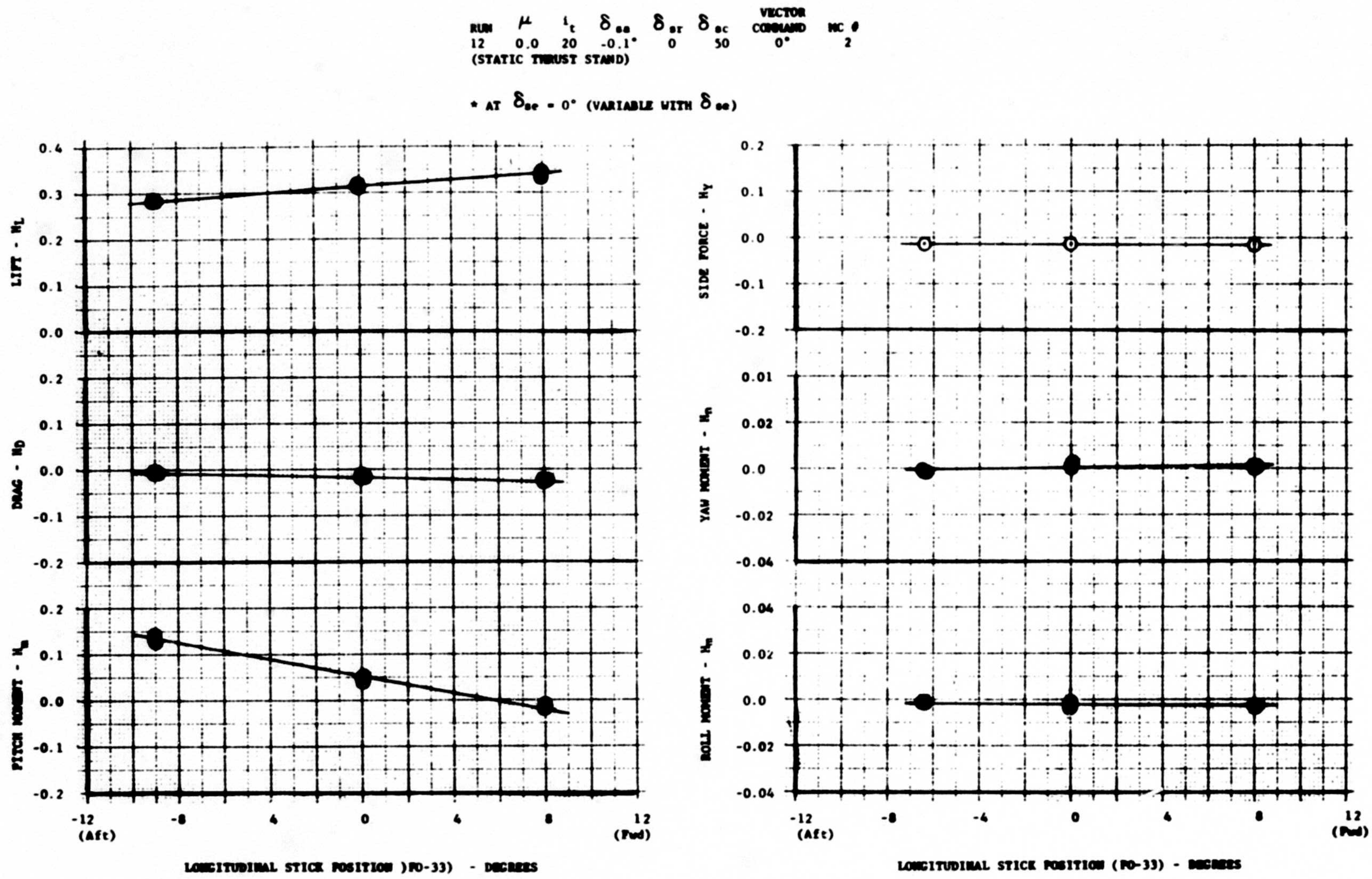

FIGURE 54

LONGITUDINAL CONTROL EFFECTIVENESS - FAN POWERED (HI-POWER) - μ = 0°

RUN	RDG	μ	i_t	δ_{sa}	δ_{sr}	δ_{sc}	VECTOR COMMAND
10	2,18-21	0.12	18.1°	0.2°*	1.8	49.6	16°

* AT δ_{se} = +7° (VARIABLE WITH δ_{se})

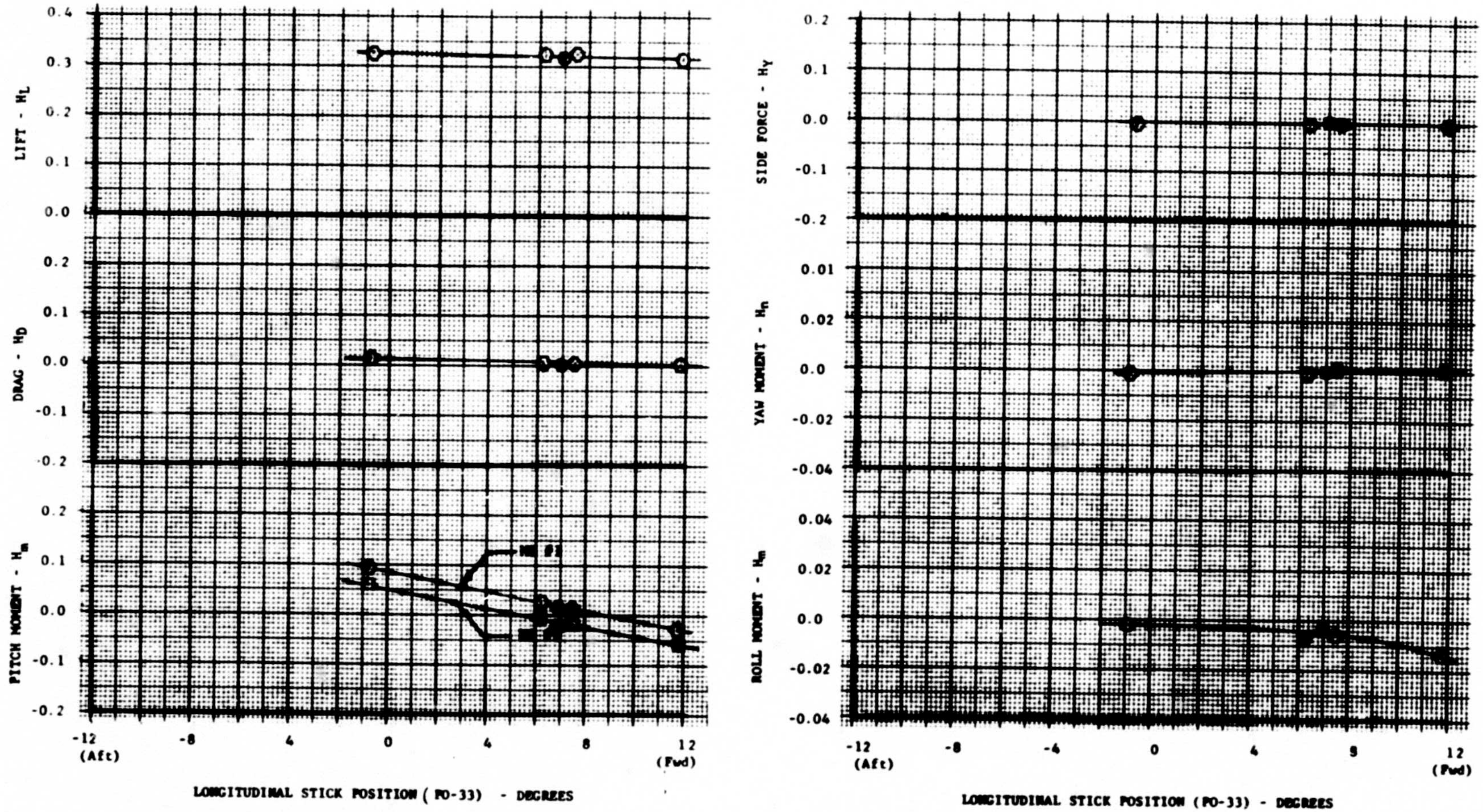

FIGURE 55
LONGITUDINAL CONTROL EFFECTIVENESS
FAN POWERED (HI-POWER)- μ= 0.12

RUN	RDG	μ	i_t	δ_{sa}	δ_{sr}	δ_{sc}	VECTOR COMMAND
11	1	0.16	17.6°	0.0°	0.8	50.5	30°
12	8-10	0.17	17.5°	-0.1°*	1.5	50.4	29°

* AT δ_{se} = +6° (VARIABLE WITH δ_{se})

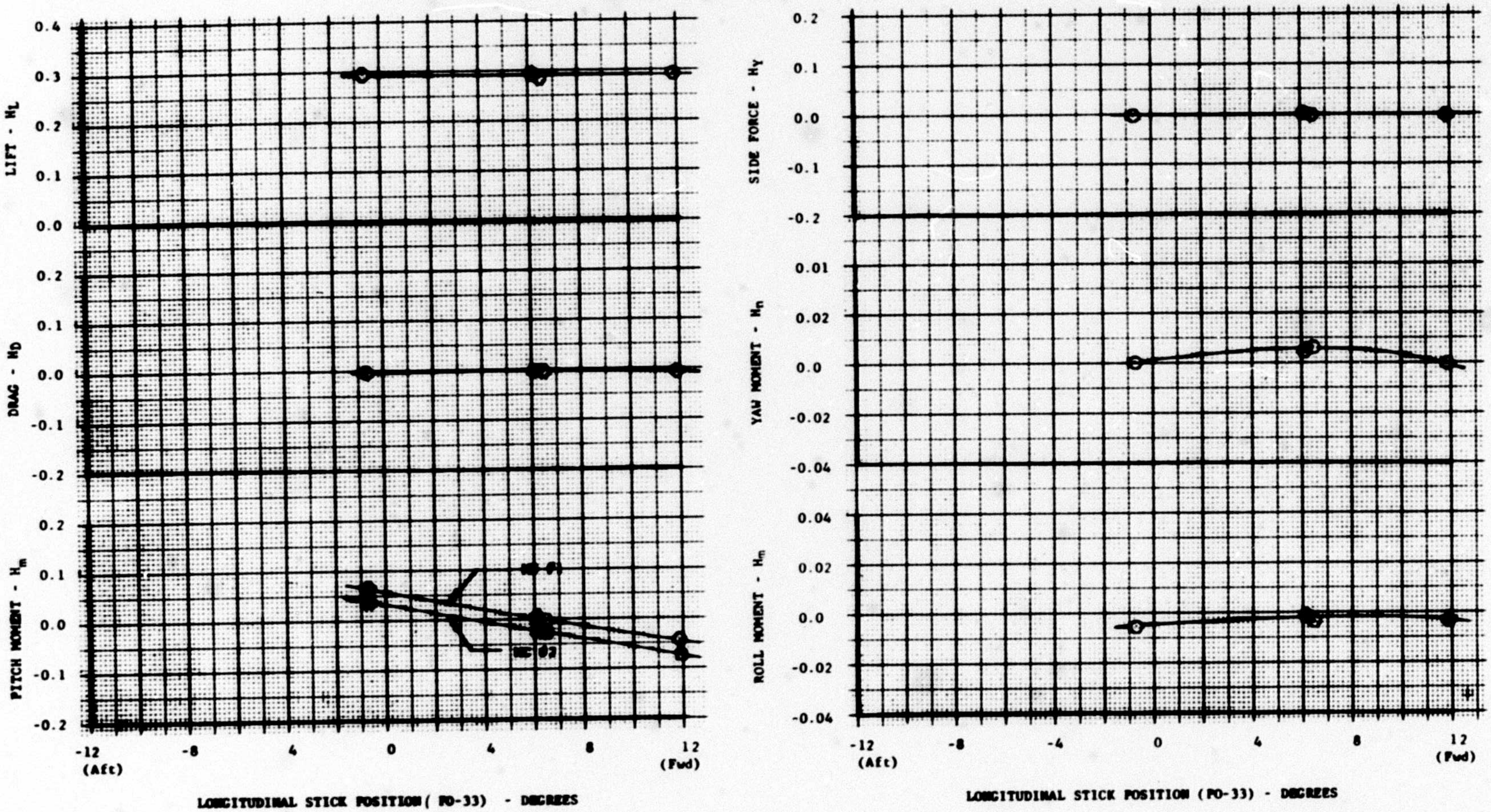

FIGURE 56
LONGITUDINAL CONTROL EFFECTIVENESS
FAN POWERED (HI-POWER) - μ= 0.17

RUN	RDG	μ	i_t	δ_{sa}	δ_{sr}	δ_{sc}	VECTOR COMMAND
13	20-23	0.22	18.1°	0.5°*	2.0	51.3	41°

* AT δ_{se} = -1° (VARIABLE WITH δ_{se})

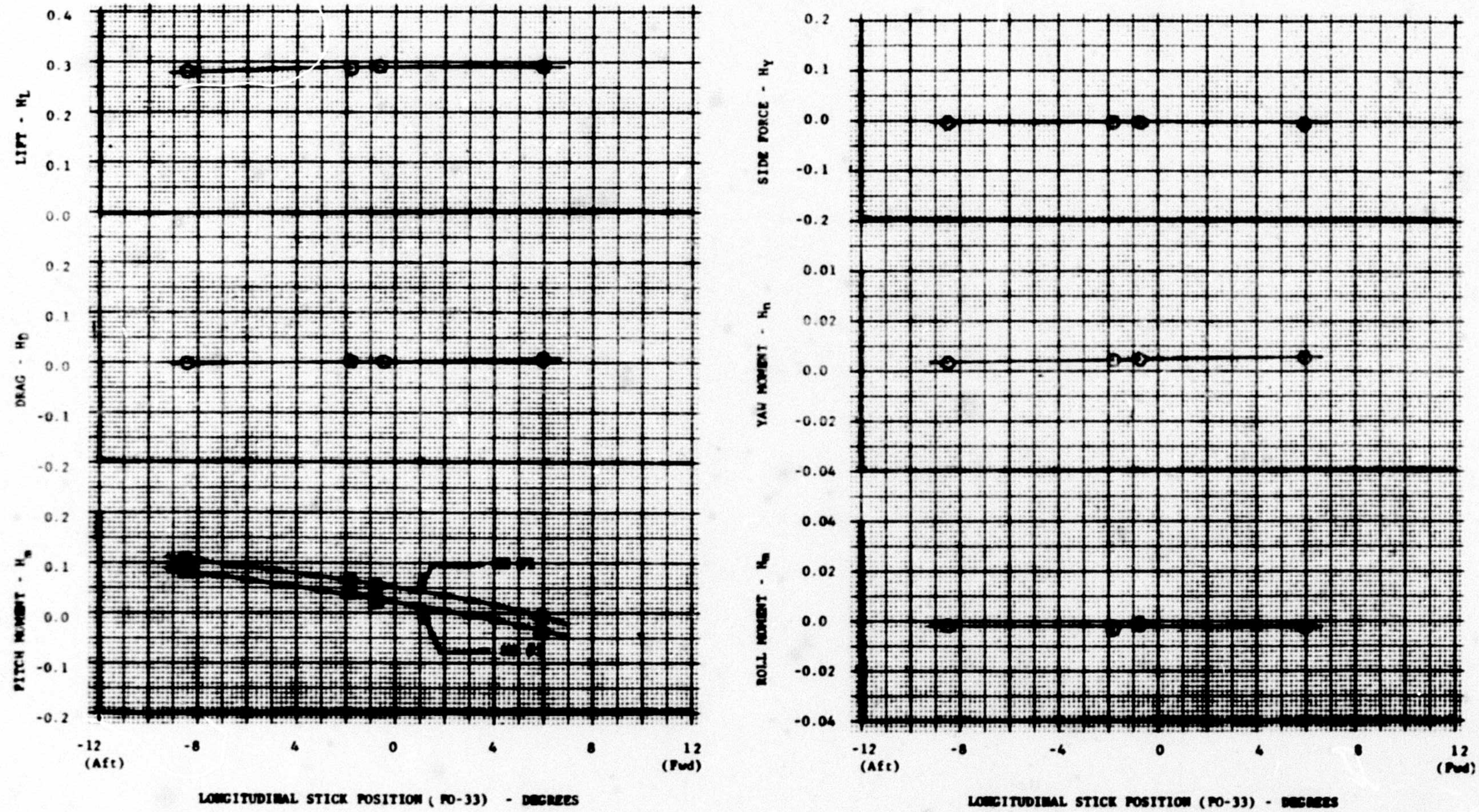

FIGURE 57
LONGITUDINAL CONTROL EFFECTIVENESS
FAN POWERED (HI-POWER) - μ = 0.22

RUN	RDG	μ	i_t	δ_{se}	δ_{sr}	δ_{sc}	VECTOR COMMAND
31	1,4,8	0.26	15.5°	VAR	0.1*	50	50°
32	1-3	0.25	16.0°	VAR	0.3**	50	50°

* AT (δ_{se} = -4.5°) VARIABLE WITH δ_{se}
** AT (δ_{se} = -8.0°)

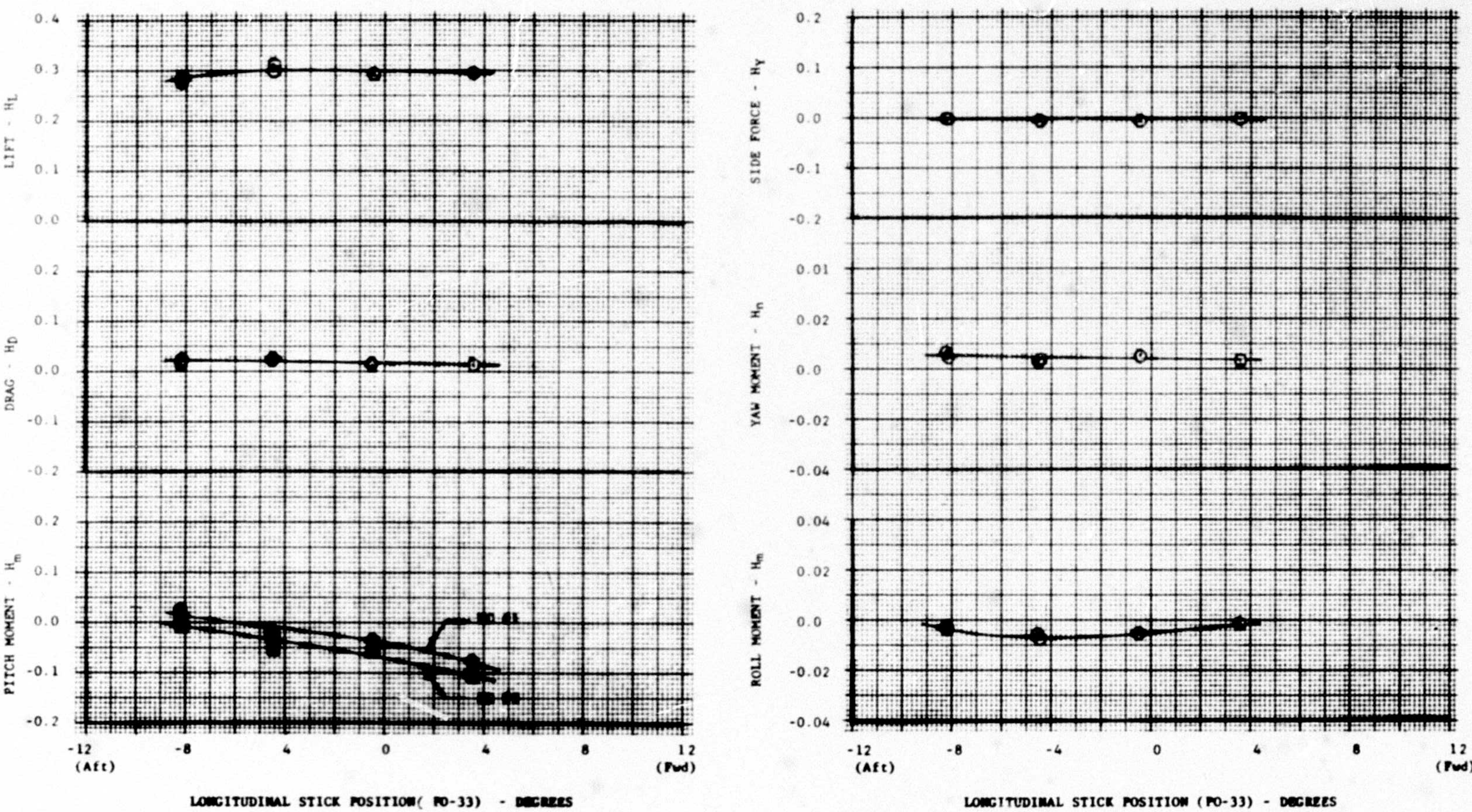

FIGURE 58
LONGITUDINAL CONTROL EFFECTIVENESS
FAN POWERED (HI-POWER) - μ = 0.25

RUN	μ	i_t	δ_{se}	δ_{sr}	δ_{sc}
3	0.0	20°	-0.3°*	0	50

* AT δ_{sa} = 0° (VARIABLE WITH δ_{sa})

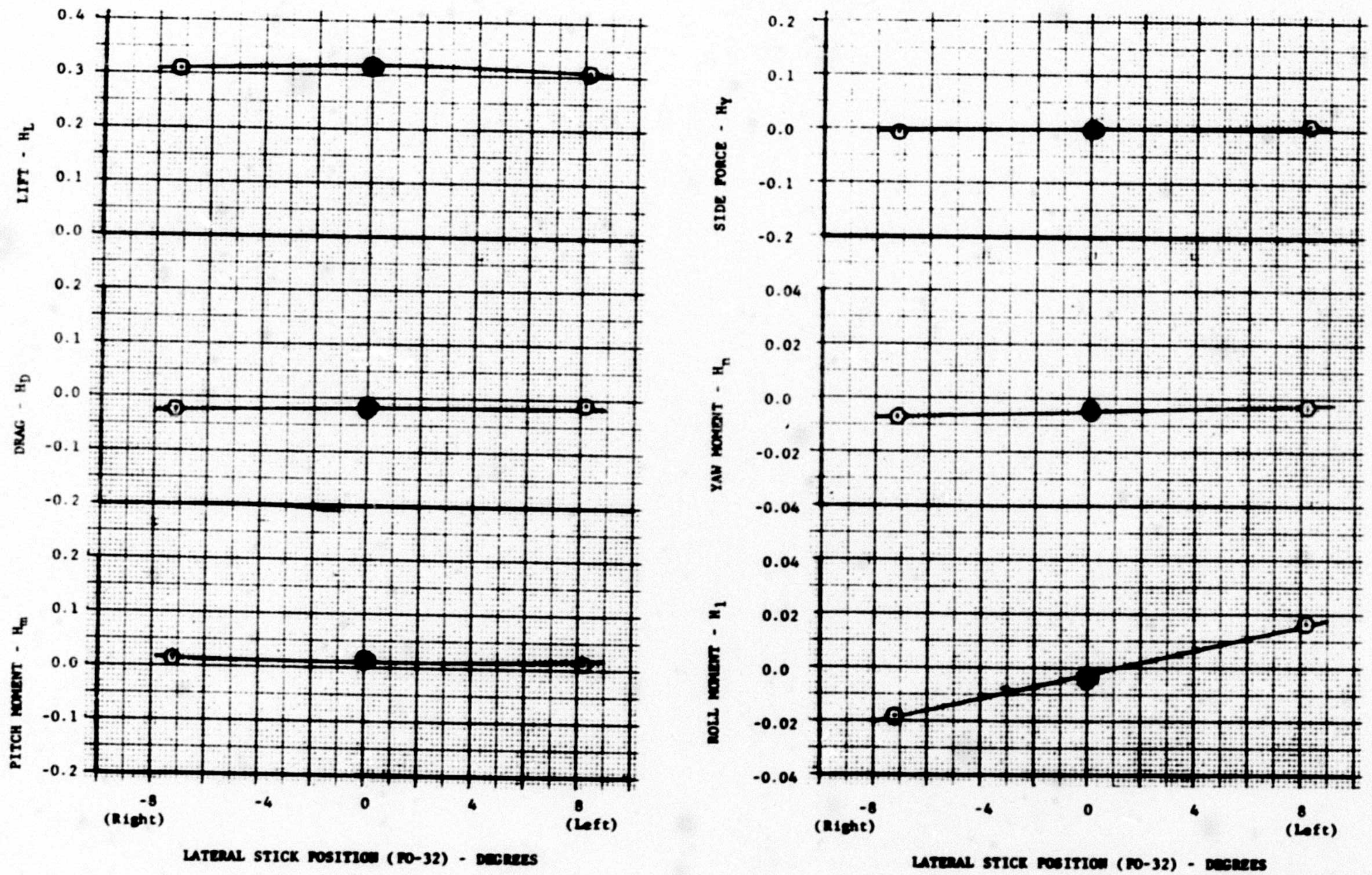

FIGURE 59
LATERAL CONTROL EFFECTIVENESS
FAN POWERED (HI-POWER) - μ = 0.0

RUN	RDG	μ	i_t	δ_{se}	δ_{sr}	δ_{sc}	VECTOR COMMAND
10	21-25	0.12	18.1°	7.5°*	+2.0	49.6	16°

* AT δ_{sa} = +1°(VARIABLE WITH δ_{sa})

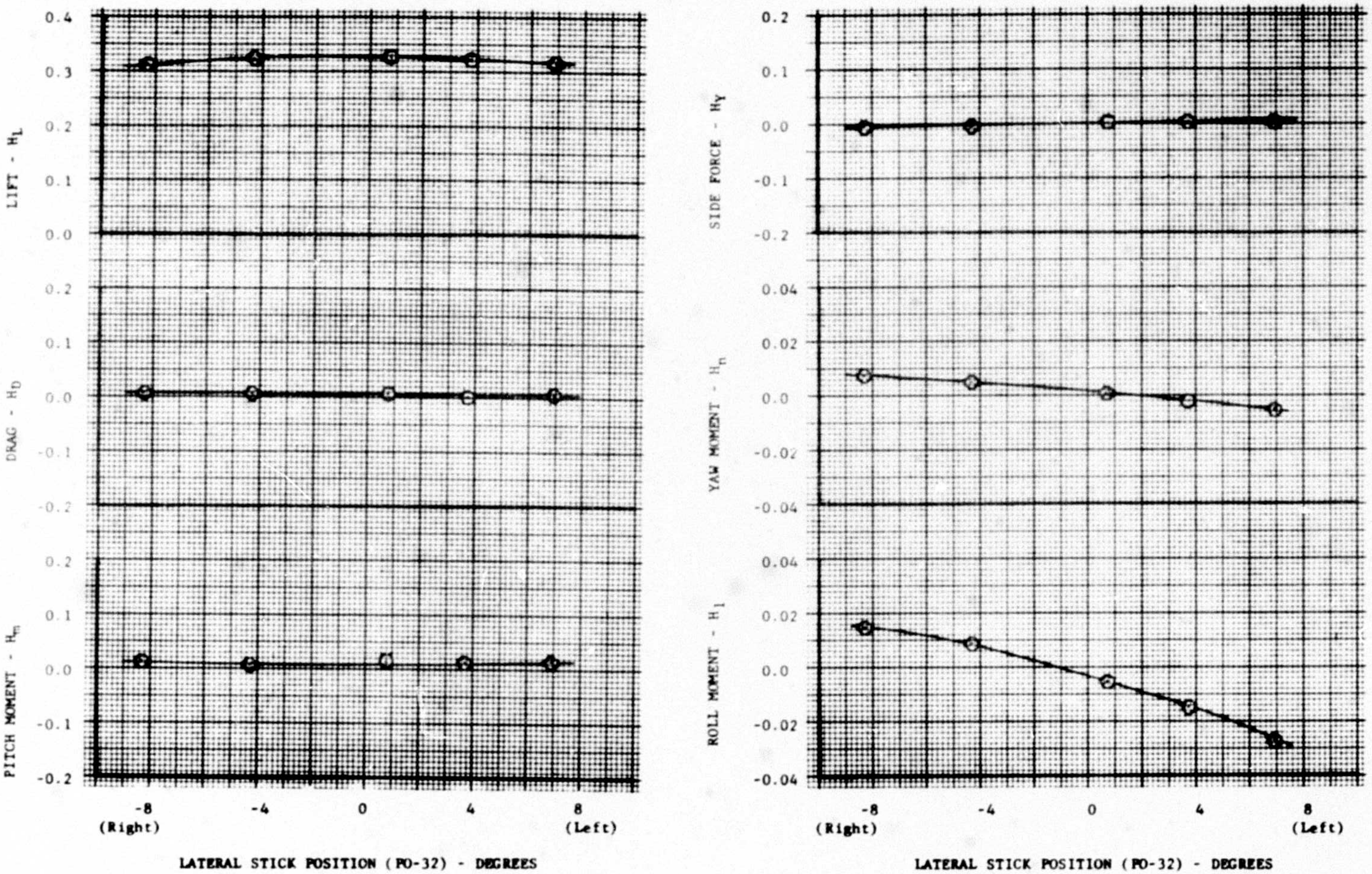

FIGURE 60
LATERAL CONTROL EFFECTIVENESS
FAN POWERED (HI-POWER) - μ= 0.12

RUN	RDG	μ	i_t	δ_{se}	δ_{sr}	δ_{sc}	VECTOR COMMAND	MC #
12	13-17	0.17	17.7°	6.9°*	2.1	50.9	29°	1

* AT δ_{sa} = 0° (VARIABLE WITH δ_{sa})

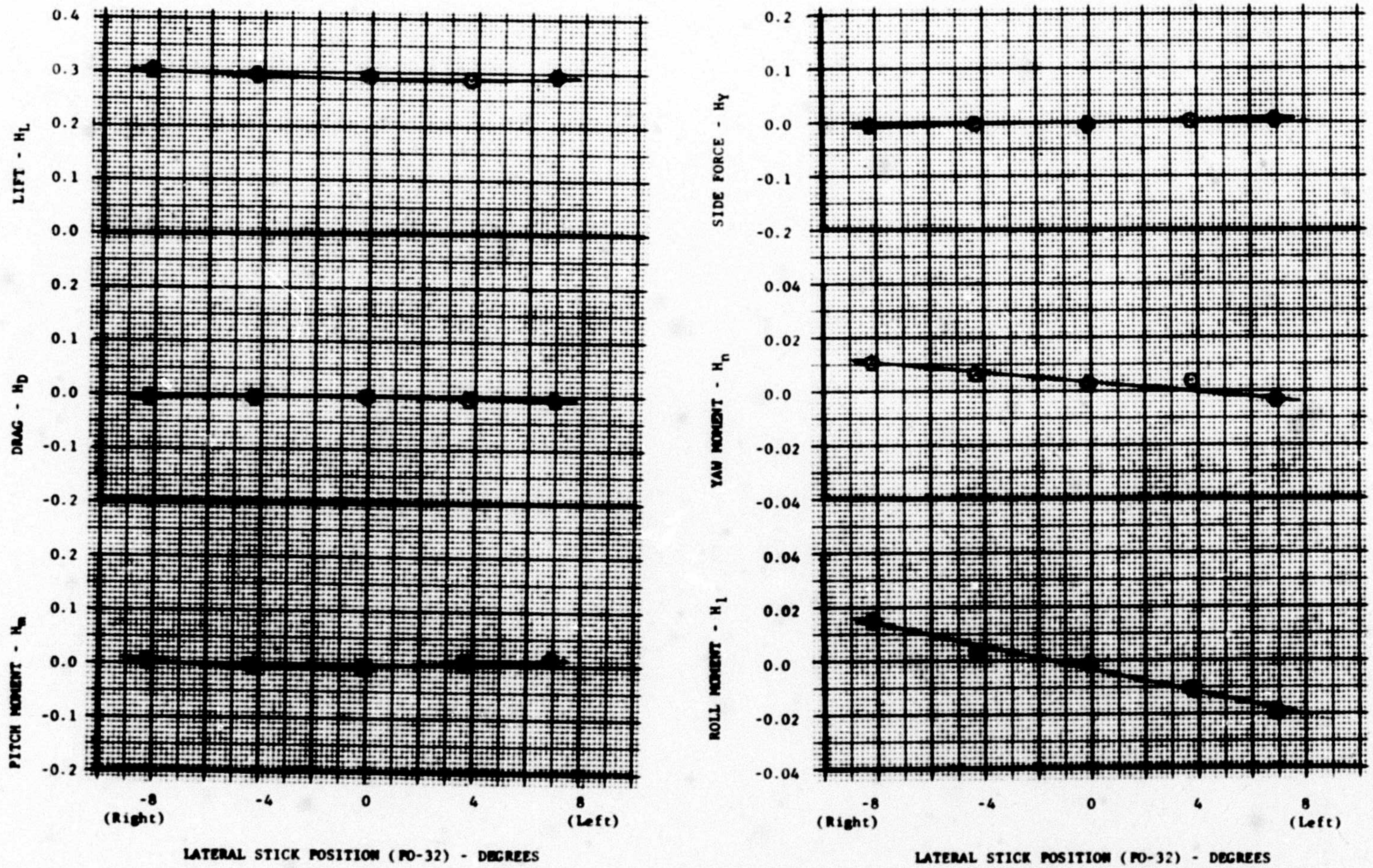

FIGURE 61
LATERAL CONTROL EFFECTIVENESS
FAN POWERED (HI-POWER) - μ = 0.17

RUN	RDG	μ	i_t	δ_{se}	δ_{sr}	δ_{sc}	VECTOR COMMAND	MC #
12	13-17	0.17	17.7°	6.9°*	2.1	50.9	29°	1

* AT δ_{sa} = 0°(VARIABLE WITH δ_{sa})

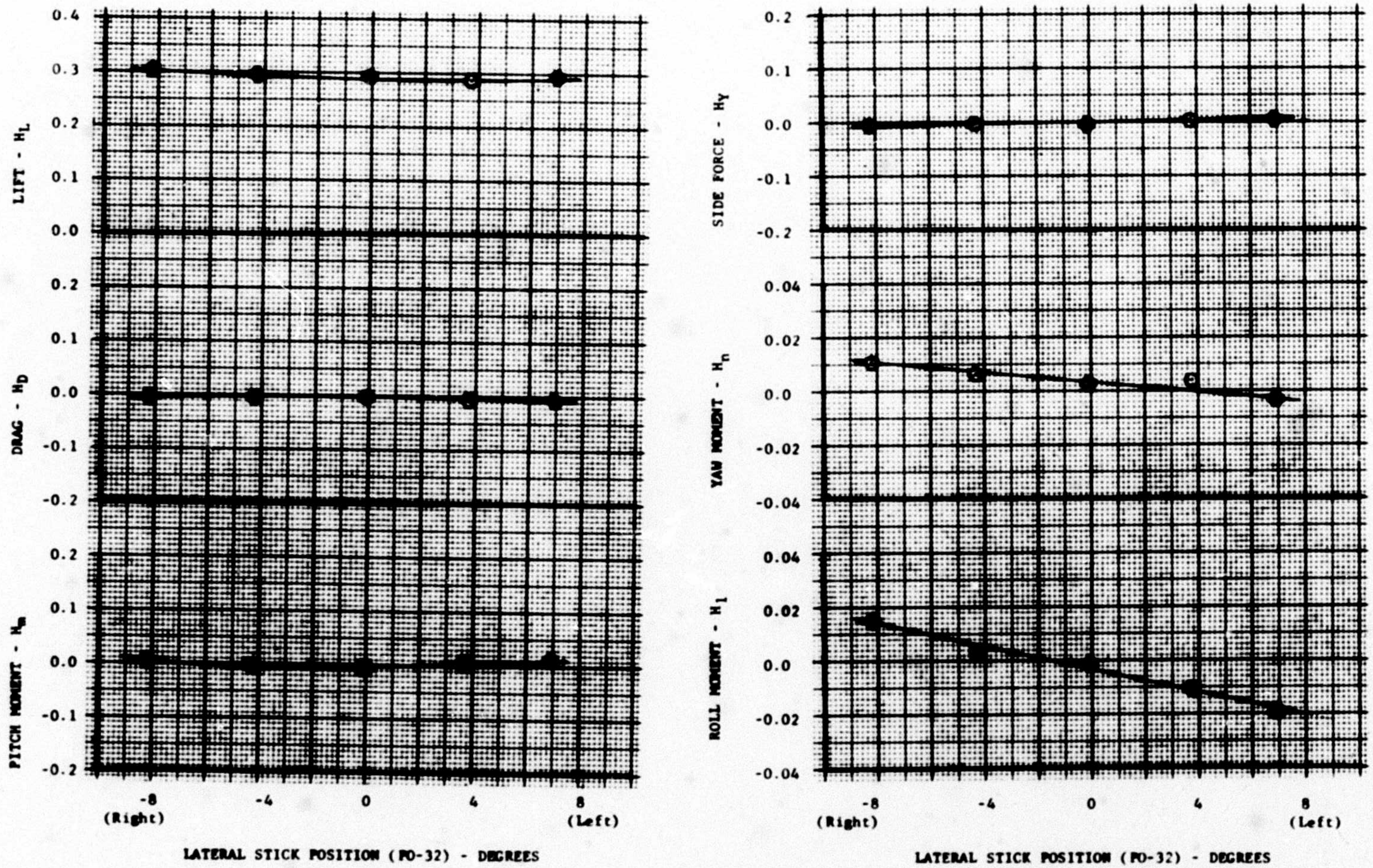

FIGURE 61
LATERAL CONTROL EFFECTIVENESS
FAN POWERED (HI-POWER) - μ = 0.17

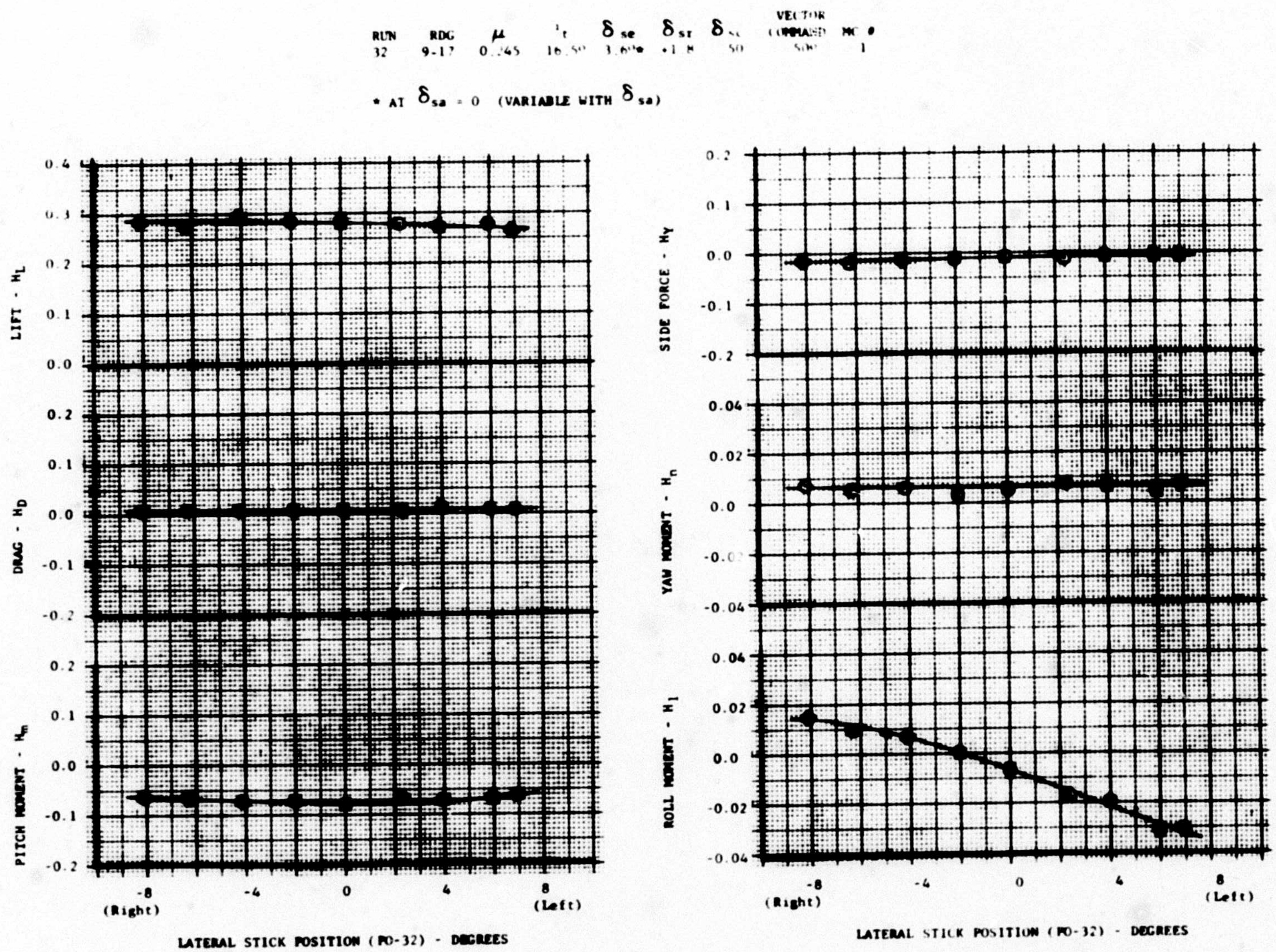

FIGURE 63
LATERAL CONTROL EFFECTIVENESS
FAN POWERED (HI-POWER) - μ= 0.245

RUN	RDG	μ	i_t	δ_{se}	δ_{sr}	δ_{sc}	VECTOR COMMAND	MC #
33	21-23	0.075	19.5°	4.2°*	1.3	50	11°	1

* AT δ_{sa} = 0° (VARIABLE WITH δ_{sa})

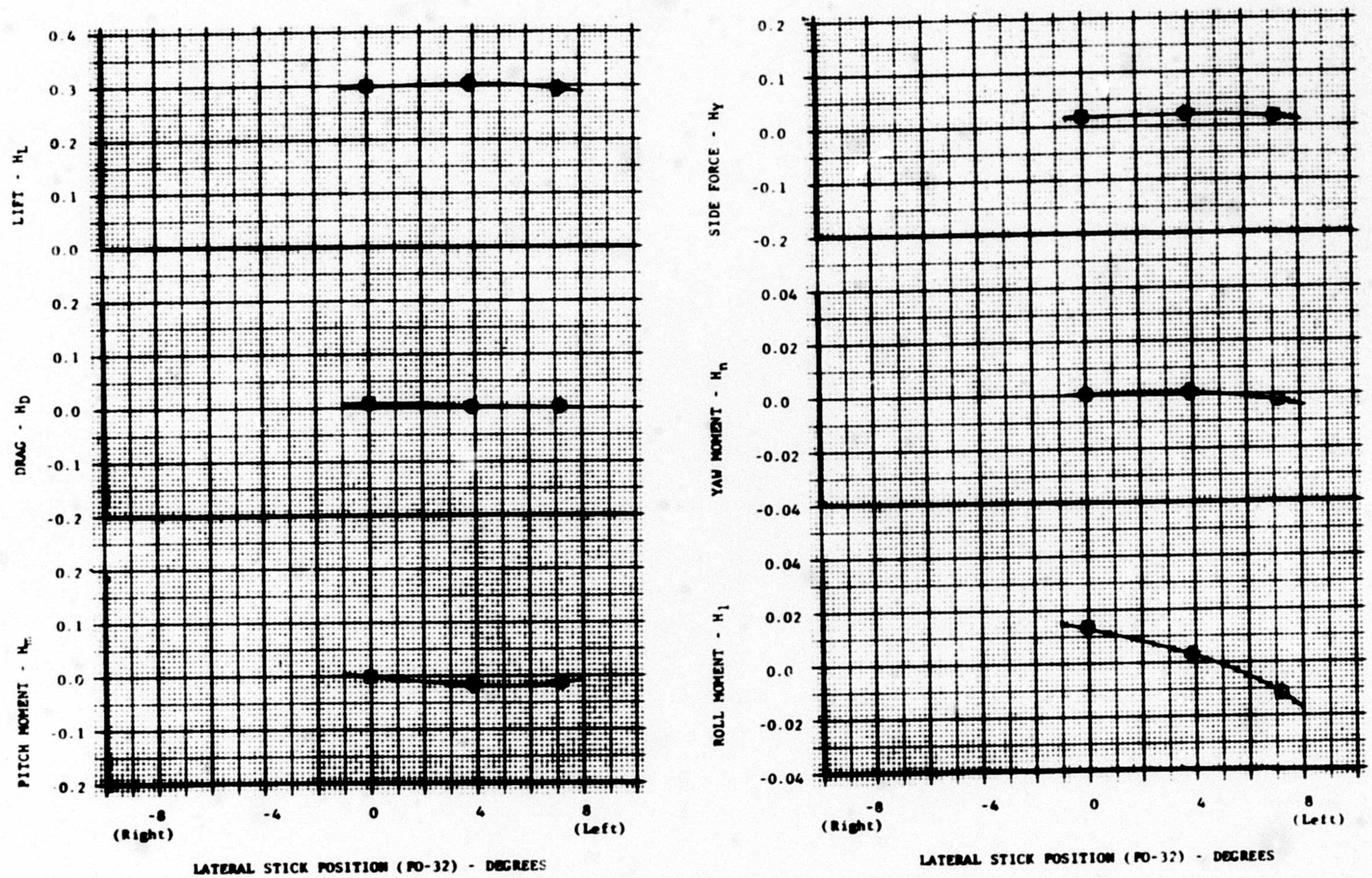

FIGURE 64
LATERAL CONTROL EFFECTIVENESS
FAN POWERED (LO-POWER) - μ= 0.075, β = -12

RUN	RDG	μ	i_t	δ_{se}	δ_{sr}	δ_{sc}	VECTOR COMMAND	MC #
33	13-15	0.11	19.6°	5.7°*	-0.5	50	17°	1

* AT δ_{sa} = 0° (VARIABLE WITH δ_{sa})

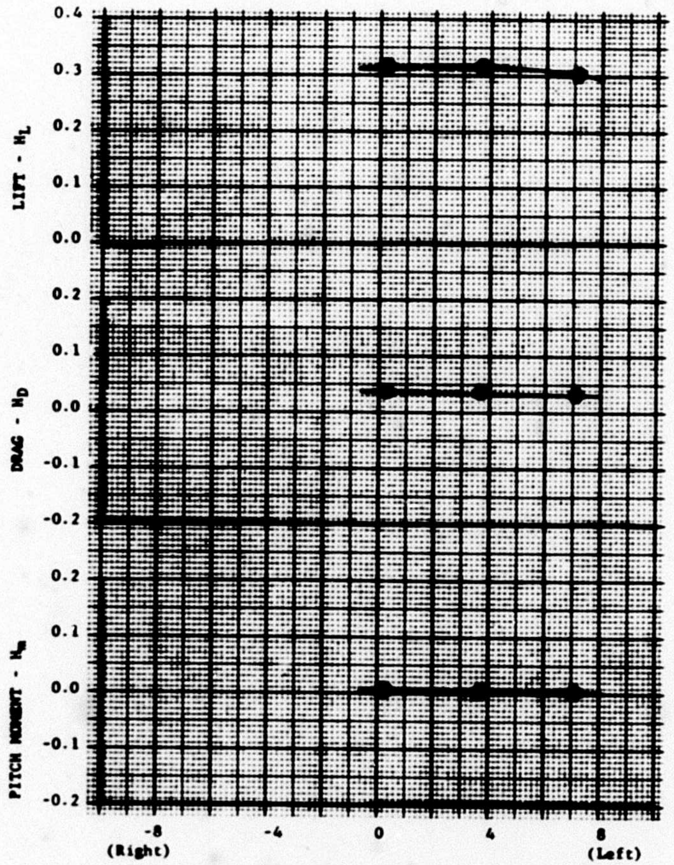

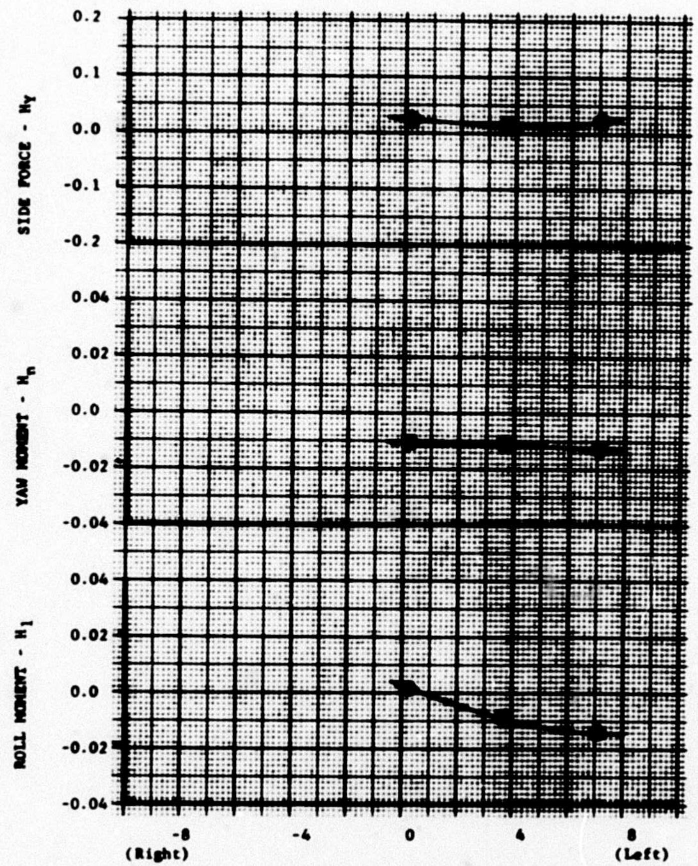

FIGURE 65
LATERAL CONTROL EFFECTIVENESS - FAN POWERED (LO-POWER)
μ = 0.11 α = 6 β = -8

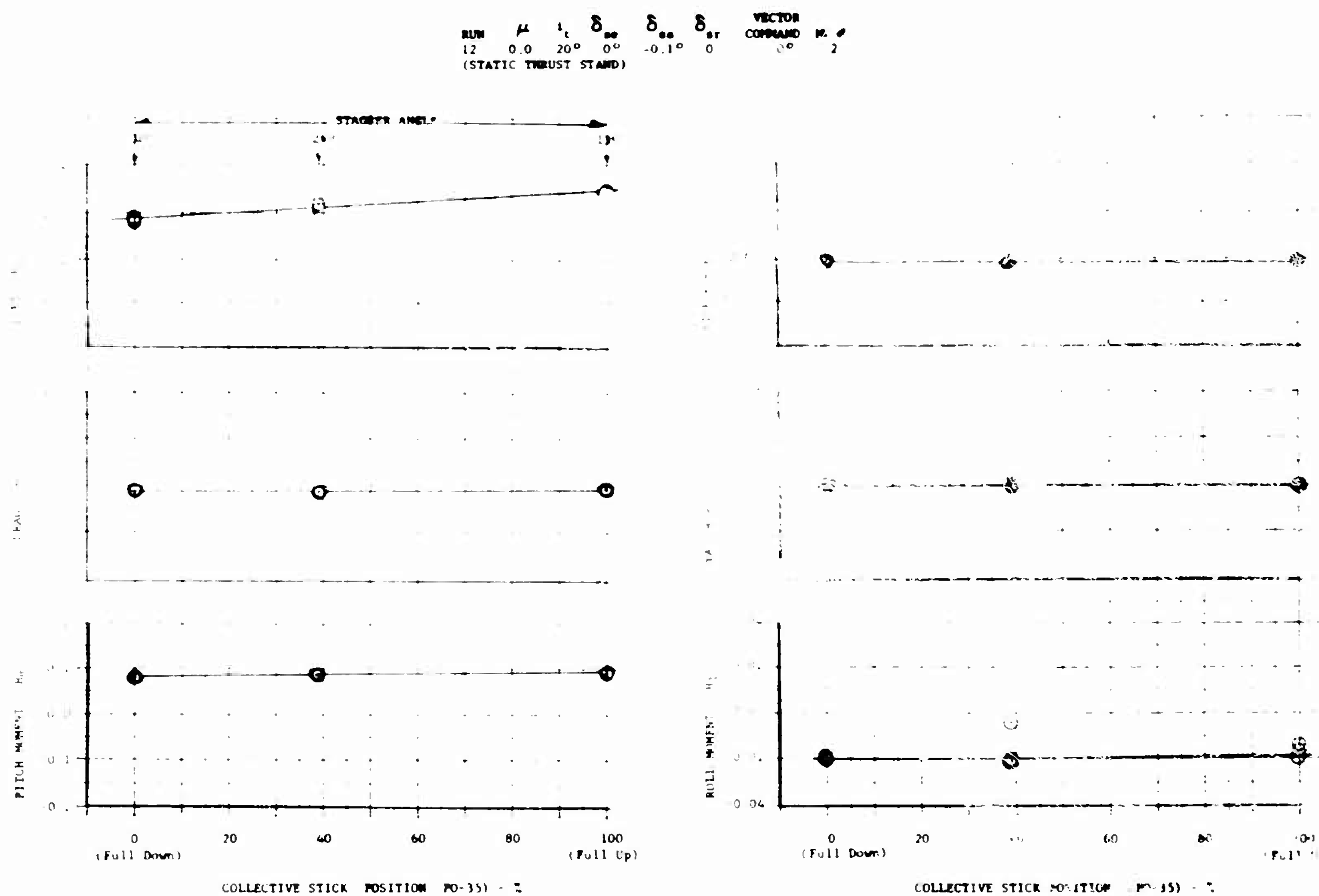

FIGURE 66
COLLECTIVE CONTROL EFFECTIVENESS - FAN POWERED (HI-POWER)
$\mu = 0.0$

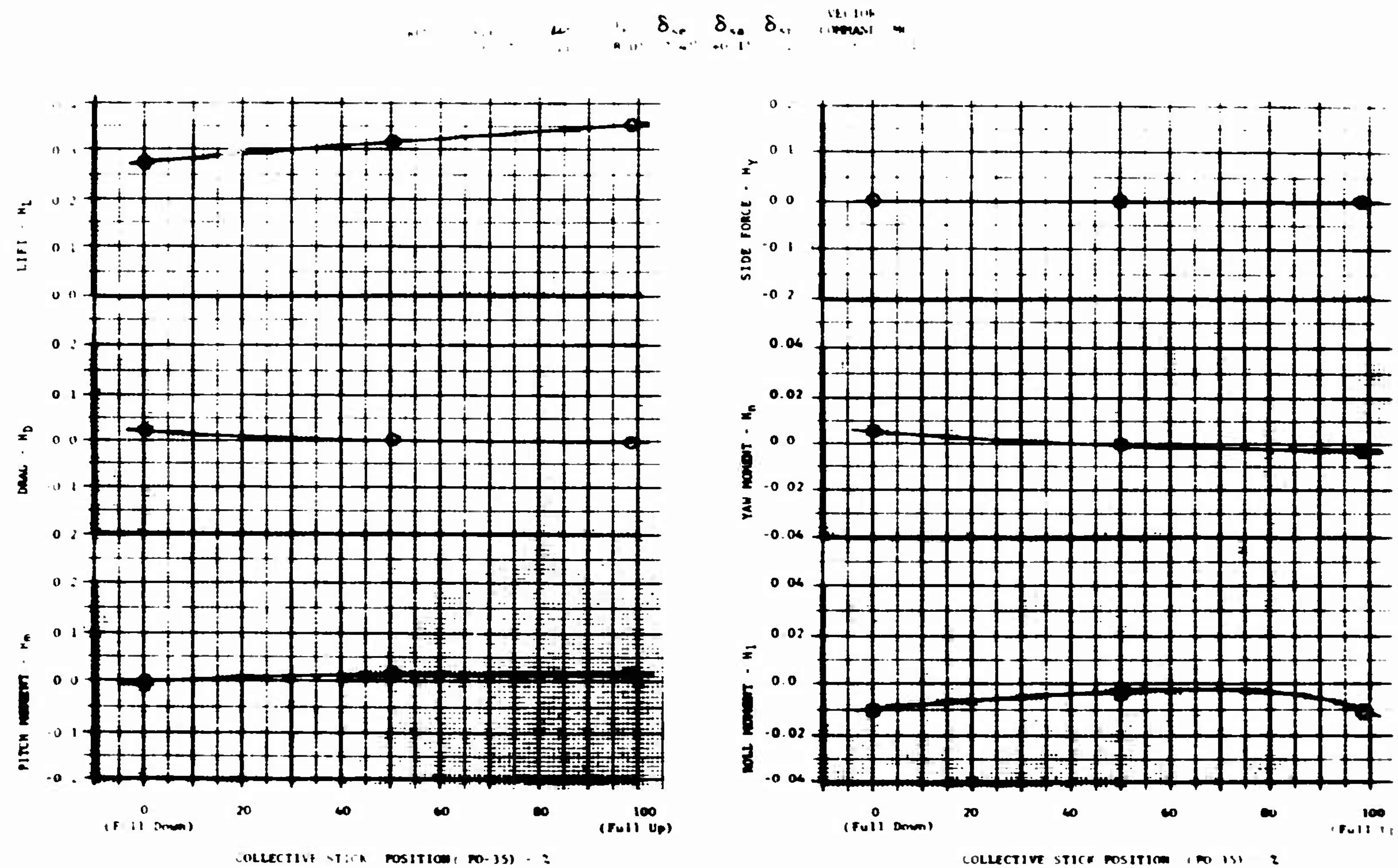

FIGURE 67
COLLECTIVE CONTROL EFFECTIVENESS - FAN POWERED (HI-POWER)
$\mu = 0.115$

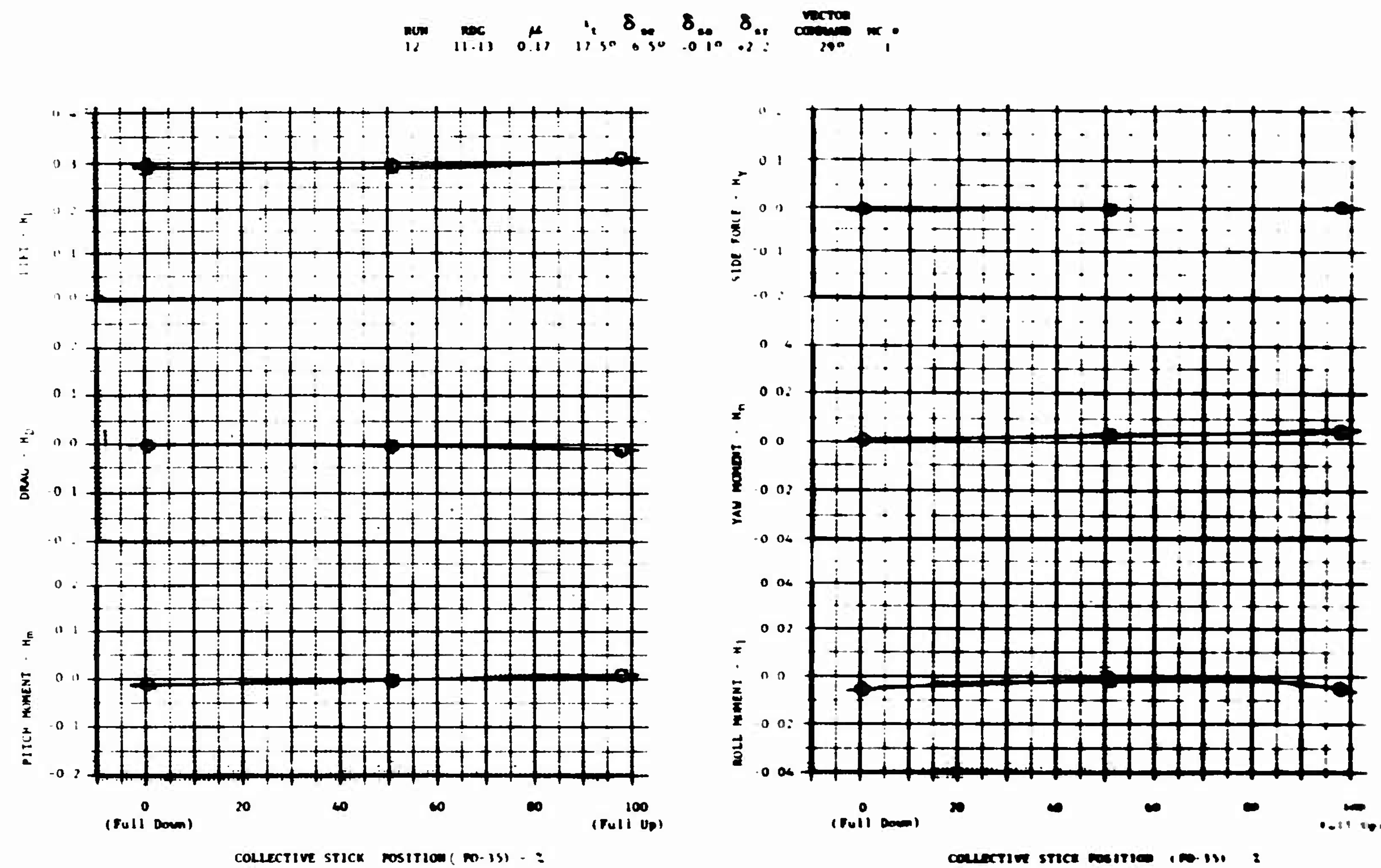

FIGURE 68
COLLECTIVE CONTROL EFFECTIVENESS - FAN POWERED (HI-POWER)
$\mu = 0.17$

	RUN	RDG	μ	i_t	δ_{se}	δ_{sa}	δ_{sc}	VECTOR COMMAND	MC #
○	10	28-32	0.12	17.6°	7.6°	-0.1°	49.5°	16°	1
□	10	25-27	0.12	17.6°	7.2°	-8.3°	49.6°	16°	1

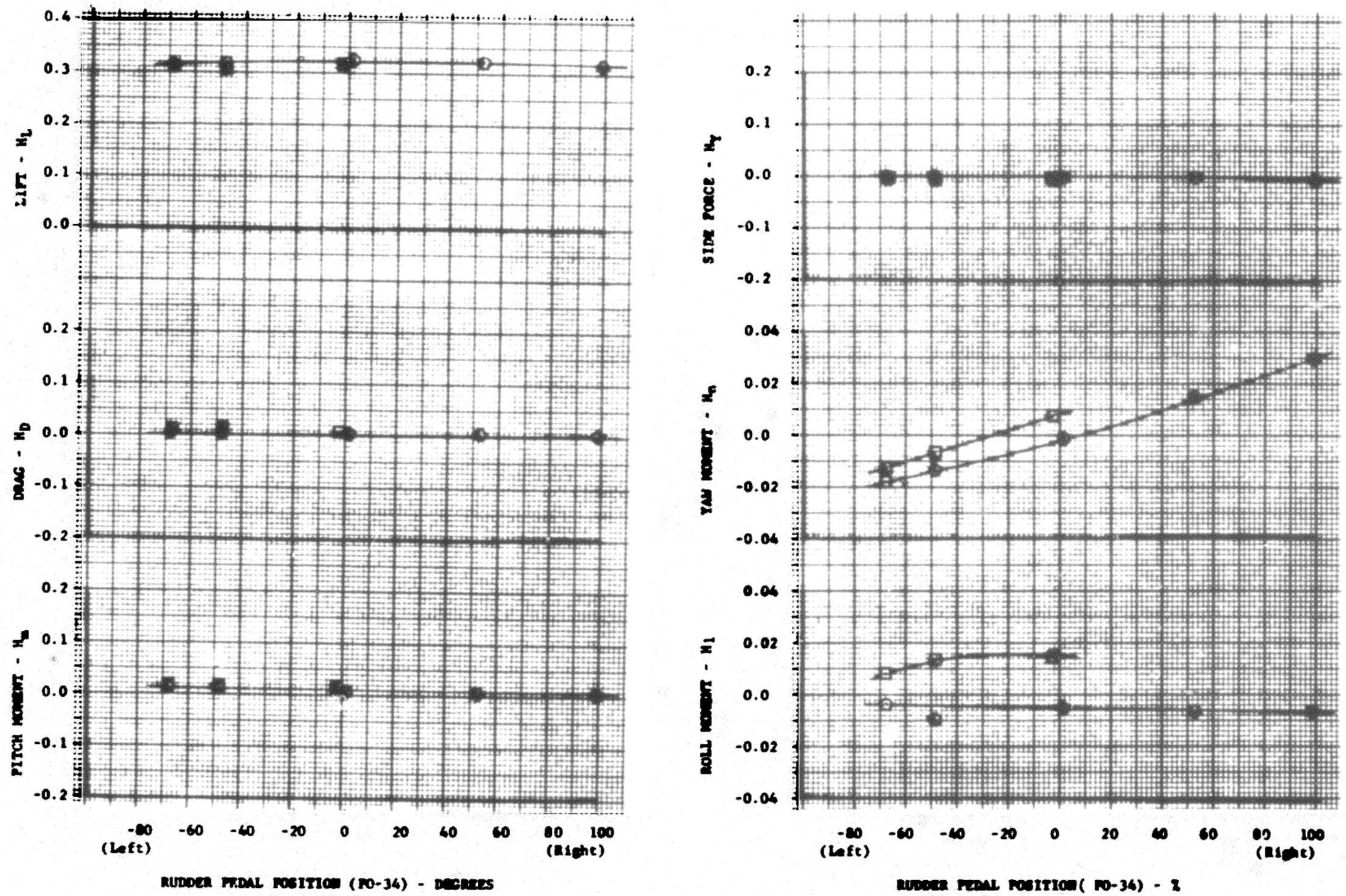

FIGURE 69
DIRECTIONAL CONTROL EFFECTIVENESS - FAN POWERED (HI-POWER)
$\mu = 0.12$

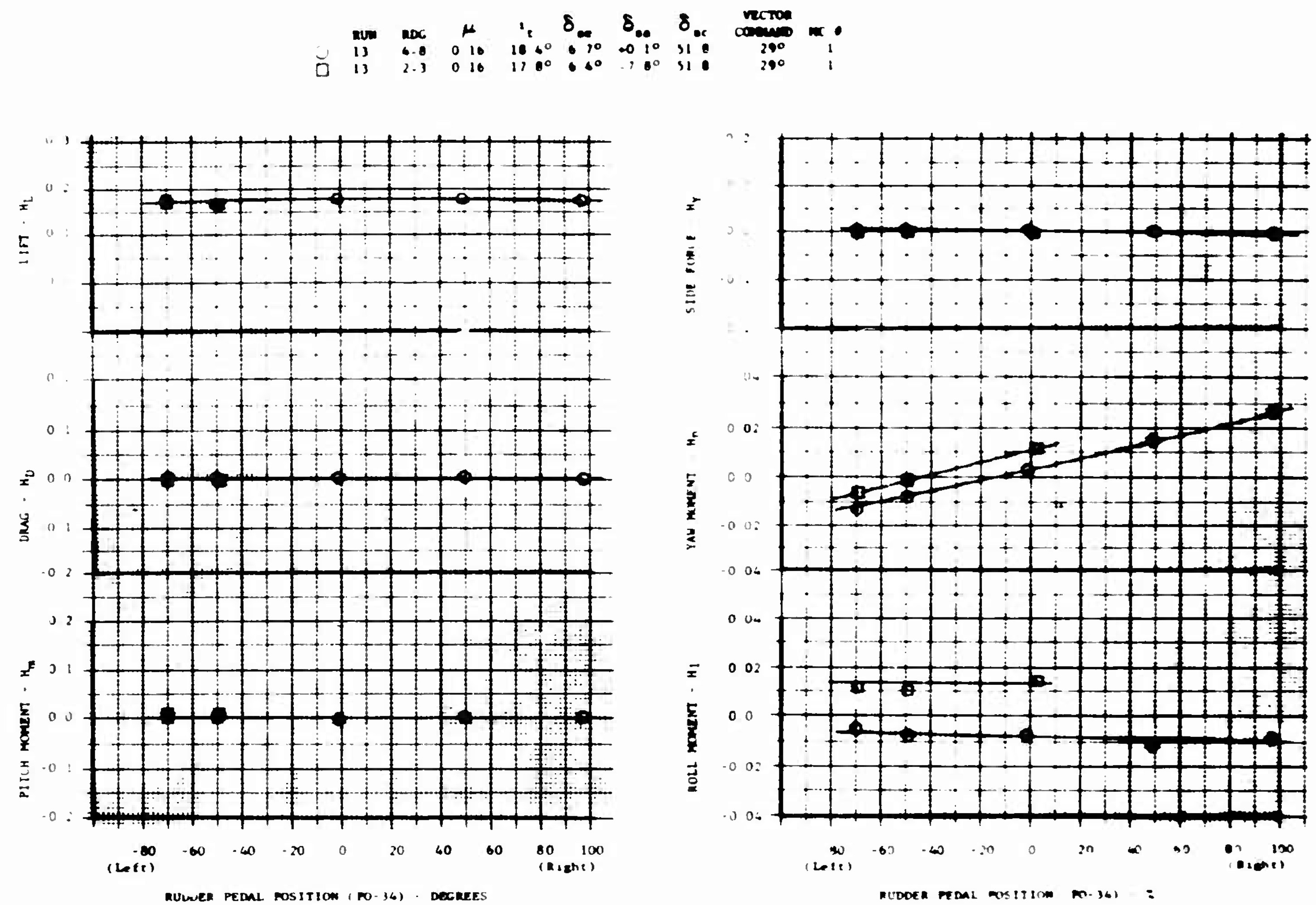

FIGURE 70
DIRECTIONAL CONTROL EFFECTIVENESS - FAN POWERED (HI-POWER)
$\mu = 0.16$

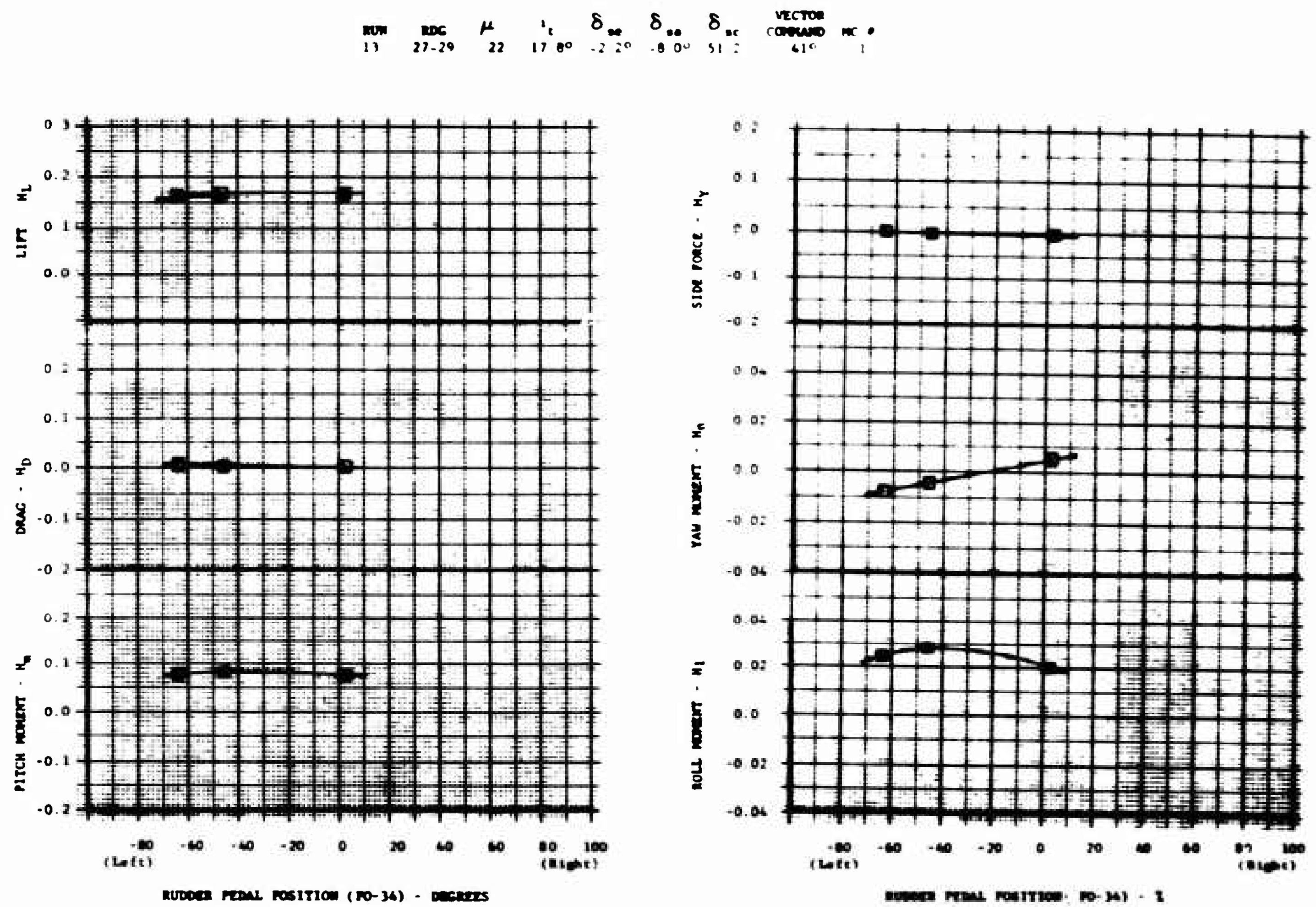

FIGURE 71
DIRECTIONAL CONTROL EFFECTIVENESS - FAN POWERED (HI-POWER)
$\mu = 0.22$

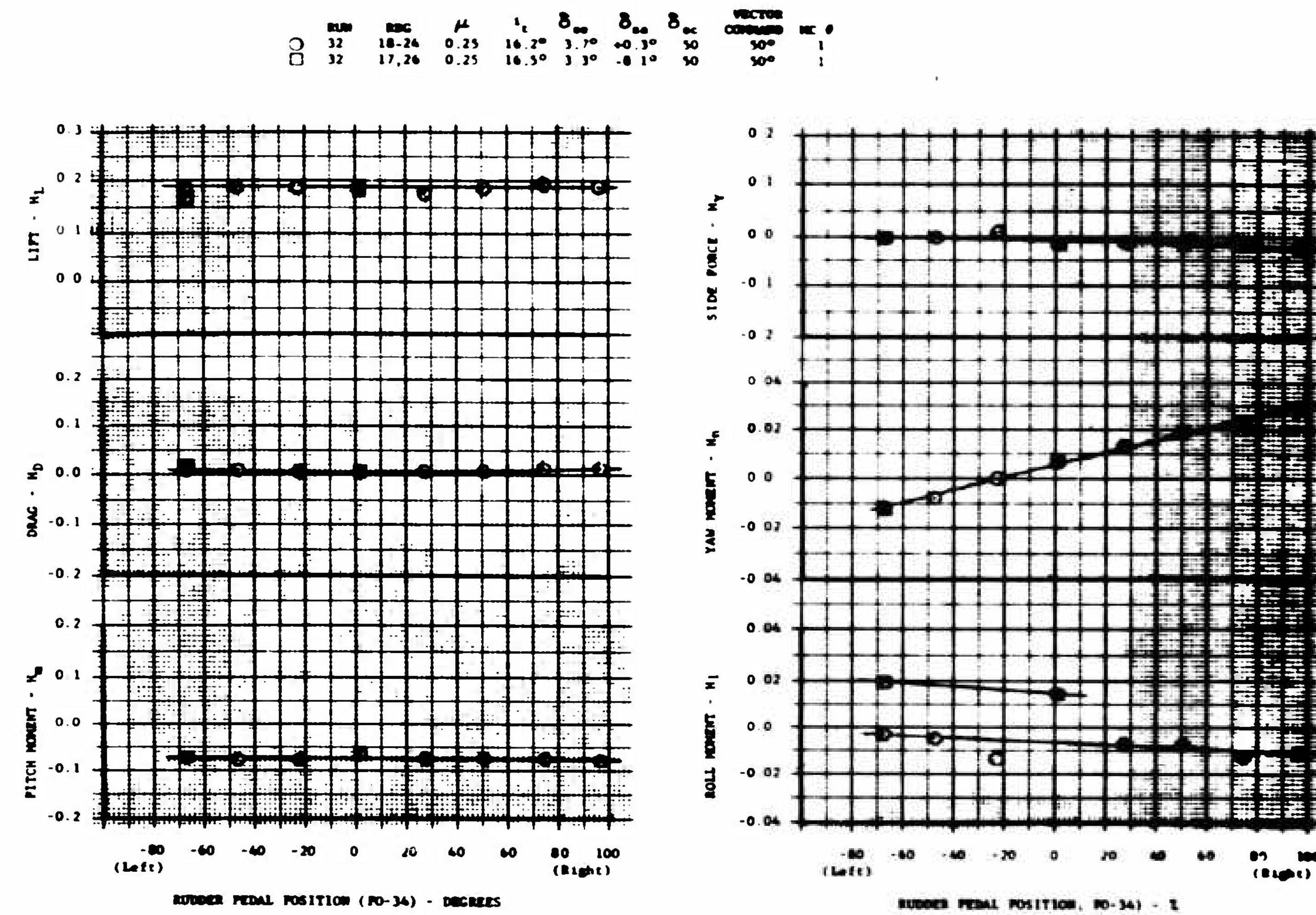

FIGURE 72
DIRECTIONAL CONTROL EFFECTIVENESS - FAN POWERED (HI-POWER)
$\mu = 0.25$

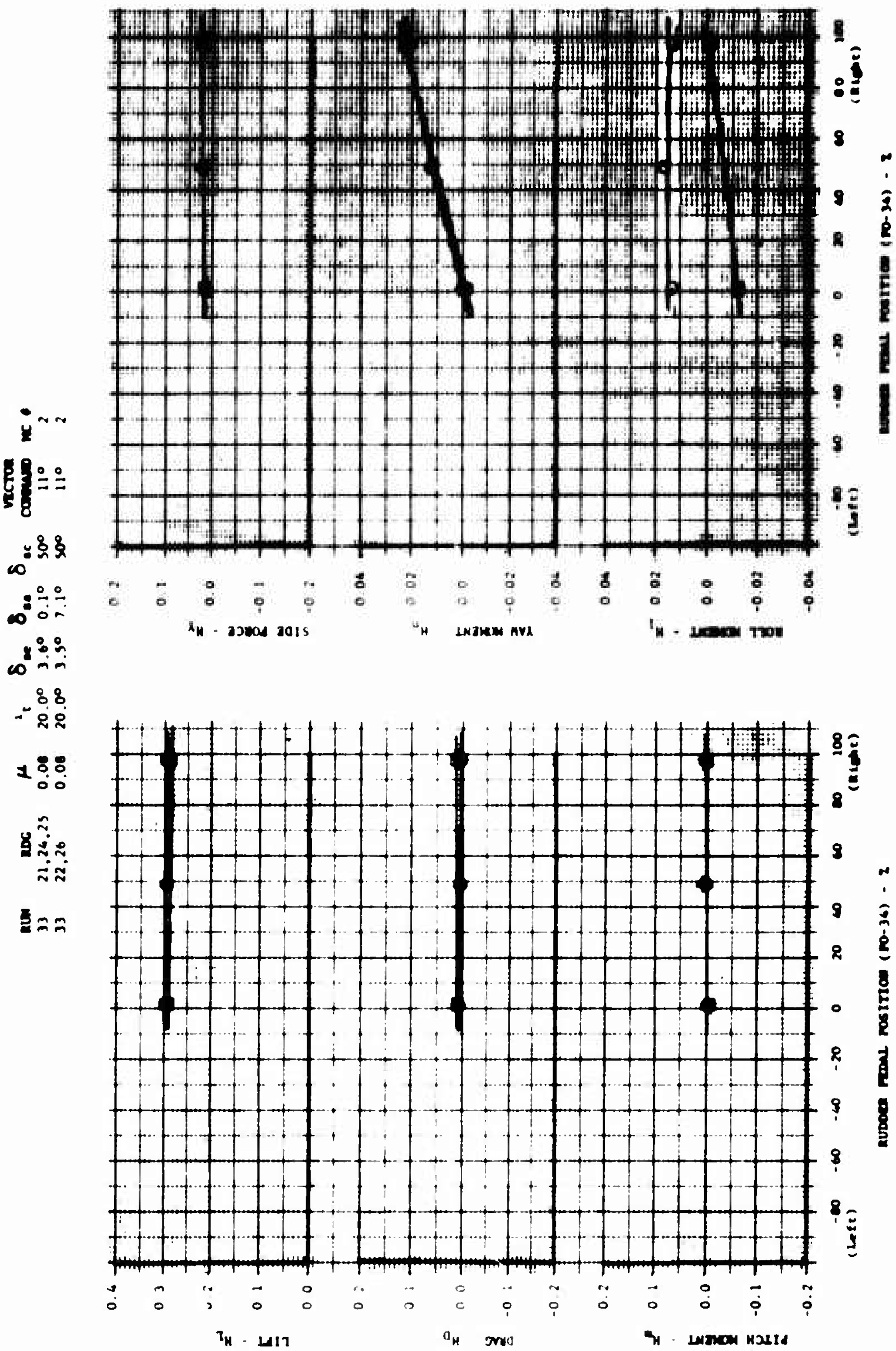

FIGURE 73
DIRECTIONAL CONTROL CHARACTERISTICS - FAN POWERED (LO-POWER)
μ = 0.08, B = -12

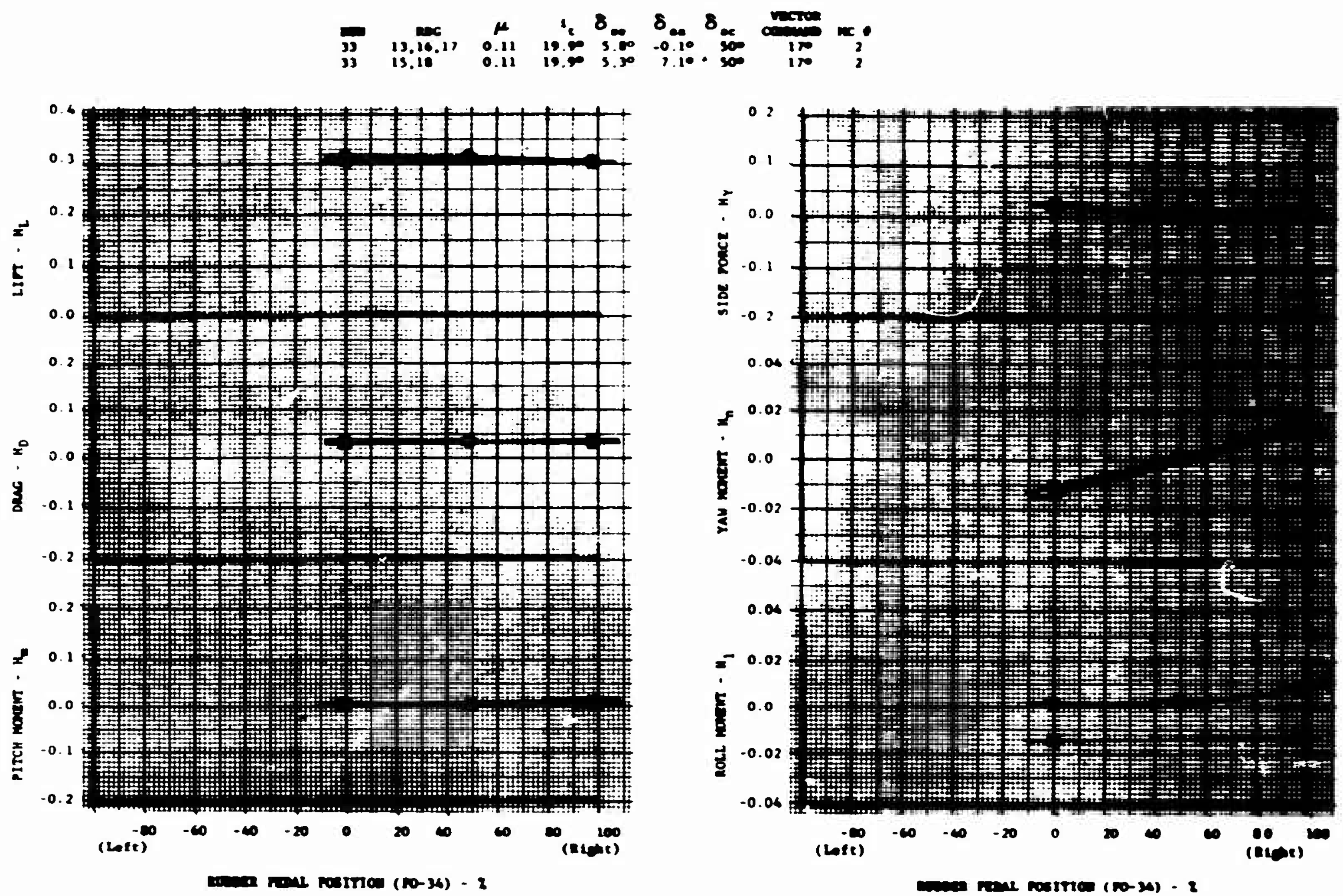

FIGURE 74

DIRECTIONAL CONTROL EFFECTIVENESS - FAN POWERED (LO-POWER)

μ = 0.11, α = +6, B = -8

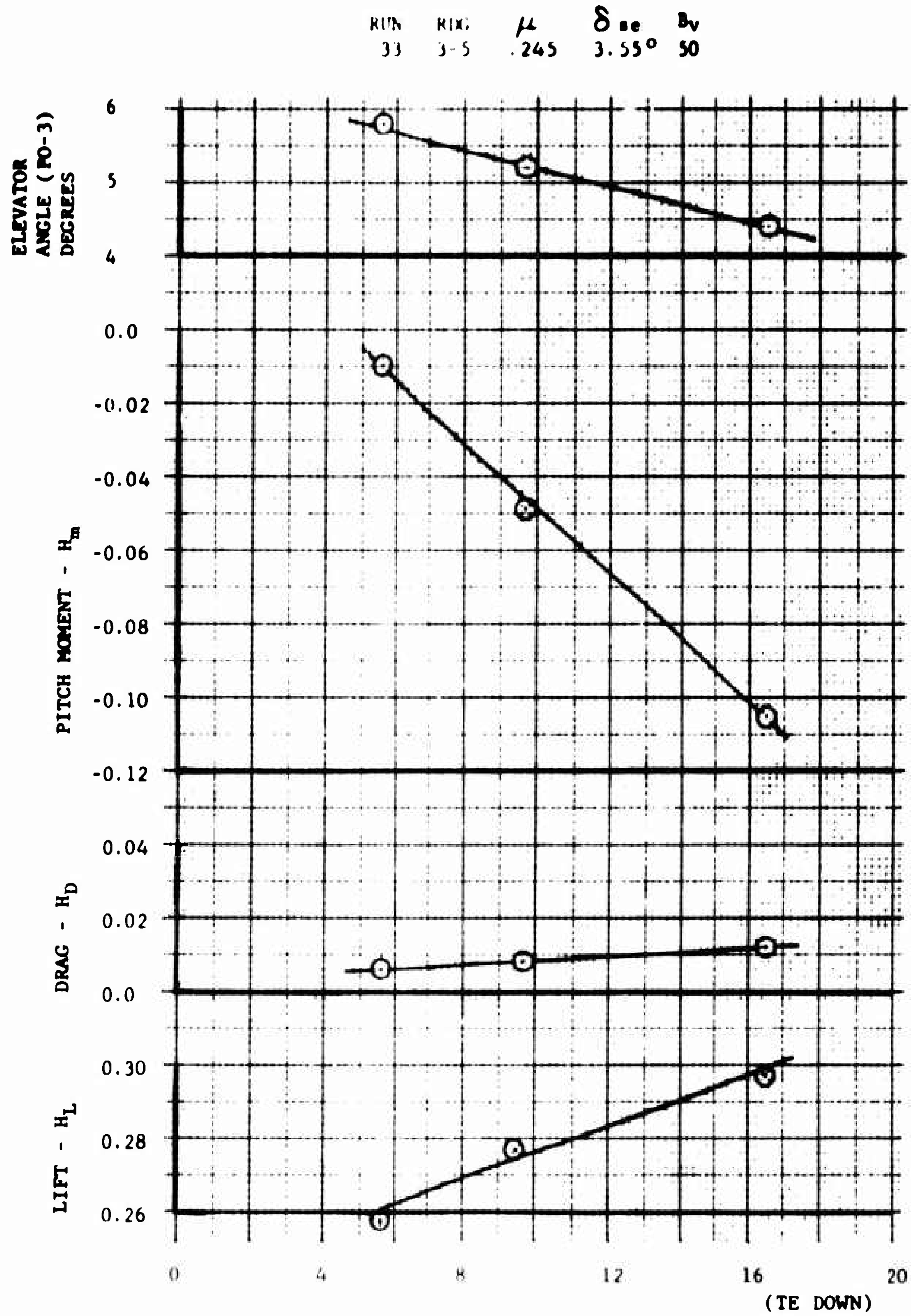

FIGURE 75

HORIZONTAL STABILIZER EFFECTIVENESS - FAN POWERED μ = 0.245

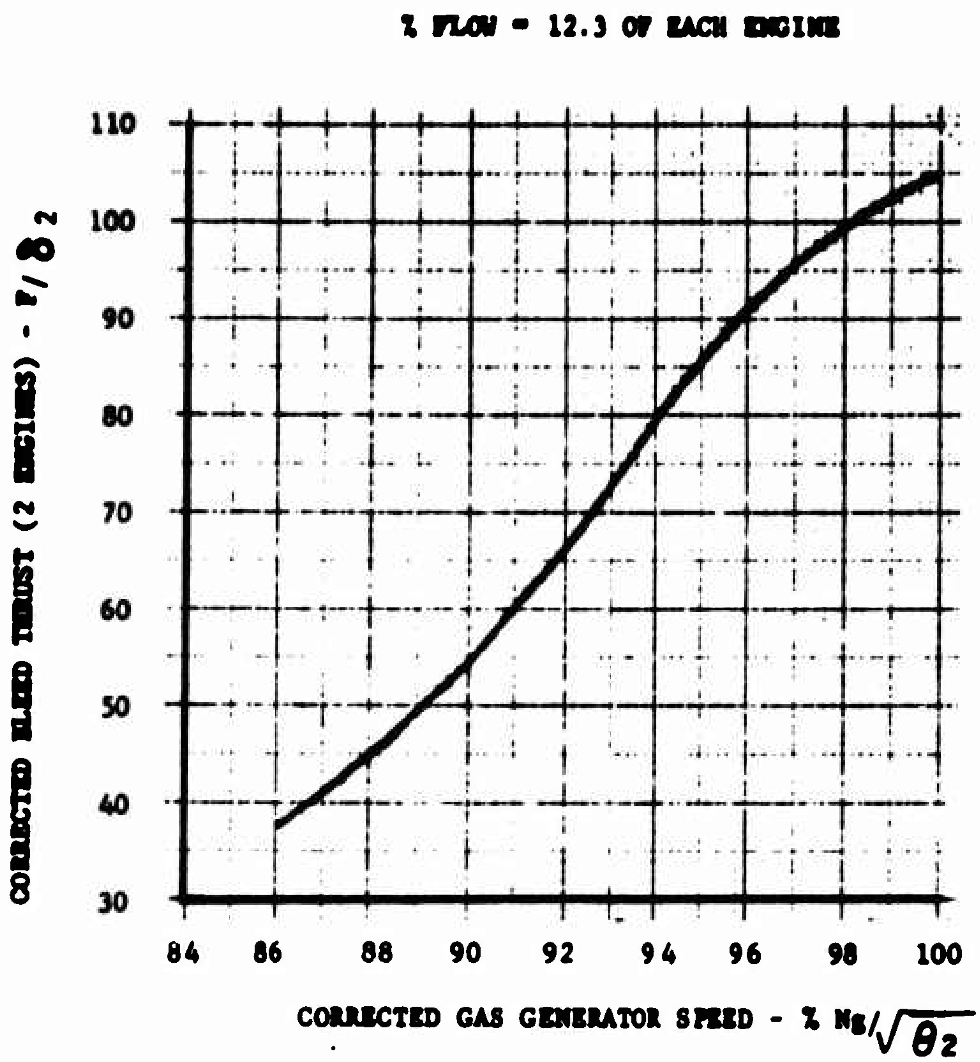

FIGURE 76A

ESTIMATED THRUST DUE TO ADDITION OF PITCH FAN FLOW INTO JET TAIL-PIPE

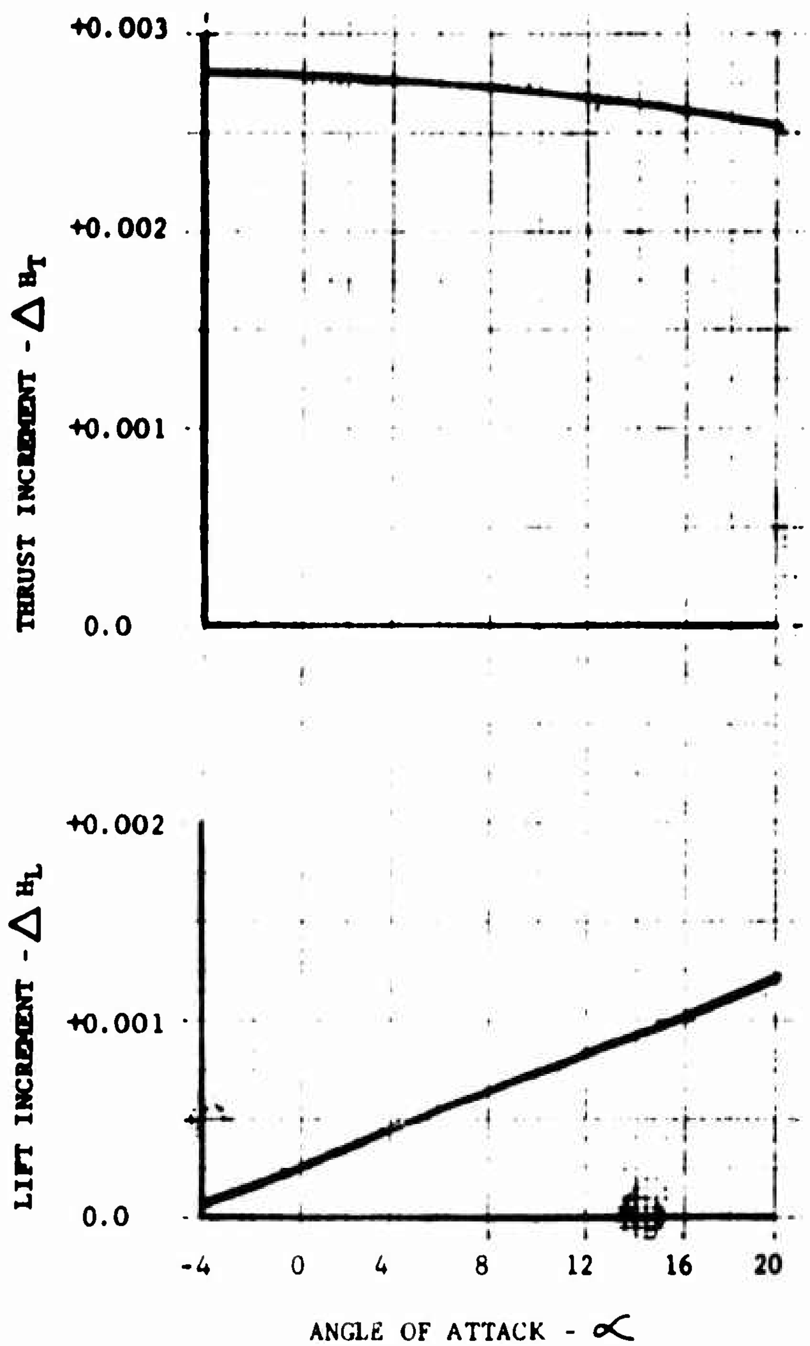

FIGURE 76B

ESTIMATED LIFT AND DRAG
INCREMENTS IN COEFFICIENT FORM DUE
TO PITCH FAN BLEED FLOW

RUN	RDG	μ	i_t	δ_{ee}	VECTOR COMMAND	PF INLET AND EXIT	POWER	MC #
25	10-20	0.15	15.2°	-0.6°	25°	OPEN	LOW	2
25	1-9	0.25	10.6°	-0.6°	47°	OPEN	LOW	2
26	1-12	0.16	1[illegible].[illegible]°	-0.3°	23°	CLOSED	HIGH	2
26	13-18	0.23	12.0°	0.0°	35°	CLOSED	HIGH	2

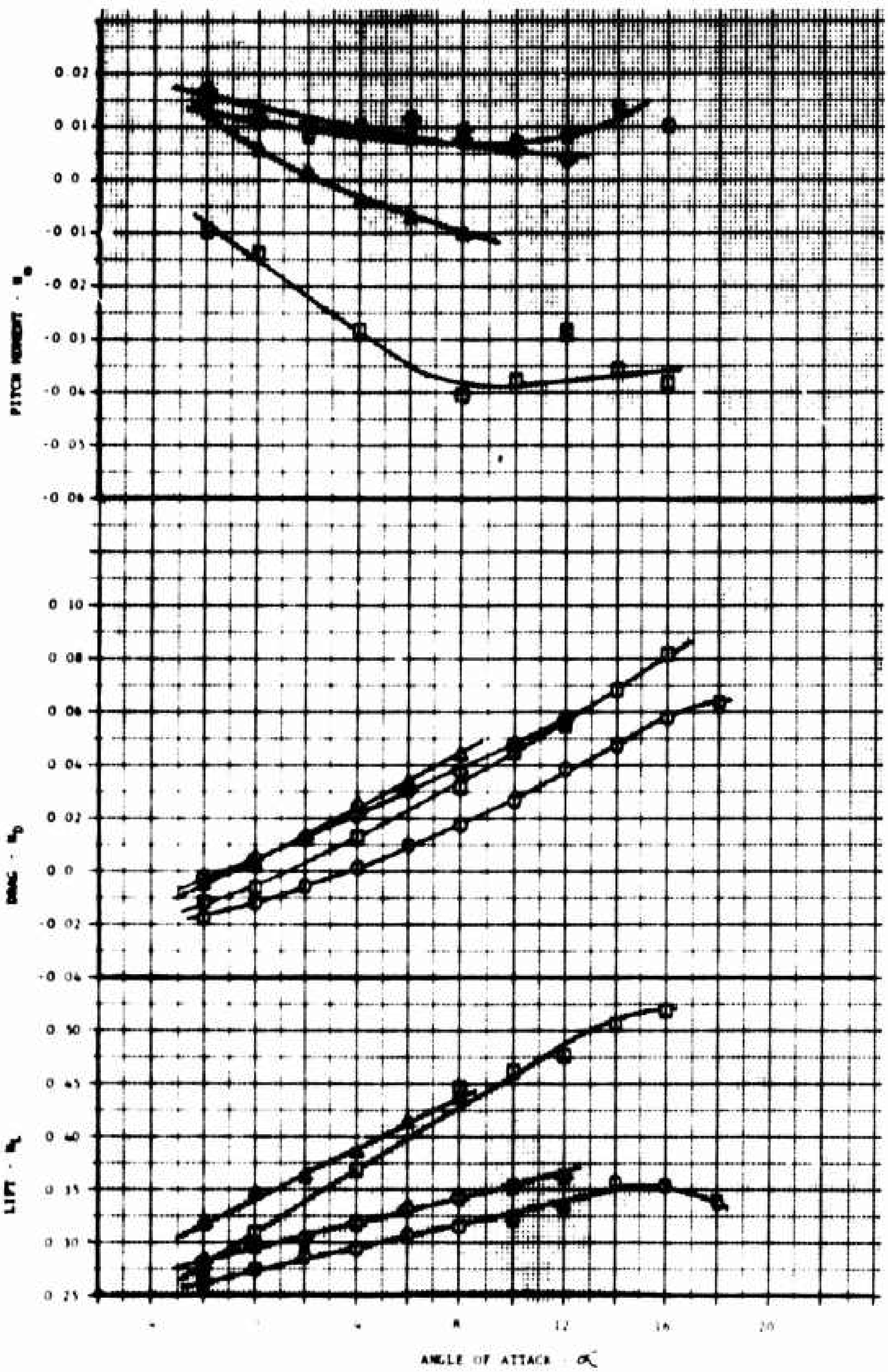

FIGURE 77
LONGITUDINAL CHARACTERISTICS
FAN POWERED - PITCH FAN "OFF"

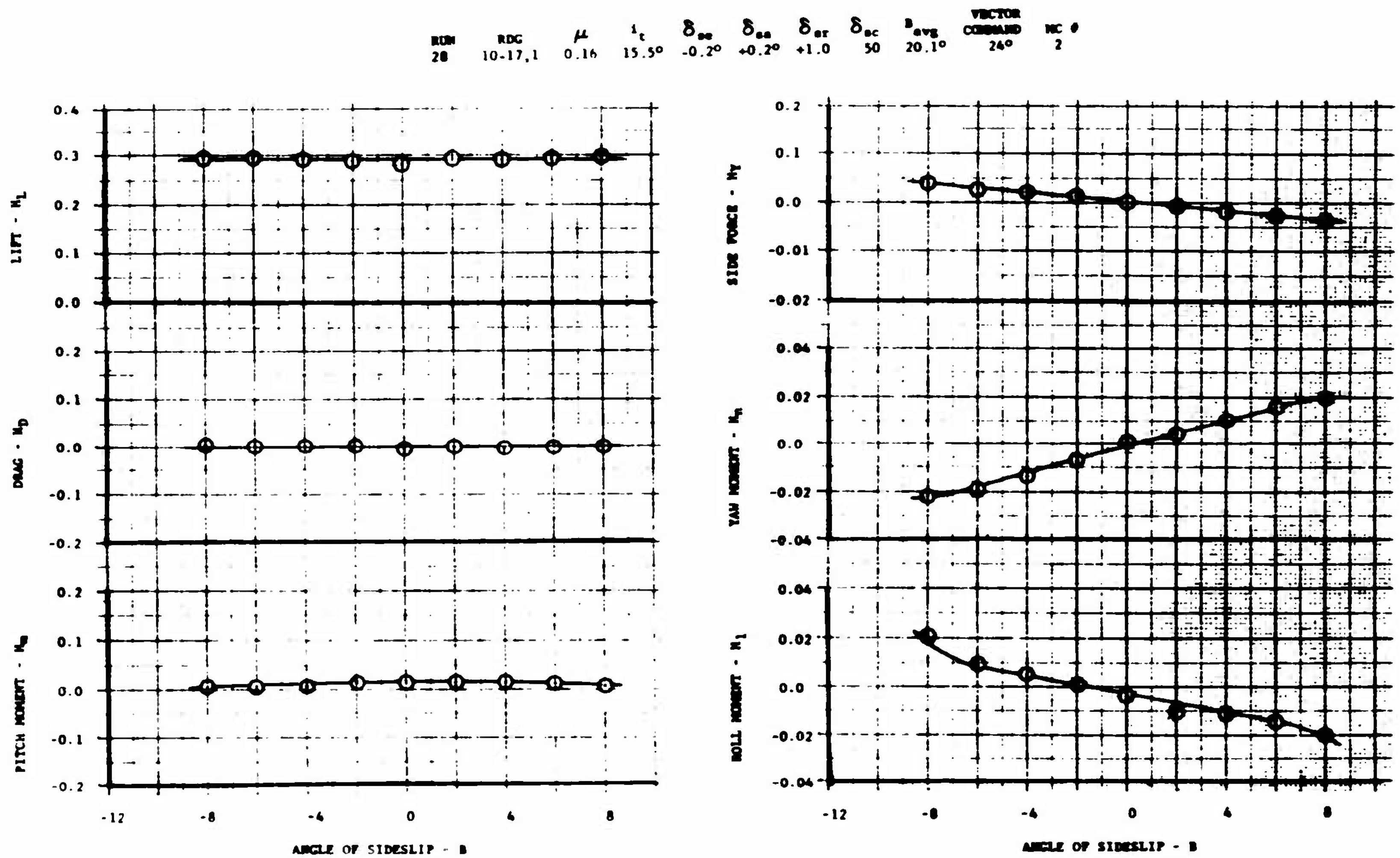

FIGURE 78
LATERAL DIRECTIONAL CHARACTERISTICS - FAN POWERED (HI-POWER)
PITCH FAN "OFF" - INLETS AND EXIT CLOSED - μ = 0.16

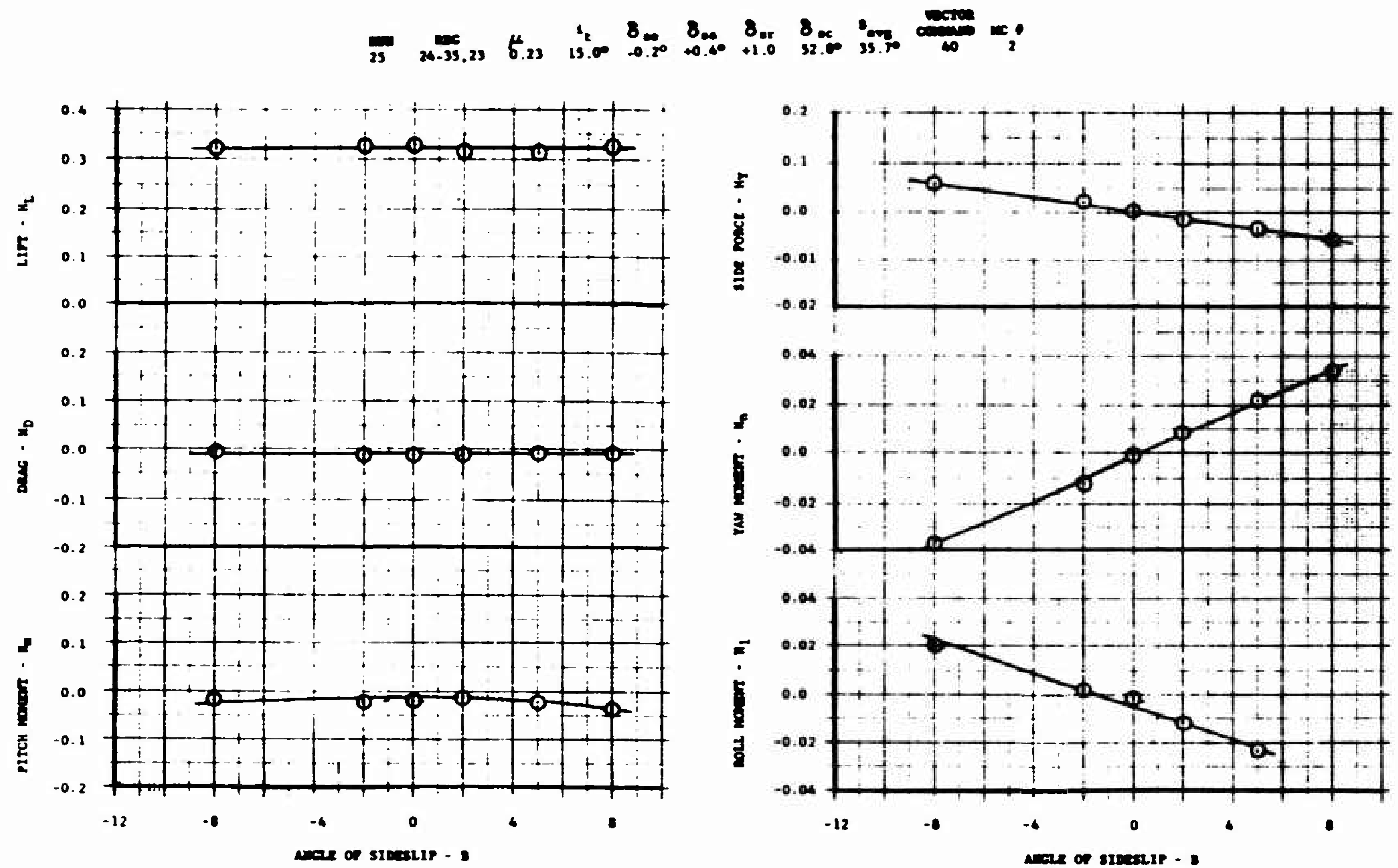

FIGURE 79
LATERAL DIRECTIONAL CHARACTERISTICS - FAN POWERED (LO-POWER)
PITCH FAN "OFF" - INLETS AND EXIT OPEN - μ = 0.23

RUN	RDG	μ	i_t	δ_{ee}	δ_{aa}	δ_{er}	δ_{ec}	MC #
25	44-47	0.12	14.7°	-0.1°	+0.3°	+1.0	52.6°	2

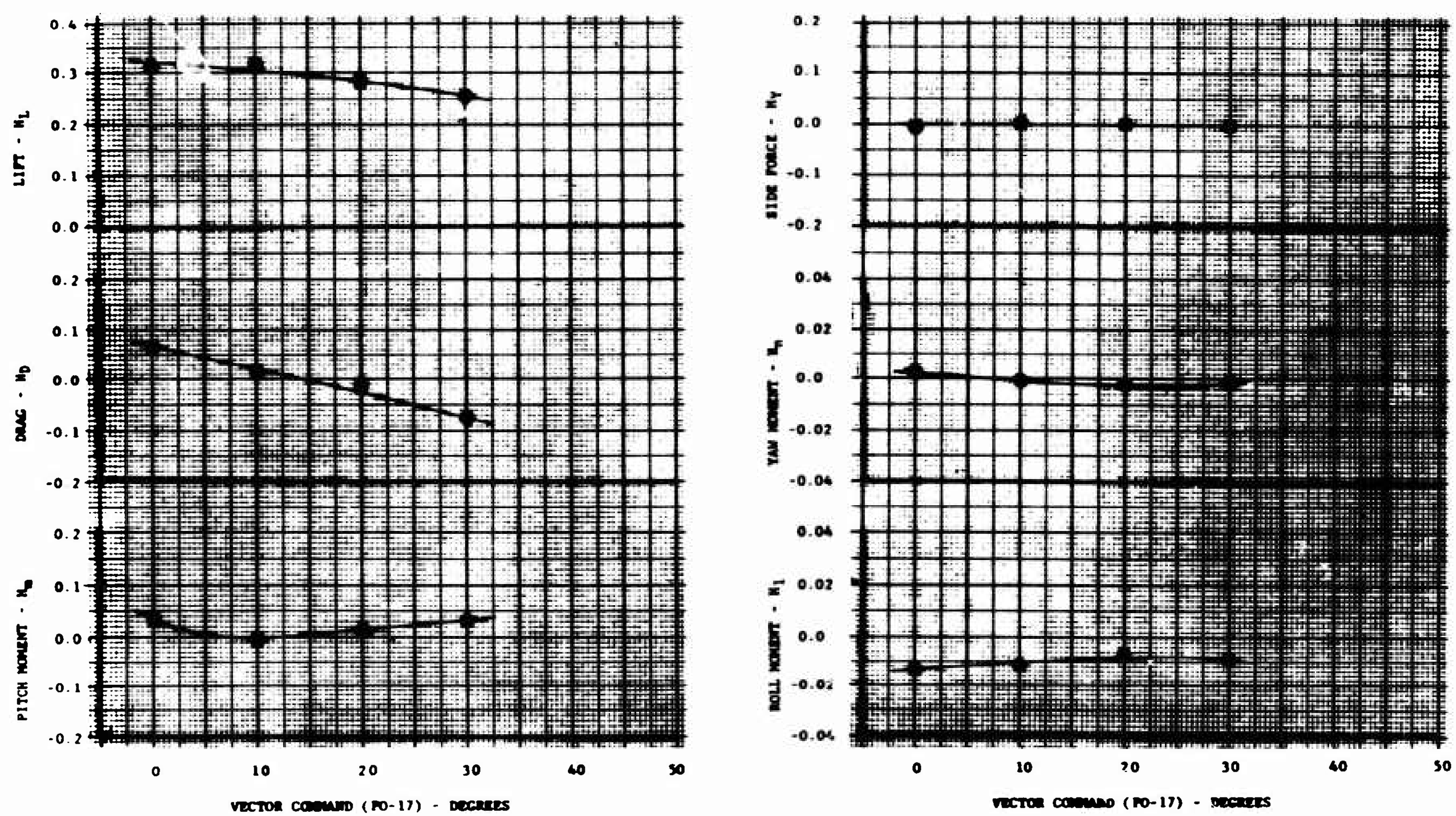

FIGURE 80
VECTOR EFFECTIVENESS - FAN POWERED (LO-POWER)
PITCH FAN "OFF" (OPEN) - μ = 0.12

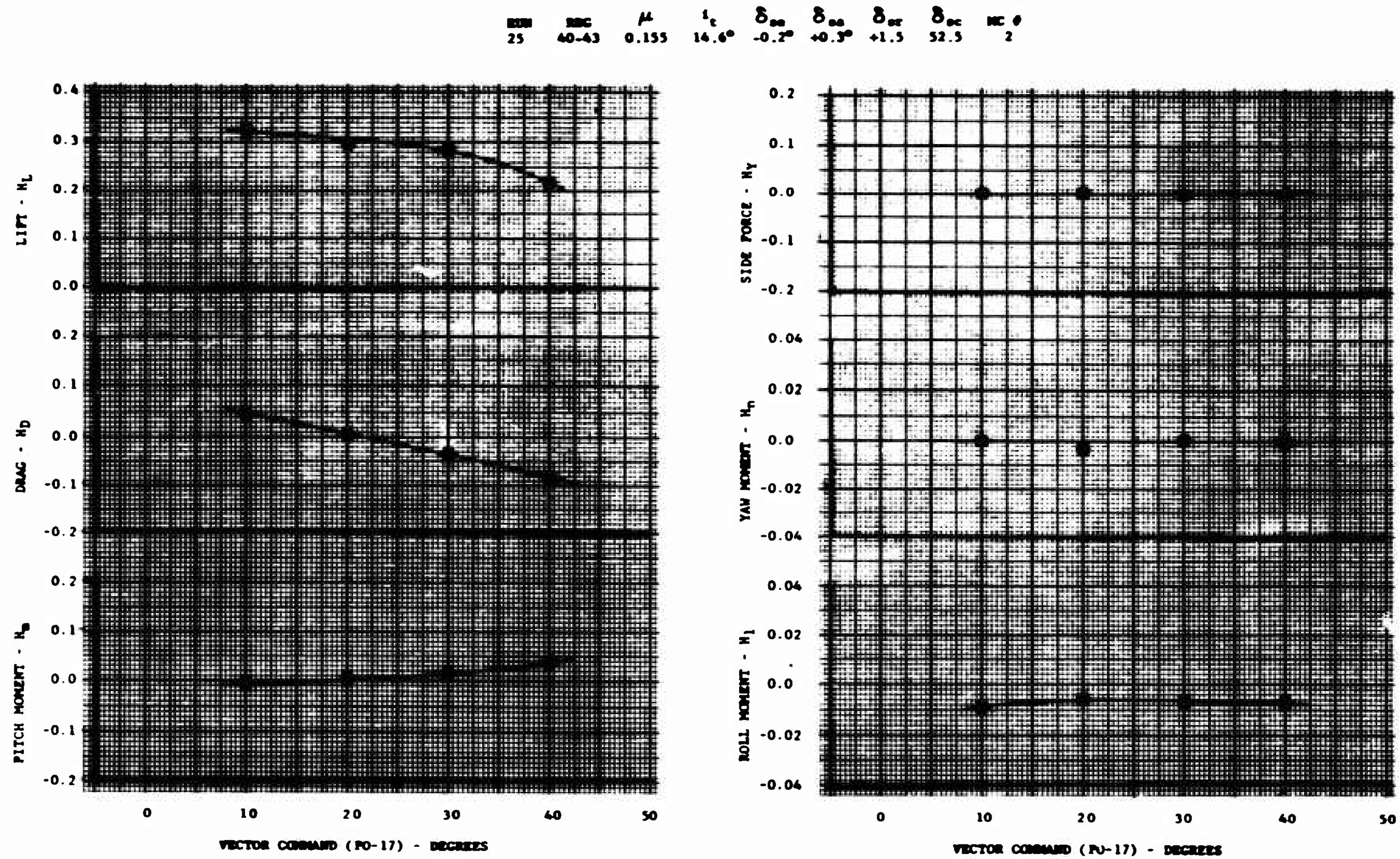

FIGURE 81
VECTOR EFFECTIVENESS - FAN POWERED (LO-POWER)
PITCH FAN "OFF" (OPEN) - μ = 0.16

82	RUN	RDC	μ	i_t	δ_{ae}	δ_{aa}	δ_{ar}	δ_{ac}	MC #
	25	36-39	0.23	14.6°	-0.2°	+0.3°	+1.5	52.5	2

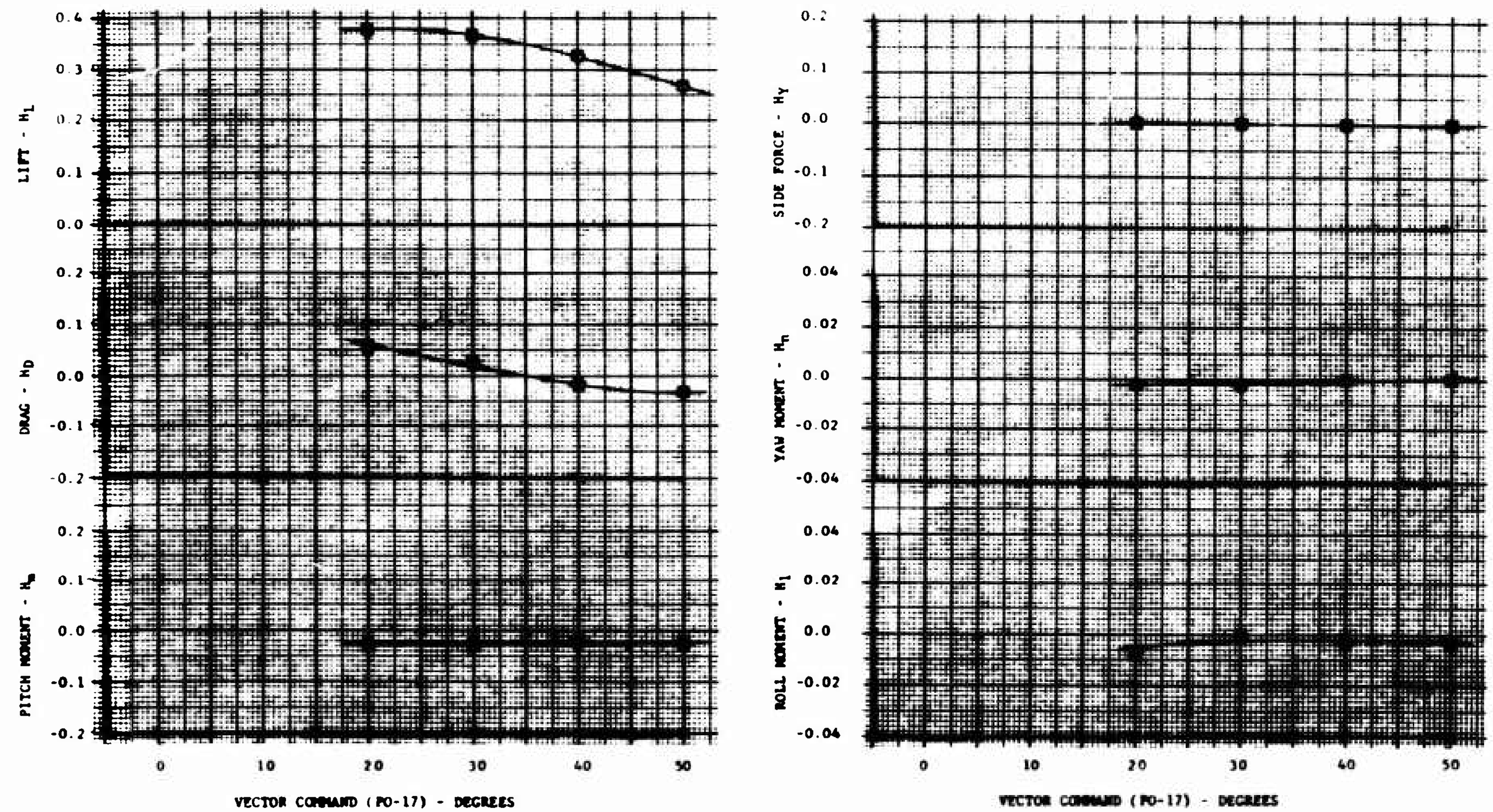

FIGURE 82
VECTOR EFFECTIVENESS - FAN POWERED (LO-POWER)
PITCH FAN "OFF" (OPEN) - μ = 0.23

RUN	RDG	μ	i_t	δ_{ae}	δ_{ee}	δ_{er}	δ_{ec}	RC #
26	31-33,14	0.23	12.3°	-0.2°	+0.3°	+2.6	50	2

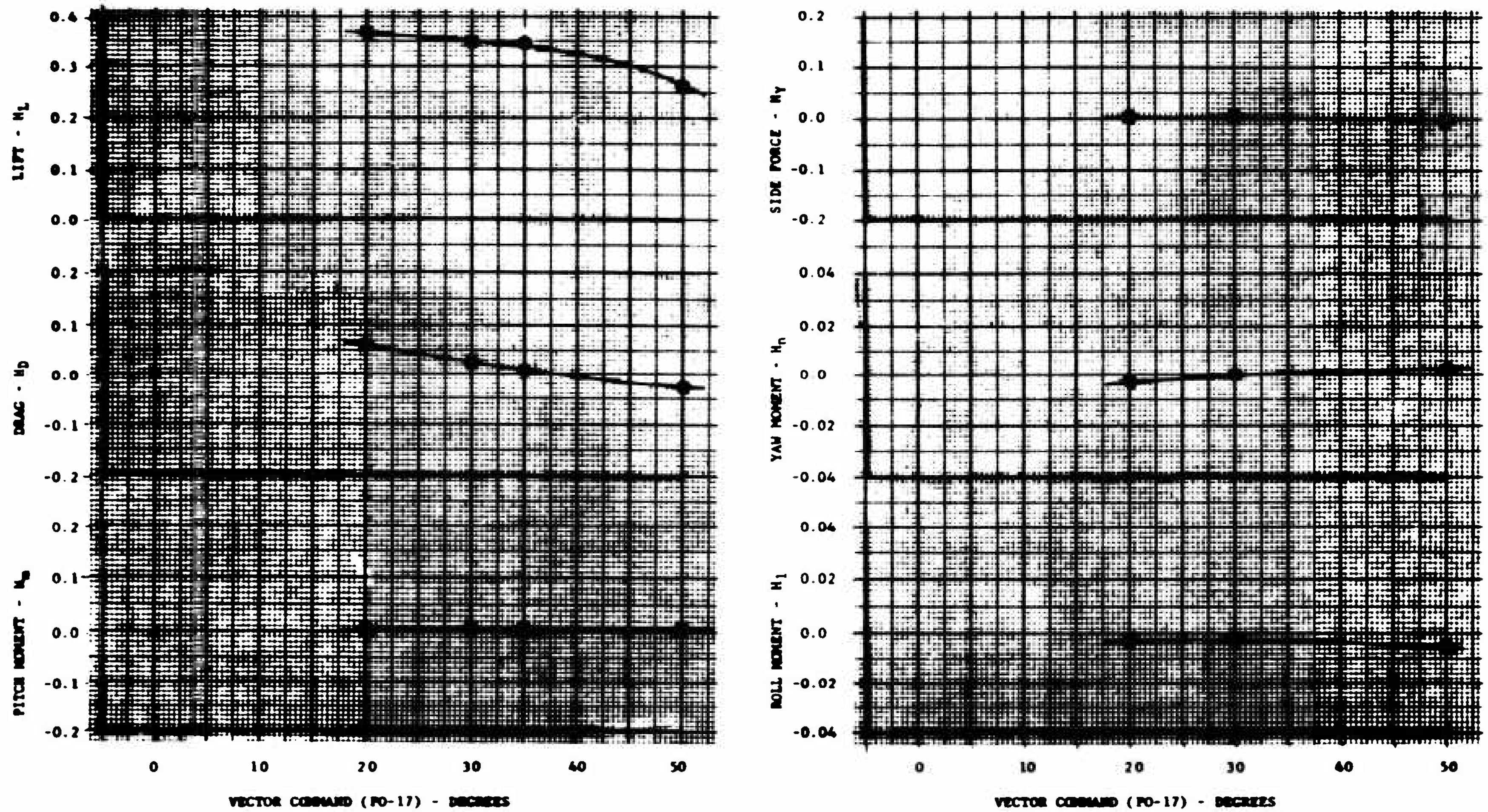

FIGURE 83
VECTOR EFFECTIVENESS - FAN POWERED (HI-POWER)
PITCH FAN "OFF" (CLOSED) - μ = 0.23

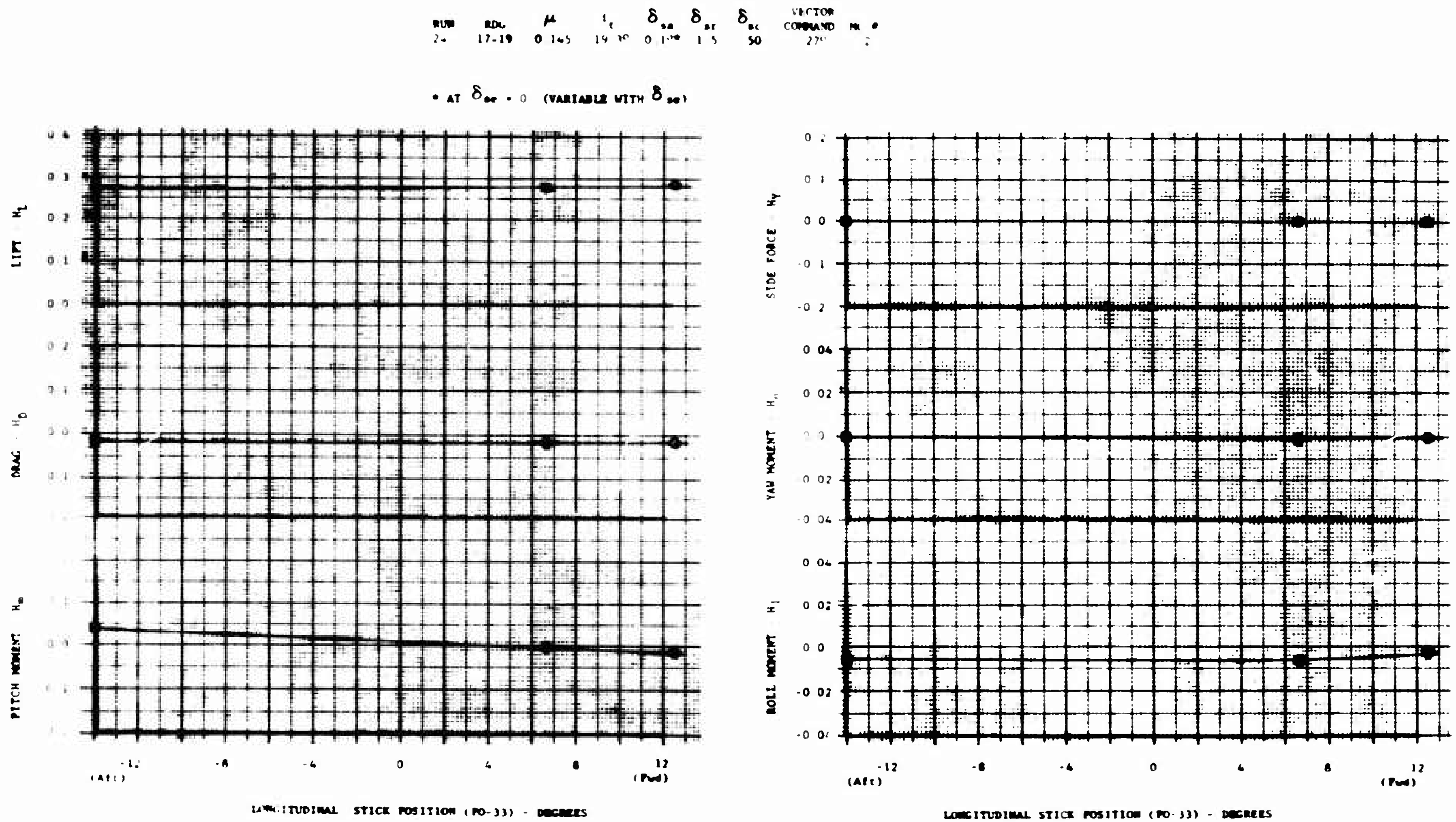

FIGURE 84
LONGITUDINAL CONTROL EFFECTIVENESS - FAN POWERED (LO-POWER)
PITCH FAN "OFF" (OPEN) - μ = 0.145

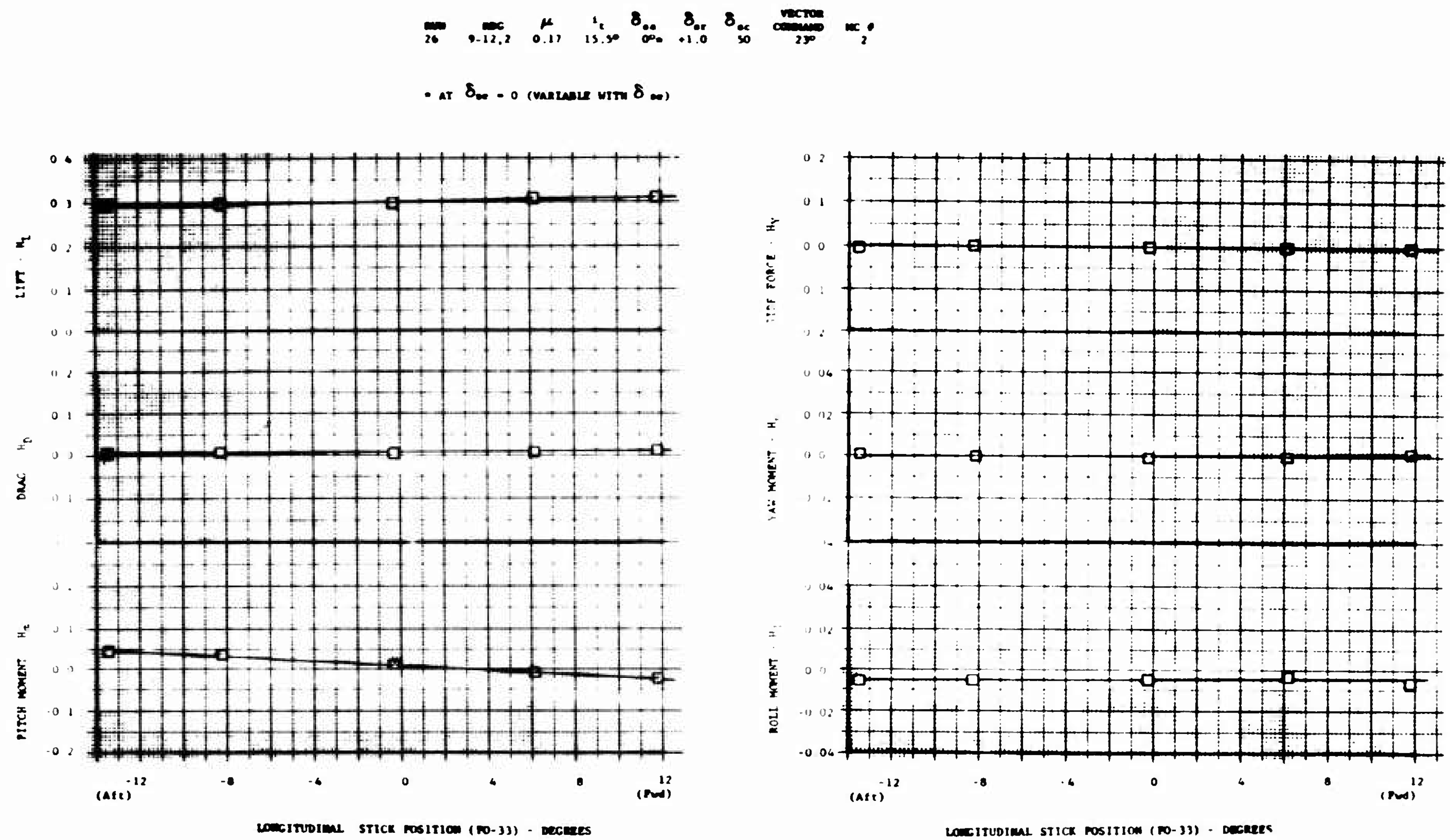

FIGURE 85
LONGITUDINAL CONTROL EFFECTIVENESS - FAN POWERED (HI-POWER)
PITCH FAN "OFF" (CLOSED) - μ = 0.17

RUN	RDG	μ	i_t	δ_{se}	δ_{sr}	δ_{sc}	VECTOR COMMAND	MC #
25	25-28,38	0.24	14.8°	0.0°*	1.0	50	40°	2

* AT δ_{se} = 0° (VARIABLE WITH δ_{se})

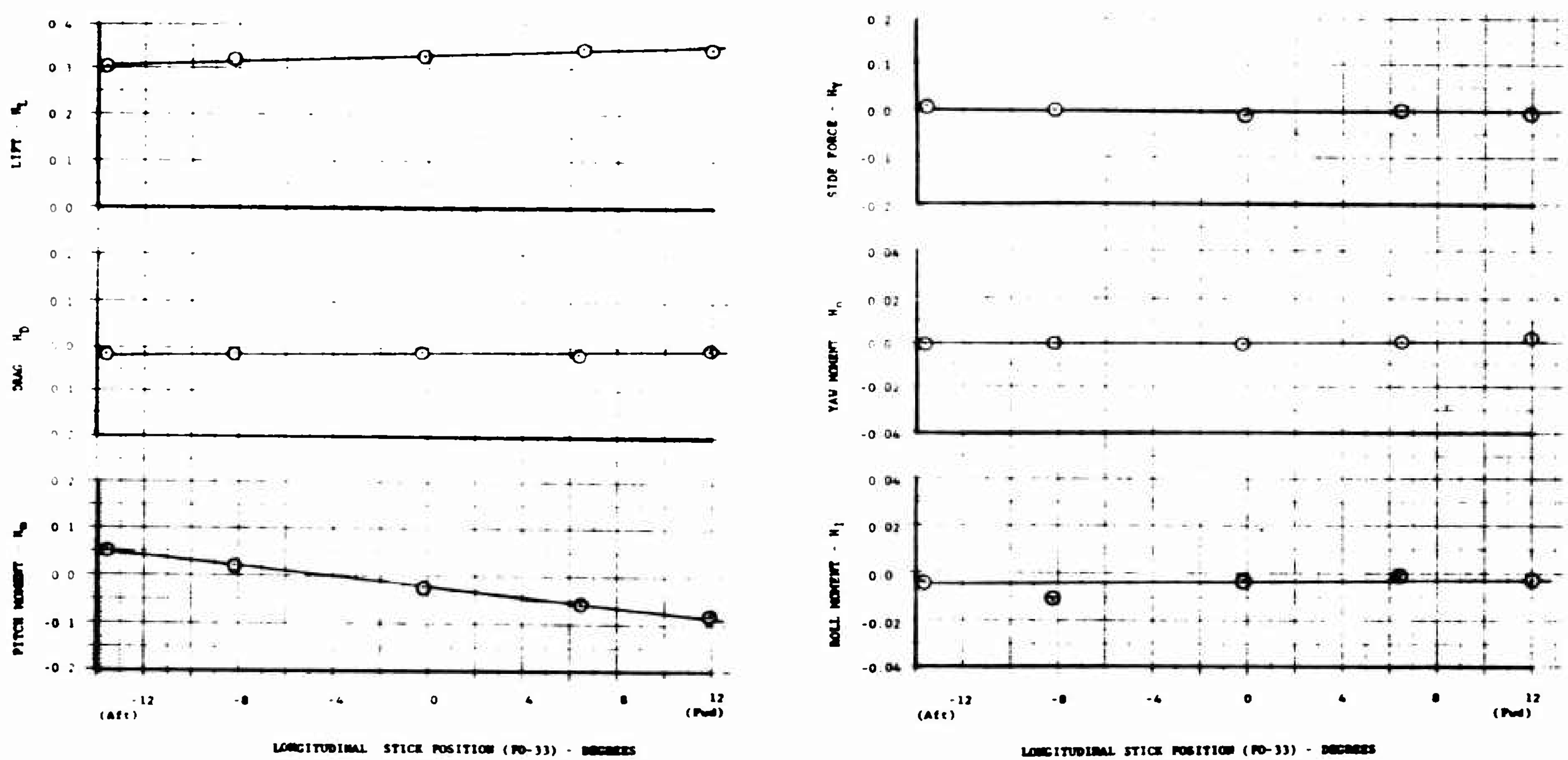

FIGURE 86
LONGITUDINAL CONTROL EFFECTIVENESS - FAN POWERED (LO-POWER)
PITCH FAN "OFF" (OPEN) - μ = 0.24

RUN	BDG	μ	i_t	δ_{se}	δ_{sr}	δ_{sc}	VECTOR COMMAND	RC #
26	19-22	0.23	11.7*	0.1°*	+1.8	50	35°	2

* AT δ_{se} = 0° (VARIABLE WITH δ_{se})

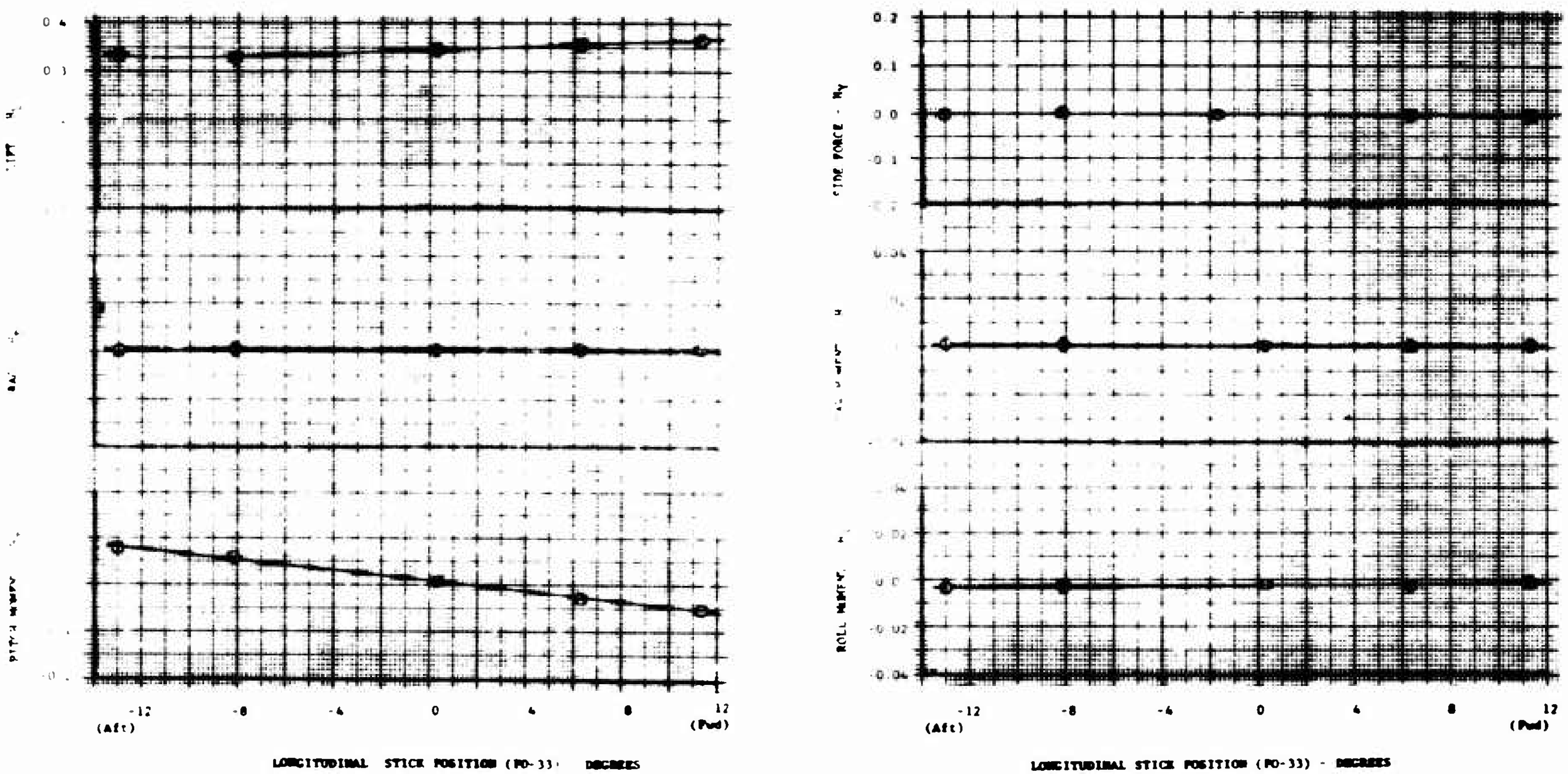

FIGURE 87
LONGITUDINAL CONTROL EFFECTIVENESS - FAN POWERED (HI-POWER)
PITCH FAN "OFF" (CLOSED) - μ = 0.23

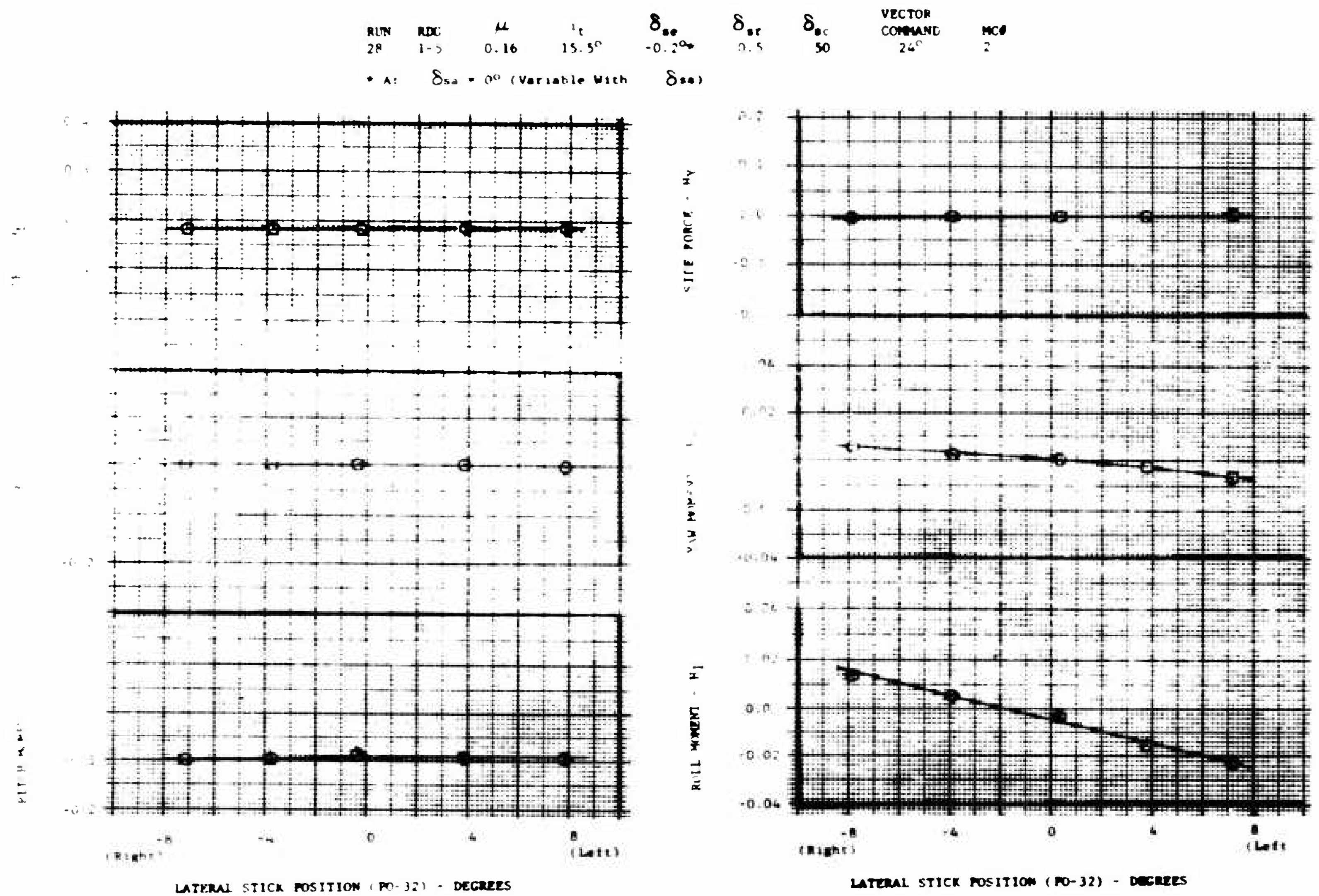

FIGURE 88

LATERAL CONTROL EFFECTIVENESS - FAN POWERED (HI-POWER)
PITCH FAN "OFF" (CLOSED) - μ = 0.16

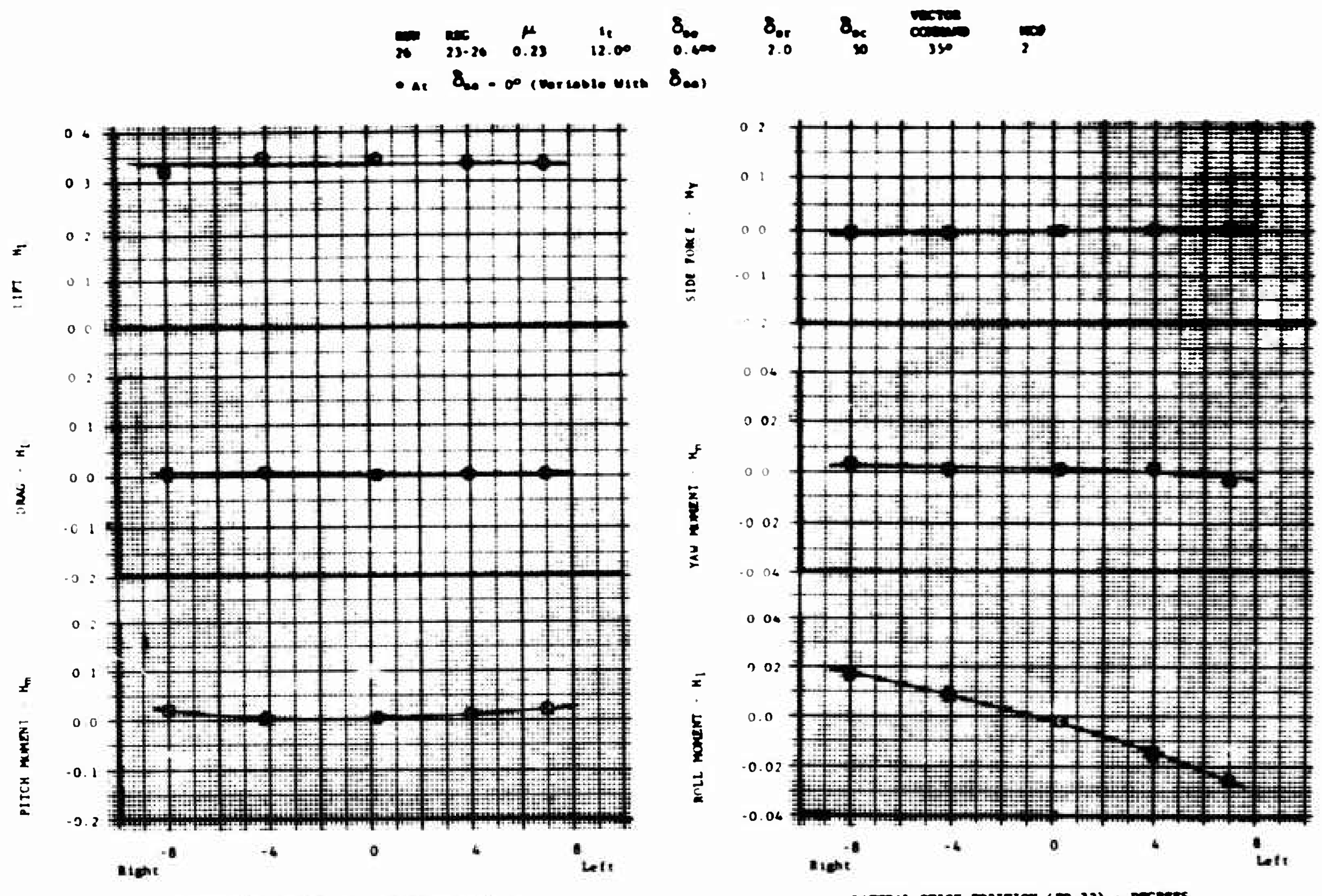

FIGURE 89

LATERAL CONTROL EFFECTIVENESS - FAN POWERED (HI-POWER)
PITCH FAN "OFF" (CLOSED) - μ = 0.23

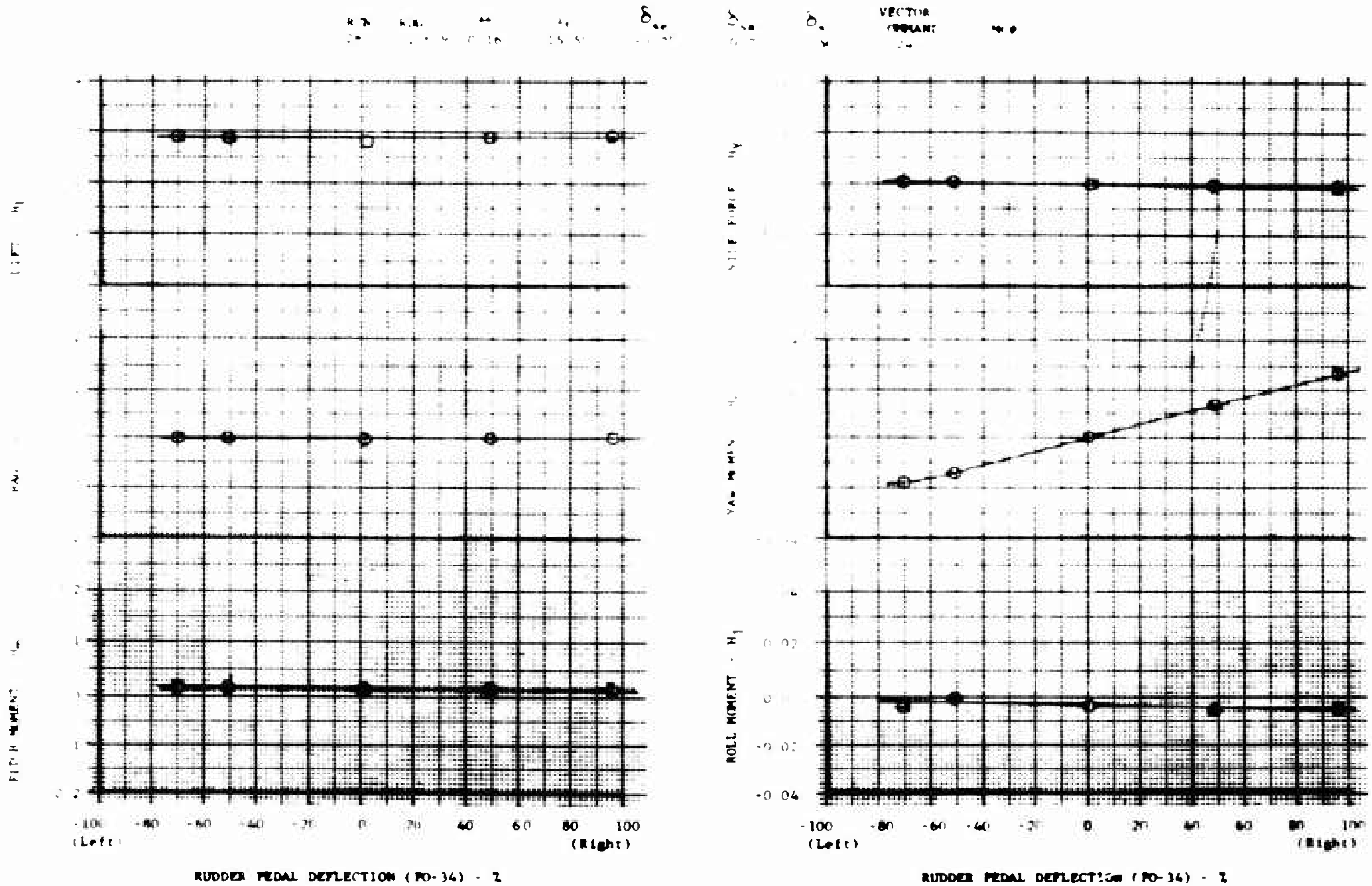

FIGURE 90

DIRECTIONAL CONTROL EFFECTIVENESS - FAN POWERED (HI-POWER)
PITCH FAN "OFF" (CLOSED) - μ = 0.16

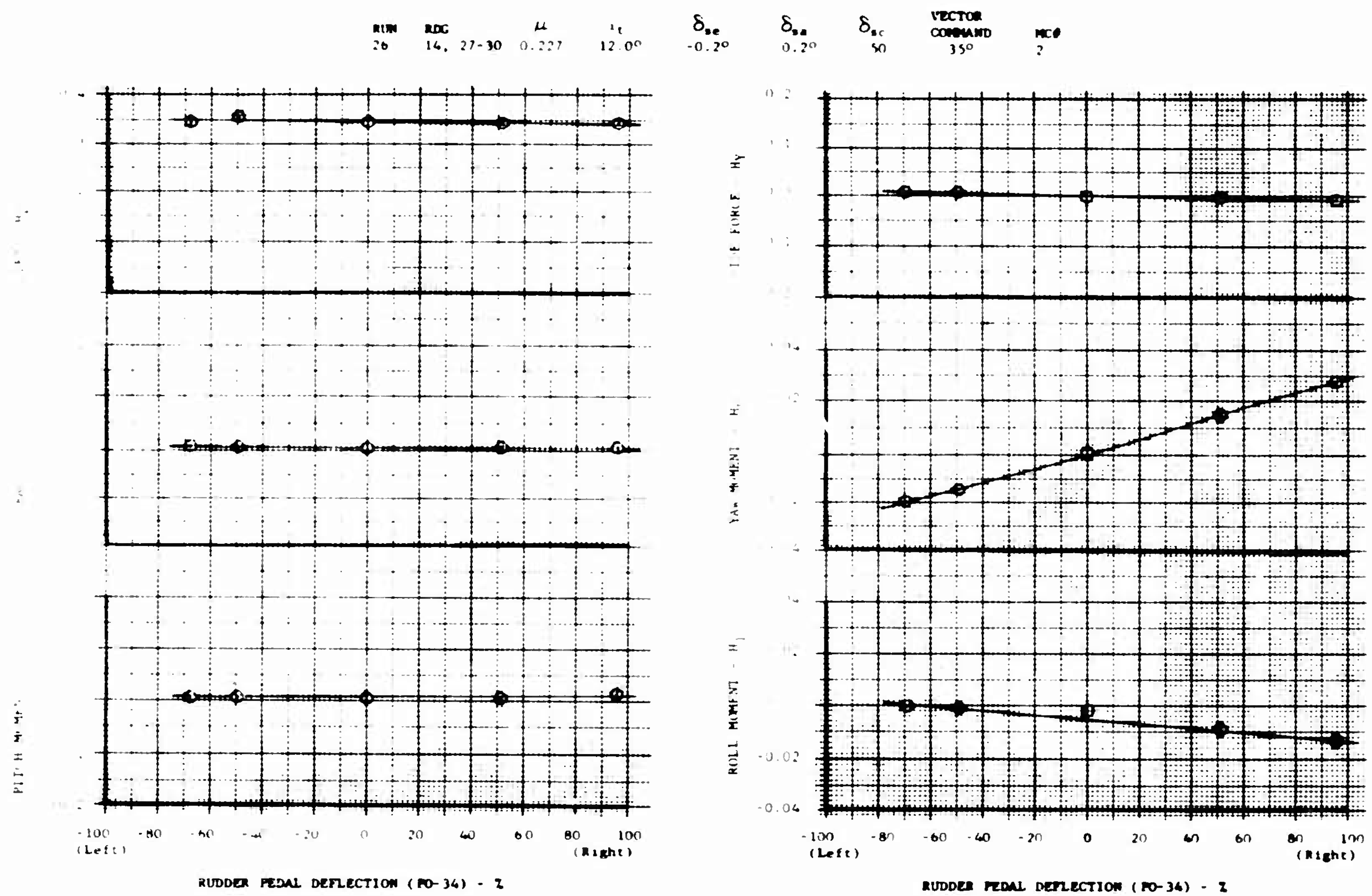

FIGURE 91

DIRECTIONAL CONTROL EFFECTIVENESS - FAN POWERED (LO-POWER)
PITCH FAN "OFF" (OPEN) - μ = 0.23

RUN	RDG	μ	δ_{se}	δ_{sa}	δ_{sr}	δ_{sc}	MC#
23	1, 27-29	0.165	-0.1°	0.2°	1.0	50	1

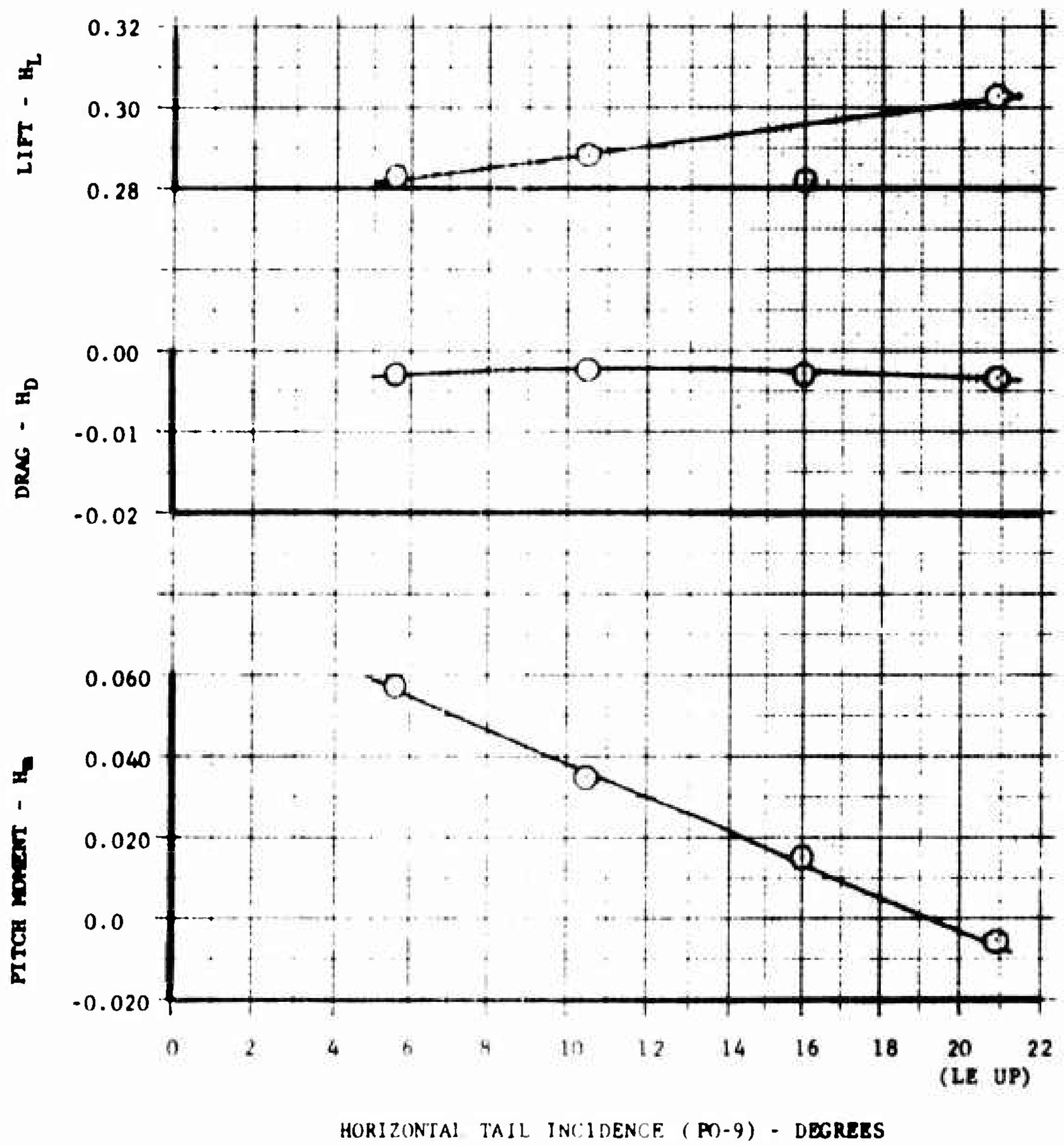

FIGURE 92

HORIZONTAL STABILIZER EFFECTIVENESS
FAN POWERED (HI-POWER) - PITCH FAN "OFF" (CLOSED) - μ = 0.165

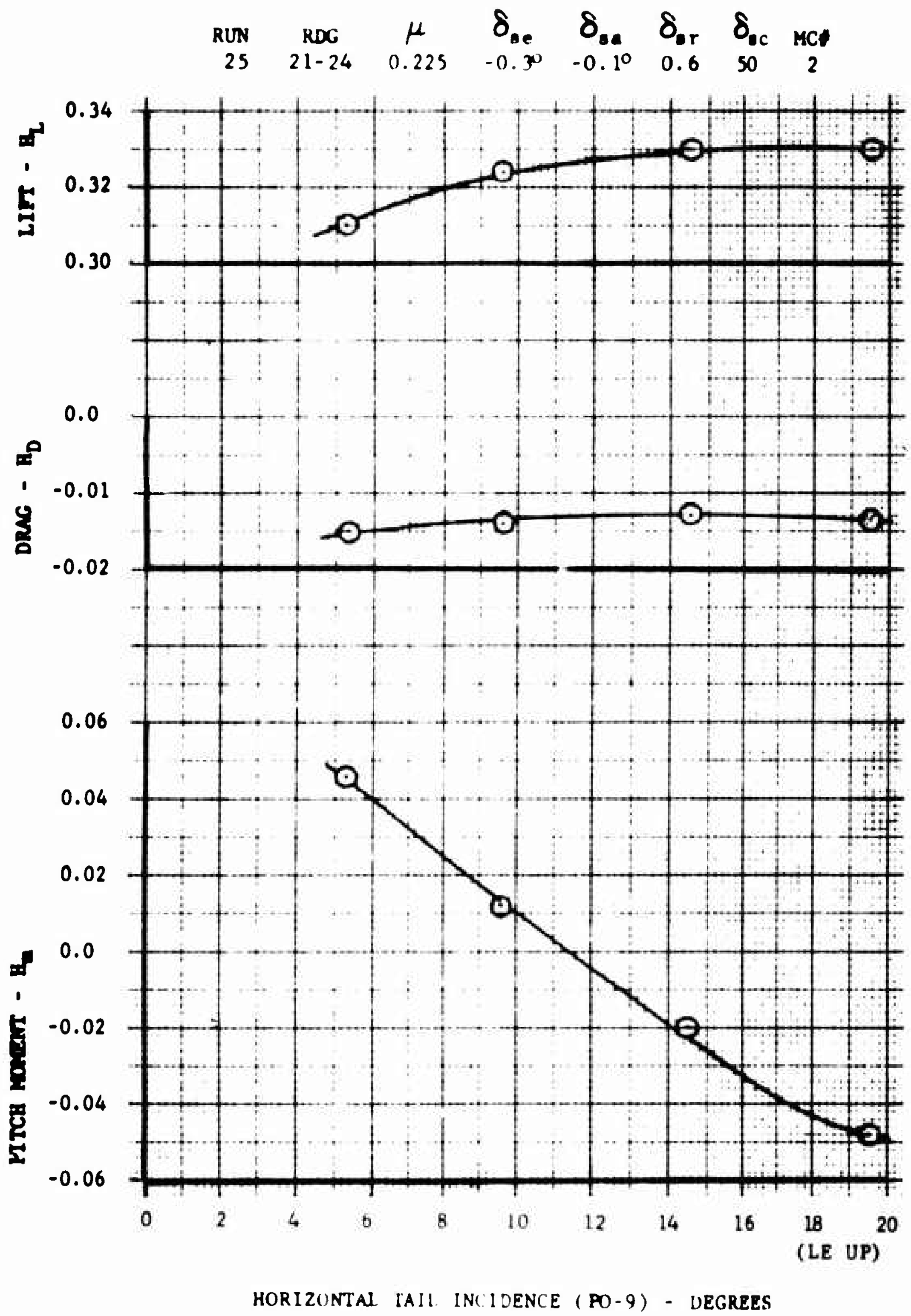

FIGURE 93

HORIZONTAL STABILIZER EFFECTIVENESS
FAN POWERED (LO-POWER) PITCH FAN "OFF" (OPEN) - μ = 0.225

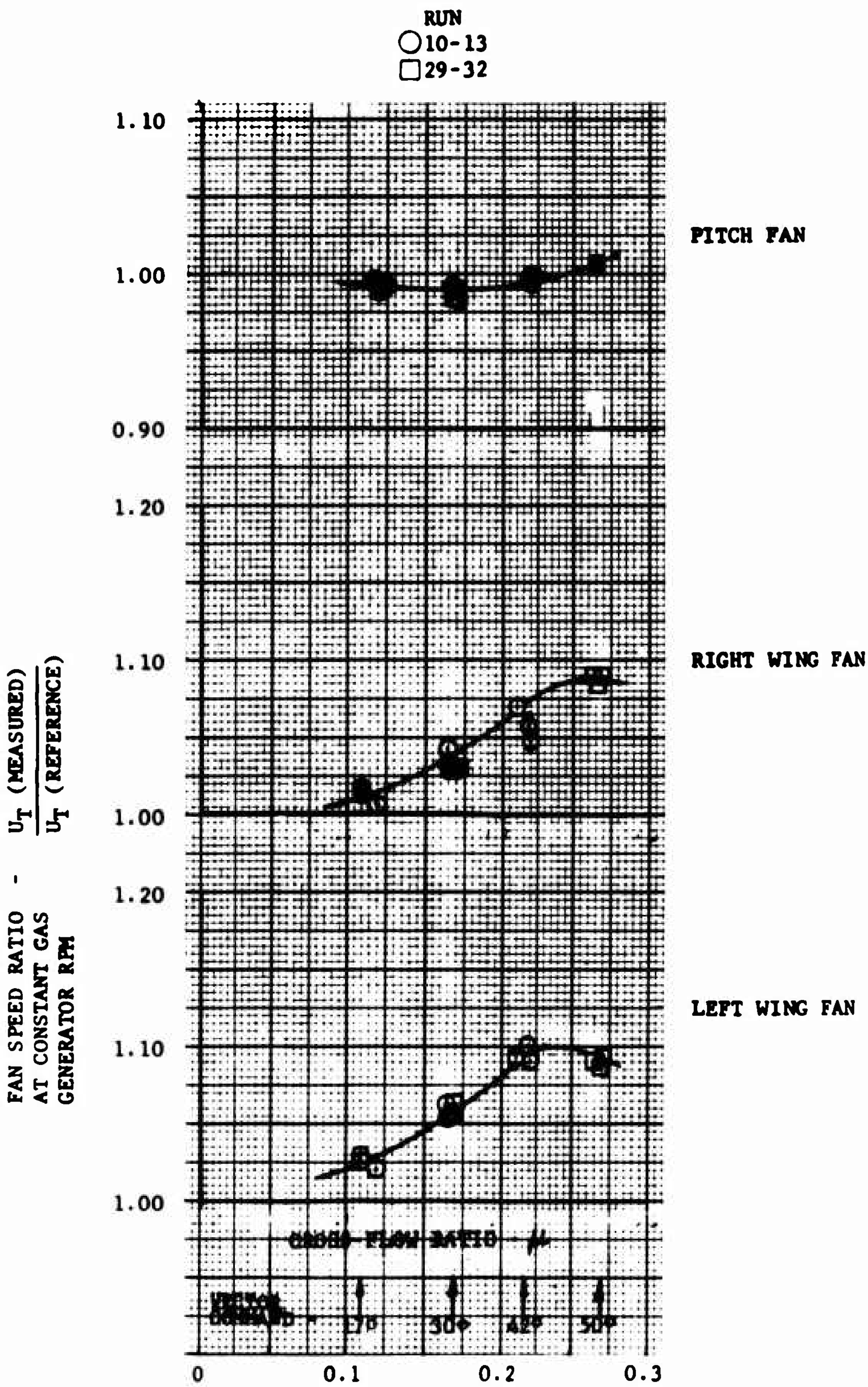

FIGURE 94

FAN SPEED RATIO VERSUS CROSS-FLOW RATIO
FOR APPROXIMATE TRIMMED (DRAG = 0) FLIGHT
HIGH-POWER - CONTROLS FIXED

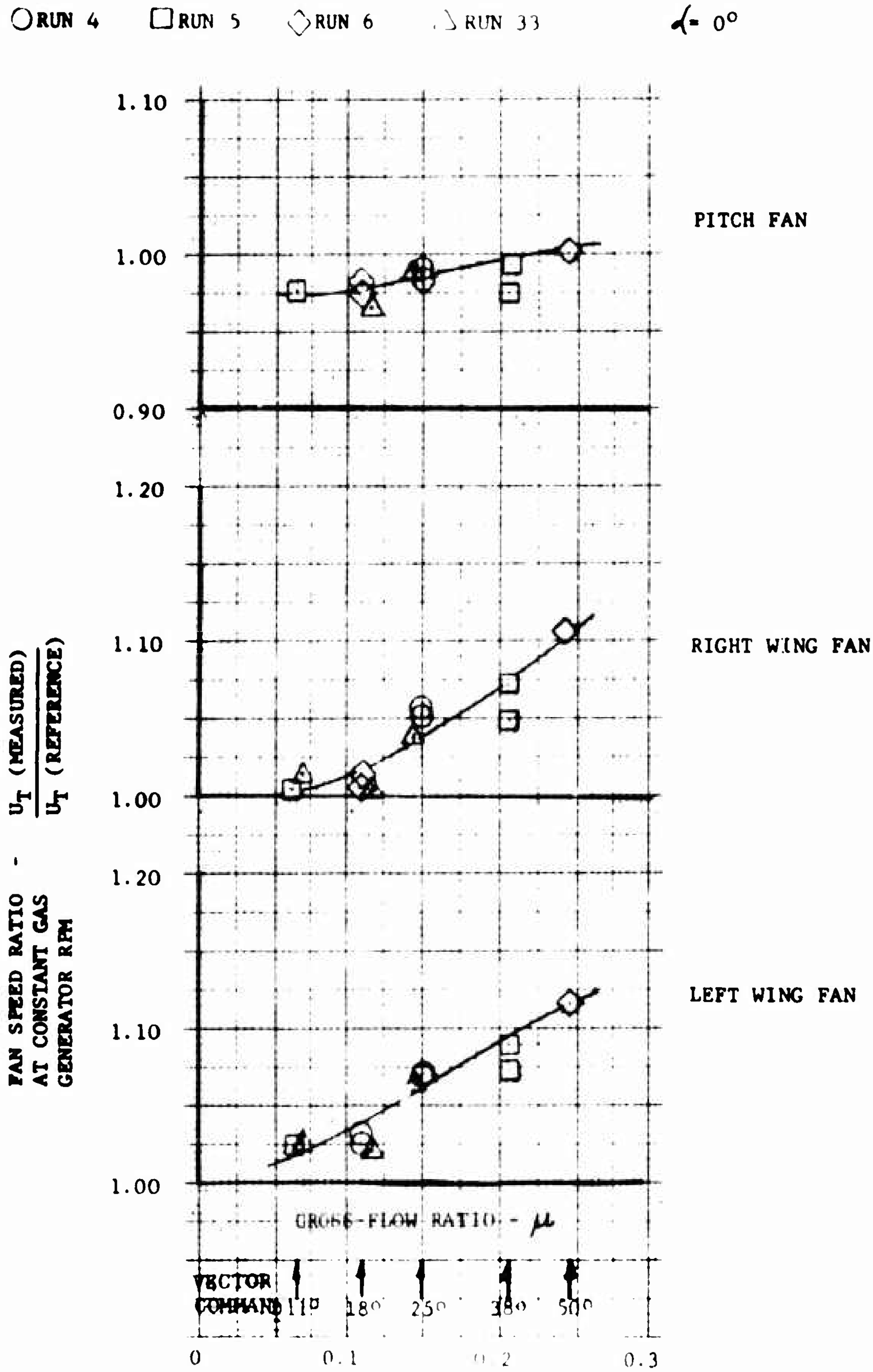

FIGURE 95

FAN SPEED RATIO VERSUS CROSS-FLOW RATIO
FOR APPROXIMATE TRIMMED (DRAG = 0) FLIGHT
LO-POWER - CONTROLS FIXED

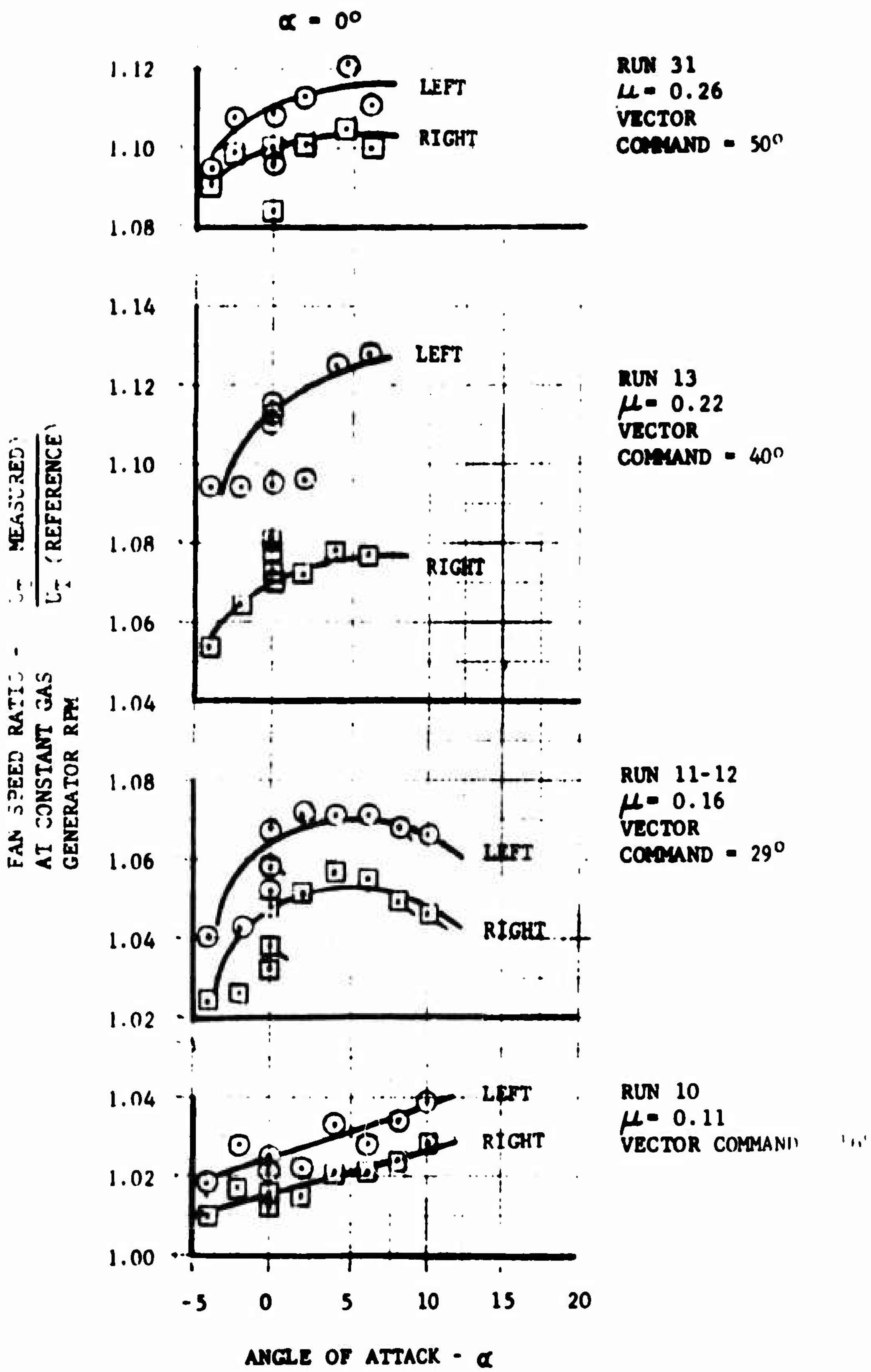

FIGURE 96

WING FAN SPEED RATIO VERSUS ANGLE OF ATTACK FOR APPROXIMATE TRIMMED (DRAG = 0) FLIGHT HI-POWER - CONTROLS FIXED

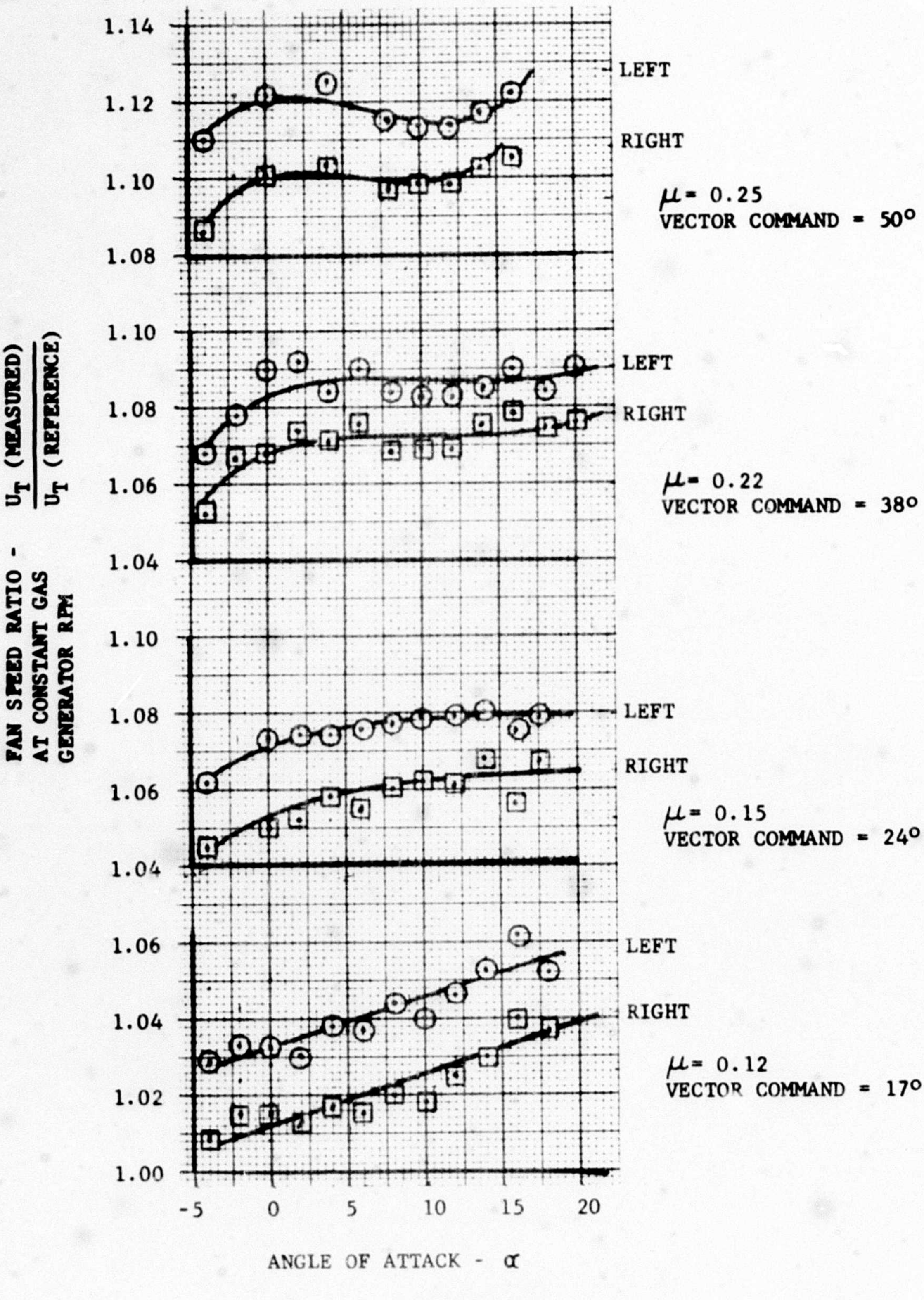

FIGURE 97

WING FAN SPEED RATIO VERSUS ANGLE OF ATTACK FOR APPROXIMATE TRIMMED (DRAG = 0) FLIGHT LO-POWER - CONTROLS FIXED

RUNS 14 - 15

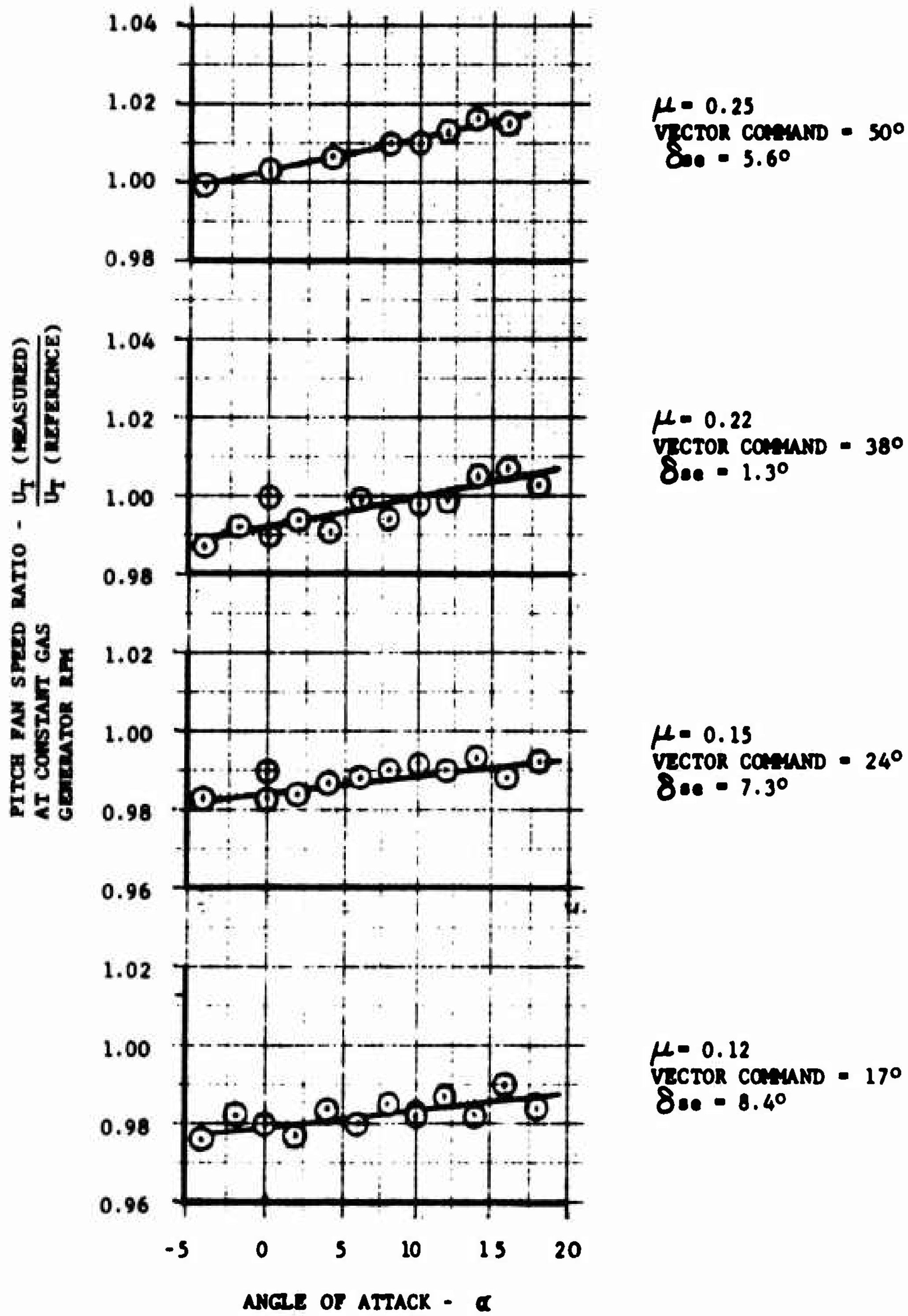

FIGURE 98

PITCH FAN SPEED RATIO VERSUS ANGLE OF ATTACK FOR APPROXIMATE TRIMMED FLIGHT - LO-POWER - CONTROLS FIXED

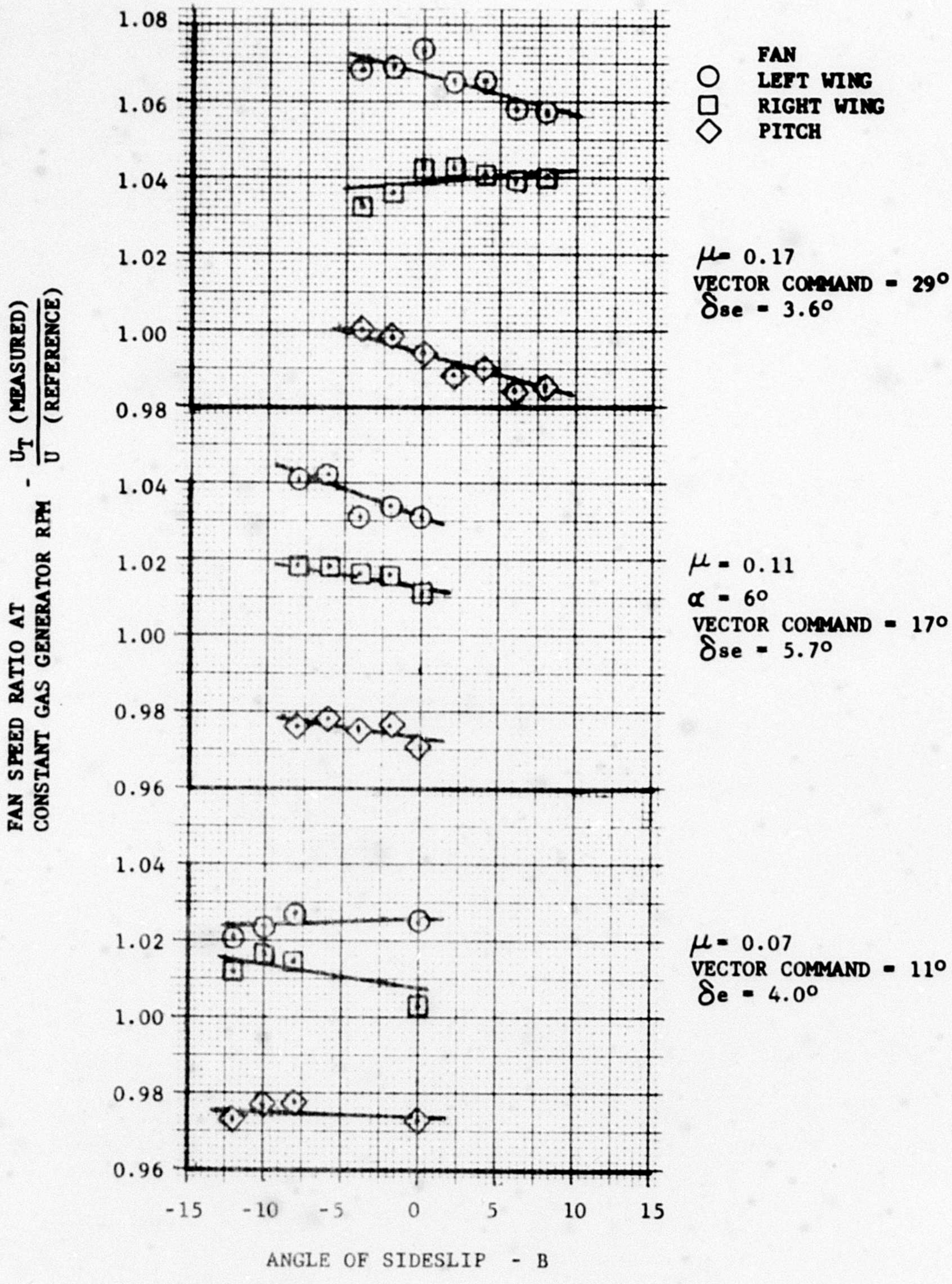

FIGURE 99

FAN SPEED RATIO VERSUS ANGLE OF SIDESLIP AT APPROXIMATE TRIMMED (DRAG = 0) FLIGHT - CONTROLS FIXED

RUNS 10 - 13, 32

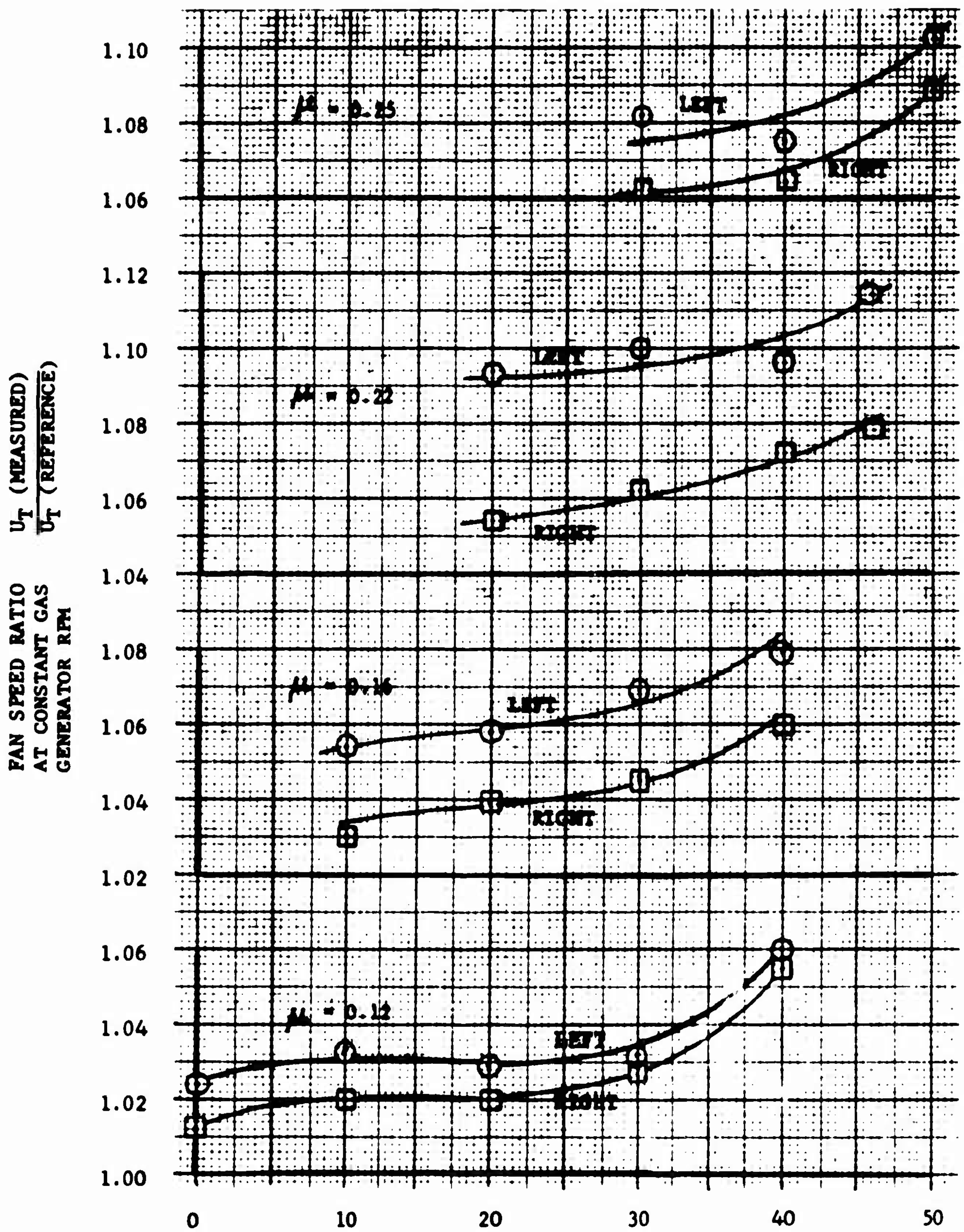

FIGURE 100

WING FAN SPEED RATIOS VERSUS VECTOR COMMAND ANGLE FOR A RANGE OF CROSS-FLOW RATIOS - HI-POWER CONTROLS FIXED

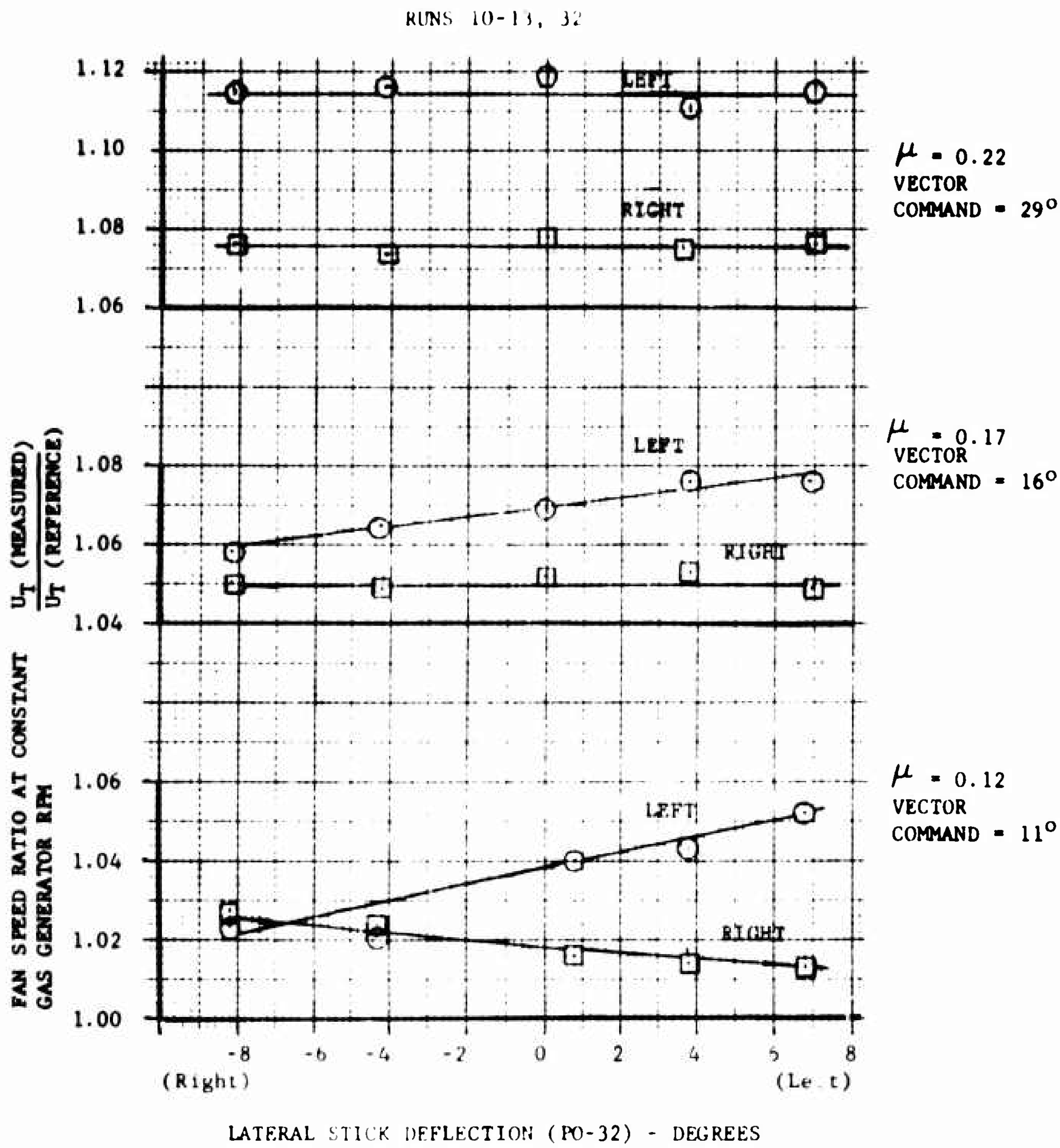

FIGURE 101

FAN SPEED RATIOS VERSUS LATERAL
STICK DEFLECTION FOR
APPROXIMATE TRIMMED (DRAG = 0) FLIGHT
HI-POWER
ALL OTHER CONTROLS FIXED

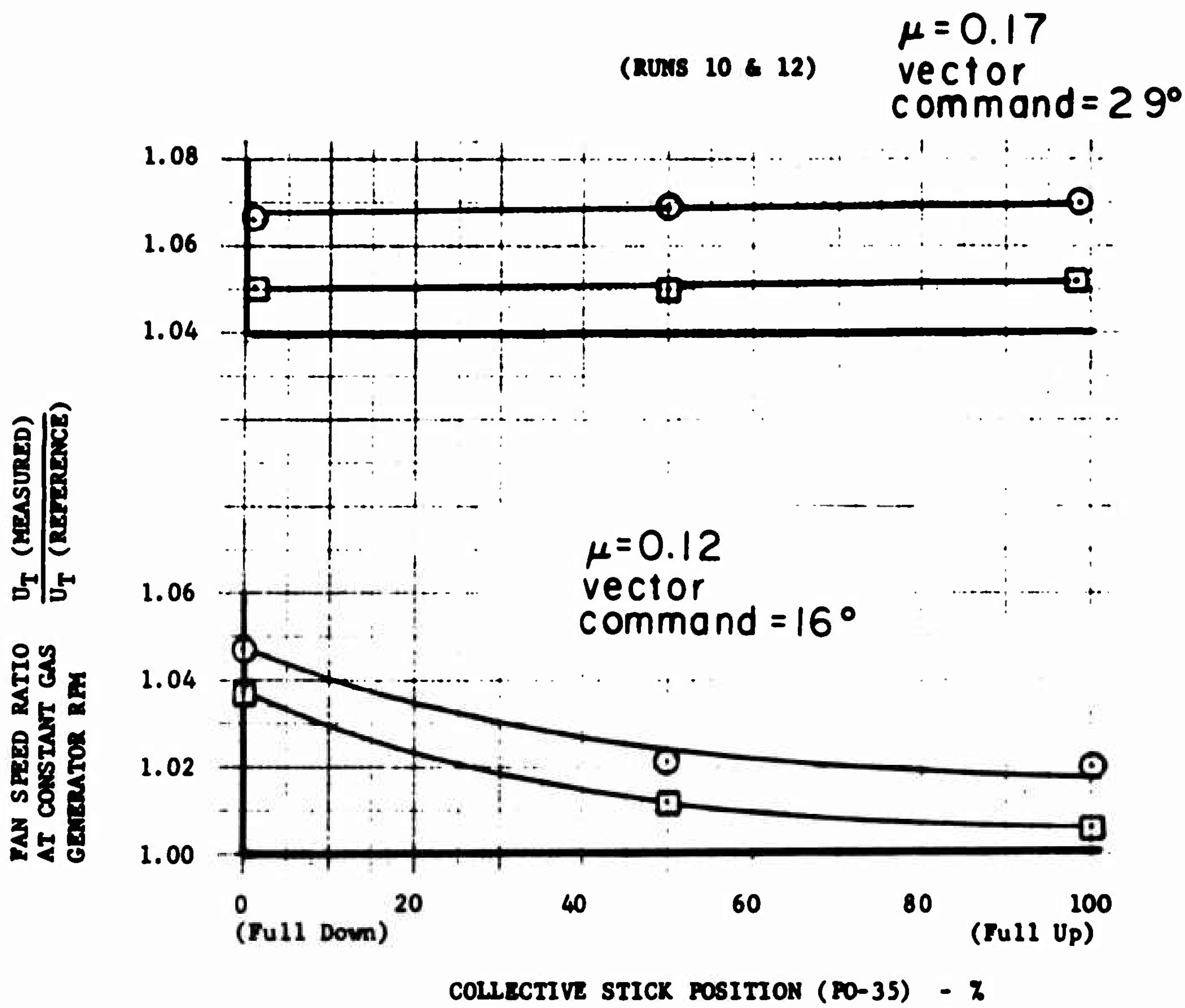

FIGURE 102

FAN SPEED RATIOS VERSUS COLLECTIVE STICK POSITION FOR APPROXIMATE TRIMMED (DRAG=0) FLIGHT

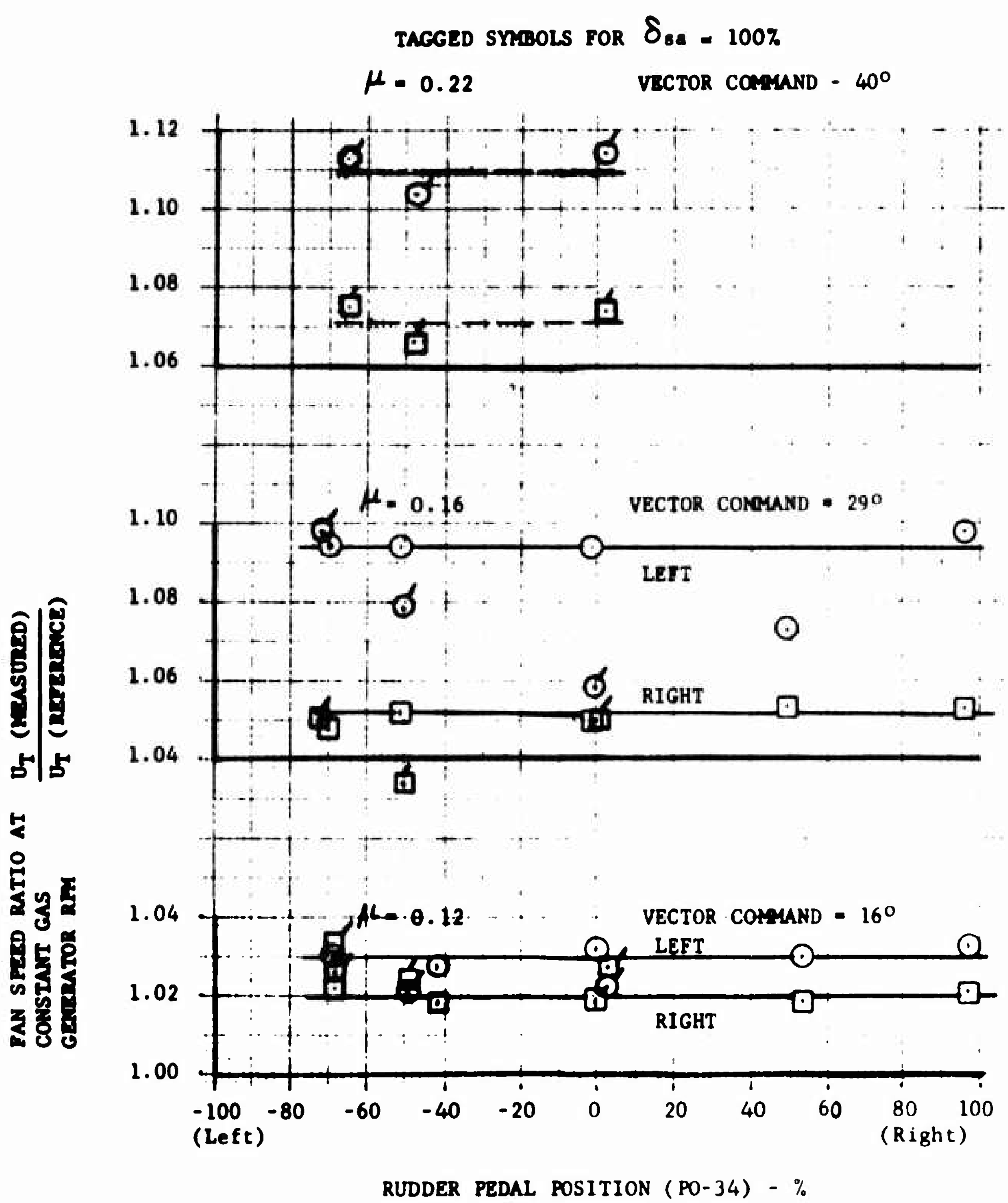

FIGURE 103

FAN SPEED RATIOS VERSUS RUDDER
PEDAL POSITION FOR APPROXIMATE
HI-POWER
ALL CONTROLS FIXED EXCEPT
AS NOTED

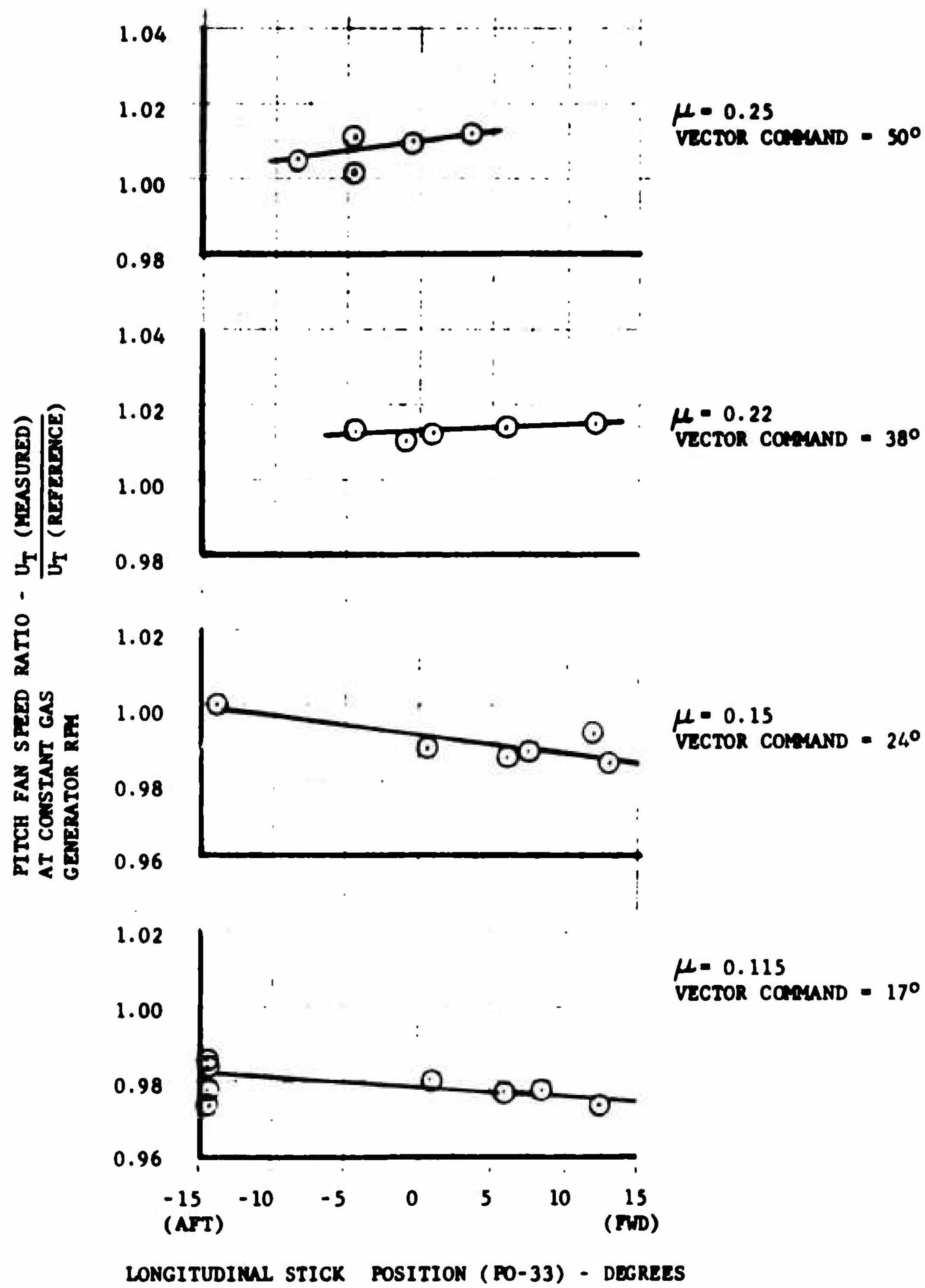

FIGURE 104

PITCH FAN SPEED RATIO VERSUS LONGITUDINAL STICK DEFLECTION FOR APPROXIMATE TRIMMED FLIGHT - LO-POWER ALL OTHER CONTROLS NEUTRAL

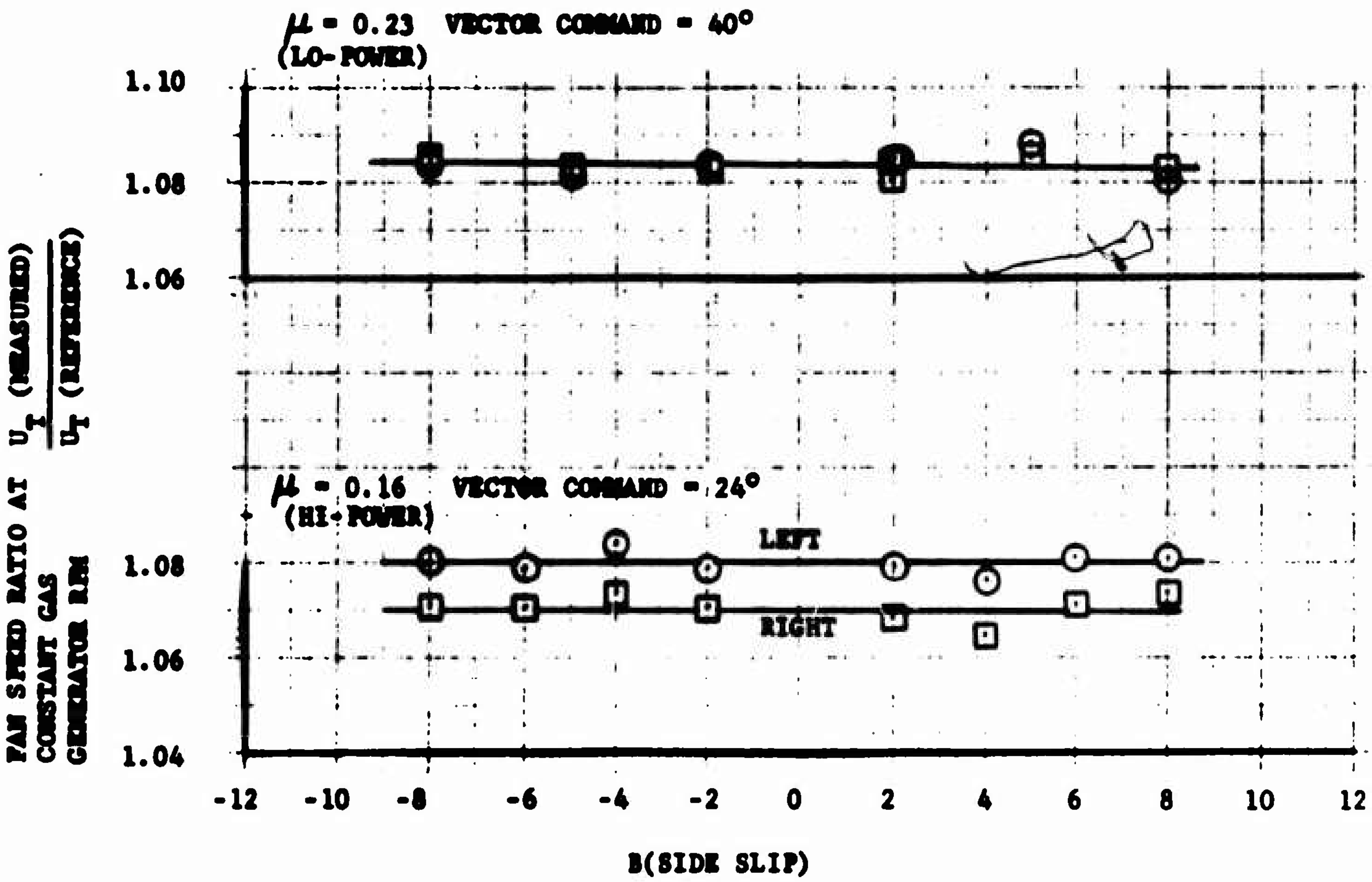

FIGURE 105

FAN SPEED RATIOS VERSUS ANGLE OF SIDESLIP AT APPROXIMATE TRIMMED (DRAG = 0) FLIGHT PITCH FAN "OFF"

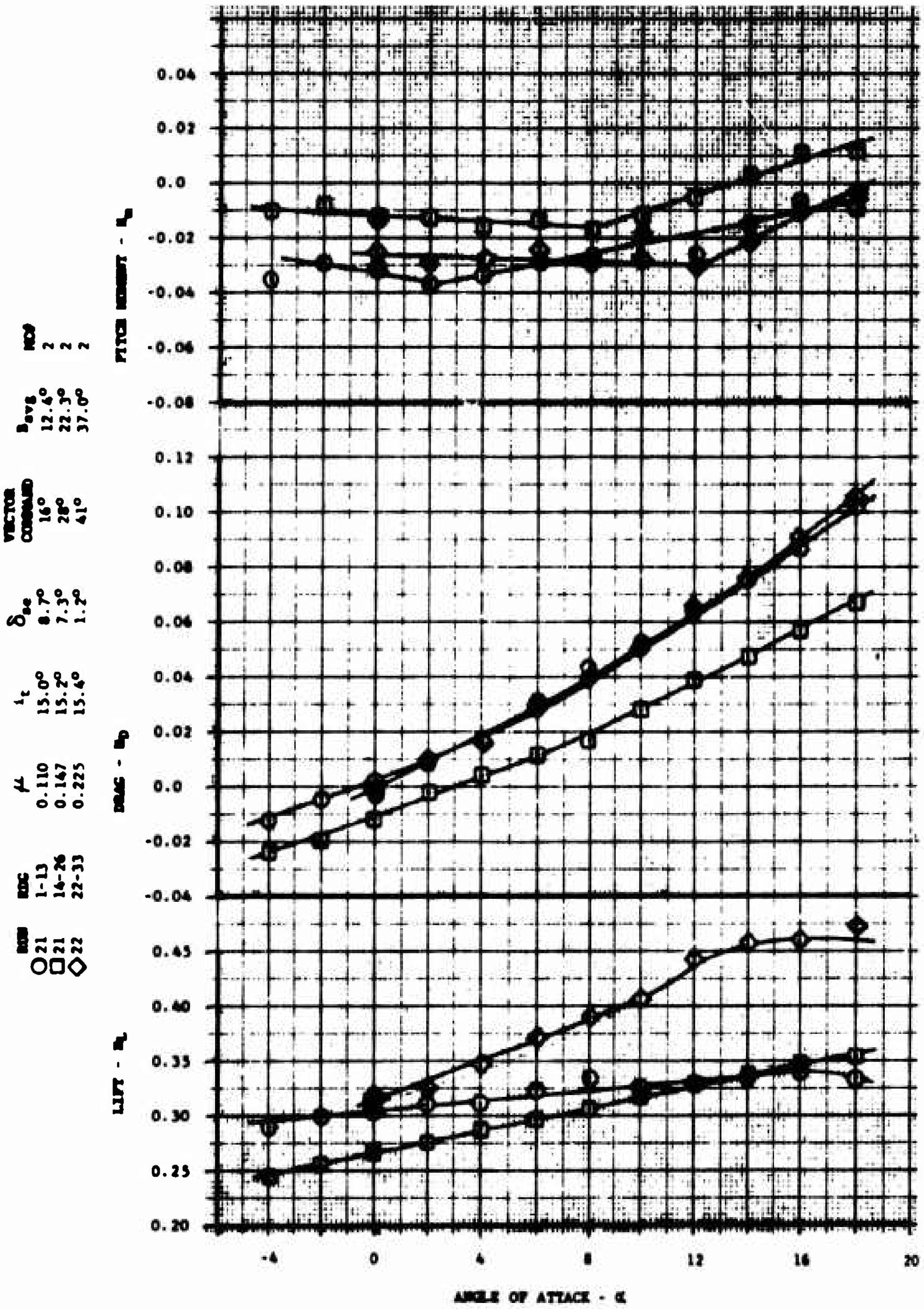

FIGURE 106

LONGITUDINAL CHARACTERISTICS - FAN POWERED (LO-POWER) - NORMAL TAIL WITH SLAT

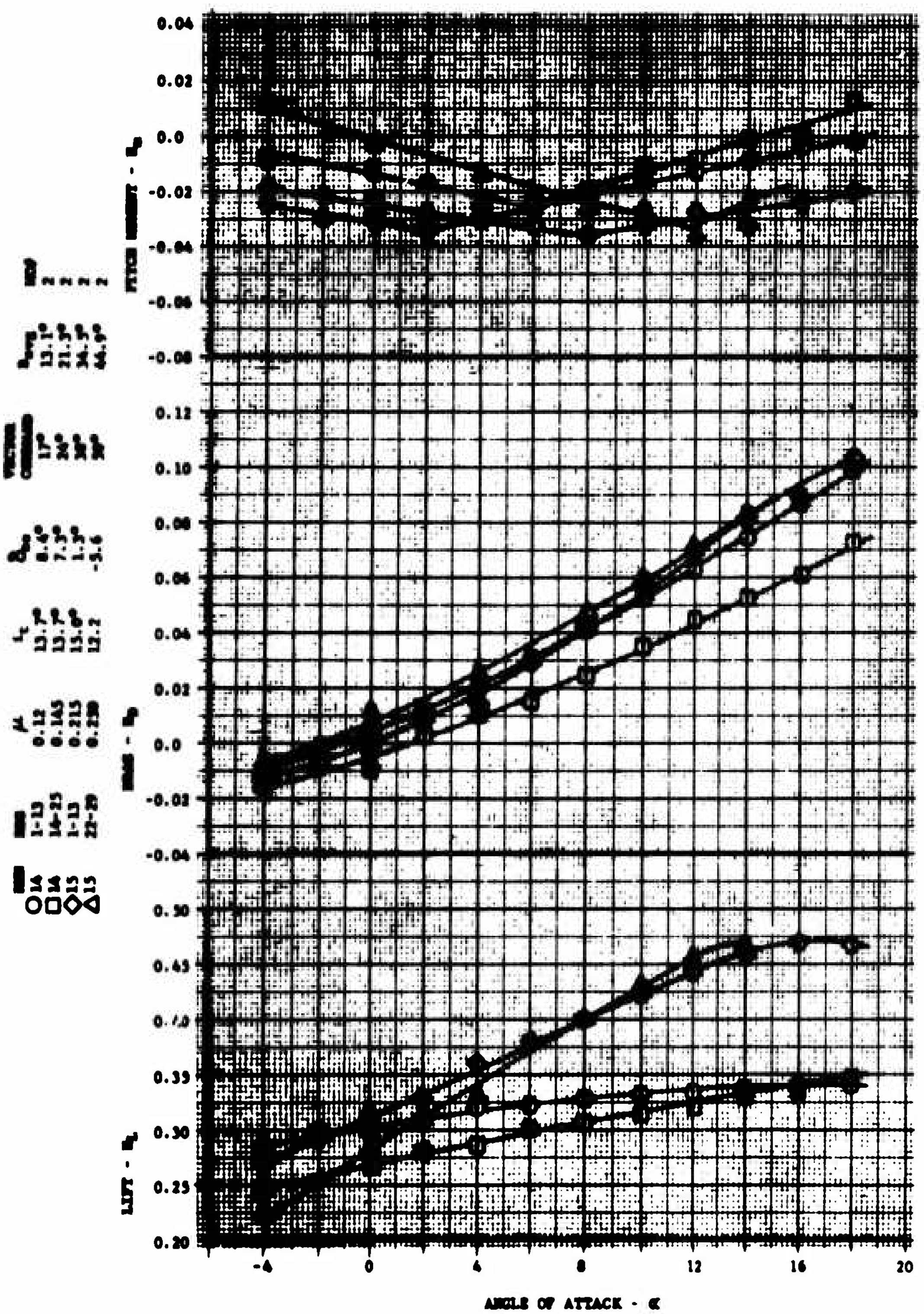

FIGURE 107

LONGITUDINAL CHARACTERISTICS - FAN POWERED (LO-POWER) - TAIL WITH TIP EXTENSIONS

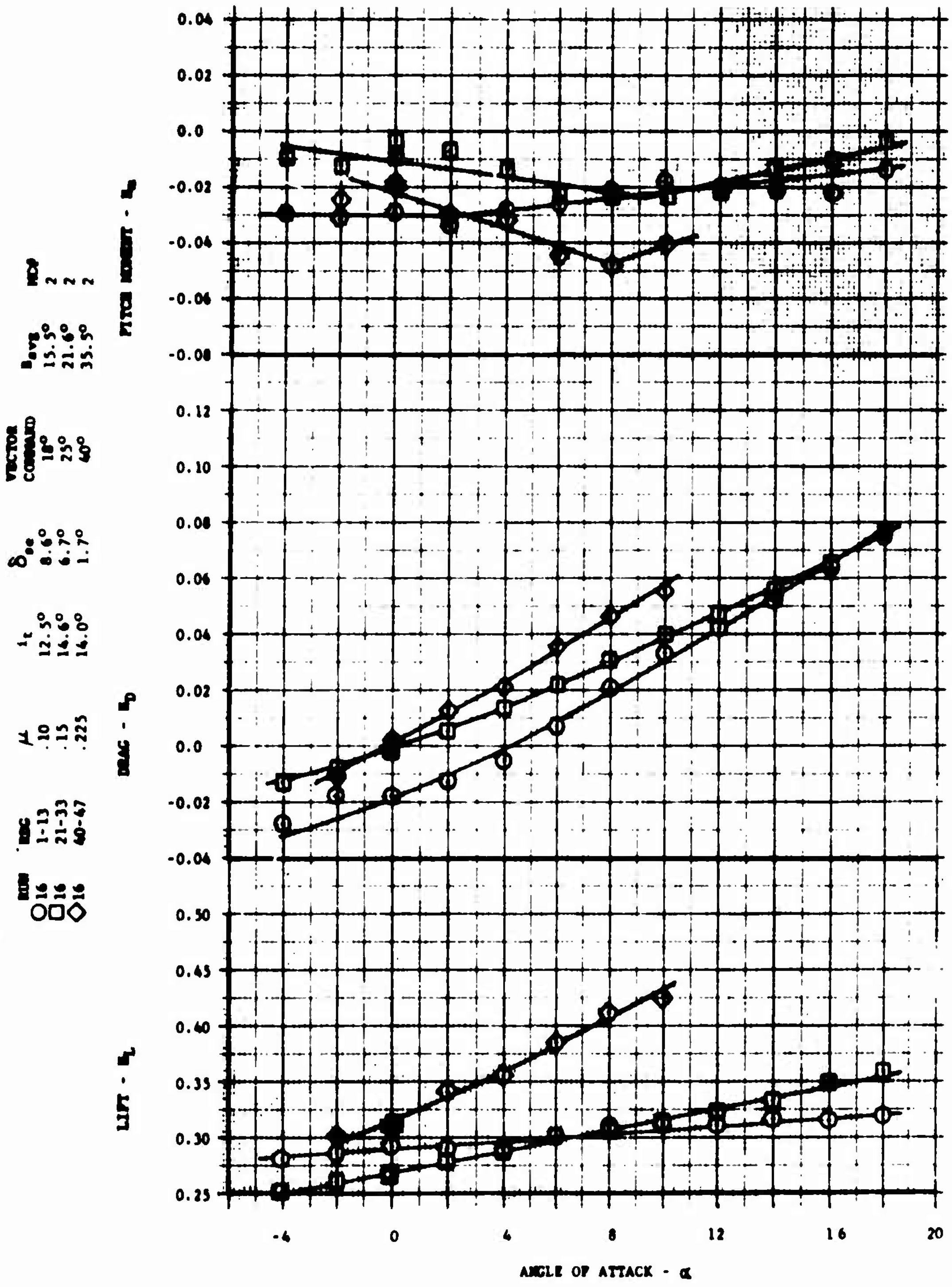

FIGURE 108

LONGITUDINAL CHARACTERISTICS - FAN POWERED (LO-POWER) - TAIL WITH TIPS AND SLAT

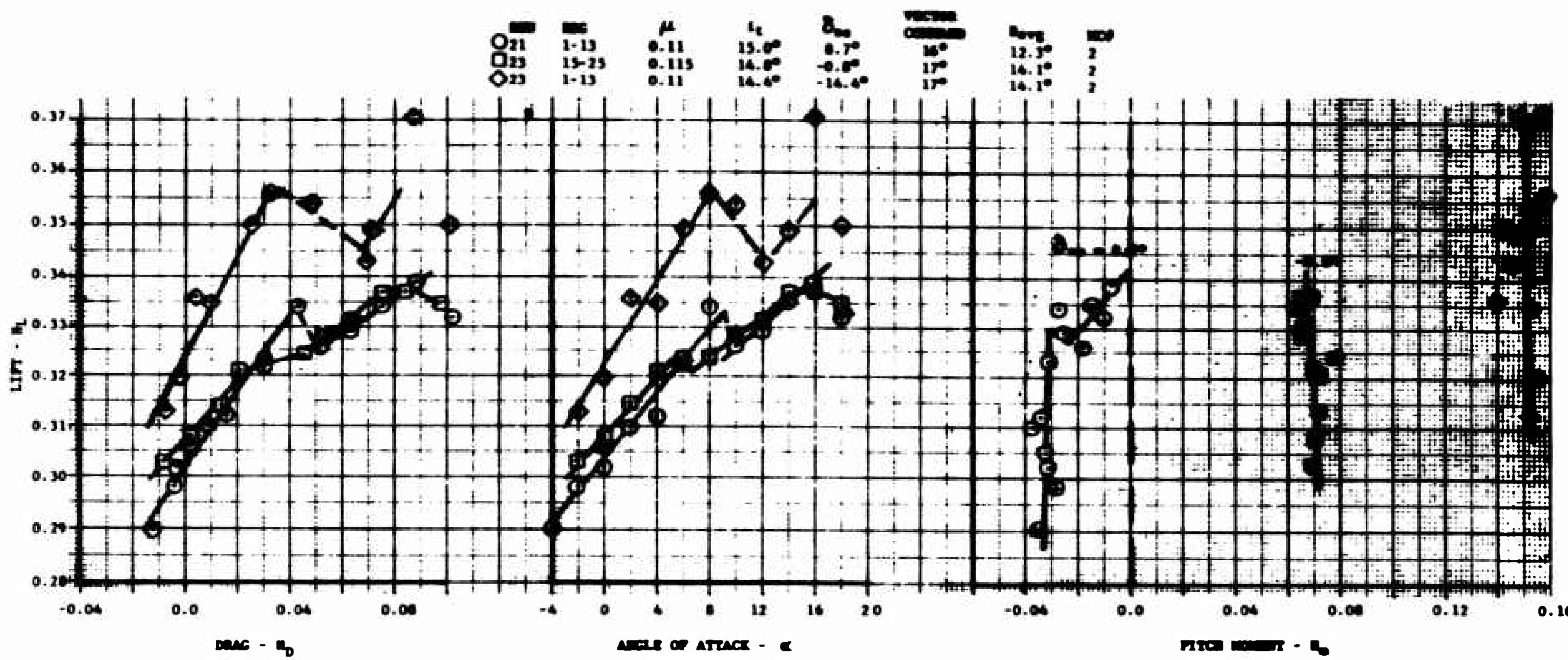

FIGURE 109

LONGITUDINAL CHARACTERISTICS FOR A RANGE OF CONTROL SETTINGS FAN POWERED (LO-POWER) - SMALL TAIL WITH SLAT - μ = 0.11

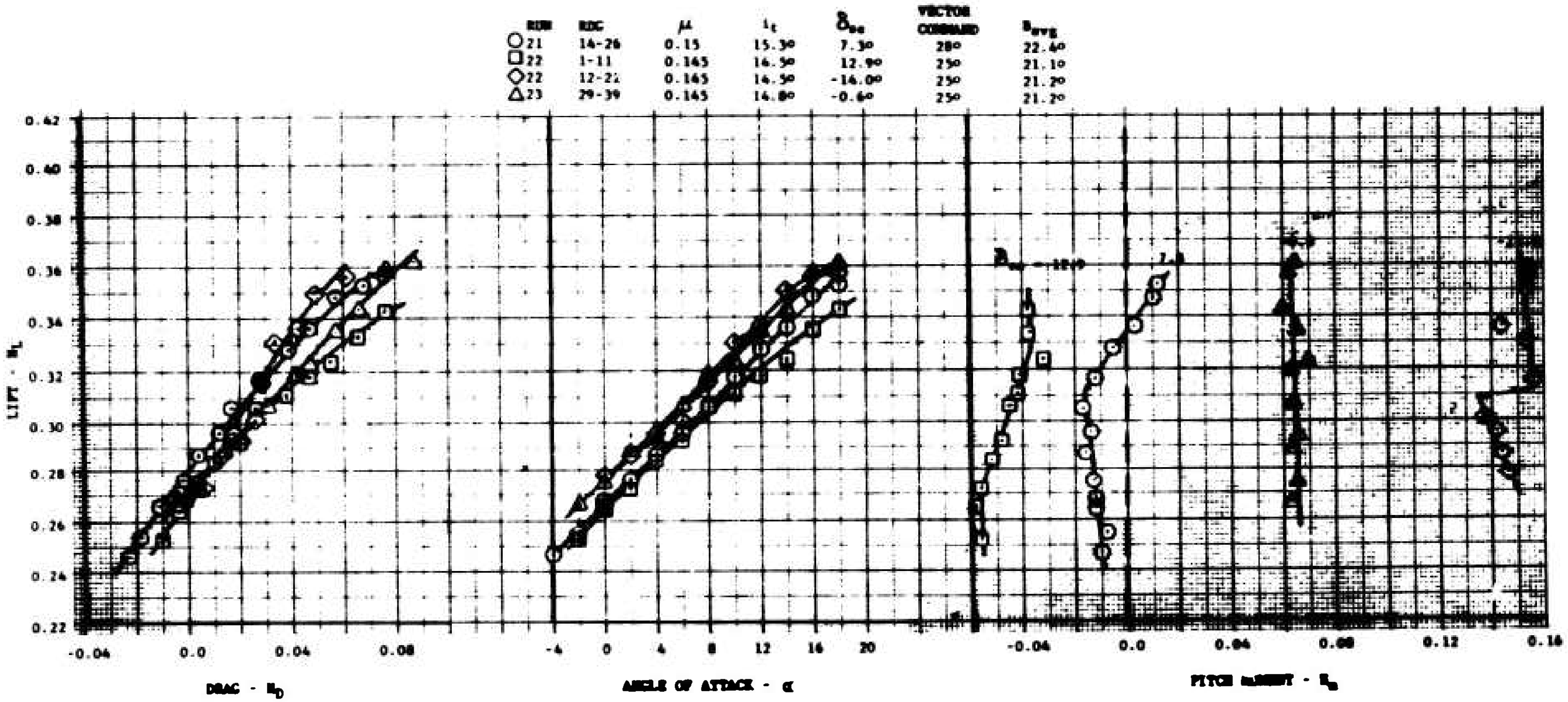

FIGURE 110

LONGITUDINAL CHARACTERISTICS FOR A RANGE OF CONTROL SETTINGS
FAN POWERED (LO-POWER) - NORMAL TAIL WITH SLAT - μ = 0.145

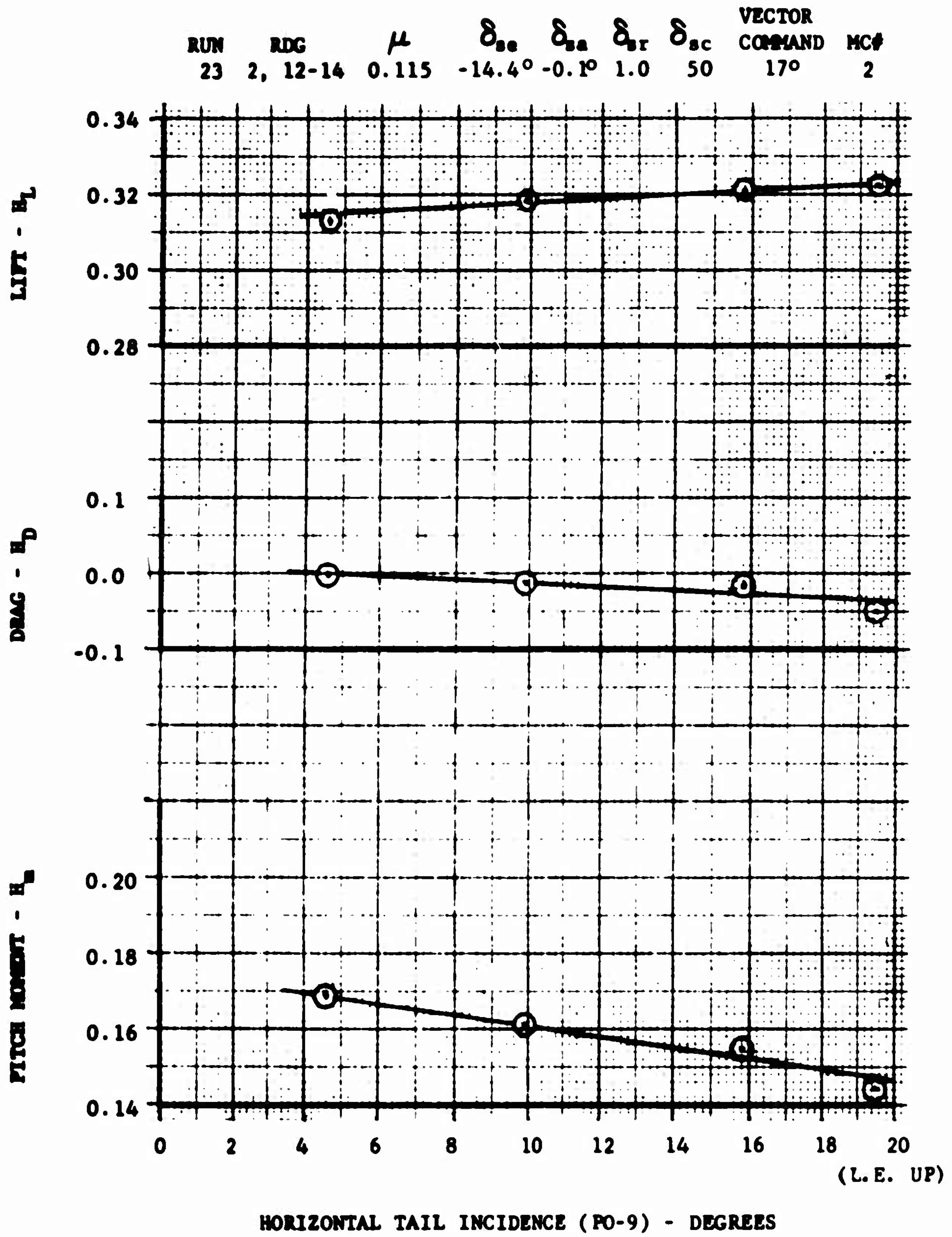

FIGURE 111

HORIZONTAL STABILIZER EFFECTIVENESS
FAN POWERED (LO-POWER)- HORIZONTAL TAIL WITH
SLAT
$\mu = 0.115$

RUN	RDG	μ	δ_{se}	δ_{sa}	δ_{sr}	δ_{sc}	VECTOR COMMAND	MC#
23	16, 26-28	0.115	-0.8°	-0.1°	2.0	52	17°	2

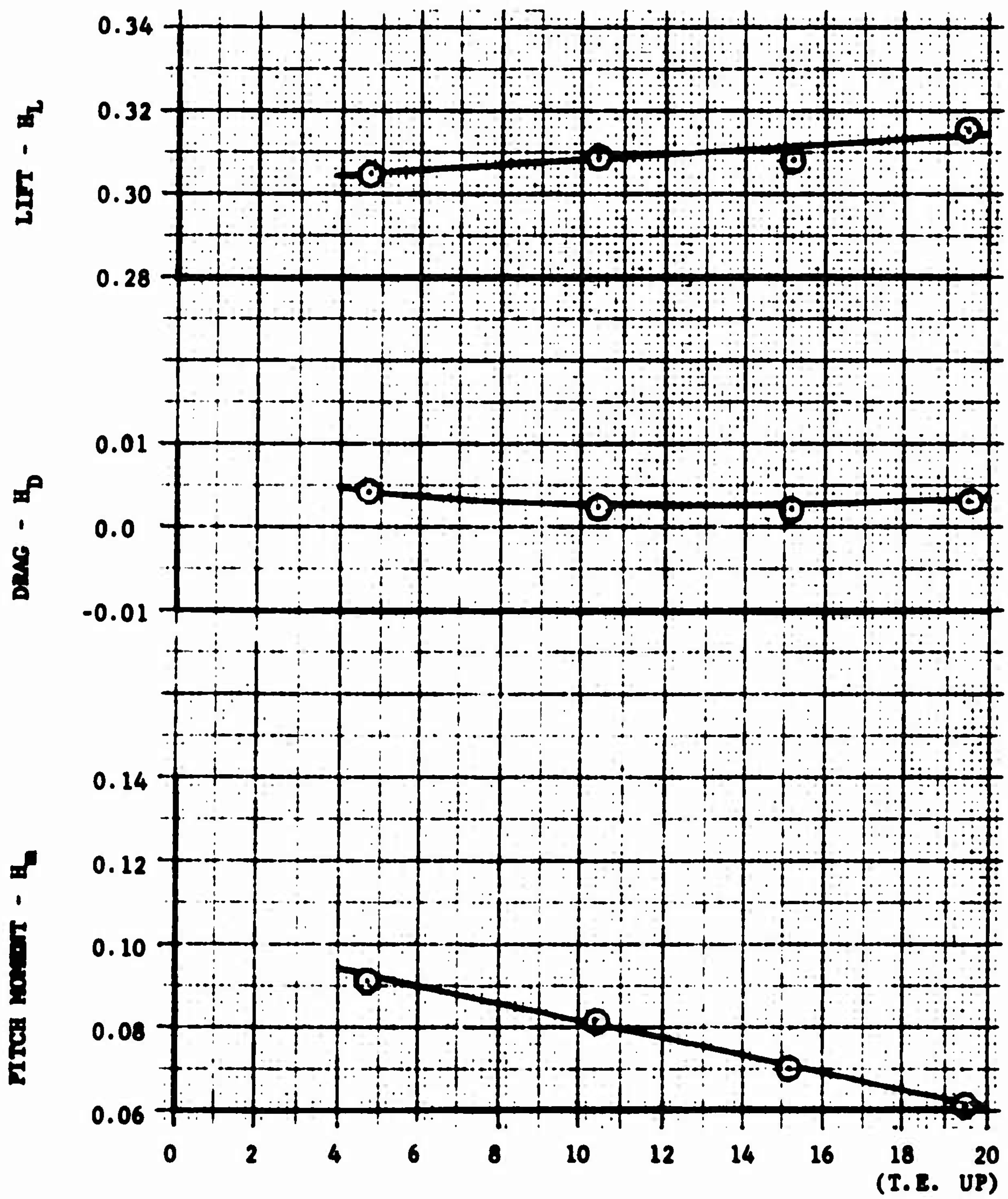

HORIZONTAL TAIL INCIDENCE (PO-9) - DEGREES

FIGURE 112

HORIZONTAL STABILIZER EFFECTIVENESS
FAN POWERED (LO-POWER) - NORMAL TAIL WITH SLAT
μ = 0.115

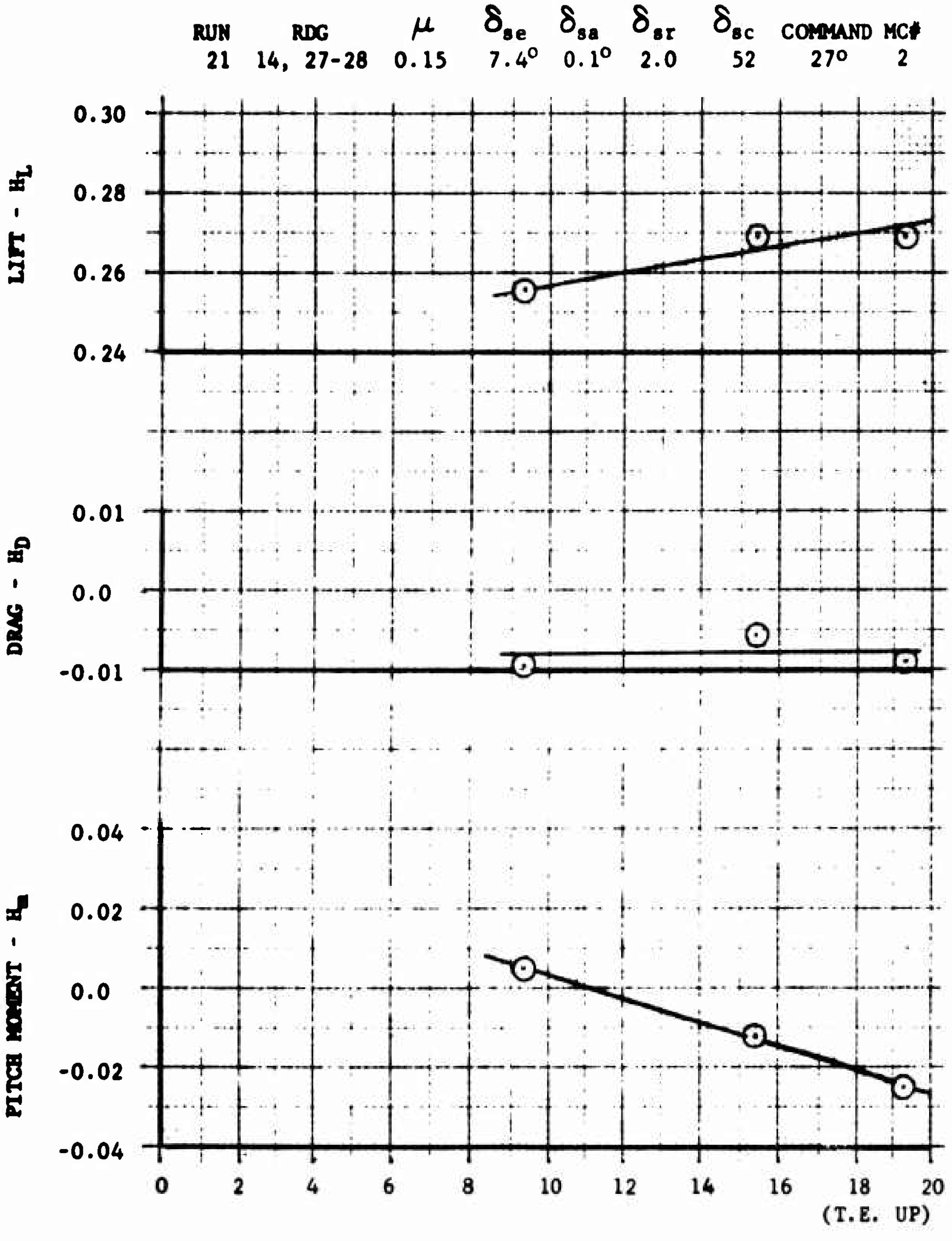

FIGURE 113

HORIZONTAL STABILIZER EFFECTIVENESS
FAN POWERED (LO-POWER) - NORMAL TAIL WITH SLAT
$\mu = 0.15$, $\delta_{se} = 7.4^{\circ}$

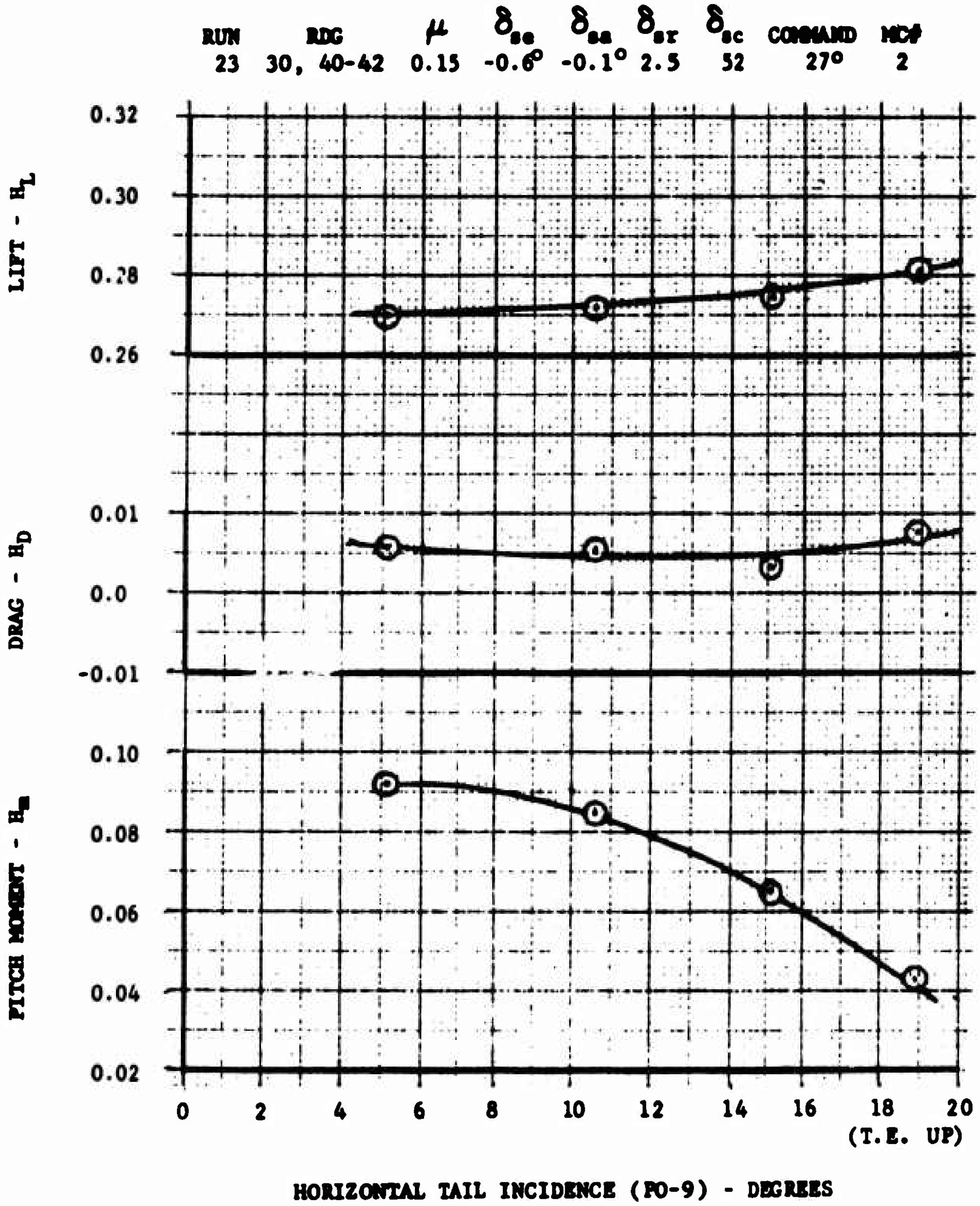

FIGURE 114

HORIZONTAL STABILIZER EFFECTIVENESS
FAN POWERED (LO-POWER) - NORMAL TAIL WITH SLAT
$\mu = 0.15$, $\delta_{se} = -.06$

RUN	RDG	μ	δ_{se}	δ_{sa}	δ_{sr}	δ_{sc}	VECTOR COMMAND	MC#
23	14, 16, 29-32	0.15	7.2°	-0.3°	2.0	51	24°	2

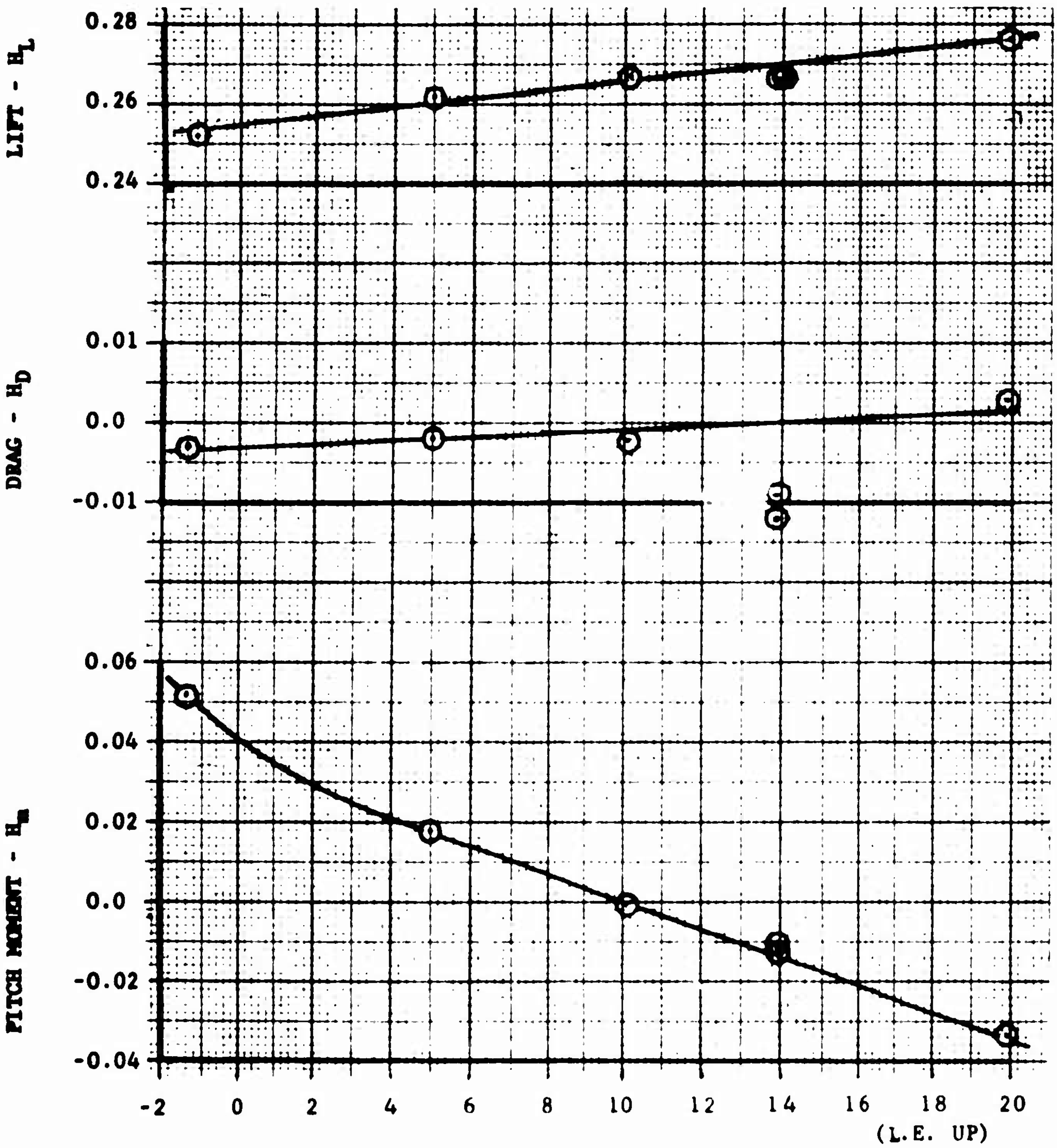

FIGURE 115

HORIZONTAL STABILIZER EFFECTIVENESS
FAN POWERED (LO-POWER) - LARGE TAIL
$\mu = 0.15$

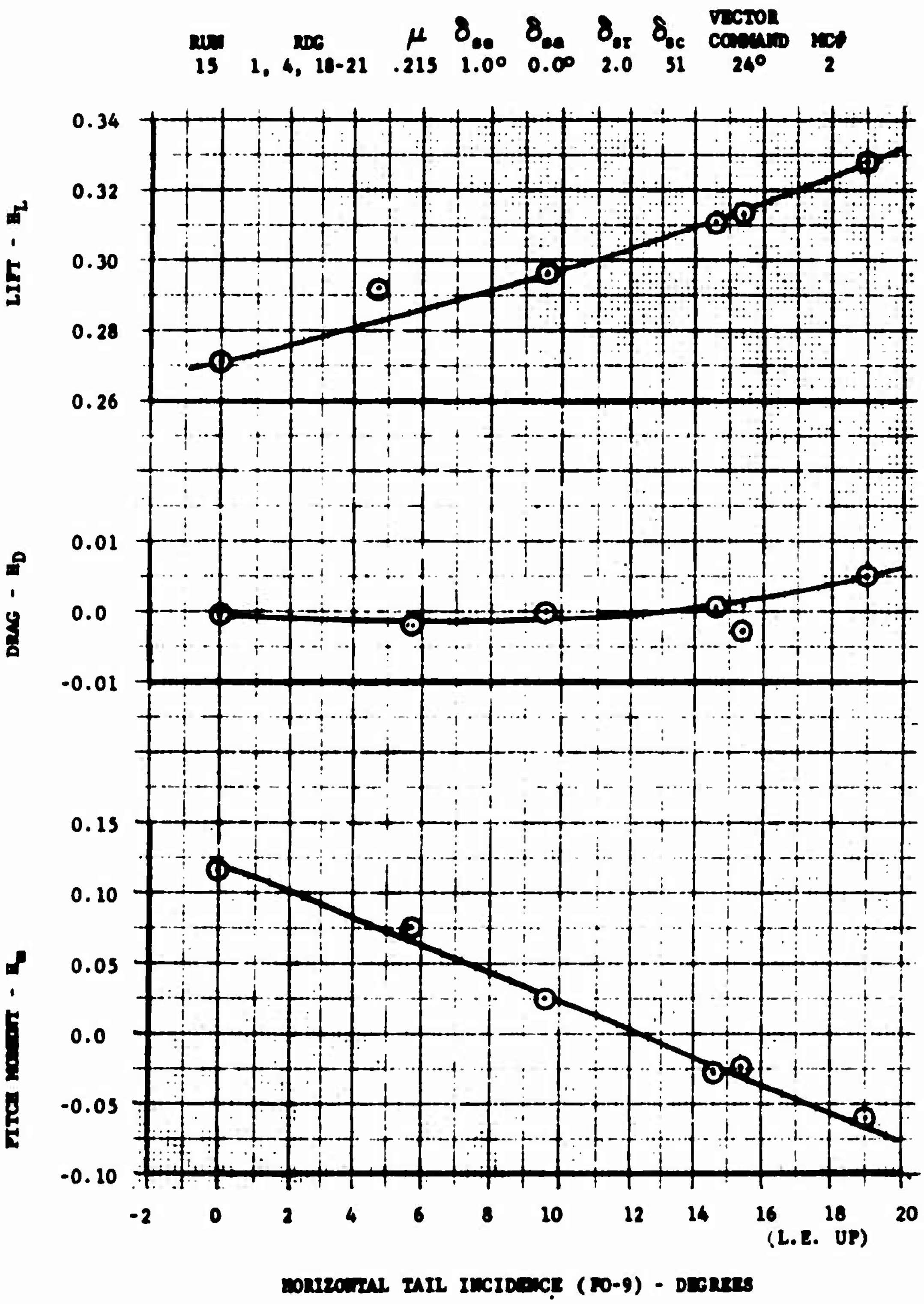

FIGURE 116

HORIZONTAL STABILIZER EFFECTIVENESS
FAN POWERED (LO-POWER) - LARGE TAIL
$\mu = 0.215$

RUN	RDG	μ	δ_{se}	δ_{sa}	δ_{sr}	δ_{sc}	VECTOR COMMAND	MC#
16	4, 17-20	0.15	8.3°	-0.1°	1.0	52°	18°	2

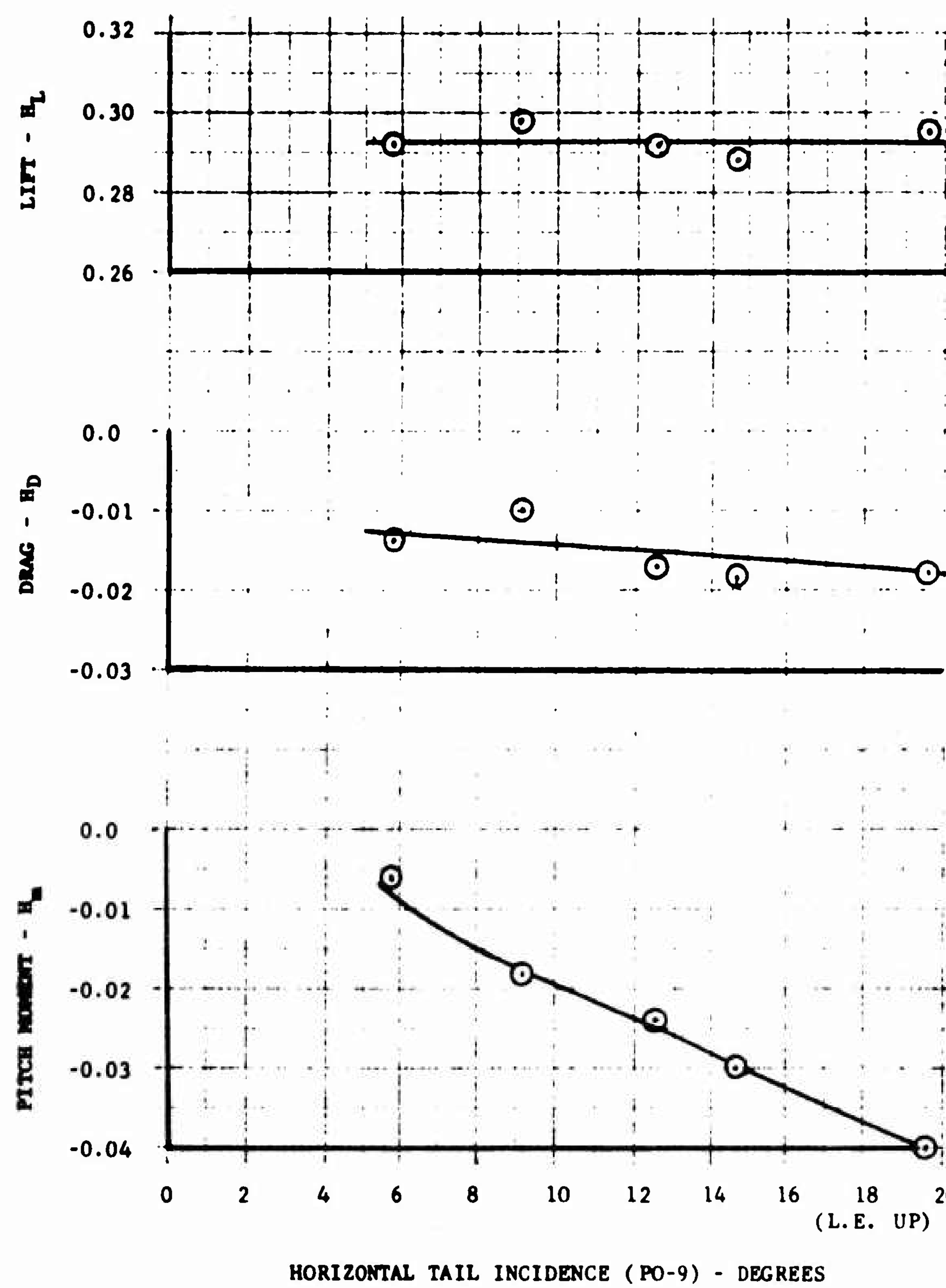

FIGURE 117

HORIZONTAL STABILIZER EFFECTIVENESS
FAN POWERED (LO-POWER) - LARGE TAIL WITH SLAT
μ = 0.115

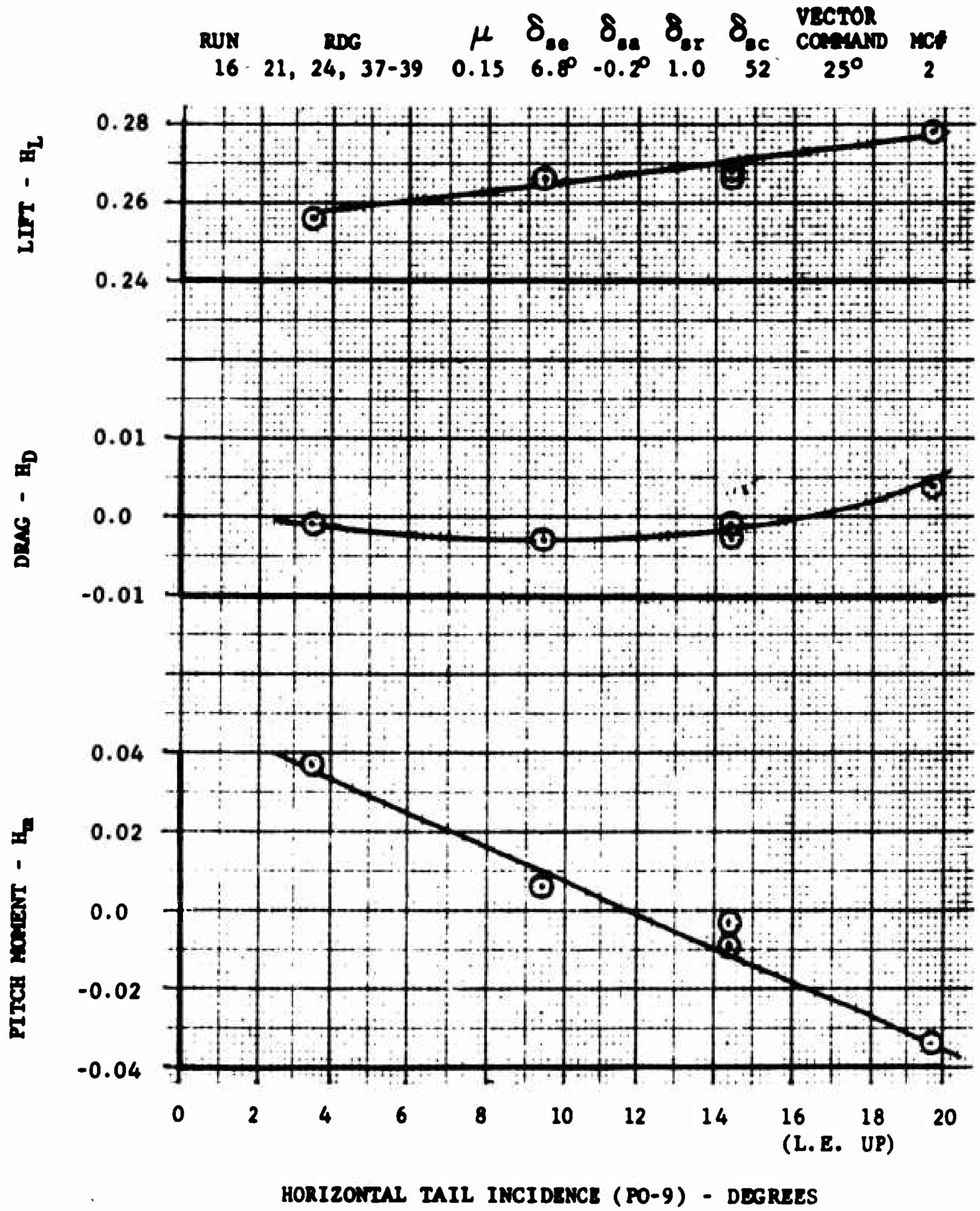

FIGURE 118

HORIZONTAL STABILIZER EFFECTIVENESS
FAN POWERED (LO-POWER) - LARGE TAIL
WITH SLAT
μ = 0.15

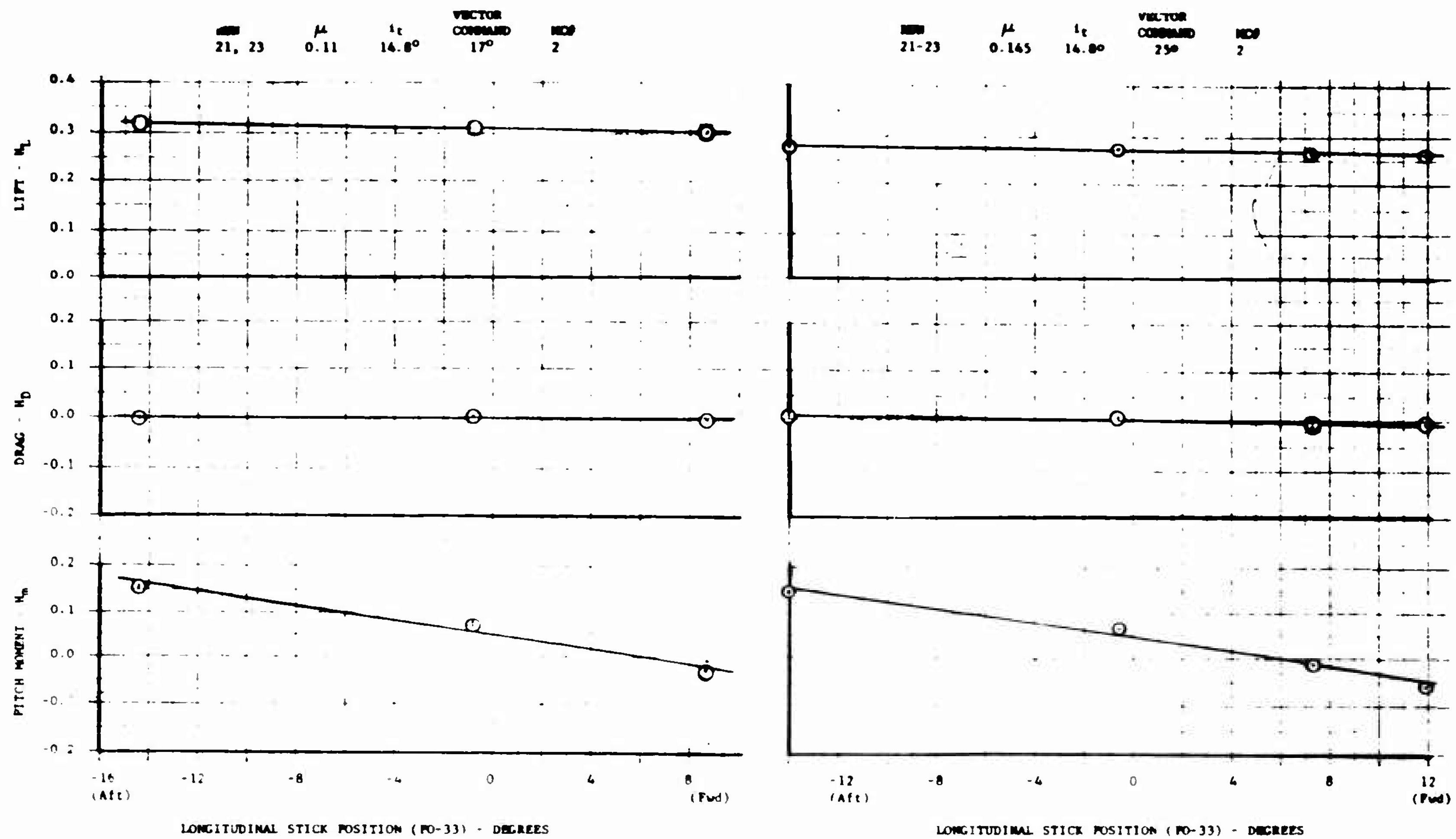

FIGURE 119

LONGITUDINAL CONTROL CHARACTERISTICS - FAN POWERED (LO-POWER)
NORMAL TAIL WITH SLAT - μ = 0.11 AND 0.145

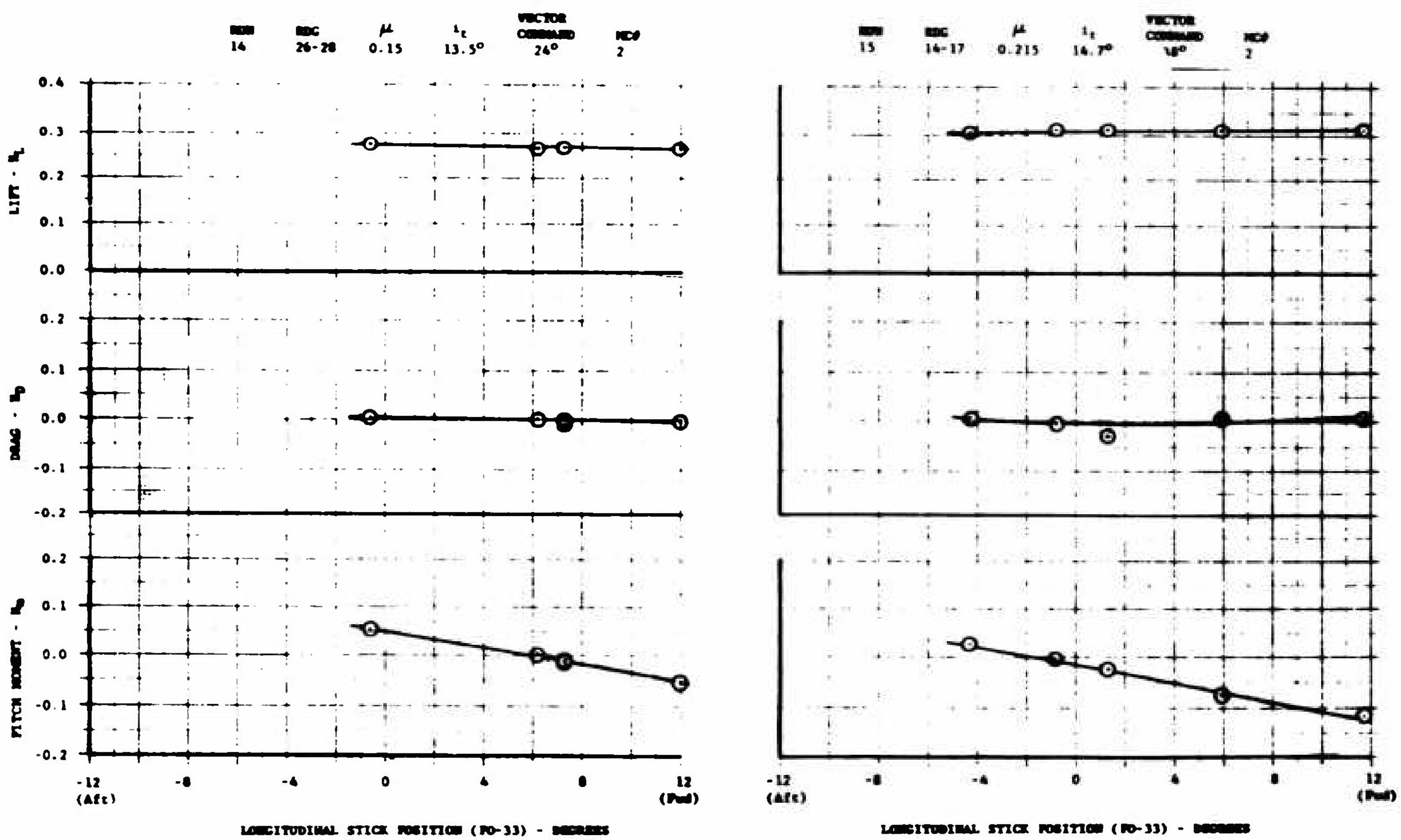

FIGURE 120

LONGITUDINAL CONTROL EFFECTIVENESS - FAN POWERED (LO-POWER)
LARGE TAIL - μ = 0.15 AND 0.215

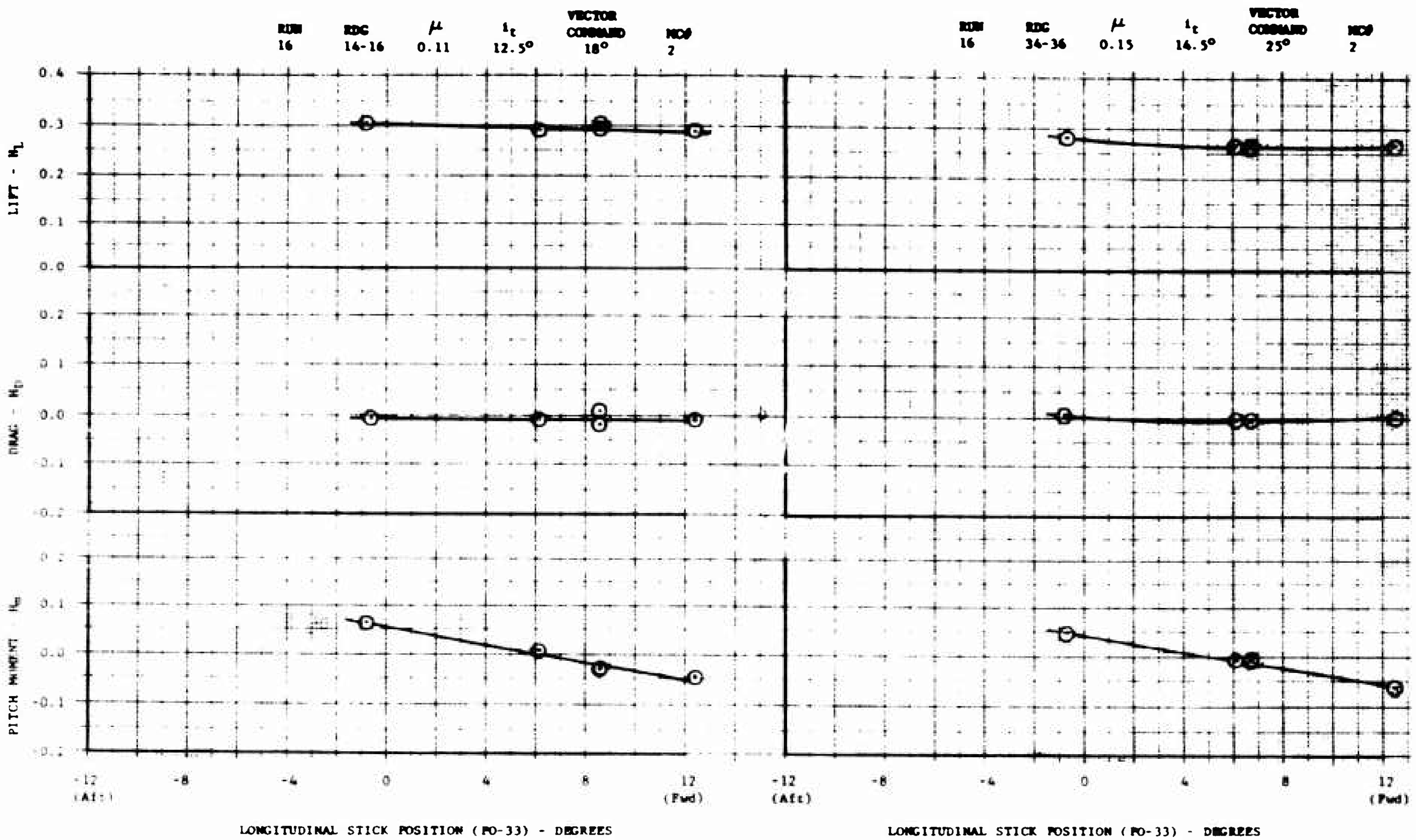

FIGURE 121
LONGITUDINAL CONTROL EFFECTIVENESS - FAN POWERED (LO-POWER)
LARGE TAIL WITH SLAT - μ = 0.11 AND 0.15

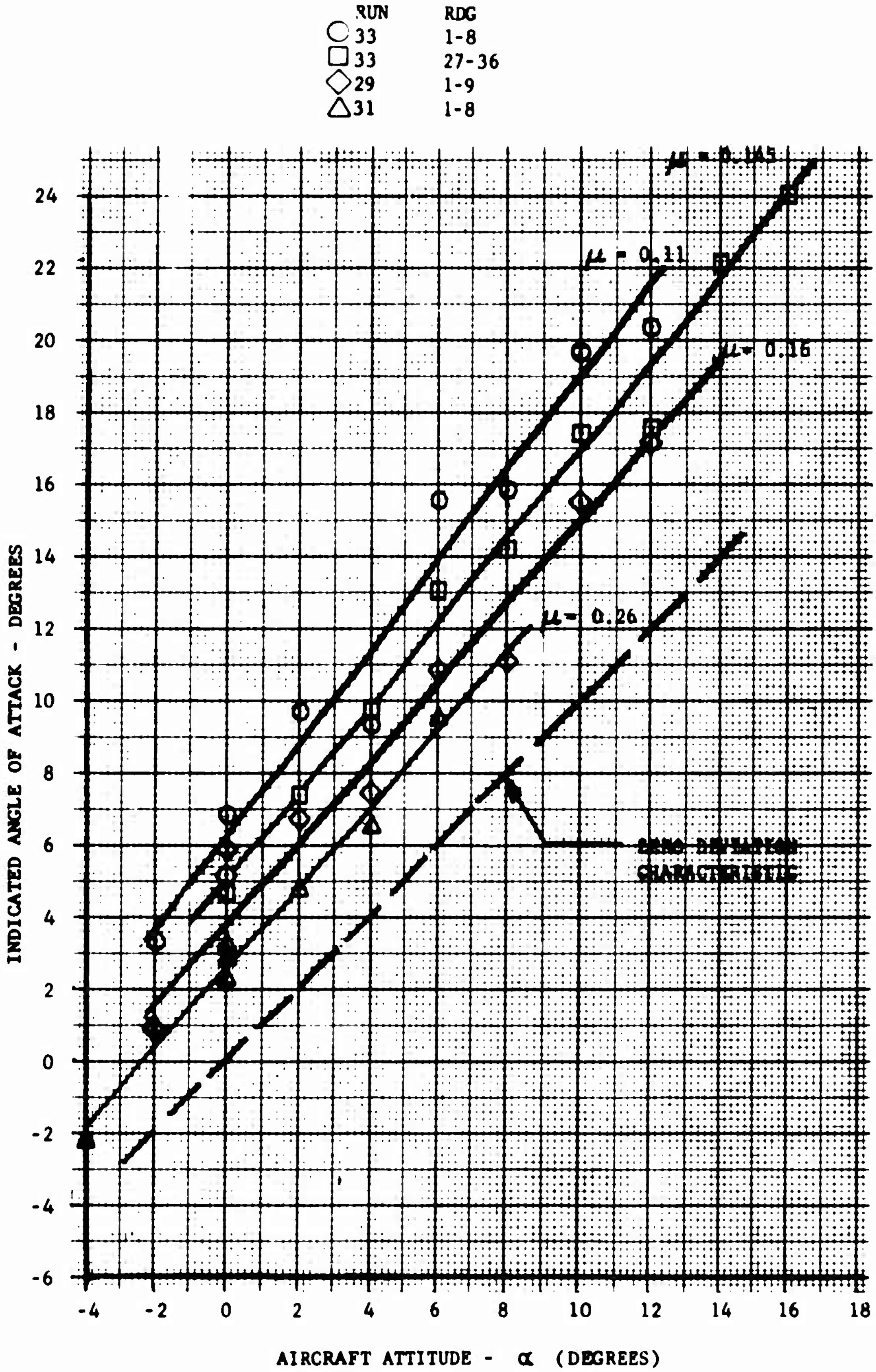

FIGURE 122

PITCH ATTITUDE INDICATOR CALIBRATION
FAN POWERED - PITCH FAN "ON"

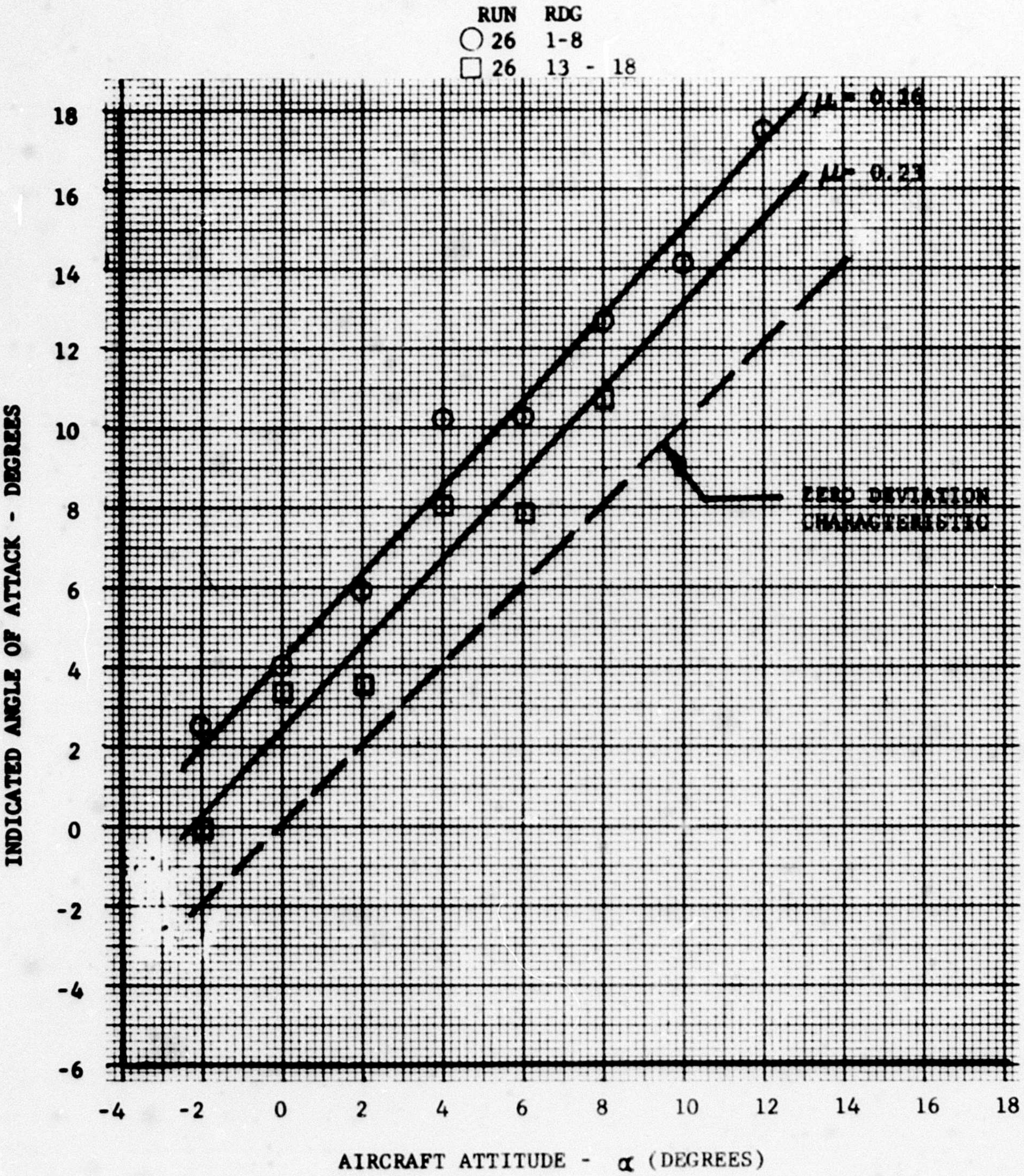

FIGURE 123

PITCH ATTITUDE INDICATOR CALIBRATION
FAN POWERED - PITCH FAN "OFF"

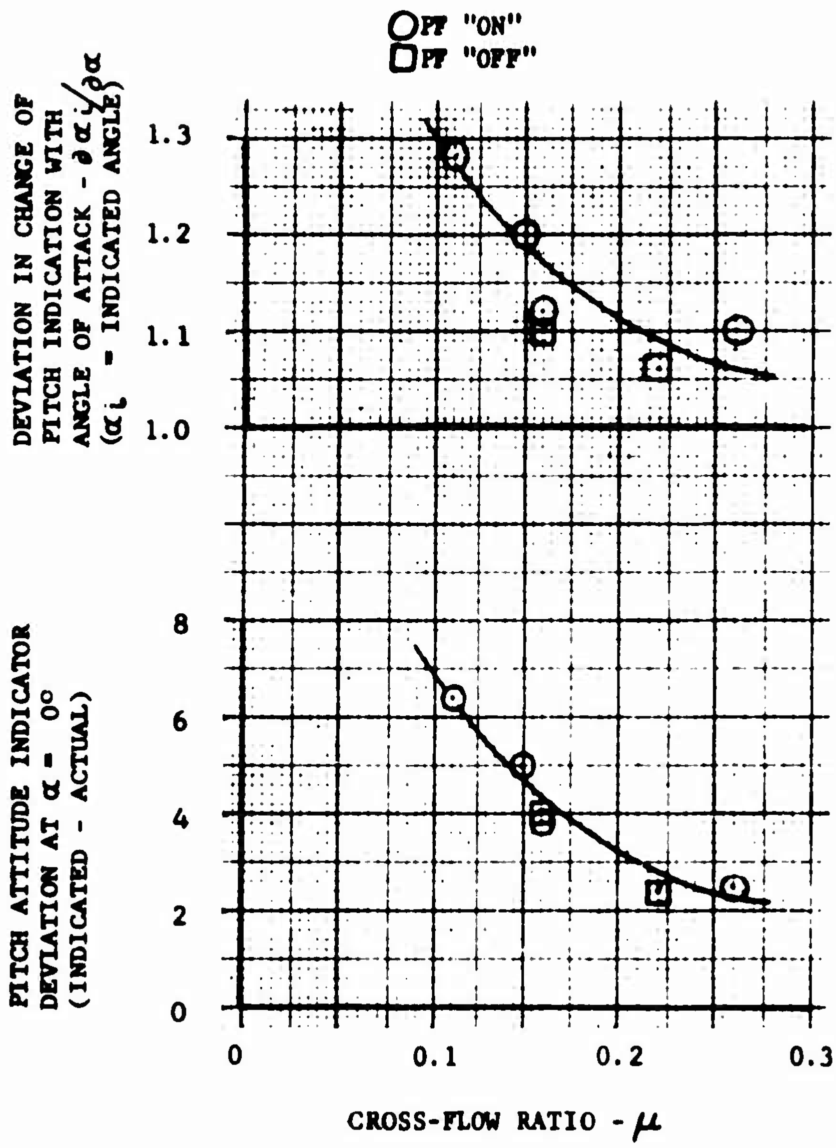

FIGURE 124

SIGNIFICANT DEVIATION FACTORS IN PITCH ATTITUDE INDICATION

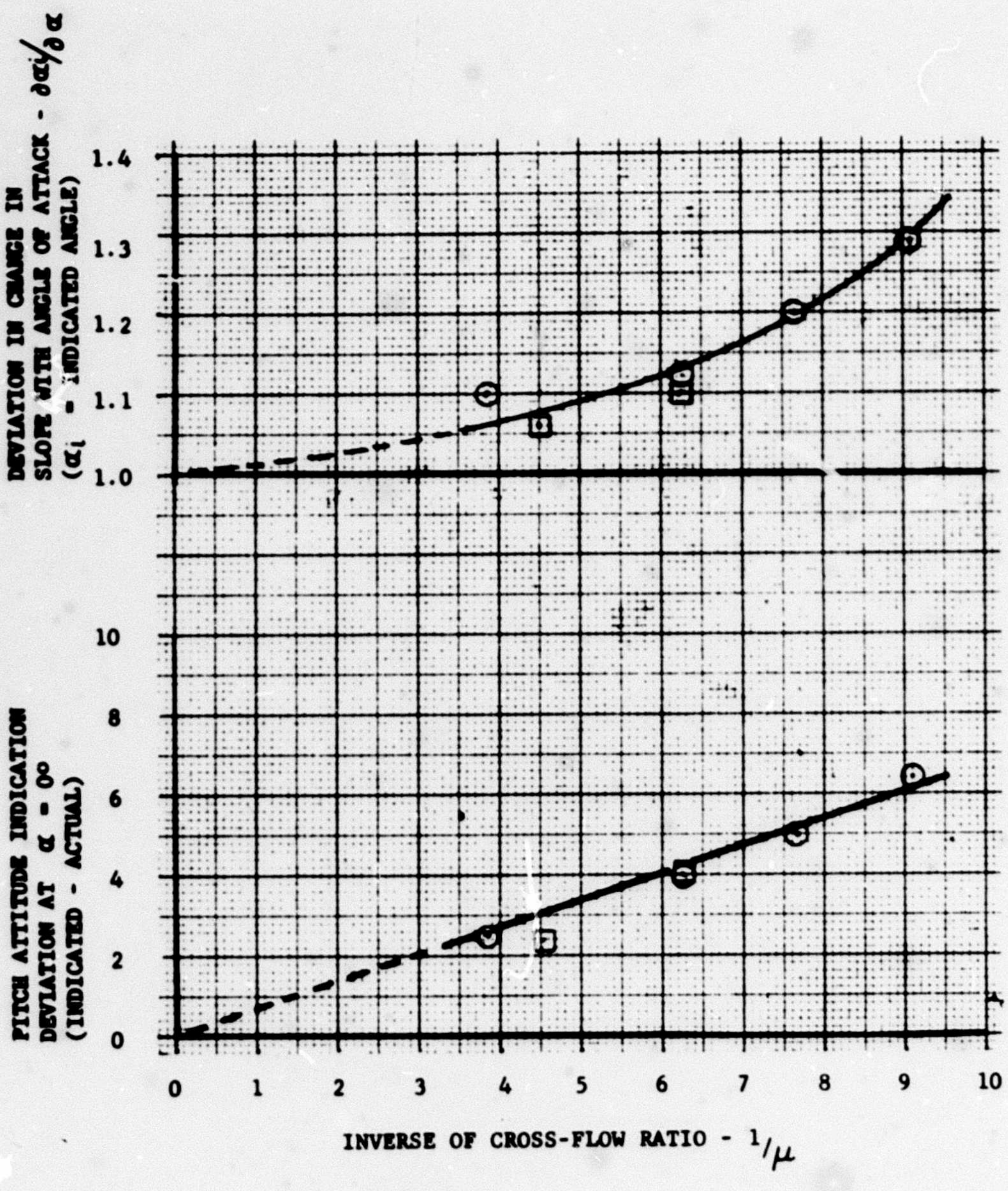

FIGURE 125

CORRELATION OF PITCH ATTITUDE
INDICATOR DEVIATIONS WITH
INVERSE OF CROSS-FLOW RATIO

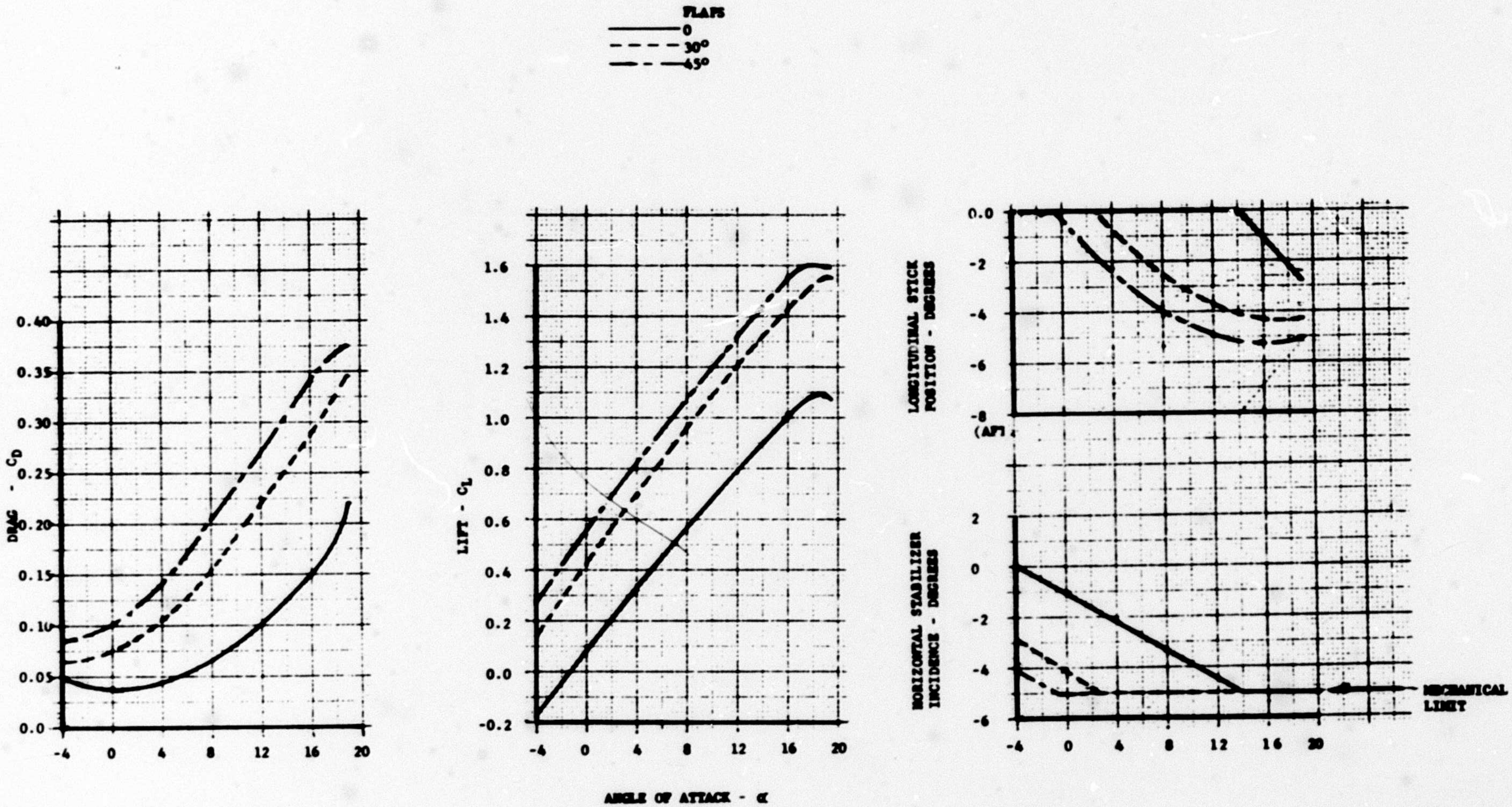

FIGURE 126

TRIMMED LIFT, DRAG AND LONGITUDINAL CONTROL
FOR A RANGE OF FLAP SETTINGS - GEAR UP

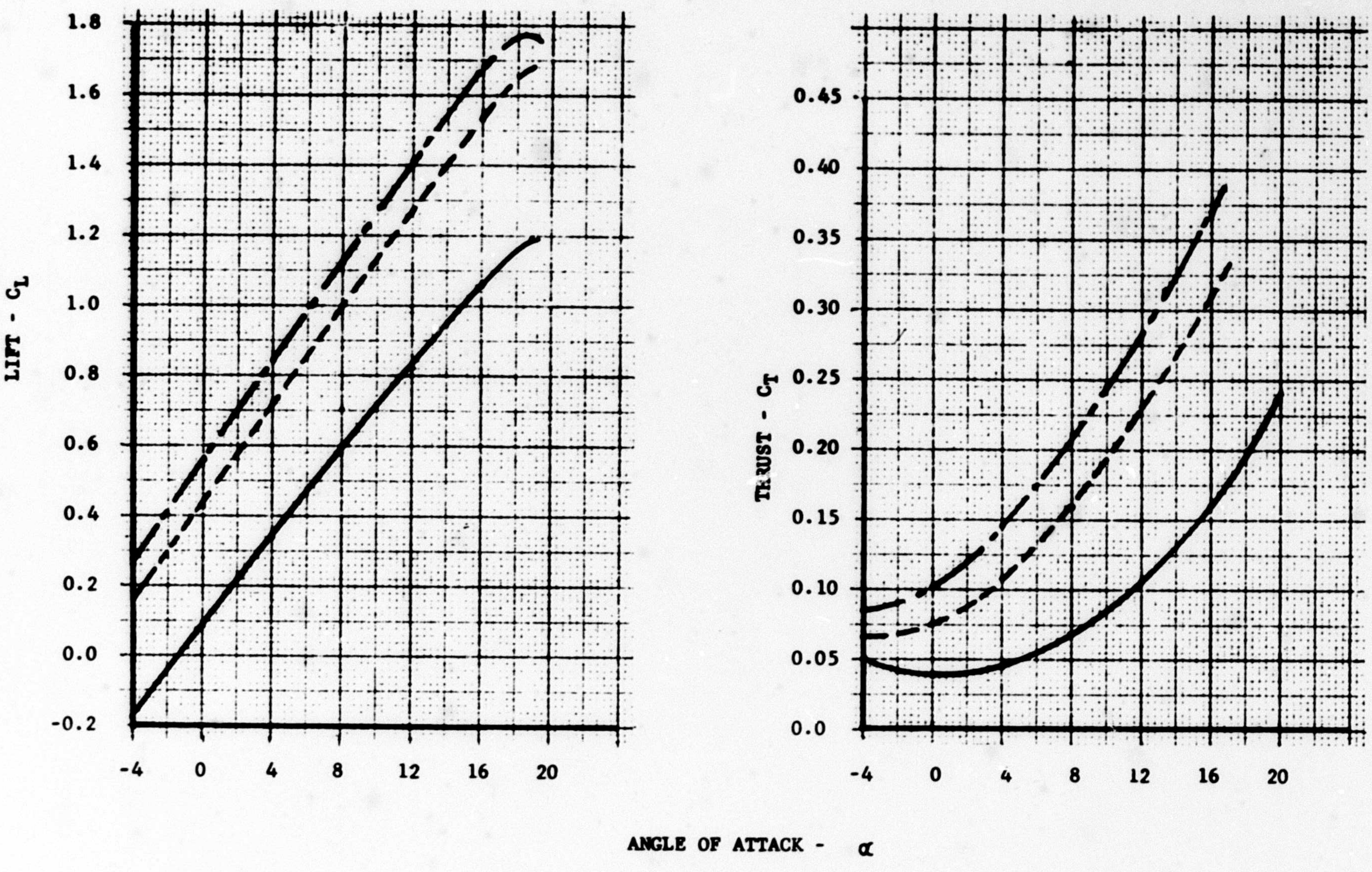

FIGURE 127

TRIMMED LIFT CHARACTERISTICS - POWER ON - CTOL - FOR A RANGE OF FLAP SETTINGS - GEAR UP

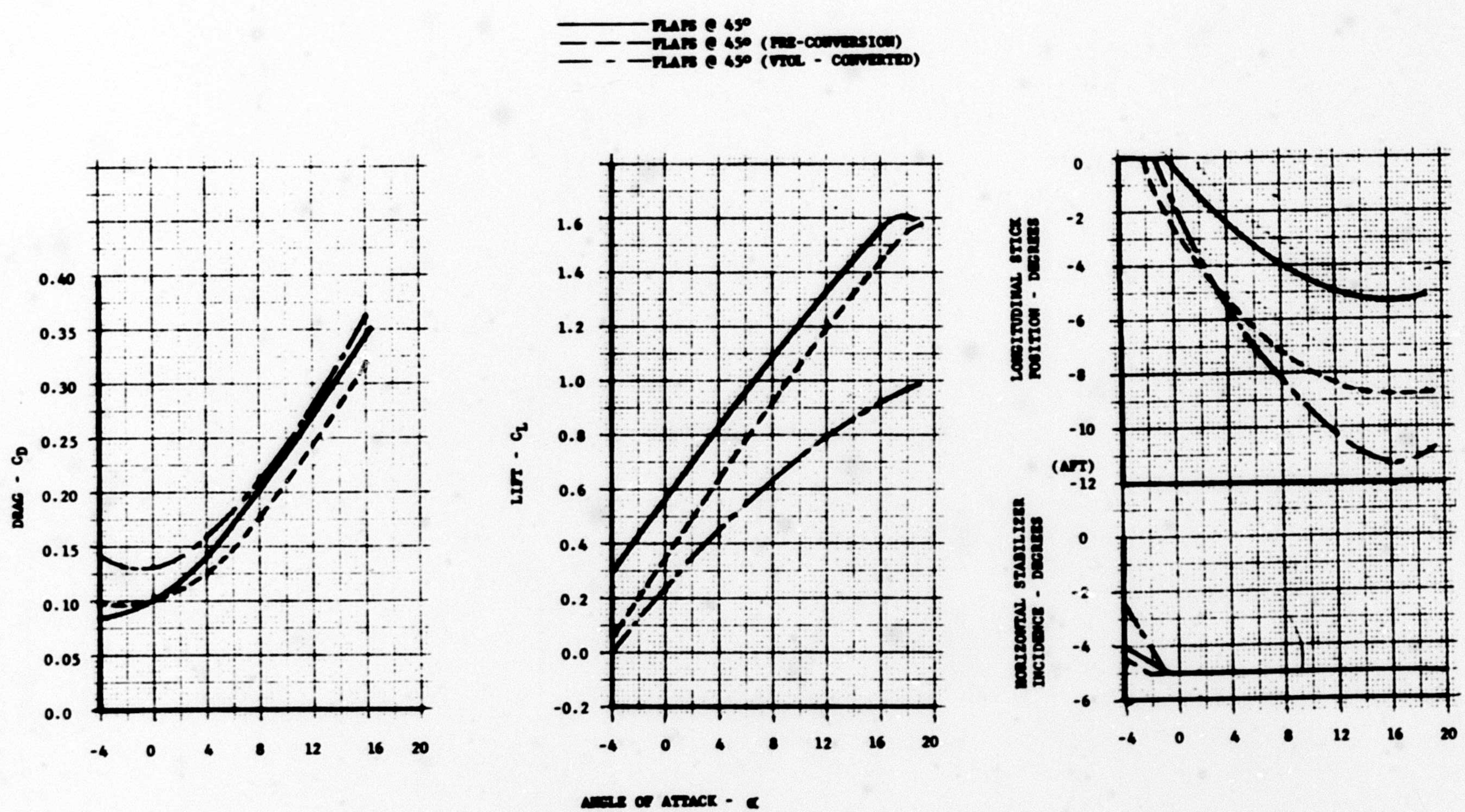

FIGURE 128

COMPARISON OF TRIMMED LIFT, DRAG AND LONGITUDINAL CONTROL
FOR THE THREE INTERMEDIATE CONFIGURATIONS DURING A CONVERSION CYCLE - GEAR UP

(TEST TYPE DOORS USED FOR GEAR DOWN AS WELL AS UP CONFIGURATION)

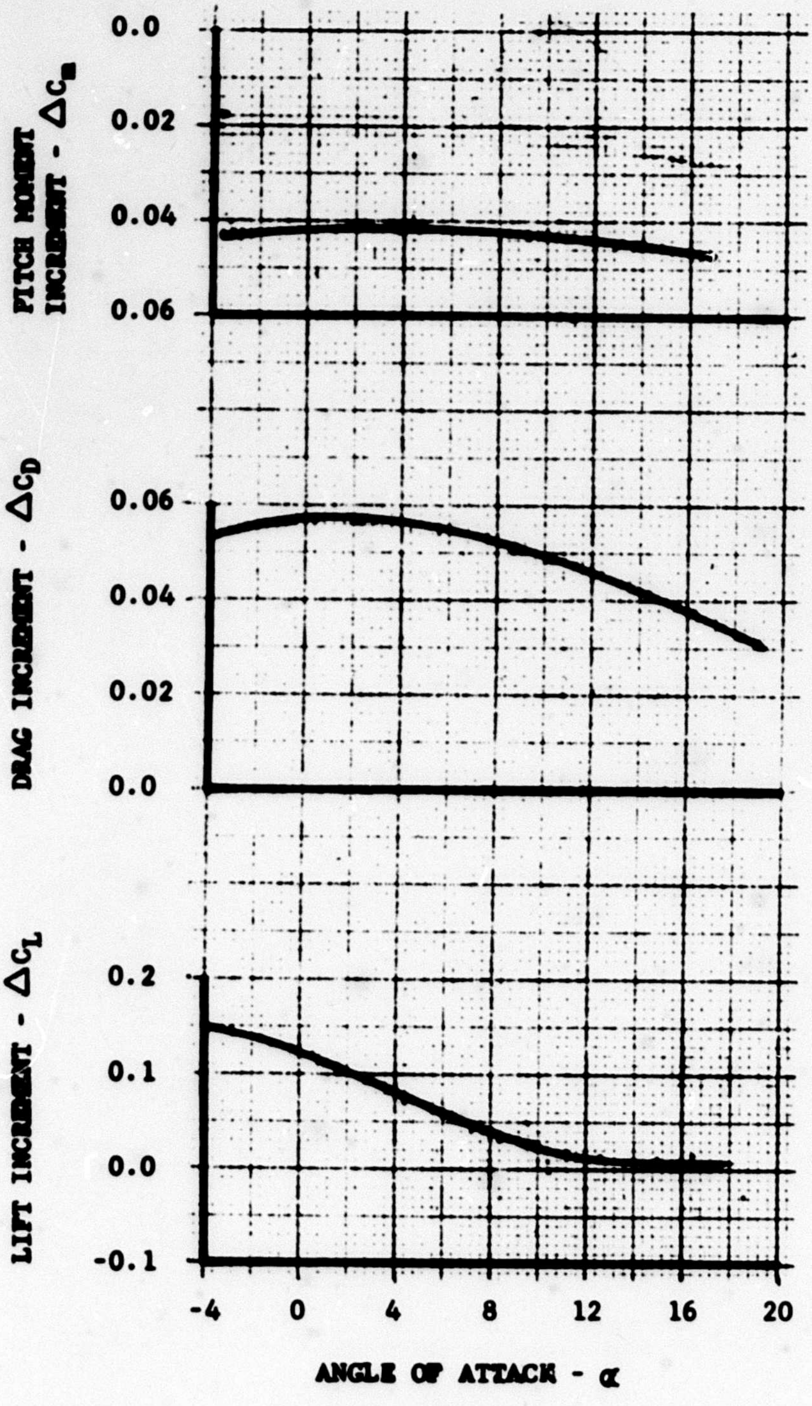

FIGURE 129

INCREMENTAL LIFT, DRAG AND PITCHING MOMENT DUE TO LANDING GEAR

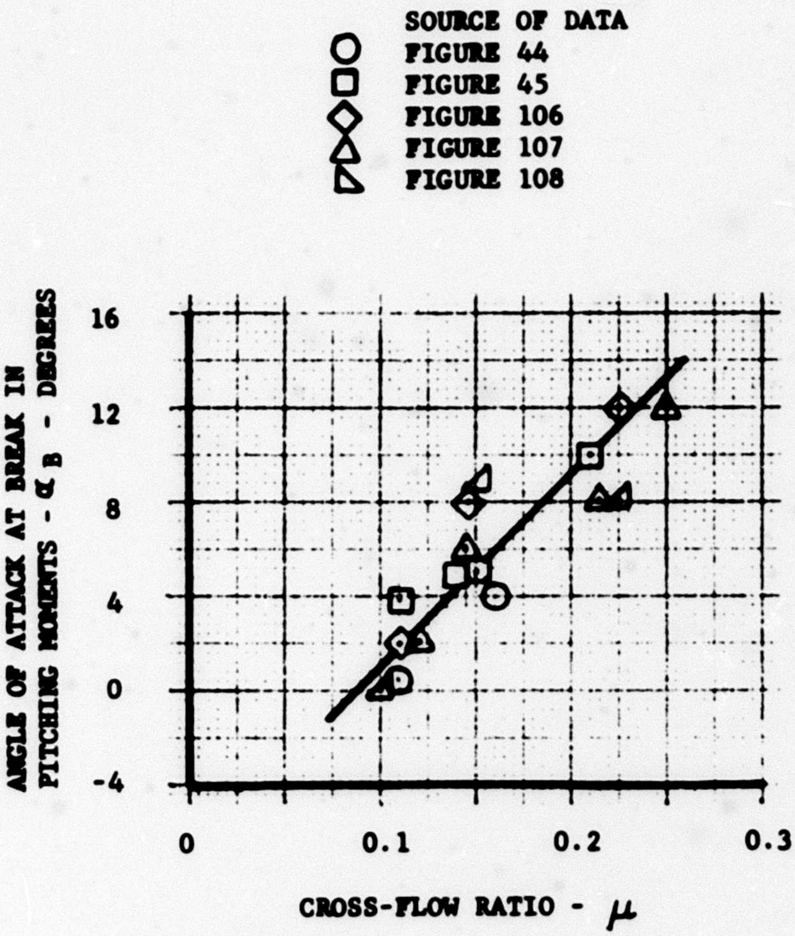

FIGURE 130

ANGLE OF ATTACK AT
BREAK IN PITCHING MOMENT -
NEAR TRIMMED CONDITIONS

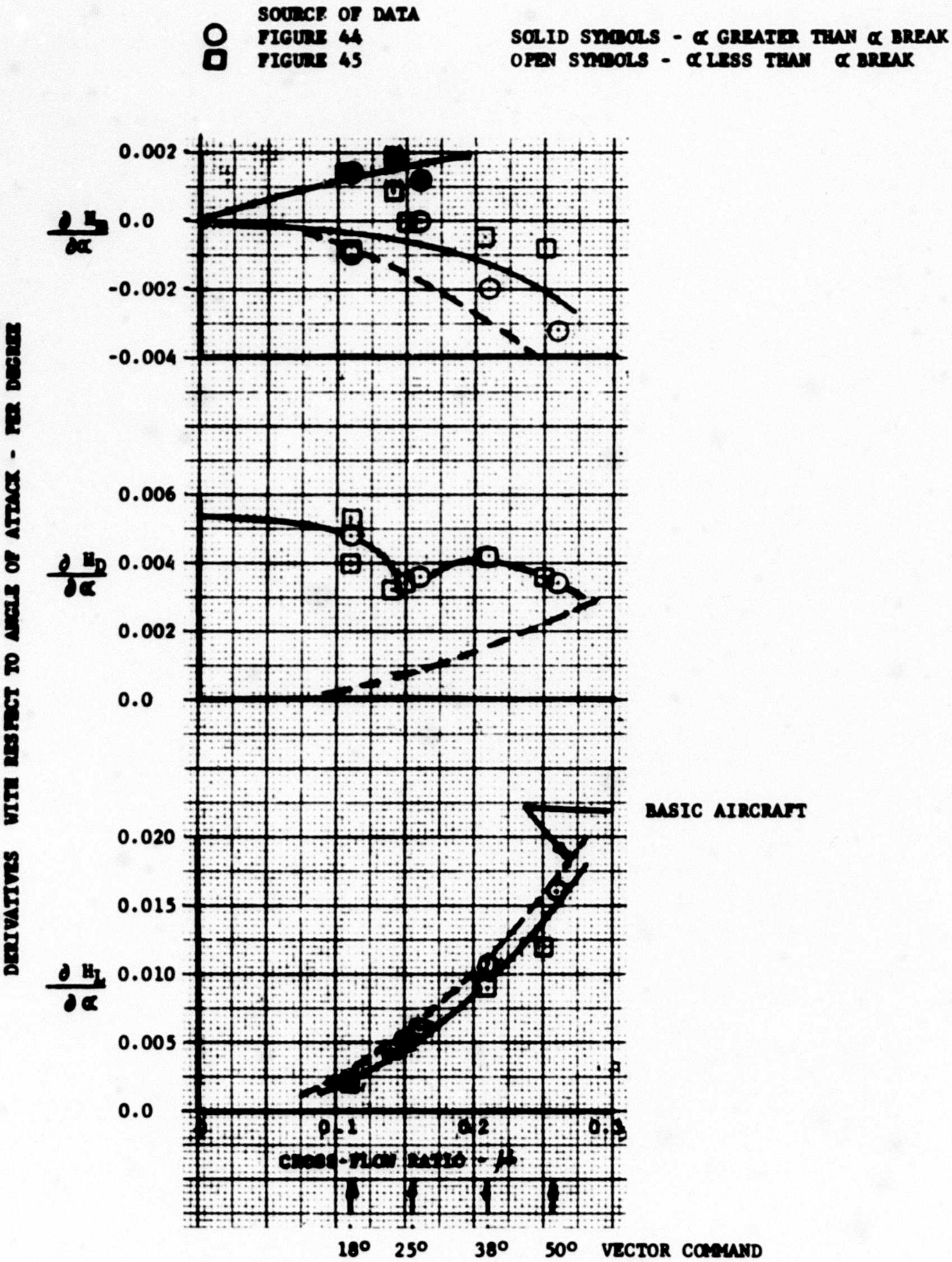

FIGURE 131

ANGLE OF ATTACK DERIVATIVES -
FAN POWERED

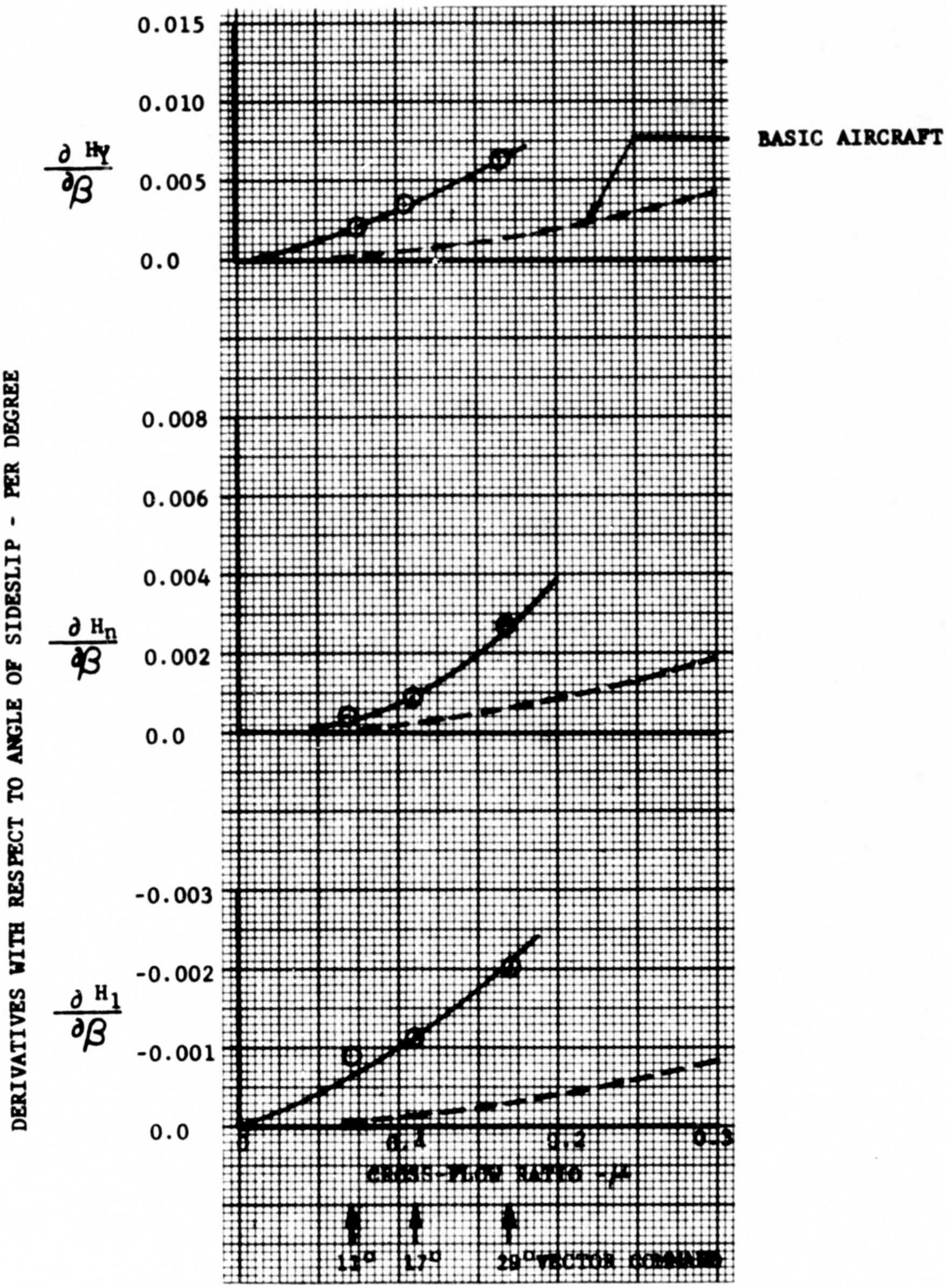

FIGURE 132

ANGLE OF SIDESLIP DERIVATIVES -
FAN POWERED (LO-POWER)

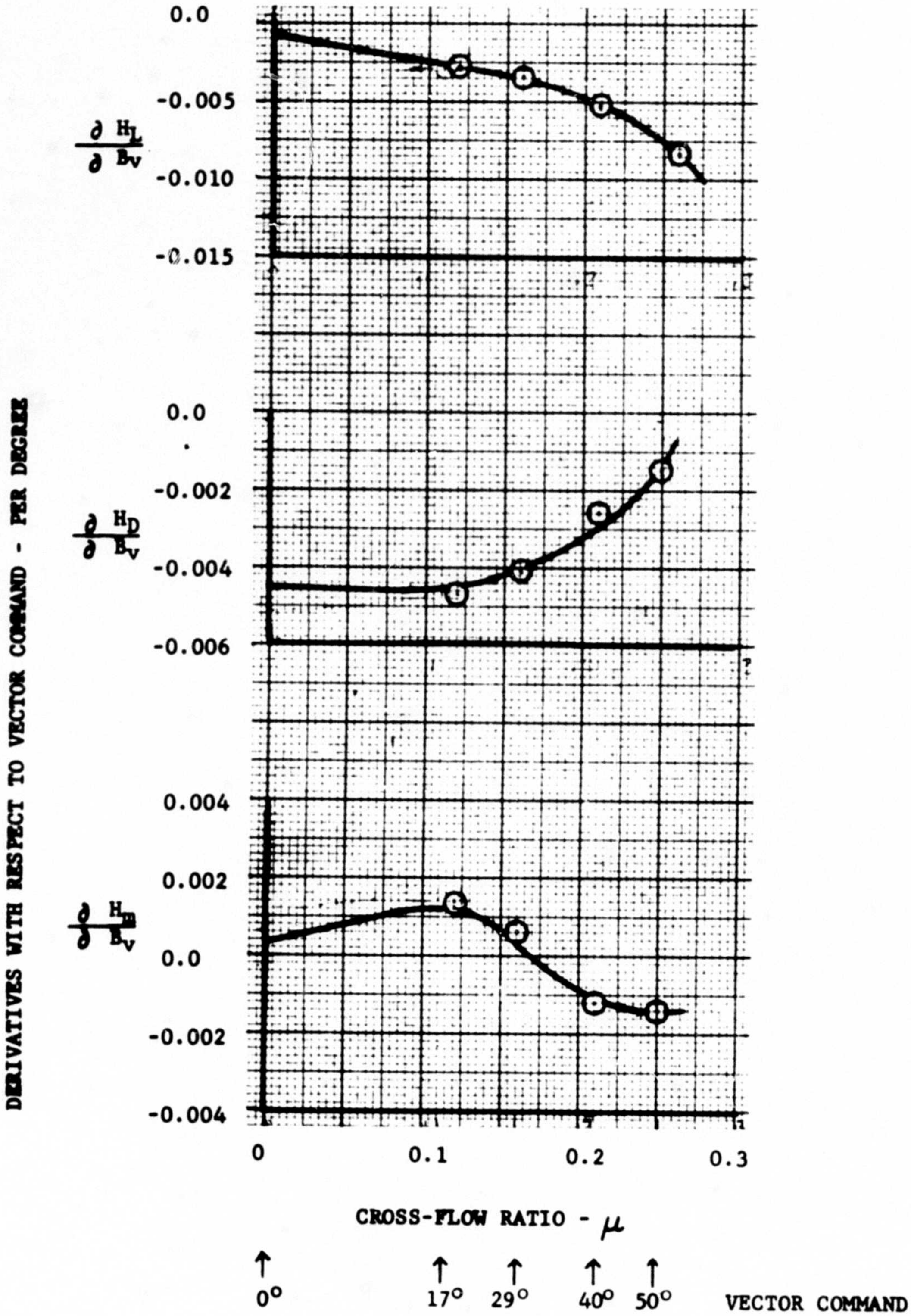

FIGURE 133

VECTOR COMMAND DERIVATIONS -
FAN POWERED (HI-POWER)

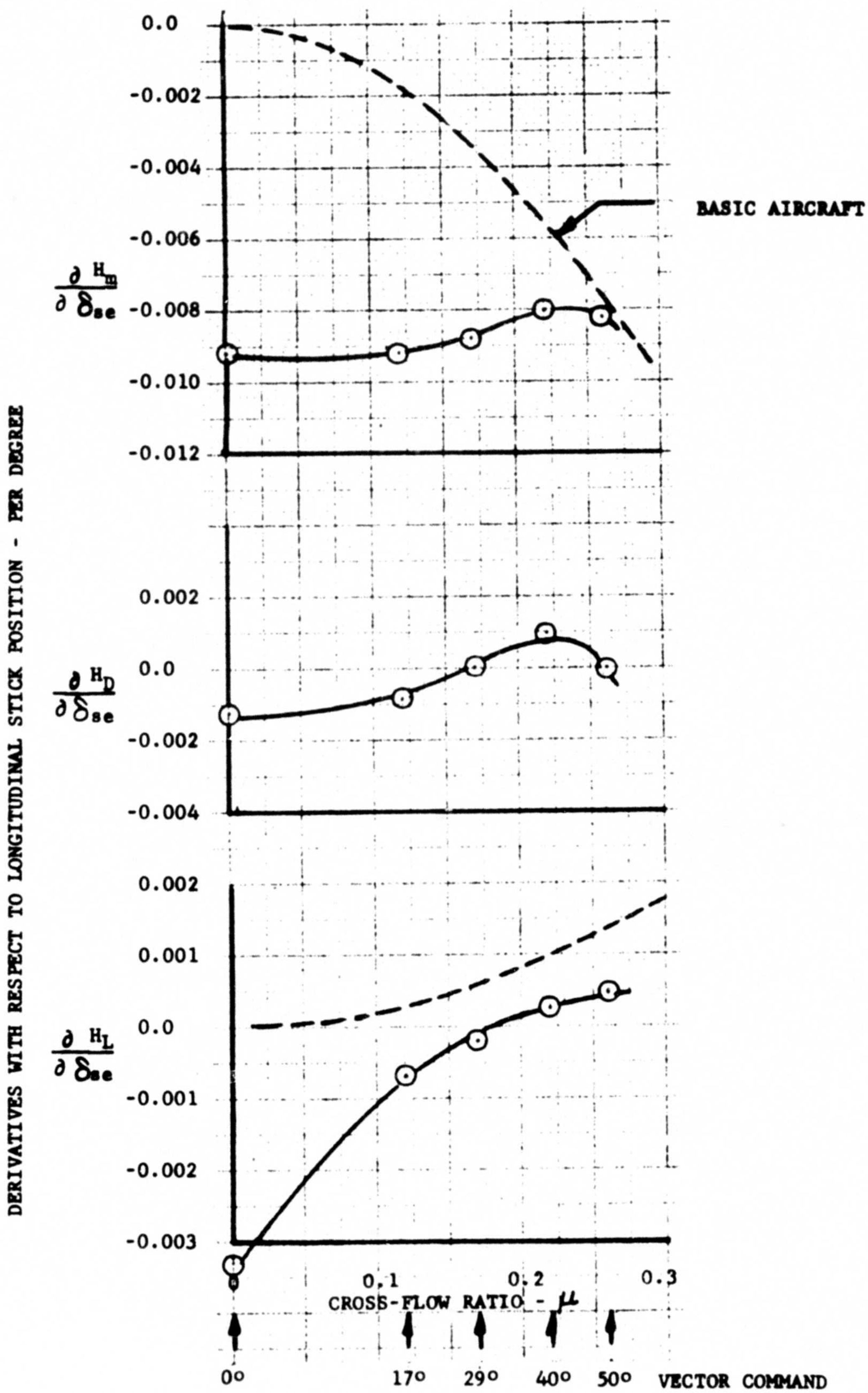

FIGURE 134

LONGITUDINAL CONTROL DERIVATIVES -
FAN POWERED (HI-POWER)

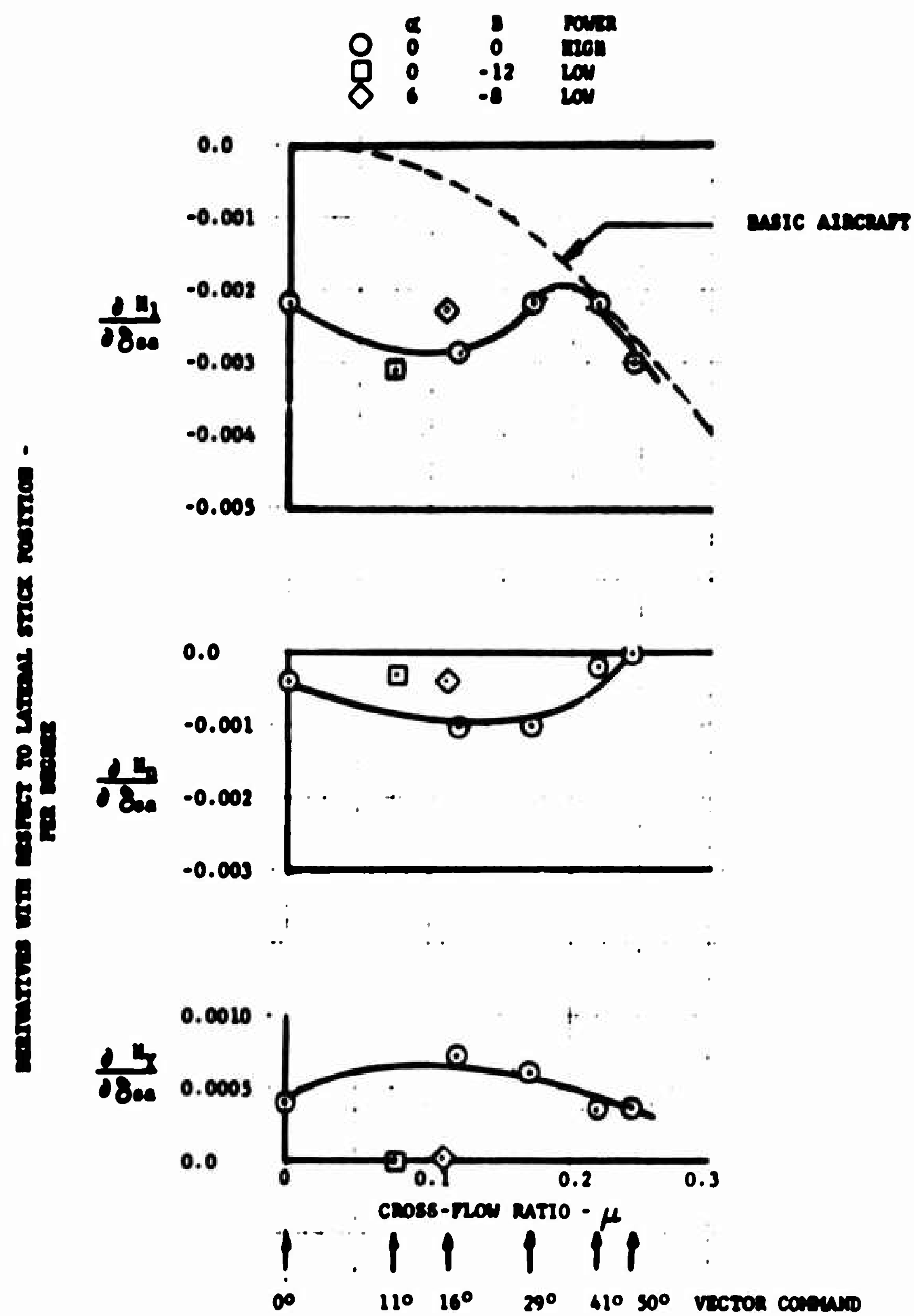

FIGURE 135

LATERAL CONTROL DERIVATIVES -
FAN POWERED

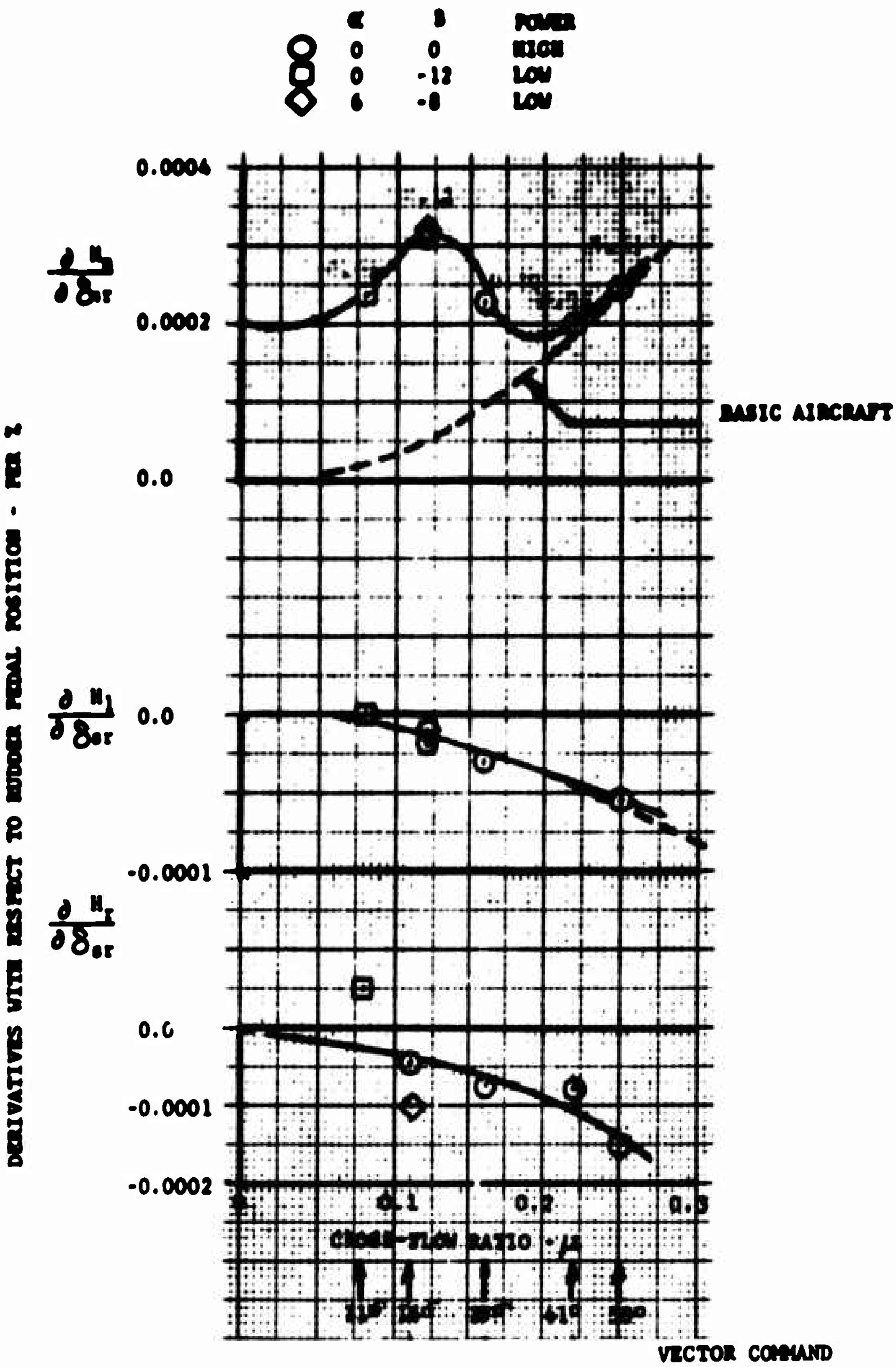

FIGURE 136

DIRECTIONAL CONTROL DERIVATIVES
FAN POWERED (HI-POWER)

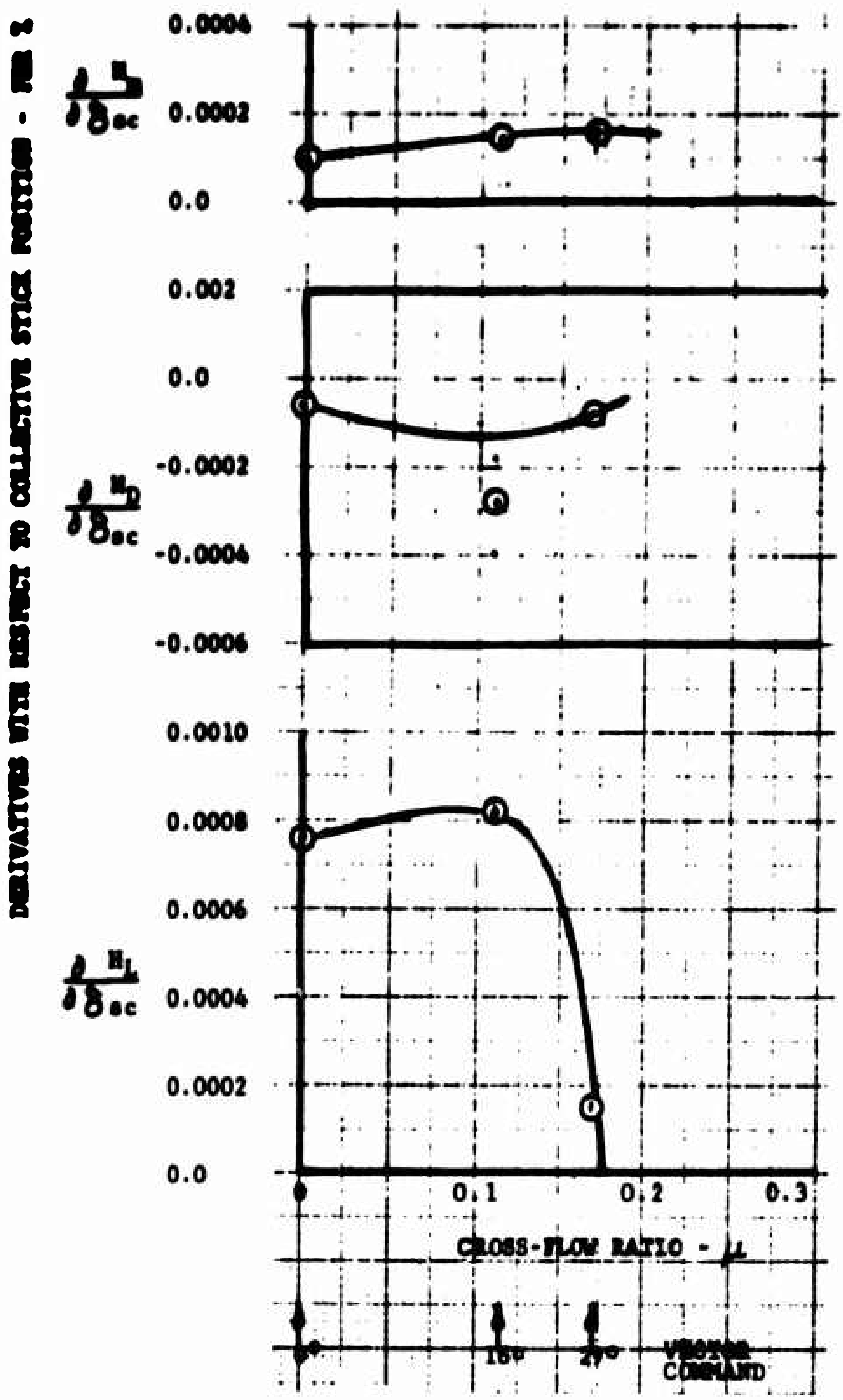

FIGURE 137

COLLECTIVE CONTROL DERIVATIVES
FAN POWERED (HI-POWER)

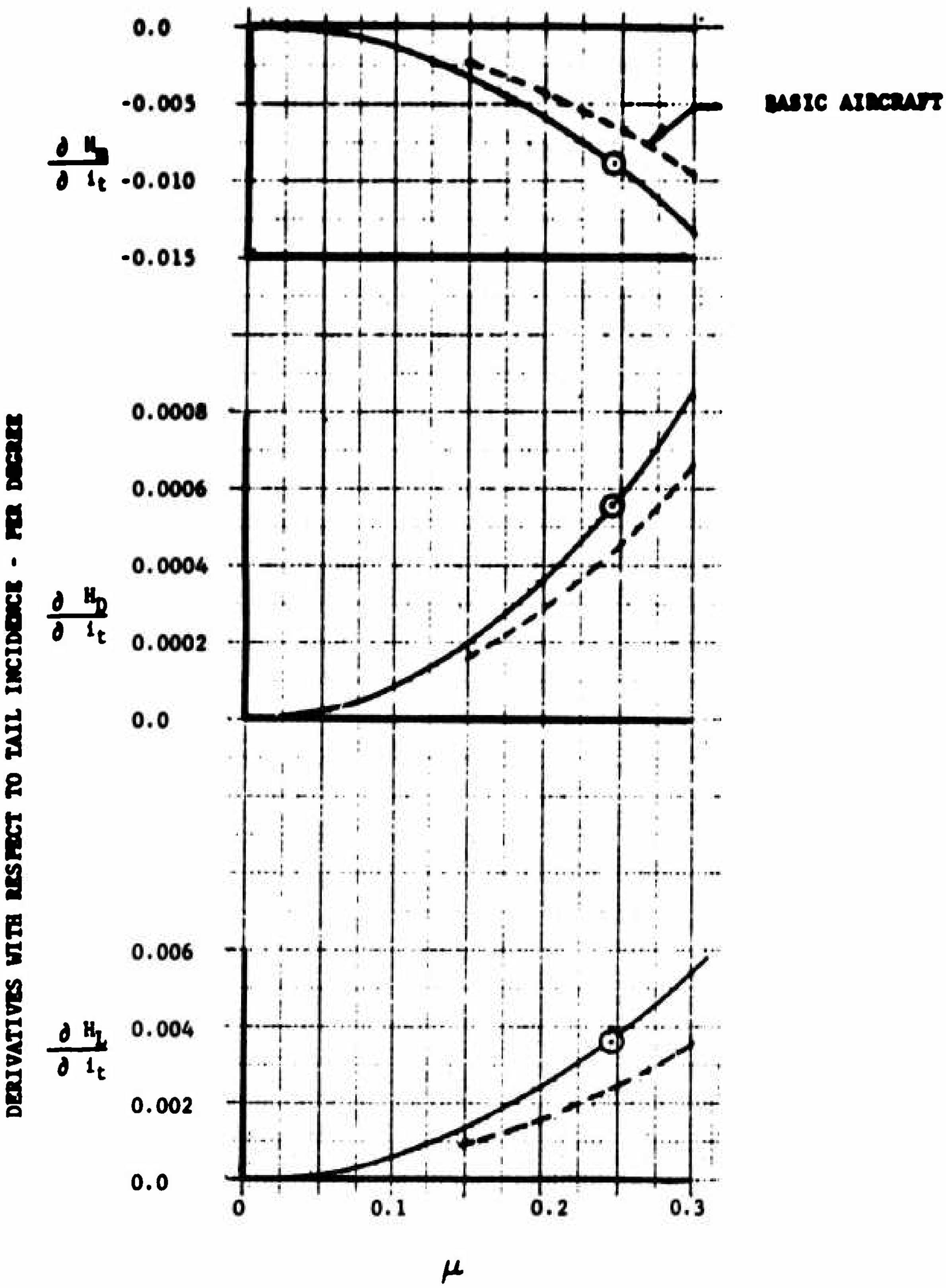

FIGURE 138

HORIZONTAL STABILIZER DERIVATIVES
FAN POWERED (HI-POWER)

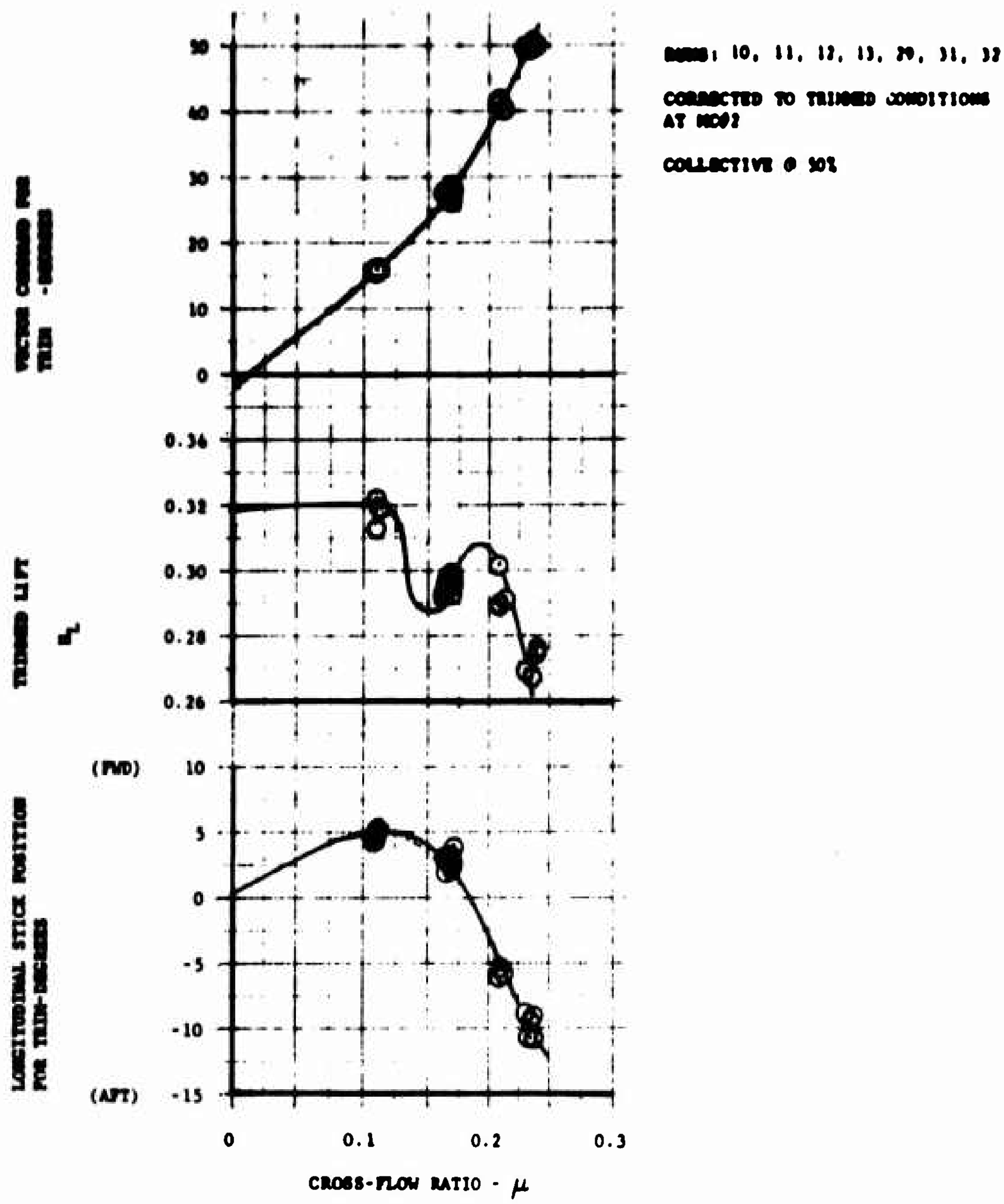

FIGURE 139

TRIMMED TRANSITION CHARACTERISTICS
FAN POWERED (HI-POWER) $\alpha = 0^\circ$ $\beta = 0^\circ$
CONTROLS "TRIMMED" $i_t = 20^\circ$

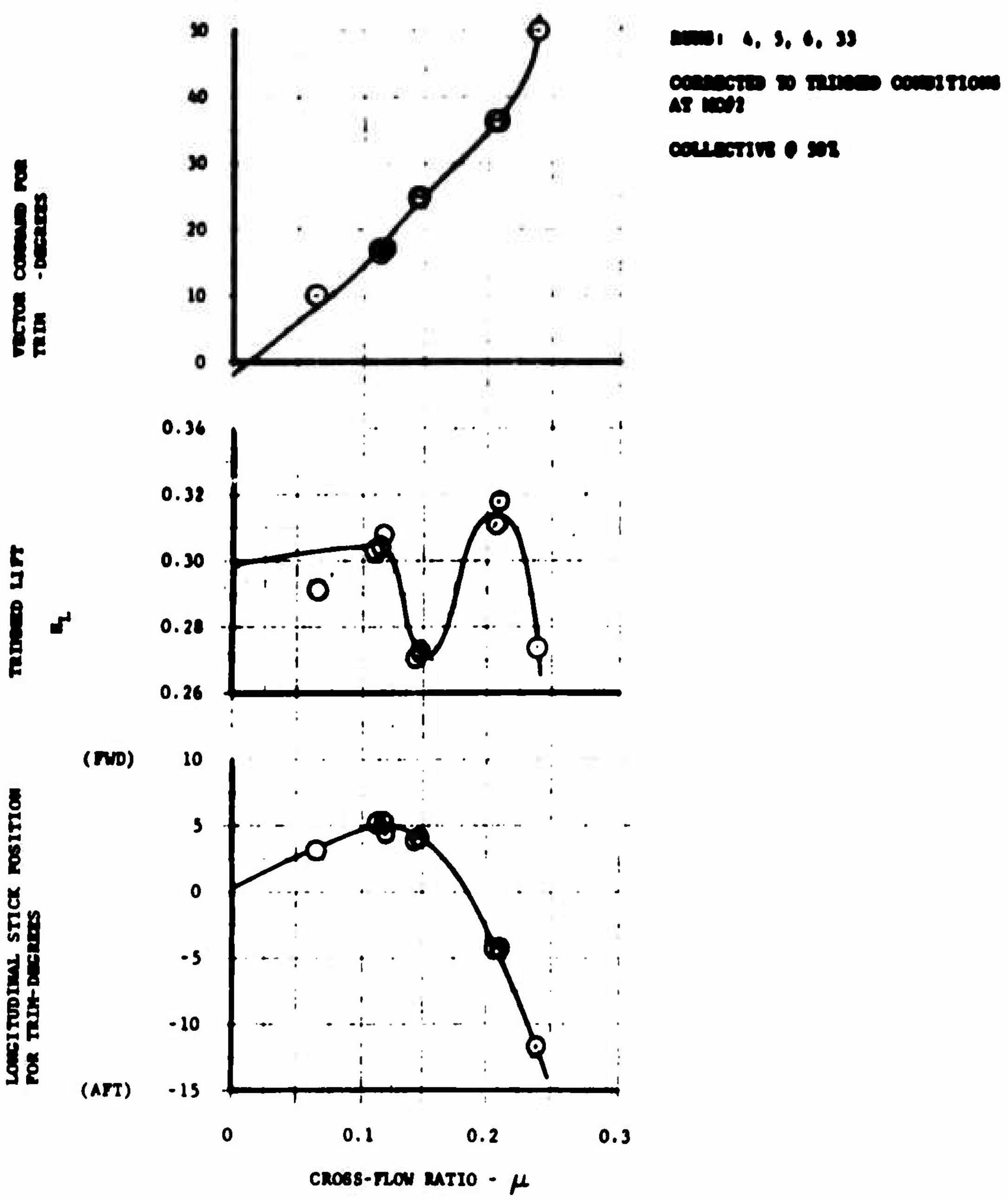

FIGURE 140

TRIMMED TRANSITION CHARACTERISTICS
LO-POWER $\alpha = 0°$ $\beta = 0°$
CONTROLS "TRIMMED" $i_t = 20°$

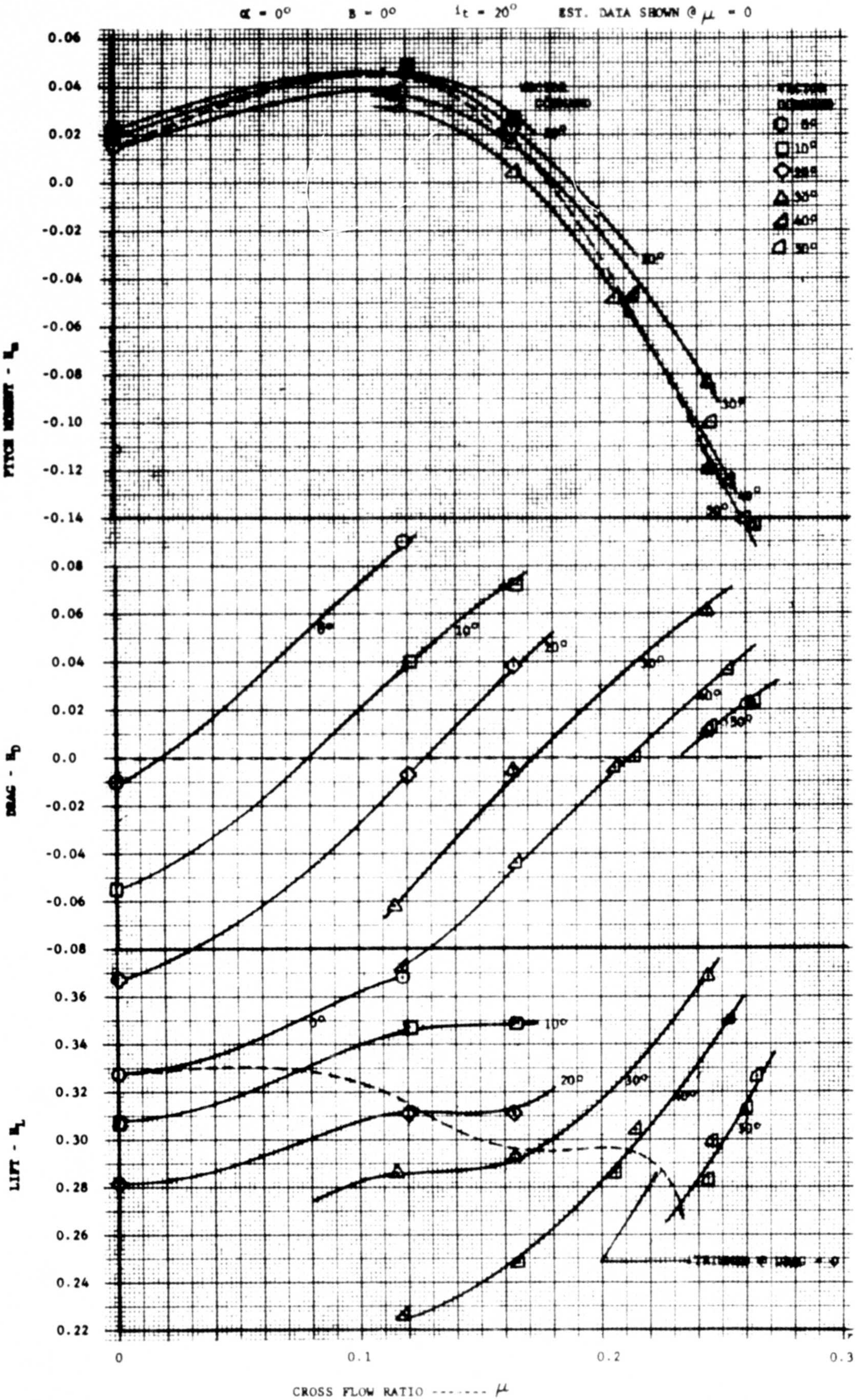

FIGURE 141

COMPOSITE FAN POWERED TRANSITION CHARACTERISTICS
ALL CONTROLS "NEUTRAL"

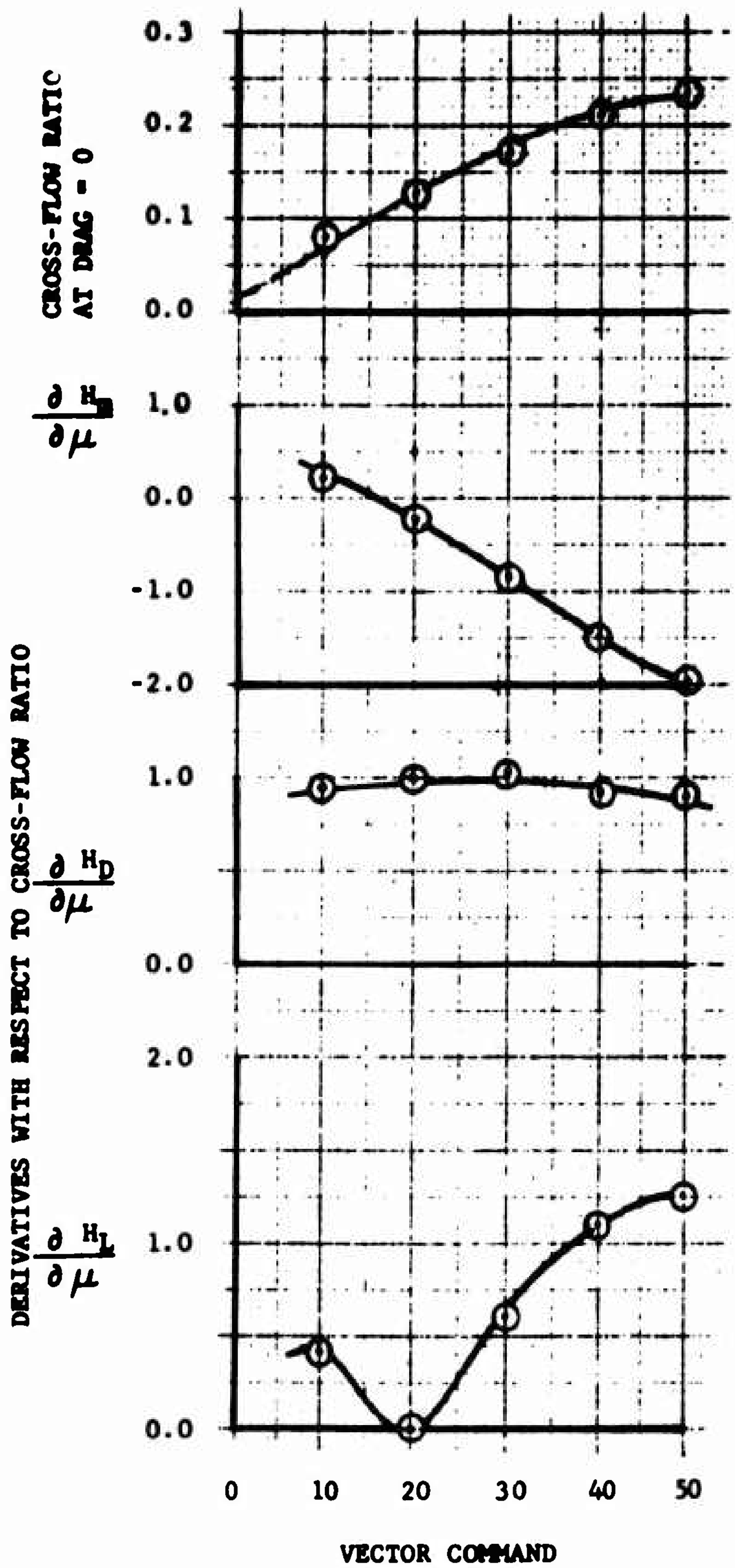

FIGURE 142

FLIGHT SPEED DERIVATIVES
FAN POWERED (HI-POWER)

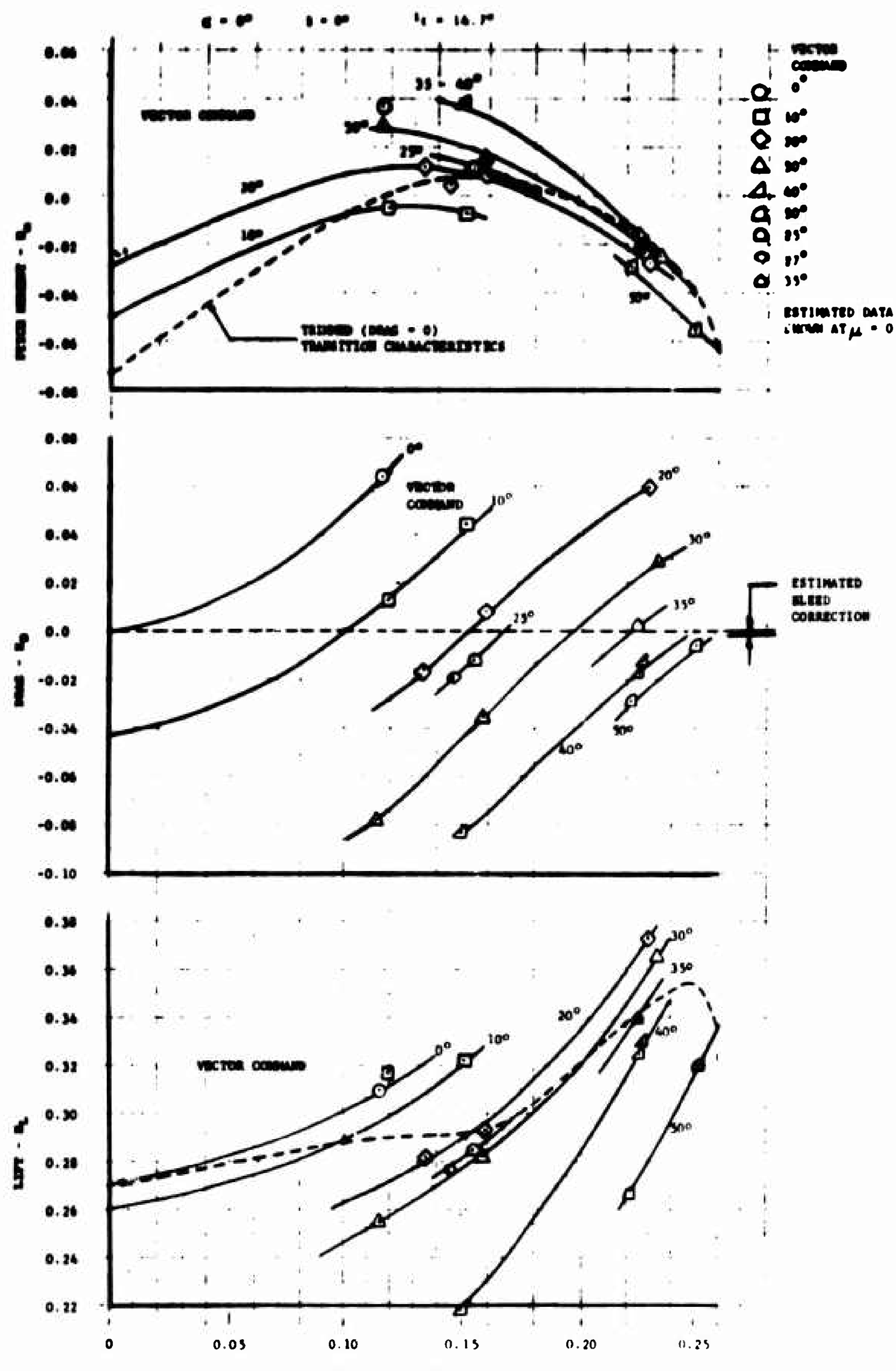

FIGURE 143

COMPOSITE FAN POWERED TRANSITION CHARACTERISTICS PITCH FAN "OFF" (OPEN) - ALL CONTROLS "NEUTRAL"

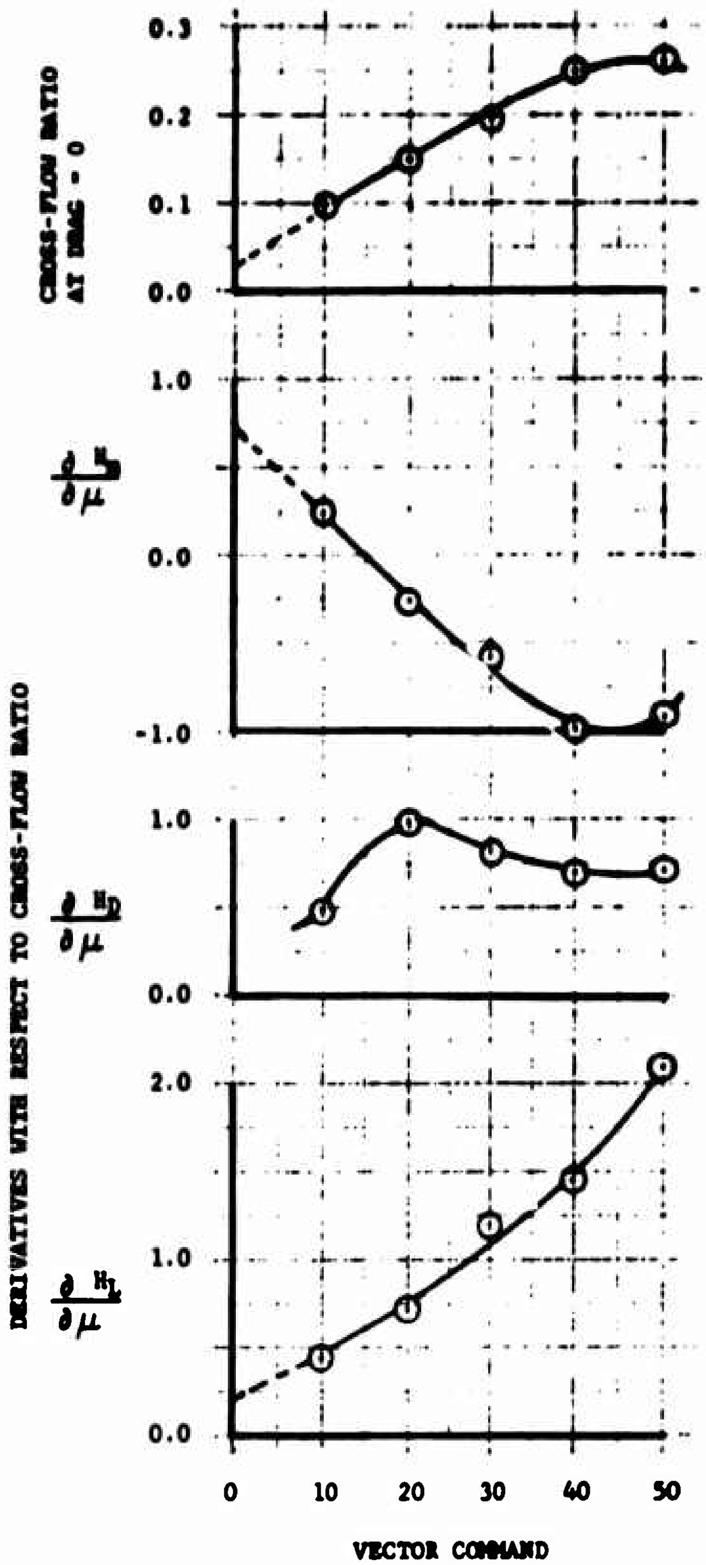

FIGURE 144

FLIGHT SPEED DERIVATIVES
FAN POWERED - PITCH FAN "OFF"

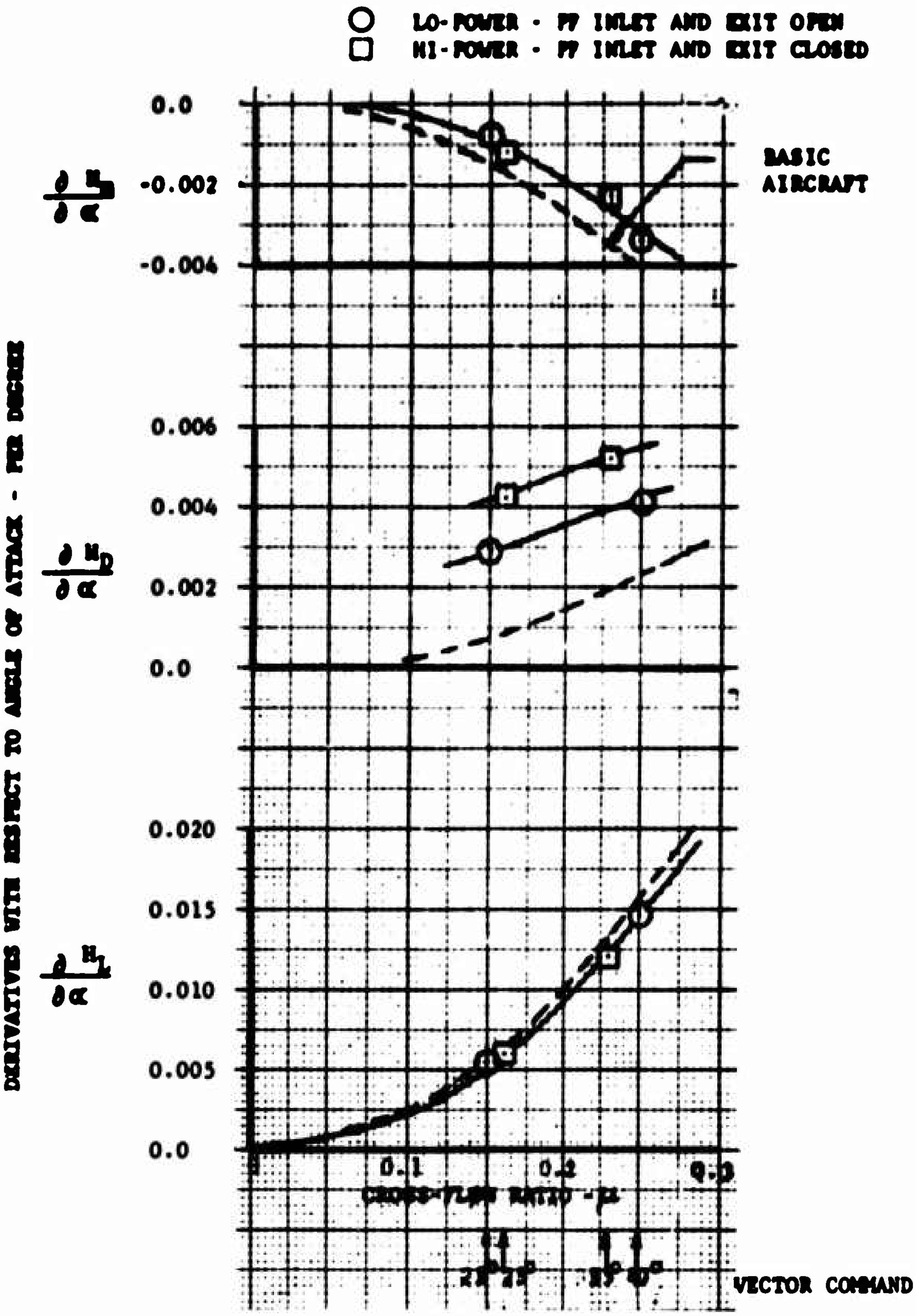

FIGURE 145

ANGLE OF ATTACK DERIVATIVES
FAN POWERED - PITCH FAN "OFF"

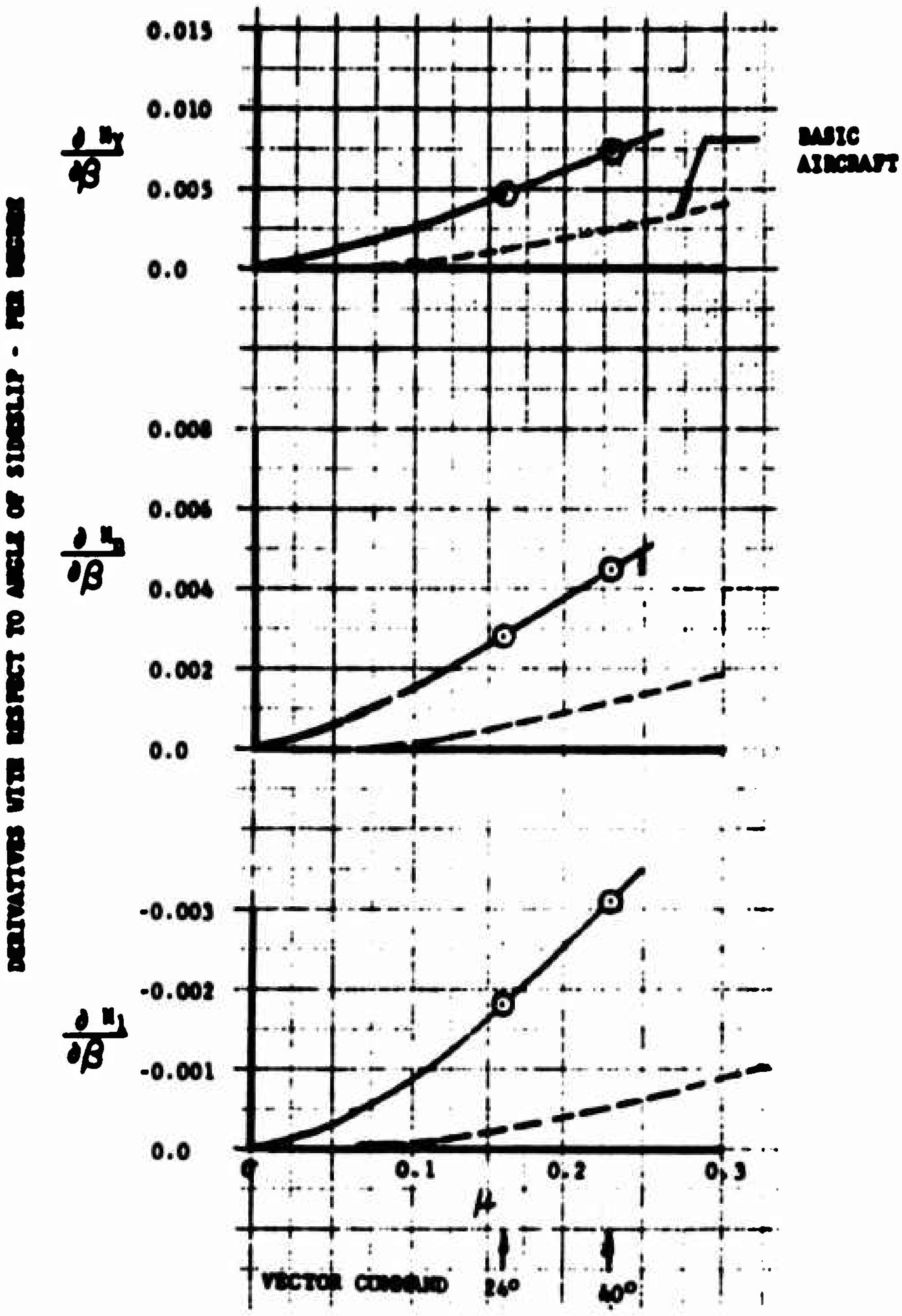

FIGURE 146

ANGLE OF SIDESLIP DERIVATIVES
FAN POWERED - PITCH FAN "OFF"

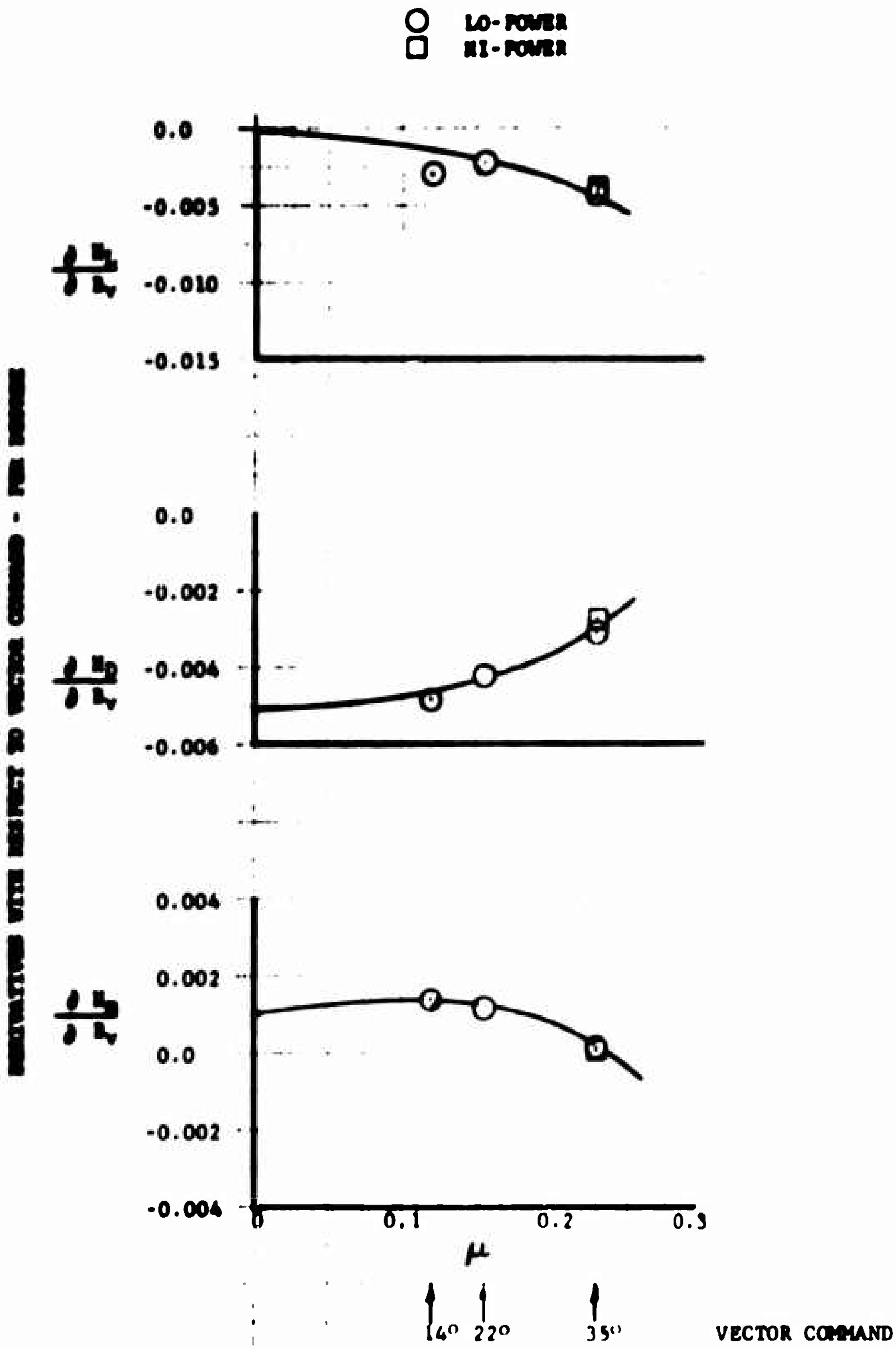

FIGURE 147

VECTOR COMMAND DERIVATIVES
FAN POWERED PITCH FAN "OFF"

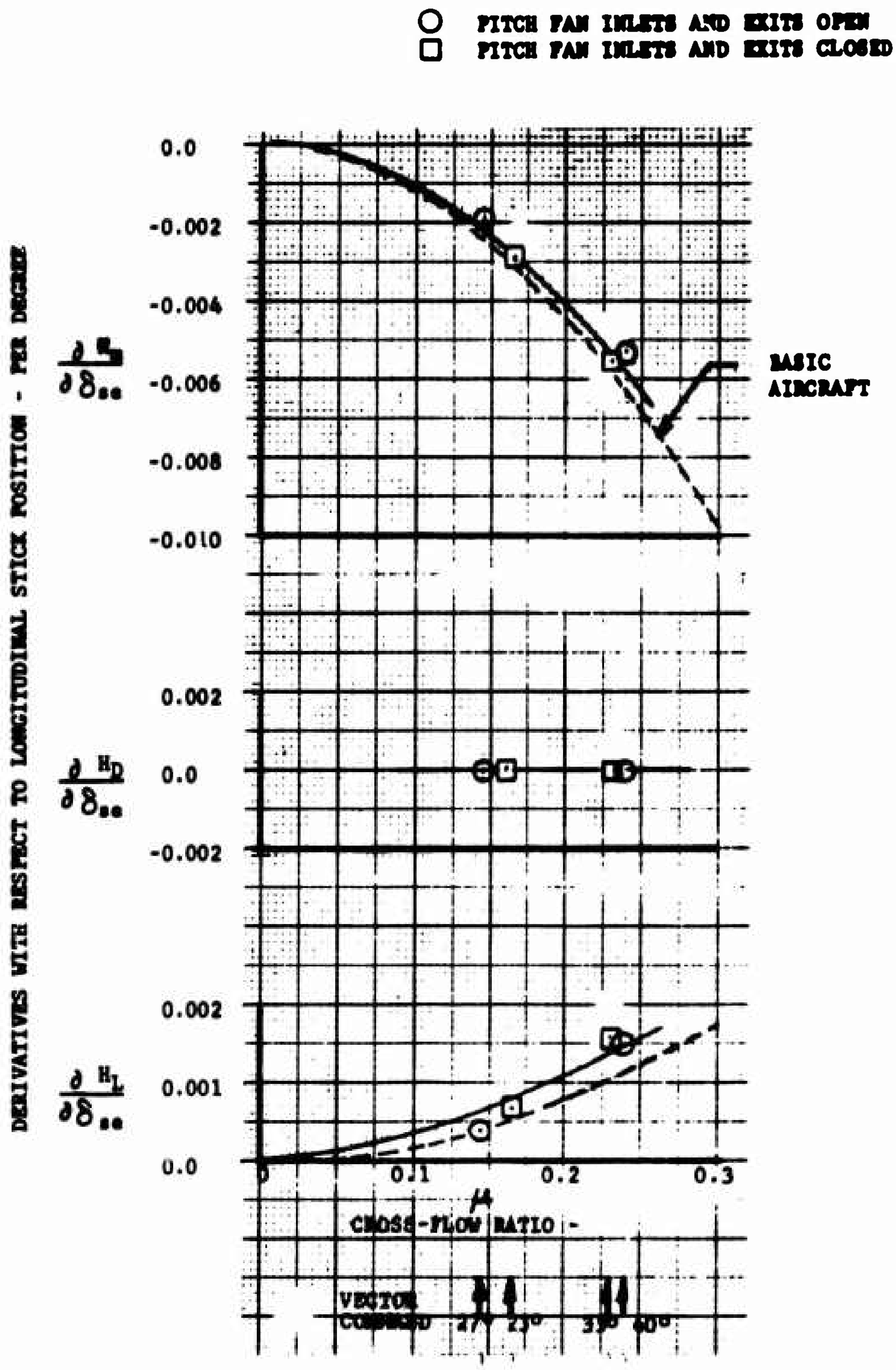

FIGURE 148

LONGITUDINAL CONTROL DERIVATIVES
FAN POWERED PITCH FAN "OFF"

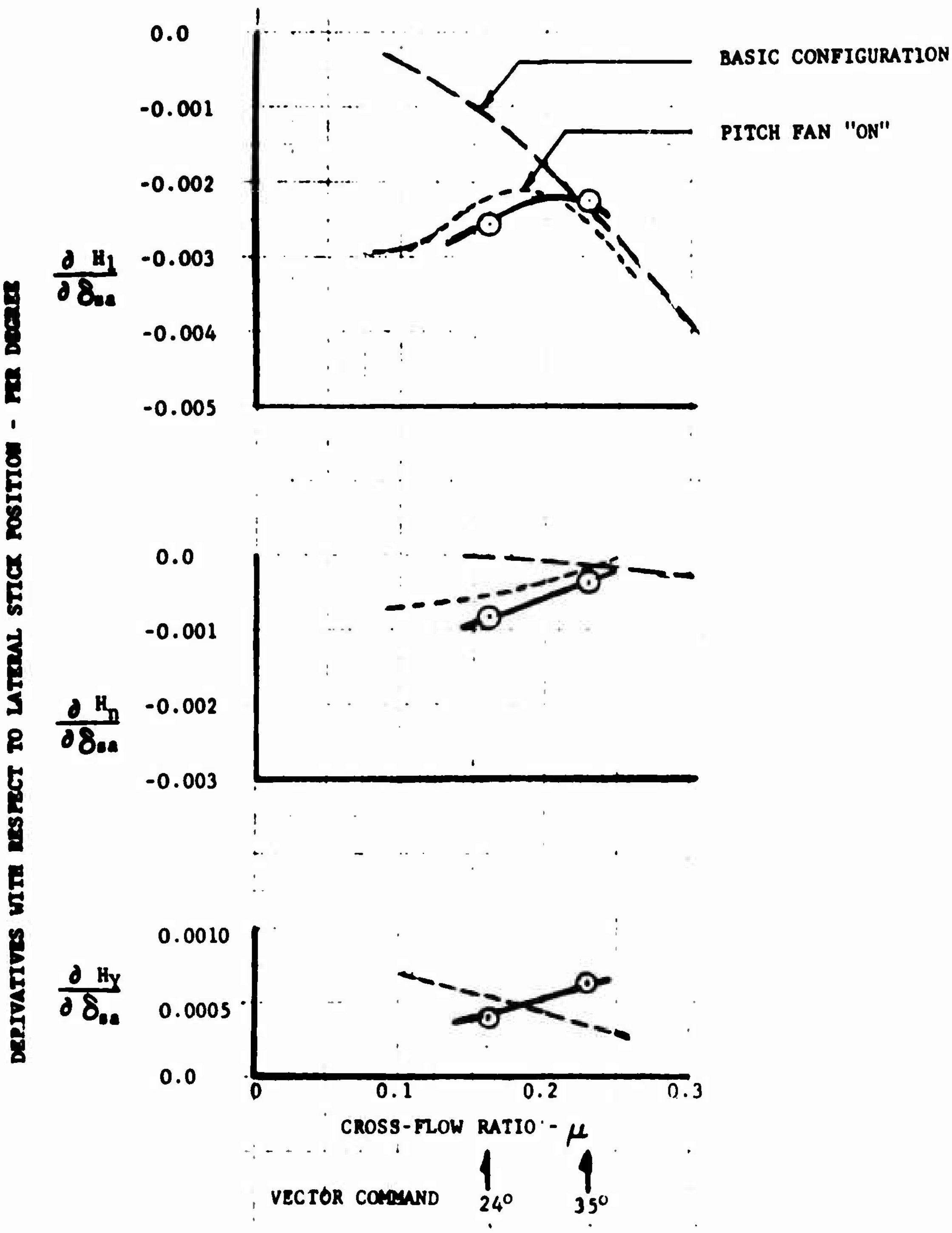

FIGURE 149

LATERAL CONTROL DERIVATIVES
FAN POWERED PITCH FAN "OFF"

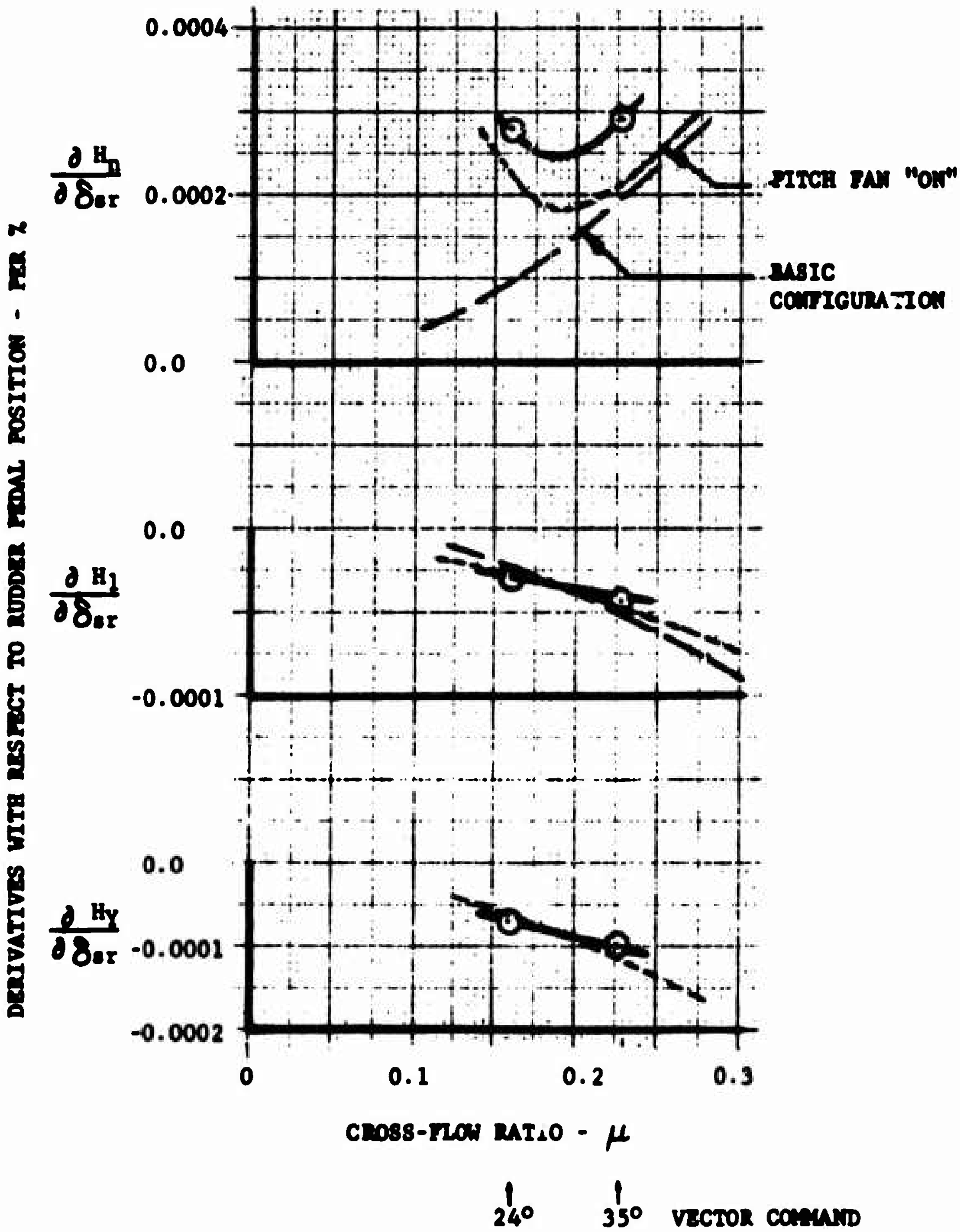

FIGURE 150

DIRECTIONAL CONTROL DERIVATIVES
FAN POWERED - PITCH FAN "OFF"

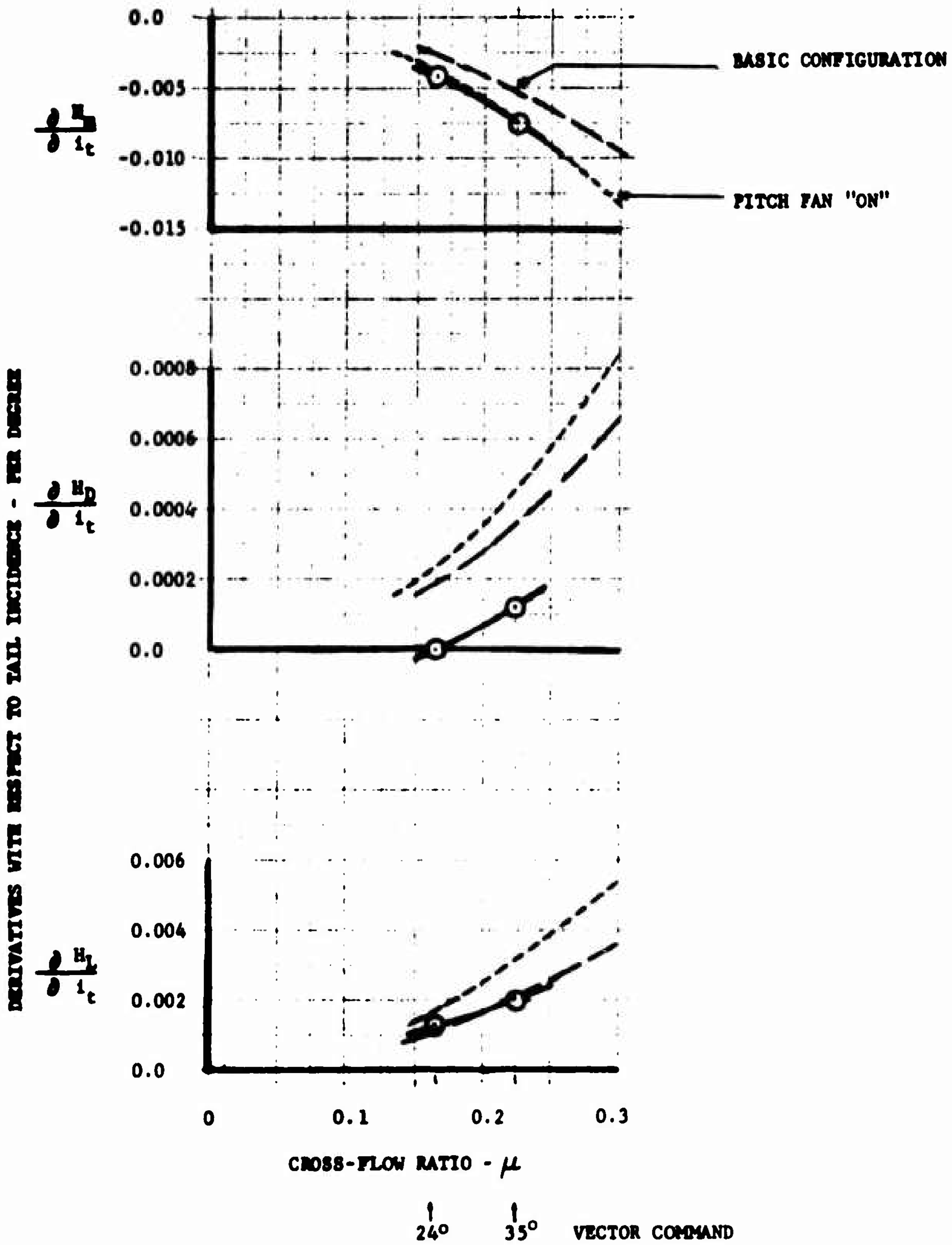

FIGURE 151

HORIZONTAL TAIL DERIVATIVES
FAN POWERED PITCH FAN "OFF"

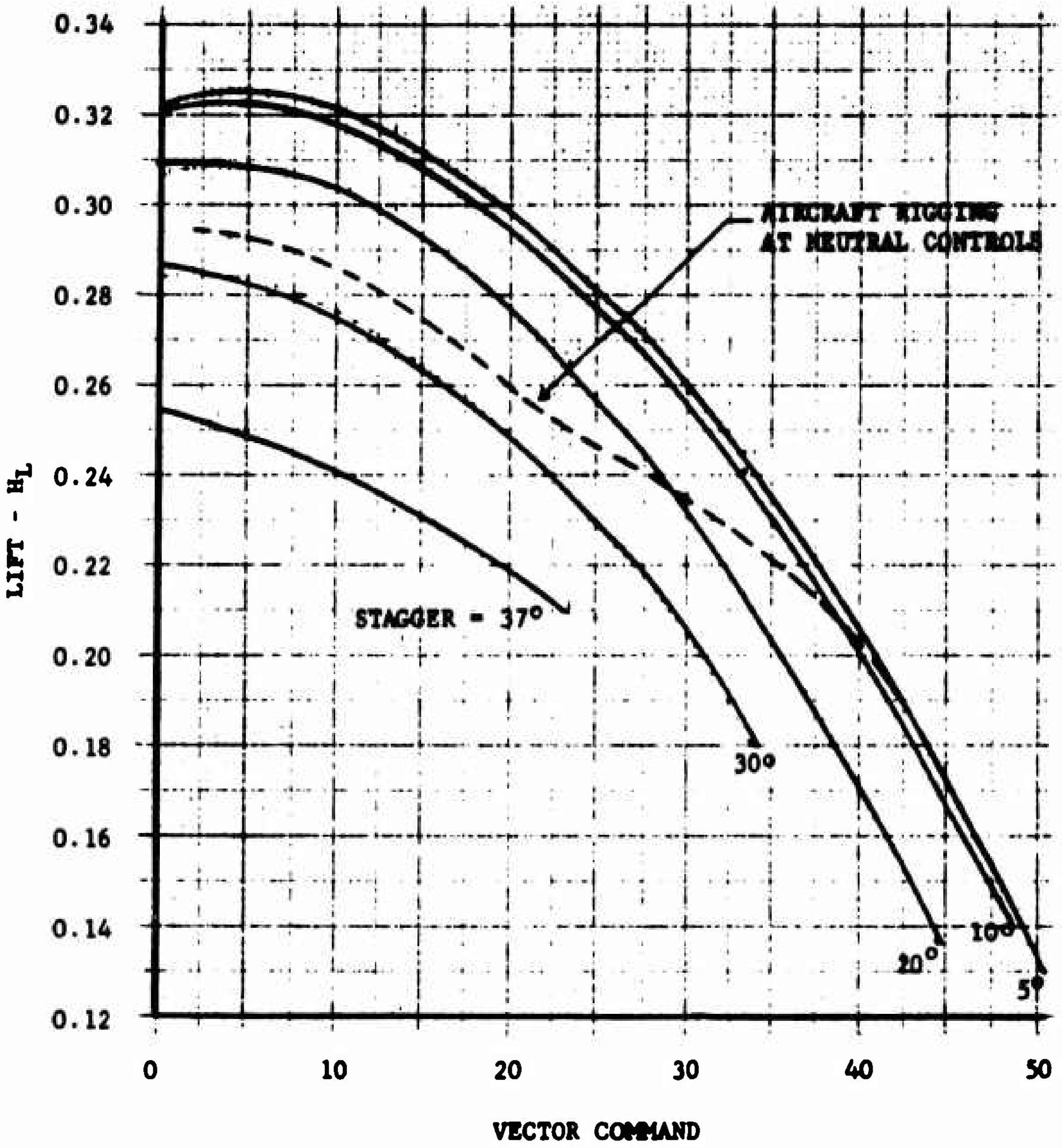

FIGURE 152

ESTIMATED STATIC VECTOR - STAGGER
LIFT EFFECTIVENESS (HI-POWER)

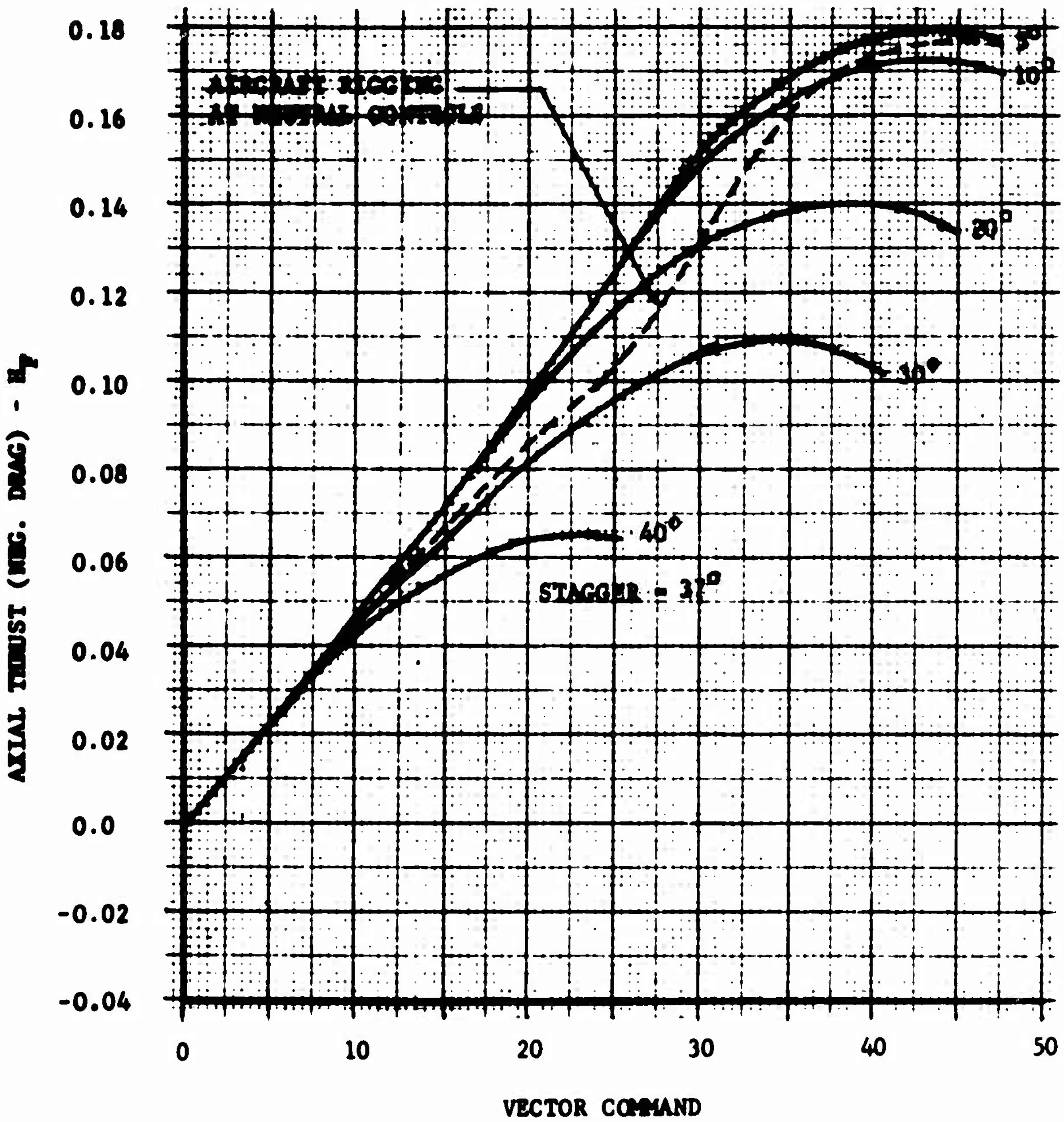

FIGURE 153

ESTIMATED STATIC VECTOR - STAGGER
THRUST EFFECTIVENESS (HI-POWER)

SOURCE OF DATA: ACCEPTANCE TESTS OF PITCH FAN WITH MODIFIED THRUST MODULATOR SYSTEM.

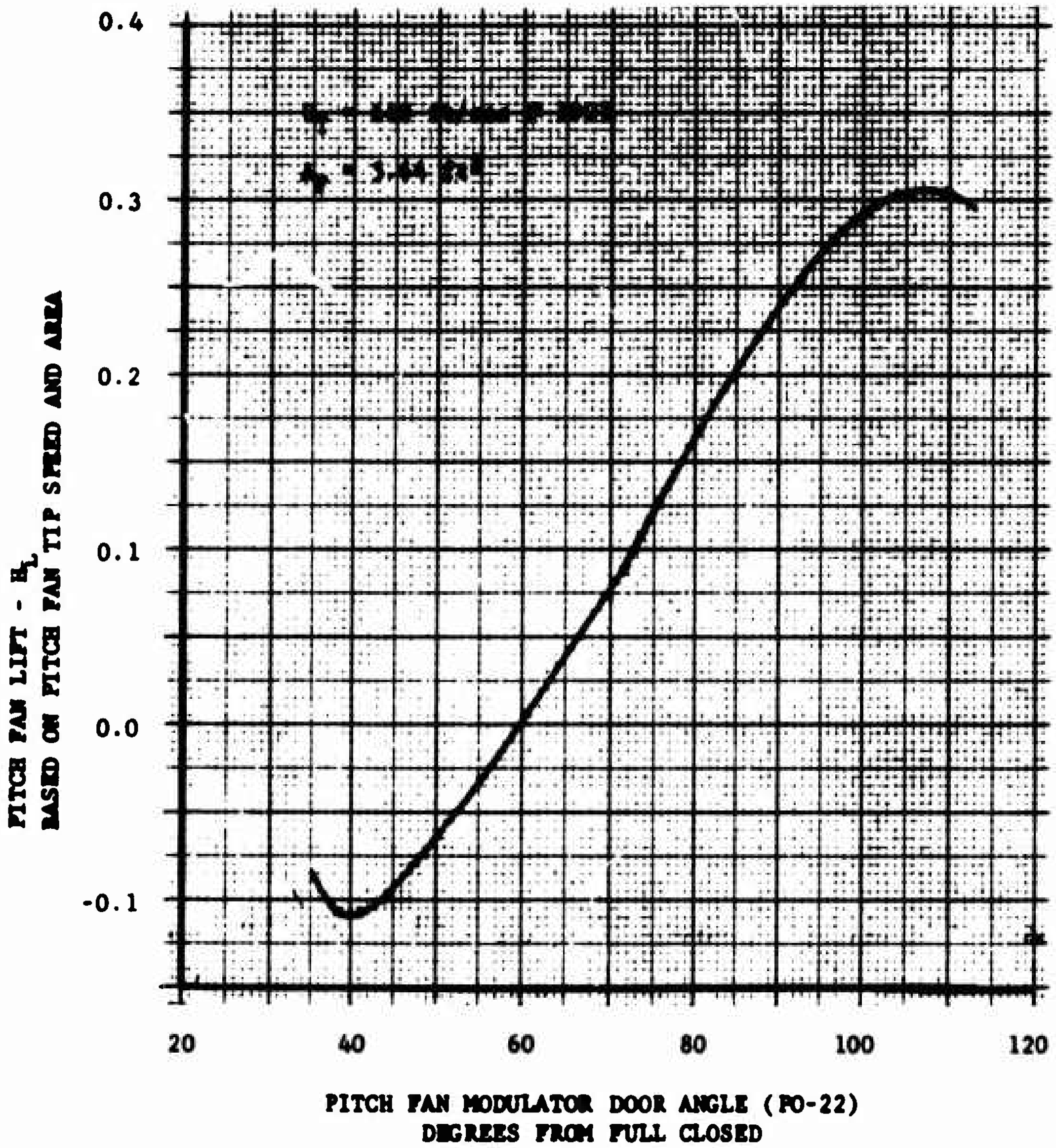

FIGURE 154

ESTIMATED PITCH FAN LIFT VERSUS MODULATOR DOOR POSITION

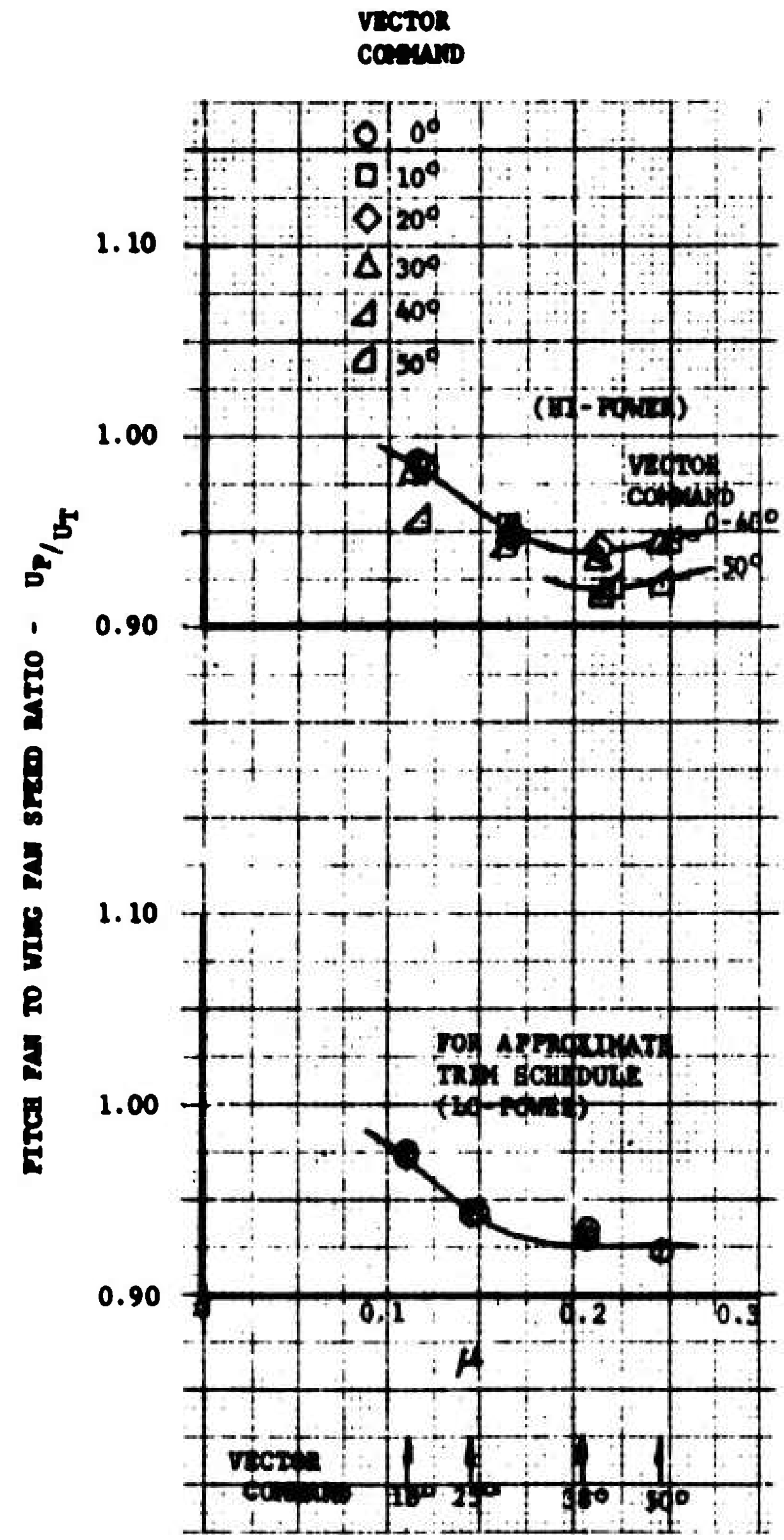

FIGURE 155

VARIATION OF PITCH AND WING FAN SPEED RATIO VERSUS CROSS-FLOW AND VECTOR COMMAND

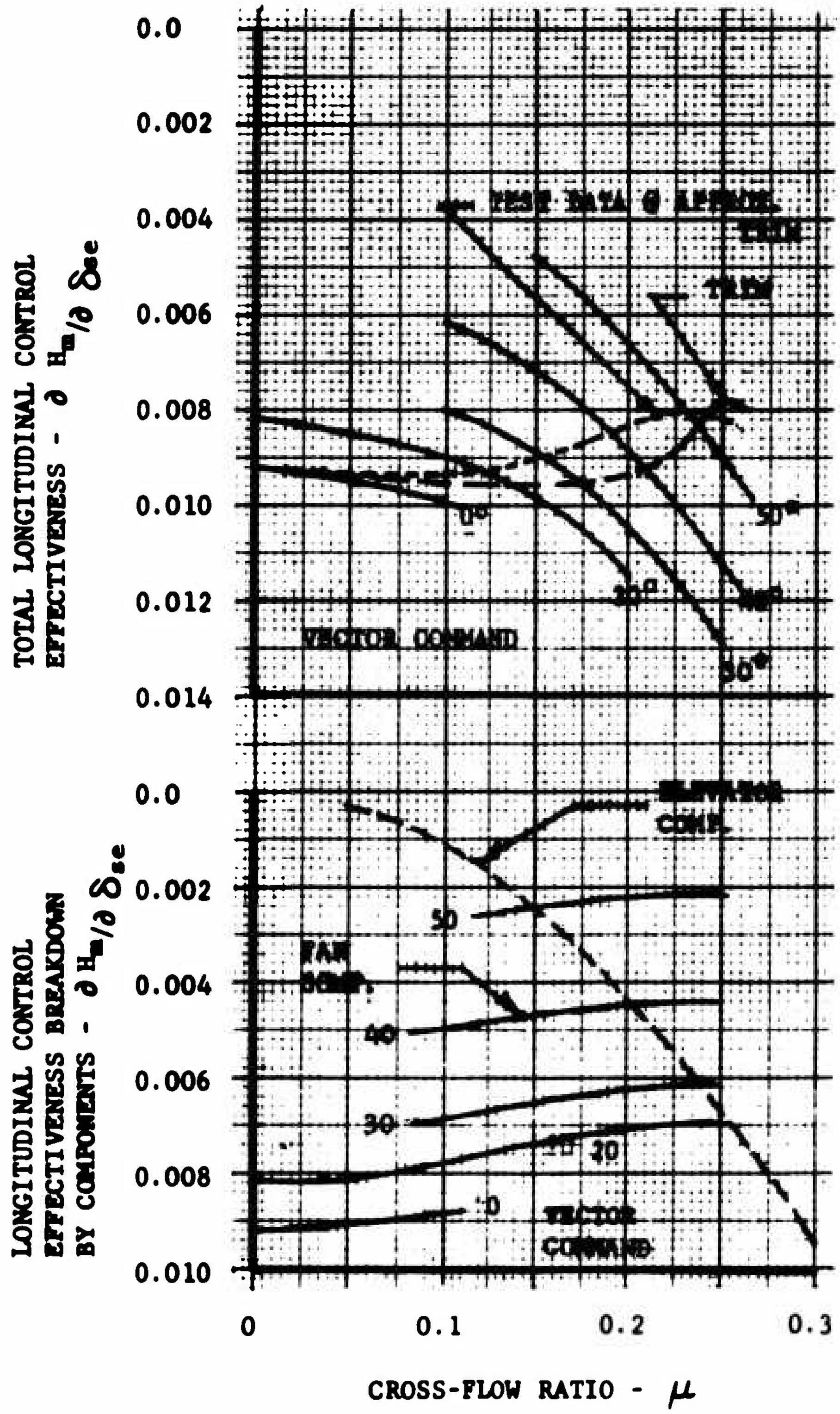

FIGURE 156

BUILD-UP OF LONGITUDINAL CONTROL EFFECTIVENESS VERSUS SPEED AND VECTOR COMMAND

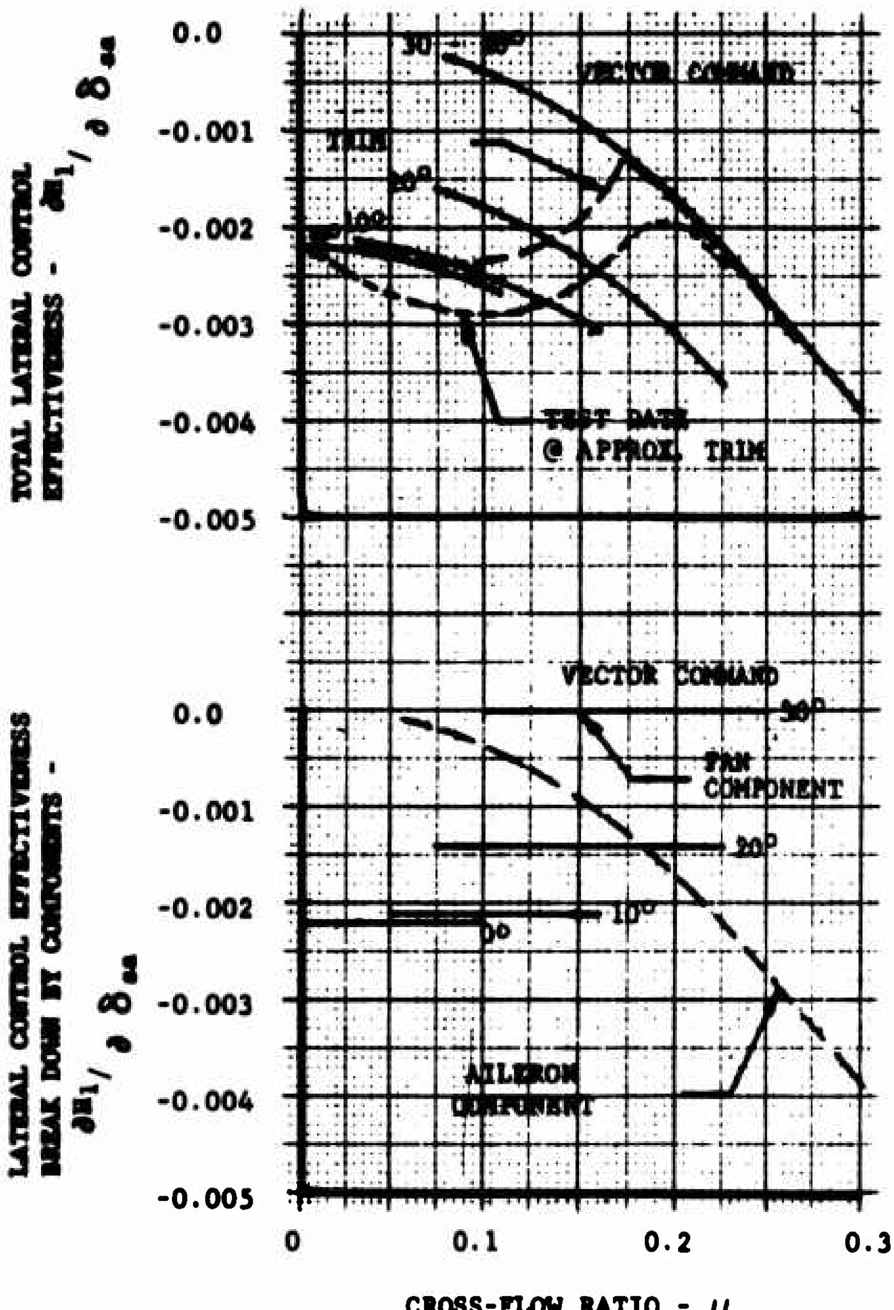

FIGURE 157

BUILD-UP OF LATERAL CONTROL EFFECTIVENESS VERSUS SPEED AND VECTOR COMMAND

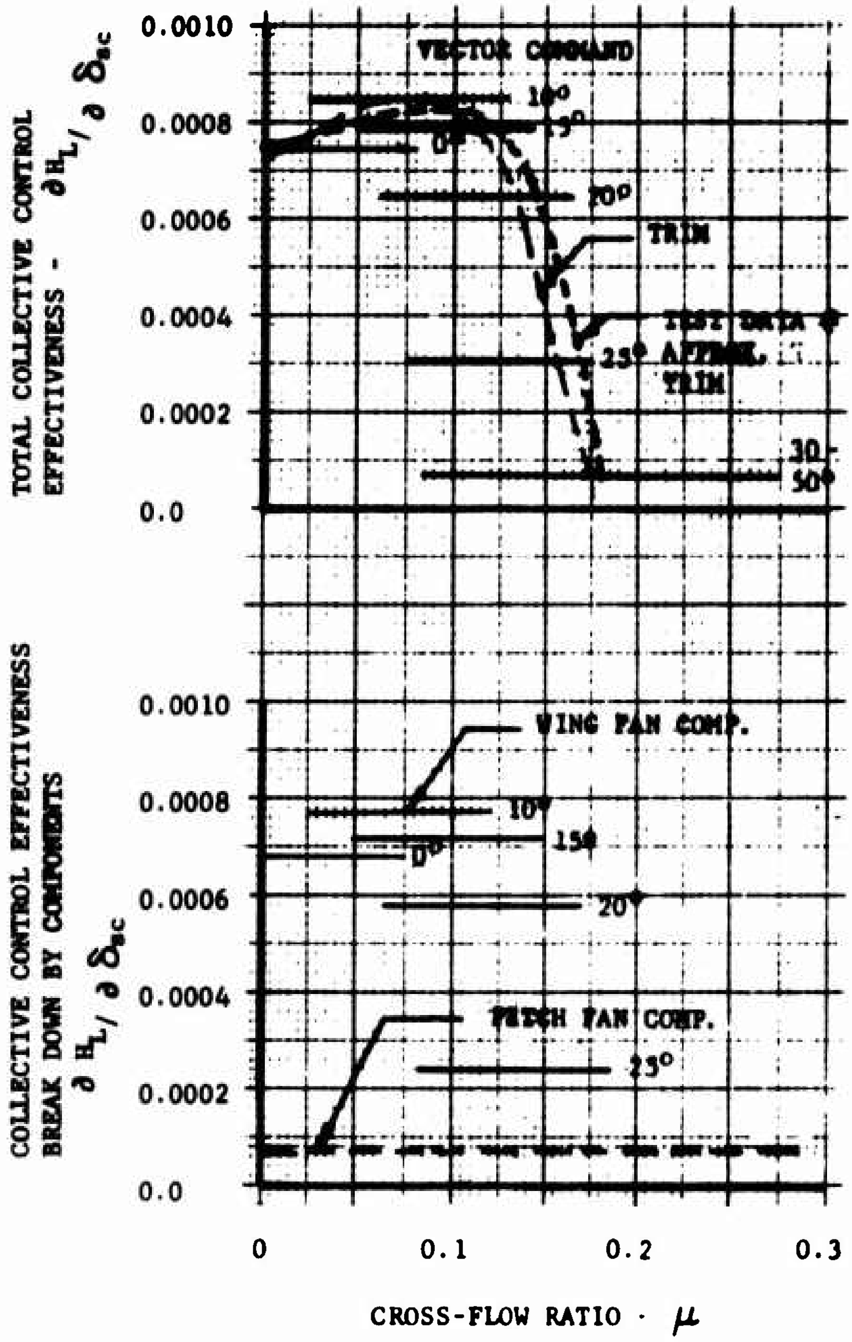

FIGURE 158

BUILD-UP OF COLLECTIVE CONTROL EFFECTIVENESS VERSUS SPEED AND VECTOR COMMAND

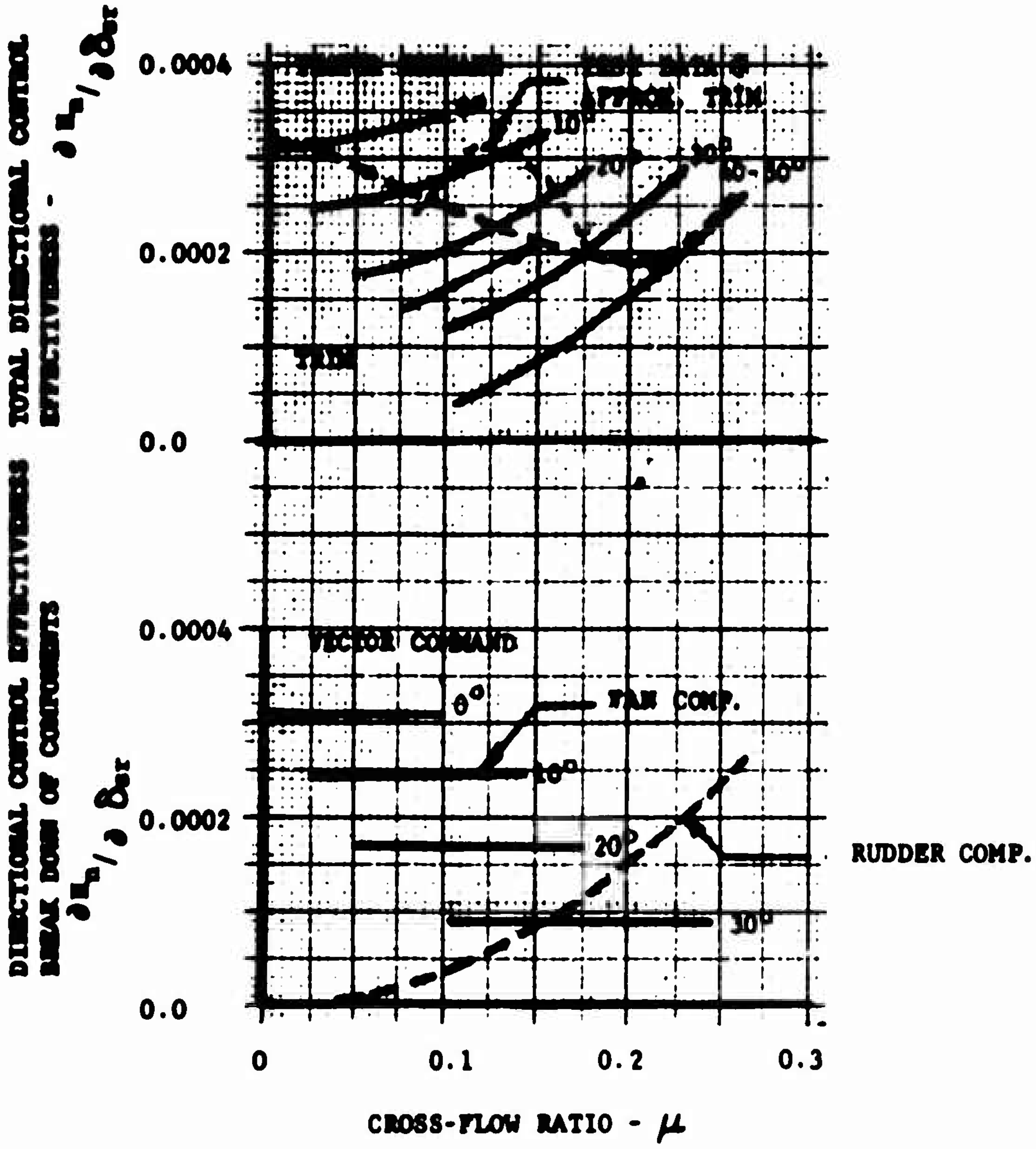

FIGURE 159

BUILD-UP OF DIRECTIONAL CONTROL EFFECTIVENESS VERSUS SPEED AND VECTOR COMMAND

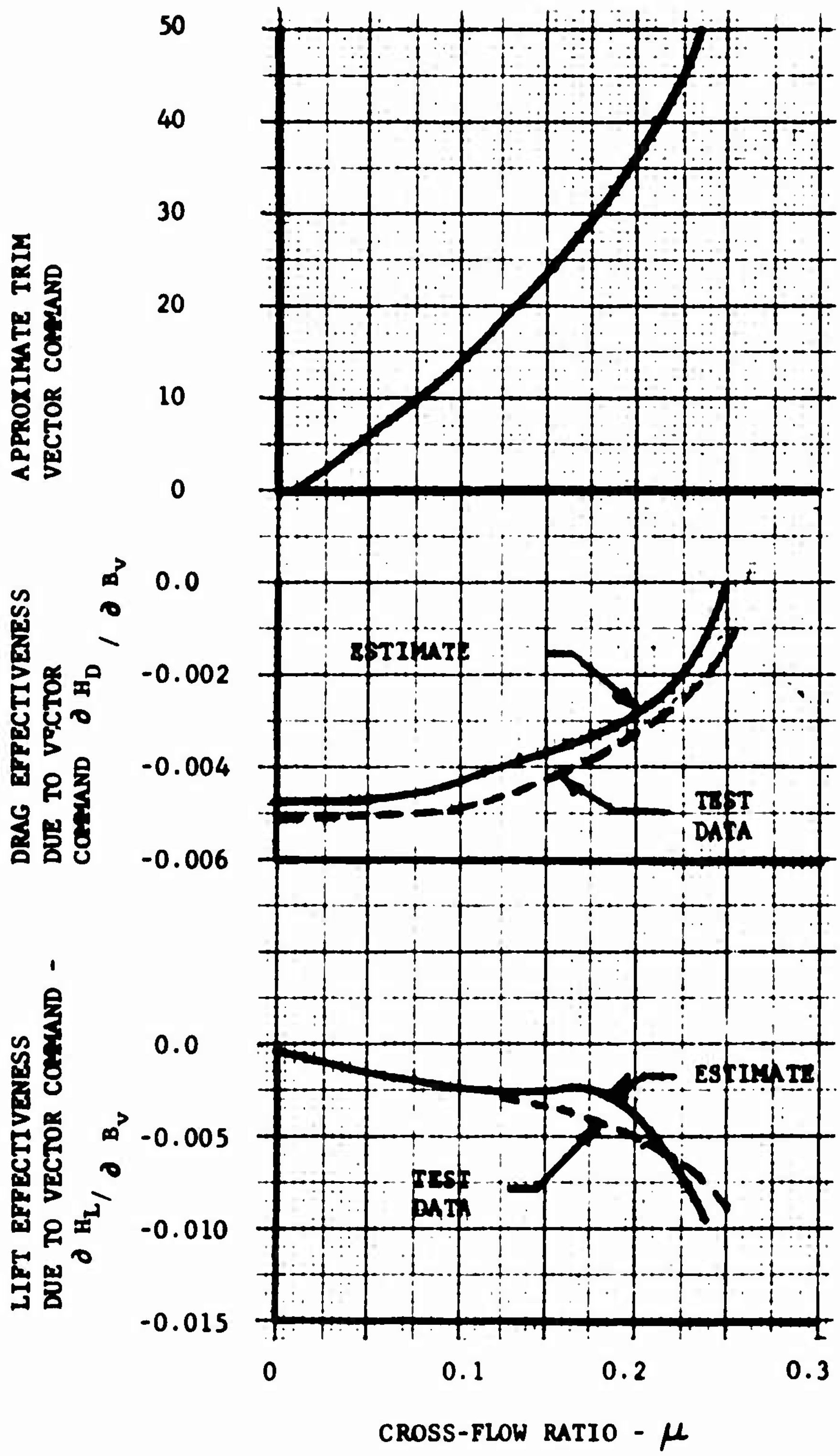

FIGURE 160

BUILD-UP OF VECTOR COMMAND EFFECTIVENESS

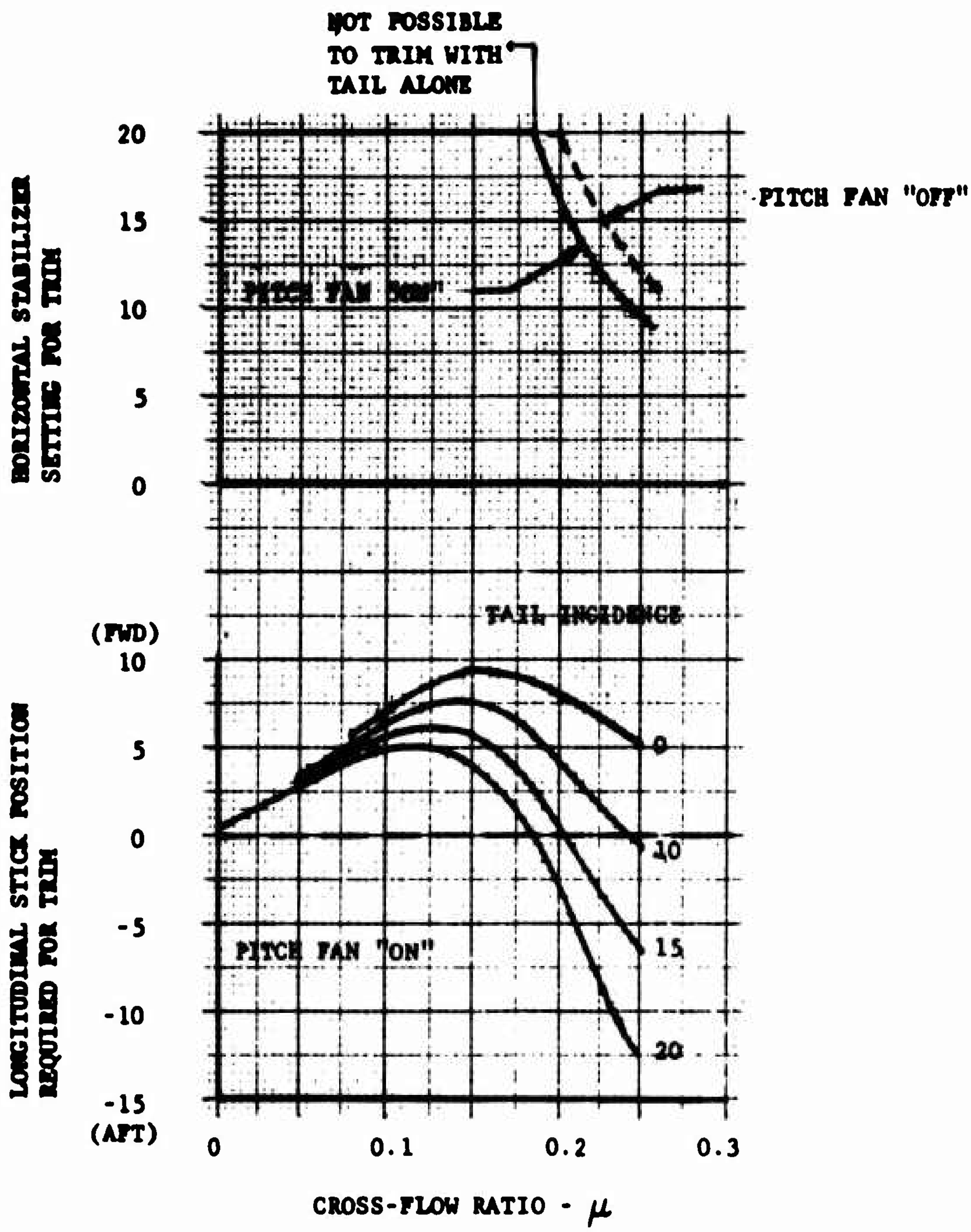

FIGURE 161

LONGITUDINAL TRIM REQUIREMENTS
DURING TRANSISTION

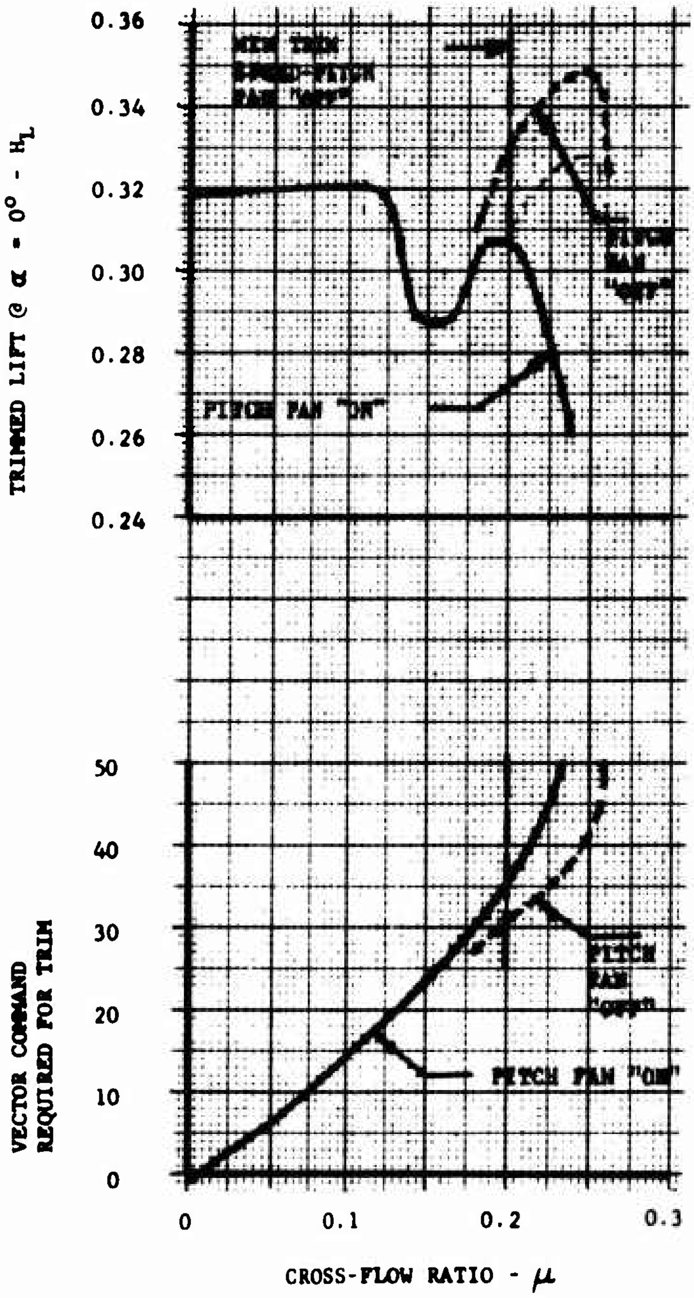

FIGURE 162

TRIMMED LIFT AND VECTOR COMMAND
DURING TRANSITION

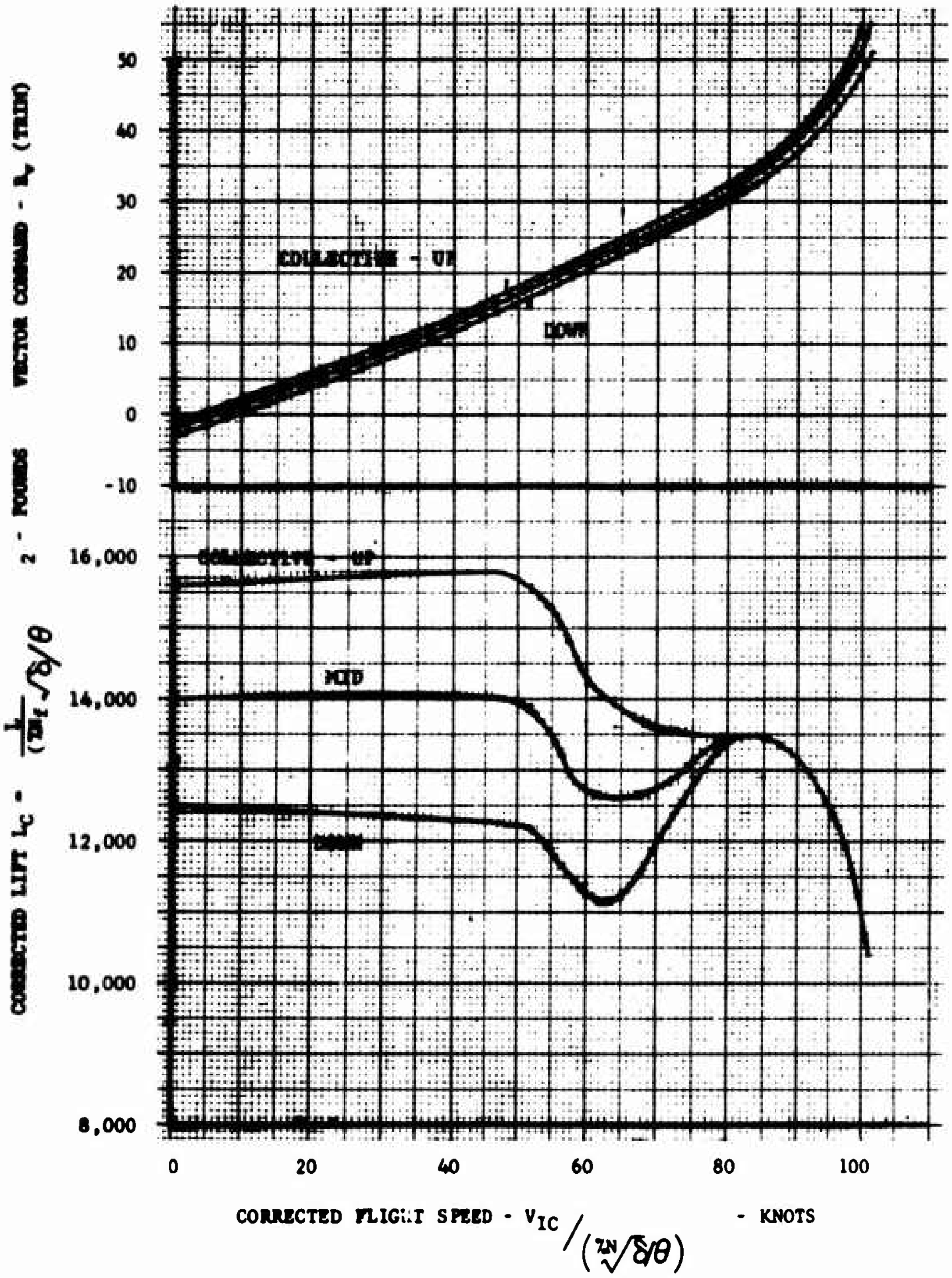

FIGURE 163A

TRIMMED TRANSITION CHARACTERISTICS - CORRECTED LIFT AND FLIGHT SPEED - ANGLE OF ATTACK = 0 DEGREES

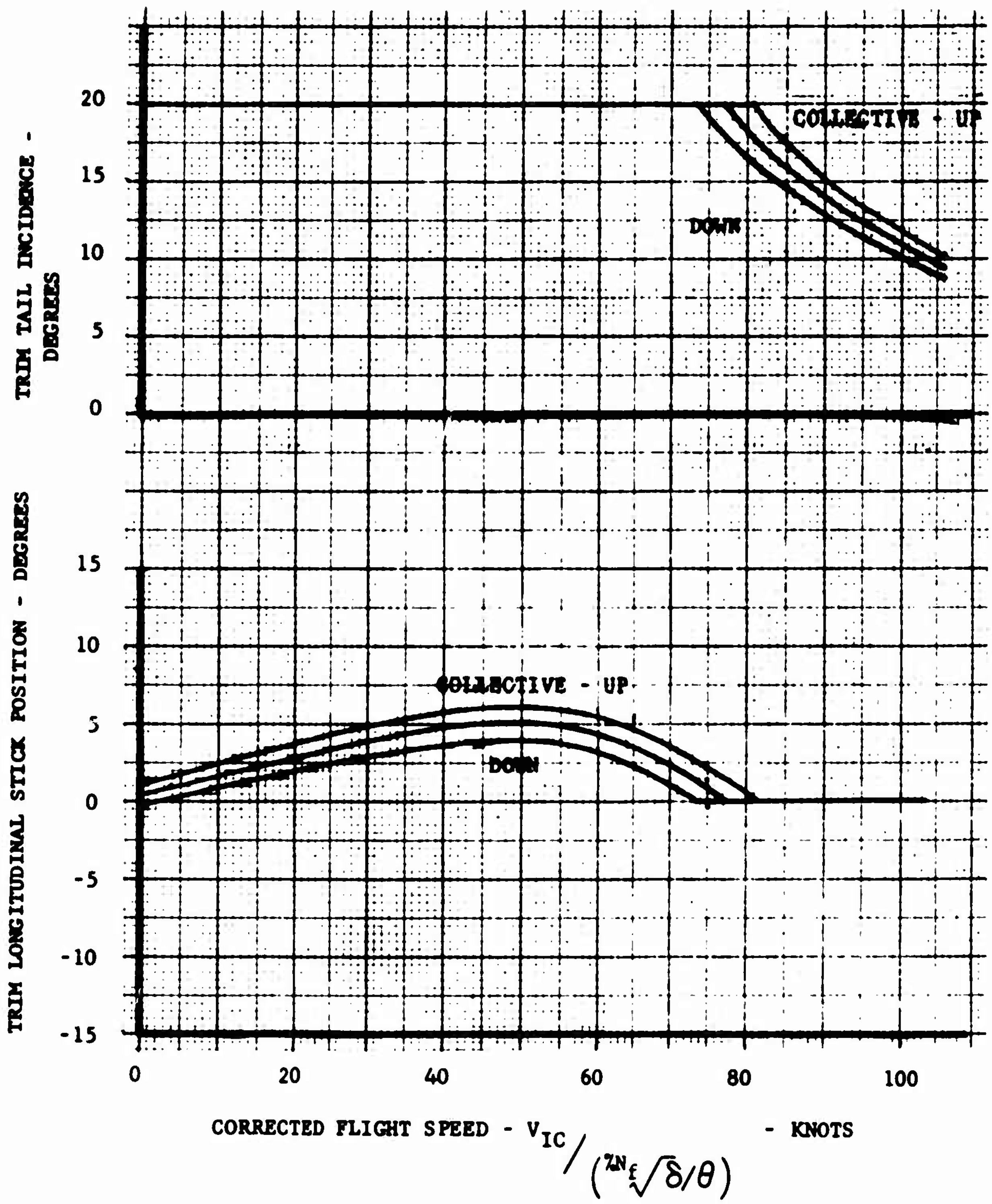

FIGURE 163B

TRIMMED TRANSITION CHARACTERISTICS -
CORRECTED LIFT AND FLIGHT SPEED

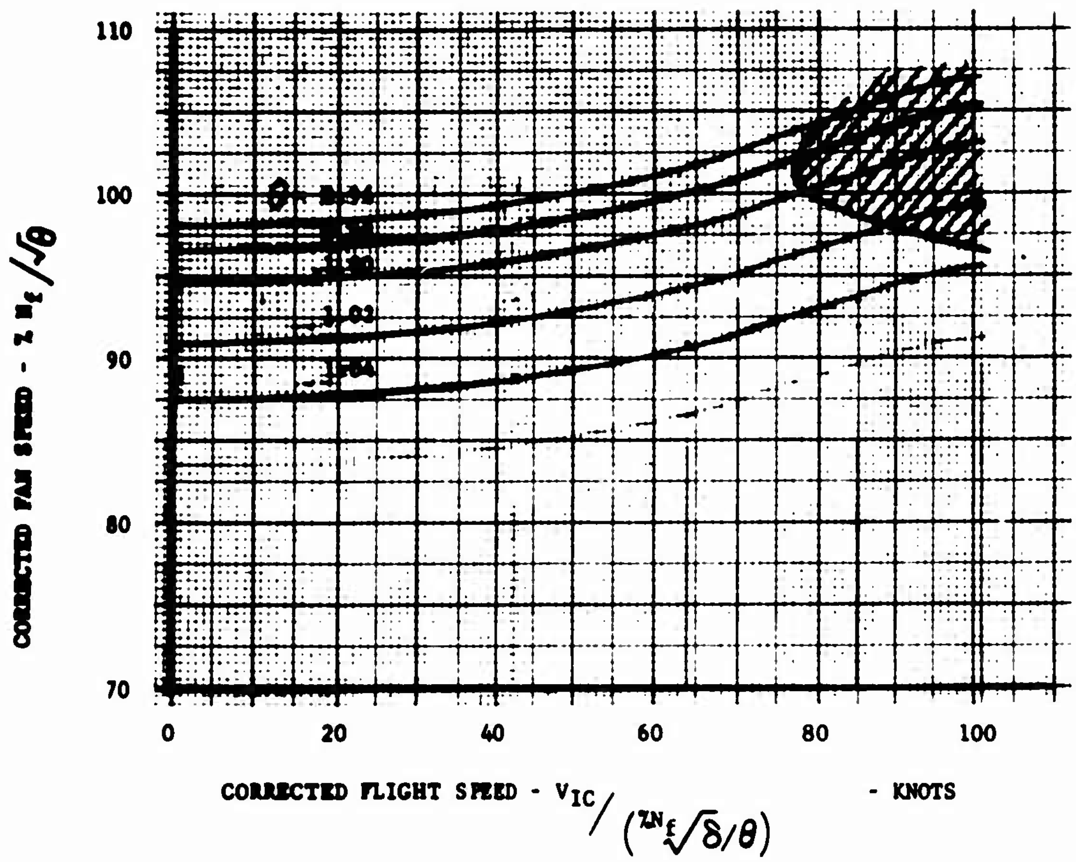

FIGURE 164

FAN SPEED CAPABILITY
AT MAXIMUM GAS GENERATOR POWER

HASHED ARES IS REGION WHERE HEIGHT CONTROL IS CHANGED FROM COLLECTIVE TO ENGINE THROTTLE

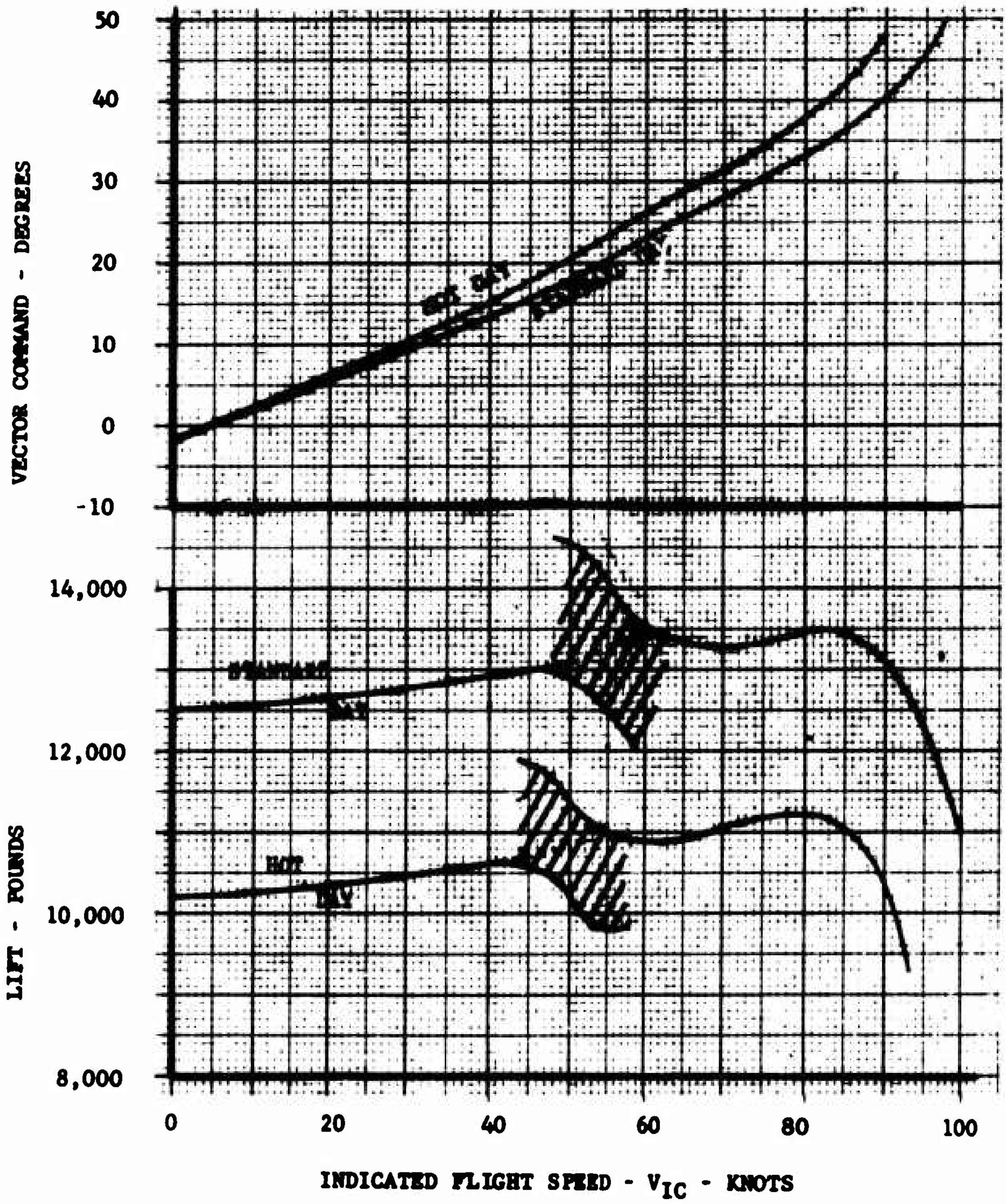

FIGURE 165A

TRIMMED LIFT CHARACTERISTICS -
SEA LEVEL STANDARD AND 2500 FT. HOT DAYS
ANGLE OF ATTACK = 0 DEGREES

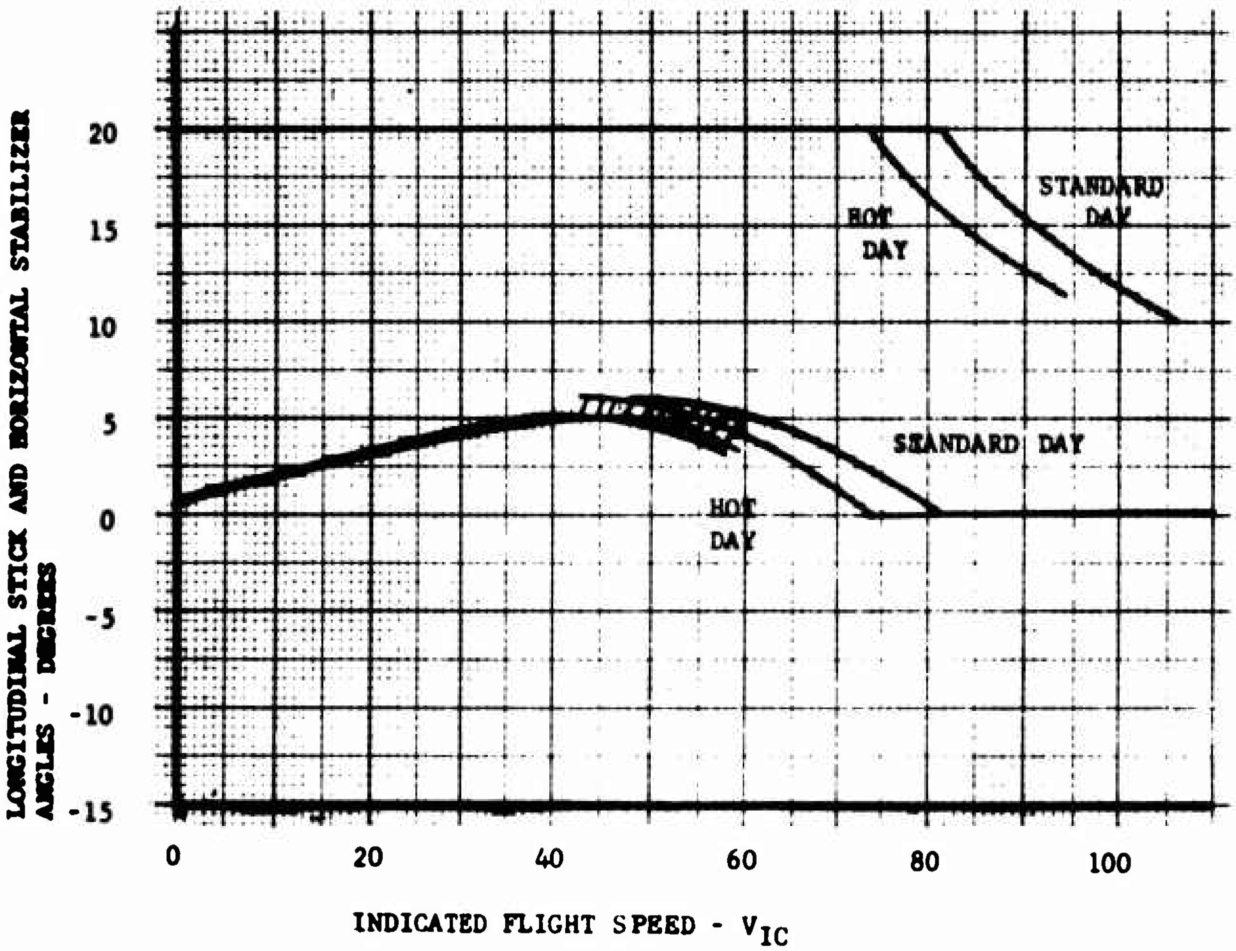

FIGURE 165B

TRIMMED LIFT CHARACTERISTICS (CONTINUED)